Equilibrium Concepts in Natural Water Systems

A symposium sponsored by
the Division of Water,
Air, and Waste Chemistry
at the 151st Meeting of
the American Chemical
Society, Pittsburgh, Pa.
March 23-24, 1966.

Werner Stumm,
Symposium Chairman

ADVANCES IN CHEMISTRY SERIES **67**

AMERICAN CHEMICAL SOCIETY

WASHINGTON, D.C. 1967

Library of Congress Catalog Card 67-27366

PRINTED IN THE UNITED STATES OF AMERICA

Advances in Chemistry Series

Robert F. Gould, *Editor*

AMERICAN CHEMICAL SOCIETY PUBLICATIONS

FOREWORD

ADVANCES IN CHEMISTRY SERIES was founded in 1949 by the American Chemical Society as an outlet for symposia and collections of data in special areas of topical interest that could not be accommodated in the Society's journals. It provides a medium for symposia that would otherwise be fragmented, their papers distributed among several journals or not published at all. Papers are refereed critically according to ACS editorial standards and receive the careful attention and processing characteristic of ACS publications. Papers published in ADVANCES IN CHEMISTRY SERIES are original contributions not published elsewhere in whole or major part and include reports of research as well as reviews since symposia may embrace both types of presentation.

PREFACE

This symposium was organized (1) to demonstrate that elementary principles of physical chemistry can be used to isolate and identify some of the pertinent variables that determine the composition of natural water systems; (2) to bring together analytical chemists, geologists, oceanographers, limnologists, and sanitary engineers who need to collaborate for a better understanding of our environment; (3) to stimulate research in aquatic chemistry and water analysis and to guide researchers in limnology, oceanography, and geochemistry.

Natural waters are complex systems whose chemistry cannot be described without considering many variables. To obviate this complexity, simplified manageable models are used to help us understand and predict real systems. As of now, the theory of the thermodynamic equilibrium appears to be the most expedient concept to facilitate identification of many variables relevant in determining the mineral relations and in establishing chemical boundaries of aquatic environments. Obviously, however, the state of equilibrium is an abstraction. Natural waters are open, dynamic systems with variable inputs and outputs of mass and energy in which true equilibrium is not attained. To be useful, a model need not be realistic as long as it produces fruitful generalizations and valuable insight into the factors that control the chemistry of natural waters.

By comparing the actual composition of sea water (sediments + sea + air) with a model in which the pertinent components (minerals, volatiles) with which water has come into contact are allowed to reach true equilibrium, Sillén in 1959 epitomized the application of equilibrium models for portraying the prominent features of the chemical composition of this system. His analysis, for example, has indicated that contrary to the traditional view, the pH of the ocean is not buffered primarily by the carbonate system; his results suggest that heterogeneous equilibria of silicate minerals comprise the principal pH buffer systems in oceanic waters. This approach and its expansion have provided a more quantitative basis for Forchbammer's suggestion of 100 years ago that the quantity of the different elements in sea water is not proportional to the quantity of elements which river water pours into the sea but is inversely proportional to the facility with which the elements in sea water are made insoluble by general chemical actions in the sea.

Although inland waters represent more transitory systems than the sea, equilibrium models are also useful here for interpreting observed facts. Even in highly dynamic systems, we can obtain some limits on the variation of the chemical composition, and we can speculate on the type of dissolved species and solid phases one may expect.

In natural waters organisms and their abiotic environment are interrelated and interact upon each other. Such ecological systems are never in equilibrium because of the continuous input of solar energy (photosynthesis) necessary to maintain life. Free energy concepts can only describe the thermodynamically stable state and characterize the direction and extent of processes that are approaching equilibrium. Discrepancies between predicted equilibrium calculations and the available data of the real systems give valuable insight into those cases where chemical reactions are not understood sufficiently, where nonequilibrium conditions prevail, or where the analytical data are not sufficiently accurate or specific. Such discrepancies thus provide an incentive for future research and the development of more refined models.

At an accelerating rate, we are altering the natural patterns of our environment, and in order to dispose of our wastes, we intervene with nature. It is my hope that the papers presented here contribute toward a better understanding of the environment and in turn will also lead to a better understanding of the way it is affected by man's pollution.

The motivation for this symposium grew out of discussions among members of the Study Section on Environmental Sciences and Engineering advisory to the Public Health Service, who gave me their encouragement and assistance. I am especially indebted to T. E. Larson and J. J. Morgan. The symposium has been supported by Grant WP 00899-01 of the Division of Water Supply and Water Pollution Control of the United States Public Health Service.

Cambridge, Mass. WERNER STUMM
January 1967

Applications and Limitations of Chemical Thermodynamics in Natural Water Systems

JAMES J. MORGAN

W. M. Keck Laboratory of Environmental Health Engineering, California Institute of Technology, Pasadena, Calif.

Studying thermodynamic relationships at constant temperature and pressure permits comparison between actual chemical composition of a natural water system and the equilibrium composition of a model closed system. Comparing the composition of the equilibrium model with that of the actual natural water system is an important step in understanding the real system. In contrast to closed-system models, for which the time-invariant state is equilibrium, the stationary state is the corresponding state of open systems. Three different chemical systems in natural waters illustrate these principles: homogeneous and heterogeneous buffer capacities in natural waters, hydrolysis reactions of aqueous aluminum, and the oxidation of reduced manganese by oxygen.

The chemistry of various natural water systems has received growing attention in the past two decades. Among others, chemical oceanographers, geochemists, limnologists, ecologists, water chemists, and water engineers have been engaged in increasing efforts to formulate adequate experimental and theoretical descriptions of the chemical behavior of ocean waters, estuaries, rivers, lakes, ground waters, soil-water systems, and various processes in water-treatment technology. Formulating equilibrium models based on the principles of classical chemical thermodynamics has occupied a prominent position in these efforts. Such formulations have occasionally yielded valuable insights into the pertinent equilibrium relationships for different natural water environments. While a comprehensive description of past developments in applying chemical thermodynamics to different natural water systems is not presented, it is appropriate to mention here the work of Sillén (32), Garrels and Christ

(*11*), Kramer (*18*), Stumm (*23, 34*), Goldberg (*13*), Holland (*16*), and Pourbaix (*27, 28*).

This paper outlines the basis for applying thermodynamic principles in studying the chemistry of natural water systems of all kinds, discusses the kinds of thermodynamic models available, and indicates some important limitations of such thermodynamic approaches. The general ideas will be illustrated by considering a few examples of chemical reactions of some interest in various kinds of natural water systems.

Natural Water Systems and Thermodynamic Systems

The general term natural water system refers to an actual system of some complexity, consisting of an aqueous phase, one or more mineral phases, and most often, a gas phase. The real natural water system quite often includes a portion of the biosphere. In general, the actual system may be inhomogeneous over-all, although it usually can be sufficiently well-characterized as consisting of a number of discrete homogeneous regions. For example, the oceans have relatively discrete regions of constant density and temperature and also contain relatively well-isolated deep basins of quite different chemical compositions. Extensive ground water formations may show pronounced spatial differences in principal mineral assemblages. Rivers and estuaries are characterized similarly by spatial differences in their physical and chemical properties.

Thermodynamic systems are parts of the real world isolated for thermodynamic study. The parts of the real world which are to be isolated here are either natural water systems or certain regions within these systems, depending upon the physical and chemical complexity of the actual situation. The primary objects of classical thermodynamics are two particular kinds of isolated systems: adiabatic systems, which cannot exchange either matter or thermal energy with their environment, and closed systems, which cannot exchange matter with their environment. (The closed system may, of course, consist of internal phases which are each open with respect to the transport of matter inside the closed system.) Of these, the closed system, under isothermal and isobaric conditions, is the one particularly applicable for constructing equilibrium models of actual natural water systems.

In addition to those attributes of real natural water systems mentioned above, there is one other which is often important. These systems are open to their environment. They receive various inputs (fluxes) of matter and energy from their surroundings and return matter and energy to their surroundings. Distinctions between closed and open systems depend largely upon the limits defined for isolation. However, large systems—*e.g.*, the lithosphere, plus the hydrosphere, plus the atmosphere

—are not reasonably expected to approach true equilibrium on time scales of interest in studying most natural water systems. Therefore, recognizing the open character of actual natural water systems, it is necessary to weigh the usefulness of equilibrium models for such systems and the possible need for applying other kinds of models.

Chemical Reactions and Equilibria in Closed, Isothermal Systems

For any chemical system the second law of thermodynamics furnishes useful equalities and inequalities which characterize the state of that system. At a state of equilibrium in a closed system, the total internal entropy production, $\sum dS_i$, is zero. For a spontaneous or natural process in any system, $\sum dS_i > 0$. The internal entropy production is a particularly pertinent variable in connection with the thermodynamic description of open systems. For the practical case of an isothermal, isobaric closed system, in which one or more chemical reactions may occur, the use of the Gibbs energy provides an equivalent and more convenient description of the state of the system with respect to the equilibrium state. The Gibbs energy of a system is defined by:

$$G = H - TS \qquad (1)$$

where G is the Gibbs energy or Gibbs free energy, H is the enthalpy, T is the absolute temperature, and S is the entropy. For a closed system of k chemical components, a particular form of the Gibbs equation for chemical transformation is:

$$dG = -SdT + VdP + \sum_{i}^{k} \mu_i dn_i \qquad (2)$$

from which the chemical potential of component i is defined as:

$$\mu_i = \left(\frac{\partial G}{\partial n_i}\right)_{T,P,n_j} \qquad (3)$$

The chemical potential is thus identical with the partial molar-free energy, $\overline{G}_i$, of component i. The total free energy of a closed system is therefore

$$G = \sum_{i} n_i \mu_i = \sum_{i} n_i \overline{G}_i \qquad (4)$$

Consider these typical examples of reactions of interest in natural water systems:

$$CaCO_3\ (s) + 2H^+ + H_2O = Ca^{2+} + H_2O + CO_2\ (g) \qquad (5)$$

$$2Fe^{2+} + 1/2\ O_2 + 5H_2O = 2Fe(OH)_3 + 4H^+ \qquad (6)$$

$$\begin{gathered} Mg_5Al_2Si_3O_{10}(OH)_8\ (s) + 10H^+ = \\ Al_2Si_2O_5(OH)_4\ (s) + SiO_2\ (s) + 5Mg^{2+} + 7H_2O \end{gathered} \qquad (7)$$

These can all be represented by the general reaction expression

$$\nu_A A + \nu_C C + \ldots = \nu_B B + \nu_D D + \ldots \qquad (8)$$

where ν_A represents the moles of component A, ν_B the moles of component B, etc. More concisely, for a closed system the stoichiometry can be written in generalized form as

$$\sum_i^k \nu_i M_i = 0 \qquad (9)$$

where M_i represents the molecular weight of component i, and ν_i is the stoichiometric coefficient of component i in a single over-all reaction. The ν_i are positive for products and negative for reactants. The free energy change of the isothermal, isobaric system as a result of the chemical reaction is:

$$dG = \sum_i^k \mu_i dn_i \qquad (10)$$

Introducing the degree of advancement of the reaction, ξ, which is defined by

$$dn_i = \nu_i d\xi \qquad (11)$$

ξ_i and $d\xi_i$ being the same for all i's taking part in the reaction, the change in the Gibbs free energy is obtained as

$$dG = \sum_i \nu_i \mu_i d\xi \qquad (12)$$

It can be readily shown (29) that the internal creation of entropy, dS_i, is given by

$$dS_i = -\frac{dG}{T} = -\frac{1}{T}\sum_i \nu_i \mu_i d\xi \qquad (13)$$

The quantity $\sum_i \nu_i\mu_i \left(= \sum \nu_i\bar{G}_i \right)$ is called the free energy change of the reaction, ΔG. The quantity $-\sum \nu_i\mu_i$ is called the affinity, A, by de Donder. Thus,

$$\Delta G = \sum \nu_i\mu_i = -A \tag{14}$$

Evidently,

$$\left(\frac{\partial G}{\partial \xi}\right)_{T,P} = \Delta G = -A \tag{15}$$

and the free energy of the reaction is precisely the rate of change of the Gibbs free energy with respect to the degree of advancement of the reaction. Since, from Equations 13 and 15

$$dS_i = -\frac{\Delta G}{T}\,d\xi = \frac{A}{T}\,d\xi \tag{16}$$

the condition for chemical equilibrium in a closed system of constant temperature and pressure is

$$\Delta G = -A = \sum_i^k \nu_i\mu_i = 0 \tag{17}$$

which corresponds to the condition that G for the system be a minimum. The driving force for a single chemical reaction is, therefore, a positive value for the affinity or a negative value for ΔG, the Gibbs free energy of the reaction.

The rate of internal entropy production, $\frac{dS_i}{dt}$, may be written

$$\frac{dS_i}{dt} = \frac{A}{T}\frac{d\xi}{dt} = \frac{A}{T}v \tag{18}$$

where $v = d\xi/dt$ is the velocity of the chemical reaction. The foregoing relationship provides a formal link between kinetic and thermodynamic descriptions of chemical reaction systems, and it is a basic one in irreversible chemical thermodynamics.

The general relationships involved for a single chemical reaction in a closed system are shown schematically in Figure 1, where the degree of advancement at point *e* corresponds to chemical equilibrium. Point *t* represents a state of the system corresponding to spontaneous chemical reaction. While the invariant condition of the closed system considered is the equilibrium state, *e*, this generally is not the case for a thermodynamic system open to its environment. For such a system, the time-

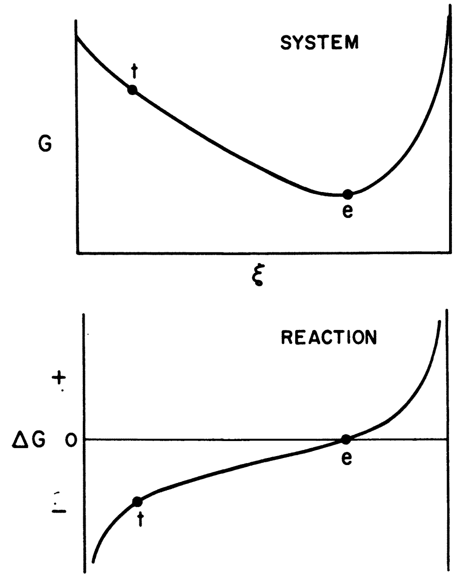

Figure 1. General relationships between Gibbs free energy variables of a chemical reaction and the degree of advancement

invariant condition is a stationary state which may be considerably far removed from that degree of advancement corresponding to chemical equilibrium in a closed system. This aspect of natural water system models is discussed further below.

The above arguments for a single chemical reaction are readily extended to the case of several simultaneous reactions in the same system. In the equilibrium state, for several reactions, I, II, . . . , *n* the affinities of all reactions are zero:

$$A_{\mathrm{I}} = A_{\mathrm{II}} = \ldots A_n = 0 \qquad (19)$$

The second law requires that the total entropy production in a system of several reactions be positive for a closed system removed from equilibrium. However, in the case of thermodynamic coupling of reactions (*26*), it is not necessary that individual reaction entropy productions be positive. Apparently such reaction systems have not yet been considered in connection with natural water systems.

The Equilibrium Constant. The relationship between the reaction free energy or the affinity for each chemical reaction and the composition of a closed system is readily obtained by applying Equation 14 for ΔG to the relationships between chemical potential, and the activity, a_i:

$$\mu_i = \mu_i^\circ + RT \ln a_i, \qquad (20)$$

where μ_i° ($= \bar{G}_i^\circ$) is the standard state chemical potential of i for each of the reaction components. The general result is

$$\Delta G = \sum_i \nu_i \mu_i^\circ + RT \sum_i \nu_i \ln a_i \tag{21}$$

or

$$\Delta G = \Delta G^\circ + RT \ln \prod_i^k a_i^{\nu_i} \tag{22}$$

where $\Delta G^\circ \left(= \sum_i \nu_i \mu_i^\circ \right)$ is the standard state Gibbs free energy of the reaction, or, in terms of Equation 8,

$$\Delta G = \Delta G^\circ + RT \ln \frac{a_B^{\nu_B} a_D^{\nu_D} \ldots}{a_A^{\nu_A} a_C^{\nu_C} \ldots} \tag{23}$$

Designating the quotient on the right hand side of Equation 22 or 23 for $\Delta G \neq O$ as Q

$$Q = \left(\frac{a_B^{\nu_B} a_D^{\nu_D} \ldots}{a_A^{\nu_A} a_C^{\nu_C} \ldots} \right) \tag{24}$$

and its corresponding value for $\Delta G = 0$ as K, the equilibrium constant

$$K = \left(\frac{a_B^{\nu_B} a_D^{\nu_D} \ldots}{a_A^{\nu_A} a_C^{\nu_C} \ldots} \right)_{\Delta G = 0} \tag{25}$$

the convenient and useful results are obtained

$$\Delta G^\circ = \sum_i \nu_i \mu_i = -RT \ln K \tag{26}$$

and

$$\Delta G = RT \ln \frac{Q}{K} \tag{27}$$

or

$$A = RT \ln \frac{K}{Q} \tag{28}$$

Equation 26 is the basis for a most important practical application of chemical thermodynamics to natural water systems: computing equilibrium constants from partial molar Gibbs free energies of formation for an almost unlimited number of reactions of interest, even though most of these reactions may not have been investigated experimentally. Adding logarithms of equilibrium constants corresponds simply to an algebraic combination of standard partial molar free energy data (Equation 26); hence, the computations are quite straightforward. A number of useful compilations of free energy data for species of interest are available (*19, 31, 33*).

Equations 27 and 28 permit a simple comparison to be made between the actual composition of a chemical system in a given state (degree of advancement) and the composition at the equilibrium state. If $Q \neq K$, the affinity has a positive or negative value, indicating a thermodynamic tendency for spontaneous chemical reaction. Identifying conditions for spontaneous reaction and direction of a chemical reaction under given conditions is, of course, quite commonly applied to chemical thermodynamic principle (the inequality of the second law) in analytical chemistry, natural water chemistry, and chemical industry. Equality of Q and K indicates that the reaction is at chemical equilibrium. For each of several chemical reactions in a closed system there is a corresponding equilibrium constant, K, and reaction quotient, Q. The status of each of the independent reactions is subject to definition by Equations 26–28.

Equilibrium Model for Natural Water Systems

The need to abstract from the considerable complexity of real natural water systems and substitute an idealized situation is met perhaps most simply by the concept of chemical equilibrium in a closed model system. Figure 2 outlines the main features of a generalized model for the thermodynamic description of a natural water system. The model is a closed system at constant temperature and pressure, the system consisting of a gas phase, aqueous solution phase, and some specified number of solid phases of defined compositions. For a thermodynamic description, information about activities is required; therefore, the model indicates, along with concentrations and pressures, activity coefficients, f_i, for the various composition variables of the system. There are a number of approaches to the problem of relating activity and concentrations, but these need not be examined here (*see, e.g.,* Ref. *11*).

The steps for constructing and interpreting an isothermal, isobaric thermodynamic model for a natural water system are quite simple in principle. The components to be incorporated are identified, and the phases to be included are specified. The components and phases selected "model" the real system and must be consistent with pertinent thermodynamic restraints—*e.g.,* the Gibbs phase rule and identification of the maximum number of unknown activities with the number of independent relationships which describe the system (equilibrium constant for each reaction, stoichiometric conditions, electroneutrality condition in the solution phase). With the phase-composition requirements identified, and with adequate thermodynamic data (free energies, equilibrium constants) available, chemical equilibrium in the closed system is then assumed (the affinity of each reaction is taken as zero), and the composition variables (activities, partial pressures, mole fractions) of the system are computed. Examples of this approach include a sea water model by Sillén (*32*), the inorganic ocean and fresh water models of Kramer (*17, 18*), a generalized fresh water model by Stumm (*34*), and Holland's discussion of the history of sea water (*16*). In some applications, the model used is in fact a series of imaginary closed systems, a few components being added in sequence and the conditions at chemical equilibrium being computed after each such addition. Alternatively, as in Kramer's approach, the assumed model is a single closed system at chemical equilibrium, and a set of simultaneous equations is solved to yield the over-all composition of the model. In either of these formal approaches, comparing the equilibrium composition of the model with that of the real natural water system is the important step in which one hopes to gain a clearer understanding of the chemical behavior of the real system.

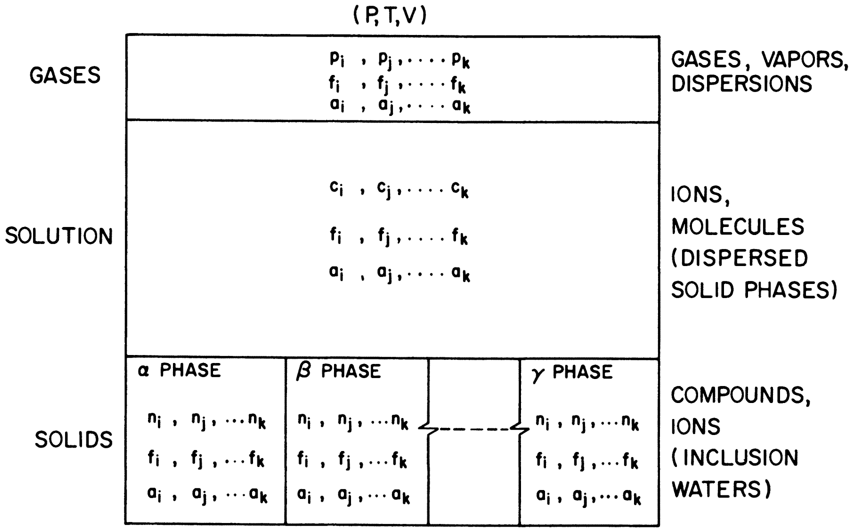

Figure 2. Generalized model for thermodynamic description of natural water systems

Significance and Applications of Equilibrium Models. Some of the value and significance of equilibrium models may be pointed out.

An idealized equilibrium model in which the essential features (pressure, temperature, predominant phases, major solution components, etc.) of the real system are accounted for is amenable to rigorous thermodynamic interpretation.

Selecting the conditions and the pertinent species and equilibria requires a critical examination of the available data for the real systems.

The equilibrium model allows certain inferences to be drawn concerning the geochemical environment which might have existed when sediments were formed, from knowledge of the thermodynamic properties of these sediments today. Thus, one can speculate about the evolution of the lithosphere, hydrosphere, and atmosphere, by assuming that equilibrium states were approached at various stages in geological history.

Comparing results for the model with data for the real system and identifying significant discrepancies help to identify gaps in our information or to reveal limitations in applying an equilibrium model. These may be of several kinds:

(a) Pertinent chemical equilibria may have been ignored in formulating the model or important species in solid or solution phases not considered.

(b) Thermodynamic data on assumed species and phases may be incorrect or inadequate.

(c) Analytical data on certain chemical elements in nature may be inadequate to distinguish between various physical and chemical forms (dissolved *vs.* suspended, oxidized *vs.* reduced, monomeric *vs.* polymeric, etc.).

(d) The rates of certain chemical reactions may be so slow that equilibrium is not attained in the real system.

(e) Temperature, pressure, and activity-concentration corrections may require refinement. Significant temperature gradients exist at times in nearly all bodies of water. Adequate data on temperature dependence of equilibria often are not available. Pressure correction requires knowing the partial molar volumes of the species involved. Extensive refinement along these lines is frequently unjustified because of greater uncertainties about other sources of discrepancy between the models and the real systems.

(f) The equilibrium model may be a poor approximation for a particular natural water system because of the flows of matter and energy in the real system. The appropriate time invariant condition might thus not be the state of thermodynamic equilibrium.

PERTINENT CHEMICAL EQUILIBRIA. The need to identify all pertinent reactions and equilibria has been sharply underlined recently by Sillén's calling attention to the likely important role of aluminosilicates in regulating the pH of sea water. In general, heterogeneous equilibria of all kinds need to be examined because of their potential significance with respect to pH regulation, metal-ion buffering, and adsorption of various organic solute species in natural waters. Ion-pair and complex formation equilibria between all pertinent anions or ligands and metal ions of interest must be recognized. There is still much ignorance in this area, although data of interest are becoming increasingly available (*12*, *33*).

For elements of several possible oxidation states (*e.g.*, sulfur, the transition metals) all relevant disproportionation equilibria need to be examined. Pseudo-equilibrium conditions may be maintained for some time, where competing oxidation-reduction systems can be involved. For example, the following kinds of reactions

$$\mathrm{Fe(II)} + \mathrm{O_2} = \mathrm{Fe(III)} \tag{29}$$

$$\mathrm{Fe(III)} + \text{reduced X} = \mathrm{Fe(II)} + \text{oxidized X} \tag{30}$$

might be proceeding at appreciable rates, but $d\mathrm{Fe(II)}/dt$ could be essentially zero. The possible significance of such systems needs to be considered, particularly in organic-rich fresh water and soil-water environments.

ADEQUACY OF THERMODYNAMIC DATA. Data on several important aluminosilicates appear to be insufficient for a detailed discussion of all equilibria. Information on the influence of solid solutions or coprecipitated phases on thermodynamic properties appears to be rather limited, as is that for metastable "non-stoichiometric" oxides (*e.g.*, of manganese) and surface complexes.

One significant reason why certain "thermodynamic" data are inadequate for equilibrium models is that they may not really be representative of equilibrium, having been obtained by experimental procedures (*e.g.*, solubility or potentiometry) which were time-dependent in themselves and in which slow kinetics were involved. This is an aspect about which not much seems definitely known.

ANALYTICAL CHEMICAL DATA FOR NATURAL WATERS. While elemental compositions of various natural waters usually can be determined with good reliability, analytical methods to distinguish between free and complex-bound species, oxidized and reduced forms, simple and polynuclear metal ion forms, and even between dissolved and colloidal or suspended phases are often lacking. Data on the nature and amounts of the individual substances which make up the total concentrations of organic material found in different natural waters are not yet extensive. These analytical deficiencies relate almost solely to the highly reactive, non-conservative elements—*e.g.*, iron, manganese, phosphorus, carbon, nitrogen, aluminum, and other metal ions.

KINETICS OF REACTIONS IN NATURAL WATERS. In considering equilibria and kinetics in natural water systems, it is usually necessary to recall that widely different time scales need to be identified with chemical reactions in different systems. Relatively short times (days to weeks) are available for approach to equilibrium in rivers, smaller lakes, reservoirs, and estuaries. Times for reaction in large lakes, seas, and perhaps typical ground waters are of the order of tens to hundreds of years. In ocean waters, the reaction time may range from thousands of years to long geological periods (millions of years). Garrels (9) has summarized much of the pertinent information on rates of geochemical reactions. Of course, highly spontaneous reactions (large positive affinity or negative Gibbs free energy of reaction) need not occur at observable rates. Familiar examples are the thermodynamic unstability of nearly all organic compounds—*e.g.*,

$$CH_3COOH = 2H_2O + 2C\ (\text{graphite}) \qquad K = 10^{18} \qquad (31)$$

and the spontaneous nature of Reaction 32.

$$1/2\,N_2(g) + 5/4\,O_2(g) + 1/2\,H_2O = NO_3^- + H^+ \qquad K > 1 \qquad (32)$$

The phenomenon of metastability depends upon a slow or negligible rate for a particular reaction of a phase or species. The same substance may, however, participate in other reactions which attain equilibrium—*e.g.*,

$$A \overset{\text{rapid}}{\rightleftarrows} B \quad (\Delta G < 0) \qquad (33)$$

$$\underset{\text{metastable}}{A} \xrightarrow{\text{extremely slow}} C \quad (\Delta G < 0) \qquad (34)$$

Thus, for certain reactions, the general point *t* in Figure 1 may represent the observable state of the system because of unfavorable chemical kinetics. The absence of any necessary relationship between thermodynamic tendencies for natural reactions and rates simply means that the kinds of models which have been considered above provide, to use an apt term of Garrels and Christ, "permissive" answers, but kinetic factors may frequently render these answers of little practical significance, even in closed systems.

Among some kinds of reactions which are "slow" on a relevant time scale and in particular environments are certain metal-ion oxidations, oxidation of sulfides, sulfate reduction, various metal ion polymerizations (*e.g.*, vanadium, aluminum), aging of hydroxide and oxide precipitates, precipitation of metal-ion silicates and carbonates (*e.g.*, dolomites), conversions among aluminosilicates (*e.g.*, feldspar-kaolinite), and solution or precipitation of quartz (9). Some of these reactions can be accelerated greatly by biological catalysis (*e.g.*, sulfate reduction, metal ion oxidations) (7).

Open Systems and Dynamic Models

Natural water systems are, in contrast to the models discussed so far, systems which are open to their environment. Therefore, what additional limitations should be expected when using equilibrium models? Figure 3 outlines some of the major features which generally need to be included in formulating either a time-invariant or dynamic open system model for any particular natural water system. The simplest model to be considered for an open system is perhaps the stationary or steady state. The time-invariant condition of a chemical reaction system which is open to its environment is the stationary nonequilibrium state (*5*, *29*).

In a closed system, the time-invariant condition is equilibrium, which is a state of zero internal entropy production. By contrast, the stationary state of an open system is one in which entropy production is occurring, subject to the external constraints upon the system (*e.g.*, fixed concentrations or affinities in the environment). Prigogine (*29*) has described the stationary state as one of minimum entropy production (least free energy dissipation), compatible with the constraints upon the system. Significant limitations to the general validity of this extremum principle have been discussed by Denbigh (*5*), among others. The possibilities of applying the variational principles await further elucidation. In any event, for open systems in which the over-all affinities are controlled by external conditions, the internal, entropy production, and hence the affinity and Gibbs energy for a chemical reaction, is not zero in the stationary state. Thus, in Figure 1, point *t* might represent the state of an open system in which a reaction is proceeding. This state is determined by the fluxes of reactants and products between system and surroundings and by the kinetics of the reaction. The literature on chemical reactors (*5*, *6*, *20*) describe some model systems which have some general relevance for studying natural water systems.

In connection with the factors mentioned in Figure 3 it would seem useful to call attention to the form of the fundamental expression describing the concentration, c_i of constituent *i* at any point (x, y, z) in a natural water system.

$$\frac{\partial C_i}{\partial t} + u\frac{\partial C_i}{\partial x} + v\frac{\partial C_i}{\partial y} + w\frac{\partial C_i}{\partial z} = \frac{\partial}{\partial x}\left(D_x\frac{\partial C_i}{\partial x}\right) + \frac{\partial}{\partial y}\left(D_y\frac{\partial C_i}{\partial y}\right) + \frac{\partial}{\partial z}\left(Dz\frac{\partial C_i}{\partial z}\right) + r_{i,\,n} \qquad (35)$$

where the $u\frac{\partial C_i}{\partial x}$, etc. are advective or convective terms, $\frac{\partial}{\partial x}\left(D_x\frac{\partial C_i}{\partial x}\right)$, etc. are diffusion or turbulent transport terms, depending upon the hydrodynamic situation, and $r_{i.\,n}$ denotes the rate of formation or disappearance of constituent *i* by process *n* in the neighborhood of the point. In the steady state for *i*, $\frac{\partial C_i}{\partial t} = 0$. Steady state models have been developed for various chemical reactions and processes in different natural water systems. Some interesting examples are provided by Berner's model (*1*) for sulfate distribution in sediments, O'Connor's models for non-conservative substances in tidal estuaries (*25*), and Riley's model for phosphorus distribution in sea water (*30*). Such models require reasonably detailed information on the flows in the system, the rates of the chemical reactions of interest, the diffusion and mixing process, etc. These kinds of models are needed for a sufficiently accurate description of the spatial distributions of chemical constituents in natural water systems involving a combination of slow reactions, high rates of material and energy flow, and complex transport processes. Indeed, even the necessary conditions for a stationary state may often not be realized, where perturbations in fluxes of matter and energy are pronounced.

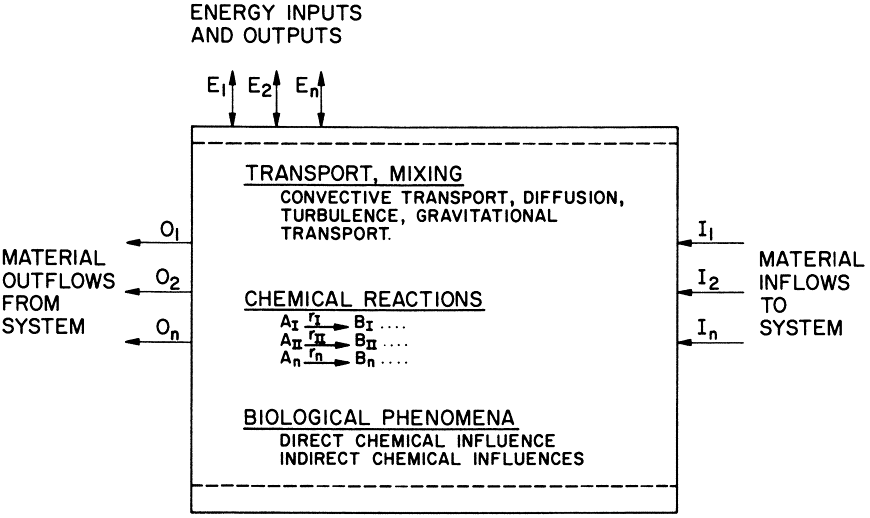

Figure 3. Generalized model for chemical dynamic description of natural water systems

In view of all of the preceding observations concerning the formal differences between closed and open systems, what general conclusions can be drawn about the applicability of equilibrium concepts in understanding and describing the chemical behavior of the elements in natural water systems? Since equilibrium is the time-invariant state of a closed system, the question is under what conditions do open systems approximate closed systems. A simple example will illustrate the relationships, which are already implicit in Equation 35. If one considers the case of a simple reaction

$$A \underset{k'}{\overset{k}{\rightleftharpoons}} B \qquad (36)$$

which takes place in a completely mixed volume V, into which A and B are introduced at concentration $(A)_0$ and $(B)_0$ and from which A and B are withdrawn, the volume rate of flow being g, then the material balance rate expressions for A and B can be written as

$$\frac{d(A)}{dt} = \frac{g(A)_0}{V} - \frac{g(A)}{V} - k(A) + k'(B) \tag{37}$$

and

$$\frac{d(B)}{dt} = \frac{g(B)_0}{V} - \frac{g(B)}{V} + k(A) - k'(B) \tag{38}$$

In the time-invariant condition

$$\frac{d(A)}{dt} = \frac{d(B)}{dt} = 0 \tag{39}$$

The ratio of (B) to (A) for this condition is

$$\frac{(B)}{(A)} = \frac{k\frac{V}{g}\Big((A)_0 + (B)_0\Big) + (B)_0}{k'\frac{V}{g}\Big((A)_0 + (B)_0\Big) + (A)_0} \tag{40}$$

The equilibrium constant and the first-order rate constants are related by

$$K = \frac{k}{k'} \tag{41}$$

It is clear from Equations 40 and 41 that the steady state ratio $\frac{(B)}{(A)}$ approaches K as the flows to the system become small with respect to the rates of chemical reaction. In the simple case where $(B)_0 = 0$, one obtains

$$\frac{(A)}{(B)} = \frac{1}{K} + \frac{1}{k\left(\frac{V}{g}\right)} \tag{42}$$

or

$$\frac{(A)}{(B)} = \frac{1}{K} + \frac{1}{\ln 2\tau_R/\tau_{1/2}} \tag{43}$$

where $\tau_R = \frac{V}{g}$ and $\tau_{1/2} = \frac{\ln 2}{k}$, the half-time of the first-order reaction.

Thus, when the residence time τ_R, is sufficiently large relative to the appropriate time scale of the reaction, $\tau_{1/2}$, the time-invariant condition of the well-mixed volume considered approaches chemical equilibrium.

This requirement would appear difficult to satisfy for the number of slowly reacting constituents in the total volume of many fresh water or estuarine systems, where residence times may be small and mixing incomplete. It probably is sufficiently well-satisfied for a number of elements in the greater part of large-volume and low-flow systems—for example, the major oceans, the Great Lakes, and certain ground water formations. Equilibrium would appear to be a reasonable assumption for such substances as sodium, potassium, magnesium, calcium, carbonate, chloride, sulfate, and fluoride in long-residence time systems (*13, 17, 18*). Holland (*16*), in reviewing previous observations on the interactions of river-transported clay minerals with ocean waters, has inferred that equilibrium is approached at least in part.

For nearly all kinds of systems it can be argued that there exist regions or environments where, at times, the time-invariant condition closely approaches equilibrium, even though gradients exist throughout the system as a whole (*35*). The concept of a local equilibrium is a fundamental assumption in thermodynamic theories of irreversible processes. Local equilibrium conditions might be expected to develop for certain kinetically rapid species and phases at sediment-water interfaces in fresh, estuarine, and marine environments. In contrast, other local environments, such as the photosynthetically-active surface regions of nearly all lakes and ocean waters and the biologically-active regions of soil-water systems are clearly far removed from total system equilibrium. Essential nutrients are incorporated into the biosphere in the euphotic regions of surface waters with locally high energy and material flux, and are transported by gravity (Figure 3). Net degradation of organic matter occurs at greater depths in some systems; reducing environments can result in various chemical changes (nitrate and sulfate reduction, iron reduction, metal ion sulfide precipitation, etc.). Consequently, pronounced vertical gradients of elements such as oxygen, phosphorus, carbon, nitrogen, sulfur, silica, iron, and manganese develop in deep bodies of water. As mentioned above, particular solutions of Equation 35 are needed to describe the over-all behavior of these elements in such situations.

Some Examples of Thermodynamic Applications To Natural Water Systems

Buffer Capacities of Natural Waters. Natural waters are buffered in different ways and to varying degrees with respect to changes in pH, metal ion concentrations, various ligands, and oxidation-reduction potential. The buffer capacity is an intensive variable and is thermodynamic in nature. Hydrogen-ion buffering in natural waters has recently been discussed in detail by Weber and Stumm (*38*). Sillén (*32*) has doubted the commonly held view that pH buffering in the oceans is caused by the CO_2–HCO_3^-–CO_3^{2-} equilibrium. Recently, Garrels (*10*) and Holland (*16*) have expanded upon the quantitative aspects of Sillén's proposal concerning the role of aluminosilicate equilibria in maintaining the pH of sea water. In the brief examples presented here, several pH-buffering systems are compared. The range is not comprehensive, and the treatment is intended only to suggest some possibilities for further studies. The practical importance of the buffer capacities, since they are based upon thermodynamics, will depend also upon those other factors already discussed, *i.e.*, kinetics and fluxes.

The buffer capacity may be considered as defined for the incremental addition of a constituent to a closed system at equilibrium—*e.g.*, adding a strong acid to a carbonate solution, CO_2 to a water solution in equilibrium with calcite, a strong acid to a sea water solution in equilibrium with both kaolinite and muscovite, etc. In general,

$$\beta^{C_i}_{C_j} = \frac{dC_i}{d\text{pH}} \tag{44}$$

where $\beta^{C_i}_{C_j}$ is the pH buffer capacity for adding C_i incrementally to a system of constant C_j. The buffer capacity is found analytically by differentiating the appropriate function of C_i for the system, with respect to pH. For example, evaluating the heterogeneous buffer capacity $\beta^{C_T}_{CaCO_3}$ involves combining the relationships

$$2(Ca^{2+}) + \sum_r Z_r C_r = (HCO_3^-) + 2(CO_3^{2-}) + (OH^-) - (H^+) \tag{45}$$

$$C_T = (H_2CO_3) + (HCO_3^-) + (CO_3^{2-}) \tag{46}$$

$$K'_c = (Ca^{2+})(CO_3^{2-}) \tag{47}$$

$$K'_1 = (HCO_3^-)(H^+)/(H_2CO_3) \tag{48}$$

$$K'_2 = (CO_3^{2-})(H^+)/(HCO_3^-) \tag{49}$$

$$K_{CO_2} = (H_2CO_3)/P_{CO_2} \tag{50}$$

$$K'_w = (H^+)(OH^-) \tag{51}$$

to obtain C_T, for specified $\sum_r Z_r C_r$, the non-carbonate alkalinity, where Z_r and C_r are the ion charge and concentration, respectively. General approaches have been described by Weber and Stumm (*38*). The buffer capacity is an intrinsic function of the pH as well as the pertinent capacity variable for the system.

Figure 4 shows a number of computed "homogeneous" (absence of solid phases) buffer capacity *vs.* pH relationships for sea water conditions and for millimolar solutions at 25°C. The various $\beta^{C_A}_{C_j}$ are the familiar buffer capacities with respect to addition of strong acid (or base), introduced by Van Slyke (*36*). The two curves of $\beta^{C_T}_{ALK}$ are for adding or removing total CO_2 (frequently denoted $\sum CO_2$) in a system of constant alkalinity (electroneutrality condition). As pointed out by Sillén, the various homogeneous buffer capacities at the pH of sea water, approximately 8, are not large, although they are certainly larger than the corresponding ones for many fresh water conditions.

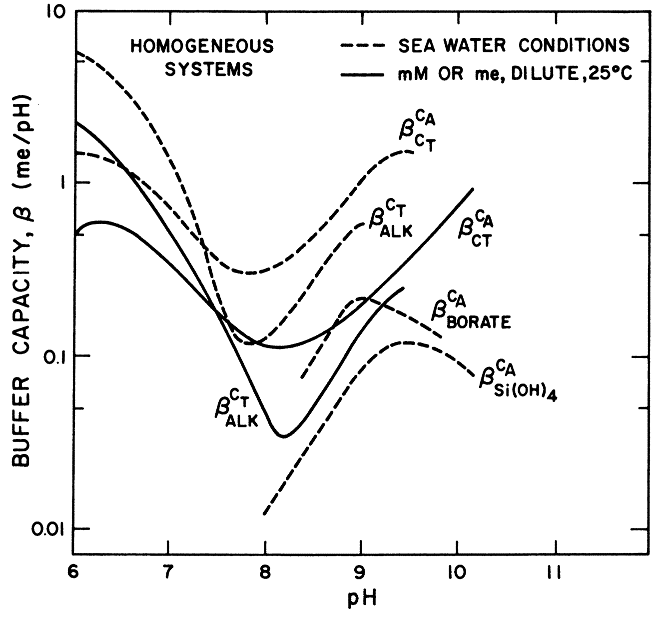

Figure 4. Buffer capacity vs. pH for some chemical systems not involving solid phases

One set of aluminosilicate equilibrium relationships for which some quantitative data are available is depicted in Figure 5. This figure (25° C) is derived from information presented and discussed by Hemley (*15*), Feth, Roberson, and Polzer (*8*), and Garrels and Christ (*11*). The dual boundaries between potassium mica (muscovite) and kaolinite reflect the roughly estimated uncertainty in the equilibrium constant. The relationship of this boundary to actual K^+–H^+ ratios in sea water may be

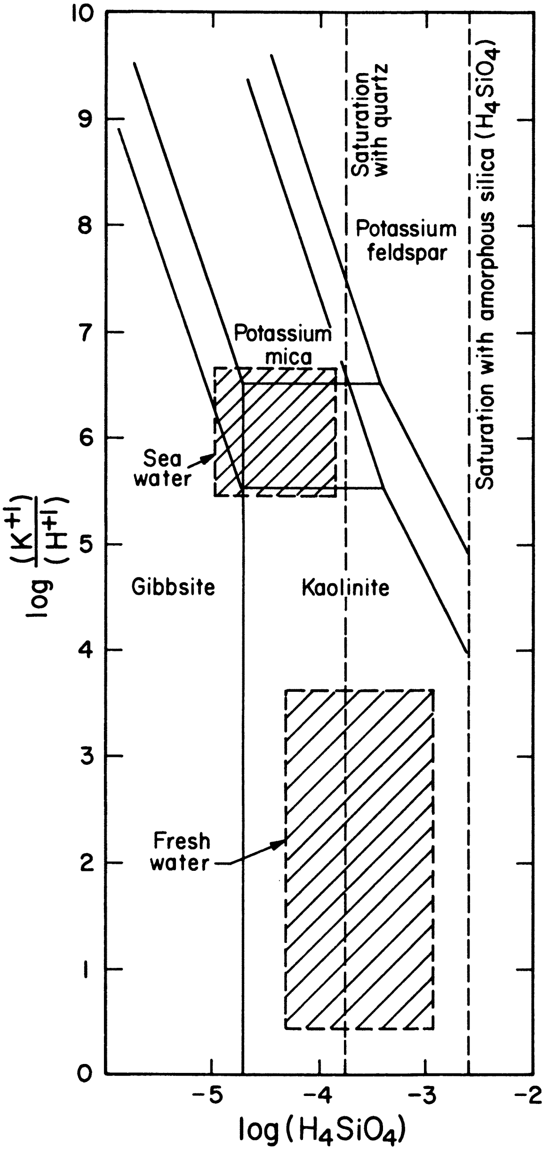

Figure 5. Equilibrium relationships and observed natural water domains for some phases in the system $KOH-Al(OH)_3-Si(OH)_4-H_2O$, at 25°C.

taken to suggest that the oceans are at least approximately in equilibrium with muscovite and kaolinite (*16*). In sharp contrast, fresh water conditions are far removed from the aluminosilicate equilibrium boundary (*8, 10, 11*).

If one considers an imaginary and highly oversimplified model for the sea water system in which the kaolinite-muscovite equilibrium is assumed to take place in a closed system to which strong acid or strong base is added incrementally, a buffer capacity can be computed. The electroneutrality would be

$$(H^+) + (K^+) = (Cl^-) + (OH^-) + C_A \qquad (52)$$

where C_A is the concentration of strong acid added (or the negative of strong base added)—*e.g.*, HCl. The potassium ion concentration, (K^+), is given by $K'(H^+)$, where K' is the equilibrium constant for the kaolinite-muscovite equilibrium,

$$KAl_3Si_3O_{10}(OH)_2 + H^+ + 3/2\ H_2O = \\ 3/2\ Al_2Si_2O_5(OH)_4 + K^+ \qquad (53)$$

Therefore, $\beta^{C_A}_{K—M}$ can be evaluated.

Buffer capacities for four heterogeneous systems are shown in Figure 6. For comparison, two homogeneous buffer capacities are also shown

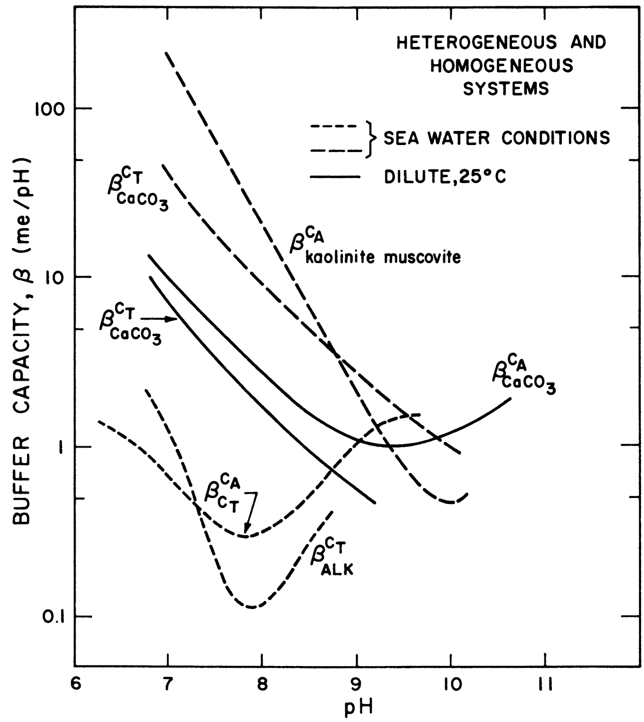

Figure 6. Buffer capacity vs. pH for some heterogenous and homogeneous chemical systems

and are seen to be relatively small. For fresh water systems, $\beta^{C_T}_{\text{CaCO}_3}$ and $\beta^{C_A}_{\text{CaCO}_3}$ are of considerable practical interest. In this illustration, $\beta^{C_T}_{\text{CaCO}_3}$ was evaluated for an assumed zero noncarbonate alkalinity. It is apparent that, for sea water conditions, both the kaolinite-muscovite equilibrium system and the CO_2-$CaCO_3$ (s) system represent large potential resistances to pH change. The buffer capacity of kaolinite-muscovite with respect to $\sum CO_2$ should be large indeed. It would seem extremely pertinent to begin to investigate the kinetic aspects of some of these buffer systems.

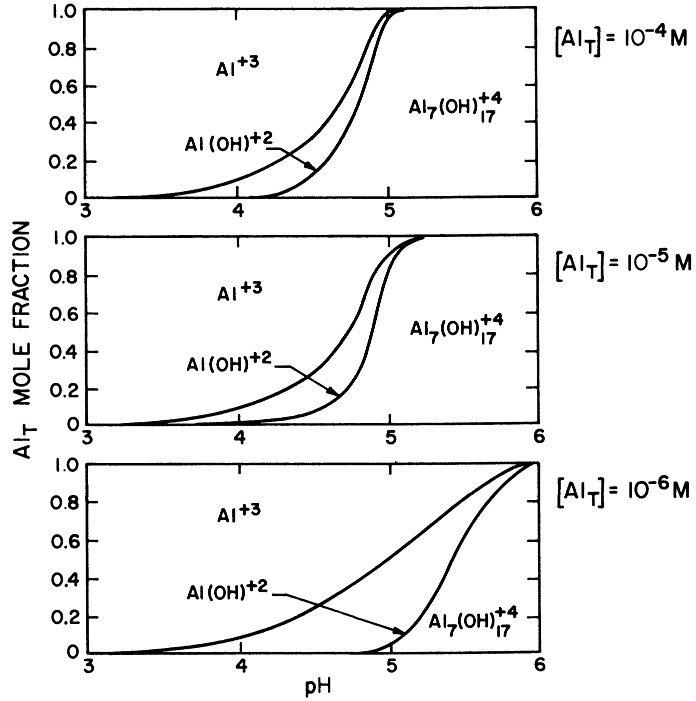

Figure 7. Relative equilibrium distributions of three aqueous Al species as a function of pH and total solution concentration

Aluminum Solute Species and Solubility. The qualitative importance of metal-ion hydrolysis in determining the solution chemistry of aluminum is generally recognized. Considerable practical and theoretical interest in the behavior of aqueous aluminum in the oceans (where it is one of the highly reactive elements), in geochemical studies of aluminosilicates and related systems, and in water treatment technology (coagulation and flocculation processes) would seem to make it an appealing subject for demonstrating the application of chemical thermodynamics to natural water systems. In a sense, however, the quantitative information on hand appears somewhat better suited to emphasizing the limitations in a thermodynamic approach to aluminum chemistry in natural waters. The simple cases mentioned cannot purport to be realistic or useful examples. They merely attempt to utilize the limited data available to give a more or less qualitative impression of what the actual situation might be like.

The earlier work of Brosset (*4*), among others, indicates that formation of soluble aluminum hydrolysis products must be a rather slow process, even at the higher temperatures used in the laboratory investigations. For the solid phases such as $Al(OH)_3$ and $Al_2O_3 \cdot 3H_2O$, the aging process is also known to be slow, at least at low temperatures (*9*).

With these kinetic factors in mind, it is still of interest to attempt to get some idea of the possible soluble species and their relationship to aluminum solubility. The data for polymeric aluminum hydrolysis products are those for 50°C. reported by Biedermann (*2*), who has described the two reactions

$$7Al^{3+} + 17H_2O = Al_7(OH)_{17}{}^{4+} + 17H^+ \qquad (54)$$

$$13Al^{3+} + 34H_2O = Al_{13}(OH)_{34}{}^{5+} + 34H^+ \qquad (55)$$

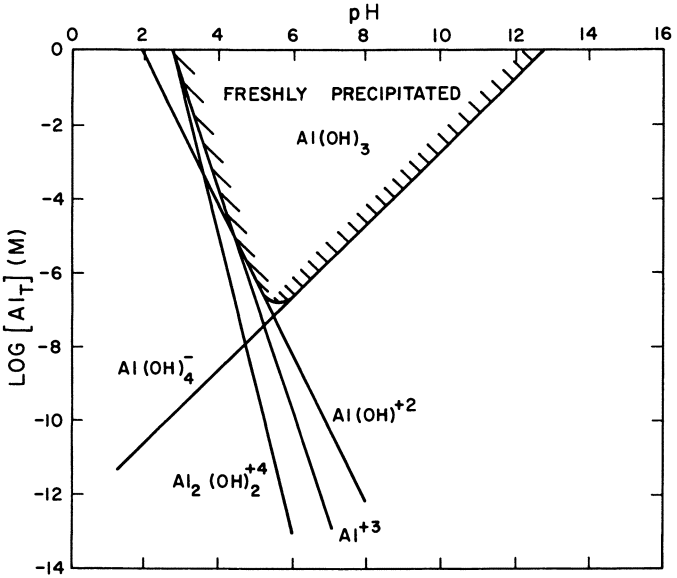

Figure 8. pH vs. concentration for monomeric and dimeric Al species assumed in equilibrium with freshly precipitated $Al(OH)_3$

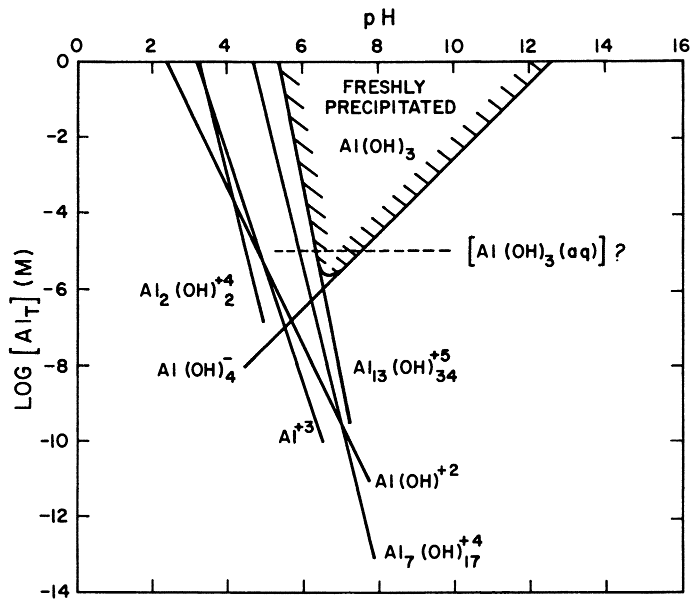

Figure 9. pH vs. concentration for various monomeric and polymeric Al species assumed in equilibrium with freshly precipitated Al(OH)$_3$

Other data have been selected from Sillén and Martell (*33*). Figure 7 presents the results of strictly illustrative calculations of the relative amounts of simple Al^{3+} ion, $AlOH^{2+}$ ion, and the polymeric cation, $Al_7(OH)_{17}^{4+}$ for varying pH at different total concentrations of soluble aluminum. Including the species $Al_{13}(OH)_{34}^{5+}$ would still further repress the calculated amounts of Al^{3+} and $AlOH^{2+}$.

The relative influence of the polymeric hydrolysis products and the simpler species needs to be examined in the light of the pertinent solid phases which might be formed in a given system. Figures 8, 9, and 10 show three different descriptions of aluminum "solubility" (activity). Figure 8 represents the region of stability for "freshly precipitated" $Al(OH)_3$ ($\log K_s = -33$), ignoring the existence of all but the simple ion, the monohydroxo species, and the dimer on the cationic side. This gives one rather familiar picture of aluminum solubility. When this description is expanded to include some of the more complex species, as in Figure 9, the domain of $Al(OH)_3$ is sharply reduced. Qualitatively, one can readily imagine that this picture may be appropriate for visualizing the conditions in short-term coagulation experiments or processes involving aluminum salts over the pH range 4–6.

For gibbsite ($\log K_s = -36.3$), considering the existence of both $Al_7(OH)_{17}^{4+}$ and $Al_{13}(OH)_{34}^{5+}$, Figure 10 shows quite a different result

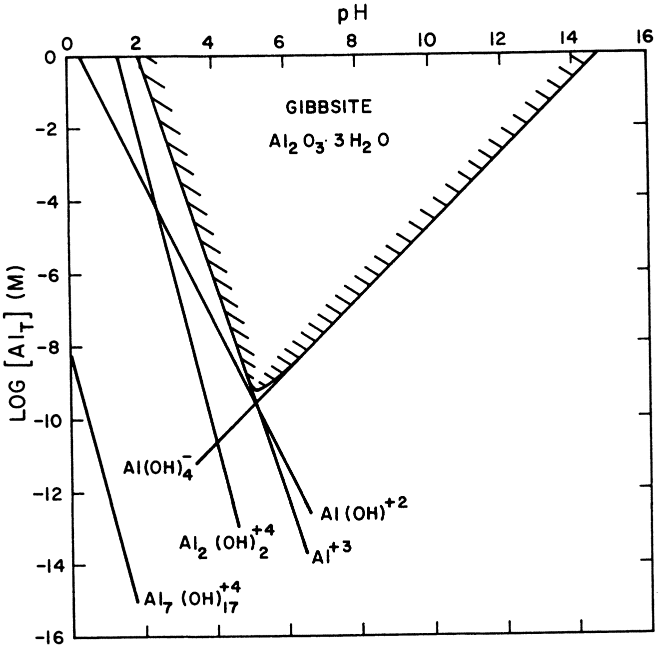

Figure 10. pH vs. concentration for various monomeric and polymeric Al species assumed in equilibrium with gibbsite

again. The influence of the polymeric forms considered is now essentially negligible, and the simpler species appear sufficient to account for solubility. The maximum solubility at the pH of sea water (neglecting concern about activity effects is certainly justified here) even appears to be of the right order, although aluminum activity might actually be controlled by aluminosilicates (*cf.* Figure 5).

What should one assume to be a true equilibrium state for aluminum under given set of conditions in a natural water system? Figures 9 and 10 may at least establish a crude range, with apparent "equilibrium" as described by Figure 9 corresponding to a short-time scale and with Figure 10 approximating true equilibrium, attainable at long times and low temperatures, or more rapidly for elevated temperatures during equilibration. Time certainly appears to be of great theoretical as well as practical importance in the chemical behavior of aqueous aluminum.

Oxidation of Manganese by O_2. Manganous manganese in simple systems is unstable with respect to oxidation by dissolved oxygen, as can be seen from the thermodynamic relationships summarized in Figure 11. For example, the overall reaction obtained by combining

$$1/2\ O_2 + 2H^+ + 2e^- = H_2O \qquad (56)$$

and

$$Mn^{2+} + 2H_2O = MnO_2 + 4H^+ + 2e^- \qquad (57)$$

is

$$Mn^{2+} + 1/2\,O_2 + H_2O = MnO_2 + 2H^+ \qquad (58)$$

The relative positions of the H_2O—O_2 boundary and the Mn^{2+}—MnO_2 boundaries for both 10^{-5} and $10^{-7}M$ activities of aqueous Mn^{2+} indicate that for pH values greater than about 4, Reaction 58 is spontaneous. Similarly, the pure solid phases $MnCO_3$ and $Mn(OH)_2$ are unstable with respect to oxidation to MnO_2. Extensive interpretations of manganese chemistry in terms of the thermodynamic properties of the oxides and on other solid phases and solution species of manganese can be found in the recent literature (*3, 14, 24*).

The kinetic behavior of Mn(II)—O_2 reactions has been studied recently (*23, 24*). Experiments covering times ranging from hours to days have indicated that, in bicarbonate-carbonate solutions of pH 9–10 (10°–25°C.), the oxygenation product ranges in composition from about $MnO_{1.3}$ to $MnO_{1.5}$. Only in highly alkaline buffer solutions (pH ~ 12) have stoichiometries corresponding to about $MnO_{1.9}$ been observed. Figure 12 shows some typical data from kinetic experiments, in which the extent of manganese oxidation has been measured in terms of total

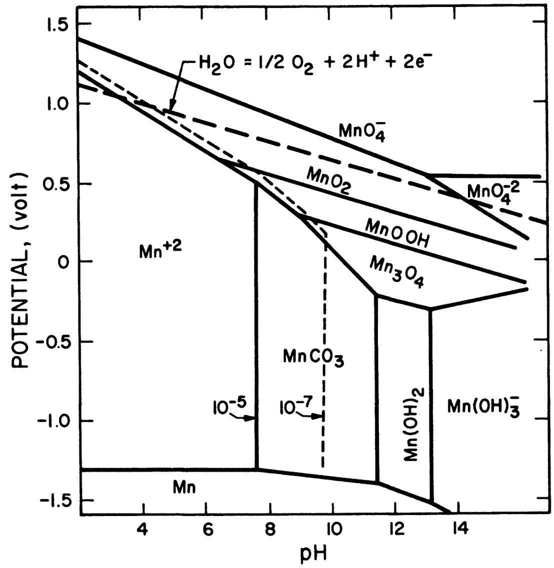

Figure 11. Some thermodynamic relationships in the systems MnO-H_2O-CO_2 and O_2-H_2O, at 25°C.

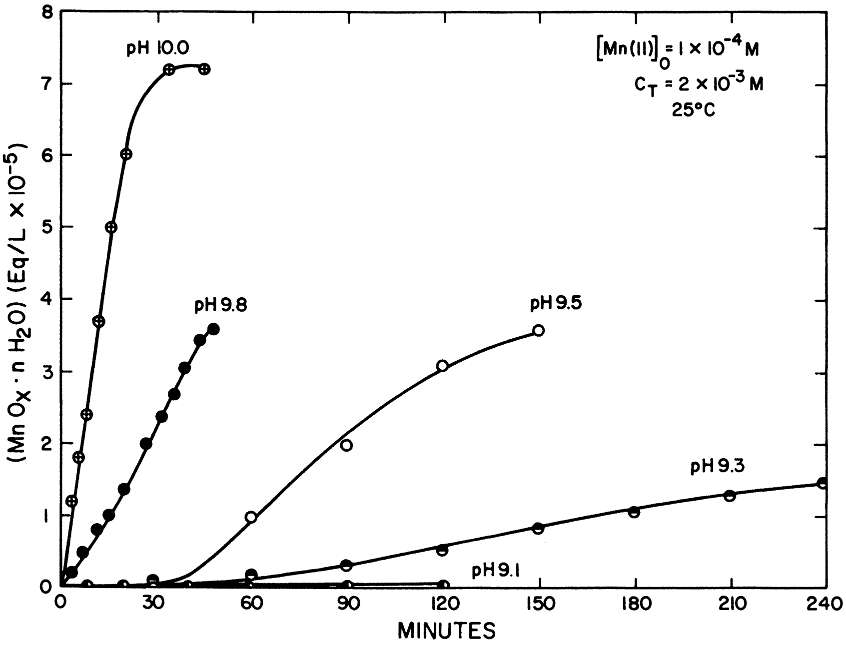

Figure 12. Oxygenation of Mn(II)

equivalents of oxidized manganese, Mn(III) + 2Mn(IV) (22). There is a strong pH effect on the reaction rate. The oxidation rate data are generally consistent with an autocatalytic expression of the form

$$\frac{-d(\mathrm{Mn(II)})}{dt} = k_o\,(\mathrm{Mn(II)}) + k_n\,(\mathrm{Mn(II)})(\mathrm{MnO}_x) \qquad (59)$$

Figure 13 compares the influence of pH on Fe(II) and Mn(II) oxygenation rates. In both instances the dependence upon OH^- concentration is found to be second order; the pH range for rapid Mn(II) oxygenation is considerably higher than that for Fe(II).

Applying the foregoing thermodynamic and kinetic information to manganese behavior in natural water systems is considerably limited because the manganese system exemplifies the difficulties discussed earlier. On the thermodynamic side, the kinds of oxide phases in natural waters may not correspond to those for which equilibrium data are available. Also, cation exchange reactions are probably important (*21*). On the kinetic side, the role of catalysis by various mineral surfaces in suspension or in sediments is not really known. Of considerable importance may be microbial catalysis of the oxidation or reduction processes, as described by Ehrlich (*7*). With respect to the real systems, relatively few data are available which would permit a reliable distinction to be made between oxidized and reduced forms of manganese. The general impression seems to be (*13, 37*) that the reduced form is predominant in most ocean waters. Obviously, considerable information is still needed concerning the composition of predominant phases in nature, the forms of manganese in solution-suspension, and the kinetic aspects under chemical and biological conditions simulating the real systems.

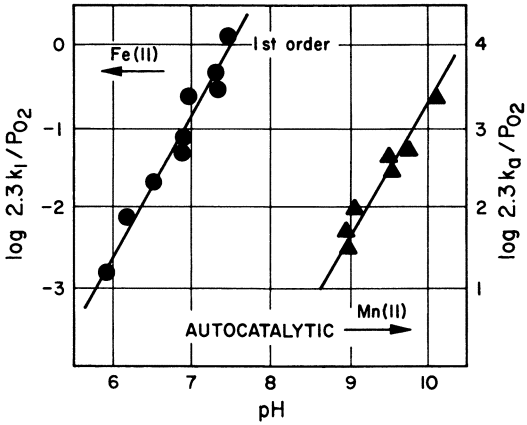

Figure 13. Effect of pH on Mn(II) and Fe(II) oxygenation rate constants at 25°C.

Even with these limitations, we may ask what our present limited kinetic data suggest about the real systems. Essentially, they suggest that extensive oxidation of *ca.* $10^{-7}M$ manganous ion in a hypothetical closed system resembling sea water (pH ~ 8, temperature ~ 5°C. P_{O_2} ~ 0.2 atm.) should be expected to take a long time. The order of the rate constants in Figure 13, extrapolated to pH 8, would make a time on the order of several hundred to a thousand years appear not unreasonable for the autocatalytic oxidation of 90% of the initial level. Such a calculation must, of course, be largely speculative in light of the uncertainties. It does, however, begin to account for the apparent pronounced discrepancy between an equilibrium model and the observed situation in the oceans and other bodies of water and may stimulate interest in other kinetic approaches in systems where equilibrium is clearly not attained.

Acknowledgment

The author acknowledges the assistance of Frank Birkner in making several of the computations. The author is grateful to Werner Stumm for many stimulating discussions about this subject.

Literature Cited

(1) Berner, R. A., *Geochim. Cosmochim. Acta* **28,** 1497 (1964).

(2) Biedermann, G., *Svensk Kemisk Tidskr.* **76,** 19 (1964).

(3) Bricker, O. P., *Am. Mineralogist* **50,** 1296 (1965).

(4) Brosset, C., Biedermann, G., Sillen, L. G., *Acta Chem. Scand.* **8,** 1917 (1954).

(5) Denbigh, K. G., "The Thermodynamics of the Steady State," Wiley, New York, 1951.

(6) Denbigh, K. G., "Chemical Reactor Theory," Cambridge University Press, Cambridge, 1965.

(7) Ehrlich, H. L., "Principles and Applications in Aquatic Microbiology," H. Heukelekian and N. C. Dondero, eds., pp. 43-60, Wiley, New York, 1964.

(8) Feth, J. H., Roberson, C. E., Polzer, W. L., *U.S. Geol. Surv. Water Supply Paper* **1535-I,** 1964.

(9) Garrels, R. M., "Researches in Geochemistry," P. H. Abelson, ed., pp. 25-37, Wiley, New York, 1959.

(10) Garrels, R. M., *Science* **148,** 69 (1965).

(11) Garrels, R. M., Christ, C. L., "Solutions, Minerals and Equilibria," Harper and Row, New York, 1965.

(12) Garrels, R. M., Thompson, M. E., *Am. J. Sci.* **26D,** 57 (1962).

(13) Goldberg, E. D., "The Sea," M. N. Hill, ed., pp. 3-25, Interscience, New York, 1963.

(14) Hem, J. D., *U.S. Geol. Surv. Water Supply Paper* **1667-A,** 1963.

(15) Hemley, J. J., *Am. J. Sci.* **257,** 241 (1959).

(16) Holland, H. D., *Proc. Natl. Acad. Sci.* **53,** 1173 (1965).

(17) Kramer, J. R., *Great Lakes Res. Div., Univ. Michigan, Publ. No.* **11,** 147-160 (1964).

(18) Kramer, J. R., *Geochim Cosmochim. Acta* **29,** 921 (1965).

(19) Latimer, W. M., "Oxidation Potentials," 2nd ed., Prentice-Hall, Englewood Cliffs, N. J., 1952.

(20) Levenspiel, O., "Chemical Reaction Engineering," Wiley, New York, 1962.

(21) Morgan, J. J., Stumm, W., *J. Colloid Sci.* **19,** 347 (1964).

(22) Morgan, J. J., Stumm, W., *J. Am. Water Works Assoc.* **57,** 107 (1965).

(23) Morgan, J. J., Stumm, W., *Proc. 2nd Intern. Water Poll. Res. Conf., Tokyo,* 103-117 (1965).

(24) Morgan, J. J., "Principles and Applications in Water Chemistry," S. D. Faust and J. Hunter, eds., Wiley, New York, in press.

(25) O'Connor, D. J., *Proc. Amer. Soc. Civ. Engrs.* **91,** SAI, 23 (1965).

(26) Pings, C. J., Nebeker, E. B., *Ind. Eng. Chem. Fundamentals* **4,** 376 (1965).

(27) Pourbaix, M., *Bull. Soc. Chim. Belg.* **54,** 10 (1945).

(28) Pourbaix, M., "Thermodynamics of Dilute Aqueous Solutions," E. Arnold, London, 1949.

(29) Prigogine, I., "Thermodynamics of Irreversible Processes," 2nd ed. Interscience, New York, 1961.

(30) Riley, G. A., *Bull. Bingham. Oceanogr. Coll.* **13,** 1 (1951).

(31) Rossini, F. D., *et al., Natl. Bur. Std. Circ.* **500,** (1952).

(32) Sillen, L. G., "Oceanography," Mary Sears, ed., pp. 549-581, AAAS, Washington, D. C., 1961.

(33) Sillen, L. G., Martell, A. E., *Spec. Publ.* **17,** The Chemical Society, London, 1964.

(34) Stumm, W., *USPHS Publ.* **999-WP-15,** 299-323 (1964).

(35) Thompson, J. B., "Researches in Geochemistry," P. H. Abelson, ed., Wiley, New York, 1959.
(36) Van Slyke, D. D., *J. Biol. Chem.* **52,** 525 (1922).
(37) Wangersky, P. J., Gordon, D. C., *Limnol. Oceanogr.* **10,** 544 (1965).
(38) Weber, W. J., Jr., Stumm, W., *J. Chem. Eng. Data.* **8,** 464 (1963).

RECEIVED May 23, 1966. Work supported in part by Research Grant WP-00941 from the Division of Water Supply and Pollution Control, USPHS.

2

Analysis of Water for Trace Metals

Present Capabilities and Limitations

DAVID N. HUME

Department of Chemistry and Laboratory for Nuclear Science,
Massachusetts Institute of Technology, Cambridge, Mass.

Many methods exist which have the needed sensitivity for determining trace metals in natural waters. When the requirements of selectivity, accuracy, reliability, convenience, economy, and applicability to real systems are added, the number of methods is greatly reduced. Most promising among those remaining are flame and plasma emission, atomic absorption, colorimetry, direct and inverse polarography, and neutron activation analysis. Applying any of these methods to natural waters is subject to the usual hazards in trace analysis: Measured quantities which may not be significantly large compared with random experimental error, and danger both of loss of material and adventitious contamination. Examples are given of the discrepancies which commonly arise in actual experimental work and the type of approach necessary to minimize them.

Determining trace elements in water is, like most trace analyses, characteristically difficult—*i.e.*, fraught with unpredictable hazards. There is no manual of standard procedures available which could be applied to a variety of situations, and reliable data showing the precision and accuracy even of the most widely accepted procedures are extremely scarce. Although a quantitative appraisal of the methods now used is not possible at present, a critical survey—if it puts various methods in perspective—may accomplish much the same purpose.

The most desirable qualities in a trace method are sensitivity, selectivity, accuracy, applicability, reliability, convenience, and economy. Possessing all of these attributes to a high degree is, fortunately, not an absolute requirement. If it were, there would be rather few elements capable of being determined at the trace level. Nevertheless, a method is seriously limited if it does not meet most of these requirements.

Sensitivity refers to the limiting amount detectable or, more practically, the limiting concentration detectable with surety. For trace analysis a sensitivity in the parts per million (p.p.m.) range is a minimum requirement. A parts per billion (p.p.b.) sensitivity is preferable and, in time, need for fractional p.p.b. sensitivities will undoubtedly arise. Ideally, the sensitivity should be high enough to preclude a concentration procedure. There is no danger that workers who specialize in developing increasingly sensitive methods will run out of significant problems in the near future.

Selectivity means the ability to discriminate one particular element from the others. Innumerable highly sensitive reactions exist which are useless because of the interfering action of other components. Accuracy is an obvious necessity, but it means much more than simple reproducibility on known samples.

Applicability sums up the effects of various factors which involve applying a method to a real problem, although these factors may not be involved when the method is tried and tested under ideal laboratory conditions. A method which performs admirably on synthetic samples may fail miserably when applied to sea water, for example, or even fresh waters which contain natural organic materials. Reliability involves the practical aspects of accuracy. Everyone encounters a method which, although demonstrably precise and accurate in the hands of its inventor, is through the effects of unidentified variables, capricious and unpredictable from person to person and even from day to day. Convenience becomes a large consideration, particularly if the work is to be done at sea, or in the field, or if many samples must be examined. An otherwise ideal method, which involves lengthy manipulations and a vibration-sensitive instrument, is of little use to a man who has to analyze hundreds of samples in a cubby-hole laboratory on a pitching ship. Economy, too, becomes important as the number of samples to be examined increases: economy in time, money, space, and equipment. When all these things are considered, the large number of methods for determining traces is considerably reduced. We must then ask what methods exist and examine the most promising.

Optical Methods

The methods under consideration for determining trace metals in water may be divided into three principal categories: optical, electroanalytical, and miscellaneous. Among optical methods, those techniques which initially suggest themselves as being most useful include emission spectroscopy, x-ray analysis, flame photometry, plasma spectroscopy, atomic absorption spectroscopy, and colorimetry. Classical emission spectroscopic techniques have proved useful for examining the residues from the evaporation of natural waters (*8*). A photographic spectrograph provides a permanent record of each sample, applicable not only to the problem at hand but to estimating the concentration of other elements which may become of interest later. Sensitivities are high, and although spectrographic results are often good only to within a factor of 2, refinement of the technique can give precision to within a few percent for some elements under the most favorable circumstances. Direct arc or spark excitation of solutions presents additional problems, particularly at the trace level, although rotating graphite disc electrodes with a spark-type source have been successfully applied to the rapid routine determination of the major constituents in natural waters (*9*). X-ray methods, both absorption and fluorescence, are likewise better adapted to solid samples. Flame photometry, plasma emission spectroscopy, atomic absorption spectroscopy, and colorimetry, on the other hand, are well suited to determining trace constituents in aqueous solutions and are suggested for serious consideration.

The advantages of flame photometry are reasonably good sensitivity, convenience, and versatility. For the alkali elements it is accepted as the standard method for water samples and can give good precision under carefully controlled conditions. The sensitivity for many elements (—*i.e.*, zinc) is poor, and there can be severe matrix problems. Not only are there many examples of enhancement and suppression by other elements, but foreign constituents as they affect the viscosity, surface tension, and volatility of the samples can affect the emission efficiency (*4, 11*).

Plasma emission spectroscopy is a new technique in which the chemical flame as an excitation source is replaced by an electrically generated plasma in an inert gas such as nitrogen (*20*). A much hotter emission source is achieved than is possible with chemical flames, resulting not only in considerably increased sensitivity but also in eliminating interferences of the sort arising from nonvolatile residues from the matrix. The technique is, however, still in an early stage and at present cannot be recommended to anyone whose primary interest is in using a dependable measuring tool to study water composition.

Atomic absorption spectroscopy is likewise a relatively new technique but one which has developed rapidly and for which a considerable choice of commercial equipment is available (*12, 13*). In this technique, the samples are vaporized in a flame, and the absorption of monochromatic light beamed through the flame from an external source is used to measure concentration. The sensitivity for many elements is excellent, and good quantitative results can be obtained. For a number of elements atomic absorption is clearly the method of choice. Nevertheless, there are still a number of limitations to the applicability of the method. Suitable light sources are not available for all the elements, scanning of the spectrum is not yet practical, and although the external interference effects are much less than are usually found in flame photometry, they are by no means entirely eliminated.

By contrast, colorimetry is relatively simple and inexpensive. Procedures exist not only for all the metals but for many nonmetallic constituents and organic compounds. It is undoubtedly the most widely applied technique in trace analysis, and the colorimeter or spectrophotometer tends to be the "work-horse" of the laboratory. Sensitivities are astonishingly great, and quantitative precision varies from a few percent to a few tenths of a percent, depending upon the method, equipment, and skill of the user. However, a colorimetric determination usually involves more steps and complications than any of the direct procedures. Often there is a separation or concentration step (*e.g.*, solvent extraction) somewhere in the procedure, and normally many reagents are used to prepare the sample. There is great ambiguity about the actual limits of sensitivity of most colorimetric methods because of the number of variables involved, and the dependence of the apparent sensitivity upon the

Table I. Estimated Detection Limits of Optical Methods (p.p.b.)

Element	*Flame Emission*[a]	*Plasma Emission*[b]	*Atomic Absorption*[c]	*Colorimetry*[d]
Al	10,000	20	100	0.2
Au	5,000	20	100	3
Bi	40,000	2000	200	10
Cd	5,000	100	10	1.4
Pb	14,000	80	50	3.1
Pt	13,000	100	500	3
Sn	25,000	200	200	100
Zn	80,000	100	5	1.6
Mg	1,900	5	3	1.1
Ca	80	5	10	1.4
Sr	70	50	20	3
Ba	1,100	80	1000	>100
Fe	1,100	15	50	2
Co	4,200	10	50	1.9
Ni	700	10	30	4
Cu	1,100	1	10	0.8

[a] Values from Whisman and Eccleston (*21*) or from Gilbert (*7*).
[b] West and Hume (*20*).
[c] Kahn (*12, 13*).
[d] Based on data in Sandell (*17*). *See* text.

apparatus and conditions. Nevertheless, many colorimetric methods have a high sensitivity indeed (*10*).

Table I compares some estimated sensitivities for various elements by the four methods under conditions chosen to make the comparisons as objective as possible. Flame or plasma emission and atomic absorption involve direct utilization of liquid sample. The actual concentration of constituent in the sample is thus the logical way of expressing detection limits and is used here. In colorimetry, however, there are usually dilution and concentration steps in the procedure which vary greatly from method to method; hence, direct comparison from element to element is difficult. The method of measurement is also far from uniform, and for this reason we have chosen to express the limit of detectability as p.p.b. (by weight) of element being determined in the final colored solution, assuming a 1-cm. light path. Detection limits generally imply the smallest amount or concentration which gives a reliably observable response above background (*e.g.*, 1% of full scale at maximum sensitivity, or some equivalent, depending on noise). Obviously, accurate quantitative determinations require much higher concentrations—*e.g.*, a factor of 100 or more.

Comparing detection limits is always a hazardous business. Different workers measure them under different circumstances and even with different definitions of the quantity being measured. Partisan bias cannot be ruled out, and reproducibility from worker to worker leaves much to be desired. Nevertheless, the figures in Table I should give a fairly realistic picture of the comparative capabilities of the four methods.

From the standpoint of quantitative accuracy at higher concentrations, any of these methods can give results good to within a few percent. For more precision and higher accuracy, much depends on the nature of the sample and the skill and effort of the operator. The first three methods depend considerably on the characteristics of an atomizing system, which in turn can be significantly affected by sample composition. Determining trace elements in the presence of macro quantities of other constituents always involves difficulties, and determining traces in sea water directly is a classic example. While it is possible to determine trace elements by flame and plasma methods by introducing sea water directly into the source, the precision is inevitably reduced, and various mechanical difficulties appear. In this respect, the atomic absorption method seems to be less affected than the others, and there are reports of measuring nickel, iron, manganese, zinc, and copper in sea water directly at concentrations less than 1 p.p.b. (*6*). For general work in fresh waters containing elements at the p.p.m. level, the flame emission technique combines speed, convenience, and economy with great versatility. Colorimetry commends itself for economical versatility and is good for organic as well as inorganic, and anionic as well as cationic constituents.

Electroanalytical Methods

A bewildering number of electroanalytical methods exist, most of which tend to be unsuited to practical analysis and need not concern us here. For determining trace metals in waters, three polarographic approaches recommend themselves from the standpoint of sensitivity, versatility, and reliability. These are conventional polarography, square wave polarography—or its variants such as pulse polarography—and inverse polarography, often called anodic stripping voltammetry (*18*).

Conventional polarography is a well-established technique for which commercial apparatus is readily available, and it is capable of detecting and determining 20 or so metallic elements. Table II summarizes the sensitivity in terms of detection limits, the range in which good quantitative results can be obtained, and the expected precision under ordinary circumstances. In general, those elements which can be determined by conventional polarography can be determined by the square wave technique with as much as a 100-fold increase in sensitivity but at a roughly 10-fold increase in cost.

Table II. Comparison of Electroanalytical Methods[a]

Technique	*Detection limits* (*-log* M)	*Quantitative Range* (*-log* M)	*Precision* (*%*)
Conventional DC Polarography	5	4–2	1–3
Square Wave Polarography	7	6–3	1
Inverse Polarography	10	9–4	5

[a] Ref. *18*.

Inverse polarography is a simple and an elegant technique in which the trace metal in the sample is concentrated by electroplating on a microelectrode for a suitable time and then measured by reversing the current and stripping the deposited metal back off into the solution. As Table II shows, there is a substantial increase in sensitivity over conventional and even square wave polarography, yet the method may be used with simple and relatively inexpensive apparatus. It should be noted that the concentrations involved here may be as low as 0.01 p.p.b. One of the advantages of these methods is that they often require a minimum of sample manipulation and reagent addition. The latter is particularly important in low-level work where it is difficult to obtain reagents which do not contain amounts of the element in question equal to or greater than the amounts in the sample.

On the other hand, these electroanalytical methods have considerably narrower applicability than, for example, some of the optical methods. They apply mainly to the metals, and then only certain ones. Some elements—copper, zinc, silver, cadmium, indium, tin, mercury, lead, bismuth, and thallium—can be determined both by direct and inverse methods. For titanium, vanadium, chromium, manganese, iron, cobalt, nickel, molybdenum, the platinum metals, gold and polonium, however, only direct polarography is applicable. The sensitivities for all these elements are of the same order of magnitude. For those elements for which it is applicable, inverse polarography has outstanding advantages which recommend it for much greater use than it has enjoyed in the past.

Published on January 1, 1967 on http://pubs.acs.org | doi: 10.1021/ba-1967-0067.ch002

Other Methods

A number of methods which cannot be classified conveniently either as optical or electroanalytical suggest themselves on the basis of sensitivity or other characteristics. Mass spectrometry is extremely sensitive and of general applicability. The results may be very good, especially when the method is combined with stable isotope dilution. However, sample preparation is difficult, and the method is both time consuming and expensive. Relatively few laboratories have the necessary equipment, and hence it is unlikely that much work will be done by this means. Catalytic reaction methods are also extremely sensitive but very limited in scope. Most chemical methods of analysis do not have the necessary sensitivity and particularly in low level work, are subject to errors by adventitious contamination.

Neutron activation is a highly sensitive technique which has special, almost unique advantages for trace analysis (3, 22). If the original sample can be irradiated without prior chemical treatment and with a

Table III. Sensitivity of Neutron Activation Analysis[a]

Element	*Detection Limit, p.p.b.*	*Element*	*Detection Limit, p.p.b.*
Al	0.02	Mg	1.3
Au	0.0004	Ca	3.0
Bi	3.2	Sr	0.09
Cd	0.07	Ba	7.0
Pb	100.0	Fe	12.0
Pt	0.1	Co	0.0006
Sn	0.4	Ni	0.6
Zn	0.06	Cu	0.003

[a] Ref. 22.

minimum of handling and exposure, the chances of contamination are tremendously reduced. Once the sample is irradiated, chance introduction of moderate amounts of the element in question do not affect the results—an advantage shared by no other method. In spite of the limitations imposed by neutron absorption cross-section and half-life, the method is applicable to a wide range of elements, and the sensitivities are extremely good (Table III). However, the equipment involved is considerable and not of the sort to be found everywhere. It is definitely not a field method, and it will long continue to be a highly specialized technique, limited to a relatively few places and practitioners.

Performance

From a casual perusal of the sensitivities and standardization precisions of the methods so far discussed, one might easily think that determining trace metals in water systems presented relatively few problems and that perhaps all that would be necessary would be to adapt general methods to the particular circumstances of specific water systems. Unfortunately, the situation is by no means that simple. To put things in proper perspective, let us look at the results of some cooperative analyses done on standard water samples in the last few years. Table IV summarizes some of the results reported by Lishka, Kelso, and Kramer (*15*) in a cooperative study by 69 participating laboratories in analyzing a standard water sample for major and minor constituents by standard methods. The laboratories included those of state, municipal, and federal agencies, industrial concerns, universities, consultants, and foreign organizations. Those participating were professionals, using their customary methods. Results showing evidence of gross error (presumed caused by dilution, calculation, etc.) were eliminated from the report. The grand averages of most of the results are reasonably close to the accepted value, indicating absence of serious bias in most of the methods, but the range of values reported is frequently disturbingly large. Table V gives the results of a similar cooperative study involving 17 laboratories in which the constituents being determined were trace metals (*14*). Again the grand averages—except for aluminum—suggest no serious bias, but the reported percent standard deviations are quite variable and indicate that the findings of different workers may differ to such an extent that conclusions of a single worker might have little significance.

Revelations of this sort shock those who are accustomed to taking at face value the claims regarding precision and accuracy of test methods. The distressingly large discrepancies observed cannot be explained by assuming a special ineptitude on the part of water chemists. The same dismal pattern of dissent has been observed in analyzing standard rock

Table IV. Results of a Cooperative Interlaboratory Evaluation

Determination	*Values Reported*	*Added p.p.m.*	*Av. of Results*
Ca^{2+} (EDTA)	122	108	105.0
Mg^{2+} (EDTA)	103	82	82.3
Hardness (EDTA)	156	610	606.0
SO_4^{2-} (gravimetric)	91	259	254.2
SO_4^{2-} (turbidimetric)	60	259	262.6
Cl^- (Mohr)	122	241	235.6
Cl^- (pot. tit.)	30	241	233.8
NO_2^- (colorimetric)	125	0.25	0.22
NO_3^- (colorimetric)	118	1.1	1.35
Na^+ (flame)	94	19.9	19.9
K^+ (flame)	88	3.1	3.2

[a] Ref. *15*.

Table V. Results of a Cooperative Inter-Laboratory Evaluation of Standard Methods for Determining Trace Metals in Water[a]

Determination	*Laboratories Reporting*	*Added p.p.m.*	*Av. Reported (p.p.m.)*	*% Std. Dev.*[b]
Iron	17	0.55	0.55	22.3
Copper	14	0.56	0.60	36.4
Manganese	17	0.20	0.20	50.0
Aluminum	12	2.00	3.44	94.0
Cadmium	7	0.16	0.18	38.1
Lead	13	0.12	0.13	33.3
Chromium	14	0.15	0.13	27.3
Zinc	11	7.47	7.73	13.1

[a] Ref. *14*.

[b] The standard deviation reported is not the usual quantity but is calculated using the sum of the squares of the deviation from the added amount instead of the average.

samples (*17*) and in unpublished interlaboratory studies of methods used in the chemical industry and between clinical laboratories. The sad fact is that this sort of thing is typical of experimental results even though we may not be aware of it. Much experimentation is done in such a way that the discrepancies never come to light, but when careful com-

of Standard Methods for Determination of Minerals in Water[a]

Low	*High*	*50% Range*[b] *(p.p.m.)*	*Std. Dev. (%)*
81	130	±2	5.9
56	102	±2	8.7
554	666	±9	2.9
195	288	±6	1.2
188	340	±9	10.9
210	272	±6	4.2
209	245	±6	1.5
0.12	0.30	±0.4	13.2
0.1	4.9	±0.4	83.0
15.0	24.0	±0.9	9.2
1.9	4.2	±0.3	15.2

[b] The 50% range is the spread about the true value which includes one-half of the reported values. Some of the most divergent values were eliminated in computing averages and standard deviations.

parisons are made—especially with difficult operations such as trace analysis—the effects can be startling.

First, it must be recognized that in analyzing a real sample the result is the product of an over-all process. Conventional figures on precision and accuracy are usually the result of an experimental program which shows a shameful lack of realism. The developer of an analytical method is most likely to measure his reproducibility under completely artificial conditions if he measures it at all. With the best of intentions he does everything possible to evade or conceal the natural variability of his method, even to throwing out results which are "obviously" not as good as they ought to be. Consequently, the figures he does obtain have no more relevance to the use of the method on a day-to-day basis with samples of unknown composition than the results of highly advertised gasoline economy runs have to the mileage which the ordinary motorist can expect in daily driving.

In the over-all process involved in analyzing a real sample, the factors we are not aware of, in the words of Sir Ronald Fisher, are "strictly innumerable." If we take the trouble to look, we find under supposedly identical conditions significant variability from day to day, from laboratory to laboratory, from instrument to instrument, and from man to man—to name only a few. A celebrated example is the measurement of the velocity of light, which has been reported by a number of workers showing marvellous internal precision and astonishing discrepancies between studies. It is only by intercomparison that one becomes aware of the magnitude of the variability, and it is only when this is realized that something can be done to track down the sources. Personal equation, as it is sometimes called, is an acknowledged part of experimental uncertainty. It is well-known, for example, that different observers cannot agree on such a simple thing as the reading of a Vernier scale and that each of us has his own particular preferences for digits in estimating the last figure on a reading. It seems that the only truly valid estimates of performance must be obtained by stealth, for it is only by stealth that we can outwit the personal equation. Unfortunately the personal equation is not limited to people; with the perversity which seems so characteristic of inanimate objects, methods, samples, reagents, laboratories, instruments, locations, and seasons have personal equations, too. In many operations, the random variability owing to unknown or uncontrolled causes is relatively small compared with the effects being measured and, therefore, does not intrude upon our consciousness. In trace analysis, the effects being measured and the variability of the measurements may be comparable in magnitude—a situation which is vexatious but not disastrous unless the worker is unaware of it. The checks and safeguards to be built into the operation and its interpretation must, however, be more stringent and comprehensive than those most workers are accustomed to.

Sources of Error

Trace analysis has its special hazards for the unwary. The most important of these are loss of material in the analytical process and contamination by outside sources. Everyone realizes that trace constituents can be lost from samples, but few are aware of the many ways in which this can occur. For example, phosphate has been observed to disappear mysteriously from water samples in polyethylene bottles (*10*). Nitric acid, used to clean plastic vials, has been observed to convert these surfaces to ion exchangers, which readily take up as much as 10^{-12} moles per sq. cm. of trace metals (*16*). Lead nitrate solutions unless made distinctly acidic, plate out much of the lead on the walls of glass bottles. While everyone realizes that formation of a precipitate is liable to carry out trace constituents either by adsorption or occlusion, it is not as well-known that vanishingly small amounts of precipitates—amounts likely to be overlooked on casual observation—may also do this. The fly-ash and soot, which seem to be inescapable components of city air, can introduce serious adsorption errors in exposed solutions (*16*). Naturally occurring organic materials in lake and river waters can sequester metal ions, inhibiting their normal reactions. Organic complexes of metals may biodegrade on storage. Trace constituents may combine with other components of the sample to form unreactive species which do not respond to the analytical method being used. Organic compounds may plate out on container walls as an oil slick.

Contamination of the sample by apparatus, reagents, and the environment in general seems to be an even more serious problem. This is particularly true when one passes from the p.p.m. to p.p.b. scale. Shain (*19*) finds that "pure" water contains copper in concentrations of the order of 10^{-8} *M* and lead and cadmium in concentrations about 10^{-9} *M*. This does not mean that other elements were not present in equal or even greater amounts. These were simply the elements for which Shain had a sensitive and convenient analytical method (inverse polarography). He also observed that 0.1 *M* solutions made up from the best available reagent-grade chemicals were invariably 10^{-7} *M* or more in heavy metals, particularly lead. Sandell (*17*) has observed that borosilicate glass gives off arsenic, zinc, and lead in appreciable amounts. Laboratory platinum is a known source of iron. Nineteen elements not counting rare earths have been found in filter paper. Matson and Roe (*16*) have observed solutions to become contaminated with lead from borosilicate glass and copper from polyethylene with resulting concentrations as high as 5×10^{-8} *M*. The same workers have observed an atmospheric fall-out up to as high as 10 micrograms per sq. meter per hour of lead in an air-conditioned urban laboratory. Plastic containers and ion exchange resins used to purify water may introduce spectrophotometrically significant amounts of organic substances (*5*). More than one worker trying to prepare highly pure reagents has discovered to his dismay that the purification process has introduced more impurity than was present initially.

When dealing with natural water, whether from river, lake, or ocean, particulate matter nearly always constitutes a problem. The trace elements in the natural system are frequently associated with the particulate phases: organic and inorganic, living and nonliving. Removing suspended mineral particles or living organisms may simplify the analytical procedure but destroy the significance of the results. Adding reagents to prevent adsorptive losses can disrupt the natural distribution of constituents between the solids and the solution. This problem has no simple solution but must be kept in mind by anyone working with natural water systems.

Conclusions

One should not conclude that trace analysis of water systems is a hopeless undertaking. It is possible to get results which are consistent and which seem to be reliable, but it does involve much effort and attention. One does not get satisfactory results without careful, critical appraisal of all conceivable variables involved. An example of the approach which is necessary is the recent work by Andersen in our laboratory on strontium and barium distribution in the Atlantic Ocean (*1*, *2*).

It was felt that a more reproducible and reliable analytical method was needed for these elements than had been available before if one were to determine whether certain apparent variations in concentration with depth were real or adventitious. A method was worked out, involving the concentration and separation of the barium and strontium in 1-liter samples of sea water, followed by quantitative determination through flame photometry. Every step in the over-all process, from the moment the sample was brought up to the deck of the ship to the final instrumental read-out in a laboratory thousands of miles away and months later, had to be checked. We had to assure ourselves that sample storage did not result in loss of the trace elements. After considerable experimentation we found that storage in polypropylene bottles was satisfactory if the sea water were made up to pH 3 with hydrochloric acid. Adding radioactive strontium and barium tracers at the time the samples were taken verified that significant losses in the storage container did not occur over a year. The samples had to be filtered to remove particulate matter before analysis, and the filtration process likewise had to be checked with tracers to show that nothing was lost in this step. The removal of the trace elements from sea water by the ion exchanger was shown to be complete, and the conditions for quantitative separation and recovery were determined using radioactive strontium and barium. In the course of this operation it was found necessary to remove and prove removal of strontium and barium impurities from the reagents and from the ion exchange resins before use.

Determination of strontium and barium by flame photometry has been known for a long time, but for the purpose at hand, not known well enough. The specific effect of all the special conditions resulting from the ion exchange separation with complexing reagents had to be investigated and the optimum conditions of flame composition, temperature, position, sample feed rate, etc., pinned down. Instrumental modifications were necessary to achieve sufficient sensitivity with barium. It had to be proved that other constituents from sea water were not entering the final separated samples to cause interference. Finally, repetitive analyses had to be done, not on synthetic samples, but on actual sea water run through the entire procedure, to determine the reproducibility of the method, and on sea water samples to which known concentrations of barium and strontium had been added to determine the accuracy. The resulting standard deviations were gratifyingly small: 0.05 p.p.m. for strontium and about 0.5 p.p.b. for barium—more than sufficient to show the existence of clear-cut variations with depth in the Atlantic Ocean. The research on the method took far more time and effort than the actual study itself, but this is only to be expected when one sets out to develop a method by which to perform a truly difficult analysis.

Abundant analytical tools exist which possess the sensitivity and a potentiality for the accuracy needed for quantitative work at the trace level in water systems. Applying these methods requires great care if the results are to be valid. Most of the methods which exist are, in their present state, limited to relatively ideal and artificial systems. They are potentially applicable to real systems, even those of considerable complexity, but the workers who use them must have skill, imagination, patience, and a feel for the statistical nature of experimental data.

Literature Cited

(1) Andersen, N. R., Ph.D. Thesis, M.I.T. Dept. of Chemistry, June 1965.

(2) Andersen, N. R., Hume, D. N., submitted to *Anal. Chim. Acta.*

(3) Atkins, D. H. F., Smales, A. A., *Advan. Inorg. Chem. Radiochem.* **1,** 315 (1959).

(4) Dean, J. A., "Flame Photometry," McGraw-Hill, New York, 1960.

(5) Delhez, R., *Chem. Anal.* **49,** 20 (1960).

(6) Fabricand, B. P., Sawyer, R. R., Ungar, S. G., Adler, S., *Geochim. Cosmochim. Acta* **26,** 1023 (1962).

(7) Gilbert, P. T., Beckman Instruments, Inc., South Pasadena, Calif., personal communication.

(8) Haffty, J., *U.S. Geol. Survey Water-Supply Paper* **1540A,** 1 (1960).

(9) Haffty, J., Helz, A. W., *U.S. Geol. Survey Profess. Paper* **424-B,** 333 (1961).

(10) Heron, J., *Limnol. Oceanog.* **7,** 316 (1962).

(11) Herrmann, R., Alkemade. C. T. J., Gilbert, P. T., "Flame Photometry," Wiley, New York, 1963.

(12) Kahn, H. L., *J. Chem. Educ.* **43,** No. 1A 40 (1966).

(13) *Ibid.,* No. 2A 132 (1966).

(14) Kroner, R. C., Ballinger, D. G., Kramer, H. P., *J. Am. Water Works Assoc.* **52,** 112 (1960).

(15) Lishka, R. S., Kelso, F. S., Dramer, H. P., *J. Am. Water Works Assoc.* **55,** 647 (1963).

(16) Matson, W. R., Roe, D. K., "Analysis Instrumentation 1966," Plenum Press, New York, 1966.

(17) Sandell, E. B., "Colorimetric Determination of Traces of Metals," 3rd ed., Interscience, New York, 1959.

(18) Schmidt, H., von Stackelberg, M., "Modern Polarographic Methods," Academic Press, New York, 1963.

(19) Shain, I., "Stripping Analysis," Treatise on Analytical Chemistry, Part I, Vol. 4, Chap. 50, Kolthoff and Elving, eds., Wiley, New York, 1963.

(20) West, C. D., Hume, D. N., *Anal. Chem.* **36,** 412 (1964).
(21) Whisman, M., Eccleston, B. H., *Anal. Chem.* **27,** 1861 (1955).
(22) Winchester, J. W., *Prog. Inorg. Chem.* **2,** 1 (1960).

RECEIVED June 17, 1966. Supported in part by the U.S. Atomic Energy Commission under Contract AT(30-1)-905.

3

Master Variables and Activity Scales

LARS GUNNAR SILLÉN

Royal Institute of Technology (KTH), Stockholm, Sweden

The infinite dilution activity scale is useful for ionic equilibria in fresh waters, but for equilibria in sea water one gains precision by applying an ionic medium activity scale. Measuring pH in sea water gives less information than total alkalinity and total carbonate. Calculations on redox equilibria are simplified by introducing the master variable $pE = -\log\{e^-\}$.

The equilibrium law (law of mass action) in its logarithmic form gives simple linear relationships between the activities of the reactants (*e.g.*, Equation 1). In the following text, the curled brackets represent activities, and the square brackets concentrations.

$$\log K_a = \log\{H^+\} + \log\{A^-\} - \log\{HA\} \qquad (1)$$

One can add or subtract log *K* values in the same way that one adds or subtracts the corresponding reaction formulas. An example is given below for 25°C., infinite dilution (*18*).

$(+)\ CaCO_3(s) + CO_2(p\text{ atm.}) + H_2O \rightleftharpoons Ca^{2+} + 2HCO_3^-$ $\qquad \log K = -5.83$

$(-)\ CO_2(p\text{ atm}) + H_2O \rightleftharpoons H_2CO_3$ $\qquad \log K = -1.46$

$(+)\ H^+ + HCO_3^- \rightleftharpoons H_2CO_3$ $\qquad \log K = 6.35$

$(-)\ H^+ + CO_3^{2-} \rightleftharpoons HCO_3^-$ $\qquad \log K = 10.33$

Summing up, one obtains:

$$CaCO_3(s) \rightleftharpoons Ca^{2+} + CO_3^{2-}$$
$$\log K = -5.83 + 1.46 + 6.35 - 10.33 = -8.35 \qquad (2)$$

The logarithmic form lends itself to graphical presentation. For example, in a system containing a number of acid-base systems of known total concentrations, the concentration of each individual species is a unique function of the master variable log [H$^+$], which may be represented in a logarithmic diagram. In Figure 1, for a system with total phosphate concentration 0.1*M*, the log (concentration) of the various species is given as a function of pH. The linear portions of the curves point toward the system points with coordinates (log total concentration, log acidity constant). Such diagrams and their uses are more fully discussed in Ref. *13*.

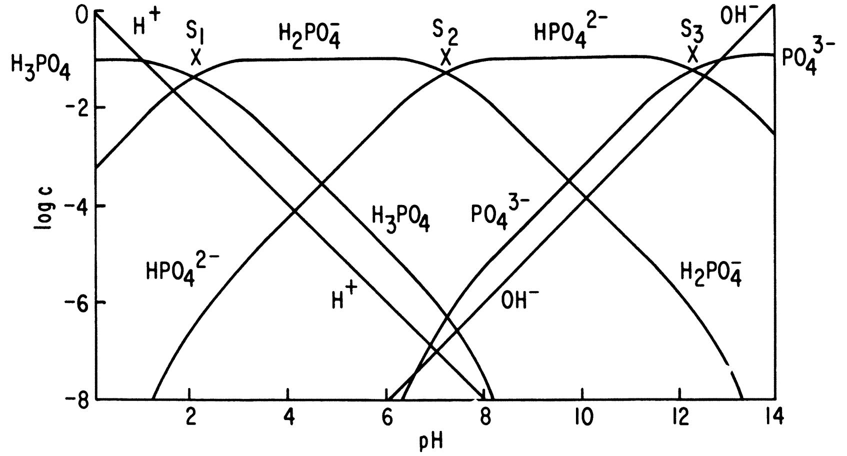

L. G. Sillén, "Treatise on Analytical Chemistry," Interscience

Figure 1. Logarithmic diagram of log c *as a function of pH for solutions with total phosphate concentration 0.1*M*, assuming* $pK_1 = 2.1$*,* $pK_2 = 7.2$*,* $pK_3 = 12.3$*, and* $pK_w = 14.0$ (13)

Another example is Figure 2, which is a diagram for a sample of sea water (7). It shows the log (concentration) for the species in the carbonate system (H_2C, HC^-, C^{2-}) and the borate system (HB, B^-) at various pH. At the log [H^+] of the sea water sample, one may read the concentrations of the two predominating species (HCO_3^- and H_3BO_3) and of the minor species. One can also determine the change in concentrations as the [H^+] is altered—*e.g.*, by adding acid. It is immediately obvious that there will be two equivalence points (points of minimum buffer capacity), namely, P_1 and P_2.

For other types of equilibria other master variables can be used—*e.g.*, log [Cl^-] or log [Br^-] for halogeno complexes, p*E* (*see below*) for redox equilibria, and log $p(O_2)$ for equilibria between oxides and gas phases (*12*).

Such diagrams of course contain the same information as used in numerical calculations—*i.e.*, equilibrium conditions for the various reactions, and the mass balance conditions. Their advantage is in giving in a single glance a clear picture of the situation.

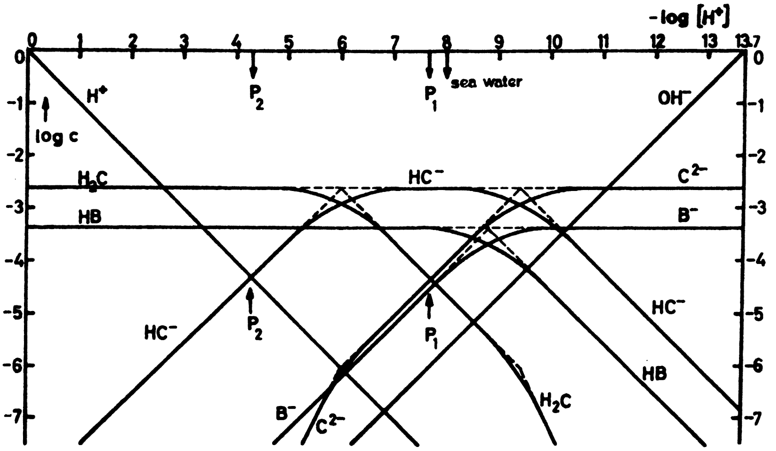

Tellus

Figure 2. Logarithmic pH diagram for sea water, assuming log $[B]_{tot} = -3.37$, *log* $C_t = -2.62$, *and the following* ($-\log K_a$) *values: 6.0 for* H_2CO_3, *9.4 for* HCO_3^- *and 8.8 for* $B(OH)_3$, *and log* $K_w = -13.7$ *(only the order of magnitude is representative). Arrows give log* $[H^+]$ *for sea water and for two equivalence points (points of minimum buffer capacity),* P_1 *(corresponding to* $HB + HC^-$*) and* P_2 *(corresponding to* $HB + H_2C$*) (7)*

The Ionic Medium Method

In Figure 2 one may ask whether concentrations or activities are meant, especially for H^+. Actually, both are since one should use a scale where they are identical.

In the last few decades an increasing number of workers interested in complicated ionic equilibria have been using the "ionic medium" method (3). Instead of water, as a solvent one uses a salt solution of fairly high concentration, such as 2*M* NaCl or 3*M* $LiClO_4$, keeping the concentrations of the reacting species much lower than that of the medium ions.

Since some reactants are usually ionic, one must decide on some mixing rule. Usually the concentration of an individual medium ion or the ionic strength is kept constant. (The mixing rule is indicated by 3*M* $Na(ClO_4)$, 3*M* $(Na)ClO_4$ in the "Tables of Stability Constants" (*18*).) Whichever rule one uses, this will not change the definitions below.

The concentrations are then used instead of the activities in various thermodynamic expressions (*e.g.*, the equilibrium law, and Nernst's equation for the e.m.f.). Some physical chemists are suspicious of this method. However, it is just as thermodynamic as the traditional one, the only difference being that another activity scale is used.

Activity Scales

Activity $\{A\}$ is defined by the chemical potential μ_A as shown in Equation 3.

$$\mu_A = \mu_A{}^* + RT \ln\{A\} = \mu_A{}^* + RT \ln \gamma_A[A] \qquad (3)$$

Here, $\mu_A{}^*$ is a constant, which defines the activity scale, and γ_A is the activity coefficient. For the moment we will disregard the units of concentration (mole fraction, moles per kg. solution, moles per kg. water). Changing to a new activity scale means that $\mu_A{}^*$ is shifted by a constant and that all activities are multiplied by the same factor.

In treating ionic equilibria in aqueous solution, two activity scales have proved especially useful. The first is the traditional infinite dilution activity scale, which is defined in such a way that the activity coefficient $\gamma_A = \{A\}/[A]$ approaches unity as the solution approaches pure water. One might refer to this scale as the fresh water scale.

The "ionic medium" activity scale, on the other hand, is so defined that the activity coefficient, $\gamma_A = \{A\}/[A]$ approaches unity as the solution approaches the pure solvent (in this case the ionic medium)—*i.e.*, when the concentrations go toward zero for all other species than water and the medium ions.

Experience shows that the activity coefficients on this scale stay near unity (usually within experimental error) as long as the concentrations of the reactants are kept low, say less than 10% of the concentrations of the medium ions. The activity (≈ concentration) of several ions, notably H^+, can be determined conveniently and accurately by means of e.m.f. methods, either with or without a liquid junction. In the latter case the liquid junction potential is small (mainly a function of $[H^+]$) and easily corrected for (*3*). The equilibrium constant for any reaction, on the ionic medium scale, may then be defined as the limiting value for the concentration quotient:

$$K = \lim Q \text{ (pure medium)} \qquad (4)$$

where *e.g.*,

$$Q = [H^+][A^-]/[HA] \qquad (4a)$$

In usual measurements at low reactant concentrations, the deviations of Q from K are usually smaller than the experimental errors; hence, it is preferable to set K equal to the average of Q rather than to extrapolate according to Equation 4.

Since no extrapolation is needed, equilibrium chemists working with an ionic medium scale have often not bothered to define rigidly the constant with which they are working. Sometimes they have used a misleading nomenclature—*i.e.*, for a thermodynamic equilibrium constant K

valid in an ionic medium, they have used the term "concentration quotient" or "apparent constant" as distinguished from the so-called "true thermodynamic equilibrium constants" on the infinite dilution activity scale. As a matter of fact, equilibrium constants on an ionic medium scale are thermodynamically as well defined as those on the infinite dilution scale, and often they can be measured much more accurately if one wishes to do so (*11*).

Since the oceans of the world contain an ionic medium of practically constant composition, ocean chemists should use the ionic medium approach when studying the equilibria of minor components, such as the carbonate species and the borate species. A model sea water might contain, in 1 kg. solution, 0.478 mole Na^+, 0.064 mole Mg^{2+}, 0.550 mole Cl^- and 0.028 mole SO_4^{2-}.

Equilibria With the Medium

Equilibrium studies in dilute aqueous solutions cannot alone help to distinguish between species that differ only by varying amounts of water. One may learn, for example, that a boron species exists with one boron atom and no charge, and another with one boron atom and the charge −1. One may write them (because of other evidence) as $B(OH)_3$ and $B(OH)_4^-$, but as far as the equilibrium data are concerned what we call $[B(OH)_4^-]$ might well be a sum of the concentration of BO_2^-, $H_2BO_3^-$, and $B(OH)_4^-$. This must also be understood when we use conventional formulas for the concentrations of, say H^+ and H_2CO_3:

$$\text{“}[H^+]\text{”} = \Sigma[H_{2n+1}O_n^+];\quad \text{“}[H_2CO_3]\text{”} = \Sigma[CO_2(H_2O)_n] \tag{5}$$

We cannot distinguish between such species simply because we do not vary the water activity $\{H_2O\}$. Working with an ionic medium, we also keep the activities of the medium ions practically constant, and so we cannot distinguish between species containing various amounts of the medium ions. Hence, one must understand that the formulas for various species include an unknown number of water molecules and medium ions. For instance, if our ionic medium is the model sea water referred to above, we would mark true concentrations by asterisks.

$$\begin{aligned}
&[H^+] = [H^+]^* + [HSO_4^-]^* + \ldots\\
&[Mg^{2+}] = [Mg^{2+}]^* + [MgSO_4]^* \ldots\\
&[CO_3^{2-}] = [CO_3^{2-}]^* + [MgCO_3]^* + [NaCO_3^-]^* + \ldots\\
&[HCO_3^-] = [HCO_3^-]^* + [MgHCO_3^+]^* + \ldots
\end{aligned} \tag{6}$$

Note that we can distinguish between HCO_3^- and CO_3^{2-} since both carbonate and H^+ are minor species and do not belong to the medium ions. The uncertainty expressed in Equation 6 might be thought of as a limitation of the ionic medium method, but it is also an advantage since one need not bother about the equilibria of complex formation with Mg^{2+} and Na^+ which are surely hard to measure accurately, and which are now eliminated by definition. The remaining equilibria (between metal ions, H^+, CO_3^{2-}, borate etc.) could, on the other hand, be determined quite accurately. Hence, in ocean chemistry one would use an ionic medium activity scale rather than the infinite dilution scale. On the other hand, for equilibria in fresh waters, the ionic concentrations are so low that one may, with some confidence, use the common approximation formulas to estimate the ionic activity coefficients on the infinite dilution scale. The fresh water scale would seem logical for such waters.

What is pH?

The quantity pH has been defined at least three different ways (*2*). Sørensen's (*16*) original definition was $\mathrm{pH} = -\log[H^+]$. Those using an ionic medium scale may use this definition since one can usually measure $-\log[H^+] = -\log\{H^+\}$ rather accurately.

The activity definition (*17*) on the "infinite dilution" scale, $\mathrm{paH} = -\log\{H^+\} = -\log \gamma_H - \log[H^+]$ was experimentally studied by Bjerrum and Unmack (*4*). This definition is not rigid because of the intrinsic uncertainty in defining individual ionic activities. Depending on the precision required, it is usually stated that the approximations used to estimate γ_H breakdown at some ionic strength between 0.01 and 0.2*M*.

An operational definition has been repeatedly suggested (*5*, *9*) and that sponsored by IUPAC is based chiefly on the work of Bates (*1*, *2*). The pH is defined in terms of a cell—*e.g.*, calomel electrode||solution|glass or hydrogen electrode.

As cell solution for this example one uses, in two different experiments, the unknown solution (x) and a standard buffer solution (s), whose pH($\mathrm{pH_s}$) has been estimated so as to approach the second definition. Comparing the e.m.f.'s gives

$$\mathrm{pH_x} - \mathrm{pH_s} = -(E_x - E_s)(RTF^{-1}\ln 10)^{-1} \qquad (7)$$

With this definition a reproducible number will always result. On the other hand the $\mathrm{pH_x}$ so obtained does not correspond exactly to the second definition since it contains the uncertainty in the definition of γ_H and in addition an unknown difference in the liquid junction potential which may be important, especially if the solution is not very dilute. If similar solutions are compared, however, differences in pH may give accurate ratios between H^+ activities or concentrations.

Many measurements of pH in sea water have been recorded, usually to within two decimals. If one used an operational definition and could teach oceangoing chemists to apply the same standards of accuracy, one should obtain pH values measured by e.m.f. that would be comparable within ±0.01 if taken at the same temperature and salinity. Even this aim does not seem to be fulfilled at present. Moreover pH will vary if a water mass is brought to a different pressure and temperature, even if there is no change in chemical composition, and it is hard to make a meaningful, accurate comparison of pH values at different pressure and temperature. It would seem better to measure quantities that are conservative and independent of p and T, such as the total carbonate concentration C_t, the total alkalinity, A_t, and the difference $(A_t - C_t)$. Both C_t and $(A_t - C_t)$ can be obtained from a single e.m.f. titration of a sea water sample with acid which gives the two equivalence points in the titration curve, P_1 and P_2 indicated in Figure 2. The amount of acid added at P_1 corresponds to $(A_t - C_t)$ and that added between P_1 and P_2 to C_t. Figure 3 gives E *vs.* ml. acid from a preliminary experiment by Dyrssen and co-workers (7). The lines are plots of Gran functions to find the equivalence points. The method is inherently quite accurate, and it seems more meaningful to collect values for C_t and $(A_t - C_t)$ for various sea water masses than to assemble large tables of pH values.

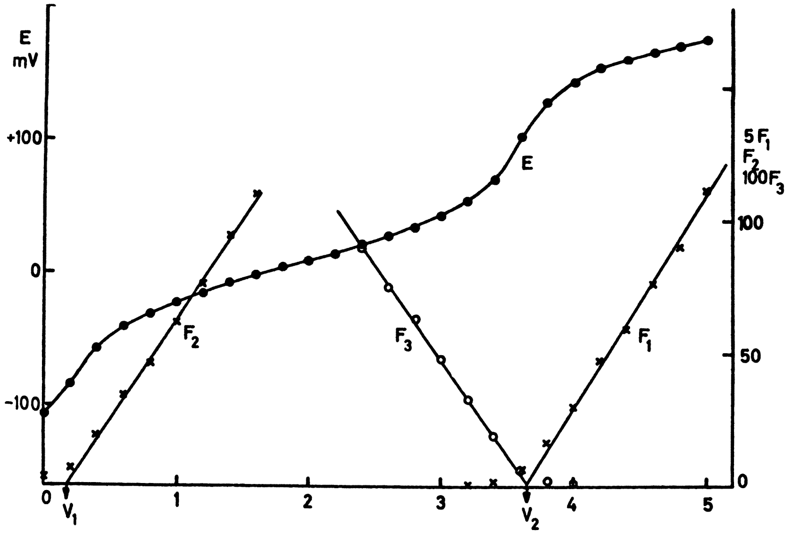

Tellus

Figure 3. E.m.f. titration curve for 154 grams sea water with v *ml. (0.1000M HCl + 0.4483M NaCl).* E *(mv.) for the cell: reference electrode|solution|glass electrode* vs. v *(ml).* F_1, F_2, *and* F_3 *are Gran functions for finding the equivalence points* v_1, v_2 *(corresponding to* P_1 *and* P_2 *in Figure 2)* (7)

Redox Equilibria

In oxidation-reduction equilibria, the common reagent is the electron e^-, and matters are simplified considerably if one treats the electron like any other reagent, H^+, Ag^+, Cl^-, etc. (Note that neither of these exists free and unhydrated in aqueous solutions). Clark has suggested (*6*) using $\{e^-\}$, and Jørgensen (*8*) has suggested the definition:

$$pE = -\log\{e^-\} \tag{8}$$

This is analogous to the second definition of pH. The electron activity scale is fixed to the hydrogen scale by $H^+ + e^- \rightleftarrows \frac{1}{2}H_2(g)$; $\log K = 0$. Hence, $pE = 0$ at a standard hydrogen electrode, and for any system at equilibrium we find the relationship between our new quantities and the reversible redox potential, e (or E_h)

$$e\ (=E_h) = -RTF^{-1}\ln\{e^-\} = (RTF^{-1}\ln 10)pE \tag{9}$$

$$pE = e/(RTF^{-1}\ln 10) \tag{9a}$$

The value of $(RTF^{-1}\ln 10)$ is 59.155 mv. at 25°C. Once the $\{e^-\}$ scale has been defined, we may begin to use equilibrium constants on that scale. For instance, inserting $\log p(O_2) = -0.68$, $\log\{H^+\} = -8.1$ and $\log\{H_2O\} = -0.01$ into the equilibrium constant for

$$\tfrac{1}{2}O_2(g) + 2H^+ + 2e^- \rightleftarrows H_2O(l); \qquad \log K = 41.55$$

we find that $pE = 12.5$ in sea water at equilibrium with air at 25°C.

Values for log K for various redox reactions are given in Ref. *18* together with the traditional standard potential values. Those who prefer to express the electron activity in volts rather than on a scale similar to that for other reagents should remember that at one time some physical chemists opposed expressing acidity by $[H^+]$ or pH. They claimed quite correctly that what one measures is really not a concentration but an e.m.f., and thus they found it more logical to measure the acidity, not by $[H^+]$ or its logarithm, but rather by the "acidity potential," a quantity in volts.

Log K values for redox reactions may be added just like any other log K values—*e.g.*, Reaction 10 (*18*).

$$(+)\ Ag_2S(s) + 2H^+ + 2e^- \rightleftarrows 2Ag(s) + H_2S(g) \qquad \log K = -1.22$$
$$(-2)\ Ag^+ + e^- \rightleftarrows Ag(s) \qquad \log K = 13.514$$

Summing up:

$$Ag_2S(s) + 2H^+ \rightleftarrows 2Ag^+ + H_2S(g)$$
$$\log K = -1.22\text{–}2 \times 13.514 = -28.25 \tag{10}$$

Reaction 11 is taken from calculations (*14*) of possible concentrations of

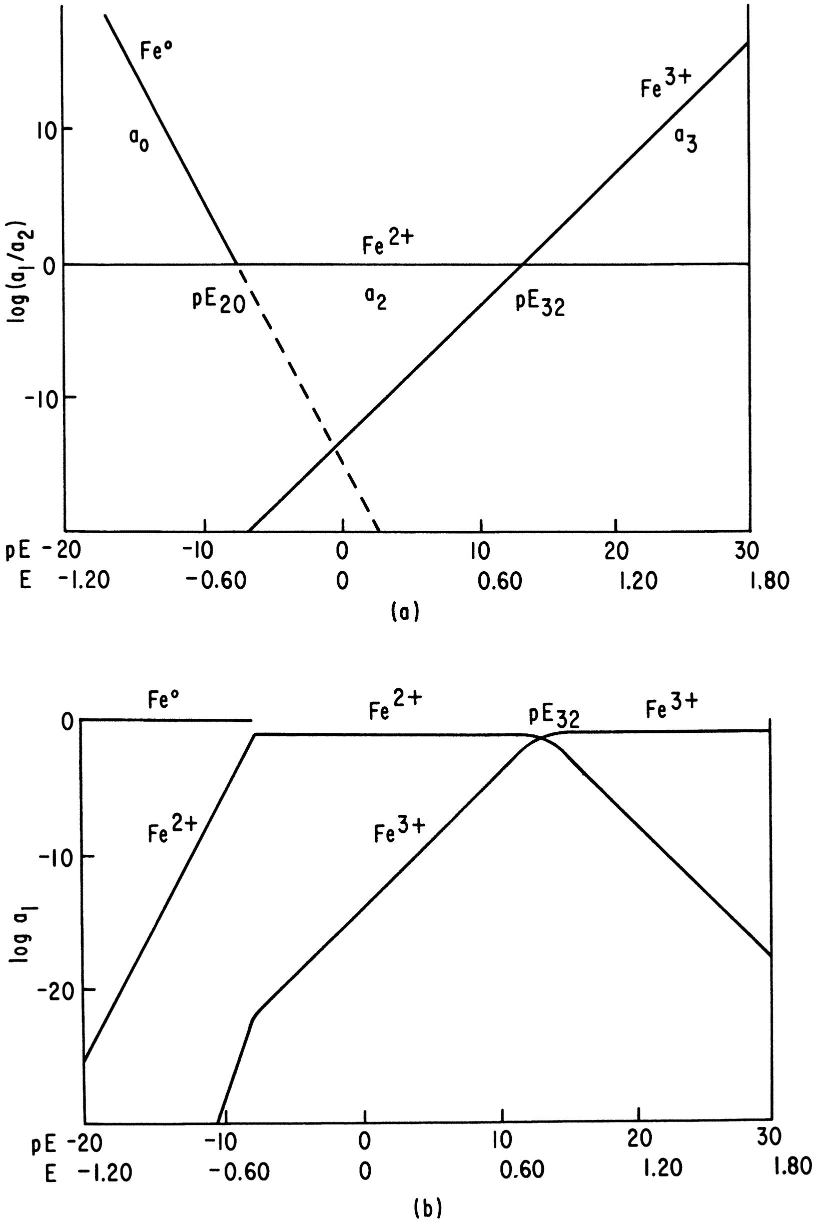

L. G. Sillen, "Treatise on Analytical Chemistry," Interscience

Figure 4. Redox diagrams for Fe. (a) Log (a/{Fe^{2+}}) as a function of pE for Fe^0, Fe^{2+} and Fe^{3+}. Where the Fe^0 line is broken, solid Fe cannot exist at equilibrium. (b) Log a as a function of pE for Fe^0, Fe^{2+}, and Fe^{3+}. The total Fe concentration is assumed to be 0.1M except in the range where solid Fe exists at equilibrium (13)

various Fe species in sea water at equilibrium with FeOOH(s). We may combine log *K* values as follows:

$$\mathrm{FeOOH(s)} + 3\mathrm{H^+} \rightleftarrows \mathrm{Fe^{3+}} + 2\mathrm{H_2O} \qquad \log K = 4.0$$
$$\mathrm{Fe^{3+}} + e^- \rightleftarrows \mathrm{Fe^{2+}} \qquad \log K = 13.0$$

Summing up:

$$\mathrm{FeOOH(s)} + 3\mathrm{H^+} + e^- \rightleftarrows \mathrm{Fe^{2+}} + 2\mathrm{H_2O} \quad \log K = 17.0 \tag{11}$$

Introducing the values of pH = 8.1 and pE = 12.5 we find $\log\{\mathrm{Fe^{2+}}\} = 17 - 3\mathrm{pH} - \mathrm{p}E = -20$, which indicates that $\mathrm{Fe^{2+}}$ is not likely to explain the measured concentration of Fe in sea water (around $10^{-7.2}M$).

Using p*E* as the master variable, one may construct logarithmic diagrams. Figure 4 shows two diagrams (*13*) for the equilibria Fe(0, II, III), at the maximum total concentration 0.1*M*. Figure 4b corresponds to the acid-base diagram in Figure 1; for p*E* > 13, $\mathrm{Fe^{3+}}$ predominates in the solution; for p*E* < 13, $\mathrm{Fe^{2+}}$ does; at low p*E*, solid Fe(s) precipitates, and the activities of the dissolved species decrease sharply. Figure

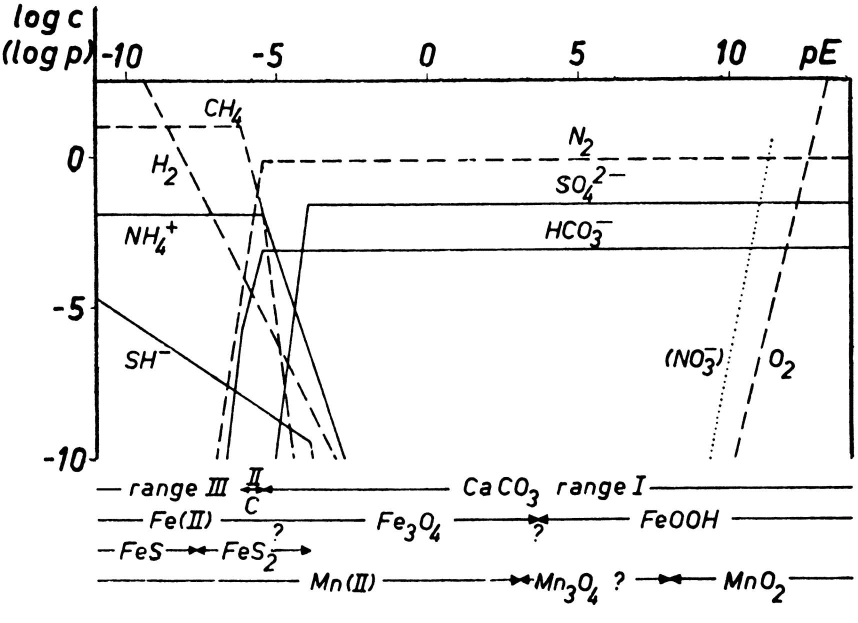

Arkiv Kemi

Figure 5. Redox diagram giving, as functions of pE, log c (solid) or log p (broken) for the main variable species in a "model system" corresponding to sea water + air + sediments. At the lower end the ranges are indicated in which various solids would be stable (15)

4a shows a relative logarithmic diagram, with $\log\{Fe^0\} - \log\{Fe^{2+}\}$ and $\log\{Fe^{3+}\} - \log\{Fe^{2+}\}$ as functions of p*E*. Figure 5 (*15*) shows for a model, representing the real system air + ocean + sediments, how the concentrations or activities of the most important species would vary with p*E*. Our present state corresponds to $pE = 12.5$, and points to the left may to some extent resemble earlier states of the system when it was oxidizing less than now. We can, for instance, see how carbon is transformed from carbonate to C(s) and CH_4; nitrogen from N_2 to NH_4^+ and sulfur from sulfate to FeS_2(s). The lower part of the diagram indicates the solid phases present in various ranges.

If one has many calculations to make on redox equilibria, it is certainly practical to change over to the p*E* scale rather than to work with voltages. When I tried to survey the equilibria in the ocean (*14*), I saved time this way even if I had to calculate all the log *K* values first. Once that was done, there were no more divisions and multiplications by multiples of 0.05916, and there was less chance of making mistakes.

The literature contains many values for E_h that have been obtained by placing a Pt electrode and a calomel electrode into the water sample (or mud). The oxidizing properties in the long run are usually determined by $[O_2]$, but E_h measured in this way for a natural sample probably never gives the reversible value for the O_2 couple but depends on some minor constituents in the solution or impurities in the electrode. This point will be dealt with more fully in another chapter (*10*). If one uses p*E* values in calculations, there is less chance that the conclusions will be compared with dubious E_h values.

Literature Cited

(1) Bates, R. G., Guggenheim, E. A., *Pure Appl. Chem.* **1**, 163 (1959).
(2) Bates, R. G., "Determination of pH," Wiley, New York, 1964.
(3) Biedermann, G., Sillén, L. G., *Arkiv Kemi* **5**, 425 (1953).
(4) Bjerrum, N., Unmack, A., *Kgl Danske Videnskab Selskab, Mat-fys Medd.* **9**, No. 1 (1929).
(5) Clark, W. M., *Ind. Eng. Chem.* **28**, 620 (1936).
(6) Clark, W. M., *Hyg. Lab. Bull.* **151**, 1 (1928).
(7) Dyrssen, D., Sillén, L. G., *Tellus* **19**, 110 (1967).
(8) Jørgensen, H., "Redox-målinger," p. 10, Gjellerup, Copenhagen, 1945.
(9) MacInnes, D. A., *Science* **108**, 693 (1948).
(10) Morris, J. C., Stumm, W., ADVAN. CHEM. SER. **67**, 270 (1967).
(11) "Recommended Symbols for Equilibrium Constants," *IUPAC Inform. Bull.* **26**, 25 (1966).
(12) Sillén, L. G., Rengemo-Anderson, T., *Svensk Papperstidn.* **55**, 622 (1952).
(13) Sillén, L. G., "Treatise on Analytical Chemistry," I. M. Kolthoff and P. J. Elving, eds., Part IB, Chap. 8, 1959.
(14) Sillén, L. G., *Am. Assoc. Advan. Sci. Publ.* **67**, 549 (1961).
(15) Sillén, L. G., *Arkiv Kemi* **25**, 159 (1966).

(16) Sørensen, S. P. L., *Medd Carlsberg Lab* 8, 1 (1909); *Biochem. Z.* **21**, 131 (1909).
(17) Sørensen, S. P. L., Linderstrøm-Lang, K., *Medd Carlsberg Lab* **15**, No. 6, (1924).
(18) "Stability Constants," *Chem. Soc. Spec. Publ.* **17** (1964).

RECEIVED April 15, 1966.

4

Gibbs Phase Rule and Marine Sediments

LARS GUNNAR SILLÉN

Royal Institute of Technology (KTH), Stockholm, Sweden

An imaginary equilibrium model of the sea water + sediment + air system is constructed by adding the components successively. The working hypothesis is proposed that in an intermediate model, with the eight components H_2O*—*HCl*—*SiO_2*—*$Al(OH)_3$*—*$NaOH$*—*KOH*—*MgO*—*CaO*, seven phases would be at equilibrium: (1) an aqueous solution of composition ≈ sea water, (2) quartz, (3) kaolinite, (4) hydromica (illite), (5) chlorite, (6) montmorillonite, (7) phillipsite or some other zeolite. The composition of the solution and of each solid phase will be fixed once p, T, and* $[Cl^-]$ *are given. Adding* CO_2 *brings* $CaCO_3$*; adding FeO and* Fe_2O_3 *bring glauconite and goethite. Studies of separated clay phases are highly desirable.*

In considering equilibrium concepts in ocean water systems, several questions immediately present themselves. Why does sea water have exactly the composition it has? Why are the ratios between Na^+, K^+, Mg^{2+}, and Ca^{2+} exactly what they are and so nearly constant? Why is the carbonate concentration about 2.3 mmoles/kg., and why does the pH in the bulk of sea water fall into a comparatively narrow range, around 8.1? In searching for an answer, my attention was turned to Goldschmidt's geochemical balance (*7*) for the formation of the sea. He suggested that for each liter of present day sea water, about 600 grams of igneous rock had reacted with about 1 kg. of volatile substance (H_2O, HCl, CO_2 etc.); during the process, in addition to the liter of sea water, around 600 grams of sediment and 3 liters of air were formed. Table I (*21*) gives Goldschmidt's figures, recalculated to the unit "moplis," which stands for moles per liter sea water, together with corresponding figures from Horn's later attempt at a geochemical balance (*16*). Since the differences are not important to the following discussion we may arbitrarily use Goldschmidt's values.

Table I. Balance of Materials for the Formation

Component		*From*	
		Primary rock	*Volatile*
H_2O			54.90
Si	(SiO_2)	6.06/12.25	
Al	$(AlO_{1.5}, Al(OH)_3)$	1.85/3.55	
Cl	(HCl)	0.01/0.02	0.54/0.94
Na	$(NaO_{0.5}, NaOH)$	0.76/1.47	
Ca	$(CaO, Ca(OH)_2)$	0.56/1.09	
Mg	$(MgO, Mg(OH)_2)$	0.53/0.87	
K	$(KO_{0.5}, KOH)$	0.41/0.79	
C[a]		0.02/0.03	0.60/2.06
	(CO_2)	0.02/0.03	0.53/1.05
	$(C(s))$		0.07/1.01
O_2[a]			0.027/0.022
Fe[a]		0.55/0.91	
	$(FeO, Fe(OH)_2)$	0.32/0.53	
	$(FeO_{1.5}, FeOOH)$	0.23/0.38	
Ti	(TiO_2)	0.06/0.12	
S[a]		0.01/0.02	0.06/0.06
F	(HF)	0.03/0.05	
P	$(PO_{2.5}, H_3PO_4)$	0.02/0.04	
Mn[a]	$(MnO_{1\text{ to }2})$	0.01/0.05	
N_2[a]			0.101/0.082

[a] Calculated from the estimates of Goldschmidt (*7*) and Horn (*16*).

Figure 1 shows an imaginary experiment (*19, 20*). To the right the real system is represented by 1 liter of sea water, the corresponding amounts of air, and sediment. We assume that Goldschmidt's values (Table I) give the amounts of the various components in this system. To the left is the imaginary model which contains the same components as the real system in exactly the same amounts, the only difference being that the imaginary system—the "equilibrium model"—has reached true equilibrium. The question now is what would the equilibrium model look like; in particular, which solid phases would it contain, and what would be the composition of the liquid and gas phases. If we knew the answer, we would like to compare this system with the real one.

Gibbs Phase Rule

Gibbs phase rule (*6*) is valid for a system that has reached complete equilibrium. It deals with the restrictions imposed on the system by the various equilibrium conditions, and it is often stated in the form:

$$F = C + 2 - P \qquad (1)$$

of 1 Liter of Sea Water[a]

Now in		
Air	*Sea water*	*Sediments*
	54.90	
		6.06/12.25
		1.85/3.55
	0.55	—/0.40
	0.47	0.29/1.00
	0.01	0.55/1.08
	0.05	0.48/0.82
	0.01	0.40/0.78
	0.002	0.62/2.09
	0.002	0.55/1.08
		0.07/1.01
0.027/0.022		
		0.55/0.91
		0.18/0.32
		0.37/0.59
		0.06/0.12
	0.03	0.04/0.05
		0.03/0.05
		0.02/0.04
		0.01/0.05
0.101/0.082		

Unit is moles per liter sea water.

The "variables" (or rather, "intensive variables"), are p (pressure), T (temperature), and the concentrations (*e.g.*, mole fractions of the components) in each separate phase. P is the number of phases present at equilibrium, and C is the minimum number of components necessary to duplicate any system that represents the equilibrium in question. (The components may sometimes be chosen in several ways). Finally, F is the number of degrees of freedom or the number of independent variables. With P phases present, one can (within limits) assign values independently of F variables, but then all other variables are fixed by the conditions for equilibrium. [For example, one may apply the phase rule to the system $CaO—CO_2—H_2O$, with one, two, three, four, or five phases, determine how many independent variables result, and decide what will be the most practical choice of variables. (Five phases might be $CaCO_3$(s), $Ca(OH)_2$(s), ice, an aqueous solution, and a gas phase.)]

It follows from Equation 1 that if a system is at equilibrium and one adds a new component, ($\Delta C = 1$), either a new phase is formed ($\Delta P = 1$) or a new free concentration variable is added ($\Delta F = 1$). For example, if N_2 is added to the system mentioned above, one obtains the new variable $p(N_2)$ in the gas phase.

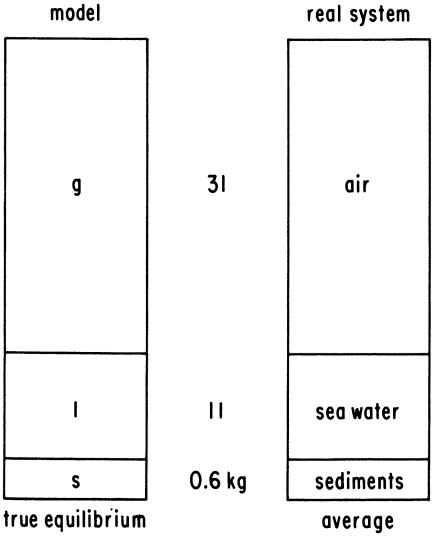

Svensk Kemisk Tidskrift

Figure 1. The true system (right) of 1 liter of sea water with the corresponding 0.6 kg. sediments and 3 liters air. On the left, the equilibrium model with the same amounts of the various components at true equilibrium (with the exception of N_2 (20)

A Simplified Ocean Model

We shall now consider the system HCl—H_2O—$Al(OH)_3$—SiO_2—KOH where $C = 5$. This system might be called an ocean model since the first two components may represent the volatile substances used to form the ocean and the three last may represent oxides in the igneous rock. It is simplified since all minor components (and even some of the main components) are missing—*i.e.*, CO_2 and sulfur compounds among the volatiles, Na, Mg, Ca, and Fe among the rock components.

In a part of this system which has been studied by Hemley (*11*), four phases can exist at equilibrium: aqueous solution, solid quartz, solid kaolinite ($Al_2Si_2O_5(OH)_4$), and potassium mica ($KAl_3Si_3O_{10}(OH)_2$). The variables are p, T, and the various concentrations $[K^+]$, $[H^+]$, $[Cl^-]$, $[Al]_{aq}$, $[Si(OH)_4]_{aq}$, etc. If we apply the phase rule (Equation 1) to equilibria of the four phases mentioned, we find $F = 5 + 2 - 4 = 3$. The most practical choice of independent variables would seem to be p, T, and $[Cl^-]$. These are easy to control, and Cl^- is the one ion that must remain in the aqueous phase since there is no place for it in the solid phases. The phase rule now states that after the values for these three variables are chosen, the other variables, such as $[K^+]$ and $[H^+]$, are fixed by the equilibrium conditions.

We can understand why this is true if we consider the equilibrium between kaolinite and K-mica:

$$1.5\ Al_2Si_2O_5(OH)_4(s) + K^+ \rightleftarrows KAl_3Si_3O_{10}(OH)_2(s) + 1.5\ H_2O + H^+ \tag{2}$$

The equilibrium condition gives

$$K = [H^+]/[K^+] (\approx 10^{-6}) \tag{2a}$$

(Ref. *11* extrapolated to 25°C. by Ref. *15*)

There is one more equation, namely the "charge condition":

$$[K^+] + [H^+] = [Cl^-] + K_w/[H^+] \tag{2b}$$

Once p, T, and $[Cl^-]$ have been chosen, then the equilibrium constants K and K_w are uniquely fixed, and Equations 2a and 2b between the two unknown variables, $[H^+]$ and $[K^+]$, are fixed. The remaining concentration variables, for species containing Si and Al, are uniquely determined by the presence of $SiO_2(s)$ and $Al_2Si_2O_5(OH)_4(s)$.

The equilibrium composition of the solution is independent of the quantities of the three solids as long as all three coexist. To a system with these four phases one may add arbitrary amounts of KOH or HCl. As long as $[Cl^-]$ is not changed and none of the three solids disappears, the system would return to the same equilibrium values for $[K^+]$ and $[H^+]$ as earlier. The system might thus be called a pH-stat rather than a buffer; its buffer capacity would be infinite as long as $[Cl^-]$ were kept constant (*20*).

How quickly equilibrium is approached is another question. Hemley made his measurements (*11*) at temperatures of 200°C. and higher, and at 25°C. one will obtain poorly crystallized products. Garrels (*5*), who has tested similar systems, states that after adding acid or base, pH may return to close to its original value in a matter of hours, even if the solid reaction products are too fine-grained to be identified by x-rays.

Intermediate Ocean Model

We may now pass from the simplified ocean model to the complete equilibrium model by adding one component after another—for each addition obtaining either a new concentration variable or a new phase. We shall concentrate on one intermediate model—namely, the system with eight components ($C = 8$) HCl—H_2O—SiO_2—$Al(OH)_3$—NaOH—KOH—MgO—CaO. Of the major components we have still excluded iron and CO_2. The latter have been withheld in the form of solid $CaCO_3$

and $MgCO_3$ (omitting the question of whether Mg exists only in a solid solution or partly in dolomite).

What is the maximum number of phases we can expect in this intermediate system? By comparing with the earlier simplified model where $C = 5$, we might suggest that the maximum F would be seven, adding one new phase for each new component. In fact, if we assume seven phases we find $F = 8 + 2 - 7 = 3$, and again the best independent variables would be p, T, and $[Cl^-]$.

For an eighth phase to be stable it would be necessary for, say, T to have a single value, determined by p and $[Cl^-]$. This does not seem likely, although in the real system the temperature may oscillate around a single value at which one phase is replaced by another. In such a case, both phases might be found in the final mixture since the time required for transformation might be larger than the times of temperature oscillations.

We shall attempt the working hypothesis that in the intermediate system equilibrium would require the maximum number (seven) of phases. This is not entirely unreasonable since the composition of sea water seems quite stable. Hence, which are the seven phases, and what evidence exists concerning the stable-phase assemblage?

Phases in Ocean Sediments. In recent years several mineralogical studies have been made on ocean sediments (*1*, *8*, *22*).

A large fraction of the marine sediments is detritus which has been carried from the continents by winds and rivers. Phases found in such detritus need not correspond to equilibrium with sea water. For example, feldspars may not be stable in contact with sea water. The chemical attack on plagioclase by fresh waters containing CO_2 is a well-documented fact, and even if I am not sure that I have seen irrefutable evidence for the degradation of plagioclase in sea water, I shall assume that those authors who believe plagioclase is unstable in the ocean are correct. On the other hand, quartz and kaolinite may well belong to the equilibrium assemblage of phases stable in sea water even if they are carried with wind and water from the continents.

From the phases found in ocean sediments, let us collect candidates for the stable equilibrium assemblage in our intermediate model and number each one.

The aqueous solution (No. 1) cannot be doubted. Quartz (No. 2) is common in sediments, and since SiO_2 is an excess component, quartz seems to be a strong candidate. Four clay minerals, kaolinite (No. 3), illite = hydromica (No. 4), chlorite (No. 5), and montmorillonite (No. 6) have been found together in various proportions in most parts of the ocean. These all seem to be good candidates. Phillipsite (No. 7), a zeolite, has been found growing in sea water (especially in the Pacific

Ocean), which makes it a good candidate, although another zeolite (clinoptilolite or heulandite) is more important in the Atlantic Ocean. Glauconite, a 1*M* mica rich in Fe, has also been found growing abundantly in the ocean under slightly oxidizing conditions (*10*), but since our intermediate model contains no Fe, we shall omit glauconite until Fe is added to the model. For similar reasons, calcite is left out; the intermediate model contains no C.

We now have seven candidates, and the phase rule allows seven phases to be stable together. We shall state as a working hypothesis that these seven phases—(1) aqueous solution, (2) quartz, (3) kaolinite, (4) hydromica (illite) (5) chlorite, (6) montmorillonite, and (7) phillipsite—are the stable assemblage in the intermediate model, and we shall test this hypothesis against various evidence. Some of these phases may prove unstable and be replaced by some other phase—*e.g.*, phillipsite by another zeolite or a feldspar. Chlorite might also be replaced by some of the magnesium silicates described by Arrhenius (*3*).

We shall also consider the possible equilibrium composition of each phase. The solid phases (except possibly SiO_2) are to some extent solid solutions, but at true equilibrium the composition of each phase should be constant, even if not ideal.

In natural aluminosilicates, a small part of the Al is often replaced by Fe; we shall consider this replacement as unessential in comparing the Fe-free intermediate model and the sediments found in nature.

Structure and Composition of Some Silicate Phases. Of the silicate phases listed above, quartz (SiO_2) and phillipsite have three-dimensional frameworks. The latter has the ideal formula $M_3Al_3Si_5O_{16}(H_2O)_6$. In samples of phillipsite from the Challenger expedition (*2*) the ratio between the metals represented by M is roughly $Na_{1.00}K_{0.86}Mg_{0.34}Ca_{0.54}$. (The content of Fe may be ascribed to a contamination of FeOOH, visible under the microscope.) The other four minerals are layer minerals [for a good survey *see* Brown (*4*)], in which Si always is surrounded by four oxygens in a tetrahedron, and Al usually by six oxygens in an octahedron, even if it can also replace Si in tetrahedral positions.

Kaolinite contains double layers (one tetrahedral layer and one octahedral), with the ideal composition $Al_2Si_2O_5(OH)_4$ (contained in a unit area corresponding to two tetrahedra). Micas, chlorite, and montmorillonite, contain triple layers—tetrahedral-octahedral-tetrahedral—of ideal composition $Al_2Si_4O_{10}(OH)_2$ (for the same unit area). An ideal mica structure is represented by muscovite, with the ideal formula, $KAl_2(AlSi_3)O_{10}(OH)_2$. The negative excess charge in the triple layers is compensated by layers of positive potassium ions. In illite (hydromica), the average charge per triple sheet is less because of substitution with Mg^{2+} or possibly removal of some Al^{3+}. An average composition (*14*) is:

$$K_{0.58}(Al_{1.38}Fe^{III}{}_{0.37}Fe^{II}{}_{0.04}Mg_{0.34})(Si_{3.41}Al_{0.59})O_{10}(OH)_2$$

Glauconite is also a mica mineral with a large part of the octahedral Al replaced by Fe(III). An average composition (*14*) is

$$M_{0.84}(Al_{0.47}Fe^{III}{}_{0.97}Fe^{II}{}_{0.19}Mg_{0.40})(Si_{3.65}Al_{0.35})O_{10}(OH)_2$$

From Jasmund's values (*17*) one may calculate $M_{0.84} \approx Na_{0.09}K_{0.62}Ca_{0.06}$.

In montmorillonite the forces between the layers are weaker than in the micas, and if montmorillonite is soaked in glycol, glycol molecules are taken up between the layers, which gives a typical shift in the x-ray diagrams. An ideal formula for Na-montmorillonite is $Na_{0.33}Al_2(Si_{3.67}Al_{0.33})O_{10}(OH)_2$. Natural montmorillonite also contains Ca and Mg in interlayer positions and Mg in octahedral positions.

Chlorite contains triple layers alternating with brucite sheets [$Mg_3(OH)_6$ in the unit area considered; Mg occupies all octahedral sites whereas Al occupies only two-thirds of them]. An ideal formula for a chlorite without Al would be $Mg_3(OH)_6Mg_3Si_4O_{10}(OH)_{10}$. In natural chlorites some Mg and some Si are replaced by Al.

Equilibrium Data. The only laboratory studies of aluminosilicate-solution equilibria in which both solid phases and aqueous solutions have been well defined seem to be those of Hemley, who has studied the K system (*11*) and the Na system (*12*) and discussed the mixed Na-K system (*13*). To obtain reasonable equilibration times with well-defined phases, it was necessary to work at temperatures higher than 150°C.

From Hemley's work on the potassium system (*11*) one may infer that kaolinite, quartz, and K-mica ($\approx$ illite) may be stable together, and the equilibrium constant $[K^+]/[H^+]$ may be extrapolated, (from $\approx$ 200°C.) to $\approx 10^6$ at 25°C.—*e.g.*, Holland's (*15*) value of $10^{6.0 \pm 0.5}$. Hemley's work on the sodium system (*12*) in the same way indicates that quartz, Na-montmorillonite, and kaolinite can form a stable assemblage, and a somewhat risky extrapolation of the equilibrium ratio $[Na^+]/[H^+]$ from $\approx$ 300° to 25°C. gives $\approx 10^{7.0}$ (*15*). These ratios are not far from the corresponding ratios in sea water. One could not expect them to be exactly the same since the hydromica and montmorillonite phases in sea water are solid solutions, containing more components than the phases in Hemley's experiments. His experiments surely do not contradict the idea that the previously mentioned phases could exist together at equilibrium.

For Ca and Mg the only data available seem to be phase studies by Peterson (*18*) on small amounts of clay minerals found together with excess of calcite and dolomite. He concluded that chlorite and montmorillonite (with mostly Mg and some Ca) form a stable assemblage, together with $CaCO_3$.

Clay Diagenesis. Holland (*15*) has summarized some evidence on the changes that clay minerals undergo as they are transported into sea water; detailed references may be found in his paper. Several authors have found ion exchange when fresh-water clays are brought into sea water, Mg^{2+}, Na^+, and K^+ replacing Ca^{2+}. The reconstitution of degraded illites and chlorites might also be described as ion exchange—replacement of H^+ by Mg^{2+} and K^+. The ion exchange processes are relatively rapid and seem to be nearly completed within about 24 hours.

There is also evidence that new clay mineral phases form. Comparisons of the clay phases carried down with a river with the clay phases deposited in the ocean outside the river mouth are suggestive but not altogether conclusive since it is hard to exclude completely the influence of rates of sedimentation, currents, etc.

Whitehouse and McCarter (*23*, *24*), however, have shown some clear-cut evidence from laboratory experiments. Even if one wished that they had changed their sea water regularly, they did analyze their various products thoroughly. They found that fresh-water illite brought into sea water underwent rapid ion exchange (75% completed within 24 hours) but that it remained illite (mica) and that no new phase could be found even after five years. The same was true for kaolinite—*i.e.*, ion exchange, 90% completed within 24 hours, but no new phase.

With fresh-water montmorillonite, most of the interaction with the solution also occurred in about 24 hours. After that, however, a slow phase transformation—or recrystallization—seemed to occur in the solids. After five years one could separate what had once been montmorillonite into four fractions, denoted by Whitehouse and McCarter as follows:

S_1 (77.6%) montmorillonitic
S_2 (10.4%) indeterminate
S_3 (8.6%) chloritic
S_4 (3.4%) illitic

The fractions were identified with x-rays and analyzed chemically.

Holland (*15*) notes that the major part of the oceanic sediments may well be detrital. Garrels (*5*) has recently estimated that to account for the stabilization of sea water composition since the birth of the ocean, only about 7% of the sediments need to have reacted.

Projection Diagram Na—K—Mg—Ca. To illustrate the composition of our seven phases with eight components at a constant p and T, we would need to draw a diagram in seven dimensions, which would cause some technical difficulties. However, we can dispense with some of the components. We may omit SiO_2 and $Al(OH)_3$ since their activities remain constant by the presence of quartz and kaolinite. The activities of H_2O and Cl^- are regulated by the aqueous phase. We omit these three phases and four components and are left with four phases and the components Na, K, Mg, and Ca, which would give a three-dimensional diagram, two projections of which are shown in Figure 2. In this diagram there should be four fixed points—one for each of the remaining solid phases in the equilibrium model—and the average composition of any mixture of these solids should be a point inside the irregular tetrahedron formed by these points.

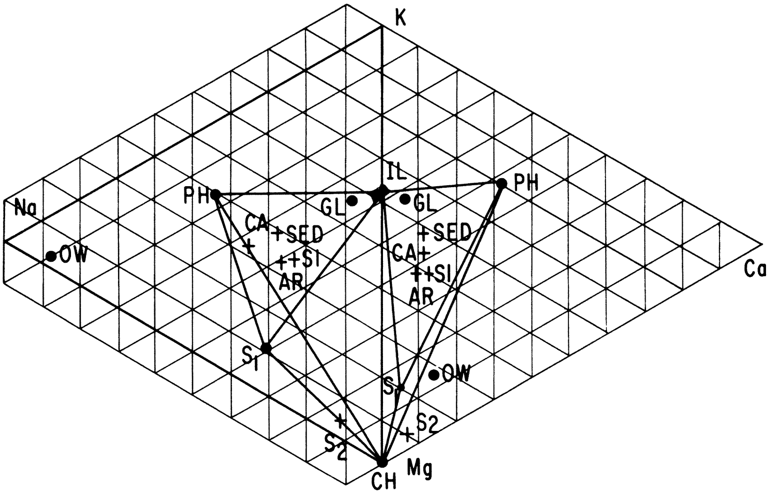

Figure 2. Projection on planes Na—K—Mg and Ca—K—Mg of the composition of possible equilibrium phases and of marine sediment minus carbonate. CH = chlorite, IL = illite (hydromica), S_1 = montmorillonite, PH = phillipsite, SED = sediments [according to Goldschmidt (7)], CA = average calcareous, SI = average siliceous, AR = average argillaceous sediments (from Ref. 22), OW = ocean water, GL = glauconite, S_2 = indeterminate fraction of Whitehouse and McCarter (23, 24)

The chlorite phase contains practically only Mg. Whitehouse and McCarter's analyses (23) for the chloritic fraction S_3 fall within the spot denoted CH in Figure 2. Even if the stable phase were some other magnesium silicate, such as sepiolite, this phase will also be represented by CH.

The mica phase contains mainly K and Mg and little Ca or Na. The field IL contains both the average composition of illites (*14*) given by Brown (*4*), the analysis of illite, treated with sea water (*23*), and that of the illitic fraction prepared from montmorillonite according to Whitehouse and McCarter (*23*). This point thus seems to be relatively accurate. Of course, there is a continuous line of possible compositions for a mica phase between IL and pure K-mica, but IL is the composition that could be at equilibrium with sea water.

The points for the two other phases are less reliable. For montmorillonite I have only one point—namely, the montmorillonitic fraction S_1 of Whitehouse and McCarter (*23*). Griffin and Goldberg (*9*) have analyzed montmorillonites from the Pacific and found practically the same composition for those of volcanic and eolic origin; unfortunately their analyses give only Fe, K, and Ca but not Na or Mg, so they could not be plotted or compared in Figure 2. For phillipsite, finally, the average from the Challenger samples was used (*2*).

As regards the sediments, the point SED (Figure 2) is the average composition for sediments minus carbonates, according to Goldschmidt (*7*). Three more points for the average composition of various types of sediments minus carbonates are taken from Wakeel and Riley (*22*)—CA = calcareous, SI = siliceous, and AR = argillaceous sediments. They all seem to be within the skew pyramid formed by the points S_1, PH, IL, and CH. Even if they had been somewhat outside, it would not have been difficult to explain—*i.e.*, the sediments still contain detrital material. Points are also given for GL (glauconite), OW (ocean water), and S_2 (the "indeterminate fraction" of Whitehouse and McCarter) (*23, 24*).

Considering the existing evidence, nothing seems incompatible with our working hypothesis that the seven stable phases in our intermediate ocean model would be those stated earlier (the items in parentheses are the components whose activities we believe may become fixed by that phase): (1) aqueous solution (H_2O, Cl), (2) quartz (Si), (3) kaolinite (Al), (4) chlorite (Mg), (5) mica = illite (K), (6) montmorillonite (Na), (7) phillipsite or some other zeolite (Ca). However, more effort should be directed toward separating oceanic sediments into fractions that might represent different mineral phases and studying these fractions chemically and by x-rays. Present x-ray analyses of a mixture of phases are a good start but do not give enough details to discuss the possible equilibria. If one could perform good separations, one might check whether each mineral phase really has roughly the same composition in various parts of the ocean, independent of origin. It would also be of interest if Hemley's studies of equilibria aluminosilicates-aqueous solutions could be extended to systems containing Mg and Ca in addition to K and Na.

Complete Ocean Model

Let us assume for the moment that our working hypothesis is true. We may then add one component after another to construct our complete ocean model (equilibrium model). If we add CO_2 and two new phases

—namely a gas phase and $CaCO_3(s)$—we have $C = 9$, $P = 9$, which gives $F = 2$. This means that if we fix T and $[Cl^-]$, then $p(CO_2)$ in the model will be determined by the equilibria and cannot vary (*19, 20*). This conclusion may irritate some workers.

Adding SO_3 will give $[SO_4^{2-}]$ as a new independent variable, which does not seem to be fixed by any new phase. On the other hand, when a small amount of BaO is added, we get $BaSO_4$ as a new phase. When we add FeO and Fe_2O_3, two new solid phases may be formed, tentatively FeOOH and glauconite. One might continue in this way, adding new phases or new concentration variables.

Two objections to this discussion may be expected. First, it is well-known that there is no true equilibrium in the ocean. Why then bother to talk about this equilibrium model? I agree that there is no complete equilibrium in the oceans and that everything interesting we observe is caused by lack of equilibrium. Nevertheless, it may be worthwhile to try to determine what the equilibrium model would look like—*i.e.*, what the solid phases and composition of the solution would be. Perhaps the equilibrium model will be a useful first approximation; the next step would then be to discuss how it is disturbed by various processes: radiation, life, transport of matter, etc. Finally, the model may be proved useless, but this has not yet been done, and perhaps one would learn many interesting things in refuting it.

Another objection is that we still have too little information to be certain of the equilibrium assemblage of minerals. Again I agree, but it may be worthwhile to advance a working hypothesis which can be checked against known facts and used as a guide for finding new facts and making new experiments. Here I have tried to give a modest start.

Literature Cited

(1) Arrhenius, G., "The Sea," Vol. 3, p. 655, Wiley, New York, 1963.
(2) Arrhenius, G., private communication, 1966.
(3) Arrhenius, G., "Abstracts of Papers," 151st Meeting, ACS, March 1966, O8.
(4) Brown, G., "The X-ray Identification and Crystal Structures of Clay Minerals," pp. 32, 54, London, 1961.
(5) Garrels, R. M., personal communications, 1962 and 1966.
(6) Gibbs, J. W., *Trans. Conn. Acad. Arts Sci.* **3**, 108, 152 (1876).
(7) Goldschmidt, V. M., *Fortschr. Mineral Krist. Petr.* **17**, 112 (1933).
(8) Griffin, J. J., Goldberg, E. D., "The Sea," Vol. 3, p. 728, Wiley, New York, 1963.
(9) Griffin, J. J., Goldberg, E. D., private communication, 1966.
(10) Hadding, A., *Lunds Univ. Årsskr. Avd.* **28** (2), 2 (1932).
(11) Hemley, J. J., *Am. J. Sci.* **257**, 241 (1959).
(12) Hemley, J. J., Meyer, C., Richter, D. H., *U.S. Geol. Surv. Profess. Paper* **424-D,** D 338 (1961).
(13) Hemley, J. J., Jones, W. R., *Econ. Geol.* **59**, 538 (1964).
(14) Hendricks, S. B., Ross, C. S., *Am. Mineralogist* **26**, 683 (1941).

(15) Holland, H. D., *Proc. Natl. Acad. Sci.* **53,** 1173 (1965).
(16) Horn, M. K., Ph.D. Thesis, Rice University, Houston, Tex., 1964.
(17) Jasmund, K., "Die silicatischen Tonminerale," p. 154, Verlag-Chemie, Berlin, 1955.
(18) Peterson, M. N. A., *J. Geol.* **70,** 1 (1962).
(19) Sillén, L. G., *Am. Assoc. Advan. Sci. Publ.* **67,** 549 (1961).
(20) Sillén, L. G., *Svensk Kem. Tidskr.* **75,** 161 (1963).
(21) Sillén, L. G., *Arkiv Kemi* **24,** 431 (1965).
(22) Wakeel, S. K. El., Riley, J. P., *Geochim. Cosmochim. Acta* **25,** 110 (1961).
(23) Whitehouse, U. G., McCarter, R. S., *Natl. Acad. Sci.-Natl. Res. Council, Publ.* **566,** 81 (1958).
(24) Whitehouse, U. G., McCarter, R. S., *Texas A & M College, Project 24,* Ref. 57-5T (1957).

RECEIVED April 15, 1966.

5

The Structure of Water and Water–Solute Interactions

W. DROST-HANSEN

Institute of Marine Science, University of Miami, Miami, Fla.

Thermal anomalies ("kinks") in the properties of water and aqueous solutions appear to be manifestations of higher-order phase transitions in structured elements of water. Some concentration-dependent anomalies are also described and discussed in terms of: (a) the occurrence of discrete structural units of water in the unaffected solvent, (b) the possible separate existence of somewhat similarly structured units in the ionic hydration atmospheres, and (c) overlapping of large (but not necessarily structured) hydration atmospheres.

An understanding of equilibrium phenomena in naturally occurring aqueous systems must, in the final analysis, involve understanding the interaction between solutes and water, both in bulk and in interfacial systems. To achieve this goal, it is reasonable to attempt to describe the structure of water, and when and if this can be achieved, to proceed to the problems of water structure in aqueous solutions and solvent-solute interactions for both electrolytes and nonelectrolytes. This paper is particularly concerned with two aspects of these problems—current views of the structure of water and solute-solvent interactions (primarily ion hydration). It is not possible here to give an exhaustive account of all the current structural models of water; instead, we shall describe only those which may concern the nature of some reported thermal anomalies in the properties of water and aqueous solutions. Hence, the discussion begins with a brief presentation of these anomalies, followed by a review of current water structure models, and a discussion of some properties of aqueous electrolyte solutions. Finally, solute-solvent interactions in such solutions are discussed in terms of our present understanding of the structural properties of water.

Thermal Anomalies in the Properties of Water

It has been suggested from time to time that the properties of water undergo more or less sudden transitions at several discrete temperatures. Mention of this phenomenon in the literature is quite scattered, however, and until recently, fairly little attention has been paid to these anomalies. Dorsey (*26*) has indicated the possible existence of anomalies in water properties while other authors have discussed one or more specific examples of unexpected temperature dependences. More recently, Drost-Hansen and co-workers (*28, 29, 30, 31, 32, 33, 34, 35*) have compiled examples of these anomalies and attempted to explain their origin qualitatively in terms of higher-order phase transitions in the structure of water.

The thermal anomalies, which have become known as "kinks," have been illustrated in the articles mentioned above. (We shall use the phrases "thermal anomalies" and "kinks" interchangeably.) In this section, we show only a few examples to indicate the diversity of aqueous systems in which they occur. We contend that the anomalies are of general occurrence and indicate transitions in the structure of water and can therefore elucidate both the problems of water structure of water itself and solute-solvent interactions.

In several previous papers, the possible existence of thermal anomalies was suggested on the basis of such properties as the density of water, specific heat, viscosity, dielectric constant, transverse proton spin relaxation time, index of refraction, infrared absorption, and others. Furthermore, based on other published data, we have suggested the existence of kinks in the properties of many aqueous solutions of both electrolytes and nonelectrolytes. Thus, solubility anomalies have been demonstrated repeatedly as have anomalies in such diverse properties as partial molal volumes of the alkali halides, in specific optical rotation for a number of reducing sugars, and in some kinetic data. Anomalies have also been demonstrated in a surface and interfacial properties of aqueous systems ranging from the surface tension of pure water to interfacial tensions (such as between *n*-hexane or *n*-decane and water) and in the surface tension and surface potentials of aqueous solutions. Further, anomalies have been observed in solid-water interface properties, such as the zeta potential and other interfacial parameters.

Before proceeding, a few comments should be made on the authenticity of these anomalies (*31, 32*). In some cases it is necessary, in order to delineate the existence of a thermal anomaly, to "sight down the line" on a graph to determine if a more or less abrupt change occurs. Usually, the difficulty is in deciding whether this is, indeed, in the nature of an abrupt change (*i.e.*, taking place over a temperature interval of 2°–3°)

or whether instead the observed points fall on a smooth curve and merely reflect a general trend. (As an example, *see* the kinetic data by Massey and co-workers on the rate of D-amino acid oxidase catalysis in Figure 12.) In other instances, it requires differentiating the data to clarify the anomaly, such as illustrated in Figure 1 for the temperature coefficient of the index of refraction of water. What is presently required to establish firmly the reality of the existence of thermal anomalies in the properties of water are precise (and preferably highly accurate) data on

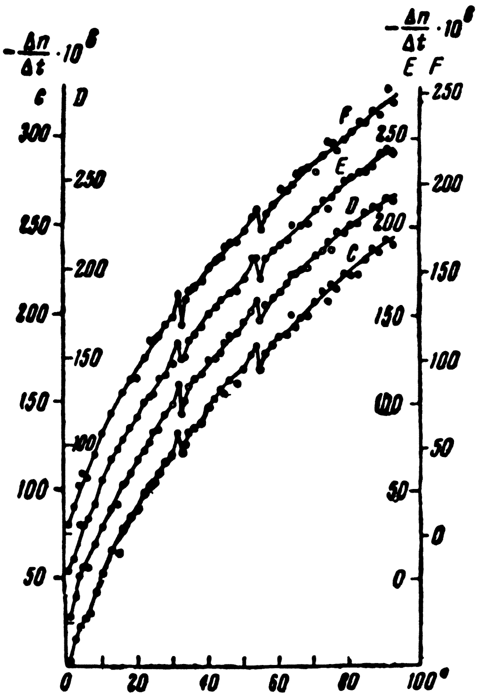

Journal of Structural Chemistry

Figure 1. Temperature coefficient of the index of refraction of water. Measurements at four different frequencies (60)

water properties (and aqueous solutions) obtained at closely spaced temperature intervals. However, even if such data were available, difficulties may still be expected, primarily owing to the fact that differentiating a general change in slope from an actual "kink" requires the demonstration of an overt discontinuity in a second-, third-, or higher-order derivative. Few data are presently available which permit such differentiation with certainty. Alternative approaches may be sought in statistical analysis of the available data. This has been attempted by Drost-Hansen in connection with the density data of water, the solubility ratio of argon to nitrogen, and the dielectric data for pure water. Ives and Marsden (*82*) have suggested a slightly different approach based on the use of orthogonal polynomials. Essentially, the analysis seeks to determine the number of terms which can reasonably be used in a power expansion to represent the data using the F-distribution as a test for fit (—*i.e.*, comparing the reproducibility of a single point with the relative increase in the precision with which the data are fitted to the power series). In the past, this author has emphasized that while few examples provide a clear cut, unequivocal evidence for the existence of the thermal anomalies, in most of the cases (where sufficiently closely spaced and precise data were available) anomalies seemed almost invariably to be indicated at essentially the same temperature ranges.

Recent criticism (*42*) of the notion of the existence of thermal anomalies has correctly pointed out that examples presented by some authors for the reality of this phenomenon lack credibility. Thus, some of the examples mentioned by Antonoff, Forslind, and others may not stand up to close scrutiny. The present author feels at this time, however, that the blanket assertion that no thermal anomalies exist is highly inappropriate and that the matter at least deserves further careful consideration, both from the point of view of added experimentation as well as from a careful review of existing data. Recently, Young (*161*) claimed that the examples presented in Ref. *31* by the present author did not constitute proof of the existence of anomalies. As a result of Young's careful study, I withdraw the example quoted in that reference (Figure 5). In this illustration of the relative temperature coefficient of the dielectric constant for water, the minimum at 60°C. does indeed indicate the likely occurrence of a structural change, but this example does not fall in the class of thermal anomalies as discussed in this connection. The temperature range over which the anomaly takes place is far too great to constitute a "more or less abrupt, sudden change" as implied in the definition. Furthermore, the graph is based on smoothed data rather than on the actual experimental points. In Figures 8, 9, and 10 in Ref. *31* a point was incorrectly plotted. These illustrations all deal with solubilities. However, when correctly plotted, I feel that the thermal anomalies are indicated. In particular, calculated values for the heats of solution based on the corrected data continue to suggest the existence of anomalies. Finally, it should be noted that Young has failed to demonstrate that anomalies are not present in all the examples I discussed.

Figure 1 shows some recent measurements by Frontas'ev and Shraiber (*60*) of the index of refraction of water as a function of temperature. Anomalies near 30° and 55°–57°C. are particularly pronounced. The existence of anomalous temperature variations of the index of refraction was discussed earlier by Tilton and Taylor (*see 31*).

Frontas'ev (59) observed an anomalous temperature dependence in the thermal conductivity of water around 30°–40°C. (Figure 2). (In this illustration the data points are those given by Frontas'ev, but I believe the curve shown gives a reasonable fit to the experimental data.) He stated specifically that an anomaly existed near 30°–40°C. and that it implies a fundamental modification in water structure in this temperature range.

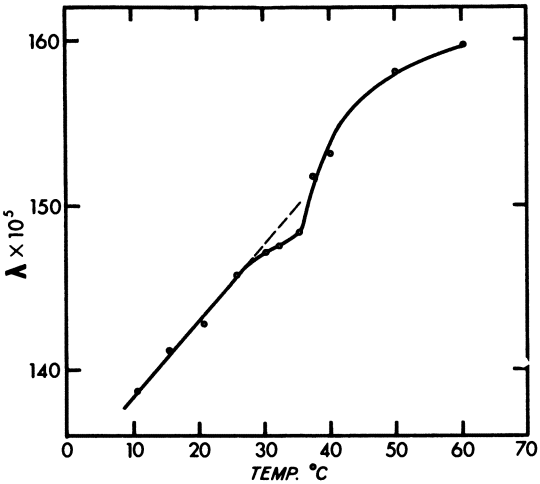

Doklady Akademii Nauk SSSR

Figure 2. Thermal conductivity of water from data of Frontas'ev (59). Curve redrawn by present author

Figure 3 shows the isothermal compressibility of water as reported by Peña and McGlashan (*117*). The compressibility goes through a shallow minimum around 50°C. While the curve may have an apparent slight "shoulder" around 40°–50°C., it is more significant that a rapid change in slope occurs above 30°C. There is little doubt that the compressibility of water does go through a minimum near 40°–50°C., as substantiated by Gibbson and Loeffler (*63*), Jessup (*85*), and Randall (*122*). Nývlt and Erdös (*114*) have determined the adiabatic compressibility for water, also by means of a piezometric method. Their results are shown in Figure 4 and indicate a break in this quantity around 30°–35°C.

Elsewhere (*31*), we have discussed Brown's measurements (*14*) on the transverse proton spin relaxation time as a function of temperature. His data suggest anomalous changes around 18°, 42°, and 60°C. Simpson and Carr (*138*) have also observed an anomaly near 40°C. on the basis of their spin relaxation studies. Simpson (*137*), in particular, reviewed other evidence for anomalies in this temperature range and noted that

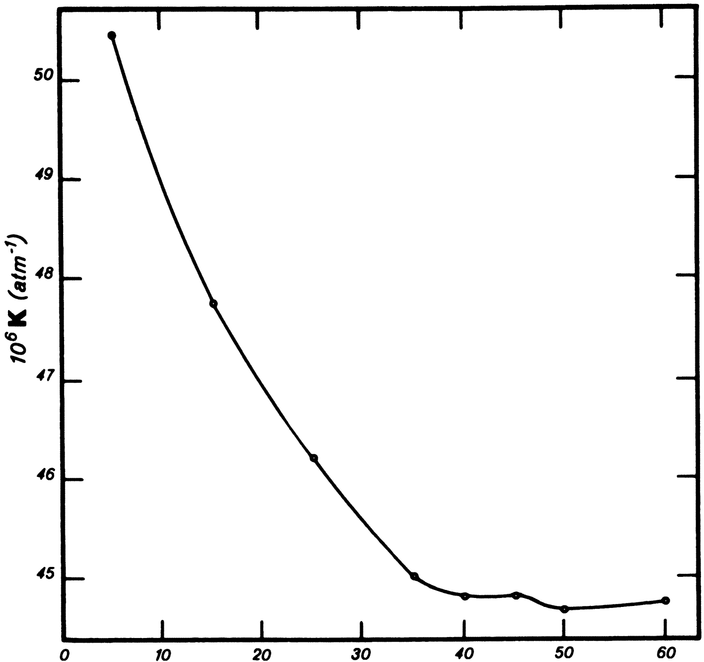

Transactions of the Faraday Society

Figure 3. Isothermal compressibility of water from data of Peña and McGlashan (117). Curve redrawn by present author

any complete theory of water should explain the observed change in activation energy in this temperature region. More recently, Glasel (*64*) measured the transverse relaxation time, and from his analysis of the activation energy for the reciprocal transverse relaxation time, he finds a distinct break near 30°C. An anomaly at this temperature has also been noted by Hausser (*74*), who observed a notable break at 30°C. Based on his measurements, Hausser calculates the following values for the self-diffusion coefficient (and the corresponding energies of activation)

$$D_0 = 7.0 \times 10^{-3} \text{ sq. cm./sec.; } \Delta E\ddagger = 3370 \pm 170 \text{ cal./gram-mole}$$
$$\text{for } T > 30°\text{C.}$$

$$D_0 = 0.131 \text{ sq. cm./sec.; } \Delta E\ddagger = 5200 \pm 260 \text{ cal./gram-mole}$$
$$\text{for } T < 30°\text{C.}$$

Woessner (*157*) has studied the relaxation in heavy water at 9.5 megacycles and notes that the data cannot be described by an Arrhenius equation. Instead, the curve appears to break around 40°–45°C.

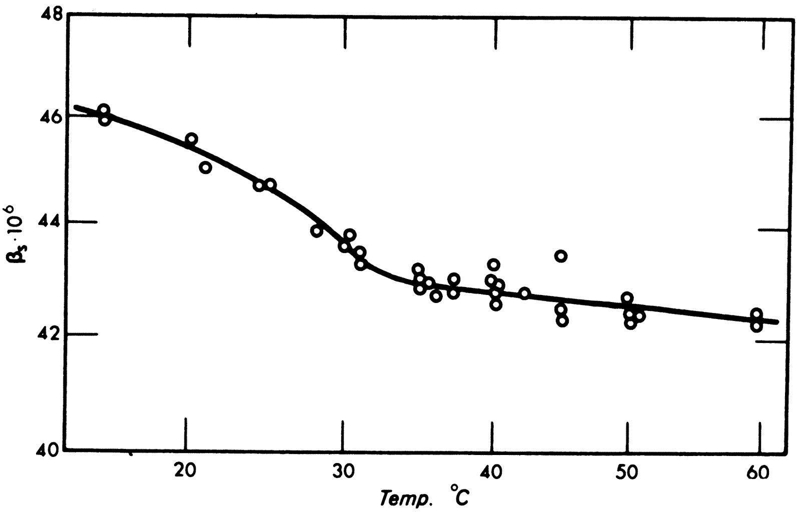

Collection of Czechoslovak Chemical Communications

Figure 4. Adiabatic compressibility of water from data of Nývlt and Erdös (114). Curve redrawn by present author

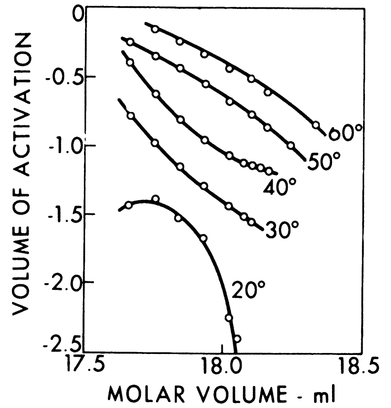

Transactions of the Faraday Society

*Figure 5. Volume of activation for conduction of 0.018*N *KCl solutions* (15)

We now consider briefly a few examples of the evidence for structural transitions as reflected by anomalous temperature dependencies in some properties of aqueous solutions.

Structural effects will probably affect kinetic properties, and as an example we mention the measurements by Brummer and Hills (*15*) of the volume of activation for potassium chloride conduction in water

(Figure 5). (*See also* Refs. *49* and *78*). The activation volume for conduction at 20°C. is negative and with large curvature away from the molar volume axis. Less negative values, but still with curvature away from the molar volume axis, are also observed at 50° and 60°C. However, at two intermediate temperatures—30° and 40°C.—the curvature is toward the molar volume axis. A change of this type is hard to reconcile with any other change than one in the structure of the solvent.

An interesting example of kinks in kinetic data is obtained from Scheurer and co-workers (*133*), who studied the dehydration of carbonic acid. Figure 6 is a plot of the log (dehydration rate) *vs.* reciprocal of absolute temperature. Note the relatively abrupt change near 31°C.

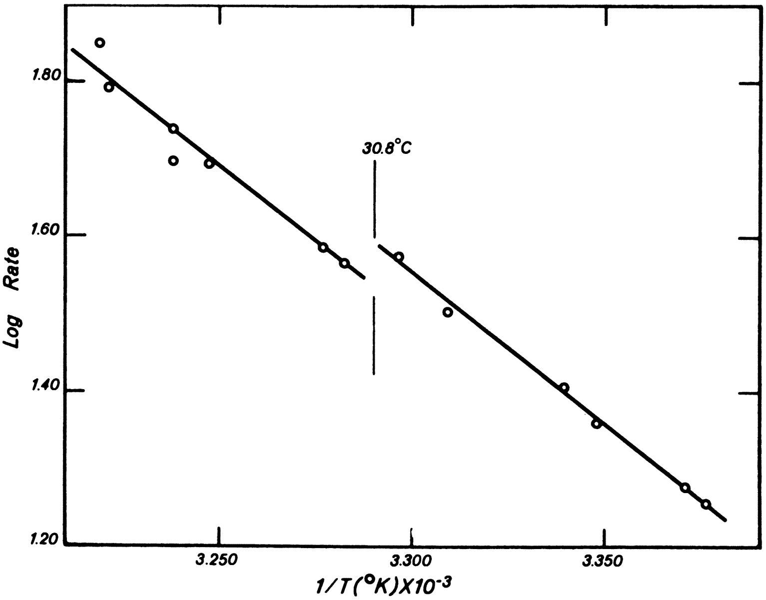

Journal of Physical Chemistry

Figure 6. Rate of dehydration of carbonic acid from data of Scheurer et al. (133)

We now turn briefly to examples of the thermal anomalies in heterogeneous systems. Shamsul Huq and Lodhi (*136*) recently determined the distribution of benzoic acid between benzene and water as a function of temperature (Figure 7). The upper set of points refers to the observed distribution coefficient based on the monomer (in the benzene phase). The data points are those obtained by Shamsul Huq and Lodhi; straight-line segments have been drawn in by the present author. Obviously, little significance can be attached to a "curve" such as this which is based on only two points for the higher temperature range, yet, it is undoubtedly significant that abrupt changes are encountered slightly above 15°C. and near 30°C.

Water properties near solid interfaces frequently reveal anomalous temperature dependencies. Thus, the zeta-potential for water flowing over a cellulose surface changes in an anomalous, abrupt manner near 30°C. (*31*). Recently, Ramiah and Goring (*121*) have noted what appears to be second-order transitions in volume *vs.* temperature near 25°C. for cellulose and other wood polymers. The anomalies were related to transitions in the layers of water adjacent to the carbohydrate molecules.

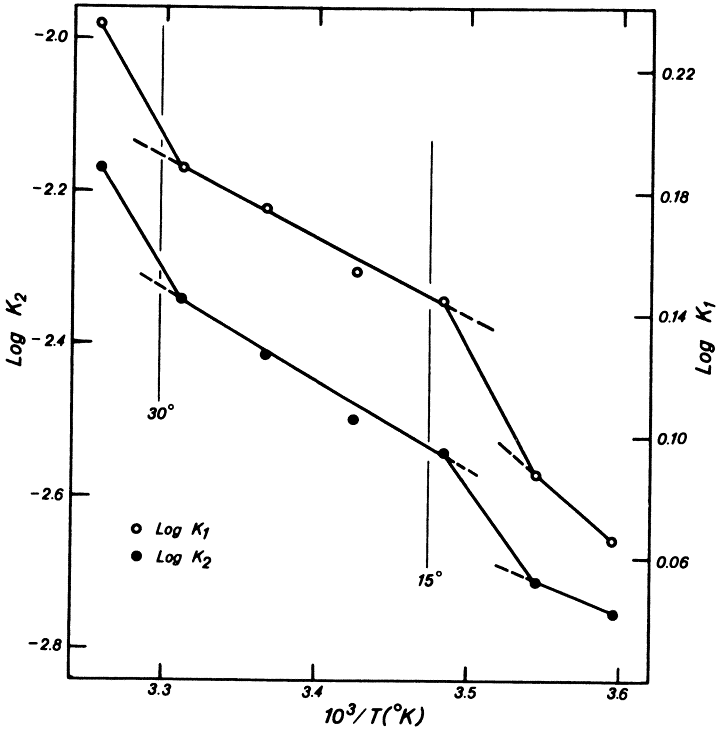

Journal of Physical Chemistry

Figure 7. Distribution coefficient of benzoic acid between water and benzene (136)

Steinert and Haase (*140*) have studied nonisothermal membrane properties using cellulose and cupriferrocyanide-impregnated cellulose membranes (Figure 8). The apparent heat of transport across the membrane was measured as a function of temperature by applying a temperature difference across the membrane. Unfortunately, more closely spaced measurements are not available; however, there is no doubt that abrupt marked transitions occur around 32° and 47°C. Anomalies were also

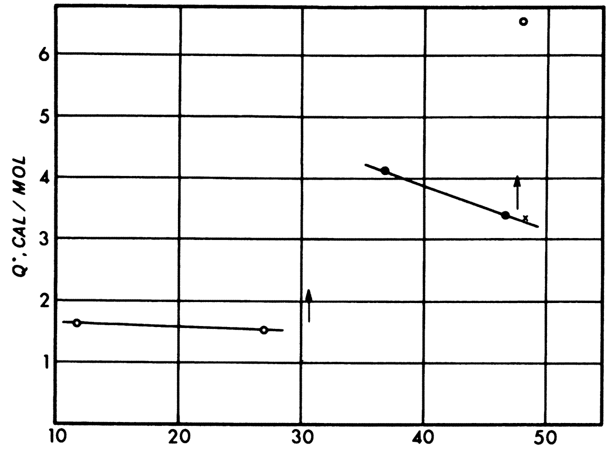

Zeitschrift fuer Physikalische Chemie

Figure 8. Heat of transfer across a cellophane membrane (140)

observed in permeability near 32.5° and 42.5°C. Steinert and Haase speculated on the origin of these anomalies, which they correctly identified as evidence of phase transitions. The authors initially assumed that the anomalies might be caused by a transition in the structure of the cellulose but were unable to find any evidence in the literature for anomalous transitions in the structure of pure cellulose at these temperatures. In view of the above, it seems reasonable to assume that the anomalies do indeed manifest phase transitions but that the structure which changes is the water associated with the membranes (*see* Ref. *143*).

Other evidence for anomalies in aqueous interfacial properties is found in measurements of membrane conductances and membrane potentials. Figure 9 shows the conductances of barium stearate multilayer membranes deposited on glass slides (*109*). Both the d.c.- and a.c.-conductances show a remarkable change in slope near 30°C., above which the conductance appears more or less temperature independent. Nelson speculates on the possibility that this change is caused by a phase transition in the multilayer, but such was not detectable in x-ray diffraction studies. This brings to mind the results by Trapeznikov (*145*), mentioned in Ref. *30,* who observed anomalous temperature dependencies in the properties of monolayers of palmitic acid spread on various salt solutions. He also suggested that these changes appear to "be connected with phase transformations in the crystals." However, as pointed out here, temperatures of the transitions, both in Nelson's and Trapeznikov's data, appear to occur at the same temperatures where we have observed anomalies in the properties of water and aqueous solutions. Hence, it

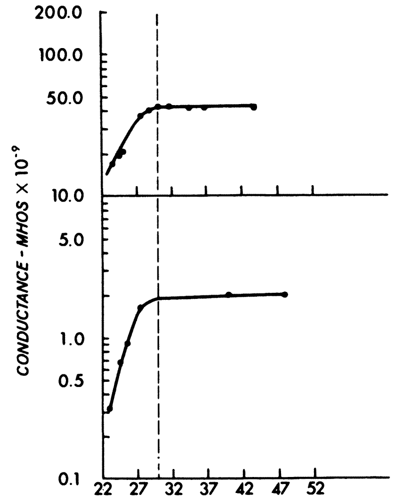

U. S. Department of the Interior, Office of Saline Water

Figure 9. Conductance of barium stearate multilayer membranes (109)

seems reasonable again to explain the observed, anomalous results in terms of the structural properties of water or, at least, of water as modified by proximity to interfaces. Finally, Nelson also observed anomalous temperature dependencies of bi-ionic potentials, using potassium oleate-impregnated collodion membranes.

We have shown a few specific examples of the nature of the thermal anomalies in water. More extensive discussion is available in the papers by this author referred to above. We add here the following general observations regarding the nature of the kinks. Two distinct types seem to exist. Centering our attention primarily on rate processes, these may be depicted schematically as shown in Figure 10. Graphs of log (rate) *vs.* the reciprocal of absolute temperature may appear as two parallel lines with a distinct displacement near the temperature of a kink (Figure 10A). As an example, note the rate data shown in Figure 6 (*133*) on the rate of dehydration of carbonic acid. Figure 10B shows schematically the corresponding energy of activation. This graph is characterized by a single, large deviation in the calculated energy of activation. As an example of such a behavior, Figure 11 shows the calculated activation energy values for hydrolysis of 2-bromo-2-chloropropane obtained from Queen and Robertson (*119*). This type of anomaly in the energy of activation is not likely to represent a "bad" point in the observed rate constants. As shown schematically in Figure 10C, the existence of a single "bad" point in the log (rate) plot would give rise to a high and a low value for the apparent energy of activation (Figure 10D).

Figure 10E shows another type of rate data. As an example, we refer to the recent kinetics data by Massey, Curti, and Ganther (*108*) on D-amino acid oxidase. Their results are redrawn in Figure 12 where the

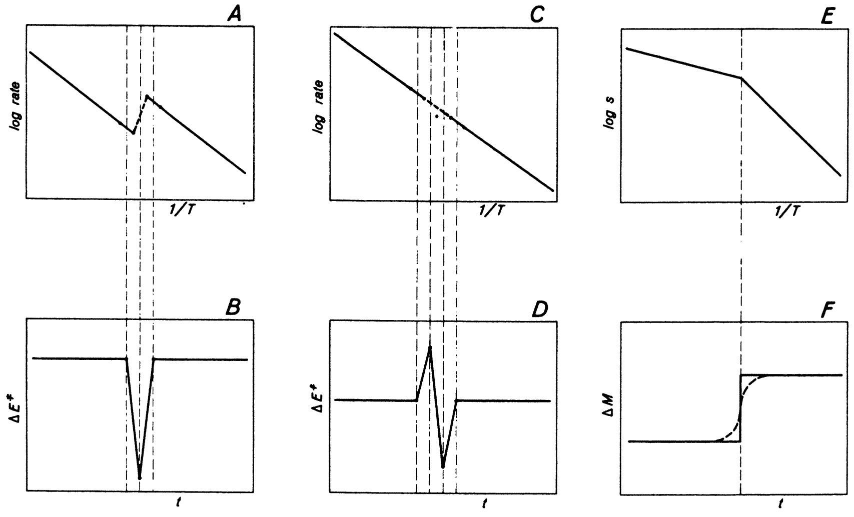

Figure 10. Types of thermal anomalies, highly schematized

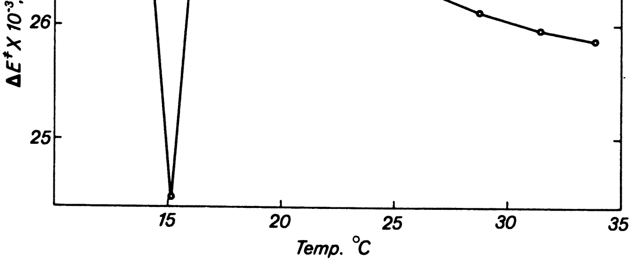

Journal of the American Chemical Society

Figure 11. Energy of activation for hydrolysis of 2-bromo-2-chloropropane (119)

ordinate is the logarithm of the rate (expressed as turnover number), and the abscissa is the reciprocal of absolute temperature. The corresponding activation energy data are shown schematically in Figure 10F; the observed activation energy will appear to have two discrete values. If precise and closely spaced data were available, the result would more likely appear as the sigmoid-shaped curve, indicated by the dash portions of Figure 10F.

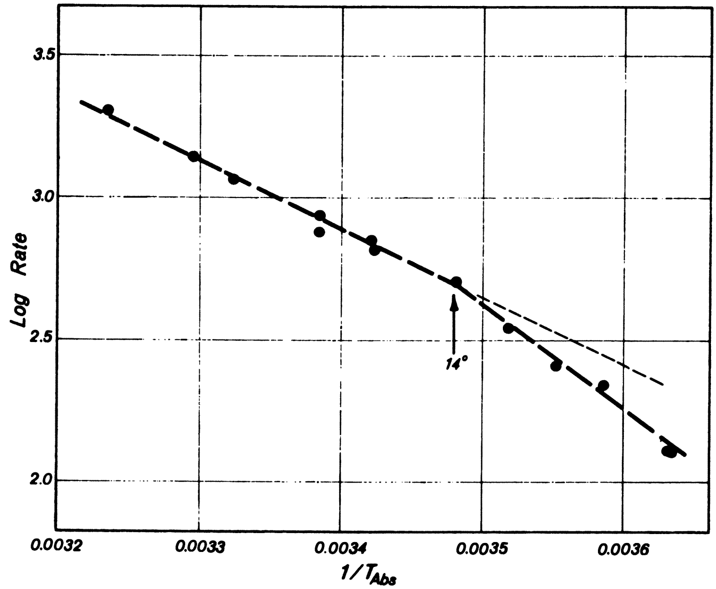

Journal of Biological Chemistry

Figure 12. Rate data for D*-amino acid oxidase catalysis* (108). *Curve redrawn by present author*

It is tempting to suggest an interpretation of these phenomena in terms of an Eyring-type rate equation. For Figure 10A, the mechanism corresponds to a reaction where the creation of the activated complex requires the same energy, practically independent of the solvent structure over the combined temperature intervals. The kink here is a manifestation of a change owing to a change in the pre-exponential factor—*i.e.*, a structural change in the solvent resulting in a change in $\Delta S^{\ddagger}$. The alternative example shown in Figure 10E suggests two different mechanisms (for the two temperature intervals) for the process under consideration. This would be expected for reactions where the mechanism depends upon the nature of the hydration of one or both of the reactants (or the activated complex) and thus reflects a change in $\Delta H^{\ddagger}$ (as well as in $\Delta S^{\ddagger}$).

Equilibrium properties also seem to show both types of anomalies illustrated in Figures 10A and 10E. As an example, we have discussed (*31*) the study by Klots and Benson (*91*) of the solubility ratio of nitrogen to argon. A solubility relation of the type shown in Figure 10A is observed in this case while other solubility data more frequently show the behavior indicated in Figure 10E.

We now summarize some generalizations regarding kinks on the basis of evidence obtained so far. (With minor exceptions, this summary is identical to the one presented in Ref. *32*).

(1) The temperatures at which the thermal anomalies are most frequently observed are approximately 15°, 30°, 45°, and 60°C. within ±1–2 degrees. In other words, the first two kinks may be centered near 13° and 31°C. while the other kinks may occur near 44° and 62°C. Hence, the unexpected symmetry which would otherwise be implied is not necessarily real, and the enumeration of the 15 degree multiples may primarily serve as a convenient mnemotechnic device for recalling the temperatures of the transitions. Each transition apparently occurs over a fairly narrow temperature interval of about 1–2 degrees on either side of the "center" of the transition temperature. It is possible and, in fact, likely that more than four kinks exist. We believe an additional kink occurs at temperatures near or above 80°C. Very likely there is also an anomaly near 140°–170°C.

(2) It is much easier to demonstrate the existence of the kinks in the properties of aqueous solutions than in the properties of pure (bulk) water. The kinks do, however, seem to occur in the properties of both. For this reason, it is believed that the kinks (at least in dilute solutions) owe their existence to some phenomena associated with the structure of water itself and that the existence of the kinks in aqueous solutions are caused by the persistence of some particular structural features of pure water, even in the presence of ionic solutes.

(3) The temperatures at which the kinks occur in aqueous solutions are rather insensitive to both the nature and the concentrations of solutes. Presently, we do not have sufficient material to state the excursions expected from the pure water values (for the temperatures of the kinks) as a function of concentration or nature of the solute. However, generally, the changes for most solutes are within 1 (or a few) degrees of the temperatures for pure, bulk water, at least for most solutions of concentrations of less than 2–5M. Only strong acids in moderate to high concentrations appear to change the temperatures of the kinks significantly. The kinks, however, remain, but the temperatures at which they occur are notably changed from the values obtained with pure water and dilute solutions.

(4) The kinks are present in both equilibrium properties and in transport phenomena.

(5) The kinks are manifested in both surface and interfacial phenomena. For these phenomena, they are often particularly noticeable although they may occur here at slightly different temperatures than those observed for bulk phenomena.

Current Water Structure Models

We now review some of the current structural theories of water, in particular, those which may allow for (although not necessarily be able to predict) thermal anomalies. [Part of the material in this section has been presented at a recent symposium (*33*).] Several reviews and monographs have appeared recently, summarizing the current status of research on the structure of water and aqueous solutions. The reader is referred to earlier theories reviewed briefly in connection with a number of different treatments of the structure of water, such as Nemethy and Scheraga (*112*), Frank and co-workers (*44, 45, 46, 47, 53*), Wicke (*156*), Eyring and Marchi (*107*), Jhon, Grosh, and Ree (*86*), and this author (*31, 32, 33*). An excellent survey is given by Kavanau (*89*); the monograph by Samoilov (*130*) also reviews a number of structural aspects of water but is primarily a presentation of Samoilov's own studies. Finally, Luck (*100*) has recently published a detailed review of water structure theories which also discusses Luck's own important contribution.

Uniformist, Average Models. We divide the current water structure models into two major categories. The first treats water essentially as an unstructured liquid while the second admits the simultaneous existence of at least two states of water—*i.e.*, the structural models which Frank has termed the "mixture models."

The basic element in the "uniformist," "average" view [adopted by Bernal and Fowler (*12*), Pople (*118*), and recently by Wall and Hornig (*155*)] is that there exists in water no local domains of structure different from that of any other arbitrarily chosen volume element in the water. In other words, in the process of averaging, the individual water molecule behaves at any time much like any other water molecule is behaving at that same time. Bernal and Fowler's original theory has commanded the greatest attention and for a long time has served well in many applications. However, it was by no means a quantitative theory. Pople's study is based on a treatment of the water molecule by Lennard-Jones and Pople (*96*), and this attempt achieved far greater quantitative insight. Wall and Hornig (*155*) draw attention to the inability of Raman spectroscopy to identify definite structures within liquid water; hence, indirectly they lend support to the "unstructured" theories such as Pople's.

Mixture Models; Broken-Down Ice Structures. Historically, the mixture models have received considerably more attention than the uniformist, average models. Somewhat arbitrarily, we divide these as follows: (1) broken-down ice lattice models (*i.e.*, ice-like structural units in equilibrium with monomers); (2) cluster models (clusters in equilibrium with monomers); (3) models based on clathrate-like cages (again in equilibrium with monomers). In each case, it is understood that at least two species of water exist—namely, a bulky species representing some type of structured units and a dense species, such as monomeric water molecules.

The water-ice mixture model, implying the existence of domains of structure resembling Ice-I (or some other type of ice) in equilibrium with monomeric water, was apparently first proposed by Rowlands and elaborated upon by Röntgen in 1892 (*see* Ref. *45*). The idea that water should be a simple mixture of ice and water has served as a useful conceptual framework for other investigators. Thus, Hall (*72*) gave a "two-state" theory of liquid water (based on ultrasonics studies), and Grojtheim and Krogh-Moe (*70*) also suggested a two-fluid model of water. The same idea was used also by Wada (*151*), who like Grojtheim and Krogh-Moe, was quite successful in making numerical predictions in agreement with observed quantities of thermodynamic interest. Samoilov (*130*) has proposed a water model in which the monomeric molecules are "tucked away" in the interstitial spaces of a lattice of ice-like geometry. Indeed, the idea of broken-down ice lattices as structure models for water has been common. Thus, without formulating a general theory, Tamman [*see* Dorsey (*27*)] suggested that there should be as many types of structures in liquid water as there are types of ice (*i.e.*, Ice-Ih, Ice-Ic, Ice-II, . . . Ice-VII). Among the most recent contributions to models of water with ice-like attributes is the x-ray diffraction study by Danford and Levy (*23*). Undoubtedly, this is the most careful x-ray diffraction work ever carried out on water. Good agreement was obtained between the calculated and the observed scattering curves, assuming a broken-down ice structure as a water model. In this theory, the monomeric water molecules occupy positions in the interstices of the ice. The model is, therefore, essentially similar to Samoilov's (*130*). It is possible, however, that in testing other models for their ability to predict the observed radial distribution function, Danford and Levy's treatment did not afford the same advantages of flexibility in the parameters for these models as was allowed in the broken-down ice model. In fact, only one other structural model was tested to any extent—namely, the Pauling clathrate-cage model. Work on the Danford-Levy model continues at Oak Ridge National Laboratory (*24*). It is disturbing, however, that the good is obtained only by means of many adjustable parameters. [Thus, three O-O distances were invoked and: "these three adjustable parameters together with associated temperature coefficients were sufficient to yield a good fit to all but the low angle region of the intensity function; ultimately this region was also fitted by introducing additional temperature coefficients associated with longer distances and by adjusting the distance characteristic of the start of the continuum. The occupancy of cavities by interstitial molecules was constrained to that required by proper density" (*24*).] Recently, Litovitz and co-workers investigated the properties of water by ultrasonic absorption. Davis and Litovitz (*25*) suggested a structure of liquid water involving elements of puckered hexagonal rings in water similar to the ice rings formed in the basal plane of the ice crystal. Density variations are accounted for by assuming that two such ring structures coexist—namely, an open-packed ice-like structure (maximum hydrogen bonding between rings) and a close-packed ring structure.

Significant Structure Theory and Eucken's Polymer Model. If we drop the restriction that the bulky species represent only Ice-I-like structures and reserve the term "ice-like" for water molecules which have merely the same spatial arrangement as ice (*i.e.*, tetrahedrally hydrogen-bonded), we may include in this two-state theory (in which we have a bulky and a dense species) the treatment by Marchi and Eyring (*107*). This is a special case of the significant structure theory of liquids and introduces, as a specific element, fluidized vacancies in addition to the individual monomers (which, in turn, are assumed capable of free rotation).

More recently, Jhon *et al.* (*86*) extended the Eyring and Marchi treatment of water (in terms of the significant structure theory). Their work recognizes the increasing amount of experimental evidence which points to a low concentration of monomeric, unbonded water molecules. The significant structures now become cage-like clusters with 46 molecules (having a density similar to that of Ice-I) and an Ice-III like structure with which equilibrium is established. Again, fluidized vacancies are produced during melting, and this process is still considered a contraction owing to the packing of single water molecules into the voids of (Ice-I) cage-like clusters. The calculated molar volumes show the observed minimum at 4°C., and the calculated vapor pressure below the boiling point agrees well with experimental data. The calculated specific heat agrees fairly well with the experimentally observed values. This structural theory was combined with Eyring's rate theory for viscous flow, resulting in a calculated pressure dependence of the relative viscosity in good qualitative agreement with the observed, complex behavior. In fact, the quantitative agreement is quite impressive.

An older water model deserves mention, if not for its likely authenticity, at least for its excellent numerical agreement between calculated and observed values. Eucken (*39*) treated water as a mixture of distinct, associated species, such as dimers, tetramers, and octamers. It now seems unlikely that this theory can be correct although Wicke (*156*) recently argued that at least near the critical point, dimers of the type implied by Eucken's theory may exist and be responsible for the anomalous behavior at that temperature (*see* Ref. *101*). Wicke (*156*) has also discussed a type of hydrogen bonding which might lead to open chain structures, planar rings and bifurcated structures. By this mechanism one might understand the existence of dimers in solution; however, these structures involve large deviations from linear OH . . . O hydrogen bonds. Until and unless calculations are forthcoming which can support the implication that such structures are energetically favorable, one must view them with some skepticism, at least as far as liquid water is concerned. Eucken's theory is interesting, however, as an example of the fact that numerical estimates obtained by such a theory may be in excellent agreement with observations, without the theory's necessarily being correct. It is undoubtedly true that a limited numerical success of a theory is no proof of the reality of the underlying model, whether or not the calculated quantities are thermodynamic parameters, the radial distribution function, or part of any other individual class of properties. Most likely a much more critical test of a water theory is its ability to predict correctly, even if only qualitatively, a large variety of widely different properties of water.

Cluster Theories. Historically, the most important study of water structure based on the existence of clusters was Stewart's x-ray diffraction work (*142*). In his theory, clusters ("cybotactic swarms") were postulated to exist, each containing on the order of 10,000 water molecules. Although this constituted an apparently reasonable theory at the time, this view has now yielded to the concept of clusters of considerably smaller sizes. It is interesting to note that without much critical analysis, Frenkel (*57*) viewed Stewart's theory of water as essentially correct. In fact, Frenkel apparently expected that further work on liquid structures in general would be along the lines Stewart advocated. Luck has discussed this in some detail (*100*). Subsequent to Stewart's papers, Nomoto (*113*) discussed a water model, based on ultrasonic studies, involving clusters of several thousand water molecules.

The most important cluster theory of water is that proposed by Nemethy and Scheraga (*112*). In a sense, their approach is similar to Eyring's theory of significant structures, although with somewhat different choices of the significant structures. The model builds on Frank and Wen's (*54*) concept of flickering clusters, for which Nemethy and Scheraga calculate the thermodynamic properties from a straightforward treatment of the partition function, assumed to be applicable to the different types of significant structures. The authors considered unbonded water molecules and water molecules with 1, 2, 3, and 4 hydrogen bonds per water molecule. The average cluster size in this theory decreases from 91 to 25 water molecules in the temperature range 0°–70°C.; at room temperature the cluster size is approximately 50. The mole fraction of non-hydrogen bonded (monomeric) molecules increases from

0.24 to 0.29 over the range 0°–70°C. However, in a more recent treatment by Griffith and Scheraga (*67, 68*) the concept of the clusters has, to some extent, been de-emphasized, and more rigorous calculations (allowing for variable spacing between the energy levels of the various states of bondedness of the water molecules) result in a far lower concentration of monomeric water molecules. This latter fact seems to be consistent with the implications of much current experimental work.

Recently, Vand and Senior (*147, 148*) have discussed the structure of water based on a partition function in which the Nemethy-Scheraga notion of energy levels for the different states of hydrogen bonding is replaced by an energy band distribution. Contrary to the treatment by Nemethy and Scheraga, in which zero-bonded (monomeric), 1, 2, 3, and 4 hydrogen-bonded water molecules were considered, Vand and Senior adopt the approach taken by Buijs and Choppin (*16*), who considered only three species of water—namely, those with neither OH group bonded, those with one OH group bonded, and those with both OH groups bonded to neighboring molecules by hydrogen bonds. Their results are quite impressive. For the Helmholtz free energy, the deviation (between the freezing and boiling points) is less than 0.5%; for the internal energy, the error (apparently a systematic deviation) is of the order of 1%, while the specific heat agrees with the observed values within approximately 0.2%. Apparently the model was not used to test temperature dependence of the molar volume. Vand and Senior pointed out that the particular model studied is not unique in being able to explain the thermodynamic properties of liquid water. Thus, they have apparently also investigated a simplified model based on one species with an energy band distribution, which also attained satisfactory results between predicted and observed thermodynamic properties of liquid water. This in a sense then approaches the sentiments of Wall and Hornig (*155*). (*See also* the recent paper by Falk and Ford (*41*), who also take issue with a formulation of water structure in terms of a mixture model.) Again, one is impressed by the wide range of current theories which can numerically predict values in excellent agreement with observed values while being mutually physically different to a significant extent.

A theory of water structure involving clusters somewhat similar to the original Nemethy-Scheraga concept has been advocated recently by Luck (*101*). In his theory, the number of water molecules in the clusters near the freezing point may exceed 100 and, in fact, may approach 700.

Clathrate-Cage Model. The final water model which is of major interest is based on clathrate hydrate cage structures. It was originally proposed by Pauling (*116*), who noted the existence of clathrate hydrates of many inert gases and suggested, by analogy to the chlorine hydrate, that water is its own clathrate hydrate. This model was subsequently taken up by Frank and Quist (*53*) and worked into a semiphenomenological, thermodynamic theory allowing them to calculate a number of parameters which could be compared directly with experimental values. The essential element of the clathrate-cage theory—as distinguished from the cluster theory—is the existence of discrete sites for water molecules and/or solute molecules in the host lattice.

One particular difficulty which has concerned Frank involves the nature of the dense species—*i.e.,* the monomeric water molecule in any of the mixture models. The difficulty is in explaining how mere van der Waals forces can provide enough attraction for the single water molecule to avoid its escaping into the vapor state [*see also* Marchi and Eyring (*107*)]. In connection with the clathrate-cage model, Frank and Quist (*53*) have pointed out that water molecules in the clathrate cages must possess unique properties. They found it necessary to assume "double occupancy" of the larger voids—*i.e.,* water dimers in the cages. It is well-known that those substances which form clathrate hydrates are nonpolar or have small dipole moments. Large dipoles are likely to interact strongly with neighboring water molecules and, therefore, tend to prevent formation of cages. Thus it is somewhat disturbing that Jeffrey (*84*), while finding ample evidence from x-ray diffraction studies for the existence of such structures as pentagonal dodecahedra of water molecules, has apparently never observed individual, single water molecules occupying the guest positions in these polyhedra. Mak (*106*), working in Jeffrey's laboratory, has demonstrated a new type of clathrate hydrate, namely, a hexamethylenetetramine hexahydrate, in which hydrogen bonding exists between the host and guest species (*see also* Franks and Ives (*55*) and the present author (*33*) on the effect of the lower aliphatic alcohols on interfacial structures in aqueous systems.)

Implications of Thermal Anomalies for Water Structure Models

It is appropriate at this point to make a few comments about the importance of the observed thermal anomalies in connection with the theories of water structure mentioned above. If the reality of the thermal anomalies is accepted, the ultimate theory of water structure must be able to allow for the existence of these anomalies and, hopefully, eventually predict their existence. If the thermal anomalies do indeed manifest higher-order phase transitions, structured elements of a certain size must be present in water. In other words, the uniformists', average structural models must definitely be ruled out. Furthermore, noting that the anomalies tend to center around discrete temperatures and apparently are completed over a few degrees, we concluded that if they do manifest "polymorphic" phase transitions, the size of the cooperating units must certainly be larger than a few molecules and probably less than the 10,000 (or larger number) implied in the structural theory of Stewart (*142*), Frenkel (*57*), and others. These considerations obviously do not apply if the anomalies are caused merely by the sudden onset of different rotational modes of the monomeric water.

As discussed elsewhere (*32*), this author believes the structural units responsible for the anomalies probably range from about 20 molecules at room temperature and up to possibly as many as 100–200. Several such structures must exist, each with its own clearly delineated thermal stability limit. Anticipating the material presented below, it is further suggested that cage-like models may have an advantage over the cluster models (to the extent to which one can distinguish between these, keeping in mind that cages, of course, are also clusters by their nature) because of their ability to provide discrete sites for a solute molecule—a statement which is suggested primarily by the behavior of nonelectrolytes in solution.

Importance of Anomalies

Frank (*44*) has recently pointed out that there are undoubtedly many experimental results which have lain dormant because they did not fit into current theories. Obviously, understanding has advanced by developing theories—*i.e.*, treatments of models which are capable of accounting for known properties and predicting other properties. Quite often, however, various experimental features have been neglected because these particular aspects, although representing reliable information, could not fit into a current theory. We are obligated to devote attention to what we understand in order to produce theories, but at the same time this should not tempt us to ignore the anomalies too long.

In discussing the value of considering anomalies, Frank points to much data which may not have received proper attention. (One of the examples of experimental results which according to Frank had not been readily explained in terms of available theories is the freezing point anomaly for the ammonium halide solutions, studied by Scatchard and Prentiss (*132*). Subsequent to Frank's discussion, these anomalous results have been the subject of an experimental reinvestigation by Garnsey and Prue (*62*). These authors have suggested that the data of Scatchard *et al.* may not necessarily be correct. However, this does not detract from Frank's general observation that one tends to ignore those anomalies which do not fit readily into existing theories.) As an example, he mentions a discontinuity in the properties of the series of alkali metal chlorides—namely, in the effect of these salts on the temperature of maximum density of solutions. The anomaly here appears to parallel the more recently discovered anomaly observed by Agar and Turner (*2*, *3*). These authors measured the heats of transport and displayed the results as a function of the crystalographic radii for the alkali and halide ions. The lithium ion appears in this comparison to be quite out of line with the behavior observed for the larger alkali ions—*i.e.*, the lithium ion appears to be a structure breaker compared with the sodium ion. Frank points out that we know the lithium ion is highly hydrated which gives the lithium ion a negative (*i.e.*, structure-making) entropy, but the heat of transport measurement suggests that the ion is a structure breaker. Frank explains this apparent contradiction in terms of a large (spherical shell) volume element of orientational disorder caused by the mismatch between the ordered hydration structure and the differently ordered, bulk water structure (the Frank-Wen (*54*) picture of hydration). Thus, when the moving ion drags with it the relatively stable hydration sphere as a kinetic unit it will create a disordered region ahead of the ion and, will thus give the net appearance of being a structure breaker. Litvimenko (*98*) observes that the lithium ion assumes an unusual position compared with the other alkali ions from his measurements on the apparent non-compressible molar volumes of the ions at infinite dilution. He explains this on the assumption that the structural changes arising from the nearest lithium ion differ significantly from the change of the other ions upon the water structure in the immediate vicinity of the ions. (Incidentally, the ammonium ion also assumes an unusual position with a positive apparent compressibility.)

Role of Water Structure in Solute–Water Interactions

In the following sections we discuss some aspects of solute-solvent interactions. This discussion is not a complete, current survey but rather an attempt to bring together some divergent experimental facets of water-solute interactions which often are not discussed by either theoreticians or experimentalists. For more detailed, general information *see* Refs. *18*, *19*, *20*, and *73*. The two essential points we wish to make are: (1) even in moderately concentrated solutions, there is evidence for the persistence of structural elements of the type found in pure water and especially in dilute solutions; (2) there is evidence for what appears to be discrete changes with concentration in the behavior of some aqueous solutions of both electrolytes and nonelectrolytes, and for nonelectrolytes this may be caused by the existence of discrete "sites" available to the solute molecules. Unfortunately, we shall be able to discuss only electrolyte-water interactions to any extent; the often more interesting nonelectrolyte-water interactions will be discussed in a later paper. This is all the more unfortunate since nonelectrolytes probably provide a more sensitive, nondestructive (or, at least, less destructive) probe of the aqueous environment.

Two water models presently being discussed in the literature may allow for the existence of cavities which, in turn, may serve as discrete sites for solute molecules. One of these is the broken down ice structure in which cavities are present in the void spaces between aligned, hexagonal rings of the ice lattice. The other model which provides for discreteness is the clathrate-cage model. We have mentioned here and discussed elsewhere (*33*) some of the arguments which tend to suggest that liquid water does not contain elements of Ice-I likeness. If the arguments stand up, a demonstration of the existence of discrete sites in the structure of water would then suggest that a clathrate-cage type model of water is most likely to be correct. In arguing our case, we shall discuss a number of different experimental results which are not readily placed in a coherent description of the structure of water or aqueous solutions.

Hydration of Ions and the Debye-Hückle Theory

The problem of ion hydration in aqueous solutions is far from being well-understood. Considering our ignorance about the structure of water, this is hardly surprising. Apparent "hydration numbers" depend strongly on the method by which they are determined. The problem is obviously important in understanding the properties of aqueous solutions. Approaches to electrolyte behavior have traditionally been through the Debye-Hückel equation and its extensions. The Debye-Hückel treatment is based on some simplifying assumptions, enumerated below.

(a) The interactions between ions are determined completely by Coulombic forces, and all other intermolecular forces can be neglected.

(b) The solvent may be considered as a continuum dielectric with a dielectric constant equal to that of the pure solvent, neglecting the effect on the dielectric constant of the solution owing to the dissolved salts.

(c) Ions are regarded as spherical and unpolarizable with spherically symmetric force fields.

(d) The effects owing to thermal kinetic energy are assumed small by comparison with the interionic attraction energy.

Pragmatically, many of the drawbacks of this approach are hidden in assigning a "mean ionic diameter" a representing the minimum distance of approach of an arbitrary ion to the central ion being considered. As examples, we recall that the potential X arising from a single charge is given by Equation 1:

$$X = \left(\frac{z_j e_0}{D}\right)\left(\frac{e^{\kappa a}}{1 + \kappa a}\right)\left(\frac{e^{-\kappa r}}{r}\right) \qquad (1)$$

where z_j = charge on central ion
e_0 = electronic charge
D = dielectric constant
r = distance from ion, j
κ = reciprocal radius of the ionic atmosphere

To calculate activity coefficients, Equation 2

$$\log f_\pm - \frac{A|z_+z_-|\sqrt{J}}{1 + Ba\sqrt{J}} + CJ \tag{2}$$

(where A [$= A(T,D)$] and B [$= B(T,D)$] are given by theory, and J is the ionic strength)
is often used, where again a and C are obtained from measurements. [Note that A and B are functions of D (dielectric constant) of the pure solvent and furthermore that D has been claimed to show kinks near 15° and possibly 30° and 60°C. (*28*). The existence of anomalies at low temperatures in the dielectric constant data, however, has recently been challenged by Rusche and Good (*124*, *125*).] The standard method for obtaining a is from empirical measurements of $f_\pm$, using Equation 2 (disregarding CJ) and plotting:

$$-\frac{A|z_+z_-|\sqrt{J}}{\log f_\pm} \quad vs. \quad \sqrt{J}$$

Since B is known, a can be calculated from the observed slope. It is, however, exactly a which in this way becomes the adjustable parameter in treating electrolyte solutions, and this quantity undoubtedly depends strongly on the nature of ion hydration.

The possibility that discrete hydration numbers exist for ions in solution has been debated for many years. It is not possible to make sharp distinctions, but it does seem as though three major views have been associated with this question. The first is that a definite, usually small number of water molecules were intimately associated with the hydrated ion. This is reflected in the hydration numbers quoted elsewhere in this paper. More recently, Samoilov (*130*) believes that hydration numbers refer in some way to the number of water molecules in the surrounding water structure whose mobility (as determined from the energy of activation for "jumping" from one position to another) had changed, owing to the influence of the force field from the ions. (If the movement of the water molecules around the ion has increased, Samoilov refers to this as negative hydration.) The third view is that the hydration numbers may in some cases be quite large—*i.e.*, as many as 60 or 70 water molecules per monovalent ion. Such large hydration numbers are, of course, unrealistic as far as definite, distinct hydration "shells" are concerned. Hence, the view has developed that what may be involved in this case are ions in structural groupings of water of the corresponding sizes.

More than 30 years ago, Scott, Obenhaus, and Wilson (*135*) suggested that for lithium chloride, a solute to solvent ratio of 1:10 corresponded to a definite composition, and they quoted earlier measurements (*134*) as indicating two distinct, definite values for the magnetic susceptibility of lithium chloride above and below the concentration, corresponding to a "decahydrate" in solution. Likewise, anomalies were also found in the density of such solutions. Scott, Obenhaus, and Wilson also quoted Hüttig and Keller (*83*) who found that the densities, refractive indices, and coefficient of extinction of lithium halide solutions showed discontinuous changes with concentration for molar ratios of water to solute of 6, 30, and 75.

Rutgers and Hendrikx (*126*) have reviewed existing hydration numbers and have provided some new values for the hydration of several cations and anions based on measurements with a membrane transference cell. Their results are hydration numbers higher than those normally assumed. Thus, apparent hydration numbers for lithium, sodium, and potassium were respectively 22, 13, and 7 while for magnesium, calcium, and zinc, values of 36, 20, and 44 were obtained.

In 1956 Owe Berg (*115*) advocated the existence in water of hydrates involving as many as 60 molecules per sodium chloride. He correctly noted that "60 water molecules could not be bound directly to one NaCl molecule (quite apart from the fact that there are no 'sodium chloride molecules' in the solution) and that the hydrates, therefore, are to be regarded as compositions of structural transformations." Horne and Birkett (*81*) have also suggested the existence of large numbers of hydration. Thus, estimates of 45–50 water molecules were obtained by different independent methods for lithium ion hydration.

The theory of Frank and Wen (*54*) for ion hydration involves the notion that some water molecules intimately contact the ion under consideration and subject to the strong centrosymmetric force field, are highly ordered. Beyond this area is a region of disorder, beyond which, in dilute solutions, unaffected water prevails. Typical literature values for "primary hydration numbers" range from 2–8 water molecules. For divalent ions, primary hydration numbers range from 10–20 water molecules while some authors have suggested hydration numbers for trivalent ions (based on compressibility data) between 20 and 30 water molecules per ion. Many attempts have been made to extend theories of this type to account better for the hydration of ions. Thus, Azzam (*7, 8*) and Horne and Birkett (*80*) have proposed a "multilayer" model of ion hydration.

We will now consider some experimental results which suggest that our concepts of ion hydration may require modification. Samoilov (*130*) has suggested a different approach to ion hydration involving only changes in the translational mobility of water molecules adjacent to ions and considering the water molecules as continuing primarily to belong to the water structure. The theory we develop in the following sections suggest that the Frank-Wen model of hydration probably still reflects essential aspects of hydration, but for more concentrated solutions this model must be expanded to allow for the effects of discrete structural entities in the water (not directly affected by the presence of the ions) as well as for the existence of discrete structural entities as part of the hydration "complexes" themselves.

Anomalous Concentration Dependencies

A most impressive, experimental study of apparent molal volumes of ions in solution has recently been completed by Vaslow (*150*). He measured the molal volumes of the alkali metal chlorides in aqueous solutions at extremely closely spaced concentration intervals over the range 0.02 to 3.5*m* at 25°C. For lithium chloride, the data above 0.1*m* can be represented (within the experimental error) in terms of two linear functions in $\sqrt{c}$ with different slopes and with a narrow transition region at about 1N. For the higher alkali chlorides, the transition region becomes wider and centered at lower concentrations; by rubidium chloride the linearity in $\sqrt{c}$ essentially disappears. Vaslow suggests that the effect is caused by a cooperative action of several ions within the solvent structure near the ions. Considering the extreme care he exercised, and the still somewhat tentative identification which can be made of the alleged transformation near 1N, it is little wonder that most previous investigators have overlooked this anomaly. However, Vaslow's data appear to establish the reality of the phenomenon. The reader is referred to the original article for an admirable discussion of the analysis of the certainty with which a more or less abrupt change in such curves can be identified. One of the most interesting results of his study, besides establishing the existence of an anomalous change in the apparent molal volumes as a function of concentration, is the observation that the concentration at which the anomaly occurs appears to depend on the nature of the solute. Thus, an independent study has shown an anomaly near 0.5*m* for tetrapropylammonium bromide while the concentrations for the anomalies for the alkali chlorides are LiCl, 1.14*m*; NaCl, 1.0*m*; KCl, 0.81*m*.

Vaslow suggested that his results were not inconsistent with water theories involving varying cluster sizes, such as those of Nemethy and Scheraga or Luck. It is not obvious, however, by which mechanism the clusters may effect a sudden change in solute behavior at a critical concentration. Vaslow dismisses the possibility that the anomalies depend on a "filling up" of one type of sites for the ions and the initiation of a different type (at transition points) since in order to obtain a sharp segregation into the different sites, a large difference in the partial molal free energy per site would be necessary. He claims that there is no evidence of such free energy changes seen in the activity coefficient curve for lithium chloride. In another connection, however, Frank (*47*) has noted that activity coefficients may not be particularly structure-sensitive: "the fact that activity coefficients in H_2O have been studied for so many decades, without an apparent need to take structure into account seems thus to be an accident, arising in part out of the nature of activity coefficients and, in part, out of the fact that, until recently, no one had looked at the tetraalkylammonium halides" (*see also* the recent article by Frank (*48*) on structural effects on activity coefficients).

The objection to the idea that the observed anomaly in apparent molal volumes reflects a distinct filling up of different types of sites should be considered in connection with Vaslow's own theory of hydration, which suggests (*see below*) that ions—at least smaller ions—may well become incorporated into existing water structure elements. Furthermore there is considerable evidence from studies on nonelectrolyte solutions that a process of filling of cavities or voids in the water structure may account for many properties of aqueous nonelectrolyte solutions. Vaslow's concentration ranges at which the anomalies occur would suggest numbers of "sites" on the order of 1 per 25 water molecules (a 1*M* solution consisting of 2 moles of individual ions thus has 2 moles of solute per $\sim$55 moles of water). Such numbers suggest the values expected if water were, indeed, a Pauling type clathrate hydrate. In connection with the objections to the filling of existing voids, one must be concerned with the question of whether or not monomeric water molecules would be displaced from the existing voids when the ions are introduced. If this is the case, one must account for equilibrium changes between the structured and monomeric species. Vaslow has argued against any simple hydration shell picture such as the possibility that the transition occurred when all of the water molecules were already in hydration shells into which further ions would need to penetrate (*see also* Ref. *111*).

Finally, Vaslow observed that in order to obtain a narrow transition region (without the need for a large partial molal free energy change), a cooperative effect among the ions must be necessary and, indeed, his expression for the apparent molal volume in terms of concentration involves the square root of the concentration to a high power. The solvent still plays a role in this connection since its structure must change (cooperatively) as the ions approach one another with increasing concentration. Notable concentration-dependent anomalies are observed also for nonelectrolytes in water in the same concentration range. This argues against the involvement of only cooperative ion-ion interactions (without cooperative ion-solvent and solvent-solvent interactions) to bring about the concentration-dependent anomalies. By the same token, one may discount (though perhaps not dismiss) the possibility that the concentration-dependent anomalies result from the interaction of "overlapping ion-hydration shells," or as an alternative, one may accept the existence of two different mechanisms of hydration (for electrolytes and nonelectrolytes respectively) creating anomalies which by chance occur in the same concentration range.

Additional evidence for the reality of concentration-dependent transitions may be obtained from a recent study by Zagorets, Ermakov, and Grunau (*162*). They investigated the structure of aqueous solutions of salts and hydrochloric acids by a proton spin-lattice relaxation technique. For dilute solutions of cobalt chloride (added to reduce the relaxation time to an experimentally convenient value) notable breaks were observed in the spin-lattice relaxation times as functions of the concentration of hydrochloric acid, potassium chloride, and sodium chloride. For NaCl sharp changes in the relaxation times as a function of concentration occurred near 1.00 and 4.15*m* (corresponding to 55 and 13.4 moles of water per sodium chloride molecule). For KCl a similarly pronounced break was observed at 0.85*m*. The values for the concentrations at which the anomalies occur (1.00 for NaCl and 0.85*m* for KCl) are, within the experimental error, the same as the values for which Vaslow found changes in the apparent molar volumes. This agreement further substantiates the existence of abrupt changes in solute properties as a function of concentration. Unfortunately, possible interpretations of this phenomenon are less well established. Vaslow considered the anomalies to reflect either cooperative effects associated with the behavior of the ions or changes in type of solvent organization (it is possible, of course, that these two alternatives are different ways of saying the same thing). Zagorets, Ermakov, and Grunau interpret the anomalies in terms of completing a two-layer "fixed" hydration shell for the ions. In connection with the studies of concentration-dependent anomalies, we might mention that the self-diffusion of sodium and chloride ions in sodium chloride at 25°C. also suggests anomalies somewhere between 0.7 and 0.9*m*. The self-diffusion coefficient (plotted as a function of $\sqrt{c}$) for sodium ions in sodium iodide also appears to show a complex functional dependence involving at least one inflection point in the concentration range of interest [*see* Adamson (*1*)]. Good (*65*) has also observed anomalous concentration dependencies in the energy and entropy of activation for viscous flow of electrolyte solutions. In particular, he noted anomalies in $\Delta E\ddagger$, and $\Delta S\ddagger$ for lithium and sodium chloride solution near 1*m* (*see* *also* his (*66*) study of the viscous properties of the alkaline earth chlorides).

Further evidence for the reality of a structural transition in the vicinity of 1*m* may be implied from a study by Satyanarayanamurty and Krishnamurty on ultrasonic velocities and compressibilities of aqueous solutions (*131*). They found that plots of the apparent molar compressibility (for metal nitrates) *vs.* square root concentration become linear only at concentrations above 1*m*.

Persistence of Water Structures in Aqueous Solutions

Thermal anomalies appear both in the properties of pure water and particularly in dilute solutions as well as in rather highly concentrated solutions of electrolytes and nonelectrolytes. We suggested that this is caused by the persistence of structured elements of water in the presence of solute—the structured elements retaining the properties characteristic of the undisturbed water structure. Elsewhere (*31*) we have mentioned the difficulties involved in this proposition when the concentration of electrolyte is sufficiently high—*i.e.*, in electrolyte solutions with a solute concentration of a few molar, the distance between neighboring ions is only a few molecular diameters of water, and hence, it seems natural to suspect that all the water molecules in such solutions would be strongly influenced by the intense electric field in the vicinity of the ions. This difficulty was overcome in Vaslow's model of ion hydration, which we discuss below. Krestov (*93*) has also suggested an unorthodox view of hydration. He proposes that some ill-defined "shielding" of the ion occurs in aqueous solutions, which apparently will allow for the elements of water structure to persist, undisturbed by the intense, local electric fields normally associated with relatively concentrated solutions of electrolytes. He believes that "hydration is accompanied by a peculiar neutralization of the ion charge and a charge redistribution over the solvent particles surrounding the ion." For this reason, Krestov and Abrosimov (*94*) chose to study the inert gases which are isoelectronic and isobaric with the ions. Vaslow (*149*) has proposed a hydration theory which may help us understand some features of the behavior of electrolytes in solution. This theory is consistent with the idea that relatively unchanged elements of water structure remain intact even in rather concentrated aqueous solutions. Vaslow's theory is based on energy of interaction values between a water dipole and an ion. For a water molecule with the H-atoms "pointing away" from the ion the variation in the energy of the ion is less than the energy of breaking a hydrogen bond. Hence, it appears that at least small ions may assume a position within the original water structure without breaking up the normal grouping of the water molecules. In other words, for some ions, the water-water interactions may be dominant despite the presence of the ions. Unfortunately, it is possible that Vaslow's hydration theory, which thus allows for the incorporation of ions into existing water structure elements, may not necessarily be correct. From a recent study by Griffith and Scheraga (*67*), it appears that the treatment by Vaslow is incomplete—*i.e.*, the contribution to the ion-water interaction of some multipole moments were neglected. In the Griffith-Scheraga theory, account is made of all the possible interactions between the ion and water based on the treatment by Coulson and Eisenberg (*21*).

In our discussion of the more likely current models of water structure, both the clathrate-cage model and the broken-down ice lattice model involve discrete sites (cavities, cages) in the water structure whereas no similar discreteness is invoked in the cluster theories. On the basis of the experiments discussed above, we suggest that the behavior of electrolytes in water can best be understood in terms of the two models involving discrete sites, and as discussed previously, the clathrate-cage model appears the most acceptable. However, we chose this model over the broken-down ice lattice models mainly by elimination—*i.e.*, based on such arguments that elements of ice-likeness do not appear consistent with many other known properties of water (supercooling, high entropy of fusion, etc.), and objections may well be made to some of these arguments.

In the present frame of reference, a concentration-dependent anomaly near 1.3*m*, would suggest one ion per 20 water molecules, or one "guest molecule" per pentagonal dodecahedron of host lattice (were such the only probable structures). Solutions of the order of 1–2*m* are rather concentrated, and one must question whether or not they should be described as concentrated solutions of solute in water or solutions of water in a crystalline hydrate melts.

Mishchenko and Dymarchuk (*111*) have studied the integral heats of reaction of cellulose with both water and aqueous solutions of electrolytes. A notable maximum in the integral heat of reaction occurs at approximately 2.5*m*. The authors visualize this sharp maximum as caused by the different behavior above and below the concentration where all the water is intimately tied up as water of hydration. Thus, assuming for calcium chloride that the hydration number is 8 for both the calcium ion and for the chloride ion, a concentration of 2.52*m* corresponds to complete hydration of the ions. Hence, they suggest that definite hydration numbers exist. It may well be argued, however, that heat of reaction with standard cotton cellulose is a poor probe to choose for studying the aqueous environment. The idea of fixed total hydration of the ions appears a somewhat unlikely interpretation if for no other reason than because these solutions still are able to flow—in fact, with a moderately low viscosity.

Additional evidence for the supposition that only the water immediately near an ion is significantly affected by the presence of the electrolyte comes from a study of proton relaxation times in alkali halide solutions by Fabricand and co-workers (*40*). Their data could be interpreted only if they assumed that the water away from an ion has the same proton relaxation time as pure water. Luz and Yagil (*103*) have studied the frequency shifts of the ^{17}O signals in aqueous solution of many diamagnetic electrolytes. One of their interesting conclusions is that the breaking of a hydrogen bond shifts the ^{17}O resonance 16 p.p.m. toward high field. Experimental data show that the shift is caused not by a general change in water structure but by direct interaction between the ion and neighboring water molecules. This is of interest in regard to our statement that the kinks appear to be unaffected by the presence of strong electrolytes, even in moderately high concentrations. Compare also this result with Vaslow's hydration theory.

There is little doubt that the water molecules in the immediate neighborhood of an ion find themselves in an extremely strong field, but apparently the water beyond the first layer (of primary) hydration is relatively unaffected. It is unfortunate for the arguments bearing on the thermal anomalies that Luz and Yagil's measurements were made in $10^{-2}m$ hydrochloric acid since hydrogen ions tend to disrupt the water structures responsible for the thermal anomalies. However, these authors stated that the line shifts were not affected in the solutions studied by adding the acid (but the lines apparently broadened if acid was not added owing to slow proton exchange).

Safford and Naumann (*128*) have shown that the time-of-flight spectra for $4.6M$ solutions of KF, KCl, CsCl, NaCl, and LiCl show peaks in the inelastic scattering region which coincide both in frequency and shape with the "ice-like" (structured) frequencies of pure water. Also, solutions of KSCN, KI, KBr, and $NaClO_4$ have lattice frequencies where they are found for water although in these cases apparently with less resolution and less intensity. Even an 18.5-M solution of KSCN showed a similar behavior. We take this to suggest that elements of water structure remain in these solutions (as discussed elsewhere in this paper, where we noted that the thermal anomalies occur at approximately the same temperatures, even for relatively concentrated solutions, as where they occur in pure water; *see also* Ref. *103*).

While on the one hand the examples mentioned above suggest the persistence of elements of water structure in the presence of solutes (electrolytes), other evidence points to a significant interaction between a small uncharged molecule (or atom) and water. While we postpone a more general discussion of aqueous nonelectrolytes to a later publication, we call attention to the entropy of solution data obtained by Krestov and Abrosimov (*94*). Although not stressed by these authors, it appears that these data, at least for the lower atomic weight inert gases, notably change at or near the temperatures of the kinks. The question is whether these changes were induced by the presence of the gas or reflect intrinsic changes in the structure of water (the pure solvent) at these temperatures. The recent study by Safford (*127*) is interesting. He studied the neutron spectra of aqueous solutions of xenon; we quote from his paper:

> In contrast with the spectra of pure water, the spectra of Xe plus H_2O at 25°C. and 1 atm shows the following features:
>
> (1) An increased structure in the region of the torsional peak and new lines not present in pure water appearing at 756, 584, 462, and 372 $cm.^{-1}$. The maximum $cm.^{-1}$ is within error of the torsional peak in pure water at 506 $cm.^{-1}$.
>
> (2) The OH . . . O stretching frequency observed for water is again present at 152 $cm.^{-1}$. However, an additional line is present in this region at 197 $cm.^{-1}$.
>
> (3) Lines at 64, 50, and 34 $cm.^{-1}$ are present as in the case of water, but appear with reduced intensity.
>
> All the lines observed for the spectra of pure water are present (although reduced slightly in intensity); therefore clusters similar to those found in pure water must be present in this liquid. However, another structure (or structures) must also be present and involve water molecules. Indeed, the presence of an additional line in the region of the OH—O hydrogen bond stretch and at a higher (210 $cm.^{-1}$) frequency than observed for H_2O (152 $cm.^{-1}$), suggests a decrease in the O—O distance and a corresponding increase in the hydrogen bond strength compared to water. Moreover, the relative sharpness of the additional structure in the vicinity of the original broad torsional peak, suggests a more unique coordination than in a water cluster.

It is apparent that introducing the inert gas does induce a local structural change in the water. At the same time lines are still observed in these solutions, characteristic of pure water. Recall again our claim that the temperatures of the kinks are largely unaffected by the presence of solute even in a moderately high concentration (of both electrolytes and nonelectrolytes.)

Further Problems of Hydration and the Intrinsic Weakness of the Debye-Hückel Theory

In connection with Vaslow's measurements (*150*) of the apparent molal volumes of the alkali metal chlorides in solutions, we call attention to the earlier measurements by Halasey on the temperature dependence of the partial molal volumes. These measurements suggest (*31*) that the partial molal volumes as functions of temperature change anomalously near the temperatures of transitions in water. This could not be predicted by the Debye-Hückel or other more current theories. Hence, the Debye-Hückel theory undoubtedly needs modification. It is natural to suggest that the Debye-Hückel theory fails because of unrealistic assumptions underlying its formalism—*i.e.*, it no longer seems adequate to consider the solvent as a continuum dielectric—or, if the formalism is to be preserved, one must at least recognize that for calculating thermodynamic functions, the correct values of the dielectric constant must be used and these probably show anomalies near 30° and 60° and possibly also 15°C. (*31, 32*) (*cf.* Refs. *124, 125*). In the case of the Debye-Falkenhagen theory for conductance, account must similarly be taken of anomalies in the temperature dependence of the viscosity (*31, 104, 105*). (A recent, still incompleted study in the author's laboratory has failed to show anomalies in the energy of activation for viscous flow of pure water at 30° and 45°C. although great care was taken with these measurements. Anomalies do seem to exist in the viscosity data for aqueous solutions, however. It is also worth noting that the viscosity of pure water is among the parameters which most often have been claimed to show anomalies. In view of the persistent occurrence of kinks in proton spin relaxation data and the close relation between these data and viscosity, it seems appropriate to worry about the proper value to be used for the viscosity in the Debye-Falkenhagen calculations.)

Issue is taken here, not with the mathematical treatment of the Debye-Hückel model but rather with the underlying assumptions on which it is based. Friedman (*58*) has been concerned with extending the primitive model of electrolytes, and recently Wu and Friedman (*159*) have shown that not only are there theoretical objections to the Debye-Hückel theory, but present experimental evidence also points to shortcomings in the theory. Thus, Wu and Friedman emphasize that since the dielectric constant and relative temperature coefficient of the dielectric constant differ by only 0.4 and 0.8% respectively for D_2O and H_2O, the thermodynamic results based on the Debye-Hückel theory should be similar for salt solutions in these two solvents. Experimentally, the excess entropies in D_2O are far greater than in ordinary water and indeed are approximately linearly proportional to the aquamolality of the salts. In this connection, *see also* Ref. *129.*

In connection with the hydration theory proposed by Vaslow (*149*) and the considerations by Krestov (93), attention is directed to the study by Blandamer and Symons (*13*). These authors note the importance of "peripheral" water interactions owing to the presence of both cations and anions. While anions may form "H-bonds" with the neighboring water molecules, the cation may interact strongly with the lone pair of a neighboring water molecule. Thus, as far as additional water molecules are concerned, the centrosymmetric force field of the ion may play a relatively minor role compared with the directional forces originating in the "first water" molecule-ion interaction. This may explain Krestov's "peculiar neutralization of the ion charge and a charge redistribution over the solvent particles surrounding the ions."

Salomaa and Aalto (*129*) have measured the free energies of transfer for some alkali halides from ordinary water to heavy water. They found that the dilute solution values for the different chlorides are all identical (210 ± 10 cal./gram mole at 25°C.), independent of the nature of the cation and stress the fact that this can be readily understood qualitatively in terms of the ion-water interaction. For the cations, the deuterium content plays a far less important role since the primary interaction is between that of the positive ion and the lone pairs of the adjacent oxygen atoms of the water molecules while for the anions, the interaction is *via* the negative ions and the partially unshielded protons (or deuterons) of the water molecules (*cf. 13*). These considerations obviously have an important bearing on the Debye-Hückel theory since the free energy of the hydrated ions must depend, even in the limiting case, on the water-solute interaction. (*See also* the discussion by Frank and Thompson (*51, 52*) of the "fine grainedness" of the ion cloud.) This, of course, is particularly important if the water structure consists of clusters and/or cages with as many as 100 water molecules.

Tikhomirov (*144*) has been concerned with the effects of ions on water structures and aqueous solution structures. He visualizes the effect of ions in a dual role, somewhat similar to the view envisioned here—namely, on the one hand, as a source of structural breakdown and, on the other hand, a source of structural stabilization. The structural breakdown simply manifests the incompatibility of the initial water structure with the centrosymmetrical force field of the ions while the reinforcing effect is caused by a hydrogen bond stabilization by the component of the field, in the direction of the hydrogen bond. This is essentially the same view as Hindman's (*79*). This is an important consideration because it seems reasonable that some electrolytes cause a definite breakdown of the water structure, undoubtedly owing to the primary hydration of these ions. At the same time, the fact that the thermal anomalies often appear greatly enhanced in fairly concentrated solutions of strong electrolytes tends to suggest that by some mechanism structural units are stabilized and enhanced in such solutions despite breakdown of the water near the ions. The present author would paraphrase Tikhomirov's view by stating that the effect of (at least some) ions is to stabilize water structures by enhancing hydrogen bonding within the structured units of the water owing to the enhancement of the hydrogen bond tendency between the water molecules belonging to the primary hydration shell and the neighboring water molecules in the latent structure in the water. This, then, implies a slightly different aspect of hydration from that emphasized by Frank and Wen, who advocate the general occurrence of a region of enhanced disorder separating the primary hydration shell from the "undisturbed" water structure at larger distances from the ion under consideration.

A somewhat intermediate view has also been adopted by Horne and Birkett (*80*), who also propose a multilayer model of hydration where both the firmly bonded, first hydration layer and the disordered zone of the Frank-Wen model are accepted. However, they suggest the existence of a second layer of water molecules (separating the primary hydration shell and the disordered zone) around the ion, consisting of "rarified" or extended clusters of water molecules with density less than water's but definitely not of Ice-I like structure. We return to this aspect later. In this connection, compare also our discussion of the studies by Vaslow (*150*), Griffith and Scheraga (*67*), and Luz and Yagil (*103*).

Gurikov (*71*) has been particularly concerned with improving the Debye-Hückel theory by an improved method of averaging the potential energy of the ion interaction. This is achieved by considering the more concentrated solutions as containing a quasi-crystalline lattice arrangement of the ions similar to the structure that the ions would possess in the equivalent form of the solid salt (*see also* the studies by Beck (*20*) of the x-ray scattering by concentrated solutions of LiCl, LiBr, and RbBr). He found that the ions were not randomly distributed in the solutions but that the structure of the solutions resembled that of the solid crystal lattice with the water molecule interspersed (*see also* remarks by Frank and Thompson (*51, 52*) on lattice aspects of solutions.) In other words, he attempts to make more nearly correct allowance for the short distance ordering in ionic solutions. The treatment resembles that presented by Kirkwood and Poirier (*90*), in which the ionic atmosphere attains a periodical structure with alternating positive and negative charges at high concentrations, again similar to the ion distribution in the corresponding salt. The treatment by Gurikov still depends crucially on the value one chooses for the Debye-Hückel constant, a, (the distance of closest approach between ions of opposite sign) and furthermore retains the unlikely assumption that the solvent is a structureless dielectric with a dielectric constant independent of the over-all effect of the solute on the dielectric properties of the solution.

Monomers in Water

We now return to some aspects of the different possible water structure models mentioned earlier. Whether water will be shown to possess a broken-down ice lattice structure, a cluster structure, or a cage structure, it appears inescapable that some of the molecules must occur as unbonded (free) monomers. The only model in which the problem of monomer concentration does not enter is that of Pople, which essentially treats the water molecule as a giant polymolecule with bent rather than broken hydrogen bonds. As mentioned earlier, this model has recently received some indirect support from the Raman studies by Wall and Hornig (*155*) and the infrared studies by Falk and Ford (*41*). However, apart from these latter studies [which may indeed be incorrect in view of the findings by Worley and Klotz (*158*), and by Luck (*102*)] practically all the evidence available suggests that water is indeed structured, and the structure undoubtedly has the attributes of the "mixture models." Hence, we must assume that monomers exist in equilibrium with structured units (with the possibility that more than one (distinct) structured species may exist at any one temperature).

The monomer concentration is undoubtedly low. If this were not true, it is hard to see how the vapor pressure of water could be as low as it actually is. Much thought and some experiments have been directed toward determining the monomer concentration. Before proceeding, a word of warning may be in order. In searching for properties which may reflect the concentration of monomers, one must remember that the properties of the monomeric water molecules in the liquid are undoubtedly different from the properties of the single water molecule in the gas phase. The water molecules in the liquid, even those which do not form any hydrogen bonds with their neighbors, still find themselves in strong fields owing to the presence of the other water molecules. This immediately reduces the utility of optical approaches in determining monomer concentration by comparisons between the spectra of water vapor and liquid water.

Stevenson (*141*) has tried recently to estimate the number of monomers in liquid water by three different approaches. He concludes that the concentration of monomers (non-hydrogen bonded water molecules) is less than 1% between 0° and 100°C. This estimate contrasts with recent theoretical values (*107, 112*). However, more recent studies (*67, 68, 86*) give lower monomer concentrations than the earlier estimates but still considerably higher values than Stevenson's. The only current theory of water which would imply small concentrations of monomers is Pople's. Stevenson's study may well be subject to some criticism—*i.e.*, the assumption that water in carbon tetrachloride should represent freely rotating monomeric water molecules. Stevenson's thermodynamic considerations may also be questioned.

Straight vs. *Bent H-Bonds*

Apart from Pople's model, few water theories accommodate the possibility that hydrogen bonds may not be linear or close to linear. Indeed, practically all major theories of water structure assume that highly bent hydrogen bonds were relatively unimportant.

Wicke (*156*) in particular, has emphasized that attention must be paid to types of aggregation other than those involving the normal tetrahedral hydrogen bonding. Among the nontetrahedral types of bonding he suggests are elements of (A) open chain structure, (B) planar rings, and (C) "bifurcated" structures. Possibly the least likely of these is structure C. Structures A and B, however, may represent configurations of minimum energy and may be responsible for any dimers which might be present in water. This type of bonding represents closer packing than the bulky, ordinary ice or the tetrahedrally constructed cluster or pentagonal dodecahedra of the clathrate hydrate cages.

Baur (*9*) has studied in some detail the nature of hydrogen bonding in crystalline hydrates. He finds that not only are many hydrogen bonds highly bent, but those such as the bifurcated bonds mentioned by Wicke also occur in crystalline hydrates. Furthermore, hydrogen atoms have apparently been found in positions where they do not form hydrogen bonds although in some of these cases it would have been geometrically possible to attain arrangements with more nearly linear hydrogen bonds. This point is particularly important in connection with our discussion of Vaslow's theory of ion hydration, which proposes that ion-water interaction may not always dominate and that structural arrangements may be possible, consistent with a more nearly unchanged water structure. Baur's article should be consulted for an interesting table listing known hydrogen bond angles differing significantly from 180°. The conclusion that strongly bent hydrogen bonds may occur in crystalline hydrates may well be valid, but the idea of bent hydrogen bonds must, of course, be applied with reservation when discussing the liquid rather than solid phase.

While it is too early to predict results from applying these notions of highly bent hydrogen bonds to water structure, it is important to remember that structures such as A and B of Wicke's could be involved in the hydration of ions.

In connection with the possibility that the hydrogen bonds in water need not be linear, Yamatera, Fitzpatrick, and Gordon (*160*) proposed that the weak interactions observed in their spectra may correspond to considerably bent hydrogen bonds, while strong hydrogen bonds correspond to the more nearly "ideal" hydrogen bonds. These authors also note the study by Lippincott, Weir, and van Valkenburg (*97*), who suggested the existence of highly bent O—H . . . O bonds from their study of ice under high pressure.

Finally, the structure of the high pressure ice polymorphs might provide additional important information regarding the abilities of water molecules to bond by means other than the hydrogen bond. Thus, Kamb (*87, 88*) has shown that Ice-VII possesses chains of distorted oxygen tetrahedra arranged so as to give chains mutually displaced by 90°, fitting into each other (self-clathrate structure) without being hydrogen bonded. For this structure Kamb shows that the van der Waals interaction is more than 50% higher than calculated by a "classical" London formula for neighboring (but not bonded) water molecules, owing to the overlap energy.

Spectroscopy of Water

Vast literature exists on the infrared spectra of water and aqueous solutions, and much information is now being collected from nuclear magnetic resonance (NMR) studies. It is somewhat disappointing that optical spectroscopy has not been more useful in elucidating the structure of water. Contradictory results have, in fact, been suggested on the basis of infrared studies. Thus, Buijs and Choppin (*16*) have studied the infrared spectra of water in the range 1.1–1.3μ, and they deduced that many of the hydrogen bonds are broken. On the other hand, Luck has interpreted the 0.96–1.1-μ region as indicating few broken hydrogen bonds and, hence, much larger aggregates of fully hydrogen bonded water molecules (*99*). Walrafen, basing his studies on Raman spectra, arrived at similar conclusions (*153*). In connection with spectroscopic studies, the recent study by Wall and Hornig (*155*) tends to suggest the absence of discrete structural elements, thus essentially lending support to the uniformists', average view, best represented by Pople. In connection with the frequent criticism by spectroscopists that liquid water at low temperatures can possess at the most a few percent of broken hydrogen bonds, interpreting infrared spectra involves some uncertainties.

A further difficulty in using infrared and Raman spectroscopic results is the scarcity of high precision data obtained at closely spaced temperature intervals. Only a few authors seem to consider this aspect (*61, 101*). Ganz observed a sharp change in the temperature coefficient of the displacement of the absorption maxima of water for the 0.77-μ band. (Ganz, incidentally, also called attention to the fact that Auer (*6*) had observed a similar anomaly in the magnetic susceptibility of water near 40° and 45°C.). Furthermore, Magat had noticed a sudden change in the infrared spectra of water near 40° or 45°C. (*105*). Apart from these studies, however, few measurements have been made at closely spaced temperature intervals. Recently, Walrafen (*154*) studied the Raman spectra of water in detail at closely spaced temperature intervals. Walrafen, in particular, studied the 175-cm.$^{-1}$ band, which shows a rapid decrease in intensity with increased temperature. Unfortunately, the scatter is too large to be useful for our problem. Currently, careful measurements at closely spaced temperature intervals are being made by Waggener and co-workers (*152*).

Chamberlain and co-workers (*17*) have noted that no distinct peak occurs in the infrared absorption spectrum of water below 193 cm.$^{-1}$. The Raman scattering does give rise to a peak near 60 cm.$^{-1}$ while slow neutron scattering give rise to a number of peaks, including a notable one at 56 cm.$^{-1}$. This discrepancy implies that a significant number of low frequency oscillations may exist in liquid water with little if any infrared activity.

The study by Chamberlain and co-workers is interesting in another connection. They concluded that a Debye process dominates at wavelengths below 1 mm., but at shorter wavelengths the "liquid lattice" modes become increasingly important. Near 30 cm.$^{-1}$ these modes account for half of the total absorption. The temperature dependence of the index of refraction is larger than would be expected from the Debye functions, and this is ascribed by the authors to a shift in the lattice band to lower frequencies upon heating. In this connection, compare the statement by Larsson and Dahlborg (*95*) that two (or possibly three) Debye functions seem to be needed to describe the neutron energy spectrum of water.

Luck (*101*) has noted the effects of electrolytes on the number of free OH groups in water. Based primarily on infrared spectra, he notes that adding 1 mole of salt changes the number of free OH groups by only 1–2%. On the other hand, he feels that as many as 100 water molecules may be involved in the secondary hydration phenomena per dissolved ion pair of salt. This leads to an apparent discrepancy considering the small change in the infrared and NMR spectra changes compared with the large effects of the salts on the solubility. Luck resolved this difficulty by noting that according to his model of the clusters, a change of 1% in the average cluster size corresponds to a decrease of about 75 molecules per cluster. By the same token, a lowering of 1% in the number of free OH groups corresponds to an increase in cluster size of about 100 molecules.

Other evidence for the existence in water of solid-like structures comes from NMR studies. Twari and Verma (*146*) studied the diffusive motion in water by a nuclear spin lattice relaxation technique. They conclude that solid-like vibrations exist in water at low temperature but that these decrease rapidly as the temperature increases from 0° to 40°C., at which temperature these solid-like motions appear to level off and remain constant up to 92°C. However, even at the boiling point about 50% of the mode of vibration is still solid-like.

As mentioned earlier, broken-down ice lattice structures as models of water continue to attract attention. The fact that structured, "crystalline-like" aggregates are present in water seems almost inescapable, and neutron diffraction data have recently supported such a view. Rahman and co-workers (*120*) have shown that solid state-like oscillations of the water molecules in liquid water are present and that these indicate that water consists of many firmly bonded aggregates. Their size is estimated as more than 7 unit cells in diameter corresponding roughly to 500 molecules. Earlier, Singwi and Sjolander (*139*) had suggested a quasi-crystalline model for water. Their remarkable observation, again based on neutron scattering, was a number of low lying energy levels (approximately equal to 4.5×10^{-3}, 5.9×10^{-3}, 26×10^{-3}, and 66×10^{-3} e.v.). One of these (66×10^{-3} e.v.) has been identified with a rotational level in the infrared spectrum (*105*) [*see also* the discussion of the study by Chamberlain and co-workers (*17*)]. Egelstaff has also studied the scattering of neutrons by water and other liquids (*36, 37*). His results strongly support a two-state model, and the structured units of his model (the "spinning globule") appear to be quite large—perhaps several hundred molecules. Further evidence for the simultaneous existence of different types of structured ("solid-like") aggregates in water may be obtained from Larsson and Dahlborg (*95*), who noted that the neutron-energies spectrum of water is best described by using two (or three) Debye spectra. More recently, Safford (*127*) has presented some suggestive evidence for assuming a broken-down ice-like structure for liquid water. While, in general, neutron scattering data have not been able to distinguish between an ice-like lattice, clusters or clathrate-cage-like lattices, Safford's results seem to suggest the presence of ice-like structures in the water. Thus, he notes that many of the lines of the neutron spectra of water occur at almost the same frequencies as in ice: lines are observed in liquid water at 88, 64, 56, and 40 cm.^{-1} as compared with 91–80, 58, 50, and 35 cm.^{-1} for ice at −25°C. The exact origin of the lines has not been determined; however, it certainly suggests a structural similarity between ice and water.

Clusters vs. *Discrete Sites*

Before proceeding, it is important to recall the significant feature which appears to distinguish the cluster model from the two other prominent mixture models—*i.e.*, the broken-down ice lattice and the clathrate hydrate cage structures. The latter two theories allow for the existence of discrete sites in water, owing to the cavities present either in the ice lattice or in the clathrate cages. No such discrete sites are allowed for in the cluster theories although Scheraga's most recent studies (Griffith and Scheraga, (*67*)) appear to de-emphasize the sharp distinction between clusters and cages.

Samoilov has pointed out that Cuddeback, Koeller, and Drickamer (*22*) observed that the activation volume for self-diffusion, $\Delta V\ddagger$, had a negative sign. Samoilov takes this to indicate that the diffusion is *via* already existing cavities between the equilibrium positions of the water molecules, *i.e.*, self-diffusion takes place *via* the cavities in the partially broken-down ice lattice. Of course, the fact that $\Delta V\ddagger$ is negative does not necessarily mean that the water molecules go into existing cavities but rather that the activated complex has a smaller molar volume than the sum of the volumes of the "reactants" in the diffusion processes. Furthermore, the fact that a negative $\Delta V\ddagger$ is obtained does not necessarily mean that the cavity into which the water might enter is necessarily that of an ice lattice. It could just as well be the cavity in the other highly structured model which provides for discreteness—namely the clathrate hydrate model. The idea that water should be a broken-down ice lattice has also been challenged by Koefoed (*92*) on the grounds that it would be difficult to account for the large entropy of fusion were the only change accompanying melting a partial breakdown of the ice lattice (*see also* Ref. *33*).

Some convincing evidence for discreteness in the structure of water comes from recent neutron inelastic scattering experiments by Safford (*127*). Essentially, he finds evidence from measurements on the xenon–water system that structures are formed involving hydrogen bonded molecules and xenon at pressures at which hydrated (micro) crystals are not expected to be stable. He concludes that the structure thus formed is different from and less complex than that of pure water and that the nature of these structures become more pronounced as external conditions (temperature and pressure) approach those at which one would expect the hydrated crystals to be stable. We have already mentioned some of the results of Glasel (*64*). In addition to pure water, he also studied the xenon–water system. Recall that the pure water data showed a notable break in the curves for the transverse relaxation time *vs.* reciprocal absolute temperature. Glasel's investigations suggest that xenon stabilizes the surrounding water structure as expected from the formation of local xenon clathrate hydrates.

An obvious difficulty in the cage model approach is the fact that there ought to be geometric limitations on the type of solutes which may enter the cages. Frank and Quist's theory should work well for small, nonpolar solutes, but larger solute molecules would present a difficulty. However, these authors do not imply that only specific, complete, pentagonal dodecahedra are involved in the cage formation in solution, but rather that the cage model merely suggests the existence of polyhedra of the nature of flickering clusters with the ability to provide discrete sites and that one is not necessarily limited to crystallographically space-filling types of polyhedra. Thus, larger and, in fact, "partial cages" may well have sufficient temporary stability to be counted as individual discrete structural units. The flexibility gained by assuming such structures, of course, immediately limits the probability that any type of "rigorous" theory is likely to be achieved.

Aqueous Nonelectrolyte Solutions

We have dealt primarily with the properties and structure of water and aqueous solutions of electrolytes. Recently, the properties of aqueous solutions of nonelectrolytes have attracted considerable attention, both in Russia and more recently in England. Franks and Ives (*45*) give an excellent review of the structural properties of aqueous alcohol solutions. They suggest that the relationships between the often anomalous properties of such systems may perhaps be explained in terms of a water structure which provides for discrete sites. These authors (*44*) have also studied the problem of the structural properties at the water–hexane interface. From their studies on the behavior of the interfacial tension as a function of the concentration of alcohol added, they suggested that the lower aliphatic alcohols might be involved cooperatively in stabilizing the water structure at the interface. Similar conclusions were reached by this author (*30*) by studying both the results of Franks and Ives' data and the surface tension of water–ethanol mixtures in the highly dilute (aqueous) region. Arnett and McKelvey (*5*) and also Arnett *et al.* (*4*) have reported that alcohol in low concentration causes an increase in the degree of structuredness of such solutions. In particular Arnett and co-workers point out that the behavior of electrolytes in mixed solvents depends critically on the nature of the solvent mixture. [The studies by Arnett and McKelvey on the pronounced effects on water structure of *tert*-butyl alcohol show that conclusions based on NMR studies of aqueous solutions using *tert*-butyl alcohol as an internal standard must be regarded with considerable reservation (*see* Ref. *43*).]

An interesting example of the "salting out" by nonelectrolytes in water was given by Grigorovich and Samoilov (*69*). They studied the solubility of praseodymium chloride and sulfate in water in the presence of various nonelectrolytes (methyl alcohol, ethyl alcohol, and diethyl ether.) Their results show that the decrease in solubility of praseodymium chloride is only of the order of a few percent but that this decrease is probably highly significant because praseodymium chloride is more soluble in pure methyl and ethyl alcohol than in pure water. (The possibility exists, however, that the observed decrease in solubility is not associated with a filling up of cavities but rather arises from a change in the heat of solution, as distinct from the entropy of solution). Many independent observations tend to confirm the notion that even in fairly concentrated aqueous solutions, elements of water structure are retained similar to those of pure water. Mikhailov (*110*) has suggested that his solubility experiments with water–alcohol and water–acetone mixtures indicate the filling in of cavities in water structure by molecules of the second component. He also mentions the x-ray diffraction studies by Ridchenko and Shestakovskii (*123*), who find that "water retains its original structure even in aqueous solutions containing methyl alcohol at relatively high concentrations (up to 30% by weight)." Mikhailov also determined the viscosity isotherms of aqueous mixtures. In all cases, he found sharp changes at discrete concentrations of nonelectrolyte which he alleged was the result of the filling in of cavities in the water structure by the molecules of the second component. The composition corresponding to the break in the concentration dependence depended only slightly on temperature, and in a composition–temperature plot the line separating the regions of different structure (for which he suggested the name, the heterostructural line) is almost vertical. This observation may possibly be reconciled with a water model involving structured clusters, which, over a certain temperature range, may retain the same geometry within one (or more) intervals of 15°C. Thus, the break appears distinctly in the viscosity isotherm for water–ethyl alcohol from 0° to 30° or 35°C. but appears to change drastically for higher temperatures (up to 80°C.) A notable change is observed in the solubility isotherms for acetanilide in water–acetone mixtures at 20° and 59°C. Since we are concerned here with a far greater range of temperature, this is hardly surprising.

Mikhailov draws attention to the fact that Persianova and Tarasov have studied compressibility of aqueous solutions of nonelectrolytes and found it necessary also to postulate the filling of cavities in a quasi-crystalline lattice of water. This again agrees with our claim that solutes —both electrolytes and nonelectrolytes—do not significantly influence the temperature at which the kinks are observed and that this must be explained by assuming that there exists in such solutions elements of water structure which are unaffected by the presence of the solute. It is possible (to be discussed elsewhere) that the structured units responsible for the kinks merely possess a latent existence in pure water and that it is indeed the presence of the solute which induces the stabilization and thus furthers rather than disrupts the original structuredness of the water.

Ben-Naim (*11*) has discussed the stabilization of water structure owing to the presence of dissolved nonelectrolytes. This theory is based on the idea that adding inert solutes to water may increase the hydrogen bonds associated with cluster formation. This is opposite to the effect of dilution in which the clusters would dissociate when an inert solute is introduced. The important point in Ben-Naim's treatment is that his discussion is based on the absence of substitution into existing cavities (associated with a "broken-down ice-like" structure or a clathrate hydrate structure as suggested by Pauling and treated by Frank and Quist), and he feels that in this respect his treatment bypasses a weakness implied in the models favored by the Russian school and the clathrate-cage model of Frank and Quist. The water model involved then is that of a cluster. However, as discussed here and elsewhere (*30, 56*) some polar molecules such as the alcohols may indeed enter into existing cavities in a cooperative fashion. Large solute molecules present a problem since it is difficult to envision these as being inserted into already existing but smaller cages. One solution is that each of these larger molecules (or nonpolar side chains on polymeric molecules) may build their own hydration hulls, or, in the language of the Nemethy-Scheraga model, may stabilize the water structure by hydrophobic bonding. Ben-Naim does not rule out the possibility that cavities may exist and become "filled up" with solute molecules. In his treatment cavities apparently are not essential for stabilizing the water structure owing to the presence of nonelectrolyte solutes.

We have mentioned these examples of the effects of nonelectrolytes on water structure only to indicate the important information which may be derived from studies of this type (*see also* Refs. *50* and *38*). Elsewhere, we will discuss the available evidence for discreteness in water structure based on the behavior of aqueous solutions of nonelectrolytes. When combined with the information about solutions of electrolytes (treated here) a better understanding of the structural properties of water in solutions may emerge.

Discussion and Summary

We have discussed some examples which indicate the existence of thermal anomalies at discrete temperatures in the properties of water and aqueous solutions. From these and earlier studies at least four thermal anomalies seem to occur between the melting and boiling points of water —namely, approximately near 15°, 30°, 45°, and 60°C. Current theories of water structure can be divided into two major groups—namely, the "uniformist, average" type of structure and the "mixture models." Most of the available experimental evidence points to the correctness of the mixture models. Among these the clathrate models and/or the cluster models seem to be the most probable. Most likely, the size of these cages or clusters range from, say 20 to 100 molecules at room temperature. Such structural elements may be responsible for the thermal anomalies which have been observed in the properties of water and aqueous solutions.

The importance of carefully considering anomalies when studying the behavior of solute-solvent interactions has been stressed. For aqueous solutions, many anomalous results presented in the literature suggest the existence of some type of discreteness in water structure. Discreteness is consistent with a view of water structure providing distinct "sites" such as those found in the models of water, implying a broken down ice lattice structure or clathrate hydrate cage-like structures.

Apparently elements of water structure persist, even in rather concentrated solutions (such as sea water), which remain unchanged from the structures associated with pure bulk water.

The problem of the structure of water seems difficult to approach through spectroscopic measurements. Little can be said with certainty at this time about the concentration of monomers in water. NMR and neutron scattering measurements seem promising as useful tools for elucidating the structure of water, especially in aqueous solutions. Further information is likely to be obtained from a comprehensive study of the effects of nonelectrolytes on the properties of aqueous electrolyte solutions. Thermal anomalies (the kinks) most probably represent the thermal stability limits of various types of different, structured aggregates, thus refuting the idea that the structure of water may best be represented by a "continuum" uniform, average structure (not withstanding some recent infrared studies). Finally thermal anomalies are often demonstrated more readily in the properties of aqueous solutions (and aqueous interfacial systems) than in the pure (bulk) phase. It remains to be clarified whether or not this is caused by the fact that the solute merely provides a more sensitive "probe" of the aqueous environment or whether latent structures in water are merely stabilized (or, in part, induced) by the presence of the solutes.

We have described several properties of aqueous solutions, some of which appear "anomalous." It is now appropriate to discuss briefly what bearing these observations have on the degree and nature of involvement of the water structure in ion hydration. Specifically, are the observed concentration-dependent anomalies determined by the nature of the hydrated structures or are they manifestations of structural changes, induced by the ions, in the pure solvent? The information which we have discussed also bears on the question of which model of hydration is most likely to be correct—the Frank-Wen (*48*) model or that of Samoilov (*115*). Some anomalies are amazingly abrupt. Vaslow's occur over rather narrow concentration ranges, and those observed by Zagorets, Ermakov and Grunau are even sharper. Sharp transitions could be expected if structured elements in the water were discretely involved. This is not to say that ions may necessarily occupy pre-existing voids or "sites" in structured units but rather that in the process of hydration structured elements of water are involved in some peripheral manner. If the anomalies were caused by the interaction of neighboring hydration shells (presumably primarily those of the cations) it is not as easy to envision sharp anomalies because of the expected gradual attenuation of the hydration structures with distance from the ion. Some of the concentration anomalies, on the other hand, depend on the nature of the solute. We are becoming increasingly aware of specific ion effects in electrolyte studies in any but the most dilute systems. The occurrence of anomalies in the concentration range from about 0.5–1m implies high degrees of hydration (or again discrete effects of structured elements of considerable size in the solvent). Large hydration numbers (40–50 molecules) have indeed been reported frequently in the literature and may have some physical significance. Observations by Luz and Yagil and by Safford and Nauman tend to suggest that even in rather concentrated aqueous solutions, elements of water structure remain unchanged in the presence of the electrolytes. This persistence in strong aqueous solutions is also suggested by the lack of any large effects on the temperatures of the thermal anomalies by the presence of the solute. In highly dilute solutions (less than $10^{-3}m$) the picture of hydration proposed by Frank and Wen may need only minor modifications (not withstanding the model of hydration proposed by Samoilov and the alleged confirmation of this model by Hertz (*75, 76, 77*)). Thus, while the Frank and Wen model of hydration may not be the final word about ionic hydration, it is certainly likely to contain a large element of truth.

It is reasonable to expect that the water molecules innermost in the hydration shell should be highly oriented and tightly bound, owing to the ion field. Thus arises the frequently reported primary hydration numbers. What happens in the next hydration "shell" is somewhat more debatable. It seems that the water molecules in the second shell must possess properties which result from the combined effects of the field at this place and the orientation of the water molecules in this layer owing to interactions with water molecules of the layer of primary hydration. This, then, is likely to be a sensitive property of ionic size and charge. If the size of the ion is small and/or the charge high, field effects will probably predominate; if the charge is unity and/or the ion size large, dipole-dipole interactions and hydrogen bonding between the first water molecules and those in the surrounding layers will determine the nature and extent of the second hydration layer (*cf. 13*). In the former case, it seems reasonable to expect that a point is reached where water molecules will not conform either to the radial symmetry of the electric field surrounding the ion or to the structured bulk elements of the water, and thus originates the disordered zone in the Frank-Wen model. On the other hand, it is possible that for ions for which the second hydration shell is determined primarily by the water-water interactions (rather than by the electric field owing to the ion), the elements which are stabilized are predominantly structured elements of water which may be related to those found in the pure bulk solvent. Any possible mismatch between these relatively similar, structured elements in the second hydration shell and the rest of the bulk solvent may present the vestiges of the disordered zone in the Frank-Wen model.

Finally, for aqueous nonelectrolyte solutions much of the available evidence suggests the involvement of discreteness in the water structure in determining the properties of such mixed solvents. This is consistent with a mixture model, especially a clathrate hydrate model.

Acknowledgment

The author wishes to express his gratitude to the Office of Saline Water for its continued support of his research on water.

Literature Cited

(1) Adamson, A. W., *J. Phys. Chem.* **58**, 514 (1954).
(2) Agar, J. N., Turner, J. C. R., *Proc. Roy. Soc.* **A255**, 307 (1960).
(3) Agar, J. N., "The Structure of Electrolytic Solutions," p. 200, Wiley, New York, 1959.
(4) Arnett, E. R., Bentrude, W. G., Burke, J. J., McDuggleby, P., *J. Am. Chem. Soc.* **87**, 1541 (1965).
(5) Arnett, E. M., McKelvey, D. R., *J. Am. Chem. Soc.* **87**, 1393, 53 (1965).
(6) Auer, H., *Ann. Physik* **18** (5), 593 (1933).
(7) Azzam, A. M., *Z. Elecktrochem.* **58**, 889 (1954).
(8) Azzam, A. M., *Neue Folge* **33**, 320 (1962).
(9) Baur, W. A., *Acta Cryst.* **19**, 909 (1965).
(10) Beck, J., *Phys. Z.* **40**, 474 (1939).
(11) Ben-Naim, A., *J. Phys. Chem.* **69**, 1922 (1965).
(12) Bernal, J. D., Fowler, R. H., *J. Chem. Phys.* **1**, 515 (1933).
(13) Blandamer, M. J., Symons, M. C. R., *J. Phys. Chem.* **67**, 1304 (1963).
(14) Brown, R. J. S., private communications; *Bull. Am. Phys. Soc. Ser. II* **3**, 166 (1958).
(15) Brummer, S. B., Hills, G. J., *Trans. Faraday Soc.* **57**, 1816, 1823 (1961).
(16) Buijs, D., Choppin, G. R., *J. Chem. Phys.* **39**, 2035 (1963).
(17) Chamberlain, J. E., Chantry, G. W., Gebbie, H. A., Stone, W. B., Taylor, T. B., Wylie, G., *Nature* **210**, 790 (1966).
(18) Conway, B. E., *Ann. Rev. Phys. Chem.* **17**, 481 (1966).
(19) Conway, B. E., Barradas, R. G., "Chemical Physics of Ionic Solutions," Wiley, New York, 1966.
(20) Conway, B. E., Verrall, R. E., Desnoyers, J. E., *Z. Physik. Chem. (Leipzig)* **230**, 157 (1965).
(21) Coulson, C. A., Eisenberg, D., *Proc. Roy. Soc.* **A291**, 445 (1966).

(22) Cuddeback, R. B., Koeller, R. C., Drickamer, H. G., *J. Chem. Phys.* **21**, 589 (1953).
(23) Danford, M. D., Levy, H. A., *J. Am. Chem. Soc.* **84**, 3965 (1962).
(24) Danford, M. D., Levy, H. A., Narten, A. H., *Ann. Progr. Rept., Chem. Div., Oak Ridge Natl. Lab.* p. 130 (1965).
(25) Davis, C. M., Litovitz, R. A., *J. Chem. Phys.* **42**, 2563 (1965).
(26) Dorsey, N. E., "Properties of Ordinary Water Substance," Reinhold, New York, 1940.
(27) *Ibid.*, p. 167.
(28) Drost-Hansen, W., *Naturwiss.* **43**, 512 (1956).
(29) Drost-Hansen, W., "Abstracts of Papers," 145th Meeting, ACS, Sept. 1963, p. 1I.
(30) Drost-Hansen, W., *Ind. Eng. Chem.* **57**, 18 (1965).
(31) Drost-Hansen, W., *Intern. Symp. Water Desalination, 1st, Washington, D.C., 1965,* in press.
(32) Drost-Hansen, W., *Ann. N.Y. Acad. Sci.* **125**, 471 (1965).
(33) Drost-Hansen, W., *J. Colloid Interface Sci.*, in press.
(34) Drost-Hansen, W., Lavergne, M., *Naturwiss.* **43**, 511 (1956).
(35) Drost-Hansen, W., Neill, H. W., *Phys. Rev.* **100**, 1800 (1955).
(36) Egelstaff, P. A., *Advan. Phys.* **11**, 203 (1962).
(37) Egelstaff, P. A., *Intern. At. Energy Comm., Symp. Inelastic Scattering Neutrons Solids Liquids,* 1962.
(38) Eley, D. G., *Trans. Faraday Soc.* **35**, 1281 (1939).
(39) Eucken, A., *Nach. Ges. Wiss. Gottingen,* **1947**, 33.
(40) Fabricand, B. P., Goldberg, S. S., Leifer, R., Ungar, S. G., *Mol. Phys.* **7**, 425 (1964).
(41) Falk, M., Ford, T. A., *Can. J. Chem.* **44**, 1699 (1966).
(42) Falk, M., Kell, G. S., *Science* **154**, 1013 (1966).
(43) Franconi, C., Conti, F., "Nuclear Magnetic Resonance in Chemistry," B. Pesce, ed., p. 349, Academic Press, New York, 1965.
(44) Frank, H. S., *Proc. Roy. Soc.* **A247**, 481 (1958).
(45) Frank, H. S., *Natl. Acad. Sci.-Natl. Res. Council Publ.* **42**, 141 (1963).
(46) Frank, H. S., *Federation Proc. Suppl. 15* **24** (2), S-1 (1965).
(47) Frank, H. S., *Intern. Symp. Water Desalination, 1st, Washington, D.C., 1965,* in press.
(48) Frank, H. S., *Z. Phys. Chem.* **228**, 364 (1965).
(49) Frank, H. S., "Chemical Physics of Ionic Solutions," p. 578, Wiley, New York, 1966.
(50) Frank, H. S., Evans, M. W., *J. Chem. Phys.* **13**, 507 (1945).
(51) Frank, H. S., Thompson, P. T., "The Structure of Electrolytic Solutions," p. 118, Wiley, New York, 1959.
(52) Frank, H. S., Thompson, P. T., *J. Chem. Phys.* **31**, 1086 (1959).
(53) Frank, H. S., Quist, A. S., *J. Chem. Phys.* **34**, 604 (1961).
(54) Frank, H. S., Wen, W. Y., *Discussions Faraday Soc.* **24**, 133 (1957).
(55) Franks, F., Ives, D. J. G., *J. Chem. Soc.* **1960**, 741.
(56) Franks, F., Ives, D. J. G., *Quart. Rev.* **20**, 1 (1966).
(57) Frenkel, J., "Kinetic Theory of Liquids," Dover, New York, 1955.
(58) Friedman, H. L., "Ionic Solution Theory," Interscience, New York, 1962.
(59) Frontas'ev, V. P., *Dokl. Akad. Nauk SSSR* **111**, 1014 (1956).
(60) Frontas'ev, V. P., Shraiber, L. S., *J. Struct. Chem. USSR, Eng. Transl.* **6**, 493 (1965).
(61) Ganz, E., *Ann. D. Phys. K.* **26**, 331 (1936).
(62) Garnsey, R., Prue, J. E., *Trans. Faraday Soc.* **62**, 1265 (1966).
(63) Gibbson, R. E., Loeffler, O. H., *J. Am. Chem. Soc.* **63**, 898 (1941).
(64) Glasel, J. A., *Proc. Natl. Acad. Sci.* **55**, 479 (1966).
(65) Good, W., *Electrochim. Acta* **9**, 203 (1964).

(66) *Ibid.*, **10**, 1 (1965).
(67) Griffith, J. H., Scheraga, H. A., personal communication, 1966.
(68) Griffith, J. H., Scheraga, H. A., "Abstracts of Papers," 150th Meeting, ACS, Sept. 1965, p. 18I.
(69) Grigorovich, A. I., Samoilov, O. Ya, *J. Struc. Chem. USSR Eng. Transl.* **3**, 446 (1962).
(70) Grojtheim, K., Krogh-Moe, J., *Acta Chem. Scand.* **8**, 1193 (1954).
(71) Gurikov, Yu. V., *J. Struct. Chem. USSR Eng. Transl.* **3**, 385 (1962).
(72) Hall, L., *Phys. Rev.* **73**, 775 (1948).
(73) Hamer, W. J., ed., "The Structure of Electrolytic Solutions," Wiley, New York, 1959.
(74) Hausser, R., Ph.D. Thesis, Technische Hochschule, Stuttgart, 1964.
(75) Hertz, H. G., "Nuclear Magnetic Resonance in Chemistry," B. Pesce, ed., p. 199, Academic Press, New York, 1965.
(76) Hertz, H. G., *Ber. Bunsenges. Physik. Chem.* **67**, 311 (1963).
(77) Hertz, H. G., Zeidler, M. D., *Ber. Bunsenges. Physik. Chem.* **67**, 774 (1963).
(78) Hills, G. J., "Chemical Physics of Ionic Solutions," Conway, Barradas, eds., p. 521, Wiley, New York, 1966.
(79) Hindman, J. C., *J. Chem. Phys.* **36**, 4, 1000 (1962).
(80) Horne, R. A., Birkett, J. D., *A. D. Little, Inc., Tech. Rept.* **18** ONR Contract No. Nonr-4424(00) (Jan. 1, 1966).
(81) *Ibid., Rept. No.* **24** (Sept. 30, 1966).
(82) Ives, J. J. G., Mardsen, P. D., *J. Chem. Soc.* **1965**, 649.
(83) Huttig, G. F., Keller, M., *Z. Electrochem.* **31**, 390 (1925).
(84) Jeffrey, G. A., "Abstracts of Papers," 144th Meeting, ACS, March-April, 1963, pp. 32P, 17R.
(85) Jessup, R. S., *J. Res. Natl. Bur. Std.* **5**, 985 (1930).
(86) Jhon, M. S., Grosh, J., Ree, T., Eyring, H., *J. Chem. Phys.* **44**, 1465 (1966).
(87) Kamb, Barclay, *J. Chem. Phys.* **43**, 3917 (1965).
(88) Kamb, B., Davis, B. L., *Proc. Natl. Acad. Sci. U.S.* **52**, 1433 (1964).
(89) Kavanau, J. L., "Water and Solute-Water Interactions," Holden-Day, San Francisco, 1964.
(90) Kirkwood, J. G., Poirier, J., *J. Phys. Chem.* **58**, 591 (1954).
(91) Klots, C. E., Benson, B. B., *J. Phys. Chem.* **67**, 933 (1963).
(92) Koefoed, J., *Discussions Faraday Soc.* **24**, 216 (1957).
(93) Krestov, G. A., *J. Struct. Chem. USSR Eng. Transl.* **3**, 137 (1962).
(94) Krestov, G. A., Abrosimov, V. K., *J. Struct. Chem. USSR Eng. Transl.* **5**, 471 (1964).
(95) Larsson, K. E., Dahlborg, U., *J. Nucl. Energy: Pt. B* **16**, 81 (1962).
(96) Lennard-Jones, J., Pople, J. A., *Proc. Roy. Soc.* **A205**, 155 (1951).
(97) Lippincott, E. R., Weir, C. E., van Valkenburg, A., *J. Chem Phys.* **32**, 612 (1960).
(98) Litvimenko, I. V., *J. Struct. Chem. USSR Eng. Transl.* **4**, 768 (1963).
(99) Luck, W., *Ber. Bunsenges. Ges.* **67**, 186 (1963).
(100) Luck, W., *Fortschr. Chem. Forsch.* **1964**, 4.
(101) Luck, W., *Ber. Bunsenges. Ges. Phys. Chem.* **69**, 626 (1965).
(102) Luck, W., personal communication, 1966.
(103) Luz, Z., Yagil, G., *J. Phys. Chem.* **70**, 554 (1966).
(104) Magat, M., *J. Phys.* **6**, 179 (1935).
(105) Magat, M., *Discussions Faraday Soc.* **33**, 114 (1937).
(106) Mak, T. C. W., *J. Chem. Phys.* **43**, 2799 (1965).
(107) Marchi, R. P., Eyring, H., *J. Phys. Chem.* **68**, 221 (1964).
(108) Massey, V., Curti, B., Ganther, H., *J. Biol. Chem.* **241**, 2347 (1966).
(109) Melpar, Inc., Final Rept. to U.S. Dept. Interior, Office of Saline Water, Contract No. 14-01-0001-387 (1966).

(110) Mikhailov, V. A., *J. Struct. Chem. USSR Eng. Transl.* **2,** 625 (1961).

(111) Mishenko, K. P., Dymarchuk, N. P., *J. Phys. Chem. (USSR)* **3,** 399 (1962).

(112) Nemethy, G., Scheraga, G. H., *J. Chem. Phys.* **36,** 3382 (1962).

(113) Nomoto, O., *J. Phys. Soc. (Japan)* **11,** 827 (1956).

(114) Nývlt, J. H., Erdös, E. H., *Coll. Czech. Chem. Comm.* **26,** 485 (1961).

(115) Owe Berg, T. G., *Acta Sci. Hung.* **8,** 439 (1956).

(116) Pauling, L., "Hydrogen Bonding," p. 1, Pergamon Press, London, 1959.

(117) Peña, M. Diaz, McGlashen, M. L., *Trans. Faraday Soc.* **55,** 2018 (1959).

(118) Pople, J. A., *Proc. Roy. Soc.* **A205,** 163 (1951).

(119) Queen, A., Robertson, R. E., *J. Am. Chem. Soc.* **88,** 1363 (1966).

(120) Rahman, A., Singwi, K. S., Sjolander, A., *Phys. Rev.* **126,** 986 (1962).

(121) Ramiah, M. V., Goring, D. A. I., *Proc. Cellulose Conf. 5th,* 27 (1965).

(122) Randall, C. R., *J. Res. Natl. Bur. Std.* **8,** 79 (1932).

(123) Ridchendo, I. V., Shestakovskii, F. K., *Russ. J. Phys. Chem.* **29,** 1457 (1955).

(124) Rusche, E. W., private communication, 1966.

(125) Rusche, E. W., Good, W. B., *J. Chem. Phys.* **45,** 4667 (1966).

(126) Rutgers, A. J., Hendrikx, Y., *Trans. Faraday Soc.* **58,** 2184 (1962).

(127) Safford, G. J., paper presented at the Cryobiology Society Meeting, Madison, Wisc., 1965.

(128) Safford, G. J., Naumann, A. W., *O.S.W. Progr. Rept.* (Jan.-March 1966).

(129) Salonaa, P., Aalto, V., *Acta Chem. Scand.* **20,** 2035 (1966).

(130) Samoilov, O. Ya., "Structure of Aqueous Electrolyte Solutions and the Hydration of Ions," transl. by D. J. G. Ives, Consultants Bureau, New York, 1965.

(131) Satyanarayanamurty, M., Krishnamurty, Bh., *J. Pure Appl. Phys. (India)* **1,** 234 (1963).

(132) Scatchard, G., Prentiss, S. S., *J. Am. Chem. Soc.* **54,** 2696 (1932).

(133) Scheurer, P. G., Brownell, R. M., LuValle, J. E., *J. Phys. Chem.* **62,** 809 (1958).

(134) Scott, A. F., Blair, C. M., *J. Phys. Chem.* **37,** 481 (1933).

(135) Scott, A. F., Obenhaus, V. M., Wilson, R. W., *J. Phys. Chem.* **38,** 931 (1934).

(136) Shamsul Huq, A. K. M., Lodhi, S. A. K., *J. Phys. Chem.* **70,** 1354 (1966).

(137) Simpson, J. H., Jr., Ph.D. Thesis, Rutgers University, 1957.

(138) Simpson, J. H., Carr, H. Y., *Phys. Rev.* **111,** 1201 (1958).

(139) Singwi, K. S., Sjolander, A., *Phys. Rev.* **119,** 863 (1960).

(140) Steinert, C., Haase, R., *Z. Physik Chem.* **21,** 270 (1959).

(141) Stevenson, D. P., *Chemistry* **69,** 2145 (1965).

(142) Stewart, G. W., *Phys. Rev.* **37,** 9 (1931).

(143) Thorhaug, A. L., Drost-Hansen, W., Abstract, Intern. Biophysics. Conf., Vienna, 1966.

(144) Tikhomirov, V. I., *J. Struct. Chem. USSR Eng. Transl.* **4,** 479 (1963).

(145) Trapeznikov, A. A., *Intern. Congr. Surface Activity, 2nd,* 109, 121 (1957).

(146) Twari, D. P., Verma, G. S., *Nuovo Cimento* **34,** 6686 (1964).

(147) Vand, V., Senior, W. A., *J. Chem. Phys.* **43,** 1869 (1965).

(148) *Ibid.,* pp. 1873-78.

(149) Vaslow, F., *J. Phys. Chem.* **67,** 2773 (1963).

(150) *Ibid.,* **70,** 2286 (1966).

(151) Wada, G., *Bull. Chem. Soc. (Japan)* **34,** 955 (1961).

(152) Waggener, W. C., Weinberg, A. J., Stoughton, R. W., *Ann. Progr. Rept., Chem. Div., Oak Ridge Natl. Lab.* p. 76 (1965).

(153) Walrafen, G. E., *J. Chem. Phys.* **40**, 3249 (1964).
(154) *Ibid.,* **44**, 1546 (1966).
(155) Wall, T. F., Hornig, D. F., *J. Chem. Phys.* **43**, 2079 (1965).
(156) Wicke, E., *Angew. Chem., Intern. Ed.* **5**, 106 (1966).
(157) Woessner, D. E., *J. Chem. Phys.* **40**, 2341 (1964).
(158) Worley, J. D., Klotz, J. M., *J. Chem. Phys.* **45**, 2868 (1966).
(159) Wu, Y-C., Friedman, H. L., *J. Phys. Chem.* **70**, 166 (1966).
(160) Yamatera, H., Fitzpatrick, B., Gordon, G., *J. Mol. Spectroscopy* **14**, 268 (1964).
(161) Young, T. F., paper presented at Southwest Regional ACS Meeting (Nov.-Dec. 1966).
(162) Zagorets, P. A., Ermakov, V. I., Grunau, A. P., *J. Phys. Chem.* **39**, 4 (1965).

RECEIVED September 14, 1966.

6

Aqueous Surface Chemistry of Oxides and Complex Oxide Minerals

Isoelectric Point and Zero Point of Charge

GEORGE A. PARKS

Stanford University, Stanford, Calif.

The isoelectric point (IEP(s)) and the zero point of charge (ZPC) are convenient references for predicting the charge-dependent behavior of oxide minerals and their suspensions. The ZPC is the pH at which the solid surface charge from all sources is zero. The IEP(s) is a ZPC arising from interaction of H^+, OH^-, the solid, and water alone. The IEP(s) of a simple oxide is related to the appropriate cationic charge and radius. The ZPC of a complex oxide is approximately the weighted average of the IEP(s)'s of its components. Predictable shifts in ZPC occur in response to specific adsorption and to changes in cation coordination, crystallinity, hydration state, cleavage habit, surface composition, and structural charge or ion exchange capacity.

The solids encountered in water suspension, whether natural or man-made colloids, sand grains or silt, are electrically charged. The charge is instrumental in determining much of their behavior—*e.g.*, the state of dispersion (*86, 87*) and the rheology (*52, 86*) of suspensions, the extent to which the solids function as adsorbents or ion exchangers, (*6, 13, 86*) and the species adsorbed. Through adsorption, the charged suspensoids can modify the composition of the aqueous phase, perhaps controlling the pH and concentrations of trace elements (*51*). Knowing the sign of the charge alone allows many useful predictions, of which only a few examples will be given. With influence of this scope, there is good reason to explore the origin of the charge. (van Olphen (*86*) mentions many properties of suspensions attributable to solid surface charge. His book has a good bibliography for those who wish more extensive treatment.)

This paper summarizes the factors controlling the sign and magnitude of surface charge on oxides and minerals in a way which permits one to predict at least the sign. To achieve working hypotheses, it has been necessary to generalize from the behavior of a few well-characterized systems and to extrapolate well beyond the limits of scientific propriety. It is hoped that the utility of the result will justify the transgression.

Oxides, especially the hydrous oxides and coprecipitated hydrous oxides and many natural minerals, especially the clay minerals, exhibit ion exchange properties (*6, 38, 94*). The ion exchange capacity of the simpler oxides arises from the existence of a pH-dependent surface charge (*6, 94*). The oxides are cation exchangers in a basic environment when the surface charge is negative. In an acid environment the surface charge is positive, and they are anion exchangers. When the surface is uncharged, they have a small capacity for both cation and anion exchange (*94*).

While surface charge is by no means the only factor responsible for electrolyte adsorption (*94*), particularly organic electrolytes (*9, 27*), the extent of adsorption of the less specifically adsorbed species, such as the simple aquo ions and, for example, primary amines and alkyl sulfonates, decreases rapidly when the sign of the oxide's surface charge is changed to that of the sorbing species (*6, 10*).

The existence of surface charge prevents coagulation in a low ionic strength suspension or sol of one solid component and thereby slows sedimentation (*86, 87*). The rate of coagulation and sedimentation can be increased by adjusting chemical conditions so that the surface charge is zero. Many examples can be found in the extensive literature of colloid and soil chemistry.

The behavior of MnO_2 can illustrate the types of predictions possible on the basis of surface charge. The illustration is not documented. MnO_2 may appear in water suspension as a result of oxidation or precipitation reactions. By analogy with some of the other oxides, particularly Fe(III) and Al(III) hydroxides (*66*), we expect that particles formed by precipitation are electrically charged, and that the charge depends on pH. The surface charge of the manganese oxides themselves is invariably negative at pH values greater than 7.6 (*36, 41, 72*). In the oceans the pH is greater than 8 (*60*), and MnO_2 will probably serve as a cation adsorbent because the surface charge is negative. In fresh waters where the natural pH may be more acid than 7, the cation-adsorption capacity of precipitated MnO_2 will be smaller, perhaps nil. Thus, although colloidal MnO_2 is probably important in determining the concentrations of trace metals in sea water (*51*), its importance in this role in fresh waters is probably reduced.

Of the many polymorphs of MnO_2, some are formed only in the presence of certain cations (*89*). Presumably, these cations are adsorbed and incorporated into the structure during precipitation. If this is true, we might expect to find different polymorphs of MnO_2 precipitated in marine and fresh water environments owing to the difference in surface charge and hence the species adsorbed and their adsorption density. Hsu (*44, 45, 46*) has reported that a similar process operates to control the species formed by hydrolysis of Al(III).

Charge can originate by processes involving components of the solid or by processes in which the solid serves primarily as a host to unrelated species adsorbed from the electrolyte. Adsorption itself can arise from electrostatic attraction alone, in which case it is relatively nonspecific or nonselective (*11, 13, 14*), or it can arise from electrostatic attraction augmented by hydrogen bonding, coordinate bonding (*17*), or London-van der Waals bonding (*9, 27*). If the contribution of any type of nonionic bonding is finite, adsorption can occur even when the surface is uncharged. Adsorption under the combined influence of ionic and nonionic bonding is called "specific adsorption."

To consolidate our discussion of the origin of surface charge, it is useful to define the zero point of charge (ZPC) or isoelectric point of the solid [IEP(s)], referring to the conditions in the aqueous phase in equilibrium with the uncharged surface. ZPC will be used here to designate the pH in any system, however complex, at which there is no net charge on the solid particles of interest. If charge is established only by H^+, OH^-, and species capable of interacting with H^+, OH^-, or H_2O to form species present in the solid lattice [*i.e.*, by potential-determining ions (PDI)], then the ZPC may be conveniently given the special name IEP(s).

Because so much of the behavior of suspensions is determined or modified by charge associated with the solid phases, ZPC may be inferred from a wide variety of experiments involving pH as a master variable. For example, coagulation and sedimentation rates are maximum at the ZPC, and anion and cation exchange capacities (measured with nonspecific, symmetrical electrolytes) are equal and minimum at the ZPC. More direct and less ambiguous are electrophoresis and streaming potential, in any of their modifications. One can estimate the IEP(s) by measuring adsorption of H^+ and OH^- if one is certain that no specific adsorption of other species occurs.

This paper will be confined largely to developing models which allow correlation of measured IEP(s)'s and ZPC's with solid composition and interpolating or extrapolating to predict values for new species. By knowing the ZPC and identifying the ions most effective in producing or modifying charge, one can, in turn, predict behavior. In developing models for charging mechanisms, we will explore many of the factors which determine the surface chemistry of the solids found in natural systems.

Simple Oxides and Hydroxides: Charging Mechanisms and IEP(s)

Interaction of Oxides with Water. Silica is one of the allegedly simpler oxides. Its surface as prepared by fracture in vacuum can be visualized as in Figure 1a. The surface contains ions which are not fully coordinated and hence are electrically charged. The net charge on a fragment from this source, however, is probably negligible. On exposure to water vapor, ionic or charged sites at the surface are converted to surface hydroxide or MOH groups (8). This process—a dissociative chemisorption—is illustrated schematically in Figure 1b.

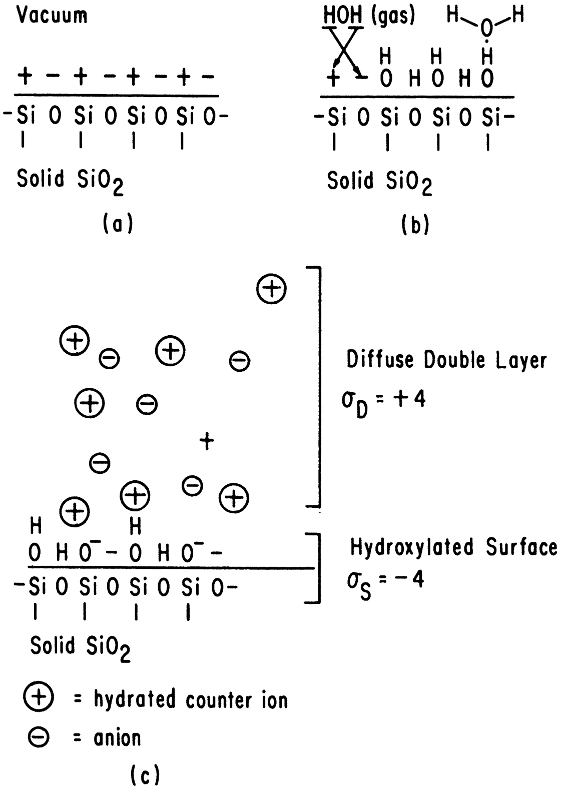

Figure 1. Schematic illustration of a silica surface in a perfect vacuum (a), in water vapor at low pressure (b), and in an electrolyte (c)

Further adsorption of water vapor results first in patches, then in coherent layers of hydrogen-bonded water (*8*). This water is probably more highly dissociated than bulk water (*30, 33*). The MOH groups function as Brönsted or protonic acids (*76*). The protons or hydronium ions donated by MOH or H_2O dissociation are mobile (*7, 33*). As the thickness of the adsorbed water increases, its properties approach those of the bulk liquid (*8, 49, 54, 95*), and eventually the solid may be considered immersed. In this state, hydrogen ions which were mobile on the gas-solid interface are free to diffuse into the bulk aqueous phase. They do so under the influence of their kinetic (kT) energy until the counter potential set up by their departure results in a diffuse, Boltzmann distribution. A negative surface and diffuse layer of positive ions are illustrated in Figure 1c. The two regions of charge collectively are called the "electrical double layer" (*86*). Mathematical description of the distribution of ions between the fixed and diffuse parts of the double layer, within the diffuse layer and between the diffuse layer and the bulk electrolyte, are well-developed and amply reported in the literature (*13, 14, 52, 86*).

When the solid is immersed directly in water, all these steps occur simultaneously. If the surface area is high, the development of the electrical double layer may lead to large changes in solution composition and pH.

Charging Hydroxylated Surfaces: Definition of IEP(s). A hydroxylated surface should be expected on all oxidic materials which have had a chance to come to equilibrium with an aqueous environment. Charge can develop on a hydroxylated surface through amphoteric dissociation of the surface hydroxide groups. Dissociation reactions can be written as follows, where underscored symbols refer to species forming part of the surface. Symbols not underscored refer to species assumed aqueous unless otherwise specified.

$$\underline{M}OH \rightleftharpoons \underline{M}O^- + H^+(aq) \tag{1}$$

$$\underline{M}OH \rightleftharpoons \underline{M}^+ + OH^-(aq) \tag{2}$$

$$\underline{M}^+ + H_2O \rightleftharpoons \underline{M}OH_2^+ \tag{3}$$

Acid dissociation (or negative adsorption of H^+) produces negative surface sites. Basic dissociation (as in Reaction 2, equivalent to positive adsorption of H^+) produces positive surface sites, which because the probability of existence of a bare $\underline{M}^+$ is small, probably occur through a combination of Reactions 2 and 3 as

$$\underline{M}OH + H^+ \rightleftharpoons \underline{M}OH_2^+ \tag{4}$$

The chief competitor of this mechanism is the adsorption of charged hydroxo complexes derived from the solid. This might occur through a sequence of reactions such as 5 and 6.

$$M_2O_3 + 3H_2O \rightleftharpoons 2M(OH)_3(aq) \qquad (5)$$

$$M(OH)_3(aq) \rightleftharpoons M(OH)_n^{3-n}(aq) + (3-n)OH^-(aq) \qquad (6)$$

and subsequent adsorption of the hydroxo complexes,

$$M(OH)_n^{3-n}(aq) \rightleftharpoons \underline{M}(OH)_n^{3-n} \qquad (7)$$

Each adsorbed positive complex ion represents a site of positive surface charge. The adsorption density must be a function of the concentration of the species which in turn depends on pH.

In both mechanisms the ions which establish surface charge are also those which would establish the potential of a reversible oxide or hydroxide electrode and hence may be called potential-determining ions (PDI). Obviously the concentrations of the PDI and the net surface charge are pH dependent, and there will be one pH at which the density of positive sites is equal to the density of negative sites—*i.e.*, at which the net surface charge is zero. This pH may be called the isoelectric point of the solid and given the acronym IEP(s) to avoid confusion with the isoelectric point of aqueous hydroxo-complex series, which will be designated IEP(aq). Recapitulating in terms of σ, the surface charge, and Γ, a net adsorption density, the IEP(s) is the pH at which either

$$\sigma = e\Gamma_H = 0 \text{ (if the PDI are } H^+, OH^-, \text{ and } e, \text{ the electronic charge)}$$

or

$$\sigma = \sum_n (n - z)e\Gamma_n = 0 \text{ (if the PDI are } M^{z+}(OH)_n^{n-z})$$

The IEP(s) has the same value as the ZPC only in the absence of adsorbed species different from the PDI. Obviously σ is negative if the pH is greater than the IEP(s) and positive if the pH is lower than the IEP(s).

It has been suggested (*61*) that the hydroxo-complex ions exclusively are the PDI when they are present and that highly charged, polynuclear hydroxo complexes play the major potential- or charge-determining role. Empirically, the IEP(aq), where:

$$\sum (Z - n)[M^{+z}(OH)_n^{z-n}] = 0$$

(brackets denote concentrations)

and the IEP(s) of the corresponding hydroxide or hydrous oxide are often the same (*72*), implying that the adsorption tendencies of the various complexes are comparable. Furthermore, the concentrations of the hydroxo complexes are usually higher than (H^+) or (OH^-). Recognizing these facts, it has been suggested that in many systems the more concentrated among H^+, OH^-, and all hydroxo-complex ions present are the predominant PDI (*72*). Inasmuch as the hydroxo-complex ion concentrations depend on pH, it is difficult to distinguish the relative importance of H^+ as the species directly concerned.

The situation is further complicated by frequent observation of IEP(s)'s which do not approximate the appropriate IEP(aq). The variability of the IEP(s) probably arises partly from the presence of multivalent, polynuclear hydroxo complexes. The compositions and concentrations of these species depend strongly on the over-all composition and history of the solution (*42, 44*). If the influence of such complexes is inordinate, the difficulty of obtaining equilibrium among them will be manifested in apparent variability of the IEP(s).

Predicting IEP(s). To correlate and predict IEP(s) on the basis of solid composition, a useful simplification can be made by taking advantage of the close analogy between dissociation reactions of surface hydroxide groups and of mononuclear hydroxyl complexes. For example,

$$M^{z+}(OH)_Z(aq) \rightleftharpoons M(OH)^+_{Z-1}(aq) + OH^-(aq) \qquad (8)$$

$$\underline{M}OH + H_2O \rightleftharpoons \underline{M}OH_2^+ + OH^-(aq) \qquad (9)$$

In both cases the same naïve electrostatic model can be used to derive a relationship between the properties of the cation, M, and the IEP(s). The model assumes that equilibrium between positive and negative surface sites is established through Reaction 10.

$$\underline{M}O^- + 2H^+(aq) \rightleftharpoons \underline{M}OH_2^+ \qquad (10)$$

If hydroxo complexes rather than H^+ are the PDI, the equilibrium reactions are:

$$\begin{aligned} &M^{z+}(OH)^-_{Z+1}(aq) + 2H^+(aq) \rightleftharpoons M^{z+}(OH)^+_{Z-1} + 2H_2O \\ &M^{z+}(OH)^-_{Z+1}(aq) \rightleftharpoons \underline{M}^{z+}(OH)^-_{Z+1} \qquad (11) \\ &M^{z+}(OH)^+_{Z-1}(aq) \rightleftharpoons \underline{M}^{z+}(OH)^+_{Z-1} \end{aligned}$$

In this case, further assumptions are necessary—namely, that no hydroxo complexes other than the two monovalent species play a significant potential-determining role and that the equilibrium constants for the two adsorption reactions are identical. The following relationship among the IEP(s) of an oxide or hydroxide, the charge or oxidation state of the cation and its radius, was derived on this basis in an earlier paper (*72*), which is also the source for much of the material in the following paragraphs;

$$\text{IEP(s)} = A - B[(Z/R) + 0.0029C + a] \qquad (12)$$

where

Z = cationic charge

$R = r_+ + 2r_o$

r_+ = cationic radius in Angstroms

r_o = oxygen ion radius

A, B = constants for all materials

C = correction for crystal field stabilization of M—OH bond

a = combined corrections for coordination number and state of hydration.

The structures of the oxides and hydroxides are arranged so that the number of oxygen ions adjacent to each metal ion—the coordination number (ν)—varies from 2 to 8 (*89, 90, 91*). In Equation 12 the empirical constant a for each ν is related to the coulombic attractive energy between the group of oxygen ions and the proton of the $\underline{\text{M}}$OH group.

Li 1,0.82,4	Be 2,0.63,4						
Na 1,1.12,4	Mg 2,0.93,6						
K 1,1.51,4	Ca 2,1.18,6 2, —,8	Sc 3,1.09,6	Ti 2, —,– 3,1.03,6 4,1.06,6	V 2, —,6 3,1.03,6 4,1.02,6 5,1.07,–	Cr 2, —,– 3,0.94,6 4, —,6	Mn 2,0.95,6 3,0.98,6 4,1.03,6	Fe 2,0.90,6 3,0.92,6
Rb 1,1.67,4	Sr 2,1.34,6	Y 3,1.13,6	Zr 4,1.08,7	Nb 4,1.02,6 5,1.04,6	Mo 4,1.00,6 6,1.03,6	Tc ——— ———	Ru 4,1.01,6
Cs 1,1.91,–	Ba 2,1.52,6	La 3,1.30,6	Hf –, —,8	Ta 5,0.99,6	W 4,0.97,6 6,0.97,6	Re ——— ———	Os 4, —,6
Fr	Ra	Ac					
		Ce 3, —,6 4,1.24,8	Pr	Nd	Pm	Sm	Eu
		Th 4,1.22,8	Pa	U 4,1.15,8	Np	Pu –, —,8	Am

Figure 2. Ionic radii and coordination numbers in oxides. Numerals

The second term, the product $B\left(\frac{Z}{R}\right)$, is a measure of the repulsive energy between the cation of radius, r_+, and charge Z, and the proton of the $\underline{M}OH$ group from which it is separated by the diameter of the oxygen $\overline{\text{ion}}$. A collection of cation radii (*37*) and corresponding coordination numbers as observed in oxides are summarized in Figure 2.

The M—OH bond for transition metal ions is stabilized by the influence of the electrical field associated with the oxygen ions coordinating M^{+z} on the electronic structure of the cation. The term *C*, is a measure of this crystal field stabilization energy, and the product 0.0029*C* corrects for this effect. Appropriate values of *C* are listed in Table I.

For arithmetic calculations and graphical correlation, it is useful to define the term:

$$\left(\frac{Z}{R}\right)_{\text{eff}} = \left[\frac{Z}{R} + 0.0029C + a\right]$$

$$\text{IEP(s)} = 18.6 - 11.5\left(\frac{Z}{R}\right)_{\text{eff}} \qquad (13)$$

Values of *a* for coordination numbers 4 and 6 and a tentative value for coordination number 8 are tabulated in Table II.

Some oxides, such as silica (*68*) and corundum (*67*) do not absorb water beyond hydroxylation of the surface. These oxides will be called

				B 3,0.64,4	C ———	N ———	O 2,1.40,–
				Al 3,0.85,6	Si 4,0.80,4	P ———	S ———
Co 2,0.90,6 3, — ,–	Ni 2,0.91,6	Cu 1,1.05,2 2,0.97,4	Zn 2, — ,4 2,1.05,6	Ga 3,0.91,6	Ge 4,0.88,6 4, — ,4	As 3,0.83,4 5,0.90,–	Se 4,1.14,4
Rh 3,0.99,6	Pd 2,1.04,4	Ag 1,1.35,2 2, — ,4	Cd 2,1.15,6	In 3,1.09,6	Sn 2,1.18,6 4,1.01,6	Sb 3,0.98,6 4, — ,– 5,1.06,–	Te 4,1.46,6
Ir ———	Pt 1,1.25,– 2,1.01,4	Au ———	Hg 2,1.30,4	Tl 3,1.26,6	Pb 2,1.38,4 4,1.16,6	Bi 3,1.14,6	Po ———
Gd	Tb	Dy	Ho	Er	Tm	Yb	Lu
Cm	Bk	Cf	E	Fm	Md	No	Lw

in sequence are oxidation state, radius in A. units, and coordination number "anhydrous" even when immersed. Hydroxides, hydrous oxides, and related species are grouped together and called "hydrous." There is a difference of about two pH units between the isoelectric points of an oxide in the hydrous and anhydrous states. Progressive dehydration from the hydrous state to the anhydrous state results in a continuous spectrum of isoelectric points between the two extremes (93). The variation of isoelectric point with hydration is also absorbed in the constant *a*.

The linear relationship between the IEP(s) and the quantity $\left(\frac{Z}{R}\right)_{\text{eff}}$, Equation 13, makes possible a convenient graphical test of the validity of the correlation. By plotting the IEP(s) as a function of $\left(\frac{Z}{R}\right)_{\text{eff}}$, a single straight line should be obtained. This correlation is shown in Figure 3. The predicted IEP(s) is a basic limit falling within one-half pH unit of the maximum observed value for most materials with coordination numbers 4 or 6. Correlation for coordination number 8 and several MO_2

Table I. Crystal Field Stabilization Energy[a] for Use with Equations 12 and 13

Metal	*Oxidation State* (II)	(III)
Mn	0	42
Fe	18	0
Co	33	42
Ni	42	—
Cu	39	—
Sc	0	0
Cr	72	70
V	73	39
Ti	68	30

[a] Units are arbitrary; information from Ref. 72.

Table II. IEP(s) Correlation Constant *a* for Use with Equations 12 and 13

Coordination	$\nu = 4$	$\nu = 6$	$\nu = 8$[a]
Hydroxides and Hydrous oxides	a = +0.21	0.0	−0.4
"Anhydrous" oxides	a = +0.39	+0.18	−0.26

[a] Constant *a* adjusted to fit IEP(s) = 9.4 for ThO_2 (*37, 60*) measured with materials assumed "anhydrous" (*43, 72*). For "hydrous" materials *a* was estimated roughly to fit the most basic observed ZPC for ThO_2 (hyd) (*72*) and still remain consistent with *a* for $\nu = 4$ and 6. Table modified from information in Ref. 72.

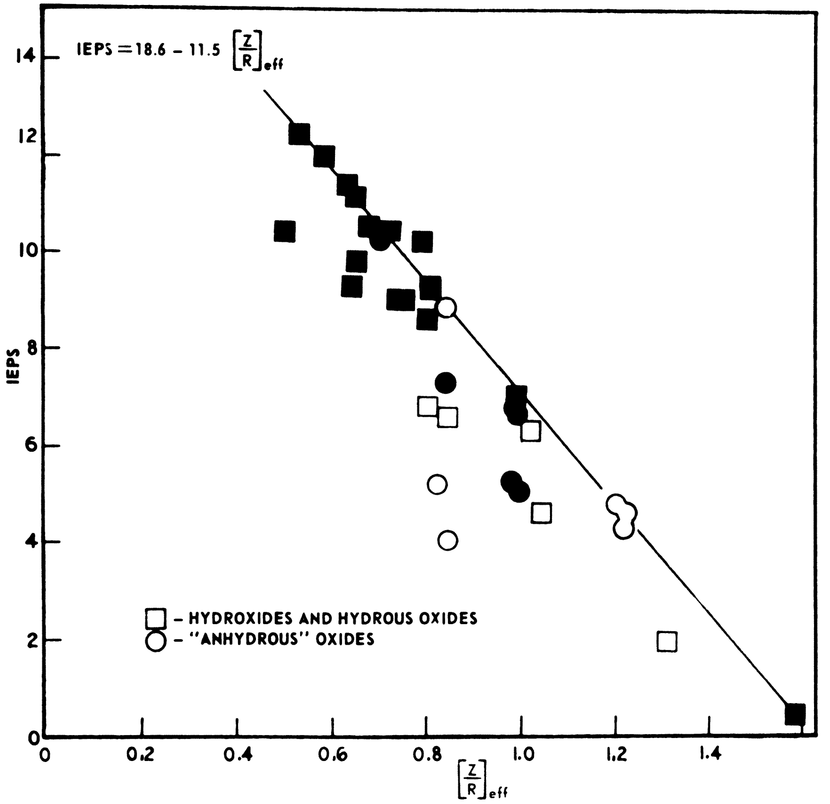

Figure 3. Correlation of experimental isoelectric points of oxides and hydroxides with $(Z/R)_{eff}$. Filled symbols represent elements with oxidation state of 2, 3, or 6. Open symbols represent oxidation state 4

oxides is not satisfactory at present. Although Equation 13 fits the most basic observed isoelectric points for many elements reasonably well, our understanding is by no means complete because for some systems, even in the relatively well-behaved group with coordination numbers 4 or 6, isoelectric points more acid than those used in Figure 3 have been observed and have yet to be interpreted satisfactorily. A partial explanation may lie in other sources of charge, discussed below.

Variability of IEP(s). VARIABILITY FROM SOURCES OTHER THAN SPECIFIC ADSORPTION. Referring to organic colloids, Abramson (*1*) has stated that a true IEP(s) can be measured in systems containing only the species H^+, OH^-, and those produced by interaction of the solid with pure water. This claim was made in response to the observation that no ionic species is totally devoid of tendency toward specific adsorption. The requirement is impossible to satisfy, of course.

Systems may be carefully chosen to approximate Abramson's stringent condition by permitting the presence only of allegedly innocuous ions such as Na^+, K^+, ClO_4^-, NO_3^-, and perhaps Cl^-. This procedure has led to considerable success in choosing IEP(s)'s which appear to be truly characteristic of the solid phase (*72*). Even in these systems, though, the choice often had to be made among a distressing multiplicity of observed IEP(s)'s. The reasons for this are not fully understood.

We have already seen that the composition and history of the electrolyte may change the concentration and composition of the PDI and hence may vary the IEP(s). While understanding of the suspect hydroxo complexes is growing, their role as PDI is at present quantitatively unpredictable.

An independent mechanism for charge development has recently come to light (*71*). There is evidence that protons diffuse from low pH electrolytes into some of the oxides, producing a positive space charge within the solid. The space charge leads to a shift in the apparent IEP(s) owing to the necessity of its compensation with surface charge to achieve zero net charge. The diffusion coefficient of H^+ in oxides and oxyhydroxides is small enough that a protonic space charge built up before an experiment (perhaps during a cleaning step) may be considered permanent and nearly constant during a rapid experiment. Hydroxides and hydrous oxides can be expected to develop a negative space charge by losing protons when aged in basic media. Onoda and de Bruyn (*71*) have observed a shift in the IEP(s) of Fe_2O_3 from about 8.3 to roughly 7.2 which was attributable to a space charge equivalent to about -3.2 microcoulombs per sq. cm.

Increasing crystallinity as observed in aging precipitates, for example, shifts the IEP(s) in the acid direction (*72*). Healy and Fuerstenau (*40*) have interpreted the wide range of IEP(s)'s (pH 2 to 7) they observed for various polymorphs of MnO_2 in terms of variation in crystallinity and a loosely defined surface field strength derived from lattice parameters. The situation may be more complex than this, however. MnO_2 will be discussed again as a possible example of the role played by defect structures manifested in ion exchange behavior.

Partial oxidation or reduction leading to nonstoichiometry in solids such as TiO_2, Fe_3O_4, or MnO_2 may be expected to shift the IEP(s) toward that characteristic of the oxidation state produced (*72*).

CHARGE REVERSAL AND VARIATION OF THE IEP(S) BY SPECIFIC ADSORPTION (*44*). To achieve zero charge in the presence of a specifically adsorbed ionic species, the pH must be shifted away from the IEP(s) to increase or decrease hydrogen ion adsorption, whichever is appropriate. The new pH at which zero charge is observed is of course not an IEP(s).

In general anionic impurities shift the ZPC to a more acid value; cationic impurities shift it to more basic values.

The ZPC in complex electrolytes may become completely unrelated to the identity of the solid phase, the ZPC being several pH units removed from the IEP(s). The best example of complete loss of influence by the solid phase is the successful measurement of correct IEP(s) values for proteins adsorbed onto quartz (*1, 53*).

Because ionic species adsorbed in response to coulombic attraction alone obviously cannot adsorb in amounts larger than those equivalent to the original surface charge—*i.e.*, they cannot reverse the sign of the surface charge—charge reversal must occur in response to specific adsorption alone. Similarly at the isoelectric point, the surface charge is zero; hence, adsorption by coulombic attraction alone will not occur. Thus, adsorption which results in a shift in the isoelectric point must be specific adsorption.

Specific electrolyte adsorption can occur on oxides by ion exchange with structural cations, with hydrogen or hydroxyl of the surface hydroxide groups, or with impurities (*92, 94*). Ions which can form insoluble compounds or undissociated complexes with a component of the solid crystal lattice adsorb more strongly than those which cannot (*2*). This does not imply or require that such complexes or compounds do or do not form. The question may be left open. It does imply that, of a series of species which form insoluble compounds with components of the solid, that which forms the least-soluble compound will be adsorbed most strongly. Thus any generalization which can be used to predict solubility or complexing tendency can be extended to predict adsorbability, at least qualitatively.

Simple multivalent cations such as Mg^{2+} and Al^{3+} are ineffective in charge reversal for coagulation (*62*) experiments and in activation for froth flotation (*35*). The related positive hydroxo complexes do function as coagulants and flotation activators and hence must be specifically adsorbed. By knowing the appropriate hydrolysis constants and the most effective species (in flotation systems apparently $M^{+z}(OH)^{+}_{z-1}$ and in coagulation, polynuclear complexes), one can predict the pH range in which each cation can be expected to adsorb strongly.

Selectivity of adsorption and the relative tendency toward adsorption may be inferred from ion exchange behavior (*6, 30, 80, 81, 84*).

Among the organic electrolytes, those with longer hydrocarbon chains form less soluble compounds and adsorb more strongly (*3, 9*). The observed order of decreasing adsorption for organic electrolytes onto Al_2O_3 (*15*) is:

$$RCOOH > RCONH_2 > ROH > RNH_2 > RCOOCH_3 > RN(CH_3)_2 > RNO_2 > ROCH_3 > RH$$

Complex Oxides: Charging Mechanisms and Zero Point of Charge

Origins of Charge. Additional charging mechanisms occur in more complicated solids (*13, 34, 38*). While the simple oxides have the general formula, A_mO_n, the group described as complex includes $A_xB_yO_n$ (*90*)—*i.e.*, oxides containing two or more cations, such as the silicates. The carbonates, orthosilicates, etc., where oxygen is present in discrete oxyanions, may be called salts as well as complex oxides. The clay minerals serve as a convenient vehicle for introducing the ZPC of these materials.

The clay minerals are layer structures (*38, 39, 86*) incorporating, for example, sheets of interconnected SiO_4 tetrahedra "cross-linked" with sheets of AlO_6 octahedra. Particles have broken bonds only on the edges of sheets. The broken bonds hydroxylate; they and structural OH on the layer surfaces can dissociate to produce a pH-dependent charge in the same way as described for the surfaces of simpler oxides. Charge from this source may be referred to as originating in the hydroxylated surface.

Isomorphic substitution of trivalent aluminum for silicon in tetrahedral sites or of magnesium for aluminum on the octahedral sites of these structures, or similar nonequivalent substitution in other structures produces an intrinsic negative charge on the framework (*13, 14, 34, 38*) unless compensated by other substitutions. In the solid clays this space charge is compensated by interlayer cations, usually Na^+, K^+, Mg^{2+} or Ca^{2+}. These are retained primarily by coulombic bonding. In suspension the interlayer cations are exchangeable and ionize or diffuse away to some extent, producing a net charge on the solid and an electrical double layer. The net charge on the solid is not confined to the surface but is distributed as a space charge. Substitution and site vacancies in defect structures such as the silica-alumina co-gels also result in intrinsic structural charge compensated by exchangeable ions (*34*). A net intrinsic structural charge from any source may be designated σ_i.

All ions in the system, whether specifically adsorbed or not, must be expected to saturate partially the ion exchange capacity arising from these relatively pH-independent sources. For this reason an isoelectric point defined in terms of hydrogen and hydroxyl ion adsorption is hypothetical, and in any real system, the pH at which zero surface charge is observed will depend upon the system composition.

Zero Point of Charge. We are operating on the assumption that pH-dependent surface charge arises predominantly from H^+ adsorption by reactions of the hydroxylated surface similar to Reactions 1 and 3. Figure 4 shows schematic H^+ adsorption isotherms illustrating the pH variation of surface charge and H^+ adsorption density, Γ_H, associated with this source. Curve a represents the total amount of adsorption on a given amount of surface area. Curve b represents more surface. In both cases, Γ_H and σ_H are zero at the same pH, the IEP(s), because the equilibrium constants for Reactions 1 and 3 are independent of the amount of surface present.

THE ZPC OF ONE-COMPONENT ION EXCHANGERS. Immersing a solid (*e.g.*, the "simple" oxide MnO_2), which has finite cation exchange capacity, results in partial ionization of the positive counter ions (*e.g.*, sodium) and partial replacement of sodium by hydrogen. The extent of ionization (hence the magnitude of σ_i) depends upon the sodium ion concentration $[Na^+]$ and hydrogen ion concentration $[H^+]$. Increasing $[H^+]$ at constant $[Na^+]$ results in further replacement of Na^+ by H^+ and ionization of fewer H^+ sites. At low $[Na^+]$, or in general, ionic strength, σ_i can be expected to decrease with decreasing pH. At high $[Na^+]$ or ionic strength sodium-hydrogen exchange is reduced, and σ_i will be less pH sensitive. The dashed lines in Figure 4 represent the pH dependence of σ_i as it might appear in NaCl and $CaCl_2$ solutions, respectively. Because the degree of ionization of Ca^{2+} from an exchanger is smaller than that of Na^+ (*14*), σ_i is smaller throughout the pH range in the Ca^{2+} system. It is assumed that σ_i in the Ca^{2+} system is less sensitive to pH as well.

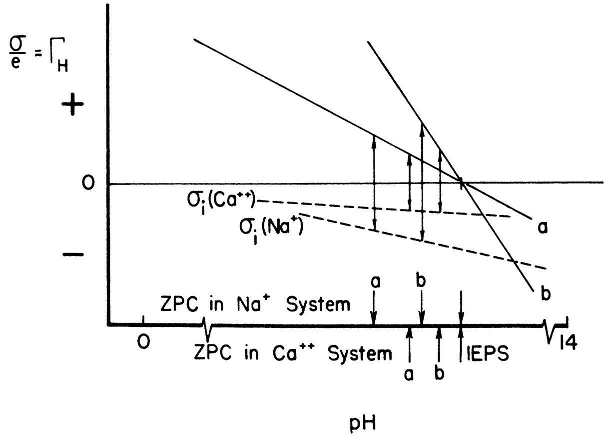

Figure 4. Schematic hydrogen ion adsorption isotherms illustrating for a one-compound system the relationship between IEP(s) and ZPC if σ_i is finite

The IEP(s) characteristic of the hydroxylated surface is the pH at which the hydrogen ion adsorption density on the hydroxylated surface sites alone is zero. To achieve zero total charge when $\sigma_i \neq 0$, however, Γ_H must be increased by adjusting the pH toward the acid side of the IEP(s) until $e\Gamma_H = -\sigma_i$; hence the ZPC is smaller than the IEP(s).

Isotherms a and b in Figure 4 again represent low and high adsorption capacity in the hydroxylated surface. The resultant ZPC decreases with decreasing relative area or adsorption site density on the hydroxylated surface or with increasing σ_i. The degree of ionization of exchangeable ions in clay systems varies with suspension concentration. By analogy we would expect the same to be true in suspensions of any ion exchanger; hence, the ZPC should be expected to vary with suspension concentration.

We may summarize the ZPC-determining role of σ_i by observing that the ZPC should be highly variable, should depend upon the solid's ion exchange capacity, the identity, concentrations, and ionization of exchangeable ions, the adsorption capacity of the hydroxylated surface and solid/liquid ratio in the suspension. For a combination of low adsorption capacity on the hydroxylated surface and high σ_i, such as might be observed if the ion exchange capacity were high and ionic strength low in a 1:1 salt system, the pH necessary to achieve $e\Gamma_H = -\sigma_i$ may be unattainably low, and a ZPC unobservable. At relatively high concentration of a strongly adsorbed exchangeable ion, σ_i may approach zero and the ZPC approach the IEP(s).

While the linear adsorption isotherms of Figure 4 are illustrative only, they are not inconsistent with reality. The simplest theory of the electrical double layer, the Gouy-Chapman approximation, predicts that if the pH is not far from the isoelectric point, the charge represented by counter ions in the diffuse double layer is related to the surface potential as follows (*4*, *52*, *86*):

$$\sigma = \sigma_D \simeq \left(\frac{n\epsilon}{2\pi kT}\right)^{1/2} Ze\Psi_0 = \left(\frac{\epsilon\kappa}{4\pi}\right)\Psi_0, \text{ if } \Psi_0 < 25 \text{ mv.} \qquad (14)$$

where:

σ = net surface charge

σ_D = net charge in the diffuse double layer

n = bulk concentration of counter ions (ions/cc.)

ϵ = dielectric constant of aqueous medium

k = Boltzmann constant

Z = Valence of counter ions, assumed symmetrical

e = electronic charge

Ψ_0 = surface potential

κ = double layer thickness

π, T have their usual meanings

De Bruyn and Agar (*16*) point out that at 25°C.

$$\Psi_0 = \frac{RT}{F} \ln \frac{(\mathrm{H}^+)}{(\mathrm{H}^+)_0} = 0.059 \; [\mathrm{pH} - \mathrm{IEP(s)}] \qquad (15)$$

where

R = gas constant

F = Faraday constant

$(\mathrm{H}^+)_0$ = Hydrogen ion concentration at the IEP(s)

Equations 14 and 15 may be combined to show that:

$$e\Gamma = \sigma = \left(\frac{\epsilon\kappa}{4\pi}\right) 0.059 \; [\mathrm{pH} - \mathrm{IEP(s)}] = K[\mathrm{pH} - \mathrm{IEP(s)}] \quad (16)$$

which is the equation of a straight line in Γ or σ and pH when the ionic strength is held constant. Of course the adsorption isotherms deviate widely from linear pH dependence when the pH is much different from the IEP(s) ($\Psi_0 > 25$ mv.), and the approximation of Equation 14 breaks down.

Combining the ion exchange capacity owing to structural charge and that of the diffuse double layer (*13, 14, 86*) associated with the charged hydroxylated surface gives some degree of anion exchange capacity on the acid side of the IEP of a cation exchanger. Because the diffuse double layer becomes a cation exchanger on the basic side of the IEP (the counter ions are positive and exchangeable), the total cation exchange capacity (CEC) will vary with pH, increasing above the IEP. This is consistent with the observation that the CEC of clays is roughly independent of pH until the pH exceeds a basic limit, after which the CEC increases (*32, 85, 88*) only if the adsorption capacity of the hydroxylated surface is small.

ZPC OF COMPLEX OXIDES. *Definition.* For compounds and co-gels with negligible intrinsic structural charge, a more quantitative approach is possible. The surfaces of such materials contain $\underline{\mathrm{M}}\mathrm{OH}$ groups of two or more types—*e.g.*, the surfaces of aluminosilicate gels or compounds contain both $\underline{\mathrm{Si}}\mathrm{OH}$ and $\underline{\mathrm{Al}}\mathrm{OH}$ groups. As a first approximation, these may be considered independent, and the IEP(s) of each type of site will be that of the corresponding pure oxide or hydroxide. The net surface charge at a pH between the two IEP(s)'s is the algebraic sum of the negative charge on the more acid sites and the positive charge on the more basic sites. The ZPC lies between the two IEP(s)'s of the end members of a binary system.

A compound AB_x, where A and B are oxides, may be taken as an illustrative example. The surface contains $\underline{\mathrm{A}}\mathrm{OH}$ and $\underline{\mathrm{B}}\mathrm{OH}$ adsorption sites. The group of sites, A, behaves independently of B sites. The charge density or H^+ adsorption density on each group of sites is independent of x, but the total particle charge attributable to each site group depends upon the relative number of each type of site—*i.e.*, on the composition of AB_x as reflected in the fraction of the total surface area occupied by each type of site. A schematic illustration of the pH dependence of charge distribution among $\underline{A}OH$ and $\underline{B}OH$ sites for AB_x is given in Figure 5. The IEP(s) of each site group is the pH at which Γ_H for that site group amounts to zero. The ZPC is the pH at which positive hydrogen ion adsorption on B (yielding, for example, $\underline{B}OH_2^+$) sites exactly balances negative hydrogen ion adsorption on A sites (yielding $\underline{A}O^-$).

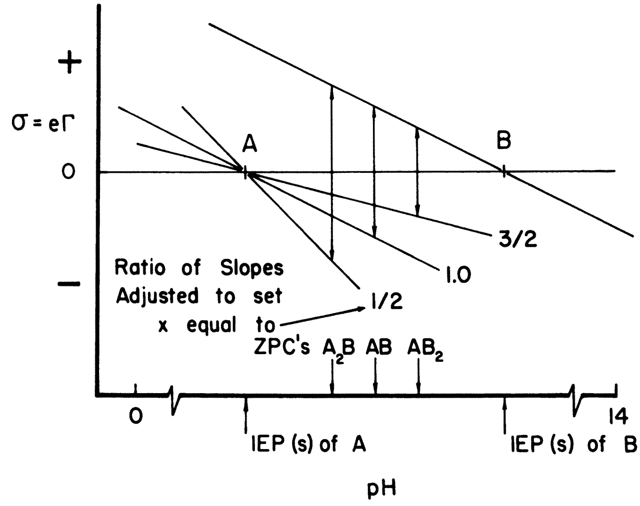

Figure 5. Schematic individual site group H^+ adsorption isotherms for complex oxide AB_x illustrating the ZPC

By applying Equation 16 to each component of a general compound or mixture of i components capable of hydroxylating and allowing for finite σ_i, the ZPC can be related to the IEP(s)'s of component site groups —*i.e.*, of component pure oxides. The total charge density σ, comprises the contributions of σ_i and of each type of hydroxylated site present in the surface at an atomic fraction f_i. Thus,

$$\sigma = \sigma_i + K_i \sum_i f_i[\text{pH} - \text{IEP(s)}_i]$$

or for compound AB_x (17)

$$\frac{\sigma}{K} = \frac{\sigma_i(x, \text{pH})}{K} + \frac{1}{1+x}[\text{pH} - \text{IEP(s)}_A] + \frac{x}{1+x}[\text{pH} - \text{IEP(s)}_B]$$

At the ZPC, $\sigma = 0$, and Equation 17 can be solved for pH to yield:

$$\mathrm{pH}_{(\sigma = 0)} = \mathrm{ZPC} = \frac{-\sigma_i}{K} + \sum_i f_i[\mathrm{IEP(s)}_i]$$

or for compound AB_x (18)

$$\mathrm{ZPC} = \frac{-\sigma_i(x,\mathrm{pH})}{K} + \frac{1}{(1+x)}[\mathrm{IEP(s)_A}] + \frac{x}{(1+x)}[\mathrm{IEP(s)_B}]$$

In the absence of σ_i, the ZPC appears according to this approximation to be simply the appropriately weighted average of the IEP(s)'s of the component oxides.

Hydrogen ion isotherms are far more complex than the linear approximations represented by Equation 14 and used in Figures 4 and 5.

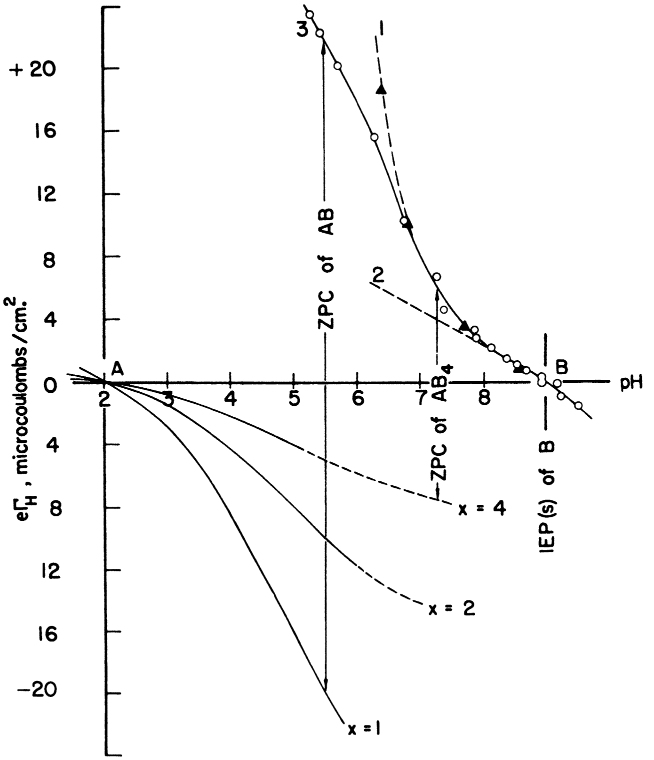

Figure 6. Theoretical and experimental H^+ adsorption isotherm and estimation of ZPC's for AB_x using nonlinear isotherms for $\sigma_i = 0$ μcoulombs/sq. cm. Curve 1, Gouy-Chapman isotherm; Curve 2, extrapolation of linear portion of Curve 1; Curve 3, experimental isotherm for adsorption of H^+ onto Fe_2O_3

Hence, the ZPC can be expected to be a more complex function of composition than represented by Equation 18. The large difference in form between isotherms based upon Equation 16 and isotherms based on the complete Gouy-Chapman relationship applied to 100-A. spherical particles is illustrated in Figure 6. The Gouy-Chapman isotherms were calculated using numerical solutions of the rigorous form of Equation 14 published by Loeb, Wiersema, and Overbeek (*57*). This book contains solutions for σ in terms of Ψ_0. The term Ψ_0 was related to pH through Equation 15. Experimental data for adsorption of hydrogen ions onto Fe$_2$O$_3$ (*73*, *74*) normalized to adjust Γ_H equal to the Gouy-Chapman prediction at [pH − IEP(s)] = −1.3, are plotted on the same graph.

To determine what change in composition dependence of the ZPC the large differences in the form of these isotherms would produce, a hypothetical case was studied. It was assumed that AB$_x$ is a compound of Fe$_2$O$_3$ (B) with an IEP(s) at pH 9, and another oxide, A (*e.g.*, SiO$_2$) with an IEP(s) at pH 2. The adsorption of hydrogen ions onto the FeOH sites was assumed to follow the isotherm actually observed for adsorption

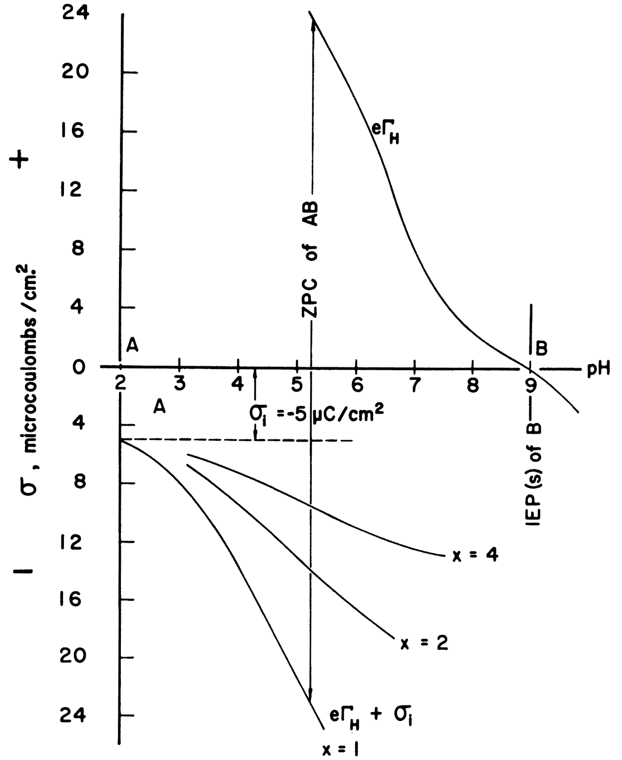

Figure 7. Isotherms used to predict variation of ZPC with composition for $\sigma_i = -5$ μcoulombs/sq. cm.

onto Fe_2O_3. It was assumed that negative hydrogen ion adsorption involving $\underline{A}OH$ sites followed an isotherm of the same form. Isotherms representing differing values of x in the chemical formula AB_x are drawn for component A. The ZPC appropriate for each composition was determined by inspection. The results are plotted in Figure 8 to illustrate the variation of ZPC with composition predicted by this somewhat more realistic model.

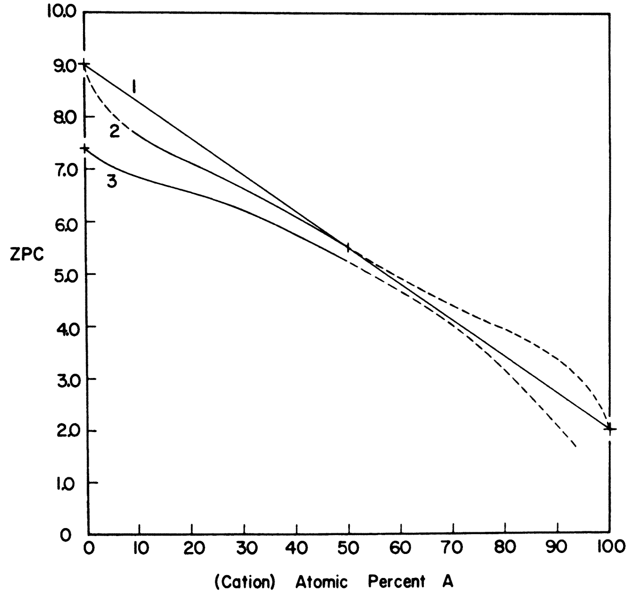

Figure 8. Composition dependence of ZPC of complex oxide AB_x. Curve 1 from Equation 18; Curve 2, $\sigma_i = 0$, graphical approximation from Figure 6; Curve 3, $\sigma_i = -5$ μcoulombs/sq. cm., approximation from Figure 7

Should the compound AB_x exhibit cation exchange capacity owing to the existence of a negative σ_i, the total negative charge will of course be the sum of σ_i and the negative charge resulting from a deficiency of hydrogen ions on A sites. Figure 7 shows the isotherms used to predict the variation of ZPC with composition in such a case. The family of curves labeled A represents the total charge density—*i.e.*, the sum of σ_i and negative $\underline{A}O^-$ sites. The variation of ZPC with composition in this system is also shown in Figure 8.

The linear relationship between the ZPC of a compound and its composition predicted in Equation 18 is surprisingly accurate when compared, as in Figure 8, with the somewhat more realistic predictions derived from Figure 7. Even assuming a rather large pH-independent σ_i

(the total surface charge of a montmorillonite (*86*) is near 11 microcoulombs per sq. cm., and hence the assumption of a constant $\sigma_i = 5$ microcoulombs/sq. cm. is extreme) leads to a ZPC differing by only one pH unit in the range 20–80% A, from the value predicted using Equation 18. Of course Equation 18 would predict the direction of the correction necessary to account for a known, finite σ_i, but a quantitative prediction is not possible since the proportionality constant, *K*, is unknown.

Experimental Data. To provide a reference list of ZPC's for complex oxide minerals and coprecipitates and to obtain examples for studying the predictive usefulness of Equation 18, experimental data were collected. Owing to the diversity of observations from which ZPC's can be inferred, sources included the literature of colloid and soil science, sanitary engineering, and mineral engineering, especially froth flotation. A thorough search would require screening by mineral species as well as by topic and therefore was judged unwarranted.

ZPC data were selected according to the criteria used to study simple oxides and hydroxides previously (*72*). The data are summarized in Table III. Insofar as possible, details of sample preparation, measurement technique, and environmental conditions are given. It is assumed that phase identification was correct.

ZPC's estimated with Equation 18 are included in the tables. As a first step in calculation it was necessary to select IEP(s)'s for the common oxide components in each of the two extreme states of hydration. In most cases the value predicted from the *Z/R* ratio agrees fairly well with experiment. For convenience, the calculated value was used. No reliable experimental data are available for oxides of phosphorus (the reason is obvious), Al(III) in tetrahedral coordination, or for Ce(IV) or Zr(IV). For these, purely hypothetical calculated IEP(s)'s were used. The IEP(s) values needed are summarized in Table IV. When it was necessary to estimate an IEP(s) for an oxide with $\nu \neq 4, 6, 8$, a value of the constant, *a*, was estimated graphically from a plot of *a vs.* ν.

SiO_2 is a component of most of the minerals studied, yet its IEP(s) is among the least well-determined. Arbiter and Fujii (*12*) experimentally justify selecting 1.8 for amorphous silica, which we will assume is also hydrous, and pH about 2.4 for crystalline quartz. These are not the IEP(s)'s they observed but averages revised from an earlier summary (*72*). This choice contradicts the prediction made on the basis of the *Z/R* ratio and pointedly illustrates the preliminary nature of this entire treatment. This choice also neglects variation of acidity with structure among the silicates. Pauling has predicted (*75*) significant differences in acidity reflecting the degree of oxygen sharing by SiO_4 tetrahedra. An attempt to unravel in detail the electrokinetic behavior of MO_2 oxides and the role played by silica in different structures is probably one of the two or three most important topics which needs careful study.

In calculating effective ZPC's with the assumed IEP(s) contributions, several additional assumptions were made, namely that;

(1) No ions other than hydrogen and hydroxyl play any potential-determining role.

(2) Additivity is on an atomic, not molar basis, and cations alone are counted.

(3) Grinding or abrasion during sample preparation produces a disturbed, disordered or amorphous surface layer which is hydrous. Acid leaching removes this material.

(4) Precipitates not subsequently dried are hydrous.

(5) The surface composition is the same as that of the bulk and is given by the idealized chemical formula.

For some minerals and for at least three reasons, even these assumptions are a gross oversimplification.

Minerals, particularly hydrous precipitates, vary notoriously in composition. In most cases, however, chemical analyses were not available; hence, an idealized composition was used. In some cases a rough average composition was calculated from analyses reported by Deer, Howie, and Zussman (*28*).

Many minerals break with well-developed cleavage along crystal planes of composition different from the average. This difference should be reflected in the IEP(s); its importance is illustrated in the data for the aluminum orthosilicates.

The third complication in assigning surface composition arises from nonstoichiometric dissolution during approach to equilibrium between the solid and solution. This subject is abundantly reported in the geological literature with regard to weathering (*50*, *55*). It appears reasonably correct to conclude that monovalent cations are quickly replaced by hydrogen ion. Bivalent cations are partially lost, probably by ion exchange with H^+, particularly if they do not form part of the structural framework of the solid.

The ZPC predictions made on this complex basis have been reasonably accurate in many cases. The complications described and a few new ones are illustrated in the experimental data contained in Table III.

The aluminosilicates, Al_2SiO_5, illustrate several key features of the treatment. Al_2SiO_5 assumes three structures differing in Al(III) coordination number (*91*) and in cleavage habit (*82*) as seen in Table V. The symbol, ν, represents coordination number.

Aluminum ions on sites of different coordination were considered different species for purposes of ZPC calculation. The IEP(s) contributions for hypothetical oxides and hydroxides containing these "species" are given in Table IV.

Table III. Zero Points

Solid	*Ground After Leaching*[c]	*Acid Leach*[c]	*Method*
		ORTHOSILICATES	
Al_2SiO_5 (Kyanite) (100) and (010) cleavage surfaces			
(1)	—	hot HCl	fl, sp
	—	no	fl, sp
(2)	—	cold HCl	fl, mep
(3)	yes	HCl	sp, mep
	no	dil. HCl	sp, mep
$Al^6Al^5SiO_5$ (Andalusite) (110) cleavage surface			
(1)	—	cold HCl	fl, mep
(2)	yes	HCl	sp, mep
	no	dil. HCl	sp, mep
$Al^6Al^4SiO_5$ (Sillimanite)			
(1)	yes	HCl	sp, mep
	no	dil. HCl	sp, mep
$Al(Al_x^4Si_{2-x})O_{11/5-x/2}$ (Mullite)			
	$2Al_2O_3 \cdot SiO_2(2/1)$		
	$3Al_2O_3 \cdot 2SiO_2(3/2)$		
(1) (3/2)	yes	HCl	sp
	no	dil. HCl	sp
$(Mg,Fe)SiO_4$, Olivine (Mg_9Fe) (*28*)			
(1)	no	—	mep
Zr^8SiO_4, Zircon			
(1)	no	6*N* HCl	mep
		CHAIN SILICATES	
$(M_{1.9}^{2+}M_{0.1}^{3+})(Si_{1.9}Al_{0.1}^{4})O_6$, Augite (*28*)			
	All cations present		
	Ca^{2+} lost from average augite		
	All M^{2+} lost		
(1)		—	mep
$LiAl^6(SiO_3)_2$, Spodumene			
	All Li^+ lost		
(1)		—	mep

of Charge of Silicates[a, b]

Zero Point of Charge			
	Calculated		
Observed	*Hydrous*	*Anhydrous*	*Source*
	6.8	5.0	
	7.4	5.9	
5.2 ± 0.1	—	—	(*18*)
6.2 ± 0.1	—	—	
6.9	—	—	(*22*)
7.9	—	—	(*67*)
6.6	—	—	
	6.3	5.1	
	6.9	5.5	
5.2	—	—	(*22*)
7.2–7.8	—	—	(*82*)
5.9	—	—	
	5.9	4.7	
6.8	—	—	(*82*)
5.6	—	—	
	7.1	5.3	
	6.4	4.9	
8.1	—	—	(*82*)
7.1	—	—	
	8.9	7.4	
4.1	—	—	(*79*)
	6.5	6.0	
5	—	—	(*24*)
	—	6.5	
	—	5.5	
	—	2.7	
4.5	—	—	(*79*)
	4.3	4.0	
2.6	—	—	(*79*)

Table III.

Solid	*Ground After Leaching*^{c}	*Acid Leach*^{c}	*Method*
SHEET SILICATES			
$(OH)_8Si_4Al_4{}^6O_{10}$, Kaolinite (*13, 14*)			
(1)		—	mep
(2)		—	mep
(3)		H-Kaolin	mep
(4)		—	Ad, Au
$(OH)_8Si_8(Al_{3.34}{}^6Mg_{0.66})O_{20}(Na_{0.66})$, Montmorillonite (*13, 14*)			
	Na^+ assumed lost		
(1)		—	mep
$(Fe,Mg)_7(Si_4O_{11})_2(OH)_2$ (*28*), Cummingtonite (analysis from Ref. *48*)			
(1)		dil. HCl	mep
$Mg_3Si_2O_5(OH)_8$, Serpentine Minerals (*28*)			
	MgOH surface		
(1)		Chrysotile	Ad, Ac
(2)		Chrysotile	mep, coag
(3)		Chrysotile	sp
(4)		Lizardite	sp
FRAMEWORK SILICATES			
$NaAlSi_3O_8$-$KAlSi_3O_8$			
	K^+,Na^+ assumed lost		
(1)		Albite	mep
(2)		Microcline	mep

[a] Abbreviations:

Ad: ZPC inferred from pH dependence of adsorption of species following
Au: Negative gold sol
Ac: Acetate ion
coag: ZPC inferred from maximum rate of coagulation or sedimentation
fl: The ZPC may be estimated roughly as the pH at which nonspecific anionic and cationic collectors give equal recovery by flotation

Average experimental ZPC's for each of the Al_2SiO_5 polymorphs are compared in Figure 9 with calculated values based on Equation 18 and several different sets of assumptions. Smolik and Fuerstenau (*82*) and Choi (*22*) have attributed the differences in ZPC among the polymorphs generally to differences in structure. Smolik and Fuerstenau went further, pointing out that the relative values were interpreted better on the basis of the Al/Si ratio in the most probable cleavage planes and the assump-

Continued

Zero Point of Charge			
	Calculated		
Observed	*Hydrous*	*Anhydrous*	*Source*
	5.5	4.8	
4.6 ± 0.3	—	—	(63)
3.3	—	—	(47)
<3.5	—	—	(83)
~5 (edges)	—	—	(32)
	5.3	4.2	
≤2.5	—	—	(47)
	6.4	6.0	
5.2 ± 0.2	—	—	(48)
	8.9	7.2	
	≤12.5	—	
10.8–11.0	—	—	(25)
10	—	—	(78)
11.8	—	—	(59)
9.6	—	—	(59)
	3.1	3.0	
2.0	—	—	(79)
2.4	—	—	(79)

mep: micro-electrophoresis
sp: streaming potential or streaming current

[b] Superscript numbers in formulae indicate ligancy. ν for M(II) and M(III) is 6; for M(IV), 4.

[c] Applies only to orthosilicates.

tion that Al is preferentially leached from the mineral surface during acid washes.

In view of evidence that the orthosilicates may dissolve congruently during initial stages of equilibration with water (55, 58), we have assumed that there is no enrichment in either Al or Si by dissolution. The following interpretation is offered instead.

Comparing experimental values (labeled G in Figure 9) and calculated values (labeled H) for all three polymorphs confirms the assumption that samples abraded or ground during preparation and not subsequently leached have a hydrous surface. The Al/Si ratio in the surface probably lies between 2 and 3 for kyanite and andalusite, implying that there is some tendency for cleavage to control exposure and that this tendency is not completely lost in the disordered surface assumed to be produced by grinding. Evidence that the surface of the ground minerals is disordered or recrystallized is found in the observation that the experimental ZPC lies between a value calculated by assuming that all of the aluminum is on sites of coordination number 6, and the value calculated by assuming that half of the aluminum is on sites with coordination number 4, as dictated by the structural formula of the mineral.

Table IV. Isoelectric Points Assumed for Component Oxides in Calculating Complex Oxide ZPC's

Surface Site	*Nominal Oxide*	*Hydrous IEP(s)*	*Anhydrous IEP(s)*
$\underline{Al}^{6}OH$	$Al_2{}^{6}O_3$	9.2	7.1
$\underline{Al}^{4}OH$	$Al_2{}^{4}O_3$	6.8	4.7
$\underline{Ba}OH$	BaO	13.3	11.2
$\underline{Ca}OH$	CaO	12.9	10.8
$\underline{Ce}^{(III)}OH$	Ce_2O_3	9.8	7.7
$\underline{Fe}^{(II)}OH$	FeO	11.8	9.7
$\underline{Fe}^{(III)}OH$	Fe_2O_3	9.3	7.1
$\underline{Mg}OH$	MgO	12.5	10.4
$\underline{Si}OH$	SiO_2	1.8	2.4
$\underline{Zr}OH$	ZrO_2	11.3	9.7
$\underline{P}OH$	H_3PO_4	−3.4	−5.4

Table V. Properties of Al_2SiO_5

Species	*Structural Formula*	*Most Prominent Cleavage Plane* (82)	*Al/Si ratio in Cleavage Plane* (82)
Kyanite	$Al_2{}^{6}SiO_5$	(100) and (010)	3
Andalusite	$Al^{6}Al^{5}SiO_5$	(110)	3
Sillimanite	$Al^{6}Al^{4}SiO_5$	(010)	2
—	$Al_2{}^{v}SiO_5$	—	–

Strong acid leaching produces the most acid experimental ZPC's. As evidenced by agreement between experimental and calculated ZPC's, the surface produced is a close approximation of an unaltered fracture surface. Cleavage planes probably do partly control the Al/Si ratio (*cf.* kyanite data), and it is important to recognize the correct site distribution of Al(III) (*cf.* andalusite data).

No strong acid leaching was attempted with sillimanite. The authors (82) determined the ZPC by streaming potential and microelectropho-

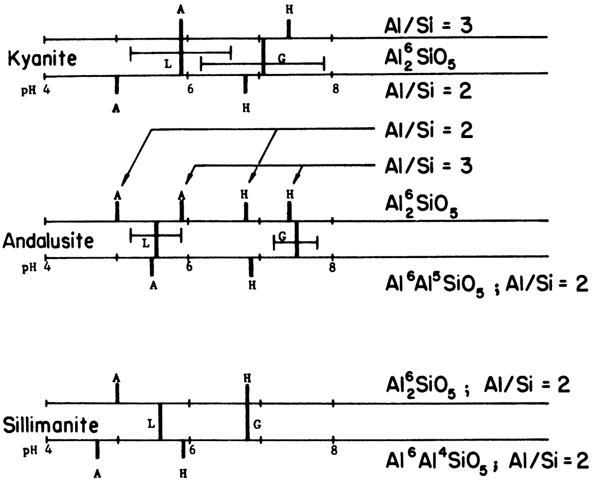

Figure 9. Experimental and calculated ZPC's for the polymorphs of Al_2SiO_5. Experimental ZPC's are labeled G if ground or abraded and not leached, L if acid leached. Calculated ZPC's are labeled A if based on the assumption of "anhydrous" substrate and labeled H if based on the "hydrous" approximation. Other assumptions are labeled in the figure

resis, interpolating between potentials and mobility measurements at pH values bracketing the ZPC. As the bracketing range was made more and more acid, the ZPC shifted in the acid direction. The value in Figure 9 is the acid extreme and may be considered the result of mild acid leaching. This experimental ZPC is intermediate between the hydrous and anhydrous approximations as might be expected if the disturbed surface were partially removed by stoichiometric dissolution.

The data for olivine illustrates an opposite extreme in stability of the metal ion in orthosilicates. Deju and Bhappu (29), whose laboratory provided the ZPC for olivine (79), report partial but stoichiometric exchange of hydrogen for magnesium under conditions similar to those used to determine the ZPC. Total replacement would presumably lead to a ZPC near the IEP(s) of silica, pH 1.8 or 2.4, depending upon the hydration state assumed. The observed ZPC lies between this value and a value calculated by assuming that the surface contains all of the magnesium and silicon expected in a fresh fracture surface, implying that more than half of the magnesium has been lost. If H^+/Mg^{2+} exchange proved reversible, Mg^{2+} would be expected to play a potential-determining role.

The calculated ZPC of zircon is a rough approximation, and little significance can be derived by comparing it with the experimental value.

Integrating the data for the aluminum, magnesium, and zirconium orthosilicates leads to the tentative conclusion that the smaller the cation valence, the more severe will be the surface alteration. In general, the calculated ZPC should most closely approximate reality for tri- and quadrivalent cations. It should represent a basic limit for mono- and bivalent cations.

The ZPC predicted from the formula composition of kaolinite (Table III) agrees reasonably well with the value inferred for the edges of the particles from studying the pH dependence of the adsorption of gold sols (*32*). Experimental ZPC's determined by electrophoresis, of course, integrate charge contributions from all sources. Because the intrinsic structural charge on the clay minerals is negative, if finite (*13, 14*), one expects effective ZPC's observed to be quite variable and more acid than the predicted value. Furthermore, the frequently reported inability to achieve positive charge on suspended clay minerals is not unexpected.

Still another complication arises in interpreting the ZPC's of serpentine minerals. There are several polymorphs (*28*). All are layer structures combining sheets of SiO_4 tetrahedra with sheets of MgO_6 octahedra. Among these, chrysotile has a fibrous habit because the structure of the mineral is strained in such a way that the crystal rolls up with the SiO_4 layer on the inside and the brucite layer on the outside (*69, 77*). The ZPC should lie between the value predicted on the basis of bulk composition and the IEP(s) of magnesium hydroxide at a pH reflecting the extent to which the SiO_4 layer is masked by the brucite layer. This is observed, but the values determined by different groups vary widely. The variability may be caused by partial breakdown of the fibers during sample preparation or by differences in habit (*28*), both effects resulting in variation of the fraction of the total surface area containing exposed SiOH. The habit of lizardite is platey (*28*); hence the composition of the fracture surface should more nearly approach the chemical formula, and the IEP(s) should, as it does, more nearly approach the predicted value.

Coprecipitates. Silica-alumina coprecipitates are immensely complicated. As a result of structural disorder and substitution of Al(III) for Si(IV) on tetrahedral sites, they exhibit cation exchange behavior (*34*). The fraction of total Al which occurs on tetrahedral sites and the CEC vary widely in response to the conditions of precipitation and subsequent sample history, especially thermal history. In general, the fraction

$$f_4 = \frac{Al^4}{Al^4 + Al^6}$$

is highest when the aluminum content of the coprecipitate is small and decreases rapidly as the aluminum content exceeds 40 atomic percent. Drying and heating the precipitate increases f_4.

In Figure 10 the experimental ZPC's of hydrous silica-alumina coprecipitates (*64*) are compared with those of dried and ignited silica-alumina catalysts (*49*), some of the previously discussed aluminosilicate minerals, and the composition dependence derived from Equation 18 assuming:

$\sigma_i = 0$

$f_4 = 1.0$ when the aluminum content is below 40 atomic percent of total structural cations.

$f_4 = 0$ when the total aluminum content is above 40 atomic percent.

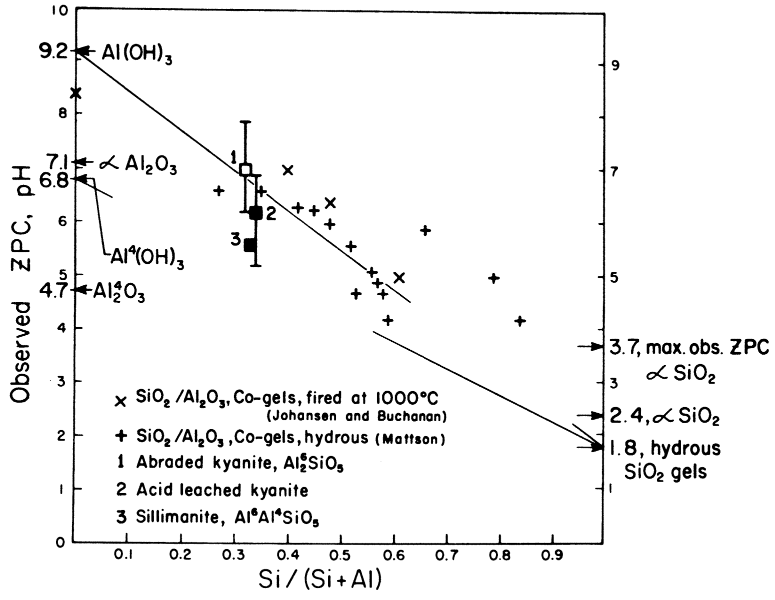

Figure 10. ZPC's of coprecipitates in the Al_2O_3-SiO_2 system. Straight lines represent Equation 18 and assumption described in text

There is sufficient doubt about the actual distribution of aluminum on sites of coordination numbers 4 and 6 and about the IEP(s) contribution of SiOH groups that detailed analysis of these results is unwarranted.

The behavior of SiO_2-Fe_2O_3 coprecipitates (*63, 64*) is similar, and the data are summarized in Figure 11. The similar behavior of coprecipitates of Al_2O_3 and Fe_2O_3 with P_2O_5 (*64*) and those containing M_2O_3, SiO_2, and P_2O_5, for which ZPC's are shown in Figure 12. The calculated ZPC's for phosphatic materials are based on an IEP(s) derived from Equation 13 for a hypothetical hydrous P_2O_5. The agreement of experimental and calculated ZPC's for minerals (discussed below) is close enough that the IEP(s) contribution $\underline{P}OH$ groups may be considered an empirically derived proportionality constant rather than a dangerous extrapolation of Equation 13.

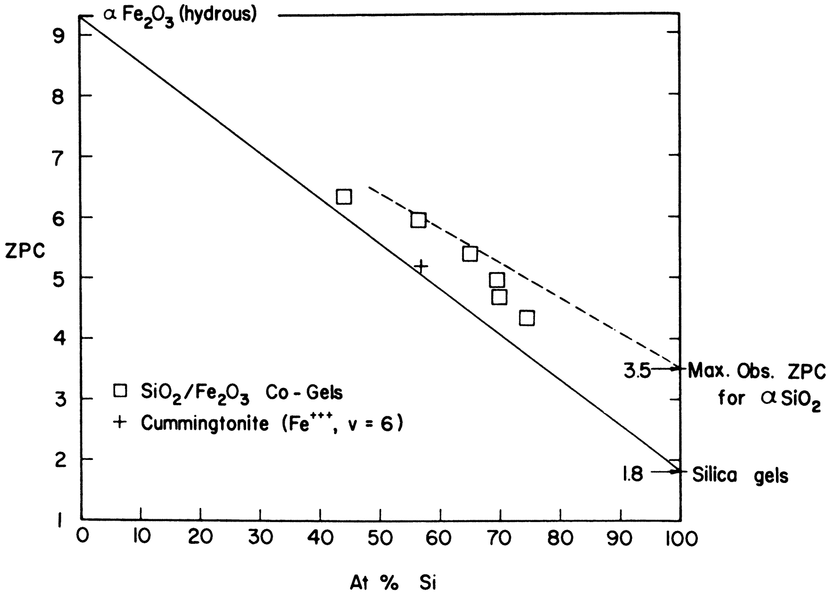

Figure 11. ZPC's of coprecipitates in the Fe_2O_3-SiO_2 system

The hydrous aluminosilicates and Zr, Th, and Ti phosphates have significant ion exchange capacity (*6*). Further interpretive study of charge development in such systems will require recognizing the ion exchange properties and measuring trivalent cation site distribution as well as adsorption and mobility.

Variability of ZPC. All sources contributing to variability of the IEP(s) of simple oxides will also contribute to that of the ZPC's of more complex solids. The important role of structural charge and the sensitivity of the degree of its compensation to environment force one to conclude that variability of the ZPC for minerals and coprecipitated hydrous oxides will be extreme. The success obtained by comparing experimental ZPC's with values calculated according to complex assumptions is sufficient to support a model of charge development based on the assumption of independent action of composition components represented in the surface. This in turn supports the application of prediction schemes known to operate in simple oxide systems to more complicated systems as well. Judging from experience with inorganic ion exchangers,

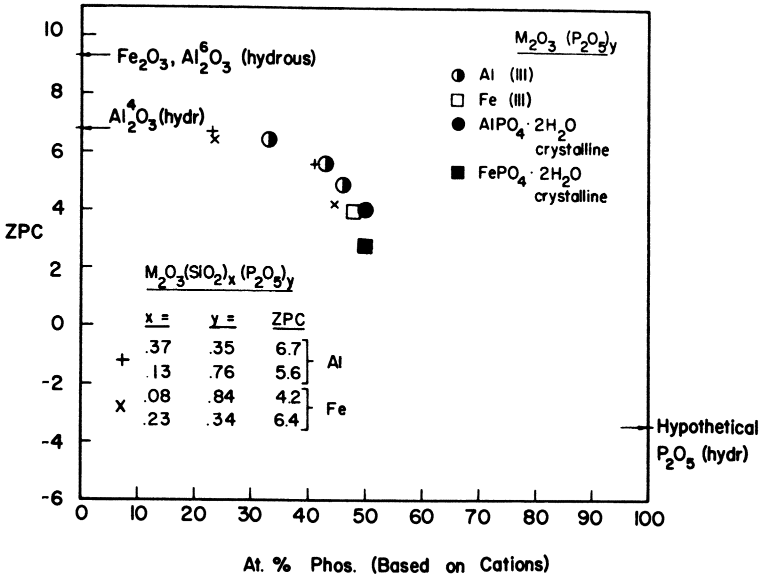

Figure 12. ZPC's of coprecipitates in the Al_2O_3-Fe_2O_3-P_2O_5-SiO_2 system

this transfer includes prediction of adsorption specificity and hence prediction of the ZPC variation with impurities.

ZPC of Non-Oxides

The zero points of charge of a group of phosphate minerals are collected in Table VI. The IEP(s) contribution of the oxy anion PO_4^{3-} is a dangerous extrapolation of Equation 13. The ZPC's, including contributions by $\overline{POH}$ groups as dictated in Equation 18, are in surprising agreement with experiment. The agreement is misleading, however. It has also been observed that the surface charge of apatite is positive at all pH values if the concentration of calcium ion is greater than about 3×10^{-3} (*5*). Similar experience has been recorded with other minerals, and ZPC's for calcium minerals are collected in Table VII. The behavior of fluorite (*21*) and apatite is similar. Two investigators found it impossible to achieve a positive charge on the surface of scheelite (*20, 70*) at any pH below about 2. Observations of this sort have led to the conclusion that the potential-determining ions of salt-type compounds are the component ions (*21, 70*). For example, there seems to be little question that the potential-determining ions for the silver halides are monovalent silver ion and the halide ion (*52*).

Owing to lack of data it is premature to attempt predictive generalizations for these materials. Nevertheless, a few useful statements can be made. The fact that a ZPC on the pH scale which agrees with predictions from Equations 13 and 18 can be observed in any system within the group under discussion, indicates that either the hydroxylated surface or hydroxo-complex adsorption charge development models probably apply under some circumstances. For some other minerals there are apparently no circumstances under which either of these models apply. Deserving of most concern is the observation that for some of these minerals, adding one of the ionic components of the solid to the system diminishes or destroys the pH sensitivity of the charge and may make it impossible to observe a ZPC on the pH scale for a mineral which did exhibit such a ZPC in the absence of the added salt (*cf.* CaF_2 data, Table VI).

In developing Equations 13 and 18 it was assumed that a hydrogen ion adsorption model would adequately describe charge development by either mechanism—*i.e.*, amphoteric dissociation of hydroxylated surfaces or adsorption of hydroxo complexes from solution. This assumption was

Table VI. Zero Points of Charge of Phosphate Minerals[a]

	Observed ZPC		*Calculated ZPC (Ca^{2+} neglected)*		
	Method	*pH*	*Hydrous*	*Anhydrous*	*Source*
Apatite, $Ca_5(PO_4)_3F$ (*89, 90, 91*)					
neglecting F	—	—	<6.9	<5.9	
(1) natural crystals	mep	4–5	—	—	(5)
(2) natural crystals if pCa < 2.5, $\sigma > 0$ at all pH.	fl	6	—	—	(5)
Hydroxyapatite, $Ca_5(PO_4)_3OH$ (*89, 90, 91*)			6.9	5.9	
If surface is $Ca_2(HPO_4)(OH)_2$			7.4	—	
(1) synthetic	mep	7			(5)
Eggonite (?), $Al^{4}PO_4 \cdot 2H_2O$ (*89, 90, 91*)			1.7	~0	
(1) synthetic	drift[b]	4	—	—	(*26*)
Strengite, $FePO_4 \cdot 2H_2O$			2.9	~1	
(ν assumed 6)					
(1) synthetic	drift[b]	2.8	—	—	(*19*)
Monazite, $(Ce,La)_{1-4/3x}Th_xPO_4$					
hypothetical $CePO_4$			3.2	1.1	
(1) natural crystals	mep	3.4 ± 0.2	—	—	(*23*)

[a] Abbreviations same as for Table III.
[b] The ZPC is the pH of a freshly precipitated suspension in which no change in pH occurs on aging.

made in recognition of the fact that the concentrations of all hydroxo complexes are interrelated by reactions involving hydrogen and hydroxyl ions. Excursion into the properties of salt-type minerals forces the realization that there are systems such as calcium and magnesium ion systems where the concentrations of hydroxo complexes in useful pH ranges are so small that the concentration of uncomplexed aquo ions are independent of pH. For example, for all pH less than about 11, the concentration of monohydroxo calcium ion is less than 1% of the aquo calcium ion concentration (*31*). In this pH range then, the calcium ion concentration is essentially constant and independent of pH unless it reacts with some species other than hydroxyl. The surface charge is relatively independent of pH under some circumstances, apparently when $(Ca^{2+})/(H^+)$ exceeds some critical value. Because the hydroxo calcium complexes, if present, have pH-dependent concentrations, Ca^{2+} must be the PDI. This behavior should also be observed for the silicates which exhibit reversible exchange of H^+ for structural cations, inasmuch as it arises from properties of the electrolyte.

Table VII. Zero Points of Charge of Calcium Salts[a,b]

	Observed ZPC			*Calculated ZPC*		
	Method	*pCa*	*pH*	*Hydrous*	*Anhydrous*	*Source*
Apatite, $Ca_5(PO_4)_3F$ *cf.* Table VI	—	$\ll 2.5$	4–5	<6.9	<5.9	(*5*)
Calcite, $CaCO_3$	fl	?	8–9	—	—	(*5*)
Fluorite, CaF_2	mep	?	7–7.5			(*21*)
	mep	2.6	>7			
	mep	3.0	~7			
	mep	3.5	~6.5			
	mep	4.0	~5.6			
Scheelite, $CaWO_4$						
(1) No pH > 4 achieves positive surface charge. Surface charge nearly independent of pH (σ by sp).						(*20*)
(2) No pH > 2 achieves positive surface charge. ZPC < 2 by extrapolation of mep. data.						(*70*)

[a] Abbreviations same as for Table III.
[b] All natural minerals.

Summary

Suspended solids are electrically charged. Many important properties of the solid and of the suspension itself are determined partly by response to the sign and magnitude of the charge. As a starting point for predicting charge and behavior, a zero point of charge on the pH scale is useful. The ZPC is variable and reflects the composition and defect structure of the solid and the identity and concentrations of components of the electrolyte in which it is suspended. These variations are predictable, at least in direction.

The isoelectric point may be conveniently defined as the ZPC expected for a pure, single component solid oxide, hydrous oxide, or hydroxide with a nondefective structure in an electrolyte totally devoid of specifically adsorbed polar or ionic species. An IEP(s) can be calculated from the charge and size of the cation using Equation 13 and the constants in Tables I and II. The maximum accuracy to be expected may be judged from the graphical correlation given in Figure 3.

The ZPC of an unaltered mixed oxide, silicate, or phosphate in a system devoid of specific electrolytes other than the PDI is approximately the average of the IEP(s)'s of its component oxides weighted on an atomic (cation) basis. Account must be taken of the correct cation coordination, cleavage and morphological habit, hydration state, and structural modification produced by abrasion. Experimental and calculated ZPC's for a group of silicate and phosphate minerals are compared in Figure 13 to show the accuracy to be expected in prediction.

Unfortunately the term "unaltered" must be left partially undefined. Roughly, it refers to a solid surface unmodified in any way by the adjacent electrolyte—*i.e.*, a surface which is not at equilibrium with its environment. Simple stoichiometric dissolution has no effect on the ZPC unless, as is apparently the case with some salt-type minerals, dissolution raises the concentration of a pH-independent PDI which usurps the potential-determining role of H^+. Alteration by hydration produces a predictable effect. Superficial compositional alteration, quite common in weathering, may occur by ion exchange involving structural cations or by nonstoichiometric dissolution. In either case the ratio of the two (or more) ZPC-determining surface sites becomes an unknown, lying between the extremes of the unaltered surface and the surface at equilibrium with the environment. These types of alteration are apparently essentially complete for compounds of M^+, so that the ZPC of a sodium feldspar for instance is expected to match the predicted ZPC for the corresponding hydrogen feldspar. Alteration is expected to be significant but not necessarily complete for M^{2+} compounds and minor for M^{3+} and higher valent cations unless long equilibrium times are involved. Useful reviews of silicate-weathering processes have been provided in recent papers by Keller (*50*) and Lagache (*55*).

Dehydration, dehydroxylation, and increased crystallinity can be expected to decrease the ZPC. The presence of anionic impurities or of pH-independent potential-determining anions will decrease the ZPC.

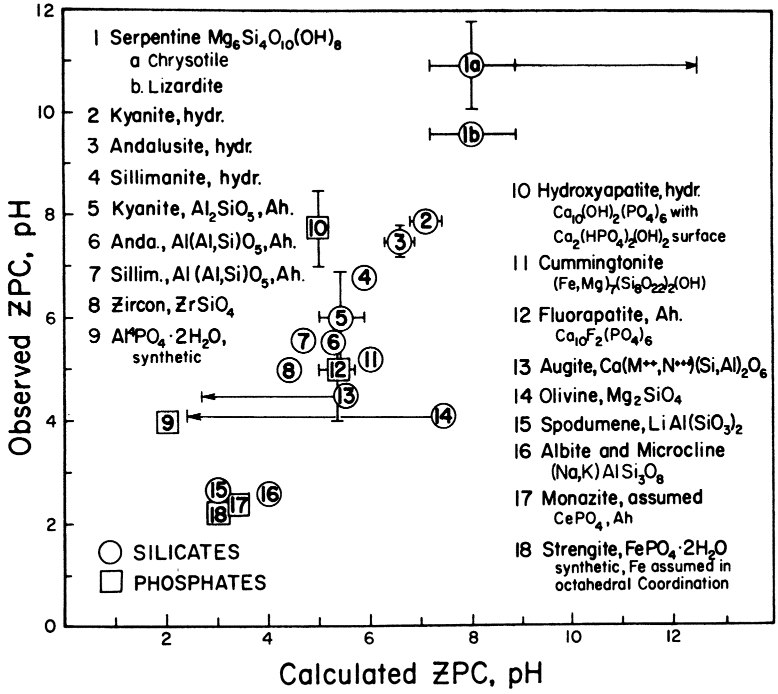

Figure 13. Experimental and calculated ZPC's for silicate and phosphate minerals. Arrows connect ZPC's calculated for the fresh fracture surface with limiting values expected to result from unusual morphology or weathering

Cationic species will increase the ZPC. The magnitude of this change is not predictable at present. An excess of a specifically adsorbed ionic species will remove pH dependence or change the ZPC to that of the impurity species.

Structures or compounds which are ion exchangers have an intrinsic structural charge, σ_i, which can be expected to shift the ZPC away from the calculated value by a variable amount. Prolonged exposure to extreme pH may result in adsorption or desorption of protons resulting in a positive or negative space charge, hence a finite σ_i. Positive σ_i may be expected to move the ZPC in the basic direction. Negative σ_i should move the ZPC in the acid direction.

In developing these prediction schemes, all aspects of the solid composition, crystal structure, morphology, and history, as well as the electrolyte composition, are reflected in changes in the surface chemistry of the solid and are manifested in the ZPC. The coulombic models used to develop the prediction scheme are grossly oversimplified, and the procedure must be used with caution and is justified only to the extent of its success.

Acknowledgments

The author thanks all the scientists whose work he used in preparing this paper. G. E. Agar, R. B. Bhappu, P. L. de Bruyn, S. Chwastiak, D. W. Fuerstenau, G. Purcell, and J. Smolik deserve special mention for providing some of the original stimulus and for advance notice of their own work. Preparation of the paper was made possible through the financial support of the U. S. Atomic Energy Commission under contract AT (04-3) 326 C.A. No. 3.

Complementary work on the interaction of oxides with water vapor and the properties of transition metal ions in mineral structures was valuable in pointing the way to some of the variables found significant. These projects are supported, respectively, by the National Science Foundation (GP172) and the Advanced Research Projects Agency, through the Stanford Center for Materials Research.

Literature Cited

(1) Abramson, H. A., Moyer, L. S., Gorin, M. H., "Electrophoresis of Proteins and the Chemistry of Cell Surfaces," p. 24 ff., Reinhold, New York, 1942.
(2) Adamson, A. W., "Physical Chemistry of Surfaces," p. 593, Interscience, New York, 1960.
(3) *Ibid.*, p. 577.
(4) *Ibid.*, p. 183.
(5) Agar, G. E., paper presented at the 95th Annual Meeting of the AIME, New York, 1966.
(6) Amphlett, C. B., "Inorganic Ion Exchangers," p. 90, Fig. 25, Elsevier Publishing Co., New York, 1964.
(7) Anderson, J. H., Ph.D. Thesis, Stanford University, 1965.
(8) Anderson, J. H., Wickersheim, K. A., *Surface Sci.* **2,** 252 (1964).
(9) Aplan, F. F., Fuerstenau, D. W., "Froth Flotation, 50th Anniversary Volume," D. W. Fuerstenau, ed., pp. 182, 184, AIME, New York, 1962.
(10) *Ibid.*, p. 187.
(11) *Ibid.*, p. 186.
(12) Arbiter, N., Fujii, Y., paper presented at the 95th Annual Meeting of the AIME, New York, 1966.
(13) Bolt, G. H., *Trans. Intern. Congr. Soil Sci., 7th, Madison, Wis., 1960,* **2,** 321, 1961.
(14) Bolt, G. H., Page, A. L., *Soil Sci.* **99,** 357 (1965).
(15) Brockman, H., *Discussions Faraday Soc.* **7,** 58 (1949).
(16) deBruyn, P. L., Agar, G. E., "Froth Flotation, 50th Anniversary Volume," D. W. Fuerstenau, ed., AIME, New York, 1962.
(17) Burwell, R. L., Jr., Pearson, R. G., Haller, G. L., Tjok, P. B., Chock, S. P., *Inorg. Chem.* **4,** 1123 (1965).
(18) Cases, J., *Compt. Rend.* **26,** 183 (1965).
(19) Chang, S. C., Jackson, M. L., *Soil Sci. Soc. Am. Proc.* **21,** 265 (1951).
(20) Choi, H. S., *Can. Met. Quart.* **2,** 405 (1963).

(21) Choi, H. S., Han, K. N., *J. So. Korea Inst. Chem.* **7,** 17 (1963).
(22) Choi, H. S., Oh, J. H., *J. Mining Met. Inst. Japan* **81,** 614 (1965).
(23) Choi, H. S., Whang, K. U., *J. So. Korea Inst. Chem.* 7, 91 (1963).
(24) Choi, H. S., Whang, K. U., *Trans. Can. Inst. Mining Met.* **66,** 242 (1963).
(25) Chwastiak, S., personal communication.
(26) Cole, C. V., Jackson, M. L., *Soil Sci. Soc. Am. Proc.* **15,** 84 (1951).
(27) Davies, J. T., Rideal, E. K., "Interfacial Phenomena," p. 79, Academic Press, New York, 1963.
(28) Deer, W. A., Howie, R. A., Zussman, J., "Rock Forming Minerals," Vols. II and III, Wiley, New York, 1962.
(29) Deju, Raul A., Bhappu, R. B., *New Mexico, Bur. Mines Mineral Resources, Circ.* 82 (1965).
(30) Dugger, D. L., Stanton, J. H., Irby, B. N., McConnell, B. L., Cummings, W. W., Maatman, R. W., *J. Phys. Chem.* **68,** 757 (1964).
(31) Feitknecht, W., Schindler, P., *Pure Appl. Chem.* **6,** 130 (1963).
(32) Follett, E. A. C., *J. Soil Sci.* **16,** 35 (1965).
(33) Fripiat, J. J., Jelli, A., Poncelet, G., Andre, J., *J. Phys. Chem.* **69,** 2185 (1965).
(34) Fripiat, J. J., Leonard, A., Uytterhoeven, J. B., *J. Phys. Chem.* **69,** 3274 (1965).
(35) Fuerstenau, M. C., Bhappu, R. B., *Trans. AIME* **226,** 164 (1963).
(36) Fuerstenau, M. C., Rice, D. A., paper presented at the 95th Annual Meeting of the AIME, New York, 1966.
(37) Green, J., *Bull. Geol. Soc. Am.* **70,** 1127 (1959).
(38) Grim, R. E., "Clay Mineralogy," Chap. 7, McGraw-Hill, New York, 1953.
(39) *Ibid.*, p. 152.
(40) Healy, T. W., Fuerstenau, D. W., *J. Colloid Sci.* **20,** 376 (1965).
(41) Healy, T. W., Herring, A. P., Fuerstenau, D. W., *J. Colloid Sci.* **21,** 435 (1966).
(42) Hem, J. D., Roberson, C. E., *U.S. Geol. Surv., Water Supply Papers,* in press.
(43) Holmes, H. F., Shoup, C. S., Secoy, C. H., *J. Phys. Chem.* **69,** 3148 (1965).
(44) Hsu, Pa Ho, Bates, T. F., *Min. Mag.* **33,** 749 (1964).
(45) Hsu, Pa Ho, Bates, T. F., *Soil Sci. Soc. Am. Proc.* **28,** 763 (1964).
(46) Hsu, Pa Ho, unpublished results.
(47) Iwasaki, I., Cooke, S. R. B., Harraway, D. H., Choi, H. S., *Trans. AIME* **223,** 97 (1962).
(48) Johansen, P. G., Buchanan, A. S., *Australian J. Chem.* **10,** 398 (1957).
(49) Jura, G., "Physical Methods in Chemical Analysis," W. G. Berl, ed., Vol. II, Academic Press, New York, 1952.
(50) Keller, W. O., "Soil Clay Mineralogy," C. I. Rich and G. W. Kunzo, eds., University of North Carolina Press, Chapel Hill, 1964.
(51) Krauskopf, K. B., *Geochim. Cosmochim. Acta* **9,** 1 (1956).
(52) Kruyt, H. R., ed., "Colloid Science," Vols. I and II, Elsevier, New York, 1949.
(53) *Ibid.*, Vol. II, p. 195.
(54) Kurosaki, S., *J. Phys. Chem.* **58,** 320 (1954).
(55) Lagache, M., *Bull. Soc. Franc. Mineral. Crist.* **88,** 223 (1965).
(56) La Mer, V. K., *J. Phys. Chem.* **66,** 973 (1962).
(57) Loeb, A. L., Overbeek, J. Th. G., Wiersema, P. H., "The Electrical Double Layer Around a Spherical Colloid Particle," The MIT Press, Cambridge, 1961.
(58) Luce, R. W., personal communication.
(59) Martinez, E., Zucker, G. L., *J. Phys. Chem.* **64,** 924 (1961).
(60) Mason, B., "Principles of Geochemistry," 2nd ed., Wiley, New York, 1962.

(61) Matijevic, E., in discussion of oral version of this paper, 151st Meeting, ACS, Pittsburgh, 1966.
(62) Matijevic, E., Janauer, G. E., *J. Colloid Interface Sci.* **21,** 197 (1966).
(63) Mattson, S., *Soil Sci.* **25,** 289 (1928).
(64) *Ibid.*, **30,** 459 (1930).
(65) *Ibid.*, **31,** 57 (1931).
(66) Mattson, S., Pugh, A. J., *Soil Sci.* **38,** 229 (1934).
(67) Milligan, L. H., *J. Phys. Chem.* **26,** 247 (1922).
(68) Moulson, A. J., Roberts, J. P., *Nature* **182,** 200 (1958).
(69) Naumann, A. W., *J. Phys. Chem.* **70,** 288 (1966).
(70) O'Connor, D. J., *Proc. Intern. Congr. Surface Activity, 2nd, London, 1957*, 319 (1957).
(71) Onoda, G. Y., de Bruyn, P. L., *Surface Sci.* **4,** 48 (1966).
(72) Parks, G. A., *Chem. Rev.* **65,** 177 (1965).
(73) Parks, G. A., de Bruyn, P. L., *J. Phys. Chem.* **66,** 967 (1962).
(74) Parks, G. A., Ph.D. Thesis, Massachusetts Institute of Technology, 1960.
(75) Pauling, L., "The Nature of the Chemical Bond," p. 558, Cornell University Press, Ithaca, 1960.
(76) Pines, H., Haag, W. O., *J. Am. Chem. Soc.* **82,** 2471 (1960).
(77) Pundsack, F. L., Reimschussel, G., *J. Phys. Chem.* **60,** 1218 (1956).
(78) Pundsack, F. L., *J. Phys. Chem.* **59,** 892 (1955).
(79) Purcell, G., Bhappu, R. B., paper presented at the 95th Annual Meeting of the AIME, New York, 1966.
(80) Russell, A. S., Gitzen, W. H., Newsome, J. W., Ricker, R. W., Stowe, V. M., Stumpf, H. C., Wall, J. R., Wallace, P., *Alcoa (Aluminum Co. Am.) Res. Lab. Tech. Paper No.* **10** (1956).
(81) Shubata, M., *Science (Japan)* **19,** 570 (1949).
(82) Smolik, J., Harman, Fuerstenau, D. W., *Trans. Soc. Mining Engrs.* **235,** 367 (1966).
(83) Street, N., Buchanan, A. S., *Australian J. Chem.* **9,** 450 (1956).
(84) Titien, H., *J. Phys. Chem.* **69,** 350 (1965).
(85) Sumner, M. E., *Clay Minerals Bull.* **5,** 218 (1963).
(86) Van Olphen, H., "An Introduction to Clay Colloid Chemistry," Interscience, New York, 1963.
(87) Verwey, E. J. W., Overbeek, J. Th. G., "Theory of the Stability of Lyophobic Colloids," Elsevier, New York, 1948.
(88) Volk, V. V., Jackson, M. L., *Proc. National Conf. Clay Minerals, 12th, Atlanta, Ga., 1963*, 281 (1963).
(89) Wells, A. F., "Structural Inorganic Chemistry," p. 472 ff., The Oxford Press, New York, 1962.
(90) *Ibid.*, p. 480.
(91) *Ibid.*, p. 792.
(92) Williams, K. C., Daniel, J. L., Thomson, W. J., Kaplan, R. I., *J. Phys. Chem.* **69,** 250 (1965).
(93) Yopps, J. A., Fuerstenau, D. W., *J. Colloid Sci.* **19,** 61 (1964).
(94) Zhabrova, G. M., Egorov, E. V., *Russ. Chem. Rev.* **30,** 338 (1961).
(95) Zimmerman, J. R., Lasater, J. A., *J. Phys. Chem.* **62,** 1157 (1958).

RECEIVED May 16, 1966.

Formation of Silicic Acid in Aqueous Suspensions of Different Silica Modifications

WERNER STÖBER[1]

Max-Planck-Institut für experimentelle Medizin, Göttingen, and Institut für Medizinische Physik der Universitat Münster, Germany

When fine powders of vitreous silica, quartz, tridymite, cristobalite, coesite, and stishovite of known particle-size distribution and specific surface area are investigated for their solubility in aqueous suspensions, final concentrations at and below the level of the saturated concentration of molybdate-active silicic acid are established. Experimental evidence indicates that all final concentrations are influenced by surface adsorption of silicic acid. Thus, the true solubility, in the sense of a saturated concentration of silicic acid in dynamic equilibrium with the suspended silica modification, is obscured. Regarding this solubility, the experimental final concentration represents a more or less supersaturated state. Through adsorption, the normally slow dissolution rates of silica decrease further with increasing silicic acid concentrations. Great differences exist between the dissolution rates of the individual samples.

In 1950 Weitz *et al.* (23) developed a sensitive colorimetric method to measure small amounts of oligomeric silicic acid in the presence of polymeric forms. Oligomeric acid in this sense comprises molecules up to hexameric chains of hydrated SiO_4 tetrahedrons, which react readily with ammonium molybdate. Hence, this fraction of a sol is frequently referred to as molybdate-active silicic acid.

In aqueous solutions, polymerization and depolymerization processes are slow under normal conditions. This, in addition to the analytical difficulties in discriminating between different degrees of polymerization,

---

[1] Present address: The University of Rochester, School of Medicine and Dentistry, Department of Radiation Biology and Biophysics, Rochester, N. Y.

accounts for the scarcity of reliable data on polymerization equilibria in the earlier literature. However, it has been shown since that a definite saturation concentration exists for molybdate-active silicic acid in a polymeric sol.

Figure 1 gives results obtained by Alexander *et al.* (*1*) and Baumann (*2*) by dissolving fine particles of commercially available vitreous silica powders in aqueous solutions. Similar data obtained in polymerization and depolymerization experiments by Scheel *et al.* (*15*) and Friedberg (*10*) indicate that the curve shown in Figure 1 represents an equilibrium concentration for oligomeric acid. It can be approached from the supersaturated state of monomeric silicic acid as well as from a solution of pure polymeric silicic acid.

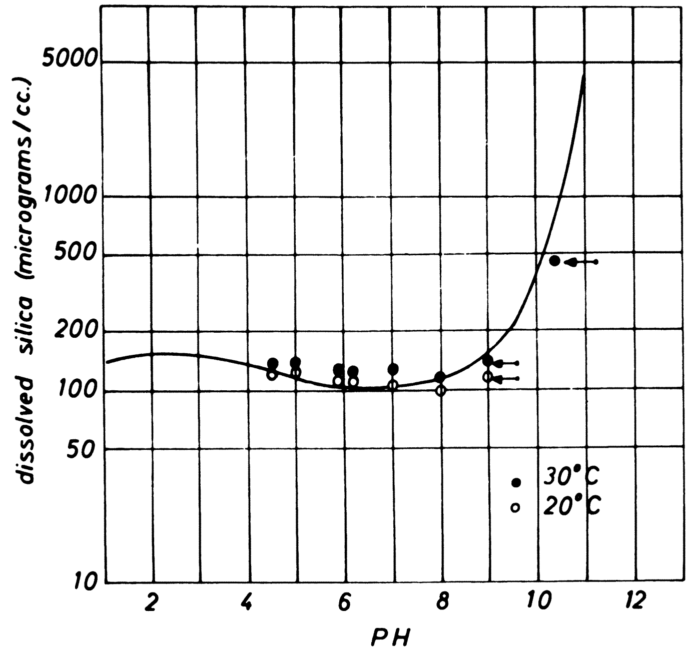

Figure 1. Solubility (saturation concentration) of oligomeric silicic acid at different pH values. Curve established by Alexander et al. (1); *data points by Baumann* (2), *arrows indicating pH shift during dissolution experiment*

Evidently, the particulate silica used in Alexander's and Baumann's experiments behaved like polymeric silicic acid. This opinion is supported by the fact that stable solutions of polymeric silicic acids have practically no polymers in the intermediate size range between oligomers and high polymers (*19*). Correspondingly, in the presence of colloidal particles of silica no noticeable amount of polymeric silicic acid is formed. The solution contains oligomers only.

With regard to a solubility equilibrium, the fact that vitreous silica behaves like a precipitate of polymeric silicic acid must be caused by the similarity between polymeric silicic acid and the hydrated surface of vitreous silica. Both forms can release silicic acid by hydrolysis and desorption, and likewise both forms are able to adsorb and condense silicic acid by means of silanol groups randomly distributed on their surfaces. Thus, in order to explain equal final states, the only assumption necessary is that the condensates will not attain the degree of dehydration of the bulk of the vitreous silica. The resulting equilibrium then relates to the two-phase system silicic acid—polymeric precipitate, and strictly speaking, this system is in a supersaturated state with respect to vitreous silica, which can be considered as an aged form of silica gel.

This interpretation poses an interesting question: if vitreous silica behaves like polymeric silicic acid or silica gel in aqueous suspension, how do the crystalline modifications of silica interact with aqueous solutions?

From the thermodynamic point of view we must take into account the fact that the lattice structure of quartz represents the solid state of lowest free energy of silica at room temperature, and accordingly, all other modifications are metastable only. Thus, in a true solubility equilibrium at this temperature, quartz will be an indispensable participant in such an equilibrium. However, the formation of quartz as well as the formation of metastable silica modifications of higher levels of free energy requires activation energies of the order of 200 kcal./mole (*21*). This condition is observed in all structural changes involving breakage and reorientation of the covalent Si—O—Si bondings of the solid framework of SiO_4 tetrahedrons. It procures the continuous existence of metastable modifications like tridymite, cristobalite, vitreous silica, coesite, and stishovite near room temperature, and it causes the low dissolution rates of most forms of silica in natural weathering processes.

Owing to this activation threshold, the first precipitation product from aqueous solutions of silicic acids will be an amorphous silica of some degree of hydration, while at room temperature the growth of vitreous and crystalline forms of silica from the precipitate (and thus the approach toward the absolute equilibrium) will proceed extremely slowly. With this understanding the data in Figure 1 are said to represent an equilibrium—*i.e.*, the reversible equilibrium between silicic acids in aqueous solution and metastable hydrated silica or polymeric silicic acid as precipitate.

The existing literature on the dissolution of crystalline silica near room temperature showed divergent data by different authors. Occasionally, reports on the dissolution of quartz in nearly neutral solutions (*12*) gave final silicic acid concentrations close to the values shown in Figure 1, but in contrast to this, extrapolating results obtained at elevated temperatures (*22*) indicated that the true equilibrium at room temperature may be an order of magnitude lower. The earlier investigations were entirely qualitative (*14*), but also in later studies poor reproducibility of results, attributed to various causes, has been reported (*11*). In order to establish some reproducible dissolution patterns and to develop a relevant theoretical model, an experimental investigation was made, utilizing all solid silica modifications available.

Experimental

Six different silica modifications were used: vitreous silica, quartz, cristobalite, tridymite, coesite, and stishovite. Two of these—cristobalite and tridymite—were prepared from fine amorphous silica powder by tempering samples at 950°C. with 1% of a mineralizer (K_2CO_3 and KH_2PO_4, respectively). Vitreous silica was obtained from fused rock crystals. All other samples were natural minerals; pure specimens of Brazilian rock crystal were used as quartz; coesite and stishovite were obtained as fine powders by isolation from Coconino sandstone of the Barringer Meteor Crater in Arizona (*4*).

The coarse materials were ground in special ball mills down to particle sizes around and below 1 micron. Samples of different specific

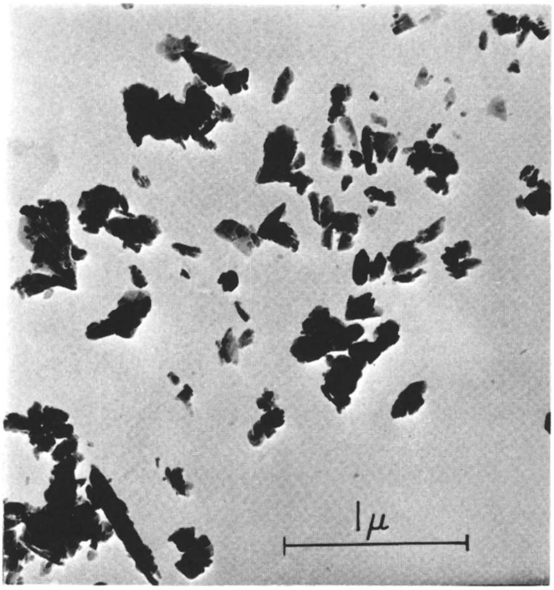

Figure 2. Electron micrograph of quartz particles of a sample of 33.6 sq. meters/gram specific surface area (×24,000)

surface area, varying between 2 and 60 sq. meters/gram were prepared by fractional centrifugal sedimentation. The surface areas were measured by BET adsorption (5). Most of the preparations were finally suspended in a series of NaOH solutions of pH values of decreasing order between 14 and 8 and subsequently washed in distilled water. Figures 2–7 show electron micrographs of some of the powders obtained.

Figure 3. Electron micrograph of the carbon shells of tridymite particles. After diffuse coating with carbon in a vacuum, the tridymite was dissolved away by hydrofluoric acid; specific surface area of this sample of relatively coarse crystals is 7.7 sq. meters/gram (×24,000)

The dissolution rates of most of the crystalline modifications in pure water are extremely slow. In addition, silica dissolved in pure water causes a shift to lower pH values. To avoid these difficulties and to obtain reliable results within an acceptable period of time, all measurements were carried out using an aqueous solution of 0.9% NaCl and 0.1% $NaHCO_3$ as solvent. This solution had several practical advantages, the most important of which was the catalytic effect of the chloride ions on the hydrolysis of Si—O—Si bondings (*10*). Together with the slightly alkaline reaction of the solution, which works in the same direction, the dissolution rates increased remarkably in preliminary tests: under the experimental conditions described below, the silicic acid level of suspensions of vitreous silica at pH 7 remained for weeks within the margin of error of the analytic procedure (0.5 μgram SiO_2/ml.), while the same amount of vitreous silica suspended in the solution used throughout this investigation established silicic acid concentrations of more than 50 μgram

SiO_2/ml. after the same period of time. Furthermore, the solution had a sufficient buffer capacity to maintain a constant pH of 8.4.

In each test, 500 ml. of this solution were mixed with the silica powder and kept in suspension by continuous but mild agitation. The apparatus was thermostatically controlled to 25° ± 0.5°C. To facilitate comparisons of individual dissolution patterns, the particulates used in

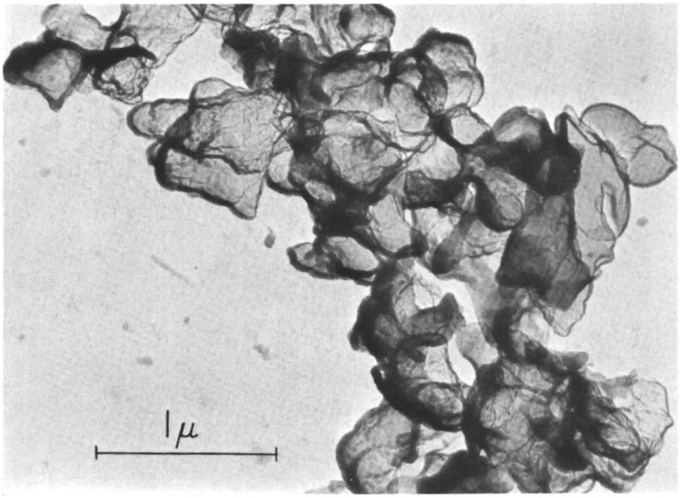

Figure 4. Electron micrograph of the carbon shells of cristobalite particles. Grains are of microcrystalline structure; specific surface area is 8.5 sq. meters/gram (×24,000)

Figure 5. Electron micrograph of carbon shells of vitreous silica. Specific surface area is 8.0 sq. meters/gram (×9600)

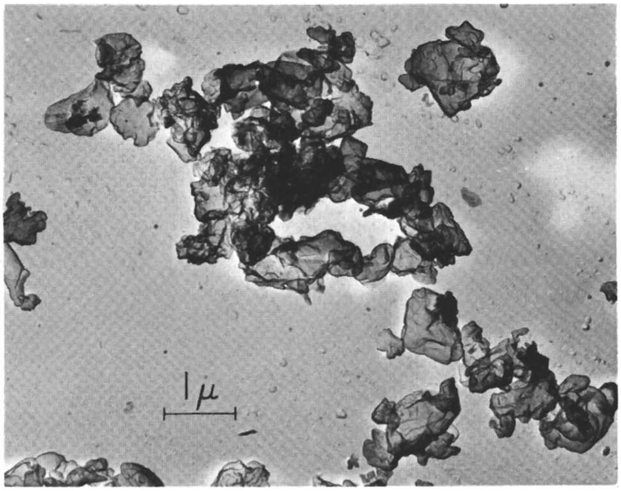

Figure 6. Electron micrograph of carbon shells of coesite. Specific surface area is 15.2 sq. meters/gram (×9600)

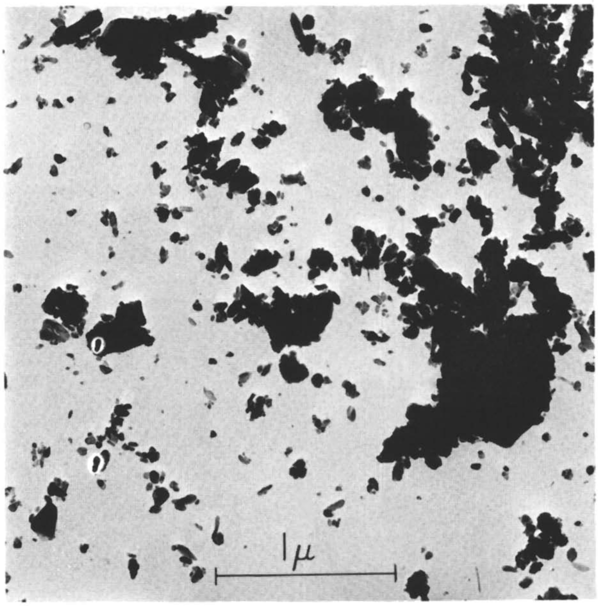

Figure 7. Electron micrograph of stishovite particles. Specific surface area is 20.6 sq. meters/gram (×24,000)

the experiments were suspended in such quantities as to provide equal surface areas exposed to the solvent in each run. Since the amount of dissolved silica was small in all cases, the loss of surface area during the experiment was negligible.

The silicic acid concentrations were analyzed at different times by withdrawing 1 ml. from the solution after a high speed centrifugation of the suspended particulates. The colorimetric determination of oligomeric silicic acid by means of the blue ammonium molybdate complex, as described by Stegemann and Fitzek (*16*), was used for the quantitative measurements.

Results and Discussion

Preliminary tests with samples of vitreous silica, quartz, cristobalite, and tridymite not treated with NaOH showed an effect which for quartz was previously described (*7*, *13*): repeated tests on the same sample did not reproduce the dissolution pattern but gave reduced values. The example in Figure 8 shows three of four repeated runs on the same cristobalite sample. Although the surface area remained constant, the concentration increase with time was always slower than in the preceding test. For quartz, some authors attribute this behavior to an amorphous surface layer of high solubility (*3*, *8*). A similar effect, however, is found for amorphous vitreous silica, and it seems more likely that the enhanced initial dissolution is caused by fine particles' adhering to the surface and to certain regions of the surface which are strongly distorted and hydrated (*20*).

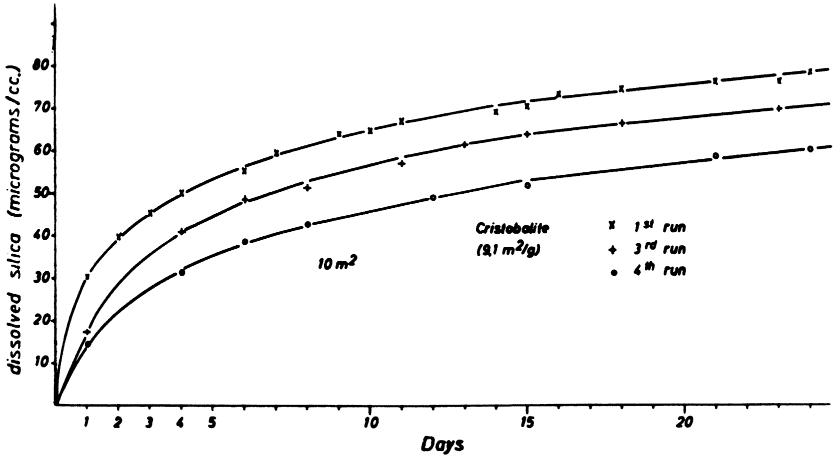

Figure 8. Repeated dissolution tests over 24 days on the same sample of cristobalite; 1.10 grams of 9.1 sq. meters/gram = 10 sq. meters of total surface area in 500 ml. of solvent.

None of the samples pretreated with NaOH solutions indicated such surface irregularities. All measurements with these preparations were quite reproducible.

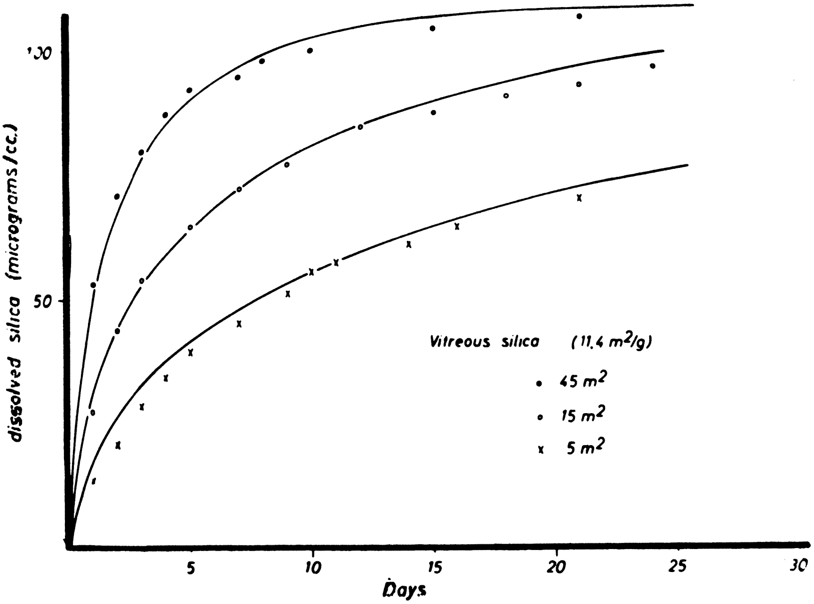

Figure 9. Dissolution patterns of vitreous silica of different quantities in suspension; 0.44 grams = 5 sq. meters, 1.32 gram = 15 sq. meters and 3.95 grams = 45 sq. meters of a powder of 11.4 sq. meters/gram in 500 ml. of solvent

Figure 9 gives some results obtained with vitreous silica. Three runs were made with 5, 15, and 45 sq. meters of total surface area in suspension. Apparently, the data indicate again the approach toward the two-phase equilibrium for polymeric silicic acid—*i.e.*, independent of the total amount of solid material, the equilibrium concentration of about 110 μgrams SiO_2/ml., as indicated in Figure 1, is approached in all three cases. Only the rate of dissolution is different, being determined by the size of the exposed surface area.

The experimental data cannot be interpreted in terms of a simple kinetic model of a zero-order hydrolysis competing with a first-order condensation of SiO_4 tetrahedrons. This is apparently because the interaction of silicic acid and the silica surface involves several different steps. At the silica surface the Si—O—Si bondings must be split by hydrolysis at an average of two bondings per SiO_4 tetrahedron. During this stage, a hydrated silicic acid molecule is formed which is still adsorbed on the surface. In a second stage, the molecule is then released into the solvent. Likewise, an adsorption stage precedes a random condensation of silicic acid onto the surface of vitreous silica. Accordingly, the following theoretical model was used, which proved to agree well with experimental data.

The model involves four basic assumptions. First, it is postulated that an adsorbed phase of silicic acid exists on the particle surface, the equilibrium of which can be expressed by a Langmuir isotherm (Equation 1, symbols are defined in table of nomenclature).

$$n_{ads} = \frac{n_0 bc}{1 + bc} \qquad (1)$$

The second assumption is that hydrolysis occurs only on sites not occupied by adsorbed silicic acid:

$$\frac{dn_H}{dt} = (n_0 - n_{ads})ke^{-\frac{A}{RT}} \qquad (2)$$

Further, the adsorption equilibrium is assumed to be established rapidly relative to the time required for the other processes. In this case the Langmuir isotherm can be inserted in Equation 2, leading to Equation 3.

$$\frac{dn_H}{dt} = \frac{n_0}{1 + bc} ke^{-\frac{A}{RT}} \qquad (3)$$

Finally, the fourth assumption requires that condensation occurs for adsorbed molecules only:

$$\frac{dn_c}{dt} = -n_{ads}k'e^{-\frac{A'}{RT}} \qquad (4)$$

Since the temperature is assumed to be constant, and no energetic evaluations are intended, the terms in Equation 5,

$$K = ke^{-\frac{A}{RT}} \text{ and } K' = k'e^{-\frac{A'}{RT}} \qquad (5)$$

may be used throughout the further calculations, and the dissolution rate can be established from the basic assumptions as shown in Equation 6.

$$\frac{dn}{dt} = \frac{dn_H}{dt} + \frac{dn_c}{dt} = \frac{n_0}{1 + bc}(K - K'bc) \qquad (6)$$

Taking into account the solvent volume, V, and the total silica surface area, F, the concentration, c, of silicic acid can be expressed as

$$c = \frac{F}{V}\int_0^t \frac{dn}{dt}\,dt - \frac{n_0 Fbc}{V(1 + bc)} + c_a \qquad (7)$$

By differentiation, an expression is obtained which relates the surface concentration changes to volume concentration changes:

$$\frac{dn}{dt} = \left\{\frac{V}{F} + \frac{n_0 b}{(1 + bc)^2}\right\}\frac{dc}{dt} \qquad (8)$$

We finally arrive at the differential equation:

$$\frac{dc}{dt} = \frac{n_0(K - K'bc)(1 + bc)}{\frac{V}{F}(1 + bc)^2 + n_0 b} \tag{9}$$

which has the analytical solution

$$t = \frac{c_e}{K}\left\{\frac{b\ln(1 + bc)}{1 + bc_e} - \frac{Vbc}{n_0 F} - \frac{bn_0F + V(1 + bc_e)^2}{n_0F(1 + bc_e)} \ln\left(1 - \frac{c}{c_e}\right)\right\} \tag{10}$$

where c_e is the equilibrium concentration for the two-phase system silicic acid–polymeric precipitate defined as

$$c_e = \frac{K}{bK'} \tag{11}$$

From this theoretical model, the three curves shown in Figure 9 have been computed by utilizing experimental data and, if not available, theoretically reasonable values for the parameters c_e, n_0, b, and K. The experimental value of 110 μgrams SiO_2/ml. was used for the equilibrium concentration c_e, a value of 600 μgrams SiO_2/sq. meter was taken for the surface concentration n_0 in accordance with a mean value of 10 μmoles/sq. meter for the adsorption sites on silica surfaces (*18*), and the values for the Langmuir constant b and the kinetic dissolution constant K were varied to match the experimental data. With b = 0.7 ml./μgram, indicating a significant adsorption at low silicic acid concentrations, and K = 30 day^{-1} corresponding to a relatively high hydrolysis rate, the curves and the experimental data were in good agreement.

The simple theoretical model does not account for whether or not silica gel and vitreous silica have the same concentration, c_e. As mentioned before, the experimental value of c_e may well constitute a supersaturated state with regard to vitreous silica, although experimental data on aging suspensions of silica gel did not indicate this and remained unchanged in oligomeric silicic acid concentration for as long as 8 months. However, a comparison with the corresponding data of quartz tests will give some more clues about the general pattern.

Figure 10 gives results obtained with quartz samples of various grain size as indicated by the different specific surface areas. Although these surface values differ by a factor of 20, the differences in the dissolution pattern for equal areas of exposed surface are barely significant. This indicates again that no difficulties in interpreting the data arise from special effects of disturbed surface layers or small particle sizes.

In all test runs final concentrations between 11 and 13 μgrams SiO_2/ml. were obtained, which apparently are close to the saturation concentration for quartz suspensions as suggested by van Lier *et al.* (*22*). Thus, it was tentatively assumed that the catalytic action of the solution used in this study would not only effect hydrolysis and recombination, but also the geometric rearrangement of Si—O—Si bondings—*i.e.*, facilitate the growth of quartz. In this case, no supersaturation phenomena would be involved, and the previous theoretical model would also hold in a case where a regular rather than a random condensation should occur. The curve in Figure 10 was computed for a saturation concentration c_e in the presence of quartz of 12 μgrams SiO_2/ml. (22), a kinetic dissolution constant K of 1.7 day^{-1}, and the same Langmuir constant b as used in the experiments with vitreous silica. The agreement with experimental data seems good.

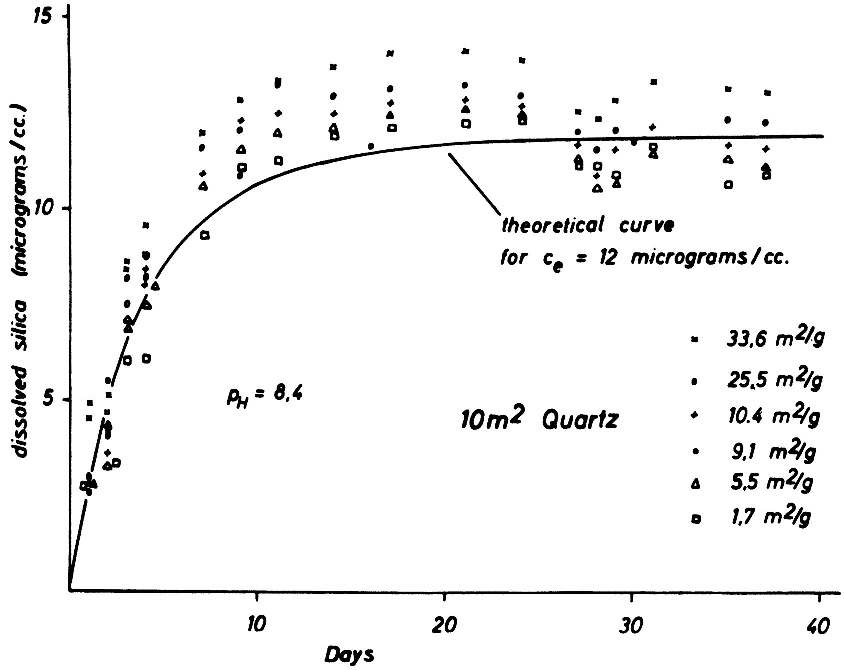

Figure 10. Dissolution patterns obtained with quartz samples of different specific surface area. Total surface area suspended in 500 ml. of solvent is 10 sq. meters

However, there is experimental evidence that despite the low constant concentrations in Figure 10 the final state after several weeks does not represent a reversible equilibrium. This became apparent in a test designed to approach the final silicic acid concentration of quartz suspensions from higher concentrations. Figure 11 shows the results of three tests with quartz suspensions of 5, 15, and 45 sq. meters of total surface area, respectively. At the beginning of the tests the solvent contained 83 μgrams SiO_2/ml. Although the silicic acid concentration dropped in all tests, the curves levelled out at different concentrations depending upon the size of the total surface area exposed. This indicates that the concentration decrease is essentially caused by adsorption of silicic acid on the quartz surface rather than by growth of quartz crystals. Hence, the same phenomenon will also greatly influence the dissolution pattern of quartz.

Apparently, the catalytic effect of chloride and hydroxyl ions found in silicic acid-polymeric precipitate equilibria does not significantly enhance crystal growth and probably might not even accelerate the growth of a dehydrated amorphous phase like vitreous silica. Accordingly, all dissolution patterns leading to a constant final concentration as in Figures 9 and 10 may be considered as indicating a steady state condition which is supersaturated to some extent with respect to the solid phase in suspension.

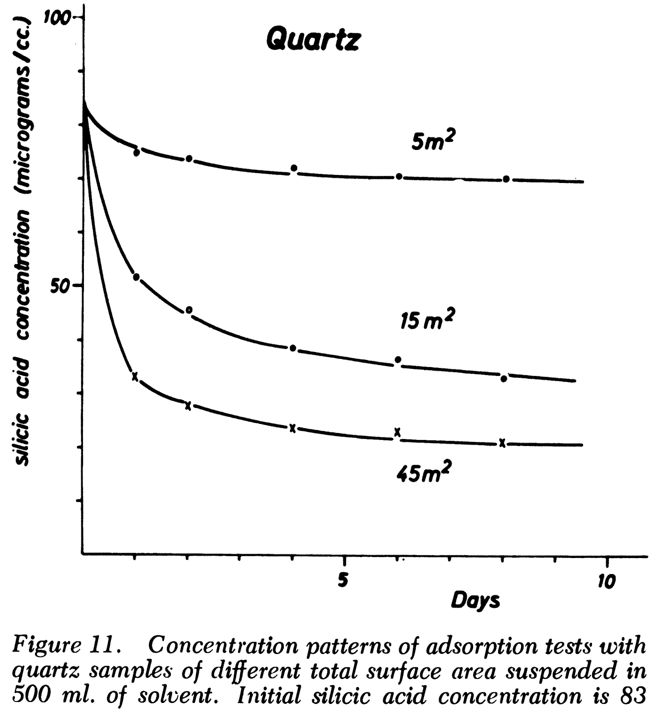

Figure 11. Concentration patterns of adsorption tests with quartz samples of different total surface area suspended in 500 ml. of solvent. Initial silicic acid concentration is 83 μgrams SiO_2/ml.

In view of this, the dissolution patterns of all other silica modifications were interpreted disregarding the condensation reaction. This seemed particularly adequate for stishovite, a high pressure, high temperature material, first produced in an autoclave by Stishov and Popova (*17*) in 1961 and detected at Meteor Crater one year later (*6*). The lattice structure corresponds to rutile so that the silicon has a coordination number of 6. Stishovite is insoluble in hydrofluoric acid, but is more soluble than any other crystalline modification in aqueous suspensions in the absence of hydrofluoric acid. The free energy level of stishovite is

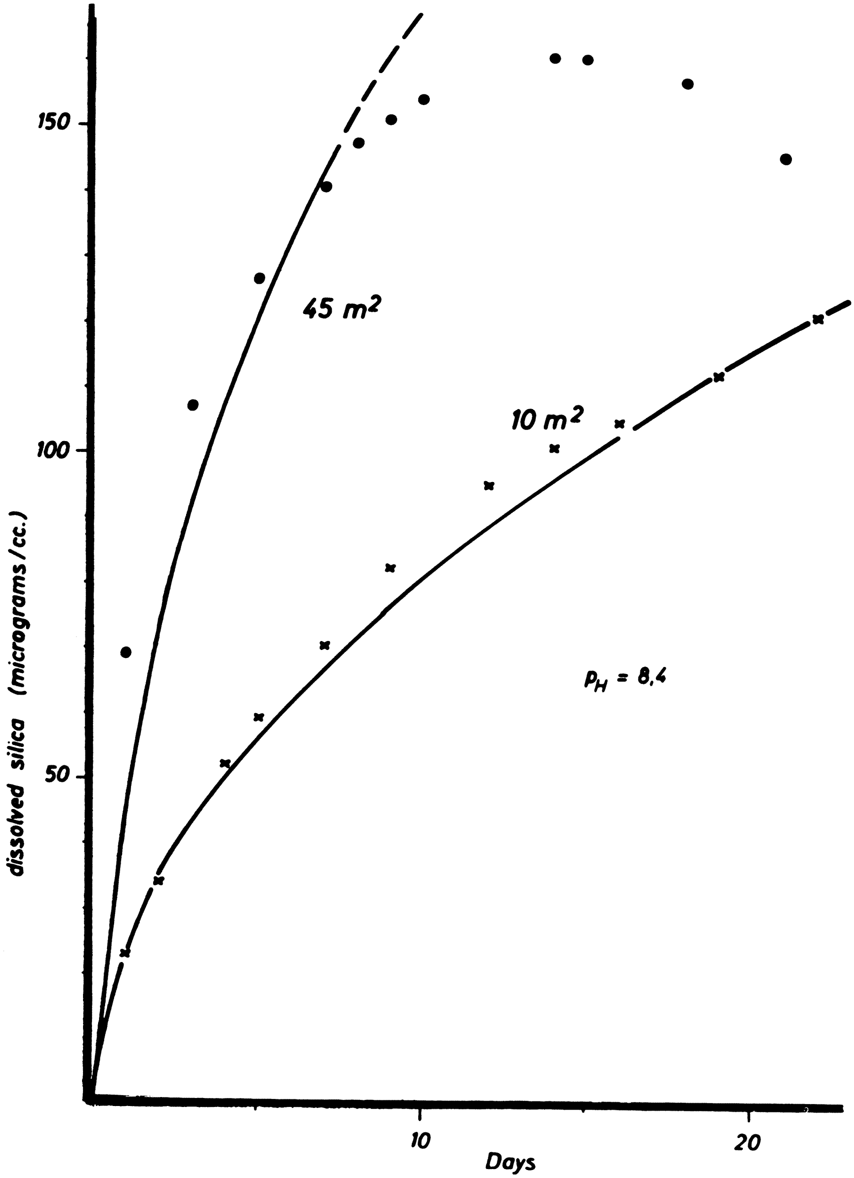

Figure 12. Dissolution patterns of two stishovite samples of 10 sq. meters and 45 sq. meters total surface area suspended in 500 ml. of solvent

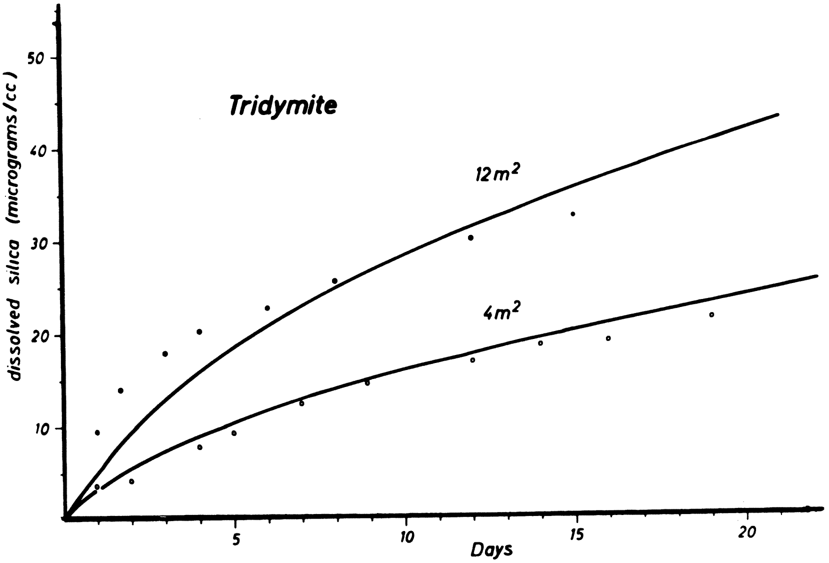

Figure 13. Dissolution patterns of two tridymite samples of 4 and 12 sq. meters total surface area suspended in 500 ml. of solvent

higher than that of vitreous silica, to which it readily converts at moderate temperatures (9). Hence, it was assumed that the adsorption of silicic acid on stishovite surfaces would be the same as for vitreous silica.

Figure 12 gives the experimental results and the theoretical curves according to this approach. For the test with a total surface area of 45 sq. meters, a supersaturation with regard to polymeric silicic acid is apparent, which, of course, is also not accounted for by the simple theoretical model. The curves were obtained for a Langmuir constant, b, of 0.7 ml./μgram and a dissolution constant K of 20 day^{-1}. The agreement with experimental points is satisfying under the circumstances.

Similar interpretations were tried for all other crystalline modifications. However, those theoretical curves matching experimental results of runs with low surface areas did not fit when properly applied to measurements with samples of high surface area and vice versa. Figure 13 gives an example for tridymite suspensions of 4 and 12 sq. meters of exposed surface area. The deviations are quite typical for all other metastable crystalline modifications.

There are several explanations for these deviations. As Figure 11 indicates, it takes some time to establish the adsorption equilibrium. Thus, the theoretical assumption concerning the adsorption equilibrium and resulting in Equation 3 may not be satisfied adequately. Here a higher initial silicic acid concentration would result. On the other hand, at high silicic acid concentrations the Langmuir isotherm is an idealization which will not properly represent experimental data of extensive adsorptive layers. Finally, the adsorption is not independent of the structure of the adsorbing surface. This is indicated by the results shown in Figure 14. In these tests, the different silica samples were suspended in a silicic acid solution of 78 μgrams SiO_2/ml. at pH = 8.4, and the decrease in concentration was measured for 5 days. As the data demonstrate there are different slopes for different substances, indicating that adsorption rates vary significantly for different modifications, quartz being the most effective. Hence the adsorption isotherms will show individual differences.

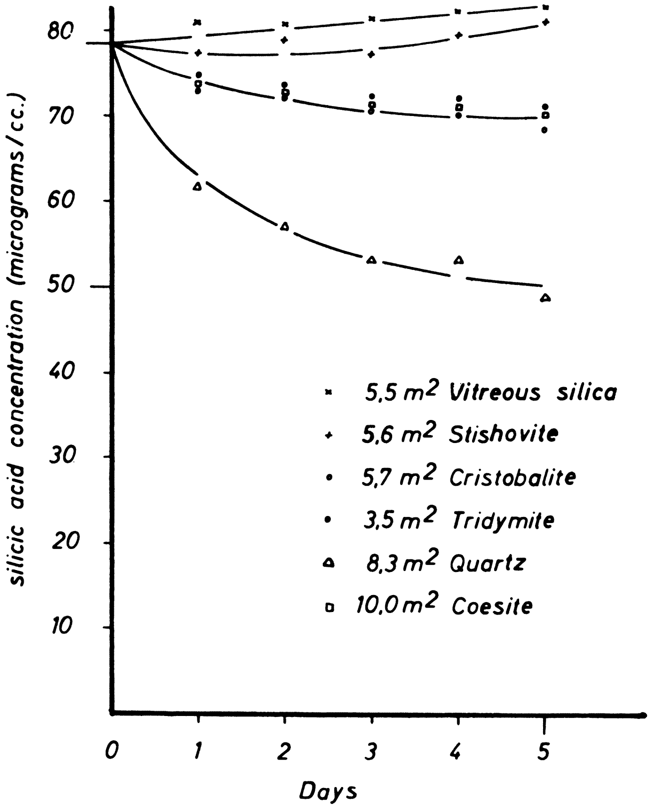

Figure 14. Concentration patterns of adsorption tests with different silica modifications. The exposed surface area is different for each sample; initial silicic acid concentration is 78 μgrams SiO_2/ml.

It is interesting, however, to compare the different dissolution constants, K, obtained with the simple Langmuir isotherm model with experimental data of dissolution rates over a 24-hour period. Figure 15 gives concentrations obtained consecutively with fresh solvent every 24

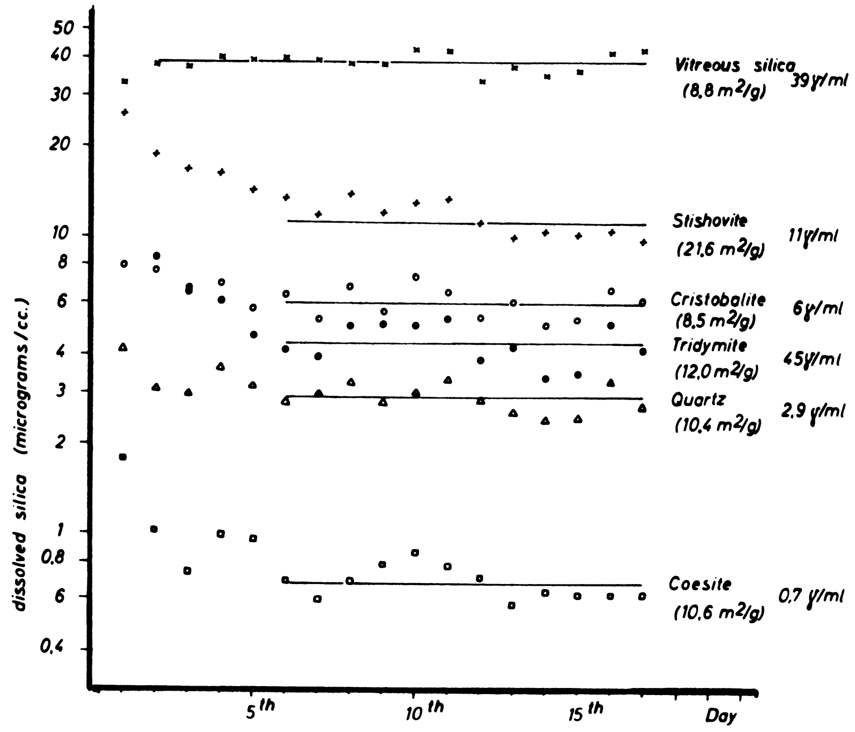

Figure 15. Daily release of silicic acid from 1 sq. meter of silica surface area into 50 ml. of fresh solvent (0.9% NaCl plus 0.1% $NaHCO_3$, pH = 8.4), repeated over 20 days for different silica modifications

hours. The average values rank from a high value for vitreous silica over stishovite, cristobalite, tridymite, and quartz to coesite. If these values are related to the lowest individual figure, they can be compared with the parameters of the theoretical model after rearranging them for a correspondingly relative scale. Table I gives such a comparison in the last two columns. Apparently, the agreement is fairly good for cristobalite, tridymite, quartz, and coesite, which all have low dissolution rates. The discrepancies for stishovite and vitreous silica are larger since the experimental dissolution period of 24 hours is already too long to be proportional to initial dissolution rates.

To investigate more thoroughly the dissolution patterns close to the asymptotic end of the concentration curve where the Langmuir isotherm becomes least reliable, long term runs were conducted with samples of extremely high total surface area (Figure 16). From these tests it becomes evident that all modifications establish specific final concentrations of silicic acid somewhere between 11 and 120 μgrams SiO_2/ml., suggesting a specific value for each modification. However, in view of the con-

Table I. Experimental and Theoretical Data of Dissolution Parameters

	K d^{-1}	K' d^{-1}	b $ml./\gamma$	n_0 γ/m^2
Quartz	1.7	0.20	0.7	600
Vitreous silica	90	1.17	0.7	600
Cristobalite	4.0	—	0.7	600
Stishovite	20	—	0.7	600
Tridymite	2.4	—	0.7	600
Coesite	0.4	—	0.7	600

[a] Solutions: 0.09% NaCl + 0.1% $NaHCO_3$;

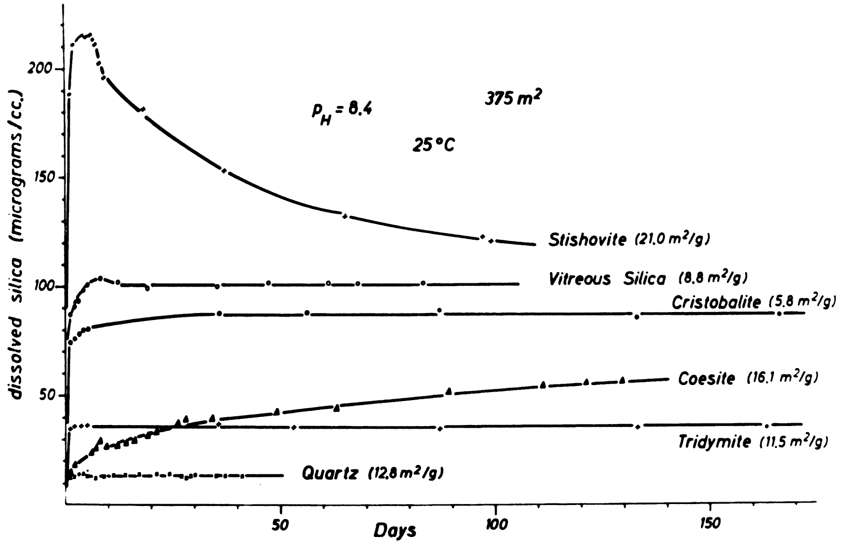

Figure 16. Dissolution patterns of different silica modifications; 375 sq. meters of total surface area suspended in 500 ml. of a solution of 0.9% NaCl plus 0.1% $NaHCO_3$ at $pH = 8.4$

centration patterns of Figure 14 neither of these final concentrations represents a reversible saturation equilibrium. As pointed out earlier, the adsorption properties are of decisive importance.

Apparently, in agreement with the second basic assumption of the theoretical model, adsorption can prevent further dissolution of silicic acid as soon as the adsorbed layer of silicic acid covers the whole surface

of Different Silica Modifications in Aqueous Solutions^a

c_e γ/ml.	$\frac{dn}{dt}_{exp.}$ γ/m² day	$\frac{dn}{dt}_{theor.}$ γ/m² day	$\frac{dn}{dt}_{exp.}$ rel.	$\frac{dn}{dt}_{theor.}$ rel.
12	145	1020	4.1	4.3
110	1950	54000	56	225
—	300	2400	8.6	10.0
—	550	12000	15.7	50
—	225	1440	6.4	6.0
—	35	240	1.0	1.0

pH = 8.4 (dissolution rate dn/dt for $c \approx 0$).

of the sample. Since the Langmuir isotherm will not reach this point for finite concentrations, it fails to represent experimental data involving extensive adsorptive layers.

If complete adsorptive molecular layers inhibit further dissolution of silicic acid, all experimental phenomena are explicable. In this case the final experimental concentration is not a saturation concentration which can be obtained also from high initial concentrations of silicic acid. Instead, the concentration will decrease only to the extent that the adsorption equilibrium is established. For sufficiently high initial concentrations of silicic acid and comparatively small surface areas, this will involve a multimolecular layer, whose equilibrium concentration is higher than the final experimental concentration of the self-inhibiting dissolution process.

Experimental evidence for this is given for quartz in Figure 11. Evaluating the concentration losses in these tests, we find that the decrease of silicic acid concentration levels off after about two or three molecular layers of acid have been adsorbed on the quartz surface. Similar results were obtained with the other crystalline modifications.

Therefore, for all crystalline forms of silica, a theoretical approach, using a more realistic adsorption isotherm is more promising. A suitable equation established by Brunauer, Emmett, and Teller (5) can be applied here:

$$n_{ads} = \left(\frac{n_0 b' c}{(c_e - c) + b'c}\right)\left(\frac{c_e}{(c_e - c)}\right) \qquad (12)$$

With this expression inserted into Equation 2, the final concentration c_f can be obtained by solving

$$\frac{dn_H}{dt} = 0$$

which results in

$$c_f = \frac{c_e}{1 + \sqrt{b'}} \tag{13}$$

This represents a simple theoretical expression of the final concentration obtainable from dissolution experiments. It implies a steady state condition in which low condensation rates are neglected. Condensation may or may not occur within the adsorptive silicic acid layer which will grow indefinitely at $c = c_e$, the equilibrium concentration of silicic acid in the presence of polymeric precipitates, thus precipitating all excessive silicic acid. The adsorption constant b' reflects the strength of the interaction between silicic acid and the particular silica modification. Values of b' for different forms of silica obtainable from Equation 13 and Figure 16 show variations by a factor of 10^3. However, owing to various simplifications, this approach provides merely a theoretical explanation of the phenomena encountered, similar to the semiquantitative way in which the van der Waals equation explains the state of real gases. Therefore, no thorough attempt has been made to match experimental data and theoretical parameters for this model. It seems evident, however, that the phenomena occurring in dissolution processes of silica are not beyond the scope of simple physical chemistry.

Conclusions

Once the surface irregularities of silica particles are removed by careful etching with sodium hydroxide, the dissolution patterns are quite reproducible and depend upon the total surface exposed in the experiment, the composition of the solvent, and the volume of the solution. The adsorptive properties and the hydrolysis rate for the different modifications then have a major influence on the dissolution pattern at room temperature. The adsorbed silicic acid finally ends further dissolution by forming an inhibiting adsorptive surface cover, thus creating specific final concentrations, which reproducibly can be reached by a dissolution process. On the other hand, starting from high concentrations of silicic acid, the concentration corresponding to the adsorption equilibrium will be established, which, depending upon the experimental conditions, might well be above the final concentration of the dissolution process.

In accordance with the thermodynamic consequences of the extreme activation energies associated with the formation of anhydrous silica modifications, the final experimental concentrations obtainable during dissolution of crystalline silica at room temperature are not two-phase equilibrium concentrations where the crystals act as solid phase. True solid members of such equilibria are randomly condensed SiO_4 tetrahedrons only—*i.e.*, some form of partially hydrated amorphous silica. This is apparently true also for quartz, although here the final concentration is of the magnitude of theoretical estimates of a two-phase equilibrium silicic acid—quartz. This may indicate, however, that the final concentrations obtained by a dissolution process do not imply a significant state of supersaturation with respect to the silica modification in suspension.

Nomenclature

A, A' = Activation energy of hydrolysis and condensation, respectively
b, b' = Adsorption constant
c = Silicic acid concentration
c_a = Initial concentration of silicic acid
c_e = Saturated concentration of silicic acid
F = Exposed surface area of silica
k, k' = Kinetic factors of surface reactions
K, K' = Rate constants of surface reactions (*see* Equation 5)
n, n_{ads} = Surface concentration of silicic acid
n_H = Silicic acid released by hydrolysis per surface unit
n_c = Silicic acid condensed per surface unit
n_0 = Surface concentration of complete layer of silicic acid
R = Gas constant
T = Temperature
t = Time
V = Volume of solvent

Literature Cited

(1) Alexander, G. B., Heston, W. M., Iler, R. K., *J. Phys. Chem.* **58,** 453 (1954).
(2) Baumann, H., *Beitr. Silikose-Forsch.* **35,** 5 (1955).
(3) Bergman, I., Cartwright, J., Caswell, C., *Brit. J. Appl. Phys.* **14,** 399 (1963).
(4) Bohn, E., Stöber, W., *Neues Jahrb. Mineral. Monatsh.* **1966,** 89.
(5) Brunauer, S., Emmett, P. H., Teller, E., *J. Am. Chem. Soc.* **60,** 309 (1938).
(6) Chao, E. C. T., Fahey, J. J., Littler, Janet, Milton, D. J., *Geophys. Res.* **67,** 419 (1962).
(7) Clelland, D. W., Cumming, W. M., Ritchie, *J. Appl. Chem.* **2,** 31 (1952).
(8) Clelland, D. W., Ritchie, P. D., *J. Appl. Chem.* **2,** 42 (1952).
(9) Dachille, F., Zeto, R. I., Roy, R., *Science* **140,** 991 (1963).
(10) Friedberg, K. D., *Beitr. Silikose-Forsch. Sonderband* **1,** 49 (1955).
(11) King, E. J., Nagelschmidt, G., *Proc. Pneumoconiosis Conf., Johannesburg,* 79 (1960).

(12) King, E. J., Nagelschmidt, G., "Die Staublungenerkrankungen," K. W. Jötten, W. Klosterkötter, G. Pfefferkorn, eds., Vol. 2, p. 84, Steinkopff, Darmstadt, 1954.
(13) Kitto, P. H., Patterson, H. S., *J. Ind. Hyg. Toxicol.* **24,** 59 (1942).
(14) Morey, G. W., Ingerson, Earl, *Econ. Geol.* **32,** 607 (1937).
(15) Scheel, L. D., Fleisher, E., Klemperer, F. W., *Arch. Ind. Hyg. Occupational Med.* **8,** 564 (1953).
(16) Stegeman, H., Fitzek, J., *Beitr. Silikose-Forsch.* **31,** 31 (1954).
(17) Stishov, S. M., Popova, S. V., *Geokhimiya* **10,** 837 (1961).
(18) Stöber, W., *Kolloid-Z.* **145,** 17 (1956).
(19) *Ibid.,* **147,** 131 (1956).
(20) Stöber, W., Arnold, M., *Kolloid-Z.* **174,** 20 (1961).
(21) Taylor, N. W., Doran, R. F., *J. Am. Ceram. Soc.* **24,** 103 (1941).
(22) van Lier, J. A., de Bruyn, P. L., Overbeek, J. Th. G., *J. Phys. Chem.* **64,** 1675 (1960).
(23) Weitz, E., Franck, H., Schuchard, M., *Chemiker-Ztg.* **74,** 256 (1950).

RECEIVED April 25, 1966.

8

The Nature of Inorganic Solute Species in Water

S. Y. TYREE, JR.[1]

University of North Carolina, Chapel Hill, N. C.

In the range of pH exhibited by most natural water and in the concentration range greater than millimolar few metal ions exist as simple hydrated cations, and relatively few oxyanions exist as simple monomeric species. The hydrated cations are good buffers toward bases, the metallate ions toward acids. As pH is raised in solutions of many hydrated cations, isopolycations are produced, and ultimately, hydrous metal oxides precipitate. As pH is lowered in solutions of many metallate ions, isopolyanions are produced, and ultimately, hydrous oxides precipitate. Salts of the intermediate isopolyions precipitate in some cases. Where the results are unambiguous, the nature of the intermediate species can be described. Kinetics are thought to have been neglected in studies of such solutions up to the present time.

In the past 20 years several physical inorganic chemistry laboratories have re-examined extensively the nature of the "simple" inorganic solutes in water. Substantial contributions to man's knowledge of the hydrolytic behavior of metal cations and metallate anions in water solvent have resulted. Various new techniques have been applied with varying degrees of efficacy. The details of the behavior, within specified conditions, of a number of solute ions are now matters of fact. In many more cases and over wider variations of conditions, all of the important variables which affect hydrolysis phenomena have not yet been identified.

We will attempt to describe broad areas of general agreement, list and comment briefly upon the techniques which have been employed, present in detail what is known of one or two solute systems within

---

[1] Present address: College of William and Mary, Williamsburg, Va.

narrow conditions, summarize—using specific examples—the variables considered important in hydrolysis phenomena, and consider the extrapolation to natural water chemistry. No attempt is made to survey comprehensively the state of knowledge of the hydrolytic behavior of all metal cations and metallate anions in water. Further the reader must bear in mind that most of the work done by physical inorganic chemists in this field has been done on solutions of metal solute concentrations greater than millimolar.

General Agreement

Metal cations, Me^{m+}, with the square root of ionic potential (7), $\sqrt{\phi}$, less than 3.2 exist as simple hydrated cations, $[Me(OH_2)_n]^{m+}$, only at low pH—*i.e.*, 1 or 2. As the pH of such solutions is raised, the hydrated cations are converted into isopolycations, $[Me_p(OH)_q(OH_2)_n]^{(pm-q)+}$. (From here on, waters of hydration will not be included in formulas since in most cases the numbers are not well established. In other words, $Me(OH_2)_n^{m+}$ will be abbreviated as Me^{m+} and $[Me_p(OH)_q(OH_2)_n]^{(pm-q)+}$ will be abbreviated as $[Me_p(OH)_q]^{(pm-q)+}$).

Many of the isopolycation-hydrated cation systems exhibit buffer capacity. For example, a solution, 0.04*M* in Ga^{3+} as the perchlorate, to which sufficient base has been added (as Na_2CO_3) so that the average gallium-containing solute species is $[Ga(OH)_{0.25}]^{2.75+}$, exhibits a pH of 2.23. When an additional 0.060 mole per liter of Na_2CO_3 is added to the solution, vigorous effervescence is observed, and the pH is raised to only 2.46. Clearly the base is bound by the gallium-containing cations, resulting in an "average" solute cation (*36*) of $[Ga(OH)_{1.75}]^{1.25+}$. Ultimately as more base is added to solutions of isopolycations, hydrous oxides or salts of isopolycations separate as heterogeneous solid phases.

Elements of $\sqrt{\phi}$ greater than 3.2 form simple metallate anions in solutions of high pH—*i.e.*, strongly alkaline solutions. As the pH of such solutions is lowered, isopolyanions are produced in many cases, ultimately yielding hydrous oxides, or salts of isopolymetallate ions as heterogeneous solid phases. Again, many of the isopolyanions exhibit buffer capacity.

A few metal ions—*e.g.*, gallium(III) ion, aluminum ion, tin(II) ion, in general those metal ions which have been described as amphoteric—are able to form both isopolycations and isopolyanions.

Techniques Used

Most of the techniques evolved by workers investigating the nature of electrolytic solutions from 1900–1950 have been applied, with varying degrees of success, in studying aqueous ion hydrolytic phenomena. In addition the physical techniques of the organic polymer chemists have been used.

Potentiometric Titration. This is probably the simplest and most straightforward way to detect aggregation coincident with hydrolysis. In practice the pH change in a solution of a given metal ion is followed carefully as base (or acid) is added, keeping the ionic strength of the solution high and constant (2 or $3M$ $NaClO_4$ or $LiClO_4$) and keeping the total metal ion solute constant. A family of such titrations over as wide a range of total metal solute concentrations as possible is obtained. In those cases where a reversible metal ion indicating electrode is known, the changes in unhydrolyzed metal ion are followed simultaneously with pH measurement. The supporting electrolyte minimizes the effect of changes in ionic strength on measured values of e.m.f. A short, yet adequate description of the treatment of the data is given by Sillén (*39*). At best, equilibrium constants relating solute hydrolysis products and the hydrated ion precursor can be obtained. At worst the average solute stoichiometry can be obtained, which is a necessary preliminary to several of the other techniques to be discussed. In general precise, reproducible data cannot be obtained from solutions containing less than a millimolar total metal solute.

The most effective proponent and practitioner of the technique has been Sillén. Contributions from him and his many co-workers in Stockholm are clearly more numerous than those from any other group studying inorganic hydrolysis in the past 15 years (*39*).

Partition Chromatography. Liquid-liquid extraction and ion-exchange techniques have both been used to infer the nature of cationic and anionic species. In both techniques, the ionic species are partitioned between two phases. The mass and/or charge balance permits one to determine solute charge from batch equilibration experiments alone. If the solute species are of several kinds, chromatograms will separate the species into fractions. In interpreting the experimental data, one must assume that the solute species cross phase boundaries unchanged. In my opinion the foregoing assumption has not always been justified.

An unambiguous example of determining the charge on a polymeric cation by the ion-exchange method is the work of Ardon and Plane (*3*) on $[Cr_2(OH)_2]^{4+}$. Using radioactive tracer metal ions, these techniques have been used in total metal concentrations as low as micromolar (*34*).

Crystal Analysis. Of course, the elemental and crystal structure analyses of crystals obtained from solutions have been used to infer structures of ionic solute precursors. Thus, Lindqvist's x-ray crystal structure analysis of $(NH_4)_6Mo_7O_{24} \cdot 4\ H_2O$ shows that the crystals contain the structural unit, $Mo_7O_{24}{}^{6-}$. Lindqvist also showed that the solutions from which the crystals are grown do contain essentially monodisperse heptamolybdate anions (*23*). On the other hand Sillén's early work on Bi(III) was interpreted in terms of a polydisperse series of isopolycations (*14*) $[Bi_{n+1}O_n]^{(n+3)+}$, which were considered as possible precursors of the $(BiO)_n$ sheets found in the crystal structures of some bismuth oxide halides. Subsequently one of Sillén's associates, Olin, found that, within limits, the solute hydrolysis product of Bi^{3+} is essentially monodispersed $[Bi_6(OH)_{12}]^{6+}$ ion.

Aveston and Johnson (*5*) report that the Raman spectra of crystals of $K_8Ta_6O_{19} \cdot 16\ H_2O$ and of saturated solutions of the crystals are the same. The light-scattering and ultracentrifuge techniques agree on the identification of the solute isopolyanion, $Ta_6O_{19}^{8-}$.

Under this category of techniques it should be noted that one is able to achieve identification of principle species only.

Diffusion. The rate of self-diffusion of a metal solute species has been used to infer the degree of aggregation of the solute species, in accordance with the postulate that the diffusion coefficient is inversely proportional to the square root of the ionic weight of the solute. An example is the study of isopolytungstates by Anderson and Saddington (*1*). However, Baker and Pope (*6*) showed that two heteropolyions, of essentially the same structure, yet differing in ionic weight by about 1000 units, have essentially the same diffusion coefficients. Thus the interpretation of diffusion data in most cases needs to be reconsidered.

Spectrophotometry. In general the edge of continuous absorption (charge transfer spectra) for solutions of both metal cations and metallate anions undergoes a red shift coincident with isopolyion formation. As well, the *d-d* spectra of transition metal ions are shifted by isopolyion formation (not always a red shift in this case). In optimum cases, equilibrium constants relating the parent solute ion and the hydrolysis product solute ions can be obtained. The work of Milburn and Vosburgh (*28*) on the Fe^{3+} hydrolysis is an excellent example.

Cryoscopy. Souchay (*40*) has summarized the application of fused salt cryoscopy to ionic solutes. Obviously two limitations are inherent in this method. Under ordinary pressures, measurements are possible at only one temperature—namely that of the transition point (*e.g., ca.* 32.38°C. in the case of $Na_2SO_4 \cdot 10\ H_2O$). Secondly, the solute is being examined in "solutions" of high ionic strength only. Isopiestic vapor pressure measurements have been used as a variation, which, in principle, eliminate both limitations. However, it does not appear that it is as yet possible to analyze such data to yield equilibrium constants (*33*). Furthermore, Tobias has cast doubt upon the inherent accuracy of the method when the polyions contain more than 3 or 4 metal ions (*41*).

Intrinsic Viscosity, Ultracentrifugation, and Light Scattering. These three techniques have been used extensively by workers investigating the properties of organic polymers and organic polyelectrolytes. Their use in studies of inorganic hydrolytic solutes has been much less extensive. By analyzing the variation of solution viscosity with solute concentration, it is possible to estimate several properties of a solute—*e.g.*, degree of aggregation and magnitude of charge. In studies of inorganic hydrolytic phenomena this method has been essentially limited to phosphate and silicate solutions. A good review of these areas has been included in Gimblett's recent book (*13*).

Kraus *et al.* (*19*) have shown that sedimentation profiles of solutions which have been centrifuged (10,000–25,000 r.p.m.) to equilibrium can be analyzed to yield good estimates of the degree of aggregation of the solute metal ion hydrolysis aggregates, a measure of the degree of polydispersity of hydrolysis products, and an estimate of the charge on the solute species. Many cation and anion hydrolysis systems have been investigated by this technique. An excellent example is the recent work of Hentz and Johnson on thorium solutions (*15*).

Debye and Naumann first showed that Rayleigh scattering could be used to estimate the molecular weight of low molecular weight solutes in aqueous solution (*9*). Since then the technique has been used to estimate the degree of aggregation in solute metal hydrolysis products for many cation and anion systems (*42*). A recent example is the study of thorium reported by Hentz and Tyree (*16*). The reader is urged to compare the results of the two studies on the same system.

None of these techniques is likely to develop so as to permit one to evaluate equilibrium constants in a polydisperse system. The ultracentrifuge is able to distinguish between monodisperse and polydisperse solutes. The light-scattering method does not give as clear a distinction between the two. Both are applicable in the range of concentration of 2–200m*M* total metal ion. The light-scattering method is easily adapted to measuring rates at which aggregation reactions take place.

Structure Determination. Levy and co-workers have shown that it is possible to elucidate the structure of solute isopolyions (*22*) in those cases where the hydrolysis product is essentially monodisperse and soluble enough to permit preparation of 2–4*M* solutions, using x-ray diffraction.

Nuclear Magnetic Resonance. Taube (*18*) has shown that two different chemical shifts in the ^{17}O NMR spectrum of $Cr_2O_7^{2-}$ solutions are observed, in the approximate ratio of non-bridging O to bridging O. However, 2*M* solutions of dichromate were used in water enriched to 1.4% H_2O^{17}, and no shifts were observed in several other cases studied.

Coagulation Effects. Matijevic and co-workers have shown that in optimum cases the effect of hydrolyzed metal ions upon the coagulation and reversal of charge of lyophobic colloids can be useful in identifying the hydrolyzed metal ion species (*25*). The same group has made the point that the critical coagulation concentrations (c.c.c.) are based upon the amounts of electrolyte added and that at the low concentrations necessary for highly charged ions, appreciable percentages of the electrolyte may be adsorbed on the colloid surface (*26*). If this is true, the actual values of c.c.c. may be much less than supposed. Furthermore, the actual solubilization and reversal of charge on the colloid takes place at concentrations only slightly greater than c.c.c. A limiting feature of this method is that it yields useful data on hydrolyzed metal ions only at concentrations well below 0.001*M*.

Examples of Techniques Used

Pb(II) Ion Hydrolysis. Below pH 8 there is general agreement upon the detailed solution chemical behavior of Pb(II) in perchlorate media. Olin (*31*), using potentiometric titration, has proposed the following series of equilibria and constants, all in 3*M* $NaClO_4$.

$$\begin{aligned}
Pb^{2+} + HOH &= [Pb(OH)]^{+} + H^{+} & K_{11} &= 1.26 \times 10^{-8}\\
4\,Pb^{2+} + 4\,HOH &= [Pb_4(OH)_4]^{4+} + 4\,H^{+} & K_{44} &= 5.6 \times 10^{-20}\\
3\,Pb^{2+} + 4\,HOH &= [Pb_3(OH)_4]^{2+} + 4\,H^{+} & K_{34} &= 1.35 \times 10^{-23}\\
6\,Pb^{2+} + 8\,HOH &= [Pb_6(OH)_8]^{4+} + 8\,H^{+} & K_{68} &= 7.2 \times 10^{-43}
\end{aligned}$$

In the 0.1–1*M* total Pb(II) region the important solute species are Pb^{2+}, $[Pb_4(OH)_4]^{4+}$, and $[Pb_6(OH)_8]^{4+}$. Furthermore, it is possible to calculate the concentrations of the several solute species present for a given set of conditions. For example, consider solutions of Pb^{2+} and 2 ClO_4^- to which sufficient base has been added so that the average number of OH^- ions bound per Pb^{2+} (hydroxyl number) is 1.00. Using Olin's constants, the fractions of total Pb(II) existing in the different solute species are calculated for three total Pb(II) concentrations in Table I.

Table I. Fraction of Total Pb(II) Existing as Different Species

Total Pb(II) molarity	Pb^{2+}	$[Pb(OH)]^{+}$	$[Pb_4(OH)_4]^{4+}$	$[Pb_3(OH)_4]^{2+}$	$[Pb_6(OH)_8]^{4+}$
0.100	0.08	0.003	0.81	0.02	0.10
0.010	0.13	0.02	0.64	0.09	0.21
0.001[a]	0.19	0.08	0.30	0.28	0.21

[a] pH 7 assumed for this concentration.

Obviously at higher than 0.10*M* Pb(II) the solute is essentially $[Pb_4(OH)_4]^{4+}$, for hydroxyl number 1.00 solutions. Both the light-scattering (*16*) and the ultracentrifugation (*10*) techniques confirm this.

As a matter of fact the structure of the isopolycation has been reported by Esval (*11*) as shown in Figure 1.

At low hydroxyl numbers Olin (*32*) subsequently agrees with the earlier findings of Faucherre (*12*) that $[Pb_2(OH)]^{3+}$ species are necessary to explain the potentiometric titration data.

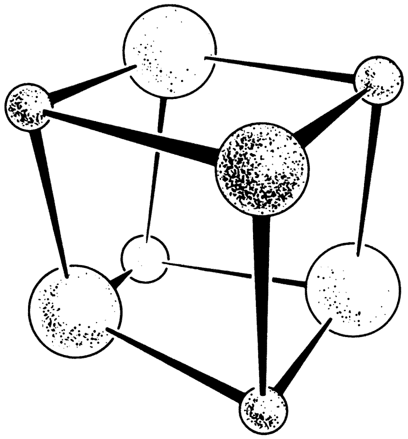

E. O. Esval, Ph.D. Thesis

Figure 1. Model of Polymeric Unit $[Pb_4(OH)_4]^{4+}$. *Lead atoms are designated by small circles. Large circles represent assumed positions for oxygen atoms* (11)

Bismuth Ion Hydrolysis. In the hydroxyl number range of 0.00–2.00, there is general agreement that the important Bi(III) species in perchlorate media are Bi^{3+} and $[Bi_6(OH)_{12}]^{6+}$ ions. For the equilibrium $6\ Bi^{3+} + 12\ HOH = [Bi_6(OH)_{12}]^{6+} + 12\ H^+$, Olin (*30*) reports log $K_{6,12} = 0.33$ in 3*M* perchlorate whereas Tobias (*41*) finds log $K_{6,12} = -0.53$ in 1*M* perchlorate. Solutions in which the hydroxyl number approaches 2.0 show hexameric bismuth cations by both ultracentrifugation (*17*) and light scattering (*44*). The structure of the isopolycation has been determined by Levy and co-workers (*22*). It has cubic symmetry, the six bismuth atoms occupying the centers of the faces of an imaginary cube, with the oxygen atoms lying at the midpoints of the 12 edges.

Important Variables

pH. Unfortunately it is rarely possible to prepare solutions of a given cation or metallate ion and vary pH conditions carefully over all the important pH ranges. Thus, in the bismuth studies as the hydroxyl

Published on January 1, 1967 on http://pubs.acs.org | doi: 10.1021/ba-1967-0067.ch008

number is raised above 2.0 (the pH being raised), heterogeneous phases separate. Furthermore, precision of pH measurement is not yet good enough to use the potentiometric technique for solutions of hydrolyzing species at total metal ion concentration below *ca.* $10^{-3}M$.

Solution Medium. It is desirable to carry out most physical measurements in 1–3*M* $NaClO_4$ in order to minimize two complications. First, activity coefficients of the hydrolyzed ionic species will not be subject to significant fluctuations in a medium of high, constant, ionic strength. Second, the anion perchlorate is thought to have insignificant ability to coordinate to the metal ions. Of course, an equilibrium constant involving highly charged ionic species might be expected to be a function of ionic strength, the more highly charged species being favored by the medium of higher ionic strength. Such seems to be the case among the few systems for which data are available at two or more ionic strengths (and the same supporting electrolyte). Thus, Olin (*31*) reported two sets of constants for the Pb(II) hydrolysis system, the differences being in the expected direction. Tobias' constant (*41*) for $[Bi_6(OH)_{12}]^{6+}$ in 1*M* ClO_4^- is smaller than Olin's constant (*30*) by almost a factor of 10 for the same system at 3*M* ClO_4^-. In their study of the Fe(III) hydrolysis, spectrophotometrically, at low hydroxyl numbers, Milburn and Vosburgh (*28*) included a fairly extensive investigation of the effect of ionic strength upon equilibrium constants. For the reaction $Fe^{3+} + HOH \leftrightharpoons [Fe(OH)]^{2+} + H^+$, $K_{1,1} = 2.89 \times 10^{-3}$ at $\mu = 0.10$; $K_{1,1} = 1.28 \times 10^{-3}$ at $\mu = 3.0$. For the reaction $2[Fe(OH)]^{2+} \leftrightharpoons [Fe_2(OH)_2]^{4+}$, $K_d = 170$ at $\mu = 0.10$ and 1600 at $\mu = 3.0$. In each equilibrium, the species with higher charge is favored by the medium of higher ionic strength, and a value of $K_d = 30$ at $\mu = 0$ was obtained by extrapolation.

Temperature and Time. It is my opinion that these two variables are of the utmost importance in any consideration of the hydrolytic behavior of metal cations and metallate anions. Furthermore, as yet it is impossible to separate the two variables in all cases. The reasons for these two statements will become apparent by considering several specific cases.

ANTIMONY (V). In a series of papers, Lefebvre and Maria (*21*) have shown that the hydrolysis of $Sb(OH)_6^-$ depends greatly on time at 25°C. Spectrophotometry, pH titration curves, and iodometric titration curves were used in the studies. It is apparent that dodecantimonates are formed in several stages of protonation when HCl is added to solutions of $(CH_3)_4NSb(OH)_6$ up to an H/Sb ratio of 0.7. However, the particular species formed depends upon the age of the solution. Solutions of the same composition but aged for different time intervals exhibit strikingly different rates of reaction with iodide and with hydroxide and have different extinction coefficients in the ultraviolet region. It is important to note that solution aging proceeds in at least three stages; the first is complete in about 2 hours, the second takes about a week, and the third continues over many months. It was concluded on the basis of one experiment that heating to 67°C. accelerates the aging process, but it cannot be regarded as certain that it did not (alternatively and/or simultaneously) result in the formation of still other species which were not important at 25°C.

ZIRCONIUM AND HAFNIUM. There is general agreement that Zr(IV) and Hf(IV) solutions in the 0.1–3*M* H^+ range are hydrolyzed to aggregates containing from 3 to 6 metal atoms per isopolycation (*2, 20, 29, 46*). On the other hand, there is no agreement in greater detail. It is not certain how many species do exist in Zr(IV) and Hf(IV) solutions at high acidities, and consequently no attempts have been made to estimate the distribution of metal among several species, as is possible for Pb(II) and Bi(III). At lower acidities—*i.e.*, solutions of $ZrOCl_2 \cdot 8\ H_2O$ in an indifferent electrolyte, the situation is even less well-defined. Some years ago it was found that solutions of Zr(IV) in Cl^- media at hydroxyl number of 2.5 underwent a 30% increase in turbidity on standing at 25°C. for one year (*37*). In the same series of experiments solutions of $ZrOCl_2 \cdot 8\ H_2O$ in pure water exhibited a 10-fold increase in turbidity upon refluxing for 4 hours and deposited a heterogeneous phase upon refluxing for an additional 2 hours. More recently a detailed study of the behavior of Hf(IV) solutions in Cl^- media was undertaken. An example of what was found is shown in Figure 2. The reciprocal of the degree

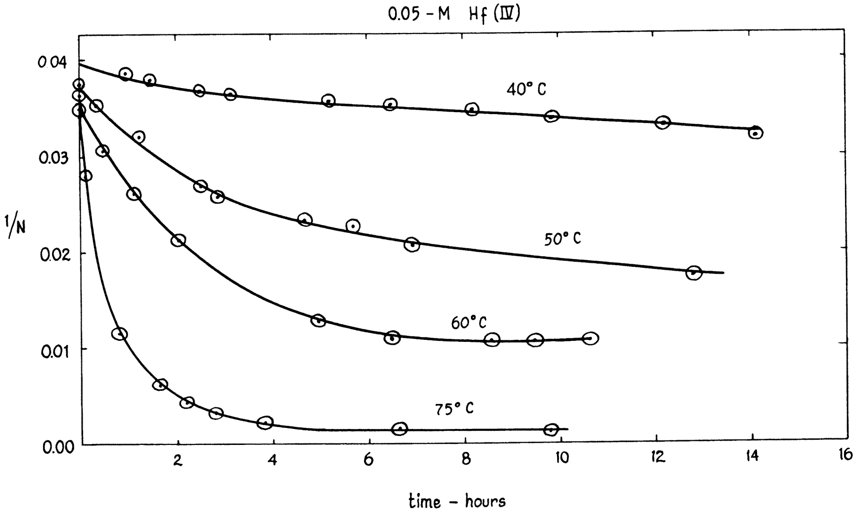

Figure 2. Reciprocal of the degree of aggregation of solute hafnium species vs. time

of aggregation of Hf(IV) *vs.* time is plotted. The particular solution is 0.05*M* Hf (made up from $HfOCl_2 \cdot 8\ H_2O$, no acid added) and NaCl added to make $[Cl^-] = 1.0M$. Two separate phenomena or a combination of the two are likely explanations. First, the temperature coefficient of the equilibrium constants can be such as to make much larger aggregates important at higher temperatures. The second possibility is that even at room temperature the solutions are unstable with respect to larger aggregates and that the half-time of approach to equilibrium is of the order of magnitude of years, perhaps many years. The second explanation is strengthened somewhat by the fact that the solutions at 75°C. retain their turbidity upon cooling to 25°C. for some months.

TUNGSTEN. When the normal tungstate is hydrolyzed by adding strong acid to a H^+/WO_4^{2-} ratio of 1.5, it is considered that the tungsten-containing species is essentially monodisperse dodecatungstate (*4, 8*). However, important time effects were discovered by the fact that the Aveston (*4*) study was done at 50°C., whereas the light-scattering study (*8*) was undertaken initially at 25°C. Solutions prepared at 25°C. obviously contain larger solute species, as yet unidentified, which are quite long-lived. Only after heating at 50°C. for 6 days do the solutions "appear" to have reached equilibrium. At the same time, solutions of WO_4^{2-} which are acidified to the same H^+/WO_4^{2-} ratio with buffers of acetic acid contain none of the larger, unidentified species (Figure 3).

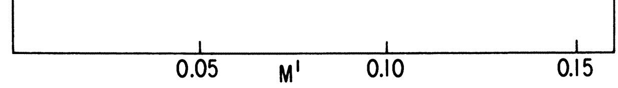

Inorganic Chemistry

Figure 3. Reciprocal of degree of aggregation of solute tungstate species vs. total tungsten molarity: △, $z' = 0$; ○, $z' = -0.2$; □, $z' = -0.4$; ——, *after heating to 50°C.;* - - - -, *25°C. solutions*

ALUMINUM. Matijevic and Tezak (*27*) found that solutions of Al^{3+} in 10^{-4} to $10^{-6}M$ range were unstable (unless acid is added) and that such solutions age unpredictably with time. They can be artificially aged by heating to 90°C., producing rather large polymeric cations which are difficult to return to simple Al^{3+} with acid at room temperature. At 10^{-1} to $10^{-3}M$ concentration the author and co-workers are currently engaged in studying the behavior of Al^{3+} as pH is increased and $Al(OH)_4^-$ as pH is lowered. In the acid solutions up to hydroxyl number 2.0 in the temperature range 25°–75°C. no time effect has been observed—*i.e.*, equilibrium is approached rapidly. On the other hand, at hydroxyl numbers in the range 2.25–2.40 instability is noted, and unpredictability is all that can be reported now. Occasionally a solution can be prepared for study. Alternatively the replication of the attempt to prepare the solution results in a gel.

GALLIUM. In the earlier quoted study of gallium hydrolysis (*36*), solutions at hydroxyl number 1.5 deposited small amounts of precipitate in days, those at hydroxyl number 1.75 in 2 weeks, those at hydroxyl number 2.00 in 4 months. Certainly the results reported cannot at all represent the equilibrium state.

History of the Solution. From the foregoing it follows that the measurements made on a solution may reflect its history a great deal, thus accounting for the inability of different workers to agree upon details in certain cases. A solution at room temperature may contain highly aggregated isopolyions as the result of a previous history of heating or if parts of it have been subjected to localized, large fluctuations in pH. Even less obvious differences in history can be important. Lefebvre (*21*) finds an appreciable difference in the behavior of isopolyantimonates in Na^+ media on the one hand and in $(CH_3)_4N^+$ media on the other. Walmsley (*45*) reports that the order of adding reagents in preparing solutions of isopolymolybdates greatly affects the time required for the solutions to come to equilibrium.

Extrapolation to Natural Water Chemistry

The chemistry of the several elements, as it occurs in natural aqueous systems, has begun to recognize some of the above-mentioned physical chemical studies, most of which have been made under carefully controlled conditions. There seem to be two important features of natural water chemistry. The first is almost always true—*i.e.*, that the pH is in the range of 6.5–8.0. The second, perhaps not so general, is that the concentrations of elements is quite low, $10^{-6}M$. A third factor of almost equal importance is that nature does not provide solutions of one or even just a few elements. For example, most natural waters will contain dissolved CO_2 and O_2. Thus, in extrapolating to natural water conditions the foregoing findings on Pb^{2+}, one would predict that at $10^{-6}M$ Pb^{2+} will be the predominant species below pH 7. However, in the presence of dissolved CO_2, carbonates of lead precipitate, and all of the results quoted above for the Pb^{2+} system at high hydroxyl number have been obtained only by rigorously excluding CO_2. Lastly, it will be difficult to ascertain in detail the previous history of natural water solutions.

In general one is justified in saying that for cationic systems, the higher the pH (going toward natural water), the larger will be the isopolycations formed. (The reverse is true for anionic aggregation.) On the other hand, the lower the concentration, the more important monomers will be. However, it is just now becoming apparent that the higher the pH, the longer it takes for the system to come to equilibrium. It is not beyond the realm of possibility for some systems in natural water to approach equilibrium with half-times of 10^n years. Both high dilution and proximity to neutrality (in the sense of pH) appear to lengthen the half-time. Such slow processes are almost certainly responsible for natural opal growth (*38*). Rubin (*35*) has found that at natural water concentration levels the precipitate flotation and ion flotation behavior of certain elements can be interpreted in terms of isopolycation species. Possibly, many inorganic solutes have not had time to come to equilibrium, and thus nonequilibrium—*i.e.,* kinetic—models might well be considered for natural water systems. Even biochemical chelating agents may be able to remove metals as chelates only slowly from isopolyhydroxometal ions.

There is every justification for using true equilibrium constants determined in the $10^{-3}M$ range for calculations in the $10^{-6}M$ range. However, I question how many true equilibrium constants are known at this time, and more importantly whether or not we are dealing with solutions at equilibrium in natural waters.

Acknowledgments

I wish to acknowledge gratefully the support of the Office of Naval Research, The Army Research Office (Durham), and the Wright Air Development Center, which have enabled us to pursue much of our solution chemistry research in Chapel Hill.

Literature Cited

(1) Anderson, J. S., Saddington, K., *J. Chem. Soc.* **1949,** 5381.
(2) Angstadt, R. L., Tyree, S. Y., *J. Inorg. Nucl. Chem.* **24,** 913 (1962).
(3) Ardon, M., Plane, R. A., *J. Am. Chem. Soc.* **81,** 3197 (1959).
(4) Aveston, J., *Inorg. Chem.* **3,** 981 (1964).
(5) Aveston, J., Johnson, J. S., *Inorg. Chem.* **3,** 1051 (1964).
(6) Baker, L. C. W., Pope, M. T., *J. Am. Chem. Soc.* **82,** 4176 (1960).
(7) Cartledge, G. H., *J. Am. Chem. Soc.* **50,** 2863 (1928).
(8) Craig, H. R., Tyree, S. Y., *Inorg. Chem.* **4,** 997 (1965).
(9) Debye, P., Naumann, R. V., *J. Chem. Phys.* **17,** 664 (1949).
(10) Esval, O. E., Johnson, J. S., *J. Phys. Chem.* **69,** 959 (1965).
(11) Esval, O. E., Ph.D. Dissertation, University of North Carolina, 1962.

(12) Faucherre, J., *Bull. Soc. Chem. France* **21,** 128 (1954).
(13) Gimblett, F. G. R., "Inorganic Polymer Chemistry," pp. 352-359, Butterworth & Co., London, 1963.
(14) Granér, F., Sillén, L. G., *Acta Chem. Scand.* **1,** 631 (1947).
(15) Hentz, F. C. Jr., Johnson, J. S., *Inorg. Chem.* **5,** 1337 (1966).
(16) Hentz, F. C. Jr., Tyree, S. Y., *Inorg. Chem.* **3,** 844 (1964).
(17) Holmberg, R. W., Kraus, K. A., Johnson, J. S., *J. Am. Chem. Soc.* **78,** 5506 (1956).
(18) Jackson, J. A., Taube, H., *J. Phys. Chem.* **69,** 1884 (1965).
(19) Johnson, J. S., Kraus, K. A., Scatchard, G., *J. Phys. Chem.* **58,** 1034 (1954).
(20) Kraus, K. A., Johnson, J. S., *J. Am. Chem. Soc.* **78,** 3937 (1956).
(21) Lefebvre, J., Maria, H., *Compt. Rend.* **256,** 1982, 2400, 3121, 4219 (1963).
(22) Levy, H. A., Danford, M. D., Agron, P. A., *J. Chem. Phys.* **31,** 1458 (1959).
(23) Lindqvist, I., *Acta Chem. Scand.* **5,** 568 (1951).
(24) Lindqvist, I., *Arkiv Kemi* **2,** 325 (1950).
(25) Matijevic, E., Janauer, G. E., Kerker, M., *J. Colloid Sci.* **19,** 333 (1964).
(26) Matijevic, E., Mathai, K. G., Kerker, M., *J. Phys. Chem.* **67,** 1995 (1963).
(27) Matijevic, E., Tezak, B., *J. Phys. Chem.* **57,** 951 (1953).
(28) Milburn, R. M., Vosburgh, W. C., *J. Am. Chem. Soc.* **77,** 1352 (1955).
(29) Muha, G. M., Vaughn, P. A., *J. Chem. Phys.* **33,** 194 (1960).
(30) Olin, A., *Acta Chem. Scand.* **11,** 1445 (1957).
(31) *Ibid.* **14,** 126 (1960).
(32) *Ibid.*, p. 814.
(33) Patterson, C. S., Tyree, S. Y., *J. Am. Chem. Soc.* **79,** 1821 (1957).
(34) Rossotti, F. J. C., Rossotti, H., *Acta Chem. Scand.* **10,** 779 (1956).
(35) Rubin, A. J., Ph.D. Dissertation, University of North Carolina, 1966.
(36) Ruff, J. K., Tyree, S. Y., *J. Am. Chem. Soc.* **80,** 5654 (1958).
(37) Ruff, J. K., unpublished observations.
(38) Sanders, J. Y. *et al., Nature* **204,** 990, 1151 (1964); **209,** 13 (1966).
(39) Sillen, L. G., *Quart. Revs.* **13,** 146 (1959).
(40) Souchay, P., *Research (London)* **4,** 11 (1951).
(41) Tobias, R. S., *J. Am. Chem. Soc.* **82,** 1070 (1960).
(42) Tobias, R. S., *J. Inorg. Nucl. Chem.* **19,** 348 (1961).
(43) Tobias, R. S., Tyree, S. Y., *J. Am. Chem. Soc.* **81,** 6385 (1959).
(44) *Ibid.* **82,** 3244 (1960).
(45) Walmsley, F., Ph.D. Dissertation, University of North Carolina, 1962.
(46) Zielen, A. J., Connick, R. E., *J. Am. Chem. Soc.* **78,** 5785 (1956).

RECEIVED April 15, 1966.

9

Heterogeneous Equilibria Involving Oxides, Hydroxides, Carbonates, and Hydroxide Carbonates

PAUL W. SCHINDLER[1]

National Bureau of Standards, Washington, D. C.

Some major and minor constituents of sea water can be classified with respect to possible control of their concentrations by simple solubility equilibria. Comparing calculated and observed data leads to the conclusion that the ocean represents a steady-state system, where the degree of oversaturation bears a reasonable relationship to the rate of sedimentation.

This paper discusses some applications of the law of mass action to systems consisting of solids, a liquid phase—mainly water—and a gaseous phase essentially similar to the earth's atmosphere. The success of such discussions is always limited by our present knowledge concerning (*a*) the chemical properties of the different phases, (*b*) some intensive properties such as temperature and pressure, and (*c*) the extent to which chemical equilibrium is approached. These restrictions hold whether we are involved in experimental work using small vessels or in studies of gigantic natural systems as represented by the sea and its surroundings. We begin, therefore, by summarizing some recent laboratory work on heterogeneous systems. Finally, a brief discussion of some properties of sea water in terms of solubility equilibria is given, based on the results of these experimental studies.

The chemical species under consideration belong to ternary systems Me^{z+}-H_2O-CO_2. Their generalized formulae are given in Table I. The general symbol $Me(OH)_{(z-2x)}(CO_3)_x$ represents a hydroxide carbonate; it includes the corresponding hydroxide ($x = 0$) and the neutral carbonate ($x = 0.5z$). Solid solutions $(Me_1, Me_2)(OH)_{(z-2x)}(CO_3)_x$ will not be considered at the moment. Furthermore, the possible occurrence

---

[1] Present address: University of Bern, Bern, Switzerland.

Table I. Chemical Species in Ternary Systems Me^{z+}-H_2O-CO_2

Solid phases	*Aqueous phase*	*Gaseous phase*
$Me(OH)_{(z-2x)}(CO_3)_x$	H_2O, H^+, OH^-	H_2O
$(Me_1,Me_2)(OH)_{(z-2x)}(CO_3)_x$	(CO_2,H_2CO_3), HCO_3^- CO_3^{2-} Me^{z+}, $Me_m(OH)_n^{(zm-n)+}$ $Me_p(CO_3)_q^{(zp-2q)+}$	CO_2

of mixed complexes is neglected. This oversimplification, though undesirable, is necessary because of the present lack of appropriate data.

Compared with the solid and gaseous phases, the aqueous solution has numerous complications. Therefore, we will first mention methods by which one can predict the composition of the solution in the presence of a given solid and gaseous phase. Later we shall remember that the formulae already attributed to the solid phases are inadequate. There is sometimes a multiplicity of solids, each having the same formula but differing from each other in chemical behavior. Within this multiplicity of solid phases, all are metastable but one. Some kinds of metastable solids and metastable equilibria will be discussed later.

Evaluation and Graphical Presentation of Solubility Data

Determining solubility constants in aqueous solutions generally involves analytical work to determine concentrations [ ] or potentiometric measurements to obtain activities { }. The ratio of activity and concentration—*i.e.*, the activity coefficient and its change with concentration—depends on the choice of the standard state. If pure water is chosen as a standard state, the activity coefficients approach unity only in dilute solutions. It is therefore necessary to express the so-called "thermodynamic" constants ^{T}K (*48*) in terms of activities. If, on the other hand, one chooses as reference an aqueous solution of comparatively high and constant ionic strength, the activity coefficients remain close to unity even at rather high concentrations of the reacting species. In this case, we may use "stoichiometric" constants K (*48*), expressed in molarities, M, and related to a particular ionic medium.

Equilibria involving hydrogen ions are sometimes characterized by mixed "constants," k; the concentrations of the acid and its corresponding base are given in molarities, and the amount of the hydrogen ions is expressed in terms of pH.

Note that the operational definition of pH is given in terms of a cell:

glass or hydrogen electrode/ solution X or
S/ saturated KCl/ calomel

The definition of pH is:

$$\mathrm{pH(X)} = \mathrm{pH(S)} + \frac{E_X - E_S}{RT \ln 10/F}$$

The term, pH(S), the value assigned to the standard buffer solution S is derived from the experimentally accessible quantity log $\{H^+\}$ γ_{Cl^-}, assuming (*2*):

$$\log \gamma_{Cl^-} = -A\sqrt{I}/(1 + 1.5\sqrt{I}) \quad (I \leqslant 0{,}1)$$

Hence, pH is not identical with – log $\{H^+\}$ since the calculation of γ_{Cl^-} is somewhat arbitrary. Furthermore, an unknown difference in liquid junction potentials may become important especially if solutions X and S differ in ionic strength and composition. Using a medium of constant ionic strength, however, it is possible to determine the hydrogen ion concentration, $[H^+]$, using a glass or hydrogen electrode. Biedermann and Sillén (*8*) extensively studied the cell:

glass or hydrogen electrode / test solution // $3M$ $NaClO_4$ /
calomel-sodium chloride half-cell (A)

The composition of the test solution was essentially

$$[H^+] = H\,M \qquad (0 < H < 0.6M)$$

$$[Na^+] = (3 - H)M$$

$$[ClO_4^-] = 3M$$

The e.m.f. of the cell was found to be

$$E_A = E'_{oA} - \frac{RT \ln 10}{F} \log H + d_1 H$$

Schindler *et al.* (*16*) investigated the cell:

Glass electrode / test solution // $0.2M$ $NaClO_4$ //
$0.19M$ $NaClO_4$, $0.01M$ NaCl / AgCl, Ag (B)

The general composition of the test solutions was

$$[H^+] = H\,M \qquad (0 < H < 0.02M)$$

$$[Zn^{2+}] = B\,M \qquad (0 < B < 0.01M)$$

$$[Na^+] = (0.2 - H - 2B)\,M$$

$$[ClO_4^-] = 0.2M$$

The e.m.f. was found to be:

$$E_B = E'_{oB} - \frac{RT \ln 10}{F} \log H + d_2 H + d_3 B$$

The constant E'_0 is obtained by extrapolation ($H \rightarrow 0$ or $B, H \rightarrow 0$); d values are available from:

$$d_1 = d(E + \frac{RT \ln 10}{F} \log H)/dH$$

$$d_2 = (\partial(E + \frac{RT \ln 10}{F} \log H)/\partial H)_B$$

$$d_3 = (\partial E/\partial \mathrm{B})_H$$

Table II summarizes the different kinds of equilibrium constants with which we shall be concerned.

Besides these few equilibrium constants we have already mentioned, there are other constants:

$$Ks_{nm} = \frac{[\mathrm{Me}_m(\mathrm{OH})_n{}^{(zm-n)+}]\,[\mathrm{CO_3}^{2-}]^{mx}}{[\mathrm{OH}^-]^{(n-zm+2xm)}}$$

$$Ks_{qp} = \frac{[\mathrm{Me}_p(\mathrm{CO_3})_q{}^{(zp-2q)+}]\,[\mathrm{OH}^-]^{p(z-2x)}}{[\mathrm{CO_3}^{2-}]^{(q-px)}}$$

describing equilibria between the solid and particular hydroxo and carbonato complexes. Since it is often easier to investigate homogeneous equilibria in homogeneous systems (since the homogeneous system has at least one more degree of freedom), we shall restrict ourselves by assuming all homogeneous equilibria to be known. All the heterogeneous constants are then available once one of them has been determined as follows:

$$\log Ks_0 = \frac{1}{m}(\log Ks_{nm} - \log \beta_{nm}) = \frac{1}{p}(\log Ks_{qp} - \log \beta_{qp}) =$$

$$\log {}^{*}Ks_0 + (z - 2x) \log K_w + x \log (Kpa_1 Ka_2) =$$

$$\log {}^{\dagger}Ks_0 + (x - z) \log Kpa_1 + x \log Ka_2 + (z - 2x) \log K_w$$

Now we must select the one appropriate solubility constant whose numerical value will serve as a basis for all subsequent calculations. Some considerations which are common to all solubility investigations may be illustrated by taking zinc carbonate as an example (*see* Table III).

Determining $[\mathrm{Zn}^{2+}]$ presents no difficulties if the solubility is not too small. As shown in Table II, $[\mathrm{Zn}^{2+}] \propto P_{\mathrm{CO_2}}[\mathrm{HCO_3}^-]^{-2} \propto [\mathrm{CO_3}^{2-}]^{-1}$. Moreover, in calculating $[\mathrm{Zn}^{2+}]$, it should be kept in mind that analytical data yield:

$$\mathrm{Zn_{tot}}^{\mathrm{II}} = [\mathrm{Zn}^{2+}] + \sum m\,[\mathrm{Zn}_m(\mathrm{OH})_n{}^{(2m-n)+}] + \sum p\,[\mathrm{Zn}_p(\mathrm{CO_3})_q{}^{2(p-q)+}]$$

Therefore, it seems favorable to operate under experimental conditions such that $[\mathrm{CO_3}^{2-}]$, $[\mathrm{HCO_3}^-]$, and $[\mathrm{OH}^-]$ are small.

Table II. Equilibrium Constants in Ternary Systems Me^{z+}-H_2O-CO_2

Homogeneous Equilibria

$$H_2O \rightleftarrows H^+ + OH^-$$

$$^{T}K_w = \{H^+\}\{OH^-\} \qquad K_w = [H^+][OH^-]$$

$$CO_2(g) + H_2O \rightleftarrows H^+ + HCO_3^{-\ a,b}$$

$$^{T}K_{pa_1} = \{H^+\}\{HCO_3^-\}P_{CO_2}^{-1}$$

$$Kpa_1 = [H^+][HCO_3^-]P_{CO_2}^{-1} \; kpa_1 = 10^{-pH}[HCO_3^-]P_{CO_2}^{-1}$$

$$HCO_3^- \rightleftarrows H^+ + CO_3^{2-}$$

$$^{T}K_{a2} = \{H^+\}\{CO_3^{2-}\}\{HCO_3^-\}^{-1}$$

$$Ka_2 = [H^+][CO_3^{2-}][HCO_3^-]^{-1} \; ka_2 = 10^{-pH}[CO_3^{2-}][HCO_3^-]^{-1}$$

$$m\mathrm{Me}^{z+} + n\mathrm{OH}^- \rightleftarrows \mathrm{Me}_m(\mathrm{OH})_n^{(zm-n)+}$$

$$^{T}\beta_{nm} = \{\mathrm{Me}_m(\mathrm{OH})_n^{(zm-n)+}\}\{\mathrm{Me}^{z+}\}^{-m}\{\mathrm{OH}^-\}^{-n}$$

$$\beta_{nm} = [\mathrm{Me}_m(\mathrm{OH})_n^{(zm-n)+}][\mathrm{Me}^{z+}]^{-m}[\mathrm{OH}^-]^{-n}$$

$$p\,\mathrm{Me}^{z+} + q\,\mathrm{CO}_3^{2-} \rightleftarrows \mathrm{Me}_p(\mathrm{CO}_3)_q^{(zp-2q)+}$$

$$^{T}\beta_{qp} = \{\mathrm{Me}_p(\mathrm{CO}_3)_q^{(zp-2q)+}\}\{\mathrm{Me}^{z+}\}^{-p}\{\mathrm{CO}_3^{2-}\}^{-q}$$

$$\beta_{qp} = [\mathrm{Me}_p(\mathrm{CO}_3)_q^{(zp-2q)+}][\mathrm{Me}^{z+}]^{-p}[\mathrm{CO}_3^{2-}]^{-q}$$

Heterogeneous Equilibria

$$\mathrm{Me(OH)}_{(z-2x)}(\mathrm{CO}_3)_x(s) + z\mathrm{H}^+ \rightleftarrows \mathrm{Me}^{z+} + (z-x)\mathrm{H_2O} + x\,\mathrm{CO_2(g)}^{b}$$

$$^{T*}K_{s_o} = \{\mathrm{Me}^{z+}\}\{\mathrm{H}^+\}^{-z}P_{CO_2}^{x} \qquad {}^{*}Ks_o = [\mathrm{Me}^{z+}][\mathrm{H}^+]^{-z}P_{CO_2}^{x}$$

$$\mathrm{Me(OH)}_{(z-2x)}(\mathrm{CO}_3)_x(s) + (z-x)\,\mathrm{CO_2(g)} + x\,\mathrm{H_2O} \rightleftarrows \mathrm{Me}^{z+} + z\,\mathrm{HCO}_3^{-\ b}$$

$$^{T}K_{s_o} = \{\mathrm{Me}^{z+}\}\{\mathrm{HCO}_3^-\}^{z}P_{CO_2}^{(x-z)} \quad \dagger Ks_o = [\mathrm{Me}^{z+}][\mathrm{HCO}_3^-]^{z}P_{CO_2}^{(x-z)}$$

$$\mathrm{Me(OH)}_{(z-2x)}(\mathrm{CO}_3)_x(s) \rightleftarrows \mathrm{Me}^{z+} + (z-2x)\,\mathrm{OH}^- + x\,\mathrm{CO}_3^{2-}$$

$$^{T}Ks_o = \{\mathrm{Me}^{z+}\}\{\mathrm{OH}^-\}^{(z-2x)}\{\mathrm{CO}_3^{2-}\}^{x} \quad Ks_o = [\mathrm{Me}^{z+}][\mathrm{OH}^-]^{(z-2x)}[\mathrm{CO}_3^{2-}]^{x}$$

[a] To distinguish from solubility equilibria, this heterogeneous equilibrium is listed with the homogeneous equilibria.

[b] Comprehensive formulae for these equilibrium constants would include factors such as $\{H_2O\}$, $\{H_2O\}^x$, $[H_2O]$, $[H_2O]^x$, etc. With reference to the normal aqueous standard state, $\{H_2O\}$ is unity. In a particular medium of constant ionic strength, $[H_2O]$ (and $\{H_2O\}$) are constants, and we are free in making the most convenient assumption $[H_2O] = 1$. Hence, there is no doubt about the correctness of our formulae. In using them as a basis for extrapolations to solutions of deviating composition, however, these conventions must be taken into account.

Table III. Solubility Constants of $ZnCO_3$

Basic Constant	*Experimental Parameters*
$^{T}Ks_o$ or Ks_o	$\{Zn^{2+}\}$, $\{CO_3^{2-}\}$ or $[Zn^{2+}]$, $[CO_3^{2-}]$
$^{T}\dagger Ks_o$ or $\dagger Ks_o$	P_{CO_2} and $\{Zn^{2+}\}$, $\{HCO_3^-\}$ or $[Zn^{2+}]$, $[HCO_3^-]$
$^{T*}Ks_o$ or $^{*}Ks_o$	P_{CO_2} and $\{Zn^{2+}\}$, $\{H^+\}$ or $[Zn^{2+}]$, $[H^+]$

The concentrations of HCO_3^- and CO_3^{2-} may be obtained from acidimetric titrations. It is sometimes best to avoid this procedure, however, since the presence of hydroxo or carbonato complexes may cause serious difficulties. We conclude that determining $^*Ks_0$ is most convenient since P_{CO_2} can be fixed and $[H^+]$ is available from measurements with a glass electrode.

We may now summarize some details of a recent experimental approach (*46*). $ZnCO_3$ was equilibrated with an aqueous phase of the original composition:

$$[ClO_4^-] = 0.0200M$$

$$[H^+] = HM$$

$$[Na^+] = (0.200 - H)M$$

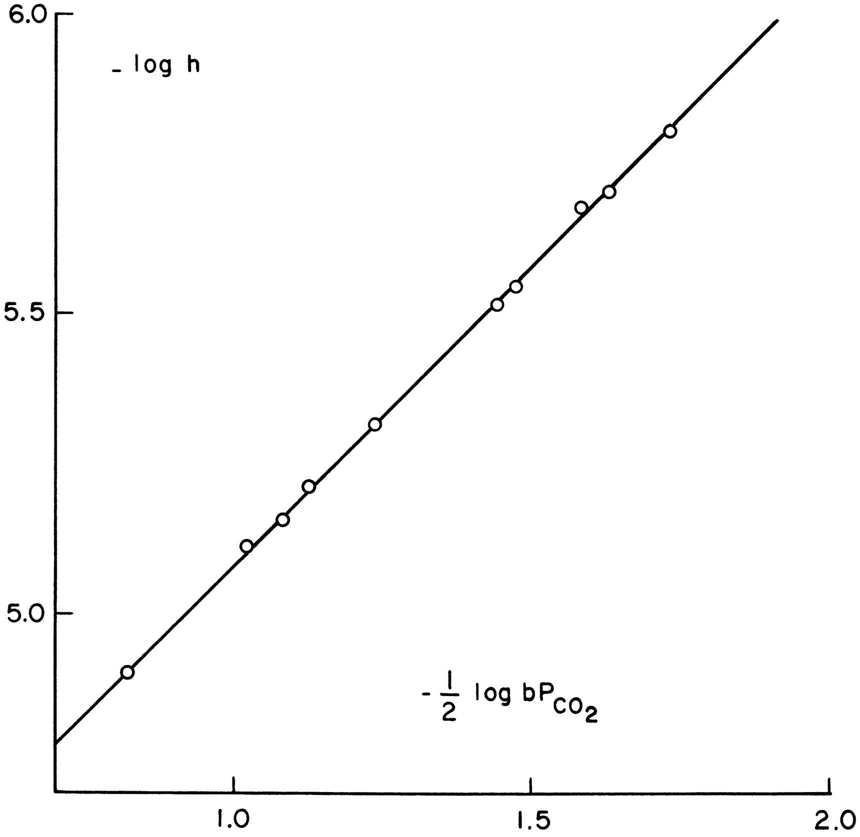

Figure 1. Solubility of $ZnCO_3$*. The straight line was calculated with log* $^*Ks_0 = 8.17$ *(25°C., I = 0.2M* $NaClO_4$*)*

and a number of different gaseous mixtures covering a range of known P_{CO_2} values. To maintain a constant ionic strength, H was always small and never exceeded 0.01M. The composition of the equilibrated solution was:

$$[ClO_4^-] = 0.200M$$

$$[Zn^{2+}] = bM$$

$$[H^+] = hM$$

$$[HCO_3^-] = Kpa_1 \cdot P_{CO_2} \cdot h^{-1} = tM$$

$$[Na^+] = (0.200 + t - h - 2b)M$$

If the analytically determined concentration of zinc is equal to b, we obtain:

$$^*Ks_o = bh^{-2}P_{CO_2} \qquad (I = 0.2 \text{ NaClO}_4)$$

In varying H and P_{CO_2} over a broad range, it was possible to check the validity of this relationship. Figure 1 shows a plot of log h vs. $\frac{1}{2}$ log (bP_{CO_2}).

This procedure enables us to determine the stoichiometric solubility constant. With a little additional information we can calculate the corresponding thermodynamic constant. For this purpose we shall consider a simple cycle:

$$Zn^{2+}{}_{(I=0.2)} + CO_2(g) + H_2O_{(I=0.2)} \rightleftharpoons ZnCO_3(s) + 2H^+{}_{(I=0.2)}$$
$$\Delta G_1 = RT\ln {}^*Ks_o$$

$$Zn(s) + 2H^+{}_{(I=0.2)} \rightleftharpoons Zn^{2+}{}_{(I=0.2)} + H_2(g)$$
$$\Delta G_2 = 2FE^\circ{}_{(I=0.2)}$$

$$C(s) + O_2(g) \rightleftharpoons CO_2(g) \qquad \Delta G_3$$

$$H_2(g) + \tfrac{1}{2}O_2(g) \rightleftharpoons H_2O(g) \qquad \Delta G_4$$

$$H_2O(g) \rightleftharpoons H_2O_{(I=0.2)} \qquad \Delta G_5 = RT\ln P_{H_2O\,(I=0.2)}$$

$$Zn(s) + C(s) + 3/2O_2(g) \rightleftharpoons ZnCO_3(s) \qquad \Delta G_6 = \Delta G_1 + \Delta G_2 + \Delta G_3 + \Delta G_4 + \Delta G_5$$

$$H_2O_{(I=0)} \rightleftharpoons H_2O(g) \qquad \Delta G_7 = -RT\ln P_{H_2O(I=0)}$$

$$H_2O(g) \rightleftharpoons H_2(g) + \frac{1}{2}O_2(g) \qquad -\Delta G_4$$

$$CO_2(g) \rightleftharpoons C(s) + O_2(g) \qquad -\Delta G_3$$

$$Zn^{2+}{}_{(I=0)} + H_2(g) \rightleftharpoons Zn(s) + 2H^+{}_{(I=0)} \qquad \Delta G_8 = -2FE^\circ{}_{(I=0)}$$

$$Zn^{2+}{}_{(I=0)} + CO_2\,(g) + H_2O_{(I=0)} \rightleftharpoons ZnCO_3(s) + 2H^+{}_{(I=0)} \qquad \Delta G_9$$
$$\Delta G_9 = \Delta G_1 + \Delta G_2 + \Delta G_5 + \Delta G_7 + \Delta G_8 = RT\ln {}^{T*}Ks_o$$

or

$$RT\ln {}^{T*}Ks_o = RT\ln {}^{*}Ks_o + RT\ln \frac{p_{H_2O(I=0.2)}}{p_{H_2O(I=0)}} + 2F\,(E^\circ_{(I=0.2)} - E^\circ_{(I=0)}) \quad (1)$$

This cycle holds for every medium. Equation 1 connects the four basic quantities ${}^{T*}Ks_o$, ${}^{*}Ks_o$, $E^\circ_{(I=0)}$, and $E^\circ_{(I)}$ without any nonthermodynamic assumptions. This enables us to evaluate solubility constants for every appropriate ionic medium using data which have been determined with reference to the usual aqueous standard state. The conversion of Ks into ${}^{T}Ks$ and vice-versa may also be performed using the Debye-Hückel equation and its extensions as shown in Equation 2.

$$\log {}^{T}Ks = \log Ks - g(z,I) \quad (2)$$

Table IV compares the values of ${}^{T*}Ks_o$ of $ZnCO_3$ as calculated from ${}^{*}Ks_o$ using Equations 1 and 2.

Table IV. Calculating[a] ${}^{T*}Ks_0$ ($ZnCO_3$) from ${}^{*}Ks_0$

Method	*log ${}^{T*}Ks_o$*
Equation 1	7.95 ± 0.05
Equation 2: $g(z,I) = \sqrt{I}$	7.72 ± 0.05
$g(z,I) = \left(\frac{\sqrt{I}}{1+\sqrt{I}}\right)$	7.86 ± 0.05
$g(z,I) = \left(\frac{\sqrt{I}}{1+\sqrt{I}} - 0.2\,I\right)$ (*14*)	7.90 ± 0.05
$g(z,I) = \left(\frac{\sqrt{I}}{1+\sqrt{I}} - 0.3\,I\right)$ (*15*)	7.92 ± 0.05

[a] Basic value: $\log {}^{*}Ks_o = 8.17 \pm 0.05$ ($I = 0.2$ $NaClO_4$, 25°C.)

In this particular example, the Davies equation (*15*) gives the same value as Equation 1; it seems to be applicable, therefore, to calculating ${}^{T}Ks$ values of oxides and carbonates of bivalent metals from Ks data in 0.2*M* $NaClO_4$. It fails, however, if applied to data which were evaluated in media of higher ionic strengths.

Next we shall consider the graphical presentation of solubility equilibria. From recent work on the system Cu^{2+}-H_2O-CO_2 (*see* appendix), we know the equilibrium constants which relate the solids CuO (tenorite), $CuCO_3 \cdot Cu(OH)_2$ (malachite), and $(Cu(CO_3))_2 \cdot Cu(OH)_2$ (azurite) with the dissolved species $H^+(OH^-)$, CO_2, HCO_3^-, CO_3^{2-}, Cu^{2+}, $CuOH^+$, $Cu_2(OH)_2^{2+}$, $Cu(OH)_3^-$, $Cu(OH)_4^{2-}$, $CuCO_3$, and $Cu(CO_3)_2^{2-}$. The data refer to pure water and hold for 25°C. Choosing $\{H^+\}$ and P_{CO_2}

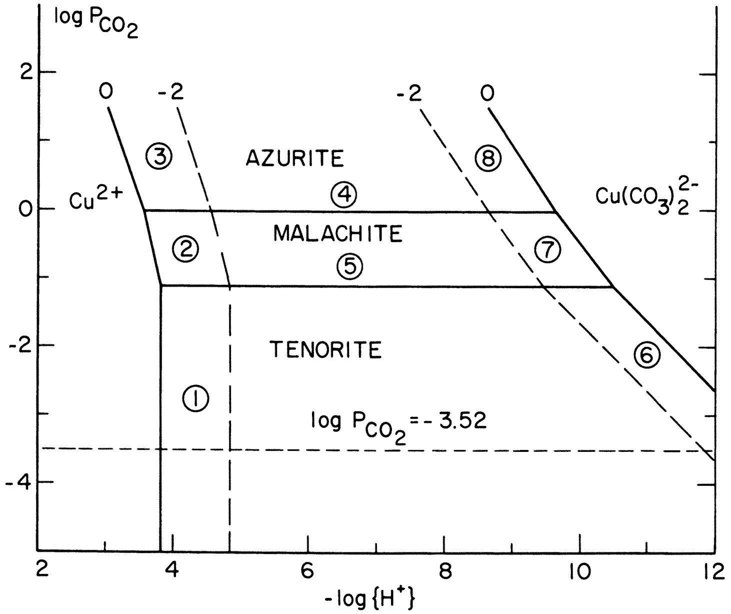

Figure 2. Predominance area diagram of the ternary system Cu^{2+}-H_2O-CO_2 (25° C., I = 0)

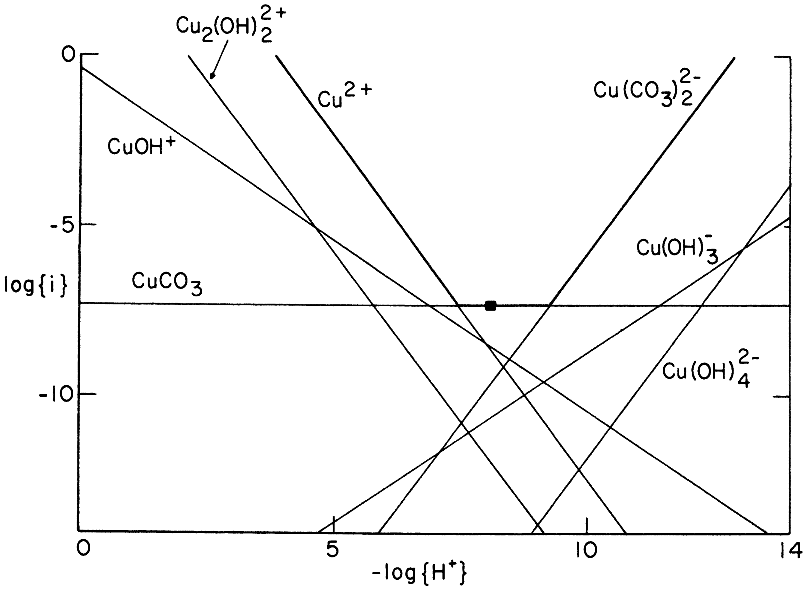

Figure 3. Solubility of CuO as a function of log {H^+} (25°C., I = 0, log P_{CO_2} = −3.52)

as chief variables, we may first construct a rough predominance area diagram (Figure 2). The straight lines 1, 2, and 3 indicate the log $\{H^+\}$ values where precipitation starts when we add a base to an acidic solution of copper ions. Lines 6, 7, and 8 give the log $\{H^+\}$ values where the different solids are in equilibrium with the carbonato complex. We may further learn that CuO is the stable solid in the presence of air ($\log P_{CO_2} = -3.52$).

Next we assume a fixed value of P_{CO_2} and investigate the composition of a saturated solution of CuO as a function of $\{H^+\}$ (Figure 3). The observed solubility must be attributed to the Cu^{2+} ion and the two carbonato complexes. Although the diagram holds only for solutions in pure water, we may assume that the activity coefficient of $CuCO_3$ remains close to unity even in sea water. The reported copper concentration in sea water is $\log[Cu_{tot}^{II}] = -7.3$ which is to be compared with the calculated value of $\log [CuCO_3] = -7.27$. Hence, we may conclude that sea water is saturated with respect to CuO, the dissolved copper being present as uncharged carbonato complex.

In most cases such solubility diagrams are calculated from solubility constants which have been evaluated for acidic or basic solutions. The results obtained by extrapolating such data to other regions should be regarded with much reserve. Figure 4 shows that for iron(III) hydroxide the observed solubility is considerably higher than that expected from solubility and hydrolysis constants. At $\log [H^+] = -8.1$, the calculated value is $\log[Fe(OH)_2^-] = -10.85$, whereas the observed value is $\log [Fe_{tot}^{III}] = -7$, which is approximately the iron concentration in sea

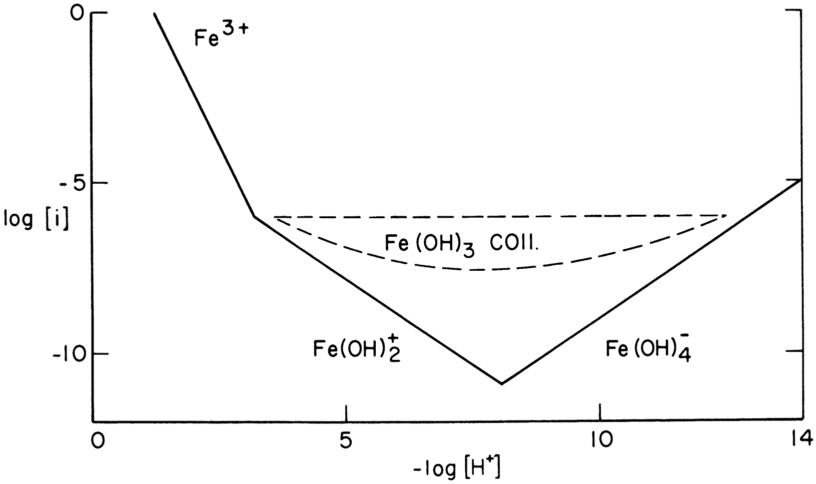

Figure 4. Solubility of amorphous iron hydroxide as a function of log $[H^+]$ *(25°C., I = 3M NaClO₄)*

water. The discrepancy is caused, as shown by using a centrifugation technique, by the presence of colloidally dispersed iron(III) hydroxide (*36*).

Metastable Solids and Metastable Equilibria

The fact that a simple formula (such as $Zn(OH)_2$) does not always account for all the chemical properties of the substance it represents may be attributed partly to the occurrence of polymorphous modifications. Differences in crystal structure may indeed cause considerable changes in thermodynamic properties (Table V).

Table V. Solubility Constants of Polymorphous Modifications

$Zn(OH)_2$ (*53*)	$\log {}^TKs_0$ (25°C.)	$CaCO_3$ (*21*)	$\log {}^TKs_0$ (25°C.)
amorphous $Zn(OH)_2$	−15.52	aragonite	−8.22
$\beta_1-Zn(OH)_2$	−16.24	calcite	−8.35
$\beta_2-Zn(OH)_2$	−16.20	$Be(OH)_2$ (*19*)	
$\gamma-Zn(OH)_2$	−16.26	amorphous $Be(OH)_2$	−20.8
$\delta-Zn(OH)_2$	−16.15	$\alpha-Be(OH)_2$	−21.1
$\varepsilon-Zn(OH)_2$	−16.47	$\beta-Be(OH)_2$	−21.5
ZnO	−16.83		

Although the difference in solubility (and Gibbs energy) may be rather large, it is often observed that some metastable solids show a high inertia in that their rate of conversion to stable solids may be extremely small. We shall return to this later.

Next, let us consider the fact that a given solid of known crystal structure has at least two additional "degrees of freedom" which may change its behavior. The presence of lattice defects, such as dislocations, and any alteration of particle size or specific surface will change its Gibbs energy. Since our present knowledge of the influence of lattice defects on solubility is rather limited, we shall restrict ourselves to a discussion of the particle size effect only.

From elementary thermodynamics we know that the reaction below has an associated change in Gibbs energy as given by Equation 3.

$$\begin{array}{ccc} \text{AB} & \rightleftharpoons & \text{AB} \\ (\text{solid}, s = 0, d = \infty, & & (\text{solid}, s, d, \text{immersed} \\ \text{immersed in aqueous solution}) & & \text{in aqueous solution}) \end{array}$$

s = molar surface
d = "particle size"

[To obtain the relationship between the "particle size" d and the molar surface s, we consider 1 mole of a finely powdered solid consisting of N uniform particles of equal size. The surface of a single particle is $S = kd^2$, where d denotes an arbitrarily chosen characteristic dimension of the particle. The volume is $V = ld^3$. Hence, the molar volume is $v = \frac{M}{\rho} = NV$, and the molar surface is $s = NS = \frac{N\alpha V}{d} = \frac{M\alpha}{\rho d}$ where $\alpha = \frac{k}{l}$]

$$\Delta G = \frac{2}{3}\bar{\gamma} s = \frac{2M}{3\rho}\alpha\bar{\gamma} d^{-1} = RT \ln \frac{Ks_o(s, d)}{Ks_o(s = 0, d = \infty)} \qquad (3)$$

where $\bar{\gamma}$ = mean Gibbs energy of the solid-liquid interface
M = formula weight of the solid
ρ = density of the solid
α = geometrical factor which depends on the shape of the crystals

From Equation 3 we obtain:

$$\log Ks_{o(d)} (\text{or } {}^*Ks_{o(d)}) = \log Ks_{o(d=\infty)} (\text{or } {}^*Ks_{(d=\infty)}) + \frac{0.2895 M\alpha\bar{\gamma}}{RT} d^{-1} \qquad (3a)$$

$$\log Ks_{o(s)} (\text{or } {}^*Ks_{o(s)}) = \log Ks_{o(s=0)} (\text{or } {}^*Ks_{o(s=0)}) + \frac{0.2895\bar{\gamma}}{RT} s \qquad (3b)$$

Equations 3, 3a, and 3b hold for monodispersed populations of uniform crystals only. Figures 5, 6, 7, and 8 show their application in some recent studies on the solubilities of ZnO, $Cu(OH)_2$, and CuO (*54*).

The quantity chiefly responsible for the measured effect is $\bar{\gamma}$ and may be calculated from experimental data. If the solubility is to be related to the particle size d, a value for $\bar{\gamma}$ is required. This demands a knowledge of α, a value difficult to estimate (*28*). It is therefore easier to calculate $\bar{\gamma}$ from a plot of Ks_0 *vs.* s.

Besides this experimental method, there is a semitheoretical method by which $\bar{\gamma}$ can be estimated. Assuming Equation 3 to be valid for any value of s and assuming that $\bar{\gamma}$ is independent of s, we may outline this method as follows. One mole of a coarse crystalline solid consisting of ions A^+ and B^- is immersed in an aqueous solution. When the large crystal is cut into small pieces, the interface s increases, and the system gains Gibbs energy. This pulverization finally yields the hydrated ions A_{aq}^+ and B_{aq}^-, and the molar surface reaches a value of:

$$s = 4\pi N_L (r_{A^+}^2 + r_{B^-}^2)$$

$$(N_L = \text{Avogadro's number})$$

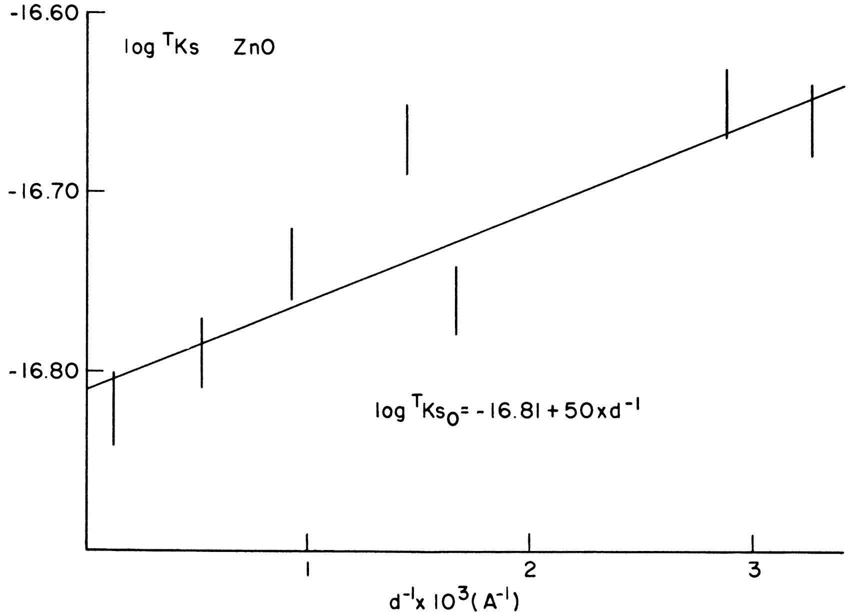

Figure 5. Solubility product of ZnO as a function of particle size d

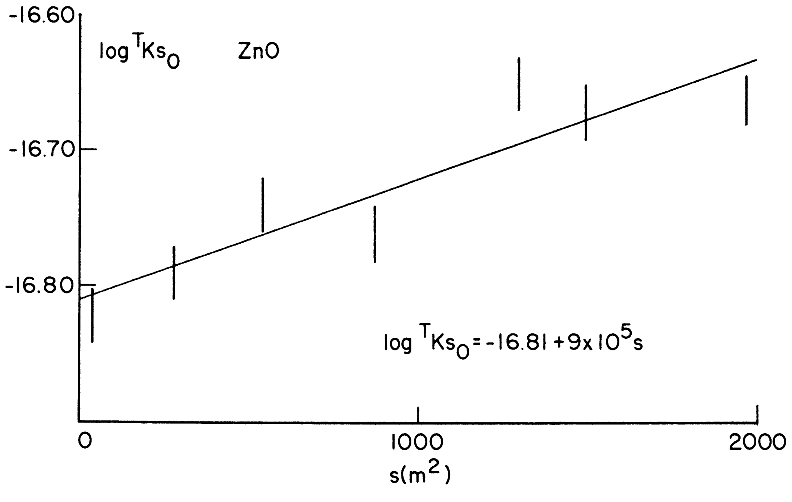

Figure 6. Solubility product of ZnO as a function of molar surface s

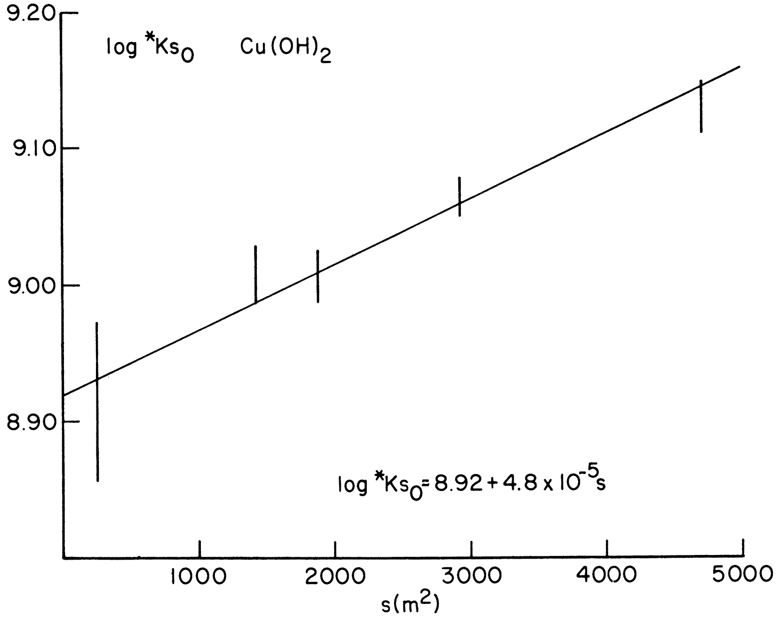

Figure 7. Solubility constant of $Cu(OH)_2$ as a function of molar surface s

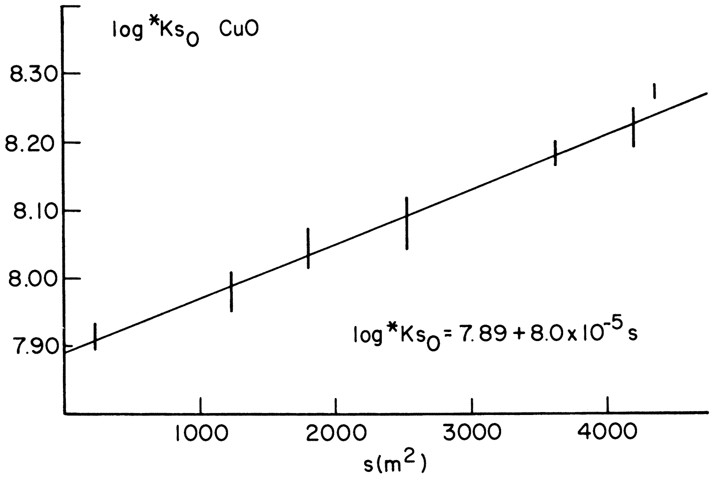

Figure 8. Solubility constant of CuO as a function of molar surface s

If the pulverization is performed in a reversible manner, the increase in Gibbs energy corresponds to the Gibbs energy of Reaction 4.

$$AB(s)_{(s=0)} \rightleftharpoons A_{aq}^{+} + B_{aq}^{-}$$

$$\Delta G \approx -RT \ln Ks_o \pm 2\,RT \ln 55 \qquad (4)$$

If A^{+}_{aq} and B^{-}_{aq} were in their standard states, the accurate value of ΔG would be available from the solubility product. However, in pulverizing and hydrating, we had to avoid any dilution. We can therefore only estimate that the activities of A^{+}_{aq} and B^{-}_{aq} are less than 1 if expressed in terms of mole fractions and equal to or greater than 1 if expressed in terms of molarities. Since mole fraction and molarity are related by a factor of about 55, the uncertainty of the calculated ΔG is, in our present example, about 2 RT ln 55. This term becomes comparatively small if ln Ks_o is large. From Equations 3 and 4 we obtain:

$$\bar{\gamma} \approx \frac{3(-RT \ln Ks_o \pm 2\,RT \ln 55)}{8\pi N_L(r_{A+}^{2} + r_{B-}^{2})} \qquad (5)$$

Table VI compares some experimentally determined and theoretically calculated $\bar{\gamma}$ values for solid-liquid interfaces.

Table VI. Gibbs Energies of Solid-Liquid Interfaces, ergs/sq. cm., 25°C.

Interface	*Experimental*	*Calculated*
ZnO 0.2*M* $NaClO_4$	770 ± 300	720 ± 235
CuO 0.2*M* $NaClO_4$	690 ± 150	890 ± 240
$Cu(OH)_2$ 0.2*M* $NaClO_4$	410 ± 130	400 ± 115
$BaSO_4$ H_2O (*41*)	121 to 153	115 ± 40
$SrSO_4$ H_2O (*18*)	84 ± 7	77 ± 41

Now, let us return to a consideration of the relative inertia of some metastable solids. As stated above, the change of the solubility product of ZnO with particle size is given by the empirical equation

$$\log {}^{r}Ks_o = -16.82 + 50\,d^{-1} \qquad (d \text{ in Angstroms})$$

Hence, in discussing the reaction below,

$$Zn(OH)_2(s)_{(metastable)} \rightleftharpoons ZnO(s)_{(stable)} + H_2O$$

we may calculate the size of the ZnO nuclei which are in equilibrium with the saturated solutions of the different modifications of $Zn(OH)_2$ (Table VII).

Table VII. Size of ZnO Nuclei in Equilibrium with the Saturated Solutions of Different Modifications of Zn(OH)₂

Hydroxide	d, A.	d^2, A.^{2}
amorphous $Zn(OH)_2$	41	1680
δ-$Zn(OH)_2$	79	6240
β_2-$Zn(OH)_2$	86	7400
β_1-$Zn(OH)_2$	92	8460
γ-$Zn(OH)_2$	95	9020
ε-$Zn(OH)_2$	150	22500

The surface of these nuclei (and therefore d^2) is a measure of the activation energy of the above reaction. We can therefore understand the common observation that only the amorphous hydroxide undergoes a spontaneous change whereas the crystalline modifications may be kept under water for a long time without being converted into ZnO. However, these considerations apply only to two-phase reactions. Oxides and hydroxides may undergo one-phase transformations as well. The above speculations must therefore be used with care.

Examining metastable solids has been restricted so far to pure phases. Still to be considered are systems consisting of an aqueous solution and a solid solution, the latter being represented by the simplified formula (A,B)L. The equilibrium is given by Equation 6.

$$\frac{x_2 f_2}{x_1 f_1} = \frac{Ks_{o(\mathrm{AL})}\,\{\mathrm{BL}\}}{Ks_{o(\mathrm{BL})}\,\{\mathrm{AL}\}} \tag{6}$$

where x_1, f_1: mole fraction and activity coefficient of AL in the solid solution

x_2, f_2: mole fraction and activity coefficient of BL in the solid solution

$\{AL\}$, $\{BL\}$: activities of AL and BL in the aqueous solution

The condition for the stability of the pure solid AL is $x_1 = f_1 = 1$, and therefore, $\{BL\} = 0$ or $f_2 = \infty$. Hence, a pure solid becomes unstable if placed in a foreign medium.

When x_2 is small, Equation 6 may be simplified to Equation 6a.

$$x_1 f_1 \rightarrow 1,\ x_2 = \frac{Ks_{o(\mathrm{AL})}}{Ks_{o(\mathrm{BL})}} f_2^{-1} \frac{\{\mathrm{BL}\}}{\{\mathrm{AL}\}} = D\frac{\{\mathrm{BL}\}}{\{\mathrm{AL}\}} \tag{6a}$$

A recently published D value (*27*) for $(Ca_{0.999}Sr_{0.001})CO_3$ will be used later. Another consequence of Equation 6 is

$$\{\mathrm{AL}\} = x_1 f_1 \, Ks_{o(\mathrm{AL})}$$
$$\{\mathrm{BL}\} = x_2 f_2 \, Ks_{o(\mathrm{BL})} \qquad (6b)$$

This indicates that the solubility of a given substance is greatly reduced when it becomes a minor constituent of a solid solution.

Solubility Equilibria of Oxides, Hydroxides, Carbonates, and Hydroxide Carbonates in Sea Water

We will now attempt to compare the reported concentrations of a few elements in the sea with calculated values, assuming certain specified solids to be in equilibrium with sea water. First, however, we must examine both the nature and reliability of the data we shall compare.

We know the analytical concentrations of the major and many of the minor elements in the ocean, but we do not know their activities with respect to the normal aqueous standard state. In particular, for the hydrogen ion we do not know, strictly speaking, either the activity or the concentration. (The acidity of the sea is reported in terms of pH values whose thermodynamic meaning in this particular medium is not well understood.) The temperature of the sea varies between 0° and 30°C., and the pressure varies between 1 and 2000 atm.

Our calculation will be based on solubility data, mainly ${}^{T}K$ values, valid for 25°C. and 1 atm. In a few cases stoichiometric constants for different media are available, but only two (for calcite and $SrCO_3$) refer to sea water. Furthermore, many of the given values are uncertain, and there are only a few systems where a complete and reliable set of solubility constants enables one to construct a solubility diagram.

Therefore, we must compare data for different ionic strengths as well as for different temperatures and pressures. Moreover, the calculated data refer to pure solids whereas the floor of the sea consists of only a few comparatively pure solids and an overwhelming mass of complicated solid solutions.

Starting with laboratory data for $I = 0$, 25°C. and 1 atm., we may find that the solubility is greater at $I = 0.7$ and an average pressure of 200 atm. Lowering the temperature to 5°C. usually reduces the solubility of a given substance with respect to both the pure solid and the solid solution. (With carbonate solids, however, the ${}^{T}Ks_0$ values generally decrease with increasing temperature.)

The deviations may cancel each other to a certain degree, and no corrections will be applied for them in the following calculations, but, it is important to realize that comparison must be restricted to a logarithmic scale considering the first decimal only.

The following tables summarize the available pertinent data. The oceanographic data are from Goldberg (22), and the appropriate equilibrium constants were selected by the author. Details of the somewhat tedious calculations and references to the literature are given in the appendix. Table VIII compares observed and calculated concentrations $[E]$ in moles per liter for some elements with low residence times.

Within this group we shall first consider iron, whose actual concentration is much higher than the calculated value. This oversaturation results in the formation of α-FeOOH or its amorphous counterpart, and the observed concentration must be attributed to the presence of these presumably colloidally dispersed solids.

A slight oversaturation is estimated for aluminum. Comparing the observed and the calculated concentrations we may conclude that 15% of the aluminum is present as $Al(OH)_4^-$ and 85% as colloidally dispersed $Al(OH)_3$. These figures compare surprisingly well with those found by Sackett and Arrhenius (*49*) who examined the nature of aluminum species in sea water.

For both iron and aluminum the low residence time agrees with the expected sedimentation rate of the coagulated solids. For the rare earth elements, we have reliable data for lanthanum hydroxide and doubtful information on the solubilities of the other lanthanide hydroxides. Whatever the reliability of these data, there is no doubt that the sea is highly undersaturated with respect to lanthanide elements. This, however, holds only for the case in which we assume that the pure hydroxides are the controlling solids. Two more possibilities must be considered. A rough estimate gives a value of 10^{-20} for the product $[La^{3+}][PO_4^{3-}]$ in sea water whereas the solubility product of lanthanum phosphate was determined as $10^{-22.43}$ [25°C., $I = 0.5M$ $NaClO_4$ (*60*)]. Hence, it seems possible that the concentrations of the lanthanide ions are controlled by the presence of sparingly soluble phosphates. On the other hand the similarity of residence times implies a possible coprecipitation of R^{3+} ions with FeOOH or $Al(OH)_3$ as vehicles. Table IX gives the relevant details for some elements with medium residence times.

As mentioned earlier, sea water seems to be in equilibrium with CuO. An apparent undersaturation is seen for Zn and Cd. Nevertheless, assuming that CuO, ZnO, and $CdCO_3$ are minor constituents of solid solutions—such as occur in manganese nodules—it is possible that the ocean is slightly oversaturated with respect to these three elements. A small oversaturation would indeed agree with the residence times given here.

Table X gives data for two elements whose equilibrium chemistry in sea water has been investigated by many workers. Although some important questions, such as the solubility of dolomite, are still open, the numbers given are probably more reliable than those in Tables VIII and IX.

Table VIII. Observed and Calculated

Element E	*Solid (assumed)*	*log*$[E]_{obs}$
Fe	am.FeOOH	−6.8
	α−FeOOH	
Al	α−Al$(OH)_3$	−6.4
Be	β−Be$(OH)_2$	−10.2
Sc	ScOOH	−9.0
La	La$(OH)_3$	−10.1
Lanthanides	R$(OH)_3$	−10.2 to −11.6

[a] 25°C., $I = 3M$ $NaClO_4$, 1 atm.
[b] 25°C., $I = 0$, 1 atm.
[c] 25°C., $I = 1M$ $NaClO_4$, 1 atm.

Table IX. Observed and Calculated

Element E	*Solid (assumed)*	*log*$[E]_{obs}$
Cu	CuO	−7.3
	$(Cu_x,Me^{II}{}_{(1-x)})O$ $(x = 10^{-2.5})$	
Zn	ZnO	−6.8
	$(Zn_x, Me^{II}{}_{(1-x)})O$ $(x = 10^{-2.5})$	
Cd	$CdCO_3$	−9.0
	$(Cd_x, Me^{II}{}_{(1-x)}CO_3$ $(x = 10^{-5})$	

[a] 25°C., $I = 0$, 1 atm.
[b] Calculated with Equation 6b, assuming $f = 1$.

Concentrations of Some Elements with Low Residence Times

$\log[E]_{calc}$	$\log \frac{[E]_{obs}}{[E]_{calc}}$	*Residence Time, years*
-10.7 ($Fe(OH)_2^+$ and $Fe(OH)_4^-$)^a	4	1.4×10^2
-12.9 ($Fe(OH)_2^+$ and $Fe(OH)_4^-$)^a	6	
-7.2 ($Al(OH)_4^-$)^b	1	$1. \times 10^2$
-8.5 ($Be(OH)_3^-$ and BeF^+)^b	-2	1.5×10^2
-7.8 ($Sc(OH)_2^+$)^c	-1	5.6×10^3
-5.1 (La^{3+})^c	-5	4.4×10^2
-3.4 to (R^{3+})^b (?) -6.0	-5 to (?) -7	1.8×10^2 to 1.8×10^3
or		
-1.4 to (RSO_4^+)^b (??) -4.0	-7 to (??) -9	

Concentrations of Some Elements with Medium Residence Times

$\log[E]_{calc}$	$\log \frac{[E]_{obs}}{[E]_{calc}}$	*Residence Time, years*
-7.3 ($CuCO_3$)^a	0	5.0×10^4
-9.8 ($CuCO_3$)^{a,b}	2	
-4.2 ($ZnSO_4$)^a	-3	1.8×10^5
-6.7 ($ZnSO_4$)^{a,b}	0	
-4.4 ($CdCl_2$)^a	-5	5.0×10^4
-9.4 ($CdCl_2$)^{a,b}	0	

Table X. Observed and Calculated Concentrations of Calcium and Strontium

Element E	*Solid (assumed)*	$log[E]_{obs}$	$log[E]_{calc}$	$log \frac{[E]_{obs}}{[E]_{calc}}$	*Residence Time, years*
Ca	$CaCO_3$(calcite)	−2.01	−2.5 (Ca^{2+})[a]	0.5	8×10^6
			−1.6 (Ca^{2+})[b]	−0.4	
Sr	$SrCO_3$	−4.04	−3.1 (Sr^{2+})[a]	−0.9	1.9×10^7
	$(Ca_{0.999}Sr_{0.001})CO_3$		−4.1	0.0	

[a] 25°C., sea water $19^0/_{00}$ Cl, 1 atm.
[b] 5°C., sea water $19^0/_{00}$ Cl, 200 atm.

Calcite will therefore precipitate in the upper layers of the sea, but it will redissolve when sedimented to depths of about 1000 or 2000 meters. There seems to be a dynamic equilibrium, which is consistent with the long residence time. The same is true for Sr where we observe equilibrium if we assume a solid solution of $SrCO_3$ in calcite as the controlling solid phase.

Conclusion

Some years ago, Sillén published (*56*) a most fundamental contribution to chemical oceanography. Assuming a simple equilibrium model he was able to obtain almost correct values for the concentrations of many major and of some minor components of sea water. In comparing Sillén's paper with our approach, the reader will find that a seven-year progress in equilibrium chemistry has generally confirmed and justified his model. There are, however, some indications that the ocean represents a steady-state system rather than a equilibrated solution. Whatever the accuracy of our calculations, the relationship between oversaturation and the rate of transport cannot be ignored.

Nevertheless, and in spite of the existence of voluminous compilations of equilibrium data, we are still far away from a real understanding of a system as complicated as the sea and its surroundings. This, in my opinion, is caused by the fact that equilibrium chemistry has been restricted to pure solids whereas the thermodynamic properties of naturally occurring minerals are at present practically unknown. Hence, a considerable additional effort in measuring stoichiometric constants for such naturally occurring solid solutions will be necessary to gain better insight into this fascinating problem.

Literature Cited

(1) Bates, R. G., *J. Am. Chem. Soc.* **61,** 308 (1939).
(2) Bates, R. G., Guggenheim, E. A., *Pure Appl. Chem.* **1,** 163 (1960).
(3) Belyavskaya, T. A., Kolosova, I. F., *Vestn. Mosk. Univ. Ser. II: Khim.* **5,** 55 (1962).
(4) Berecki-Biedermann, C., *Arkiv Kemi* **9,** 175 (1956).
(5) Berner, R. A., *Geochim. Cosmochim. Acta* **29,** 947 (1965).
(6) Biedermann, G., Kilpatrack, M., Pokras, L., Sillén, L. G., *Acta Chem. Scand.* **10,** 1327 (1956).
(7) Biedermann, G., Ciavatta, L., *Acta Chem. Scand.* **16,** 2221 (1962).
(8) Biedermann, G., Sillén, L. G., *Arkiv Kemi* **5,** 425 (1953).
(9) Bjerrum, J., *Kem. Maanedsblad* **26,** 24 (1945).
(10) Brosset, C., Orring, J., *Svensk. Kem. Tidskr.* **55,** 101 (1943).
(11) Choppin, G. R., Unrein, P. J., *Inorg. Nucl. Chem.* **25,** 387 (1963).
(12) Connick, R. E., Mattern, K. L., quoted in Connick, R. E., McVey, W. H., *J. Am. Chem. Soc.* **75,** 474 (1953).
(13) Connick, R. E., Hepler, L. G., Hugus, Z. Z., Kury, J. W., Latimer, W. M., Tsao, M. S., *J. Am. Chem. Soc.* **78,** 1827 (1956).
(14) Davies, C. W., *J. Chem. Soc.* **1938,** 2093.
(15) Davies, C. W., "Ion Association," p. 41, Butterworth and Co., London, 1960.
(16) Davies, W. G., Otter, R. J., Prue, J. E., *Discussions Faraday Soc.* **24,** 94 (1957).
(17) Davis, G. G., Smith, W. M., *Can. J. Chem.* **40,** 1836 (1962).
(18) Enüstün, B. V., Turkevich, J., *J. Am. Chem. Soc.* **82,** 4502 (1960).
(19) Feitknecht, W., Schindler, P., *Pure Appl. Chem.* **6,** 130 (1963).
(20) Gamsjäger, H., Stuber, H. U., Schindler, P., *Helv. Chim. Acta* **48,** 723 (1965).
(21) Garrels, R. M., Thompson, M. E., Siever, R., *Am. J. Sci.* **258,** 402 (1960).
(22) Goldberg, E. D., "Chemical Oceanography," J. P. Riley, G. Skirrow, eds., Vol. 1, p. 164, Academic Press, London, 1965.
(23) Harned, H. S., Hamer, W. J., *J. Am. Chem. Soc.* **55,** 2194, 4496 (1933).
(24) Harned, H. S., Brinkley, S. R., *J. Am. Chem. Soc.* **63,** 1706 (1941).
(25) Harned, H. S., Davis, R., *J. Am. Chem. Soc.* **65,** 2030 (1943).
(26) Hedström, B. O. A., *Arkiv Kemi* **6,** 1 (1953).
(27) Holland, H. D., cited by A. Lerman, *Geochim. Cosmochim. Acta* **29,** 977 (1965).
(28) Hostettler, P. B., *Am. J. Sci.* **261,** 238 (1963).
(29) Ingri, N., Lagerström, G., Frydman, M., Sillén, L. G., *Acta Chem. Scand.* **11,** 1034 (1957).
(30) Kelley, K. K., Anderson, C. T., *U.S. Bur. Mines Bull. No.* **384** (1935).
(31) Kramer, J. R., *J. Sediment. Petrol.* **29,** 465 (1959).
(32) Kury, J. W., Hugus, Z. Z., Latimer, W. M., *J. Phys. Chem.* **61,** 1021 (1957).
(33) La Mer, V. K., Parks, G., *J. Am. Chem. Soc.* **53,** 2040 (1931).
(34) Leden, I., Ph.D. Thesis, Lund, 1943.
(35) Lengweiler, H., Buser, W., Feitknecht, W., *Helv. Chim. Acta* **44,** 796 (1961).
(36) *Ibid.*, p. 805.
(37) Marcus, Y., Maydan, D., *J. Phys. Chem.* **67,** 979 (1963).
(38) Mattern, K. L., Ph.D. Thesis, University of California, 1957.
(39) Nanda, R. K., Aditya, S., *Z. Phys. Chem.* (Frankfurt) **35,** 139 (1962).
(40) Näsänen, R., Meriläinen, P., *Soumen Kem.* **33B,** 149 (1960).
(41) Nielsen, A. A., "Kinetics of Precipitation," p. 18, Macmillan, New York, 1964.

(42) Owen, B. B., Brinkley, S. R., *Chem. Rev.* **29**, 461 (1941).

(43) Paul, A. D., Ph.D. Thesis, University of California, 1955.

(44) Paul, A. D., *J. Phys. Chem.* **66**, 1248 (1962).

(45) Perrin, D. D., *J. Chem. Soc.* **1962**, 4500.

(46) Reinert, M., Ph.D. Thesis, University of Bern, 1965.

(47) Robinson, R. A., Stokes, R. H., "Electrolyte Solutions," p. 400, Butterworth and Co., London, 1955.

(48) Rossotti, F. J. C., Rossotti, H., "The Determination of Stability Constants," pp. 27, 28, McGraw-Hill, New York, 1961.

(49) Sackett, W., Arrhenius, G., *Geochim. Cosmochim. Acta* **26**, 955 (1962).

(50) Schindler, P., *Helv. Chim. Acta* **42**, 2736 (1959).

(51) Schindler, P., *Chimia* **17**, 313 (1963).

(52) Schindler, P., Michaelis, W., Feitknecht, W., *Helv. Chim. Acta* **46**, 444 (1963).

(53) Schindler, P., Althaus, H., Feitknecht, W., *Helv. Chim. Acta* **47**, 982 (1964).

(54) Schindler, P., Althaus, H., Hofer, F., Minder, W., *Helv. Chim. Acta* **48**, 1204 (1965).

(55) Shedlovski, T., MacInnes, D. A., *J. Am. Chem. Soc.* **57**, 1705 (1935).

(56) Sillén, L. G., *Am. Assoc. Advan. Sci. Publ. No.* **67**, 549 (1961).

(57) Silman, J. F. B., Ph.D. Thesis, Harvard University, 1958.

(58) Skirrow, G., "Chemical Oceanography," J. P. Riley, G. Skirrow, eds., Vol. 1, pp. 650, 651, Academic Press, London, 1965.

(59) Spedding, F. H., Jaffe, S., *J. Am. Chem. Soc.* **76**, 882 (1954).

(60) Tananaev, I. V., Vasil'eva, V. T., *Zh. Neorg. Khim.* **8**, 1070 (1963).

(61) Vanderzee, C. E., Dawson, H. J., *J. Am. Chem. Soc.* **75**, 5659 (1953).

(62) Woods, M. J. M., Gallagher, P. K., King, E. L., *Inorg. Chem.* **1**, 55 (1962).

(63) Yates, L. M., Ph.D. Thesis, Washington State College, 1955.

RECEIVED April 4, 1966.

Appendix

Selected Equilibrium Constants

Reaction	*log K*	*T, °C.*	*I*	*P, atm.*	*Reference*
$H_2O = H^+ + OH^-$	−14.00	25	0	1	(*23*)
	−13.77	25	1 $NaClO_4$	1	(*40*)
	−14.22	25	3 $NaClO_4$	1	(*29*)
$CO_2(g) + H_2O = H^+ + HCO_3^-$	−7.82	25	0	1	(*25, 55*)
	−7.5	25	s.w.	1	(*58*)[a]
	−7.3	5	s.w.	200	(*42, 58*)
$HCO_3^- = H^+ + CO_3^{2-}$	−10.33	25	0	1	(*24*)
	−9.0	25	s.w.	1	(*58*)[a]
	−9.1	5	s.w.	200	(*58, 42*)

Selected Equilibrium Constants. Continued

Reaction	*log K*	*T, °C.*	*I*	*P, atm.*	*Reference*
β – $Be(OH)_2(s) + 2H^+ = Be^{2+} + 2H_2O$	6.5	25	0	1	[b]
$Be^{2+} + 3OH^- = Be(OH)_3^-$	18.6	25	0	1	[b]
$Be^{2+} + 4OH^- = Be(OH)_4^{2-}$	18.4	25	0	1	[b]
$Be^{2+} + F^- = BeF^+$	5.06	25	0.5 $NaClO_4$	1	(*63*)
$Be^{2+} + 2F^- = BeF_2$	8.84	25	0.5 $NaClO_4$	1	(*63*)
$Be^{2+} + 3F^- = BeF_3^-$	11.81	25	0.5 $NaClO_4$	1	(*63*)
$Be^{2+} + SO_4^{2-} = BeSO_4$	0.72	25	0.5 $NaClO_4$	1	(*3*)
$CaCO_3$(s,calcite) $= Ca^{2+} + CO_3^{2-}$	−8.35	25	0	1	(*21*)
	−6.1	25	s.w.	1	(*31*)[a]
	−5.6	5	s.w.	200	(*31, 42*)[a]
$Ca^{2+} + F^- = CaF^+$	1.04	25	0	1	(*43*)
$SrCO_3(s) = Sr^{2+} + CO_3^{2-}$	−9.03	25	0	1	(*30*)
	−6.8	25	s.w.	1	[c]
$Sr^{2+} + CaCO_3$(s,calcite) $=$ $(Ca_{x1}, Sr_{x2})CO_3 + Ca^{2+}$	−0.89 $\left(= \log\left(x_2\frac{[Ca^{2+}]}{[Sr^{2+}]}\right)\right)$	25	dil	1	(*27*)
$ScOOH(s) + 3H^+ = Sc^{3+} + 2H_2O$	10.5	25	1 $NaClO_4$	1	(*51*)
$Sc^{3+} + OH^- = ScOH^{2+}$	8.7	25	1 $NaClO_4$	1	(*6*)
$Sc^{3+} + 2OH^- = Sc(OH)_2^+$	17.3	25	1 $NaClO_4$	1	(*6*)
$Sc^{3+} + F^- = ScF^{2+}$	6.18	25	0.5 $NaClO_4$	1	(*43*)
$Sc^{3+} + 2F^- = ScF_2^+$	11.45	25	0.5 $NaClO_4$	1	(*43*)
$Sc^{3+} + 3F^- = ScF_3$	15.52	25	0.5 $NaClO_4$	1	(*43*)
$Sc^{3+} + 4F^- = ScF_4^-$	18.03	25	0.5 $NaClO_4$	1	(*43*)
$Sc^{3+} + Cl^- = ScCl^{2+}$	1.07	25	0.5 $NaClO_4$	1	(*44*)
$Sc^{3+} + 2Cl^- = ScCl_2^+$	2.11	25	0.5 $NaClO_4$	1	(*44*)
$La(OH)_3(s) + 3H^+ = La^{3+} + 3H_2O$	19.19	25	1 $NaClO_4$	1	(*46*)
$La^{3+} + F^- = LaF^{2+}$	2.68	25	0.5 $NaClO_4$	1	(*32*)
$La^{3+} + Cl^- = LaCl^{2+}$	−0.12	25	1 $NaClO_4$	1	(*12*)
$La^{3+} + SO_4^{2-} = LaSO_4^+$	1.40	25	1 $NaClO_4$	1	(*38*)
$R(OH)_3(s) + 3H^+ = R^{3+} + 3H_2O$	21.9 to 18.3	25	0	1	[b]
$R^{3+} + F^- = RF^{2+}$	4	25	0	1	[d]
$R^{3+} + Cl^- = RCl^{2+}$	0	25	0	1	[e]
$R^{3+} + SO_4^{2-} = RSO_4^+$	3.6	25	0	1	(*59*)
am.$FeOOH(s) + 3H^+ = Fe^{3+} + 2H_2O$	3.55	25	3 $NaClO_4$	1	(*52*)
α – $FeOOH(s) + 3H^+ = Fe^{3+} + 2H_2O$	1.6	25	3 $NaClO_4$	1	(*35, 52*)
$Fe^{3+} + OH^- = FeOH^{2+}$	11.17	25	3 $NaClO_4$	1	(*26*)
$Fe^{3+} + 2OH^- = Fe(OH)_2^+$	22.13	25	3 $NaClO_4$	1	(*26*)
$Fe^{3+} + 4OH^- = Fe(OH)_4^-$	34.11	25	3 $NaClO_4$	1	(*35, 52*)
$Fe^{3+} + F^- = FeF^{2+}$	5.17	25	0.5 $NaClO_4$	1	(*13*)
$Fe^{3+} + 2F^- = FeF_2^+$	9.09	25	0.5 $NaClO_4$	1	(*13*)

Selected Equilibrium Constants. Continued

Reaction	*log K*	*T, °C.*	*I*	*P, atm.*	*Reference*
$Fe^{3+} + 3F^- = FeF_3$	12.00	25	0.5 $NaClO_4$	1	(*13*)
$Fe^{3+} + Cl^- = FeCl^{2+}$	0.46	25	1 $HClO_4$	1	(*62*)
$Fe^{3+} + SO_4^{2-} = FeSO_4^+$	2.31	25	0.5 $NaClO_4$	1	(*17*)
$CuO(s) + 2H^+ = Cu^{2+} + H_2O$	7.65	25	0	1	(*54*)
$Cu(OH)(CO_3)_{0.5}(s) + 2H^+ = Cu^{2+} + \frac{3}{2}H_2O + \frac{1}{2}CO_2(g)$	7.08	25	0	1	(*46*)
$Cu(OH)_{0.67}(CO_3)_{0.67}(s) + 2H^+ = Cu^{2+} + \frac{4}{3}H_2O + \frac{2}{3}CO_2(g)$	7.08	25	0	1	(*46*)
$Cu^{2+} + OH^- = CuOH^+$	6.0	18	0	1	(*4*)
$2Cu^{2+} + 2OH^- = Cu_2(OH)_2^{2+}$	17.0	18	0	1	(*4*)
$Cu^{2+} + 3OH^- = Cu(OH)_3^-$	15.2	25	0	1	(*54*)[b]
$Cu^{2+} + 4OH^- = Cu(OH)_4^{2-}$	16.1	25	0	1	(*54*)[b]
$Cu^{2+} + F^- = CuF^+$	1.23	25	0.5 $NaClO_4$	1	(*44*)
$Cu^{2+} + Cl^- = CuCl^+$	0	22	0	1	(*9*)
$Cu^{2+} + SO_4^{2-} = CuSO_4$	2.3	25	0	1	(*16*)
$Cu^{2+} + CO_3 = CuCO_3$	6.77	25	0	1	(*57*)
$Cu^{2+} + 2CO_3^{2-} = Cu(CO_3)_2^{2-}$	10.01	25	0	1	(*57*)
$ZnO(s) + 2H^+ = Zn^{2+} + H_2O$	11.18	25	0	1	(*53*)
$ZnCO_3(s) + 2H^+ = Zn^{2+} + H_2O + CO_2(g)$	7.95	25	0	1	(*46*)
$Zn(OH)_{1.2}(CO_3)_{0.4}(s) + 2H^+ = Zn^{2+} + 1.6\ H_2O + 0.4\ CO_2(g)$	9.80	25	0	1	(*46*)
$Zn^{2+} + OH^- = ZnOH^+$	5.04	25	0	1	(*45*)
$Zn^{2+} + 3OH^- = Zn(OH)_3^-$	13.9	25	0	1	(*53*)[b]
$Zn^{2+} + 4OH^- = Zn(OH)_4^{2-}$	15.1	25	0	1	(*53*)[b]
$Zn^{2+} + F^- = ZnF^+$	1.26	25	0	1	(*43*)
$Zn^{2+} + Cl^- = ZnCl^+$	0.43	25	0	1	(*37*)
$Zn^{2+} + 2Cl^- = ZnCl_2$	0.61	25	0	1	(*37*)
$Zn^{2+} + 3Cl^- = ZnCl_3^-$	0.53	25	0	1	(*37*)
$Zn^{2+} + 4Cl^- = ZnCl_4^{2-}$	0.20	25	0	1	(*37*)
$Zn^{2+} + SO_4^{2-} = ZnSO_4$	2.38	25	0	1	(*47*)
$Cd(OH)_2(s) + 2H^+ = Cd^{2+} + 2H_2O$	13.61	25	0	1	[f]
$CdCO_3(s) + 2H^+ = Cd^{2+} + H_2O + CO_2(g)$	6.14	25	0	1	(*20*)
$Cd^{2+} + OH^- = CdOH^+$	3.8	25	3 $LiClO_4$	1	(*7*)
$Cd^{2+} + F^- = CdF^+$	0.46	25	1 $NaClO_4$	1	(*34*)
$Cd^{2+} + Cl^- = CdCl^+$	2.00	25	0	1	(*61*)
$Cd^{2+} + 2Cl^- = CdCl_2$	2.70	25	0	1	(*61*)
$Cd^{2+} + 3Cl^- = CdCl_3^-$	2.11	25	0	1	(*61*)
$Cd^{2+} + Br^- = CdBr^+$	2.15	25	0	1	(*1*)
$Cd^{2+} + SO_4^{2-} = CdSO_4$	2.29	25	0	1	(*33*)
$\alpha - Al(OH)_3(s) + 3H^+ = Al^{3+} + 3H_2O$	8.2	25	0	1	[b]

Selected Equilibrium Constants. Continued

Reaction	*log K*	*T, °C.*	*I*	*P, atm.*	*Reference*
$Al^{3+} + 4OH^- = Al(OH)_4^-$	32.5	25	0	1	[b]
$Al^{3+} + F^- = AlF^{2+}$	6.13	25	0.53 KNO_3	1	(*10*)
$Al^{3+} + 2F^- = AlF_2^+$	11.15	25	0.53 KNO_3	1	(*10*)
$Al^{3+} + 3F^- = AlF_3$	15.00	25	0.53 KNO_3	1	(*10*)
$Al^{3+} + SO_4^{2-} = AlSO_4^+$	2.04	30	0	1	(*39*)

[a] Calculated from Ref. *5*.
[b] Calculated from Ref. *19*.
[c] Calculated from $\log {}^{T}Ks_o = -9.03$ assuming $\gamma\pm(SrCO_3) = \gamma\pm(CaCO_3)$.
[d] Estimated from data given by Ref. *43*.
[e] Estimated from data given by Ref. *11*.
[f] Calculated from Ref. *50*.

Calculations

The solubilities of oxides and hydroxides were calculated with log $\{H^+\}$ or log $[H^+] = -8.1$. The solubilities of carbonates and hydroxide carbonates were calculated assuming log $\{H^+\}$ or log $[H^+] = -8.1$ and $\{HCO_3^-\} + 2\,\{CO_3^{2-}\}$ or $[HCO_3^-] + 2\,[CO_3^{2-}] = 2.36 \cdot 10^{-3}M$. Similar figures are obtained by taking $\log P_{CO_2} = -3.52$.

All the calculations have been made, accounting for complexing with the most abundant ligands—*i.e.*, Cl^-, F^-, Br^-, SO_4^{2-}, and OH^-. (Our knowledge of the stabilities of complexes in sea water is poor and moreover, the concentrations of the free ligands are not exactly known since complexing between major species—*i.e.*, Mg^{2+}-SO_4^{2-}—should be considered.

The following figures were accepted:

$$\log [F^-] = -4.15$$

$$\log [Cl^-] = -0.26$$

$$\log [Br^-] = -3.08$$

$$\log [SO_4^-] = -1.55$$

$$\log [OH^-] = -5.9$$

The subsequent criteria were applied (charges omitted):

(a) Predominance of MeL_n over Me_{aq}: $\log \beta_n[L]^n > 0$

(b) Predominance of $MeL_{(n+1)}$ over MeL_n: $\log \beta_{(n+1)}[L]^{(n+1)} > \log \beta_n[L]^n$

(c) Predominance of $Me(L_1)_p$ over $Me(L_2)_q$: $\log \beta_p[L_1]^p > \log \beta_q[L_2]^q$

10

Origin of the Chemical Compositions of Some Springs and Lakes

ROBERT M. GARRELS

Northwestern University, Evanston, Ill.

FRED T. MACKENZIE

Bermuda Biological Station for Research, St. George's West, Bermuda

The spring waters of the Sierra Nevada result from the attack of high CO_2 soil waters on typical igneous rocks and hence can be regarded as nearly ideal samples of a major water type. Their compositions are consistent with a model in which the primary rock-forming silicates are altered in a closed system to soil minerals plus a solution in steady-state equilibrium with these minerals. Isolation of Sierra waters from the solid alteration products followed by isothermal evaporation in equilibrium with the earth's atmosphere should produce a highly alkaline $Na\text{-}HCO_3\text{-}CO_3$ water; a soda lake with calcium carbonate, magnesium hydroxysilicate, and amorphous silica as precipitates.

As natural waters circulate in the water cycle, their compositions change continuously. Evaporation occurs, solid materials react, gases are gained or lost, differential diffusion of components occurs through permeable and semipermeable media, and organisms absorb or lose constituents. Our only hope of gaining some insight into the genesis of various types of water bodies is to study some carefully chosen systems in which relatively few processes are involved and which can be isolated sufficiently from their surroundings to make some approximate mass balances.

We have chosen to study the genesis of the spring waters of the Sierra Nevada because of the availability of a careful set of analyses of the waters plus determinations of the primary igneous rock minerals and of the soil minerals derived from them (3). As we will demonstrate, the Sierra system emerges as one in which a few primary igneous rock minerals are being attacked by soil waters high in dissolved CO_2, but otherwise nearly pure, to yield soil minerals plus spring water. The system is apparently "closed"; there is little loss or gain of H_2O or CO_2 during the interaction of soil water and primary silicates. Furthermore, the chemical composition of the igneous rocks of the Sierra is reasonably representative of rocks of the continental crust; consequently, relations in the Sierra system may have widespread application to rock-water systems important in space and time.

Weathering Relations

Feth *et al.* (*3*) carefully studied the Sierra Nevada spring waters. We will summarize their results before extending some of their interpretations.

The granitic rocks from which the springs issue range from quartz diorite to quartz microcline gneiss. Feldspars and quartz are the major minerals in the rocks, with accessory hornblende and biotite. The K-feldspar and plagioclase feldspars, although differing widely from place to place, are about equally abundant; the plagioclase ranges in composition from oligoclase (An_{26} minimum) to andesine (An_{40} maximum). Andesine is the dominant plagioclase. The dissolved content of the springs comes almost entirely from attack of CO_2-rich soil water on these silicates, especially on the plagioclase. An aluminosilicate residue, stripped of alkali and alkaline earth metals, is left behind. Traces of gibbsite are found as well as some mica and montmorillonite. Although kaolinite was identified as an important alteration product in almost all instances, the bulk of the residue apparently averages out near the composition of kaolinite. Table I gives the mean values for the compositions of ephemeral and perennial springs.

The ephemeral springs are on the average aggressive waters with a calculated CO_2 pressure of about $10^{-1.8}$ atm. (as compared with $10^{-3.5}$ atm. for ordinary air) and have reacted sufficiently with the rock minerals to use up about half of the original dissolved CO_2 picked up while the waters pass through the soil zone. The perennial springs apparently average about the same initial CO_2 pressure, but about three-fourths of the CO_2 has been changed into HCO_3^- by reaction. Figure 1 (*1*) shows that the sodium content and the pH of the ephemeral springs are consistent with the reaction of CO_2-containing water with a plagioclase feldspar to form kaolinite in a closed system.

Reconstruction of Original Minerals. To test the conclusions of Feth (*3*) concerning the weathering reaction, allow an average spring water to back-react with kaolinite, the chief weathering product, and see if the original rock minerals can be formed. The reactions and products

Table I. Mean Values for Compositions of Ephemeral and Perennial Springs of the Sierra Nevada[a]

	Ephemeral Springs		*Perennial Springs*	
	p.p.m.	*molality × 10^4*	*p.p.m.*	*molality × 10^4*
SiO_2	16.4	2.73	24.6	4.1
Al	0.03	—	0.018	—
Fe	0.03	—	0.031	—
Ca	3.11	0.78	10.4	2.6
Mg	0.70	0.29	1.70	0.71
Na	3.03	1.34	5.95	2.59
K	1.09	0.28	1.57	0.40
HCO_3	20.0	3.28	54.6	8.95
SO_4	1.00	0.10	2.38	0.25
Cl	0.50	0.14	1.06	0.30
F	0.07	—	0.09	—
NO_3	0.02	—	0.28	—
Dissolved solids	36.0		75.0	
pH	6.2[b]		6.8[b]	

[a] Ref. 3, p. 16. [b] Median Value.

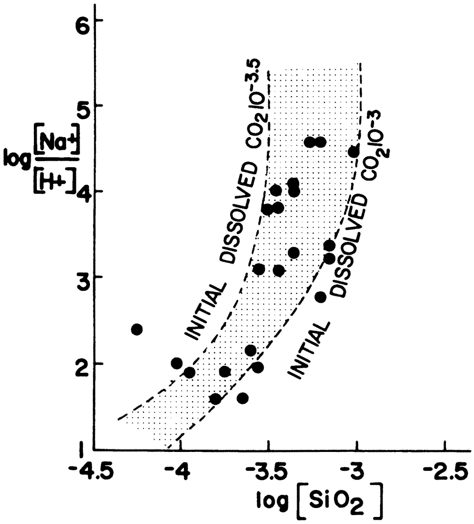

Figure 1. Logarithm of the ratio of Na^+ to H^+ in Sierra spring waters vs. logarithm of silica content. Solid circles are based on water analyses; dashed lines are theoretical compositions that should result from the attack of CO_2-bearing water on plagioclase to yield solution plus kaolinite

are shown in Table II. First the cations and anions in snow water were subtracted from the spring water solutes to determine the materials derived from the rock. Because mean compositions were used, a slight deficiency of anions resulted; this was corrected by giving HCO_3^- a slightly higher value than that realized by subtracting the mean concentration of HCO_3^- in snow from that of the springs. Otherwise no corrections were made. Then enough Na^+, Ca^{2+}, HCO_3^-, and SiO_2 reacted with kaolinite to make plagioclase, using up all the Na^+ and Ca^{2+}. The resultant calculated plagioclase does in fact have a composition similar to that found in the rocks.

Next all Mg^{2+} and enough K^+, HCO_3^-, and SiO_2 reacted with kaolinite to make biotite, leaving a small residue of K^+, HCO_3^-, and SiO_2 to form K-feldspar. Some silica remained—about 4% of the original concentration. Thus, the mass balance is probably within the limits of error of the original values of concentration used for the median composition of spring waters.

The reactions work out too well to leave much doubt that we are indeed dealing with a closed system reacting with CO_2 and that the weathering product is kaolinite or a material with a composition close to kaolinite in terms of the Al to Si ratio and the balance of alkali or alkaline earth cations.

Some Quantitative Aspects of the Weathering Process. The success of reconstructing the original rock minerals leads to several important conclusions.

First, there is at most a slight excess of silica over that needed to form the original silicates. Thus, the conclusion of Feth *et al.* (3) is re-emphasized—*i.e.*, the silica in the water came from the breakdown of the silicates and an insignificant amount from direct solution of quartz. The silica represents CO_2, changed into HCO_3^- by the weathering process.

Second, Feth *et al.* (3) observe that the waters gain much of their silica in a few feet of travel, showing that it is the action of the high CO_2 water that produces "kaolinite." The rock minerals react, forming "kaolinite" continuously in the system, and the "kaolinite" controls the water composition by its presence. If the aluminum analyses were not so low, and hence analytically suspect, an attempt could be made to calculate an equilibrium constant for the substance formed. All that can be said at the moment is that the values of SiO_2 and Al concentrations and of pH are reasonable for those controlled by an aluminosilicate of the approximate stability of kaolinite.

Third, Table II illustrates that about 80% of the rock-derived dissolved constituents in the ephemeral springs can be accounted for by the breakdown of plagioclase alone. Even though K-feldspar is abundant in the rocks, little breakdown occurs; the high Na to K ratio in these waters apparently is related to the differential rate of weathering of the feldspars rather than to K^+ adsorption after release upon clay minerals, as is often assumed. In the Sierra, the residual material left after initial attack of the aggressive waters on the rock minerals should be chiefly a mixture of quartz, K-feldspar, and kaolinite, and perhaps small amounts of aluminum oxide hydrates.

Some insight into what happens after the original strong attack on the silicates can be gained by subtracting the ephemeral spring analyses from those of the perennial springs. The perennial springs circulate deeper and have higher pH values when they encounter the rocks. Table III shows the "pick up" of constituents by continued circulation.

It is immediately apparent that the constituents added by deeper circulation are different from those derived by initial attack in some important ways. The ratio of SiO_2 to Na^+ in the increment is nearly 1 to 1. Because weathering of plagioclase to kaolinite releases dissolved SiO_2 and Na^+ in a ratio of 2 to 1 (*see* Table II) and plagioclase is the only reasonable source of Na^+, a solid other than kaolinite is being produced. Table IV is an attempt to deduce the reactions that occur during deeper

Table II. Source Minerals

	Ephemeral Springs	
Reaction (coefficients × 10^4)	*Na^+*	*Ca^{2+}*
Initial concentrations in spring water	1.34	0.78
Minus concentrations in snow water	1.10	0.68
Change kaolinite back into plagioclase Kaolinite $1.23\ Al_2Si_2O_5(OH)_4 + 1.10\ Na^+ + 0.68\ Ca^{2+} + 2.44\ HCO_3^- + 2.20\ SiO_2 =$ Plagioclase $1.77\ Na_{0.62}Ca_{0.38}Al_{1.38}Si_{2.62}O_8 + 2.44\ CO_2 + 3.67\ H_2O$	0.00	0.00
Change kaolinite back into biotite Kaolinite $0.037\ Al_2Si_2O_5(OH)_4 + 0.073\ K^+ + 0.22\ Mg^{2+} + 0.15\ SiO_2 + 0.51\ HCO_3^- = 0.073$ Biotite $KMg_3AlSi_3O_{10}(OH)_2 + 0.51\ CO_2 + 0.26\ H_2O$	0.00	0.00
Change kaolinite back into K-feldspar $0.065\ Al_2Si_2O_5(OH)_4 + 0.13\ K^+ + 0.13\ HCO_3^- + 0.26\ SiO_2 =$ K-feldspar $0.13\ KAlSi_3O_8 + 0.13\ CO_2 + 0.195\ H_2O$	0.00	0.00

circulation. With the thought that Cl^- is derived from NaCl, and SO_4^{2-} from $CaSO_4$, enough Na^+ and Ca^{2+} are removed to balance these anions. This assumption is weak, but fortunately the concentrations of SO_4^{2-} and Cl^- are so low that this step is not important.

Next it seems reasonable to use up Mg^{2+} and K^+ along with kaolinite to make biotite, inasmuch as the ratio of K^+ to Mg^{2+} in the waters is nearly that of a K-Mg biotite. This leaves Na^+ equal to SiO_2, so the remaining SiO_2 was apportioned between the reconstruction of kaolinite to plagioclase and that of montmorillonite to plagioclase. The montmorillonite composition chosen was that of a calcium beidellite of average cation exchange capacity. Beidellites seem to be prevalent under weathering conditions, and at such low concentrations of Na^+ and K^+ it is almost certain that the exchange positions are primarily occupied by Ca^{2+}.

After these steps, a considerable amount of Ca^{2+} and HCO_3^- remain, and we believe that with deep circulation, the waters which have lost much of their original aggressiveness, pick up Ca^{2+} (and perhaps some Mg^{2+}) from minor amounts of carbonates encountered en route.

for Sierra Nevada Springs

(concentrations moles/liter × 10^4)

Mg^{2+}	K^+	HCO_3^-	SO_4^{2-}	Cl^-	SiO_2	*Products moles/liter × 10^4*
0.29	0.28	3.28	0.10	0.14	2.73	
0.22	0.20	3.10	—	—	2.70	Derived from rock
	minus plagioclase					
0.22	0.20	0.64	0.00	0.00	0.50	1.77 $Na_{0.62}Ca_{0.38}$ feldspar
	minus biotite					
0.00	0.13	0.13	0.00	0.00	0.35	0.073 biotite
	minus K-feldspar					
0.00	0.00	0.00	0.00	0.00	0.12	0.13 K-feldspar

Table III. Effects of Deeper Circulation on Spring Waters[a]

	SiO_2	*Ca^{2+}*	*Mg^{2+}*	*Na^+*	*K^+*	*HCO_3^-*	*SO_4^{2-}*	*Cl^-*
Perennial Spring	4.10	2.60	0.71	2.59	0.40	8.95	0.25	0.30
Ephemeral Springs	2.73	0.78	0.29	1.34	0.28	3.28	0.10	0.14
Increment	1.37	1.82	0.42	1.25	0.12	5.67	0.15	0.16

[a] Analyses are mean values in moles/liter × 10^4.

The over-all picture of what happens to the soil waters, as illustrated by Tables II and IV, is that initially they rapidly attack the rocks, kaolinizing chiefly plagioclase plus biotite and K-spar. As they penetrate more deeply, the reaction rate slows down, and both kaolinite and montmorillonite are weathering products. Also, an important part of the Ca^{2+} comes from solution of small amounts of carbonate minerals.

Before attempting to document the formation of montmorillonite, a few remarks on weathering rates are of interest. Roughly one-half the initial CO_2 seems to be expended in the soil zone, and most of the rest alters rock minerals at deeper levels. The total reacting capacity is about

Table IV. Source Minerals and

	Concentrations in	
Reaction (coefficients × 10^4)	*Na^+*	*Ca^{2+}*
Initial concentrations (perennial minus ephemeral)	1.25	1.82
Remove $Ca^{2+} = SO_4^{2-}$, and $Na^+ = Cl^-$	1.09	1.67
Adjust HCO_3^- = total electrical charge of cations	1.09	1.67
Change kaolinite back into biotite		
$0.07\ Al_2Si_2O_5(OH)_4 + 0.42\ Mg^{2+} + 0.14\ K^+ + 0.28\ SiO_2 + 0.98\ HCO_3^- = 0.14\ KMg_3AlSi_3O_{10}(OH)_2 + 0.98\ CO_2 + 0.49\ H_2O$	1.09	1.67
Change kaolinite back into plagioclase		
$0.26\ Al_2Si_2O_5(OH)_4 + 0.235\ Na^+ + 0.144\ Ca^{2+} + 0.47\ SiO_2 + 0.52\ HCO_3^- = 0.38\ Na_{0.62}Ca_{0.38}Al_{1.38}Si_{2.62}O_8 + 0.52\ CO_2 + 0.78\ H_2O$	0.85	1.53
Change montmorillonite back into plagioclase		
$0.81\ Ca_{0.17}Al_{2.33}Si_{3.67}O_{10}(OH)_2 + 0.85\ Na^+ + 0.38\ Ca^{2+} + 0.61\ SiO_2 + 1.62\ HCO_3^- = 1.37\ Na_{0.62}Ca_{0.38}Al_{1.38}Si_{2.62}O_8 + 1.62\ CO_2 + 1.62\ H_2O$	0.00	1.15
Precipitate $CaCO_3$		
$1.15\ Ca^{2+} + 2.30\ HCO_3^- = 1.15\ CaCO_3 + 1.15\ CO_2 + 1.15\ H_2O$	0.00	0.00

9×10^{-4} equivalents per liter and corresponds to the destruction of about 3.5×10^{-4} moles of plagioclase, 0.2×10^{-4} moles of biotite, and about 0.2×10^{-4} moles of K-spar. The annual precipitation in this part of the Sierra averages about 100 cm./year. Therefore, the rate of chemical weathering is about 3.6×10^{-5} moles/year/sq. cm. If the rock consists of one-third plagioclase by volume, the rock should be disintegrated to an average depth of one meter in about 9000 years, and the residue would be chiefly a rubble of quartz, K-feldspar, and kaolinite.

Phase Control of Water Composition. The conclusion that kaolinite forms quickly and continuously during weathering, plus the strong suggestion that the deeper circulating waters are forming montmorillonite as well, can be tested qualitatively by predicting the compositional genesis of the waters, especially in terms of Ca^{2+} and Na^{+}. If one assumes that the CO_2-bearing waters continuously react with plagioclase to form first "kaolinite" and then "montmorillonite" and that these phases maintain equilibrium with the waters as they are continuously fed from the feldspar, then observed compositions can be compared with those based on these assumptions.

Weathering Products of Deeper Circulation

moles/liter $\times 10^4$

Mg^{2+}	K^+	HCO_3^-	SO_4^{2-}	Cl^-	SiO_2	*Mineral altered and product (moles/liter × 10^4)*
0.42	0.12	5.67	0.15	0.16	1.37	
0.42	0.12	5.67	0.00	0.00	1.37	
0.42	0.12	5.39	0.00	0.00	1.37	
0.00	0.02	4.41	0.00	0.00	1.09	0.14 biotite 0.07 kaolinite
0.00	0.00	3.89	0.00	0.00	0.62	0.38 plagioclase 0.26 kaolinite
0.00	0.00	2.27	0.00	0.00	0.01	1.37 plagioclase 0.81 montmorillonite
0.00	0.00	0.03	0.00	0.00	0.01	1.15 calcite

For the reaction of montmorillonite to kaolinite,

$$2H^+ + 3Ca_{0.33}Al_{4.67}Si_{7.33}O_{20}(OH)_4 + 7H_2O = 7Al_2Si_2O_5(OH)_4 + 8SiO_{2aq} + Ca^{2+}$$

the equilibrium constant is

$$K = \frac{[Ca^{2+}][SiO_2]^8}{[H^+]^2}$$

Thus, for a montmorillonite of the average composition shown and neglecting changes in the activity of water, a water undersaturated with respect to montmorillonite but saturated with respect to kaolinite should have a value for the quotient less than K, and all waters saturated with respect to both phases should have a constant value of the quotient. Figure 2 shows a plot of the compositions of Sierra springs, in which the

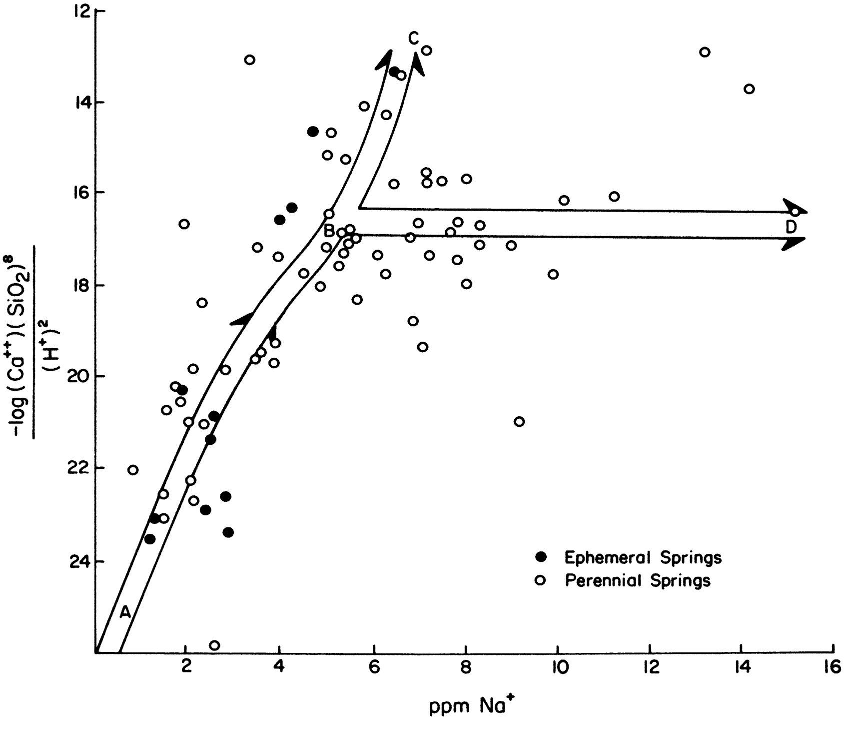

Figure 2. pK′ for equilibrium between Ca-beidellite and kaolinite plotted as a function of Na content of Sierra Nevada spring waters. Arrow ABC is the path of water evolution calculated for the reaction from $Na_{0.62}Ca_{0.38}$ plagioclase to kaolinite in a closed system with an initial dissolved CO_2 of 0.0006 moles per liter. Arrow ABD is the expected path if evolution is also controlled by the two-phase equilibrium kaolinite-montmorillonite

logarithm of the quotient $\frac{m_{Ca^{2+}} m^8_{SiO_2}}{m^2_{H^+}}$ (p*K'*) is plotted against p.p.m. Na^+. The arrow ABC is calculated assuming that only kaolinite results from decomposition of plagioclase, whereas the arrow ABD is the predicted evolution if kaolinite is formed first, but that montmorillonite also forms when the waters gain sufficient SiO_2, Ca^{2+}, and a high enough pH. The position of the arrow for kaolinite-montmorillonite equilibrium has been estimated from the boundary on Figure 3 and the exchange constants for Na-Ca montmorillonites. Despite the scatter, it is clear that the ephemeral springs alter feldspar chiefly to kaolinite and that many of the perennial springs, although their evolution is to kaolinite, have compositions that suggest a halt in that path of evolution and possible control by equilibration with both phases.

If this is true, and it must be regarded as a highly tentative conclusion, then the upper limits of silica content of many natural waters, which are far less than saturation with amorphous silica ($\cong$ 115 p.p.m.), may well be controlled by equilibrium between the waters and various silicate phases. This does not mean that the controlling solids are well-crystallized, clearly distinguishable substances, but there is definitely an interplay between the waters and solid aluminosilicates. Furthermore, the aluminosilicates apparently differ from each other in important compositional steps, and are not simply continuous gradations resulting from progressive adsorption and alteration as water compositions change. This generalization from the Sierra studies is more strikingly shown by Bricker and Garrels (*1*). Figure 3 is adapted from their work and shows that the compositions of dilute ground and surface waters in silicate-bearing rocks are contained within a set of phase boundaries derived from equilibrium relations among silicate phases.

An idealized water, derived from the attack of CO_2-bearing water on a typical felsic rock to produce only kaolinite, should have the following characteristics, expressed in terms of molar concentrations:

(1) HCO_3^- should be the only anion, except for small concentrations of Cl^- and SO_4^{2-} from fluid inclusions in the minerals, oxidation of pyrite, and other minor sources.

(2) Na^+ and Ca^{2+} should be the chief cations, and the ratio of Na^+ to Ca^{2+} should be the same as that in the plagioclase of the rock.

(3) The total of Mg^{2+} and K^+ should be less than about 20% of the total of Na^+ and Ca^{2+}. The ratio of Mg^{2+} to K^+ should range around 1 to 1, with higher values related to higher percentages of mafic minerals, and lower values to higher ratios of K-feldspar to mafic minerals.

(4) The ratio of SiO_2 to Na^+ should be about 2 to 1, with somewhat higher ratios from rocks unusually high in K-spar and/or mafic minerals.

(5) The ratio of Na^+ to K^+ should be 5 to 1 or higher because of the abundance and high weathering rate of plagioclase, as opposed to the

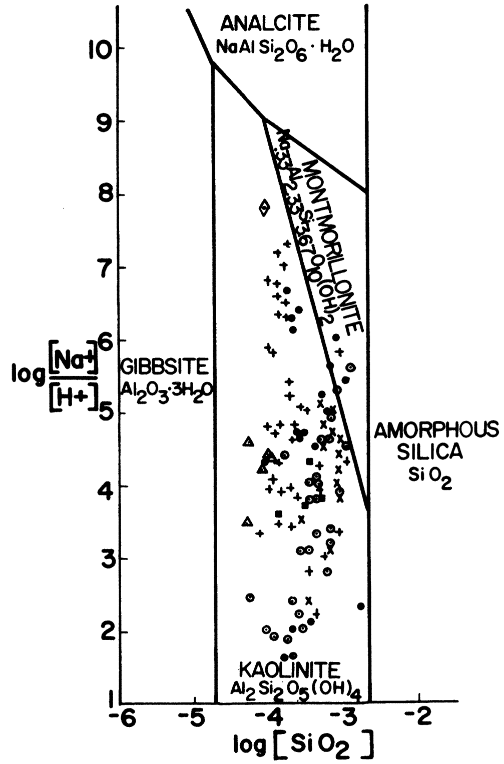

Figure 3. Stability fields of some minerals in the Na_2O-Al_2O_3-SiO_2-H_2O system at 25°C. as a function of Na^+, H^+, and dissolved silica. Points are from ground water analyses of siliceous rocks

⊙ = *granite, rhyolite*
■ = *andesite, diorite*
△ = *Jamaican bauxites*
× = *basalt, gabbro*
◇ = *sea water*
● = *siltstone, clay, shale*
+ = *sandstone, arkose, graywacke*

low weathering rate of K-feldspar and the generally low abundance of micas or other K-bearing phases.

Table V compares the Sierra waters with some waters from other felsic rocks. The fundamental similarities are clearly apparent as well as the minor variations that show the imprint of the details of rock mineralogy and small additions of constituents from various other sources.

Evaporative Concentration of Sierra Waters

The alteration of the igneous rocks of the Sierra was treated as an example of the genesis of waters in an essentially closed system. There

Table V. Compositions of Waters from Various Igneous Rocks (mole %)

	Sierra Ephemeral Springs[a]	*Sierra Perennial Springs*[a]	*Springs from Sierra Volcanic Rocks*[a]	*Ground Water from Granite, R.I.*[b]	*Ground Water from Rhyolite, N. M.*[b]
SiO_2	33.8	21.0	19.5	19.9	38.6
Ca^{2+}	8.5	13.0	10.3	9.6	4.6
Na^+	13.8	13.0	10.3	15.6	20.0
Mg^{2+}	2.8	3.5	8.0	6.6	2.5
K^+	2.5	2.0	1.4	1.2	1.3
HCO_3^-	38.7	45.0	48.5	38.0	28.0
Cl^-	—	1.5	1.4	8.4	2.5
SO_4^{2-}	—	1.5	0.2	0.6	0.8
pH	6.2	6.8	7.0	7.6	7.2

[a] Data from Ref. 3. [b] Data from Ref. 8.

was no indication from an analysis of the processes involved that a "final" equilibrium had been attained. Although the rates of altering the primary silicates diminished as CO_2 was used up and the concentration of dissolved solids increased, primary rock-forming silicates definitely are unstable in any waters produced. It would be interesting to attempt to deduce the final composition of waters and solids if a given quantity of CO_2-charged water were permitted to react indefinitely with a felsic rock, but the real situation seems to be that the waters emerge from the closed system when they have reached compositions similar to those of the Sierra and begin to lose and gain constituents from other sources.

Perhaps the next step in trying to understand the complexities of the genesis of natural waters is to see what might happen if the Sierra springs were isolated from the parent rock and solid alteration products and permitted to evaporate isothermally in equilibrium with the CO_2 of the earth's present atmosphere. In terms of a natural situation, this process might resemble the fate of waters discharged to the east of the Sierra and evaporated in a playa of the California desert. It is, of course, impossible to have a real situation without adding reactive solids from some source, but such interference could be treated afterwards in terms of additional variables. Also, this particular situation might shed some light on the effects of the "igneous rock component" of natural waters during the evaporative processes that change stream waters into oceans.

Table VI gives the mean composition of the perennial springs of the Sierras. We have chosen to ignore Fe, Al, NO_3, and F and restricted ourselves to the following analysis (Table VI).

Calculations and Procedures. The general procedure we have used is to calculate the effects of concentrating the waters by various factors

Table VI. Composition of Sierra Spring Water Used in Evaporation Study (3)

	p.p.m.	*moles/liter* × *10^4*
SiO_2	24.6	4.10
Ca^{2+}	10.4	2.60
Mg^{2+}	1.70	0.71
Na^+	5.95	2.59
K^+	1.57	0.40
HCO_3^-	54.6	8.95
SO_4^{2-}	2.38	0.25
Cl^-	1.06	0.16[a]

pH (median) = 6.8; ionic strength = 0.0013

[a] Cl^- has been diminished by 0.14 from the calculated 0.30 derived from 1.06 p.p.m. given in the analysis to correct initial electrical imbalance between anions and cations. This change is important in the compositions calculated but not in the general pattern of change to be presented.

up to 1000-fold, determining the stages at which various solids should precipitate from the system, and determining the effects of removing solids on composition and pH.

The conditions imposed are that the water remains in equilibrium with a CO_2 pressure of $10^{-3.5}$ atm., that the temperature remains constant at 25°C., and that pure water (except for a little CO_2) is continuously removed from the system. It is further assumed that any solids formed remain in equilibrium. As it turns out, the question as to whether precipitated solids are isolated after formation or continue to react is not important here, although it is important in many comparable systems.

To keep track of the minerals that might form, we tried to assess the possible combinations of dissolved species to form solids. Table VII

Table VII. Solids Considered as Possible Precipitates in Concentrated Spring Water

Species	*Solid*	*Equilibrium Constant*
Na^{2+}	None	None
K^+	None	None
Ca^{2+}		
gypsum	$CaSO_4 \cdot 2H_2O$	$a_{Ca^{2+}}a_{SO_4^{2-}} = 10^{-4.62}$
calcite	$CaCO_3$	$a_{Ca^{2+}}a_{CO_3^{2-}} = 10^{-8.35}$
Mg^{2+}		
brucite	$Mg(OH)_2$	$a_{Mg^{2+}}a^2_{OH^-} = 10^{-11.15}$
magnesite	$MgCO_3$	$a_{Mg^{2+}}a_{CO_3^{2-}} = 10^{-8}$
hydromagnesite	$Mg_4(CO_3)_3(OH)_2$	$a^4_{Mg^{2+}}a^3_{CO_3^{2-}}a^2_{OH^-} = 10^{-34.9}$
sepiolite	$MgSi_3O_6(OH)_2$	$a_{Mg^{2+}}a^3_{SiO_2}a^2_{OH^-} = 10^{-24}$
SiO_2		
amorphous silica	$SiO_2 \cdot 2H_2O$	$a_{SiO_2} = 10^{-2.7}$

shows the species we considered and some data concerning them. The values for the equilibrium constants, except for sepiolite, have been calculated from the free energy values given by Garrels and Christ (*4*). The value for sepiolite is discussed in the text.

A few notes on our selections and on some of the other mineral possibilities may help to clarify the use of these particular species. Gypsum seems to be the most likely sulfate phase. It is stable with respect to anhydrite, is a common precipitate from low temperature natural waters, and except in highly concentrated brines, double sulfates would not be expected. Calcite was chosen in preference to aragonite or possibly a whole variety of magnesian calcites because it is the stable phase and commonly precipitates directly from dilute solution. Also, the difference in solubility between calcite and aragonite is not great enough to influence the general picture. Dolomite is certainly a possibility in the system, as is the metastable mineral huntite ($CaMg_3(CO_3)_4$), but even at 1000× concentration of these waters the conditions apparently necessary in nature to precipitate dolomite (evaporation of sea water to a dense brine, gypsum precipitation, and $\frac{Mg^{2+}}{Ca^{2+}}$ ratio ≥ 30 (*2*) are not approached). The low Al (Table I) precludes more than traces of aluminosilicates, and Mg is the only cation likely to make a silicate species. Hostetler (*5*), after reviewing the occurrence of the Mg-silicates, concluded that sepiolite tends to form in most natural solutions at room temperature in preference to serpentine or talc, especially in a high silica environment, and he cites many occurrences of sepiolite plus magnesite and amorphous silica. Furthermore, Siffert (*7*) synthesized sepiolite within a day at room temperature at pH values of about 8.8 in high SiO_2/MgO solutions. Our greatest difficulty was in assigning an equilibrium constant for sepiolite. From Siffert's work and using the formula in Table VII, we get a *K* value of about 10^{-22} for the reaction:

$$3H_4SiO_4 + Mg^{2+} + 2OH^- = MgSi_3O_6(OH)_2 + 6H_2O$$

On the other hand, we precipitated a magnesium silicate from sea water by adding sodium metasilicate that gave an approximate *K* of 10^{-24} after aging. Siffert's material was freshly precipitated and could be expected to age significantly, like other poorly crystalline silicates. Consequently, the value chosen is open to considerable doubt.

Some other phases considered were nesquehonite ($MgCO_3 \cdot 3H_2O$), artinite ($Mg_2CO_3(OH)_2 \cdot 2H_2O$), and lansfordite ($MgCO_3 \cdot 5H_2O$), but all are rare and according to Hostetler (*5*) are not stable.

Our procedure was to follow the changes in concentrations and ionic strength as the water is evaporated, and by correcting ion molalities by activity coefficients, keep track of the ion activity products of the various

Table VIII. Calculated Ion Activity Products of Various Concentration

	Calcite *$CaCO_3$*	*Gypsum* *$CaSO_4 \cdot 2H_2O$*	*Brucite* *$Mg(OH)_2$*
Initial water in equilibrium with atmosphere	8.8	8.3	15.7
Concentrated by a factor of			
1.25	Saturated	8.1	15.5
2.0	Saturated	8.0	15.1
5.0	Saturated	7.7	15.9
10.0	Saturated	7.9	15.9
100.0	Saturated	8.3	15.9
1000.0	Saturated	8.8	15.4
Equilibrium Constant	8.35	4.62	11.15

[a] Products are expressed as negative logarithms (pK').

solids as shown in Table VIII. If an ion activity product reached the equilibrium constant value, we then maintained equilibrium with that solid during continuing concentration. Sample calculations show the procedure used.

Sample Calculations. The first step was to determine if the water analysis represents a solution in equilibrium with the atmosphere. For the reaction

$$CO_2 + H_2O = HCO_3^- + H^+$$

the equilibrium constant is

$$\frac{a_{HCO_3^-}\, a_{H^+}}{a_{CO_2}\, a_{H_2O}} = K_{CO_2} = 10^{-7.82} \qquad (1)$$

Rearranging, and writing in terms of activity coefficients and molalities and assuming the pH is a measure of a_{H^+}

$$a_{CO_2} = \frac{\gamma_{HCO_3^-}\, m_{HCO_3^-}\, a_{H^+}}{K_{CO_2}\, a_{H_2O}} \qquad (2)$$

In all solutions considered, the activity of water is greater than 0.99 and was considered unity throughout. The ionic strength (I) of the original water is only 0.0013 and that of the final water 0.408, so that individual ion activity coefficients calculated from Debye-Hückel equations (*4*) were used throughout to estimate ion activities. The calculated a_{CO_2}, or P_{CO_2}, using the median pH of 6.8 is shown in Equation 3.

Possible Solid Compounds in Sierra Water as a Function of by Evaporation[a]

Magnesite $MgCO_3$	*Hydromagnesite* $Mg_4(CO_3)_3(OH)_2$	*Sepiolite* $Mg(SiO_2)_3(OH)_2$	*Silica Gel* SiO_2
9.4	43.6	25.9	3.4
8.8	42.5	25.3	3.3
8.7	40.2	24.3	3.1
9.6	44.6	Saturated	3.0
9.6	48.9	Saturated	Saturated
9.6	44.0	Saturated	Saturated
9.0	42.5	Saturated	Saturated
8.0	34.9	24.0	2.7

$$P_{CO_2} = \frac{0.97 \times 10^{-3.04}10^{-6.8}}{10^{-7.82}} = 10^{-2.0}\text{ atm.} \qquad (3)$$

The CO_2 pressure of the water is considerably above the atmospheric value of $10^{-3.5}$ and therefore the initial water is not in equilibrium with the atmosphere.

The next step, which is representative of all pH calculations, is to find the pH and the accompanying changes in dissolved carbonate species when the water comes to equilibrium with the atmosphere with respect to P_{CO_2}. As CO_2 is lost, the pH will rise.

The equation for electrical neutrality is:

$$\begin{aligned} 2m_{Ca^{2+}} + 2m_{Mg^{2+}} + m_{Na^+} + m_{K^+} + m_{H^+} &= \\ 2m_{SO_4^{2-}} + m_{Cl^-} + m_{HCO_3^-} + 2m_{CO_3^{2-}} + m_{OH^-} & \end{aligned} \qquad (4)$$

Rewriting to put pH-dependent species on the right

$$\begin{aligned} 2m_{Ca^{2+}} + 2m_{Mg^{2+}} + m_{Na^+} + m_{K^+} - 2m_{SO_4^{2-}} - m_{Cl^-} &= \\ m_{HCO_3^-} + 2m_{CO_3^{2-}} + m_{OH^-} - m_{H^+} & \end{aligned} \qquad (5)$$

The terms on the right of Equation 5 can be expressed in terms of pH, equilibrium constants, P_{CO_2}, and ionic activity coefficients; the terms on the left are known from the water analysis (Table VI). Rearranging Equation 2 gives Equation 6.

$$m_{HCO_3^-} = \frac{K_{CO_2}P_{CO_2}}{\gamma_{HCO_3^-}a_{H^+}} = \frac{10^{-7.82}10^{-3.5}}{\gamma_{HCO_3^-}a_{H^+}} = \frac{10^{-11.32}}{\gamma_{HCO_3^-}a_{H^+}} \qquad (6)$$

The parallel equation for CO_3^{2-} is

$$m_{CO_3^=} = \frac{K_{HCO_3^-}K_{CO_2}P_{CO_2}}{\gamma_{CO_3^{2-}}a_{H^+}^{2}} = \frac{10^{-10.33}10^{-7.82}10^{-3.50}}{\gamma_{CO_3^{2-}}a_{H^+}^{2}} = \frac{10^{-21.65}}{\gamma_{CO_3^{2-}}a_{H^+}^{2}} \qquad (7)$$

and for OH^-

$$m_{OH^-} = \frac{K_{H_2O}}{\gamma_{OH^-}a_{H^+}} = \frac{10^{-14}}{\gamma_{OH^-}a_{H^+}} \qquad (8)$$

Substituting analytical values of molality for the terms on the left of Equation 5, Debye-Hückel activity coefficients in the right-hand terms, and neglecting m_{H^+}

$$0.00052 + 0.000142 + 0.00026 + 0.00004 - 0.000050 - 0.000016 =$$

$$\frac{10^{-11.32}}{0.97a_{H^+}} + \frac{2(10^{-21.65})}{0.86a_{H^+}^{2}} + \frac{10^{-14}}{0.97a_{H^+}}$$

collecting terms,

$$0.000896 = \frac{10^{-11.32}}{a_{H^+}} + \frac{10^{-21.28}}{a_{H^+}^{2}} + \frac{10^{-14.0}}{a_{H^+}}$$

solving for a_{H^+},

$$a_{H^+} = 10^{-8.26};\ pH = 8.26.$$

From this value of pH, the values for $m_{HCO_3^-}$, $m_{CO_3^{2-}}$, and m_{OH^-} are obtained from Equations 6, 7, and 8, and the total water analysis can be determined. The only important change is in pH, which rises from 6.8 to 8.26; the change is accompanied by a loss in dissolved CO_2 and a slight increase in CO_3^{2-}—actually not enough to be worth showing in the analysis.

The next step is to determine whether or not the water as a result of the pH change has become saturated with respect to any of the solid phases considered (Table VII). For this, ion activity products are computed for each phase and compared with the equilibrium value (Table VIII). The calculation for calcite is given to illustrate the procedure. The ion activity product is

$$\gamma_{Ca^{2+}}m_{Ca^{2+}}\gamma_{CO_3^{2-}}m_{CO_3^{2-}} = K'$$

The value of $\gamma_{CO_3^{2-}}m_{CO_3^{2-}}$ is obtained from the pH and Equation 7:

$$\gamma_{CO_3^{2-}}m_{CO_3^{2-}} = \frac{10^{-21.65}}{(10^{-8.26})^2} = 10^{-5.13}$$

The Debye-Hückel equation yields 0.88 for $\gamma_{Ca^{2+}}$, and $m_{Ca^{2+}}$ is 2.60×10^{-4} or $10^{-3.59}$ (Table VI). Thus K' is $(0.88)(10^{-3.59})(10^{-5.13}) = 10^{-8.78}$.

Consequently, because the equilibrium value of the ion activity product is $10^{-8.35}$, the water is slightly undersaturated with respect to calcite, its Ca^{2+} content is fixed by CO_2 pressure and pH; in other words, because the product of $a_{Ca^{2+}}$ and $a_{CO_3^{2-}}$ is a constant, $a_{Ca^{2+}}$ and hence $m_{Ca^{2+}}$ can be expressed as a negative term on the right side of the electrical balance equation. After sepiolite precipitates, it can be handled similarly. The

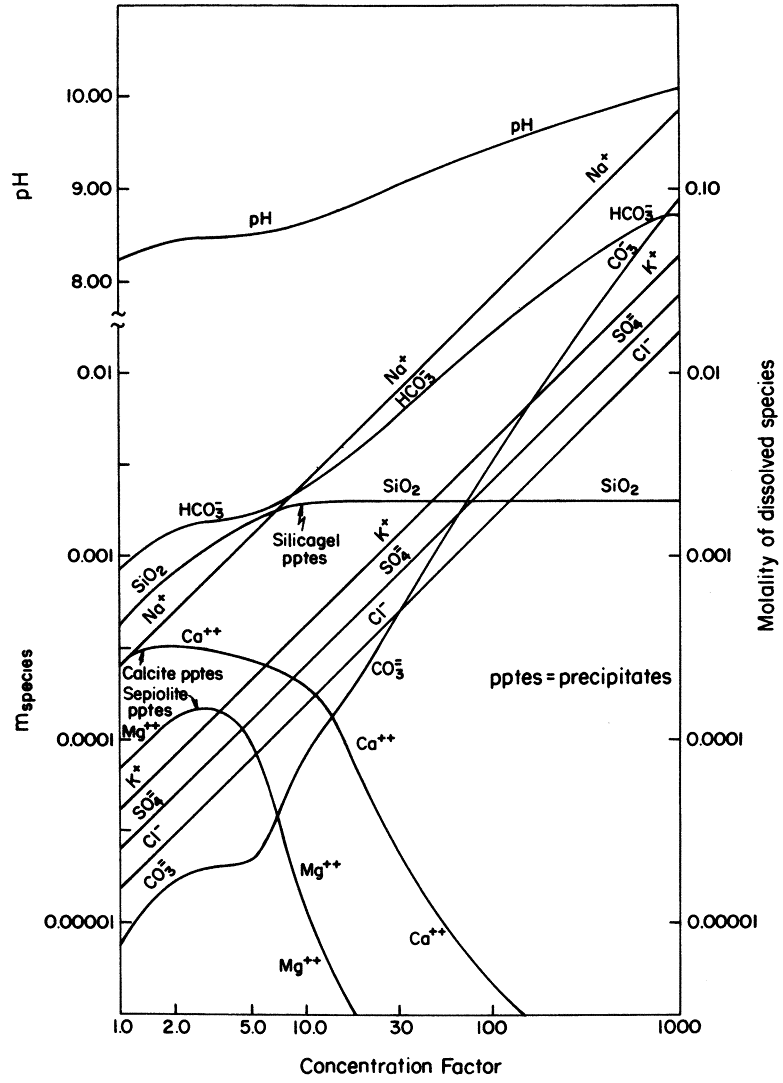

Figure 4. Calculated results of evaporation of typical Sierra Nevada spring water at constant temperature in equilibrium with atmospheric CO_2

analytical expression, after the water becomes saturated with calcite, sepiolite, and silica, is

$$m_{Na^+} + m_{K^+} - 2m_{SO_4^{2-}} - m_{Cl^-} = m_{HCO_3^-} + 2m_{CO_3^{2-}}$$
$$+ m_{OH^-} - 2m_{Ca^{2+}} - 2m_{Mg^{2+}},$$

or

$$m_{Na^+} + m_{K^+} - 2m_{SO_4^{2-}} - m_{Cl^-}$$
$$= \frac{10^{-11.32}}{\gamma_{HCO_3^-} a_{H^+}} + \frac{2(10^{-21.65})}{\gamma_{CO_3^{2-}} a_{H^+}^2} + \frac{10^{-14}}{\gamma_{OH^-} a_{H^+}} - \frac{2(10^{13.3} a_{H^+}^2)}{\gamma_{Ca^{2+}}} - \frac{2(10^{12.1} a_{H^+}^2)}{\gamma_{Mg^{2+}}}$$

In calculating for a given degree of water concentration, the ionic strength is estimated, and tentative activity coefficients for the ions are obtained. After an approximate pH is obtained and values can be assigned for the molalities of the pH-dependent species, new values for the ionic strength and activity coefficients are obtained, and the electrical balance equation is solved again. One such iteration usually suffices to provide satisfactory results. Using the Debye-Hückel activity coefficients obviously leads to an increasing uncertainty in γ_i values with increasing ionic strength, and the values calculated for 1000× concentration should be regarded as rough approximations.

Discussion. A summary of the calculated changes in water composition during evaporation is shown in Figure 4. In essence, evaporation changes the water from a nearly neutral Na-Ca-HCO_3 water to a highly alkaline Na-HCO_3-CO_3 water. Calcium and magnesium are removed by early precipitation of calcite and sepiolite, and their concentrations diminish to small values as the values of CO_3^{2-} and OH^- rise. Because of the initial high silica, there is enough silica to permit the water to precipitate silica gel at about 10× concentration. Na^+, K^+, Cl^-, and SO_4^{2-} concentrate without forming solids.

Table IX. Analyses of Various

	Na^+	*K^+*	*Ca^{2+}*
Sierra 100 ×	595	159	0.2
Lower Alkali Lake, Eagleville, Calif.[a]	370	11	6.9
Amargosa River, Nev.[a]	423	17	2.0
Kurusch Gol, Iran[a]	730	29	11
Keene Wonder Spring, Calif.[b]	1040	25	23
Sierra 1000 ×	5950	1590	0
Soap Lake, Wash.[a]	12,500	12,500	3.9
Lenore Lake, Wash.[a]	5360	5360	3.0

[a] Analyses from Ref. 6, Chapter G.
[b] Analyses from Ref. 8, Chapter F.

Buffering of pH during the early heavier precipitation of calcite and sepiolite is clear and is reflected in a near constancy of HCO_3^- and CO_3^{2-}. However, after Ca^{2+} and Mg^{2+} are substantially reduced, the pH again rises with further concentration. Because the Sierra waters are so low in sulfate, gypsum does not precipitate; abstraction of Ca^{2+} as calcite never permits the solubility product of gypsum to be exceeded.

The 100× and 1000× waters resemble some natural waters. Table IX compares, in p.p.m., the hypothetical Sierra waters with several natural water bodies.

Summary of Genesis and Evaporation of Sierra Waters

The preceding study of the origin of the composition of spring waters in felsic rocks and the results of evaporating the waters in the absence of the solid weathering residues show that the processes are highly asymmetric. The weathering study showed that dissolved silica comes chiefly from the incongruent solution of silicate minerals rather than from congruent solution of quartz, and as a result the univalent and bivalent cations in solution derived from these silicate minerals are balanced by HCO_3^-. During evaporation in equilibrium with the atmosphere, the bivalent ions tend to form insoluble carbonates or hydroxysilicates, and the pH of the evaporating solution remains relatively constant until the silicates have been largely removed. The univalent ions, on the other hand, do not form similar compounds of low solubility, and concentrate continuously with a concomitant increase in HCO_3^-, CO_3^{2-}, and pH. Therefore, waters maintained in equilibrium with the atmosphere and separated from decomposition products, with univalent ions originally derived from incongruent solution of silicates will inevitably become highly alkaline if concentrated greatly.

Saline Waters, p.p.m.

Mg^{2+}	HCO_3^-	CO_3^{2-}	SO_4^{2-}	Cl^-	SiO_2	pH
0	990	212	240	56	120	9.45
0.9	1200	1200	307	1160	63	?
0.2	639	639	257	109	70	?
25	1200	1200	306	342	?	?
38	1070	29	796	567	57	8.4
0	4250	4500	2400	560	120	10.02
23	11,270	5130	6020	4680	101	?
20	6090	3020	2180	1360	22	?

It is obvious that the silica present in these waters, if denied the opportunity to react with aluminous minerals, must precipitate as amorphous silica or as silicates of the bivalent cations, as illustrated by sepiolite in the example chosen. In nature the silica may be removed by organisms, such as diatoms, but they do not change the gross chemistry.

Acknowledgments

We have benefitted greatly from discussions with many colleagues in many places. We especially want to thank Roland Wollast of the University of Brussels, Harold Helgeson of Northwestern University, Charles Christ of the United States Geological Survey, and Owen Bricker of The Johns Hopkins University for reading the manuscript and for offering many useful suggestions and criticisms.

Literature Cited

(1) Bricker, O. P., Garrels, R. M., *Proc. Ann. Rudolphs Conf., 4th, 1965*, Rutgers Univ., New Brunswick, 1967.
(2) Deffeyes, D. K., Lucia, F. J., Weyl, P. K., *Science* **143,** 678 (1963).
(3) Feth, J. H., Roberson, C. E., Polzer, W. L., *U.S. Geol. Surv. Water Supply Paper* **1535-I,** 170 (1964).
(4) Garrels, R. M., Christ, C. L., "Solutions, Minerals, and Equilibria," Appendix 2, p. 450, Harper and Row, New York, 1965.
(5) Hostetler, P. B., Ph.D. thesis, Harvard University, 1960.
(6) Livingstone, D. A., *U.S. Geol. Surv. Profess. Paper* **440-G,** 61 (1963a).
(7) Siffert, B., *Geol. Alsace Lorraine* **21,** 32 (1962).
(8) White, D. E., Hem, J. D., Waring, G. A., *U.S. Geol. Surv. Profess. Paper* **440-F,** 14 (1963).

RECEIVED April 28, 1966. Work supported by grants from the National Science Foundation (GP-4140) and the Petroleum Research Fund of the American Chemical Society. Contribution No. 390, Bermuda Biological Station for Research.

11

Equilibrium Models and Composition of the Great Lakes

JAMES R. KRAMER

Department of Geology, Syracuse University, Syracuse, N. Y.

To a good first approximation, the Great Lakes fit a model involving the equilibrium of calcite, dolomite, apatite, kaolinite, gibbsite, Na- and K-feldspars at 5°C., 1 atm. total pressure with air of $P_{CO_2} = 3.5 \times 10^{-4}$ *atm. and water. Dynamic models, considering carbon dioxide pressure and temperature as variables (but gross concentrations fixed), show that cold waters contain excess carbon dioxide and are unsaturated with respect to calcite, dolomite, and apatite, whereas warm waters are nearly at equilibrium with the atmosphere but somewhat supersaturated with respect to calcite, dolomite, and apatite.*

Chemical equilibrium concepts are valuable in considering a dynamic fresh water regime for several reasons: (1) relating actual conditions to equilibrium model results helps to isolate important biological, physical, and chemical processes; (2) the lack of fit of equilibrium model predictions to actual situations emphasizes areas for further investigation; (3) organization of systems into models allows for generalization and simplification of empirical water chemistry data.

The rationale for using equilibrium models for Great Lakes chemistry rests upon the principle that the lithosphere (mineralogical materials) is the ultimate source of all solution materials and that these materials are obtained in the liquid phase by equilibration of rain water running over the mineralogical materials, dissolving, modifying, and causing precipitation to occur. Approach to equilibrium should be good as the time available for mixing ranges from less than 10 years to more than two centuries (9). Hence the Great Lakes should represent a much better equilibrium bath than can be found in the laboratory!

Equilibrium calculations predict only initial and final states for a particular system, whereas actual environments must be concerned with dynamic conditions and the actual paths taken in arriving at a final state. In both situations, however, probabilistic considerations regarding a reaction must be considered, and the resultant thermodynamic demands cannot be violated whether we are discussing simple ligands, complex ligands, or biological processes. It may well be true in this context that the over-all chemistry of a system may actually approach reversible equilibrium, whereas particular sub-systems not at equilibrium (such as biological processes) may represent differing paths taken to reach the equilibrium.

Equilibrium Models

The procedure used to define an equilibrium model is to (1) define all the variables and (2) define independent equilibria as a function of phase equilibria. The variables are defined as the chemical parameters typically measured in water chemistry. For the major constituents and some of the more important minor constituents, these are calcium, magnesium, sodium, potassium, silica, sulfate, chloride, and phosphate concentrations as well as alkalinity (usually carbonate alkalinity) and pH. To this list we would also add temperature and pressure. The phase equilibria are defined by compiling well-known equilibria between gas-liquid phases and solid-liquid equilibria for the solids commonly found forming in nature in sedimentary rocks. Within this framework, one can construct different equilibrium models depending upon the mineral chosen; actual data concerning the formation of specific minerals therefore must be ascertained to specify a particular model as valid.

The Gibbs phase rule is the basis for organizing the models. In general, the number of independent variables (degrees of freedom) is equal to the number of variables minus the number of independent relationships. For each unique phase equilibria, we may write one independent relationship. In addition to this (with no other special stipulations), we may write one additional independent relationship to maintain electroneutrality. Table I summarizes the chemical constituents considered as variables in this study and by means of chemical reactions depicts independent relationships. (Throughout the paper, activity coefficients are calculated by the Debye-Hückel relationship). Since there are no data available on pressure dependence, pressure is considered a constant at 1 atm. Sulfate and chloride are not considered variables because little specific data concerning their equilibria are available. Sulfate may be involved in a redox reaction with iron sulfides (*e.g.*, hydrotroilite), and/or it may be in equilibrium with barite ($BaSO_4$) or some solid solution combinations. Chloride may reach no simple chemical equilibrium with respect to a phase. Therefore, these two ions are considered only to the extent that they affect electroneutrality balance. Two values—1.2 and 13×10^{-4} equiv./liter—are assumed in the calculations for the sum of the chloride and sulfate ion charges. These values represent lower and upper limits for Great Lakes waters.

A further assumption of the model is that liquid, solid, and gas phases are in equilibrium with one another. This assumption demands a relatively rapid and high degree of mixing of atmosphere, lithosphere, and hydrosphere. Under this assumption, the carbon dioxide content of the atmosphere may be considered constant and equal to 3.5×10^{-4} atm.

Table I. Variables and Independent Phase Relationships for Determining the Number of Independent Variables

Variables Measured	*Phase Relationship*	*Equilibrium Constant (5°C.)*	*Reference*
Ca^{2+}	$2H^+ + CaCO_3(s) = Ca^{2+} + CO_2(g) + H_2O(l)$	$10^{10.19}$	*2, 3, 4, 11*
Mg^{2+}	$CaMg(CO_3)_2(s) = Ca^{2+} + Mg^{2+} + 2CO_3^{2-}$	$10^{-16.6}$	
Na^+	$Na^+ + KAlSi_3O_8(s) = K^+ + NaAlSi_3O_8(s)$	$10^{-1.08}$	*1*
K^+	$2KAlSi_3O_8(s) + 2H^+ + 9H_2O(l) = Al_2Si_2O_5(OH)_4(s) + 4H_4SiO_4(l) + 2K^+$	$10^{-13.2}$	*1*
Alkalinity	$P_{CO_2} = 3.5 \times 10^{-4}$ atm.		
H_4SiO_4	$5H_2O(l) + Al_2Si_2O_5(OH)_4(s) = 2Al(OH)_3(s) + 2H_4SiO_4(l)$	$10^{-9.6}$	*1*
Total pressure[a]	$Ca_{10}(PO_4)_6(OH)_2(s) = 10Ca^{2+} + 6PO_4^{3-} + 2OH^-$	10^{-112}	*10*
pH	sum of positive charges = sum of negative charges		
Temperature			

[a] Total pressure = 1 atm. Sum of sulfate and chloride ion equivalents assumed constant at either 1.2 or 13×10^{-4} equiv./liter.

With these stipulations, the model reduces to one more variable than there are relationships. Therefore, if temperature is considered constant, the model would become invariant; otherwise we may consider a dynamic situation with temperature varying independently (as a function of meteorological conditions, heat flow, etc.). The actual temperature distribution of the Great Lakes (except for Lake Erie and shallow areas of other lakes) is quite limited relative to volume distribution, and to a first approximation it approaches a constant of about 5°C. This conclusion may be readily ascertained by realizing the typical depth of water above the thermocline (where there is a temperature gradient) is from 10–20 meters, whereas depth equivalent to water below the thermocline (where maximum temperature change is 3°–4°C.) varies from 100–300 meters.

Other models considering the same variables but different equilibria may be considered. Empirical data outlining the phases present in a specific environment will lend support to a particular model as being valid. The solids chosen here are commonly found in the sedimentary rock environment, both ancient and recent.

Table II summarizes the degrees of freedom comparable to the models outlined in the above discussion. On a graph, a point, a curve, and a surface would represent 0, 1, and 2 degrees of freedom, respectively.

Table II. Models and Number of Independent Variables

Model No.	*Description*	*Variance*
1	Constant temperature, pressure and P_{CO_2}	0
2	Constant pressure and P_{CO_2}	1
3	Constant pressure	2

[a] For details of definition of models, *see* Table I.

The actual arithmetic involved in the calculations may be done easily by starting with the general expression for electroneutrality and substituting equilibrium expressions (9). Using the equilibrium constants of Table I and assuming that activities equal concentrations, we obtain for 5°C. and an invariant condition (model No. 1) the following data:

$(Cl^- + 2SO_4^{2-}) = 1.2 \times 10^{-4}$ *equiv./liter*

$Ca^{2+} = 10^{-3.15}$ mole/liter (27 p.p.m.)
$Mg^{2+} = 10^{-3.60}$ (6 p.p.m.)
$K^+ = 10^{-5.4}$ (0.15 p.p.m.)
$Na^+ = 10^{-4.3}$ (1.2 p.p.m.)
$H_4SiO_4 = 10^{-4.8}$ (0.95 p.p.m. SiO_2)
pH = 8.40
$\Sigma P = 10^{-7.0}$ (3 p.p.b. P)
Alkalinity $= 10^{-2.77}$ equiv./liter

$(Cl^- + 2SO_4^{2-}) = 13 \times 10^{-4}$ *equiv./liter*

$Ca^{2+} = 10^{-3.00}$ mole/liter (40 p.p.m.)
$Mg^{2+} = 10^{-3.45}$ (8.5 p.p.m.)
$K^+ = 10^{-5.3}$ (0.20 p.p.m.)
$Na^+ = 10^{-4.2}$ (1.4 p.p.m.)
$H_4SiO_4 = 10^{-4.8}$ (0.95 p.p.m. SiO_2)
pH = 8.32
$\Sigma P = 10^{-7.14}$ (2.4 p.p.b. P)
Alkalinity $= 10^{-2.85}$ equiv./liter

The arithmetic is exactly the same for model No. 2 with one independent variable as in the invariant case except that calculations are carried out for more than one temperature. The only difference therefore is in the value of the various equilibrium constants. Arithmetic for model No. 3 with two independent variables would be an extension of the above, but both P_{CO_2} and temperature would be systematically varied.

Equilibrium and Lake Water Chemistry

We may now examine specific information from chemical analyses of the Great Lakes (*7, 8, 13*) to determine to what degree the variations of the proposed model fit the actual data. Rather than consider all of the variables at once, it is simpler to consider smaller portions to get a better idea of what actually is happening. We shall look at calcium carbonate equilibria, dolomite equilibria, phosphate equilibria, and silicate equilibria.

Calcium Carbonate Equilibria. Values of the ion product, $(Ca^{2+})(CO_3^{2-})$, are plotted in Figure 1 as a function of temperature. These values represent samples from Lake Erie and Lake Ontario for all depths of water, all areas of the two lakes, and all seasons. In addition to the point plot of actual samples, the equilibrium products for calcite and aragonite solubility are plotted as a function of temperature. Three conclusions are worth mentioning: (1) most of the lake water most of the

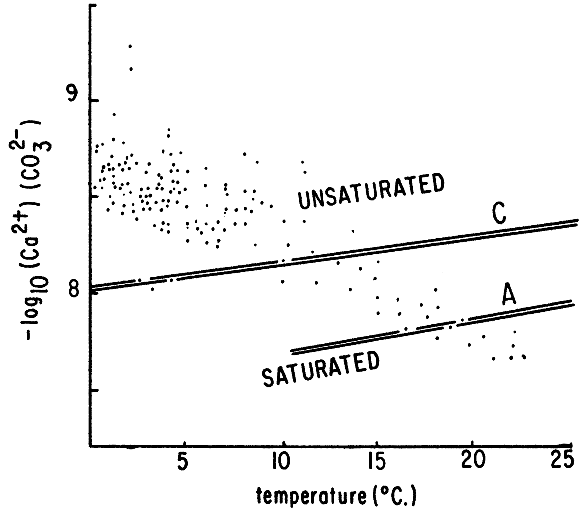

Figure 1. Saturation of lake water with respect to calcite. Double line (C for calcite, A for aragonite) represents the solubility product as a function of temperature

time is not at equilibrium with calcite or aragonite; (2) lake water reaches an average equilibrium at approximately 13°C. for calcite and 20°C. for aragonite in a dynamic environment; (3) lake water tends to be saturated with respect to calcium carbonate at high temperatures and unsaturated at low temperatures. Comparison between the actual situation and equilibrium shows that there is an alteration between saturation and unsaturation with respect to calcite. Only rarely is aragonite saturated in Great Lakes waters. This alteration is a function of both depth and season. It is curious to note that the equilibrium temperature (13°C.) is nearly the temperature at the thermocline for most Great Lakes waters.

If the chemistry of lake waters followed a univariant trend only (model No. 2, Table II), the actual data would fall along a straight line. There is a strong tendency for this to occur at higher temperatures, but scatter occurs at lower temperatures. Therefore, we must conclude within the definitions of the variables and relationships of Table I that the Great Lakes follow model No. 3, a divariant model, but approach model No. 2 a univariant model, at higher temperature. In real terms, this means at higher temperatures, assuming a constant P_{CO_2} is valid, but at lower temperatures, P_{CO_2} varies quite a bit. This is reasonable because

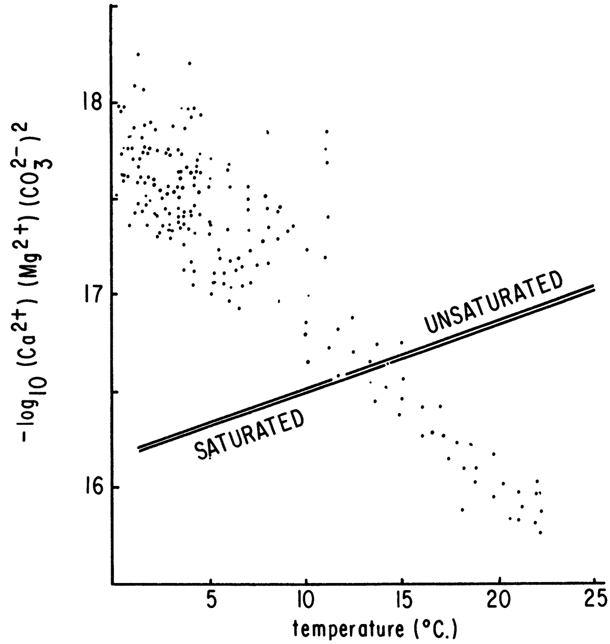

Figure 2. Saturation of lake water with respect to dolomite

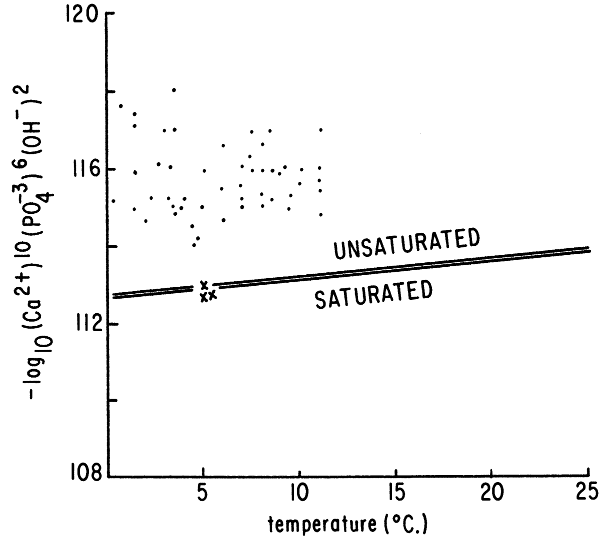

Figure 3. Saturation of lake water (winter only) with respect to hydroxyapatite as a function of temperature

deep waters are colder and tend to be poorly mixed with respect to the atmosphere, whereas warmer waters, representing surface waters, do tend to be well-mixed with respect to the atmosphere.

Dolomite Equilibrium. Figure 2 is a plot of the ion product, $(Ca^{2+})(Mg^{2+})(CO_3^{2-})^2$, as a function of temperature. Saturation of lake waters with respect to dolomite is similar to the results for calcium carbonate. The same general conclusions are apparent. Dolomite tends to be saturated with respect to lake water at 14°C.

Phosphate Equilibria. Figure 3 is a plot of the ion product, $(Ca^{2+})^{10}(PO_4^{3-})^6(OH^-)^2$, as a function of temperature. Unfortunately only data are available for low temperature (winter) waters. Samples shown by X are from water extracted from sediment in winter and are just at saturation with respect to hydroxyapatite.

Silicate Equilibria. The following equilibria are depicted at constant temperature and pressure (25°C., 1 atm. total pressure) in Figure 4.

$$2\,KAl_3Si_3O_{10}(OH)_2(s) + 2\,H^+ + 3\,H_2O(l) = 3\,Al_2Si_2O_5(OH)_4 + 2\,K^+$$

$$Na_2Al_8Si_{10}O_{33}\cdot 3\,H_2O(s) + 8\,H_2O(l) + 2\,H^+ = 4\,Al_2Si_2O_5(OH)_4(s) + 2\,H_4SiO_4(l) + 2\,Na^+$$

$$2\,(Na,K)AlSi_3O_8(s) + 2\,H^+ + 9\,H_2O(l) = 2\,(Na^+,K^+) + Al_2Si_2O_5(OH)_4(s) + 4\,H_4SiO_4(l)$$

$$5\,H_2O(l) + Al_2Si_2O_5(OH)_4(s) = Al_2O_3\cdot 3\,H_2O(s) + 2\,H_4SiO_4(l)$$

$$SiO_2(\text{amorph.},s) + 2\,H_2O(l) = H_4SiO_4(l)$$

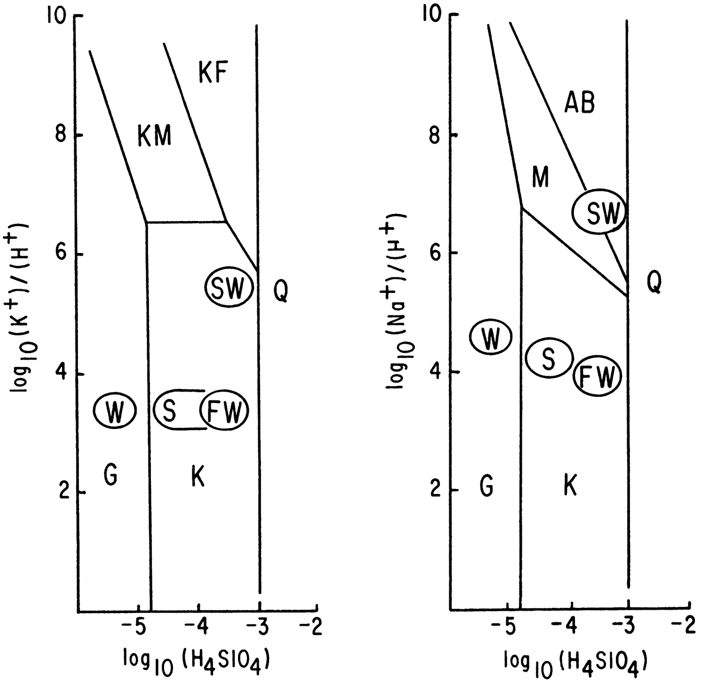

Figure 4. Silicate stability. KF, KM, G, K, and Q are K⁺-feldspar, K⁺-mica, gibbsite, kaolinite, and amorphous silica, respectively. M and AB are montmorillonite and albite. W, S, FW, and SW represent areas of winter lake data, summer lake data, extracted fresh water sediments, and extracted sea water sediments, respectively

Silica, Na^+, K^+, and H^+ analyses have been plotted for winter conditions on Lake Ontario (W on Figure 4) and have been plotted for summer conditions on the Great Lakes (*14*) (S on Figure 4). Both plots are near the gibbsite-kaolinite boundary, with the winter analyses in the gibbsite field and the summer analyses in the kaolinite field. Analyses of water extracted from bottom sediment in Lake Ontario (FW in Figure 4) in the winter lie entirely in the kaolinite field. This may be compared with the results of Siever *et al.* (*12*) for water extracted from ocean sediments (SW on Figure 4) which plot in the kaolinite and albite-montmorillonite fields with the silica concentration approaching the saturation of amorphous silica.

Note that the data used in compiling Figure 4 (*1*) do not agree with other available data (*5, 6*); the variations may be caused by determinations on different stoichiometries by different investigators. Further, the data are plotted for one temperature (25°C.) whereas most of the lake and sea water analyses are from environments of approximately 5°C.

Apparently winter lake waters are stable with respect to gibbsite relative to kaolinite, the micas, montmorillonite, and the feldspars whereas bottom sediments seem to be stable with respect to kaolinite. Kaolinite has been determined in bottom sediments of the Great Lakes as a major phase, but gibbsite has not been found so far.

Dynamic Temperature Model

The preceding discussion has pointed out that Great Lakes waters approach equilibrium at constant temperature and with respect to the atmosphere, but because of seasonal changes in temperatures and vertical mixing of waters of different temperature and because of poor mixing of bottom waters with the atmosphere, the actual system is divariant, with neither temperature or P_{CO_2} fixed. As a framework to sense modifications in lake chemistry, it is worthwhile to consider bulk composition fixed and let P_{CO_2} and temperature vary. The change in dissociation constants as a function of temperature will determine how a compositionally closed liquid will respond to temperature change. Again it is more practical to carry out the calculations for specific portions of the system.

Calcium Carbonate and Dolomite. We may consider gross chemistry of the lakes constant over temperature, pH, and P_{CO_2} changes which

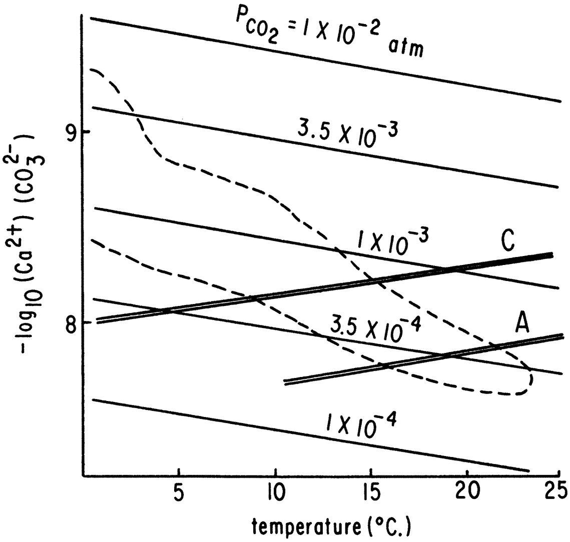

Figure 5. Ion product for calcite (C) and aragonite (A) as a function of temperature and P_{CO_2}. Areas outlined by dashed line bound lake water analyses, and double line represents solubility constants

would correspond to seasonal changes. We can then calculate a family of curves (for varying P_{CO_2}) which show the ion product, $(Ca^{2+})(CO_3^{2-})$, as a function of temperature. This dynamic system may then be compared with the results for Figures 1 and 2—the actual data for calcite and dolomite in the Great Lakes.

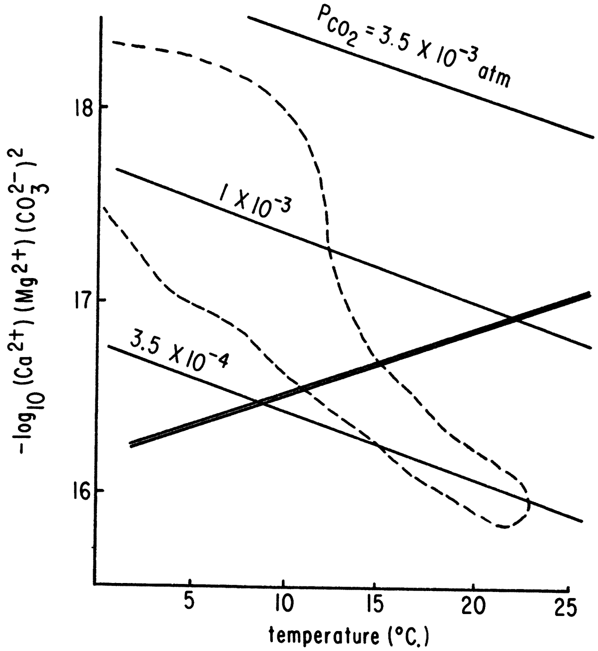

Figure 6. Ion product for dolomite as a function of temperature and P_{CO_2}. Areas outlined by dashed line bound lake water analyses, and double line represents solubility constants

For the calculations, averages of the results of the two 5°C.-equilibrium models of Ca^{2+} = 35 p.p.m., Mg^{2+} = 7 p.p.m., and alkalinity = 1.55×10^{-3} equiv./liter are used. Solubility data of Larson and Buswell (*11*), carbon dioxide solubility data of Harned and Davies (*2*), and the carbonate ionization data of Harned and Hammer (*3*) and Harned and Scholes (*4*) are used. Linear interpolations are made for dolomite between pK(soly) = 16.3(5°C.) and 17.0(25°C.). Equations outlining the calcite and dolomite calculations are:

$$CO_2(g) + H_2O(l) = HCO_3^- + H^+;\ HCO_3^- = CO_3^{2-} + H^+$$
$$CaCO_3(s) = Ca^{2+} + CO_3^{2-};\ CaMg(CO_3)_2(s) =$$
$$Ca^{2+} + Mg^{2+} + 2\,CO_3^{2-}$$

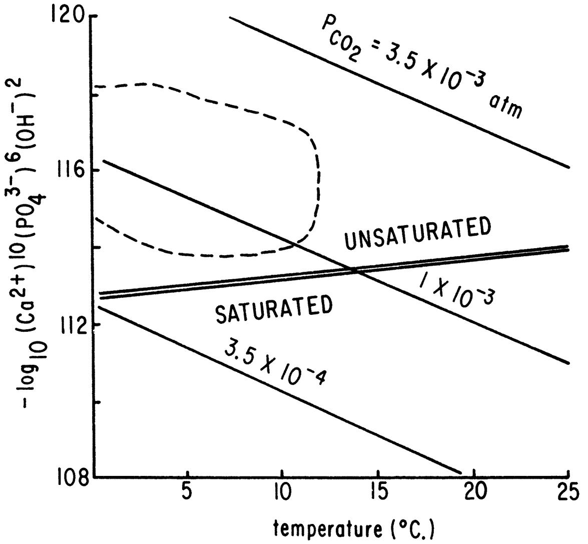

Figure 7. Ion product for hydroxyapatite as a function of temperature and pressure. Area outlined by dashed line bounds winter lake data, and double line represents solubility constant

Figures 5 and 6 show the results of the calculations, and they are compared with the actual data distribution as shown by a dashed bounding line. With both calcite and dolomite, colder waters match conditions of carbon dioxide pressure greater than atmospheric, and high temperature conditions match carbon dioxide pressure nearly the same as the atmosphere. It appears the degree of mixing and the rate of carbon dioxide diffusion is of prime importance when considering approach to liquid, gas, and solid equilibrium.

Apatite Equilibrium. The calculations are similar to those above. Since phosphates represent a negligible concentration compared with the carbonate system, carbonate equilibria may be considered in establishing pH values. Total phosphate is considered as 3.0 p.p.b.(P) in the calculations; ionization constants involving PO_4^{3-}, HPO_4^{2-}, and $H_2PO_4^-$ are from Van Wazer (*16*) and Vanderzee and Quist (*15*); solubility data for hydroxyapatite are from Kramer (*10*). Assumptions involving calcium and magnesium concentrations and alkalinity are the same as in the calcite and dolomite models. Equations summarizing the calculations are:

$$CO_2(g) + H_2O(l) = HCO_3^- + H^+;\ H_2PO_4^- = HPO_4^{2-} + H^+$$
$$HPO_4^{2-} = PO_4^{3-} + H^+;\ Ca_{10}(PO_4)_6(OH)_2(s) =$$
$$10\ Ca^{2+} + 6\ PO_4^{3-} + 2\ OH^-$$

Figure 7 shows the results of the calculations. Although temperature trends for lake water chemistry with respect to apatite have not been established yet, it appears that a similar situation may develop for apatite saturation as for the carbonates relative to P_{CO_2} and temperature.

Silicates. Thermochemical data are not well enough known as a function of temperature nor is the silicate mineralogy well enough understood to warrant any calculations as a function of temperature and P_{CO_2}.

Literature Cited

(1) Feth, J. H., Roberson, C. E., Polzer, W. L., *U.S. Geol. Surv. Water Supply Paper* **1535-I** (1965).
(2) Harned, H. S., Davies, R. D., *J. Am. Chem. Soc.* **65,** 2030 (1943).
(3) Harned, H. S., Hammer, W. J., *J. Am. Chem. Soc.* **55,** 2194 (1933).
(4) Harned, H. S., Scholes, S. R., *J. Am. Chem. Soc.* **63,** 1706 (1941).
(5) Kelley, K. K., *U.S. Bur. Mines Rept. Invest.* **5901** (1962).
(6) Kittrick, J. A., *Am. Mineralogist* **51,** 1457 (1966).
(7) Kramer, J. R., *Univ. Mich., Gt. Lakes Res. Div. Publ.* **7,** 27 (1961).
(8) *Ibid.,* **9,** 21 (1962).
(9) *Ibid.,* **11,** 147 (1964).
(10) Kramer, J. R., *Science* **146,** 637 (1964).
(11) Larson, T. E., Buswell, A. M., *J. Am. Water Works Assoc.* **34,** 1667 (1942).
(12) Siever, Raymond, Beck, K. C., Berner, R. A., *J. Geol.* **73,** 39 (1965).
(13) Sutherland, J. C., Kramer, J. R., Nichols, Lee, Kurtz, T. D., *Proc. 4th Conf. Great Lakes Res., Chicago* (1966).
(14) Thomas, J. F. J., Gale, R. M., *Can. Mines Branch Mono.* **870** (1965).
(15) Vanderzee, C. E., Quist, A. S., *J. Phys. Chem.* **65,** 118 (1961).
(16) Van Wazer, J. R., "Phosphorus and Its Compounds," Vol. I, Interscience, New York (1958).

RECEIVED April 29, 1966.

Coordination Chemistry of the Oceans

DEAN F. MARTIN

University of South Florida, Tampa, Fla.

The coordination chemistry of sea water represents a new and useful approach to understanding the chemical properties of sea water. The coordination chemistry of sea water differs from contemporary coordination chemistry in the following respects: most complexes involve pretransition metals, most complexes are labile, the ligands are simpler (water, hydroxide, chloride, carbonate, sulfate), and time and space are important parameters. Principles of coordination chemistry are applied to contemporary research in marine science in four areas: analysis of constituents of natural waters, the nature of metallic species in the oceans, the Red Tide problem, and carbonate geochemistry.

Not long ago, it was suggested (*28*) that ours is a world of coordination compounds. Since the oceans and other natural waters cover 71% of our world, these bodies of water represent a realm of coordination compounds which unfortunately has been almost studiously ignored by most coordination chemists. Even a cursory examination of aspects of marine science reveals many areas which would provide exciting research problems for those who have a background in coordination chemistry. This paper considers some pertinent aspects of coordination chemistry and shows how these principles might be useful in studying some contemporary problems in marine science. These problems include analyzing constituents of natural waters, the nature of metallic species in the ocean, the Red Tide problem, and carbonate geochemistry.

Let us review those principles of coordination chemistry that are pertinent to ocean studies.

Some Special Aspects of the Coordination Chemistry of the Ocean

A coordination entity results when a metal ion or atom accepts a share in an electron pair from some donor atom. In this sense, then, any solvated metal ion may be regarded as a coordination entity. (A more detailed introduction to the chemistry of coordination compounds may be found in monographs by Bailar (*2*), Basolo and Johnson (*3*), Jones (*24*), Lewis and Wilkins (*27*), and Murmann (*31*), among others.) A somewhat different, though useful definition is advanced by those interested in nomenclature:

> In its oldest sense, the term *coordination entity* generally refers to molecules or ions in which there is an atom (A) to which are attached other atoms (B) or groups (C) to a number in excess of that corresponding to the classical or stoichiometric valency (*23*).

From this definition, certain terms emerge. The metal atom (A) is termed the nuclear atom, the central atom, or, sometimes, the center of coordination. All other atoms directly attached are called coordinating atoms, and atoms (B) and groups (C) are called ligands. A group containing more than one potential coordinating atom is called a multidentate ligand and is said to be a chelate when attached to the metal through two or more coordinating atoms. A bridging ligand is attached to more than one center of coordination.

For coordination entities and the ocean, we should consider (a) the metal, whether a transition metal or not, the charge, and the size; (b) the ligands, whether uni- or multidentate, perhaps whether organic or inorganic; (c) the coordination number—*i.e.*, the number of donor atoms attached to the metal. The metal and the ligands surrounding it comprise the coordination sphere, which is represented by the bracket-enclosed formula.

It is important to note that the coordination chemistry of our air-conditioned laboratories is remarkably different from that of a large body of salt water in several respects, among which are the following.

Different Metals. Typically the coordination chemistry of the laboratory deals with the transition metals, usually of the *d* type, and the coordination chemistry of the metals of Groups I and II is commonly neglected. In contrast, the coordination chemistry of the ocean would, at first, seem to be the exclusive province of the pretransition metals; this is seen clearly by looking at an average composition of an ocean (Table I) (*36*).

More Metals. The apparent simplicity of the problem is misleading because although the concentration of transition metal ions is small, the ocean assuredly contains trace quantities of all naturally occurring metals. We now recognize two results of coordination: the properties of the metal are altered, and, equally important, the properties of the ligand are altered (coordinated ammonia is less basic, cyanide ion is less toxic) (*5*). Most of the catalytic activity of coordination entities recently summarized involved coordination entities of transition metal ions; examples involving magnesium ion constitute the main exceptions (*24*).

Simpler Ligands. Composition data (Table I) of the sea include aquo, halo (Cl^-, Br^-, F^-), carbonato, and sulfato complexes. Since the pH of our average ocean is 8.1, hydroxo complexes would also be important, as might be phosphate complexes. Except for the halides, ligands important to marine science are almost routinely overlooked by most coordination chemists. Fortunately there are exceptions, as noted from the papers in this volume.

Table I. Average Composition Data for Major Constituents of Sea Water (*36*)

Metals, Molar		*Ligands, Molar*	
Na^+	0.47015	H_2O	54.90
Mg^{2+}	0.05357	Cl^-	0.54830
Ca^{2+}	0.01024	SO_4^{2-}	0.02824
K^+	0.00996	HCO_3^-	0.00234
Sr^{2+}	0.00015	Br^-	0.00083
		F^-	0.00007
		(H_3BO_3)	0.00043
		Organic compounds	10^{-5}–10^{-4}

Some Complicated Ligands. Many ligands in the ocean are chelating agents, some with complicated structures (*42*). These would include amino acids, probably organic acids such as citric acid, vitamins, porphyrins, and related materials, complicated species such as humic acids and tannins. Presumably many of these materials would be present in considerably greater concentrations in inland waters and in estuaries than in the oceans. No doubt many of these chelating agents would play more important roles in estuarine processes than marine processes—*e.g.*, transporting trace metals from the land to the ocean *via* rivers and estuaries.

While the organic materials present are of considerable interest, it appears that their sources might be even more important—in particular, the excretion of organic compounds by specific organisms. The amount of carbon as dissolved organic matter is far greater than the amount incorporated into marine organisms; the ratio ranges from 300:1 in early analyses to about 100:1 in more recent work (*43*). The dissolved fraction, determined by wet combustion methods, usually is of the order of 0.5–0.12 mg. C/liter or $10^{-4.4}$–$10^{-4.0}M$. (Wangersky (*43*) has discussed the limitations of this and dry combustion.) Several explanations of the large dissolved-organism carbon ratios have been advanced for the secretion of organic materials by phytoplankton organisms during normal growth. One possibility is the removal of toxic trace metals by chelation;

however, many of the excreted compounds are not chelating agents, and this remains an unknown but intriguing area.

Labile Coordination Entities. Commonly, metal complexes are classified as to stability *vs.* instability or lability *vs.* inertness (*33, 41*). Solution stability is a thermodynamic property and describes an equilibrium of the type shown in Equation 1.

$$\mathrm{M} + n\mathrm{A} \rightleftharpoons \mathrm{MA}_n \tag{1}$$

Equation 1 occurs in the step-wise fashion:

$$\mathrm{M} + \mathrm{A} \rightleftharpoons \mathrm{MA} \tag{2}$$

$$\mathrm{MA} + \mathrm{A} \rightleftharpoons \mathrm{MA}_2 \tag{3}$$

$$\mathrm{MA}_{n-1} + \mathrm{A} \rightleftharpoons \mathrm{MA}_n \tag{4}$$

For each equation an equilibrium expression may be written—*e.g.*, the last equilibrium:

$$K_n = \frac{(\mathrm{MA}_n)}{(\mathrm{MA}_{n-1})(\mathrm{A})} \quad \text{or} \quad Q_n = \frac{[\mathrm{MA}_n]}{[\mathrm{MA}_{n-1}][\mathrm{A}]} \tag{5}$$

where K_n is the "thermodynamic equilibrium constant" using activities of the species, indicated by parentheses, and where Q_n is the "molarity quotient" or "concentration stability constant" for which activities have been replaced by concentrations of the species, indicated by brackets. A large K or Q value indicates a large solution stability. The reciprocal of the stability constant is known as the instability constant and is frequently encountered in qualitative analysis textbooks.

In contrast to stability, lability and inertness are kinetic quantities. A labile (or robust) complex is quite reactive; an inert entity is quite slow to react. A criterion has been suggested by Taube (*41*): "labile" is applied to those systems where reactions are complete within time of mixing—*i.e.*, within 1 minute at room temperature; "inert" is applied to systems in which reactions are too slow to measure or occur at measurable (by conventional techniques) rates.

Because the stability constant is the ratio of the specific rate constants for the forward and reverse reactions, respectively, both rate constants could be large, and the ratio could also be large. In short, a coordination entity might have a high solution stability and yet be very labile.

For our purposes, the prominent coordination entities must involve the derivatives of the populous metal ions listed in Table I. All are labile, most are probably stable, though more information is needed for coordination entities involving phosphate and carbonate ions.

Knowing the stability constants (actually, molarity quotients or stoichiometric constants are more useful here), it is possible to say which coordination entities are most likely present. Sillén (*36*) gives the following results.

HYDROXO COMPLEXES. Here, one considers hydroxide *vs.* chloride *vs.* fluoride coordination. For the equilibrium involving first complex formation with a metal ion of unspecified charge, we may write Equations 6, 7, 8.

$$M + OH^- \rightleftharpoons MOH \qquad Q_{OH} = \frac{[MOH]}{[M][OH^-]} \tag{6}$$

$$M + Cl^- \rightleftharpoons MCl \qquad Q_{Cl} = \frac{[MCl]}{[M][Cl^-]} \tag{7}$$

$$M + F^- \rightleftharpoons MF \qquad Q_F = \frac{[MF]}{[M][F]} \tag{8}$$

CHLORIDE COORDINATION. This predominates over hydroxide coordination—*i.e.*, [MCl] > [MOH] only if Equation 9 is valid.

$$\log Q_{Cl} - \log Q_{OH} > \log[OH^-] - \log[Cl^-] \cong -5.4. \tag{9}$$

This is true only for: silver(I), mercury(II), gold(I), and possibly cadmium and lead ions. At the pH of the ocean, hydroxide coordination is important for all ions having an oxidation number greater than 2 (*36, 37*).

FLUORIDE RATHER THAN HYDROXIDE COORDINATION. This would be expected for magnesium ion since the necessary condition (Equation 10) is fulfilled,

$$\log Q_F - \log Q_{OH} > \log [OH^-] - \log [F^-] \cong -1.5 \tag{10}$$

For the magnesium-hydroxide system, log Q_{OH} = 2.1 and log Q_F = 1.3. Otherwise, there appears to be no other ions which exist chiefly as fluoride complexes.

Similarly some degree (5–10% of the reported concentrations) of complex formation might be expected for such metal ions as magnesium or cobalt(II), but apparently there are no examples of extensive sulfato entities.

Time and Space. In the land-locked laboratory, a coordination chemist is not usually troubled by space and time as parameters. His results can be duplicated in adjacent buildings at a different time. [There is an exception to this in the reported resolution of $[Co\{CH_3COCHC(CH_3)NCH_2CH_2N(CH_3)CCHCOCH_3\}(NH_3)_2]^+$. After separation into optical enantiomers was completed and once the inactive (trans) salt was obtained, optically active salts were never again obtainable (*28*).] This is not true for the ocean, and the variation with space and time of sea water composition is necessary to obtain a proper view of the processes involved. Great strides have been made in applying analytical methods to oceanography—*e.g.*, recently Dyrssen and Sillén (*12, 13*) have demonstrated the application of Gran's graphical method to an e.m.f. titration of sea water with an acid. The method permits rapid determination of both the total carbonate concentration and total alkalinity in units of M_w ($=$ mole/kg. sea water) so that the quantities are independent of sample pressure and temperature, both *in situ* and during the titration. With this background in mind, let us turn our attention to applications of coordination chemistry.

Analysis of Natural Water Constituents

The grasp of processes occurring in the oceans and other natural waters depends upon accurate analyses for constituents. The background and limitations of present analytical methods in natural waters has been considered by Morgan (*30*), Hume (*20*), and Riley and Skirrow (*32*).

It is now possible to indicate the role of coordination chemistry by means of a single example—the problem of determining calcium in sea water (*4, 6*).

Calcium is usually determined by precipitation as the oxalate; the precipitate is dissolved in sulfuric acid, and oxalic acid is titrated with potassium permanganate, or the oxalate precipitate is ignited to the oxide and weighed. However, precipitating calcium oxalate quantitatively is difficult in the presence of magnesium and strontium ions. In sea water, the ratio of magnesium and strontium to calcium is 3 (Mg): 0.03 (Sr): 1.0 (Ca) on a weight basis and is 5 (Mg): 0.015 (Sr): 1 (Ca) on an equivalent basis. Even though multiple precipitation techniques are used, some coprecipitation of calcium and magnesium oxalates is unavoidable; the oxalate procedures are tedious and not subject to rigorous interpretation.

The compleximetric determination of calcium has been described (*4*) using ethylenediaminetetraacetic acid (EDTA), but the procedure is not specific for calcium, and separation is necessary to prevent interference by other metal ions. The separation of calcium from other ions present in sea water has been studied by Carpenter (*6*). Ion exchange, using aqueous ammonium acetylacetonate ($NH_4^+CHAc_2^-$) as an eluent, permitted quantitative separation of magnesium, calcium, and strontium in sea water samples. In practice, magnesium was eluted readily with 0.2*M* ammonium acetylacetonate, and 1*M* solutions of the reagent were used to elute calcium ion. The reagent in the aqueous effluent was quantitatively decomposed (acetic acid or ammonium acetate and acetone) by boiling at 95°C. for 95 minutes. Calcium was then determined using EDTA. Four samples could be analyzed in about 8 hours. The method is summarized in Table II, and details are given elsewhere (*6*).

Oceanic Metallic Species

In an interesting and imaginative treatment, Sillén has proposed (*36*) an equilibrium model of the ocean. By considering known equilibria and principles of coordination chemistry, he has been able to deduce the metallic species which are most likely present in an average ocean. (Average values (*36*) for the bulk of the ocean include: $\mathrm{pH} = 8.1 \pm 0.2 = -\log(\mathrm{H}^+)$; $\mathrm{pE} = 12.5 \pm 0.2 = -\log(e^-)$; density = 1.024 grams/ml.; temperature = 5°C.) Hence, 1 liter of a typical ocean then would include the following transition metals (with —log [species] in brackets): iron, mainly as FeOOH (s) [0.26] or $Fe(OH)_3$ (?) [6.0–7.9]; titanium as TiO_2 (s), probably as rutile [1.25], and maybe uncharged $Ti(OH)_4$ [$6.7 > 8$] as the dissolved species; manganese as MnO_2 [1.95] and in solution as some uncharged hydroxide species—*e.g.*, $Mn(OH)_3$ or $Mn(OH)_4$ [6.7–7.9].

Table II. Ion-Exchange Separation of Magnesium, Calcium, and Strontium (*6*)

Column:	8 x 80 mm. Dowex 50 column (100-200 mesh 8% cross-linkage)
Constituents:	10 mg. Mg^{2+}; 4 mg. Ca^{2+}; 1 mg. Sr^{2+}
Conditions:	Flow rate, 0.5 ml./min.
Separation:	
	(1) $0.2M$ NH_4CHAc_2 35 ml. elutes 10 mg. magnesium No calcium in first 250 ml. of effluent
	(2) $1.0M$ NH_4CHAc_2 27 ml. elutes 4 mg. calcium (use 50 ml.) No strontium in first 60 ml. of effluent
	(3) $2.0M$ NH_4CHAc_2 50 ml. removes 1 mg. Sr
	(4) Or, remove Sr with 50 ml. $2M$ NH_4Cl
	(5) Decompose reagent (heat 90 min. at 95°C.)

Estimates of the total gold concentration vary but are typically 10^{-10}–$10^{-10.7}M$ (in some cases $10^{-8}M$), and some have suggested that this is present as dispersed metal. Sillén (*36*) has considered this point and concluded that the metallic gold would not be stable for long periods in contact with sea water. The dissolved species would be $AuCl_2^-$, mainly, with gold(III) as hydroxo species $Au(OH)_4^-$, $Au(OH)_3Cl^-$. This is based upon the equilibria represented by Equations 11–13 (20°C., zero activities).

$$AuCl_2^- + e^- \rightleftharpoons Au(s) + 2Cl^- \qquad \log K = 19.2 \qquad (11)$$

$$AuCl_4^- + 3e^- \rightleftharpoons As(s) + 4Cl^- \qquad \log K = 51.3 \qquad (12)$$

$$Au(OH)_4^- + 4H^+ + 4Cl^- \rightleftharpoons AuCl_4^- + 4H_2O \qquad \log K = 29.4 \qquad (13)$$

Using sea water values ($pH = 8.1$, $\log [Cl^-] = 0.26$, and $pE = 12.5$ and neglecting activities), Sillén estimates the following concentrations:

$$\log [AuCl_2^-] = -7.2, \log [AuCl_4^-] = -14.8,$$
$$\log [Au(OH)_4^-] = -11.0.$$

$AuCl_2^-$ would predominate at equilibrium, and the concentration would be significantly greater than the reported concentration of gold.

The Red Tide

The Red Tide, as Humm (*21*) has noted, is not a tide and is not really red, but it is certainly a problem. It results from a sporadic occurrence of certain microorganisms which in large concentrations (*ca.* 10^6 organisms per liter) cause discoloration of water. Outbreaks of luminescent water in various parts of the world (*8, 9, 34*) have occurred off the coasts of Florida, California, New Jersey, Virginia, Maryland, Chile, Africa, and Japan. Some have suggested (*8, 34*) that the phenomenon may have been described in the Bible (*14*):

> . . . and all the waters that were in the river were turned to blood. And the fish that was in the river died; and the river stank, and the Egyptians could not drink of the water of the river; and there was blood throughout all the land of Egypt.

Outbreaks in various parts of the Gulf of Mexico have been observed, though they are especially localized along the West Coast of Florida, from the Florida Keys to Tarpon Springs. The Florida Red Tide is a fish-killing phenomenon and is always associated with dense populations of the microorganism *Gymnodinium breve* (*G. breve*), an unarmored dinoflagellate. Mass mortalities of marine life are observed when the concentration of *G. breve* reaches 250,000 per liter; concentrations of 75×10^6 *G. breve* per liter of water were reported during a 1957 Florida Red Tide bloom. Under certain conditions of wind direction and rough seas, water droplets containing *G. breve* particles become air-borne to inland locations, and human discomfort results from temporary respiratory irritations (*8, 22, 45*). The background of the problem has been covered by Humm (*21*), LaCossitt (*26*), and others (*8, 34*).

The factors that influence the Florida Red Tide are undoubtedly largely interrelated and variable. The seasonal occurrence of *G. breve* in lethal concentrations is sporadic, but initial outbreaks are likely in late summer through fall. There appears to be a strong association between the outbreaks and preceeding periods of heavy rainfall and river drainage. Possibly there is a correlation with salinity since the optimum salinity range for growth of cultured *G. breve* was reported to be 31–34$^{0}/_{00}$ by Hela (*18, 19*) and 27–37$^{0}/_{00}$ by Aldrich and Wilson (*1*). The latter workers reported upper and lower limits; optimum growth of cultured *G. breve* did not occur with salinities greater than 44$^{0}/_{00}$ or less than 24$^{0}/_{00}$. The lower value may be a limiting factor in estuaries.

An additional association of rainfall and Red Tide bloom has been suggested, and here coordination chemistry may be important. The coincidence of *G. breve* outbreaks and the location of rich phosphate beds has been a suspicious source. Also, some attention has been focused on the role of iron in the growth pattern of *G. breve,* and apparently this metal definitely stimulates the growth; in contrast, copper ion is lethal to *G. breve* at a minimum level of about 0.5 μg. atom/liter (*44*). Apparently Florida west coastal waters are enriched with nutrients and metals following periods of heavy rainfall. The Peace River not only carries large quantities of iron but is also acidic. Moreover, tannic acid, humic acids, and related products—all chelating agents—are common to this and other area streams. Ingle (*39*) noted one cause of the increase in iron content in the Peace River during periods of high rainfall—*i.e.,* during dry periods, nearby bogs, which are well-known accumulators of iron, are cut off from streams; during high rainfall periods, large concentrations of iron are leached or washed out.

As a result of recent discussions on the Red Tide, several areas of research were proposed—studies of the growth requirements of *G. breve* and related plankters under controlled conditions and under natural conditions, characterization of the toxin of *G. breve,* evaluation of potential control methods in pilot studies, among others. Considering only these areas of research, it might be appropriate to speculate on the possible use of principles of coordination chemistry.

First, one would not suggest that coordination compounds would be successful in controlling Red Tide outbreaks in the sense that ligands or coordination entities might be added to stop or prevent outbreaks. Consider the cost of adding an inexpensive (20 cents/lb.) but reasonably lethal (0.125×10^{-6} gram/liter) coordination compound to an extremely small outbreak area (perhaps 30 acres and a 10-meter depth). (Marvin and co-workers (*cf., 39*) used as a criterion of acute toxicity—100% mortality within a 24-hour period at a concentration level of 0.01 p.p.m.)

Under these fairly optimum conditions, the cost of chemicals alone would be $70. A number of assumptions have been made.

(1) Small area, although *G. breve* outbreaks have been found as far as 78 miles offshore, and the 1952 Red Tide covered an area of about 400 square miles at its peak (*34*).

(2) Reasonable cost, although one effective compound out of 4700 screened in a recent study cost $100 per gram (*38*).

(3) Uniform effectiveness, although considerable variation in the toxicity of a chemical in different lots or from different manufacturers has been observed (*37*).

(4) Effectiveness in the ocean, although comparative tests of toxicants on *G. breve* cultured in an artificial medium and in sea water from Florida suggested that the Florida water contained an inhibitor that reduced the effectiveness of the toxicants (*38*).

(5) Benevolent toxicity—*i.e.*, the compound would be lethal only to *G. breve*. In actual practice this would be unrealistic, and it might be practical to require that only the compound not kill more than 50% of any indicator organisms (such as small fish and crabs) at a 10-fold lethal dosage.

(6) Timeliness and duration: certain control methods are effective only in earliest stages of a bloom, and the effect is short-lived. Copper sulfate pentahydrate, has been found to be effective in killing off small patches of *G. breve* in early stages of a bloom, but copper sulfate cannot be used to control the organism when blooms cover many square miles of the sea. The cost estimates vary, but a value of about $1050 per square mile was reported. Using activated charcoal to absorb hormones and vitamins required by *G. breve* has been suggested, and cost estimates (based on 3 tons of activated charcoal) are $150–810 per square mile (*34*).

Despite the obvious problems indicated here, research in using coordination entities as control agents could be fruitful—certainly, at least in the sense that an insight into the life history of the organism would be gained. This might permit outbreaks to be predicted and possibly controlled in early stages. Also, the studies of the role of chelating agents might be guided by a pessimistic point of view that control measures may have to be preventative rather than curative. For example, flood control or water management might be able to change effectively the rate at which iron and nutrients are transported to the ocean. However, the important questions of the role of iron in outbreaks and the mechanism of iron transport among others must be answered before effective control could be anticipated. The nature of iron phosphate species deserves study, as does a study of the effect on the growth rate of *G. breve* of model metal-chelate systems. Of particular interest would be the metal derivatives of hydrolysis products of tannins—*e.g.*, gallic acid and *m*-galloyl gallic acid. Such laboratory studies need to be correlated with surveys of the concentrations of tannin derivatives (and related materials) as a function of time and location.

Finally, investigations of the neurotoxin of *G. breve* are in progress. It would be premature to suggest where these studies might lead, but perhaps a parallel might arise. Dwyer observed (*11*) that metal-chelate compounds were "ideal pharmacological tools with which to study many functional systems of the living cell." Hence, it is possible that a similar observation might be made in connection with the toxin of *G. breve.*

The Red Tide problem is one that has broad scientific, social, and economic ramifications. [The estimated loss to Clearwater which was in the 1953-54 outbreak was $3,750,000; the estimated loss to Fort Myers was $500,000, though this city was not in the outbreak area (*26*).] The cause-and-effect relationships are such as to challenge some of the outstanding contemporary scientists. The problems in human discomfort as well as the effect on the fishing and/or tourist industries in some areas of the world are serious and far reaching. It seems likely that coordination chemistry will be used to help solve these problems.

Carbonate Geochemistry

Another aspect of marine science that broadly affects our daily lives is the origin of carbonate deposits. Limestone and dolomite are important industrial commodities, are host rocks for ore and oil sources, and are geochemical indices (*7*). The importance of carbonate rocks is unquestioned. The chemical origin is of scientific interest, and a considerable body of background information is available. (*7, 10, 15, 16, 17, 40*).

The background of the problem may be summarized as follows. The sites on which ancient limestones were deposited are similar to the sites of modern carbonate deposition—*i.e.*, warm, shallow, tropical, and subtropical seas (the Bahama Banks and the Australian Great Barrier Reef among others). These modern unconsolidated deposits are composed principally of metastable carbonate minerals (aragonite and high-magnesium calcite, with minor amounts of low-magnesium calcite); ancient (at least older than Pliocene) deposits are made up largely of two stable minerals—calcite, $CaCO_3$, and dolomite, $CaMg(CO_3)_2$. If ancient deposits were mainly metastable minerals, then nearly all limestones have undergone recrystallization. Two modes of recrystallization are plausible: dissolution of the metastable form and reprecipitation as stable forms or solid-phase recrystallization. Preservation of delicate structures of many fossils found in ancient carbonate rocks suggests that these old carbonates must have been lithified shortly after deposition; commonly, lithification has not occurred among modern sediments. Whether rates of lithification have altered or whether present chemical environments are unfavorable to lithification is not known.

The interplay of factors leading to the formation of carbonate rocks is extremely complicated, but several avenues of investigation have yielded fruitful results. These approaches include studies of surface energies, isotopic composition and radiochemistry (including the use of carbon-14 to study the rates of carbonate deposition), solubilities under ambient conditions, and the effect of magnesium-calcium ratios in the solutions from which carbonate minerals are precipitated.

Some interesting results have emerged from studying the effects of Mg-Ca ratios.

(1) The precipitation of protodolomite under 100°C. from solutions of calcium and magnesium chlorides has been reported, and it seems plausible to suggest that, given sufficient time, dolomite would result from recrystallization of protodolomite. Siegel (*35*) found that protodolomite was produced at 25°C. when calcium and magnesium ions were entrapped in activated charcoal and could react with carbonate ion at a low rate; he also found that sulfate ion was involved in dolomite formation.

(2) Taft (*40*) has demonstrated that magnesium ions play an important role in controlling the form of carbonate which is precipitated from sea water and its persistence. Table III summarizes the conversion time—i.e., the days required for the complete conversion of aragonite to calcite. The conversion time obviously depends on the solutions with which the aragonite is in contact. This does not appear to be solely an ionic-strength effect. Sodium and potassium chloride solutions increase the rate of recrystallization of aragonite to calcite; magnesium and strontium retard the recrystallization, but the inhibiting concentrations of strontium are greater than would be found in the ocean, and calcium ion increases the rate of conversion to calcite.

Table III. Aragonite in Contact with Solutions Containing Various Salts[a] (*40*)

Solution	*C_M 10^3 gram ions/liter*	*Initial wt. p.p.t., grams*	*Temp., °C.*	*Conversion Time, days*	*Mineralogy[b] wt% Aragonite*
KCl	84	0.2000	23	25	0
KCl	505	0.2011	23	6	0
$MgCl_2$	0.08	0.2011	23	86	0
$MgCl_2$	0.21	0.2010	23	>100	99
$SrCl_2$[c]	5.75	0.5100	37	>143	99
$CaCl_2$	10.0	0.2008	23	46	—
$CaCl_2$	62.5	0.2008	23	13	0

[a] Volume, 50 ml.
[b] wt% aragonite + wt% calcite = 100%
[c] Volume, 40 ml.

At this point, one concludes that the apparent lack of recrystallization of aragonite in unconsolidated modern carbonate sediments can be ascribed to high concentration of magnesium ions in the surrounding medium. Taft (*40*) suggests that if the relatively high concentration of magnesium ions persists, the preserved metastable carbonate sediments should be cemented by aragonite. Consequently, original textures would remain, and extensive recrystallization to calcite (*via* aragonite dissolution and calcite precipitation) would be precluded. Some dolomite formation might be favored if aragonite were preserved in carbonate sediments for an extended time.

This serves to rationalize many of the observations about the carbonate problem, but it does not answer the intriguing question: what is the explanation for the effect of magnesium and strontium ions in retarding recrystallization of aragonite? As noted, the effect is not caused by simple ionic-strength effects. Further, the concentrations are probably too low to cause the precipitation of the carbonate of the non-common metal ion, although the presence of small amounts of high magnesium calcite (*ca.* 1%) would not be detectable by the method of analysis used.

Sufficient data are not available for anything beyond speculation. However, it seems plausible that the greater effectiveness of magnesium ions *vis-a-vis* strontium may be caused by the greater coordinating tendency and that either ion is altering the pertinent equilibria (Equations 14–17).

$$\underset{\text{(aragonite)}}{CaCO_3\ (s)} \rightleftharpoons Ca^{2+} + CO_3^{2-} \rightleftharpoons \underset{\text{(calcite)}}{CaCO_3\ (s)} \tag{14}$$

$$CO_3^{2-} + H_2O \rightleftharpoons HCO_3^- + OH^- \tag{15}$$

$$M^{2+} + HCO_3^- \rightleftharpoons [M \cdot HCO_3]^+ \tag{16}$$

$$M^{2+} + OH^- \rightleftharpoons MOH^+ \tag{17}$$

Recrystallization would be retarded by any process that tends to decrease the concentration of either calcium ion (perhaps through sequestration) or carbonate ion (directly through complex formation or indirectly through alteration of the carbonate-bicarbonate equilibrium). For example, it is possible that magnesium ion decreases the concentration of carbonate ion by forming a complex $[Mg \cdot HCO_3]^+$ (Equation 16), but the evidence for such a complex is contradictory for magnesium ion and without support for strontium. Hydroxide complexing by a metal, however (Equation 17), would also alter the equilibrium, and this appears to be a better possibility. The values of log K_1 for MOH^+ (at 25°C. and $\mu \rightarrow 0$) are 2.58 and 0.85 for magnesium and strontium, respectively.

Clearly, at this point, there is a need for additional data concerning the effect of other metal ions on the recrystallization of aragonite. Without doubt these data will become available. Also, data concerning the effect of sequestering agents on the recrystallization rate would be of interest. A significant start in this direction has been made by Kitano and Hood (25), who studied the influence of organic material on the rate of precipitation and crystal form of calcium carbonate precipitated from solutions of calcium bicarbonate. Those sequestering agents which greatly reduced the rate of precipitation favored the precipitation of calcite; those which moderately reduced the rate, influenced the crystal form to a moderate extent; and those which had little influence on rate also had little influence on crystal form of the precipitate.

Acknowledgment

The helpful criticisms and suggestions of William H. Taft are gratefully acknowledged.

Literature Cited

(1) Aldrich, D. V., Wilson, W. B., *Biol. Bull.* **119**, 57 (1960).
(2) Bailar, J. C., ed., "Chemistry of the Coordination Compounds," Reinhold, New York, 1956.
(3) Basolo, F., Johnson, R. C., "Coordination Chemistry," Benjamin, New York, 1964.
(4) Blaedel, W. J., Meloche, V. W., "Elementary Quantitative Analysis," 2nd ed., p. 590, Harper & Row, New York, 1963.
(5) Busch, D. H., ADVAN. CHEM. SER. **37**, 1 (1963).
(6) Carpenter, J. H., *Limnol. Oceanog.* **2**, 271 (1957).
(7) Cloud, P. E., Jr., *U.S. Geol. Surv. Profess. Papers* **350** (1961).
(8) Connell, C. H., Cross, J. B., *Science* **112**, 359 (1950).
(9) *Ibid.*, **113**, 250 (1951).
(10) Degens, E. T., "Geochemistry of Sediments," Prentice-Hall, Englewood Cliffs, 1964.
(11) Dwyer, F. P., Mellor, D. P., "Chelating Agents and Metal Chelates," Academic Press, New York, 1964.
(12) Dyrssen, D., *Acta Chem. Scand.* **19**, 1265 (1965).
(13) Dyrssen, D., Sillén, L. G., *Tellus*, in press.
(14) *Exodus*, 7: 20-21.
(15) Fairbridge, R. W., *Soc. Econ. Paleontologists Mineralogists, Spec. Publ.* **5** (1957).
(16) Garrels, R. M., "Mineral Equilibrium," Harper & Row, New York, 1960.
(17) Garrels, R. M., *Science* **148**, 69 (1965).
(18) Hela, I., *Bull. Marine Sci. Gulf Caribbean* **5**, 269 (1955).
(19) *Ibid.*, **6**, 74 (1956).
(20) Hume, D. N., ADVAN. CHEM. SER. **67**, 30 (1967).
(21) Humm, H. J., *Science News Letter* **62**, 374 (1952).
(22) Ingle, R. M., *Univ. Miami Marine Lab., Spec. Serv. Bull.* **9**, 1 (1954).
(23) IUPAC, *J. Am. Chem. Soc.* **82**, 5523 (1960).
(24) Jones, M. M., "Elementary Coordination Chemistry," pp. 376-390, Prentice-Hall, Englewood Cliffs, 1964.
(25) Kitano, Y., Hood, D. W., *Geochim. Cosmochim. Acta* **29**, 29 (1965).
(26) La Crossitt, H., *Saturday Evening Post*, p. 28 (Aug. 14, 1954).

(27) Lewis, J., Wilkins, R. G., eds., "Modern Coordination Chemistry," Interscience, New York, 1960.
(28) Martin, D. F., Martin, B. B., "Coordination Compounds," p. 90, McGraw-Hill, New York, 1964.
(29) Morgan, G. T., Main Smith, J. D., *J. Chem. Soc.* **1925**, 2030.
(30) Morgan, J. J., ADVAN. CHEM. SER. **67**, 1 (1967).
(31) Murmann, R. K., "Inorganic Complex Compounds," Reinhold, New York, 1964.
(32) Riley, J. T., Skirrow, G., eds., "Chemical Oceanography," 2 vols., Academic Press, New York, 1965.
(33) Rossotti, F. J. C., Rossotti, H., "The Determination of Stability Constants," McGraw-Hill, New York, 1961.
(34) Rounsefell, G. A., Nelson, W. R., *U.S. Fish Wildlife Serv. Spec. Sci. Rept., Fisheries* **535** (1967).
(35) Siegel, F. R., *Bull. Geol. Surv. Kansas* **152**, 127 (1961).
(36) Sillén, L. G., *Am. Assoc. Advan. Sci. Publ.* **67**, 549 (1961).
(37) Sillén, L. G., Martell, A. E., *Chem. Soc. (London) Spec. Publ.* **17** (1964).
(38) Sykes, J. E., *U.S. Fish Wildlife Serv. Spec. Sci. Rept., Fisheries* **521** (1965).
(39) *Ibid.*, p. 3.
(40) Taft, W. H., "Carbonate Rocks," G. V. Chilinger, H. J. Bissell, eds., Chap. 5, Elsevier, 1967.
(41) Taube, H., *Chem. Rev.* **50**, 69 (1952).
(42) Vallentyne, J. R., *J. Fisheries Res. Board., Can.* **14**, 33 (1957).
(43) Wangersky, P. J., *Am. Scientist* **53**, 358 (1965).
(44) Wilson, W. B., manuscript cited by Dragovich, A., May, B. Z., *U.S. Fish Wildlife Serv., Fishery Bull.* **62**, 175 (1962).
(45) Woodcock, A. J., *J. Marine Sci.* **7**, 56 (1948).

RECEIVED April 13, 1966.

13

Redox Equilibria and Measurements of Potentials in the Aquatic Environment

J. CARRELL MORRIS and WERNER STUMM

Division of Engineering and Applied Physics, Harvard University,
Cambridge, Mass.

Equilibrium models are valuable in interpreting the stability relations of pertinent redox components in natural water systems. Unfortunately, concentrations of oxidizable or reducible species may be far from those predicted thermodynamically because many redox reactions are slow. Maintenance of life resulting directly from a steady input of solar energy is also a major cause of nonequilibrium conditions. Nonphotosynthetic organisms, however, tend to restore equilibrium by catalytically decomposing, through energy-yielding redox reactions, the unstable ultimate products of photosynthesis. Measuring redox potentials frequently yields results that are not amenable to unambiguous interpretation. Quantitative interpretation with respect to solution composition is frequently not justified because the required electrochemical reversibility is usually not attained. Moreover, the point of zero-applied current is not necessarily the equilibrium potential. Most E_H*-measurements on natural waters represent mixed potentials.*

Theoretical equilibrium models can be established for oxidation-reduction systems in natural waters in much the same way that acid-base or solubility models have been developed and found useful in interpreting observed concentrations of ions and other materials. To relate the theoretical models for redox processes to observed conditions and processes in the aquatic environment is, however, much more difficult and cannot be done as rigorously. Primarily this situation occurs because true oxidation-reduction equilibrium is not observed in any natural aquatic system; this is partly because of the extreme slowness of most oxidation-reduction reactions of interest in the absence of suitable biochemical catalysis and partly because of the continuous cyclic input of photosynthetic energy that disturbs the trend toward equilibrium conditions.

The need for biological mediation of most redox processes encountered in natural waters means that approaches to equilibrium depend strongly on the activities of the biota. Moreover, quite different oxidation-reduction levels may be established within biotic microenvironments than those prevalent in the over-all environment; diffusion or dispersion of products from the microenvironment into the macroenvironment may give an erroneous view of redox conditions in the latter. Also, because many redox processes do not couple with one another readily, it is possible to have several different apparent oxidation-reduction levels in the same locale, depending upon the system that is being used as reference.

Additional difficulties occur with attempts to measure oxidation-reduction potentials electrochemically in aquatic environments. Values obtained depend on the nature and rates of the reactions at the electrode surface and are seldom meaningfully interpretable. Even when suitable conditions for measurement are obtained, the results are significant only for those components behaving reversibly at the electrode surface.

Natural waters are in a highly dynamic state, with regard to oxidation-reduction, rather than in or near equilibrium. In a typical lake there is a marked difference in redox environment between the surface in contact with the oxygen of the atmosphere and the deepest layers that bathe the sediments. In between are numerous localized intermediate zones resulting from imperfections in mixing or diffusion and from varying biological activities, none of which is truly at equilibrium. Therefore, detailed, quantitative exposition of redox conditions and processes will depend ultimately on understanding the dynamics of aquatic systems—the rates of approach to equilibrium—rather than on describing the total or partial equilibrium compositions.

Nonetheless, equilibrium considerations can greatly aid attempts to understand in a general way the redox patterns observed or anticipated in natural waters. In all circumstances equilibrium calculations provide boundary conditions toward which the systems must be proceeding, however slowly. Moreover, partial equilibria (those involving some but not all redox couples) are approximated frequently, even though total equilibrium is not approached. In some instances active poising of particular redox couples allows one to predict significant oxidation-reduction levels or to estimate properties and reactions from computed redox levels.

Valuable insight is gained even when differences are observed between computations and observations. The lack of equilibrium and the need for additional information or more sophisticated theory are then made clear.

Equilibrium Redox Potentials and Treatment of Data

The equilibrium redox potential, the free energy change per mole electron for a given reduction, represents the oxidizing intensity of the couple at equilibrium. It is conveniently expressed for many applications in terms of the parameter, pE, as proposed by Jörgensen (8) and popularized by Sillén (*14*). This parameter is defined by the relation,

$$\mathrm{pE} = \frac{F_y}{(\ln 10)\,RT}\,E_{\mathrm{H}} \tag{1}$$

where E_{H} is the redox potential on the hydrogen scale in accord with the Stockholm convention.

Conceptually pE can be regarded as the negative logarithm of a relative electron activity, just as pH is the negative logarithm of a relative proton activity. Large, positive values of pE (low electron activity) represent strongly oxidizing conditions while small or negative values (high electron activity) correspond to strongly reducing conditions. The range of pE values in aquatic systems is about +14 to −10, again comparable with the range for pH values except for the extension at the negative end.

From Equation 1 the relations,

$$\mathrm{pE} = -\frac{1}{n_e\,RT\ln 10}\,\Delta G \tag{2}$$

$$\mathrm{pE}^{\circ} = -\frac{1}{n_e\,RT\ln 10}\,\Delta G^{\circ} \tag{3}$$

may also be written. If the redox process (half-reaction or couple) is written in the form

$$(\Sigma_i n_i A_i) + n_e e = 0 \tag{4}$$

where the A_i designate the participating species and the n_i their numerical coefficients, positive for reactants and negative for products, then

$$\mathrm{pE} = \mathrm{pE}^{\circ} + (1/n_e)\log \Pi(A_i)^{n_i} \tag{5}$$

and

$$\mathrm{pE}^{\circ} = (1/n_e)\log K_{\mathrm{eq}} \tag{6}$$

where n_e is the number of mole electrons transferred according to the equation. The quantity, pE°, is then the relative electron activity when all species other than the electrons are at unit activity.

Relationships are even simpler and more comparable with one another if all the couples are written for transfer of a single mole electron in the form

$$\Sigma_i (n_i/n_e) A_i + e = 0 \tag{7}$$

Then

$$\mathrm{pE} = \mathrm{pE}^\circ + \log \Pi(A)_i^{(n_i/n_e)} \tag{8}$$

and

$$\mathrm{pE}^\circ = \log K \tag{9}$$

where K of course is given by Equation 10,

$$K = \log \Pi(A_i)^{-(n_i/n_e)} \tag{10}$$

with the A_i at their equilibrium activities.

A subsidiary symbol, pE°(W), is convenient for considering redox situations in natural waters. This quantity is defined by Equation 11.

$$\mathrm{pE}^\circ(\mathrm{W}) = \mathrm{pE}^\circ + (n_\mathrm{H}/2) \log K_\mathrm{W} \tag{11}$$

Hence, it is analogous to pE° except that (H^+) and (OH^-), when they appear in the redox couples, are taken at their activities in neutral water rather than at unity. Values of pE°(W) for 25°C. thus apply to unit activities of oxidant and reductant at pH 7.00.

Table I presents pE°(W) values for several couples pertinent to consideration of redox relationships in natural waters and their sediments. Data for E°_H or ΔG° were taken principally from the second edition of "Stability Constants" (*13*).

Redox Conditions in Natural Waters

As indicated by Table I only a few elements—C, N, O, S, Fe, Mn—are predominant participants in aquatic redox processes. Water that is in solubility equilibrium with atmospheric oxygen has a well-defined pE = 13.6 (for $P_{\mathrm{O}_2} = 0.21$ atm., $E_\mathrm{H} = 800$ mv. at pH 7 and 25°C.). Calculations from the pE° values of Table I show that at this pE all of the other elements should exist virtually completely in their highest oxidation states: C as CO_2, HCO_3^- or CO_3^{2-} with reduced organic forms less than 10^{-35}; N as NO_3^- with NO_2^- less than 10^{-7}; S as SO_4^{2-} with SO_3^{2-} or HS^- less than 10^{-20}; Fe as FeOOH or Fe_2O_3 with Fe^{2+} less than 10^{-18}; and Mn as MnO_2 with Mn^{2+} less than 10^{-10}. Even the N_2 of the atmosphere should be largely oxidized to NO_3^-.

Since in fact N_2 and organic matter, at least, persist in waters containing dissolved oxygen, no total redox equilibrium is found in natural water systems, even in the surface films. At best there are partial equilibria, treatable as approximations to equilibrium either because of slowness of interaction with other redox couples or because of isolation from the total environment as a result of slowness of diffusional or mixing processes.

Photosynthesis is a major cause of nonequilibrium conditions in natural waters. By trapping light energy and converting it to chemical energy, photosynthesis produces reduced states of higher free energy and thus nonequilibrium concentrations of C, N, and S compounds. In the context of this paper, photosynthesis may be conceived as a process producing localized centers of highly negative pE. As shown in Table I, the conversion of CO_2 to glucose at unit activities requires pE°(W) = —7.2; although this value may be modified somewhat for the actual intracellular activities, it does represent approximately the negative pE level that must be reached during photosynthesis.

Table I. Potentials of Redox Processes for Aquatic Conditions

	Reaction	*pE°(W)*
(1)	$1/4\,O_2(g) + H^+(W) + e - 1/2\,H_2O$	+13.75
(2)	$1/5\,NO_3^- + 6/5\,H^+(W) + e - 1/10\,N_2(g) - 3/5\,H_2O$	12.65
(3)	$1/2\,MnO_2(s) + 1/2\,HCO_3^-(10^{-3}) + 3/2\,H^+(W) + e -$ $1/2\,MnCO_3(s) - 3/8\,H_2O$	(8.5)[a]
(4)	$1/2\,NO_3^- + H^+(W) + e - 1/2\,NO_2^- - 1/2\,H_2O$	7.15
(5)	$1/8\,NO_3^- + 5/4\,H^+(W) + e - 1/8\,NH_4^+ - 3/8\,H_2O$	6.15
(6)	$1/6\,NO_2^- + 4/3\,H^+(W) + e - 1/6\,NH_4^+ - 1/3\,H_2O$	5.82
(7)	$1/2\,CH_3OH + H^+(W) + e - 1/2\,CH_4(g) - 1/2\,H_2O$	2.88
(8)	$1/4\,CH_2O + H^+(W) + e - 1/4\,CH_4(g) - 1/4\,H_2O$	−0.06
(9)	$FeOOH(s) + HCO_3^-(10^{-3}) + 2H^+(W) + e -$ $FeCO_3(s) - 2H_2O$	(−1.67)[a]
(10)	$1/2\,CH_2O + H^+(W) + e - 1/2\,CH_3OH$	−3.01
(11)	$1/6\,SO_4^{2-} + 4/3\,H^+(W) + e - 1/6\,S(s) - 2/3\,H_2O$	−3.30
(12)	$1/8\,SO_4^{2-} + 5/4\,H^+(W) + e - 1/8\,H_2S(g) - 1/2\,H_2O$	−3.50
(13)	$1/8\,SO_4^{2-} + 9/8\,H^+(W) + e - 1/8\,HS^- - 1/2\,H_2O$	−3.75
(14)	$1/2\,S(s) + H^+(W) + e - 1/2\,H_2S(g)$	−4.11
(15)	$1/8\,CO_2(g) + H^+(W) + e - 1/8\,CH_4(g) - 1/4\,H_2O$	−4.13
(16)	$1/6\,N_2(g) + 4/3\,H^+(W) + e - 1/3\,NH_4^+$	−4.68
(17)	$1/2\,(NADP^+) + 1/2\,H^+(W) + e - 1/2\,(NADPH)$	−5.5[b]
(18)	$H^+(W) + e - 1/2\,H_2(g)$	−7.00
(19)	Oxid. Ferredoxin + e − Red. Ferredoxin	−7.1[c]
(20)	$1/4\,CO_2(g) + H^+(W) + e - 1/24$(glucose) $- 1/4\,H_2O$	−7.20[d]
(21)	$1/2\,HCOO^- + 3/2\,H^+(W) + e - 1/2\,CH_2O - 1/2\,H_2O$	−7.68
(22)	$1/4\,CO_2(g) + H^+(W) + e - 1/4\,CH_2O - 1/4\,H_2O$	−8.20
(23)	$1/2\,CO_2(g) + 1/2\,H^+(W) + e - 1/2\,HCOO^-$	−8.73

[a] These data correspond to $(HCO_3^-) = 10^{-3}$ rather than unity and so are not exactly pE°(W); they represent more nearly typical aquatic conditions than pE°(W) values do.
[b] Reference *4.*
[c] Reference *1.*
[d] Reference *10.*

The NADP or TPN system, ubiquitous in living organisms and believed to play a major role in electron transport during photosynthesis, exhibits pE°(W) = —5.5. Moreover, various ferredoxins, now widely considered to be the primary electron receptors from excited chlorophylls (*1*), show pE°(W) values in the range —7.0 to —7.5. The coincidence of this range with the pE°(W) value for conversion of CO_2 to glucose is suggestive.

In contrast the respiratory, fermentative, and other nonphotosynthetic reactions of organisms tend to restore equilibrium by catalyzing or mediating reactions releasing free energy and thus increasing the mean pE level.

The ecological systems of natural waters are thus more adequately represented by dynamic than by equilibrium models. The former are needed to describe the free energy flux, absorbed from light and released in subsequent redox processes (7). Equilibrium models can only depict the thermodynamically stable state and describe the direction and extent of processes tending toward it.

When comparisons are made between calculations for an equilibrium redox state and concentrations in the dynamic aquatic environment, the implicit assumptions are that the biological mediations are operating essentially in a reversible manner at each stage of the ongoing processes or that there is a metastable steady-state that approximates the partial equilibrium state for the system under consideration.

It is important to bear in mind that, with regard to the chemistry of the substances in natural waters, the organisms act only as mediators or

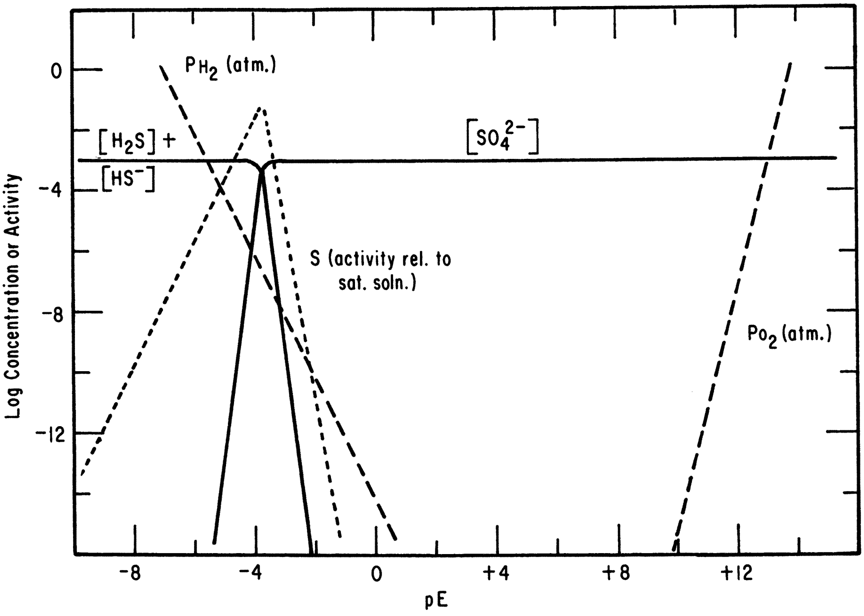

Figure 1. Equilibrium distribution of sulfur compounds as a function of pE at pH 7 and 25°C. Total concentration of compounds is $10^{-3}M$. P_{H_2S} in atm. is about 50 times ($[H_2S]$ + $[HS]$)

catalysts for reaction or electron transfer between the oxidizing and reducing substances. Thus, in their nonphotosynthetic activities, organisms can induce only those reactions that are thermodynamically possible—*i.e.*, those leading to a decrease in free energy.

Sulfur System. The reduction of SO_4^{2-} to H_2S or HS^- provides a good example of the application of equilibrium considerations to aquatic relationships. Figure 1 shows relative activities of SO_4^{2-} and H_2S at pH 7 and 25°C. as a function of pE when the total concentration of sulfur is one millimolar. It is apparent that significant reduction of SO_4^{2-} to H_2S at this pH requires $pE < -3$. The biological enzymes that mediate this reduction with oxidation of organic matter must then operate at or below this pE. Because the system is dynamic rather than static, only an upper bound can be set in this way, for the excess driving force in terms of pE at the mediation site is not indicated by equilibrium computations. Since, however, many biologically mediated reactions seem to operate with relatively high efficiency for utilizing free energy, it appears likely that the operating pE value is not greatly different from the equilibrium value.

Reduction of SO_4^{2-} to H_2S in aquatic systems is usually accompanied by oxidation of organic matter. A typical over-all process is obtained by combination of Reactions 12 and 22 from Table I as follows:

$$1/8\, SO_4^{2-} + 5/4\, H^+(W) + e - 1/8\, H_2S(g) - 1/2\, H_2O = 0;$$
$$pE^\circ(W) = -3.50$$

$$1/4\, CO_2(g) + H^+(W) + e - 1/4\, CH_2O - 1/4\, H_2O = 0;$$
$$pE^\circ(W) = -8.20$$

$$1/8\, SO_4^{2-} + 1/4\, CH_2O + 1/4\, H^+(W) - 1/8\, H_2S(g) -$$
$$1/4\, CO_2(g) - 1/4\, H_2O = 0; \log K = 4.70$$

This may also be written

$$SO_4^{2-} + 2CH_2O + 2H^+(W) = H_2S(g) + 2CO_2(g) +$$
$$2H_2O; \log K = 37.6$$

Since Δ pE°(W) or log *K* is positive, the reaction is thermodynamically possible in neutral aqueous solution at standard concentrations. Also, because the numbers of molecules of sulfur-containing and carbon-containing species do not change as a result of the reaction, the same results will hold for any equal fractions of unit activity. In addition, the pE values of the individual couples are quite insensitive to changes in activity ratio of the redox species so that qualitatively similar results will obtain with most measureable ratios of SO_4^{2-}/H_2S and CH_2O/CO_2; the former ratio must change by a factor of 10^8 to give unit change in pE, the latter one by a factor of 10^4.

Combining Reactions 11 and 14 (Table I) gives:

$$1/6\,SO_4^{2-} + 1/3\,H^+(W) + 1/2\,H_2S(g) - 2/3\,S(s) - 2/3\,H_2O;\ \Delta pE^\circ(W) = 0.81$$

or:

$$SO_4^{2-} + 2H^+(W) + 3H_2S = 4S(s) + 4H_2O;\ \log K = 4.86$$

This equation indicates a possibility of formation of solid elemental sulfur in the reduction of sulfate at pH 7 and standard concentrations. A concentration of 1*M* sulfate is unusual, however. If the concentration of SO_4^{2-} is reduced to about 0.018*M* (about 1600 mg./liter) and the H_2S activity is taken correspondingly as 0.09 atm. (H_2S is about half-ionized at pH 7, and the solubility of H_2S at 1 atm is about 0.1*M*; thus this condition means about 0.018*M* total sulfide) then ΔpE is negative, and solid sulfur cannot form thermodynamically at pH 7.

The solubility of $CaSO_4$ is about 0.016*M* at 25°C. According to this rough calculation sulfur should form in the reduction of SO_4^{2-} in saturated $CaSO_4$ only if the pH is somewhat below 7. There are some indications

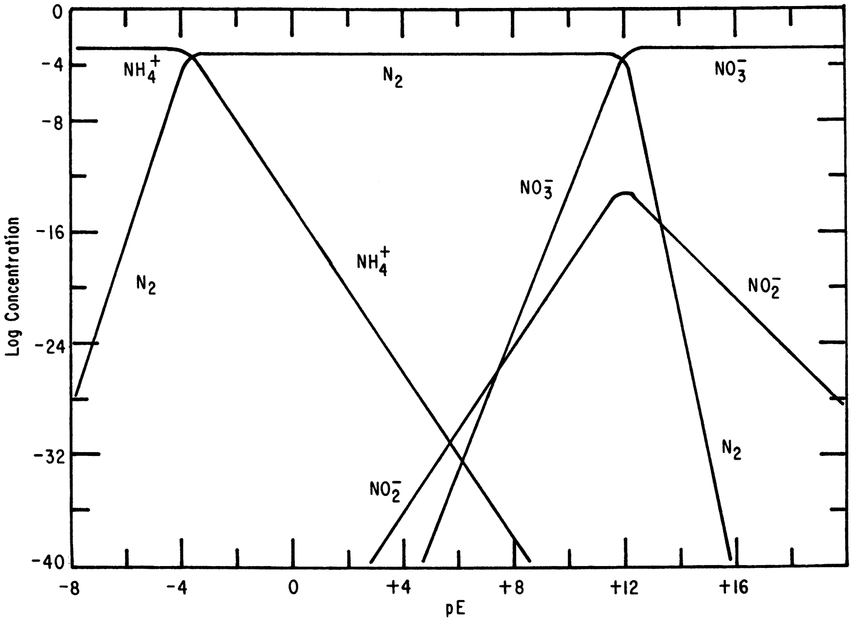

Figure 2. Equilibrium distribution of nitrogen compounds as a function of pE at pH 7 and 25°C. Total concentration is 10^{-3} gram atoms of N per liter. Maximum N_2 concentration is therefore 5 × $10^{-4}M$, corresponding to about P_{N_2} of 0.77 atm.

that this conclusion agrees with conditions of natural sulfur formation. The theoretical situation is depicted in Figure 1.

Nitrogen System. Figure 2 shows relationships among several oxidation states of nitrogen as a function of pE for a total atomic concentration of nitrogen-containing species equal to $10^{-3}M$. For most of the aqueous range of pE, N_2 gas is the most stable species, but at quite negative pE values ammonia becomes predominant, and for pE greater than +12 nitrate dominates at pH 7. The fact that nitrogen gas has not been converted largely into nitrate under prevailing aerobic conditions at the land and water surfaces indicates a lack of efficient biological mediation of the reverse reaction also, for the mediating catalysis must operate equally well for reaction in both directions. It appears then that denitrification must occur by an indirect mechanism such as reduction of NO_3^- to NO_2^- followed by reaction of NO_2^- with NH_4^+ to produce N_2 and H_2O.

Because reduction of N_2 to NH_4^+ at pH 7 can occur substantially when pE is less than about —4.5, the level of pE required is not as negative as for the reduction of CO_2 to CH_2O. It is not surprising then that blue-green algae are able to mediate this reduction at the negative pE levels produced by photosynthetic light energy. What is perhaps surprising is that nitrogen reduction does not occur more widely among photosynthetic organisms and proceed to a greater extent as compared with CO_2 reduction. Kinetic problems in breaking the strong bonding of the N_2 molecule probably are major factors.

It may also be noted that the pE values indicate the thermodynamic possibility of N_2 reduction accompanied by CH_2O oxidation. This is the gross mechanism mediated by nonphotosynthetic nitrogen-fixing bacteria.

Figure 2 also shows the shifts in relative predominance of the three species, NH_4^+, NO_2^- and NO_3^-, all within the rather narrow pE range from 5.8 to 7.2. That each of the species has a dominant zone within this range would seem to be a contributing factor to the observed highly mobile characteristics of the nitrogen cycle.

Carbon System. A diagram has not been given for the carbon system since the major feature is simply a conversion of predominant CO_2 to predominant CH_4 with the half-way point at $pE(W) = -4.13$. At this pE value, where the other oxidation states exhibit maximum relative occurrence, the equilibrium concentration of $HCOO^-$ is just $6 \times 10^{-10}M$, that of CH_2O only $5 \times 10^{-17}M$ and that of CH_3OH only $10^{-14}M$. Formation of solid carbon is thermodynamically possible close to $pE = -4.13$, but its inclusion does not change other relationships significantly.

Methane fermentation may be considered a reduction of CO_2 to CH_4 accompanied by oxidation of any one of the intermediate oxidation states to CO_2. Since all of the latter have pE°(W) less than —6.2 (this for

CH_3OH), each can in its oxidation provide the negative pE level required thermodynamically for reduction of CO_2 to CH_4.

Alcoholic fermentation, exemplified here by the reduction of CH_2O to CH_3OH, can occur with $pE < -3.0$. Because the concomitant oxidation of CH_2O to CO_2 has $pE^\circ(W) = -8.2$, there is no thermodynamic problem.

Although, as has been stressed, conclusions regarding dynamics may not generally be drawn from equilibrium considerations, it appears that all of the reactions discussed, except those involving N_2, are sufficiently biologically mediated in the presence of abundant biota that as the pE level is lowered gradually, successive reactions tend to occur in the order of their thermodynamic possibility. In a closed aqueous system containing organic material—say CH_2O—oxidation of the organic matter will occur first by reduction of O_2 ($pE(W) = 13.8$). This will be followed, as the pE level decreases, by reduction of NO_3^- (7.15, 6.15) and NO_2^- (5.8). Reduction of MnO_2, if present, should occur at about the same pE level. Reduction of FeOOH to $Fe^{(II)}$ should occur next. Finally, when sufficiently negative pE levels have been reached, reduction of CO_2 to CH_4 (−4.1) and SO_4^{2-} to HS^- (−3.8) may occur almost simultaneously, and ammonification may begin at about the same level (−4.7). The described sequence is mainly that observed for the vertical distribution of components in a well-eutrophied lake and also is in general the temporal succession in a closed system containing excess organic matter, such as a batch digester.

Measuring Electrode Potential

Direct measurement of pE values for natural water environments involves complex theoretical and practical problems in spite of the apparent simplicity of the electrochemical technique. Even when reproducible numbers are obtained, they often do not represent reversible Nernst potentials. Although aqueous systems containing oxygen or similar oxidizing agents will usually give positive E_h values and anaerobic systems will usually give negative ones, detailed quantitative interpretation is unjustified in most instances.

Since natural waters are generally in a dynamic rather than an equilibrium condition, even the concept of a single oxidation-reduction potential characteristic of the aqueous system cannot be maintained. At best, measurement can reveal an E_h value applicable to a particular system or systems in partial chemical equilibrium and then only if the systems are electrochemically reversible at the electrode surface at a rate that is rapid compared with the electron drain or supply by way of the measuring electrode. Electrochemical reversibility can be characterized principally by the magnitude of the exchange current, i_o, at the electrode surface.

When measurement of E_h for a system such as:

$$Fe^{3+} + e = Fe^{2+}$$

is performed with a platinum or other "inert" metal electrode, the balance point at zero applied current does not indicate zero electron exchange but only that the rates of the opposing processes are equal. The amount the potential must be shifted to obtain an indication with the measuring instrument, and hence the sharpness or reproducibility of the measurement, is determined by the slope of the net exchange current in the vicinity of the balance point. Exact measurement is possible only if $(\Delta i/\Delta E)_{i=0}$, the slope of the polarization curve, is sufficiently great.

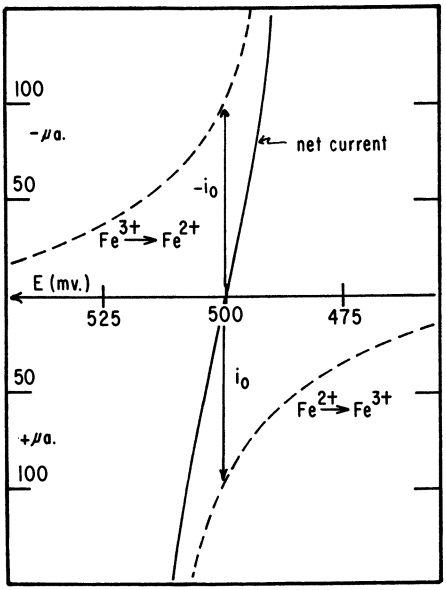

Figure 3. Electrode polarization curve for Fe^{2+}–Fe^{3+} system at a ($Fe^{2+} = Fe^{3+}$) concentration of $10^{-3}M$ and pH of 2. Curves are schematic but based on experimental data at significant points. Electrode area, 1 sq. cm., i_0 = exchange current, ($+i_0$) anodic, ($-i_0$) cathodic

This slope is related to the exchange current by:

$$(\Delta i/\Delta E)_{i=0} = \frac{nF}{RT} i_0 \qquad (12)$$

while i_o is also given by:

$$i_o = AnFK' \, C_{ox}^{(1-\alpha)} \, C_{red}^{\alpha} \tag{13}$$

where α is the transfer coefficient, often close to 0.5, K' is the reaction rate constant at the electrode surface with units of cm., sec.$^{-1}$ when C_{ox} and C_{red} are expressed in moles per cc., and A is the area of the electrode surface in sq. cm. (*5*, *16*).

Under favorable circumstances, with modern instrumentation for which the current drain is quite low, reliable potential measurements can be made with systems giving i_o greater than about 10^{-7} amp. For the Fe^{3+}–Fe^{2+} system K' at 25°C. has been determined to be about 10^{-3} cm., sec.$^{-1}$ in approximate agreement with other work (*15*). This represents a rather rapid electrode reaction. This value of K' gives $i_o = 10^{-4}$ amp. for 10^{-3} concentrations of Fe^{3+} and Fe^{2+} and for an electrode area of 1 sq. cm. Thus, the exchange current and the slope of the polarization curve amply provide accurate measurement of E_h, as shown in Figure 3. If concentrations smaller by ten-fold of both ions are present, i_o and the slopes are only one-tenth as great, but with $i_o = 10^{-5}$ reliable measurements can still be made, as shown in Figure 4. If the concentration of only one ion is decreased, the drop in i_o is not as great and E_h, the potential corresponding to equal cathodic and anodic currents, is shifted, as shown by Figure 5. If both Fe^{3+} and Fe^{2+} are at $10^{-6}M$ concentrations (*ca.* 0.05 mg./liter), i_o is 10^{-7} amp., and measurements are no longer precise. Actually, because of other effects caused by trace impurities, it becomes difficult to obtain measurements in accord with simple Nernst theory when either ion concentration is less than about $10^{-5}M$.

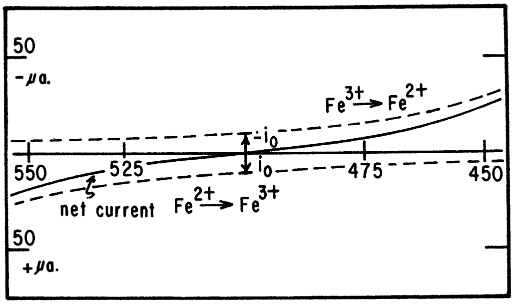

Figure 4. Electrode polarization curve for Fe^{2+}–Fe^{3+} system at ($Fe^{2+} = Fe^{3+}$) concentration of $10^{-4}M$, pH of 2. Other conditions same as for Figure 3

According to Equation 13, more precise measurements can be obtained at very low concentrations with an increase in the electrode area, *A*. Electrodes with large areas are advantageous in this way but also tend to magnify the effects of trace impurities or other reactions on the electrode surface itself, such as adsorption of surface active materials leading to reduction in K'.

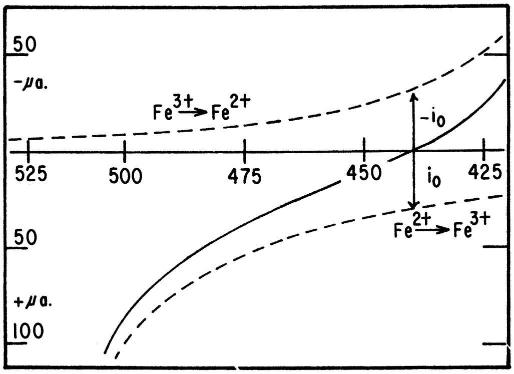

Figure 5. Electrode polarization curve for Fe^{2+}–Fe^{3+} system at concentration of $Fe^{2+} = 10^{-3}M$, $Fe^{3+} = 10^{-4}M$, pH of 2. Other conditions same as for Figure 3

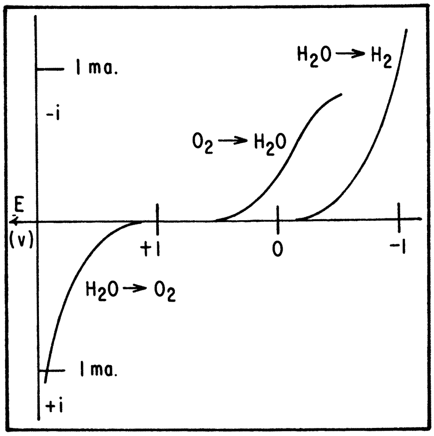

Figure 6. Electrode polarization curves for oxygen-containing solutions in otherwise-pure water. Curves are schematic but in accord with available data at significant points

It has been estimated that for O_2 (1 atm.) the specific exchange current, i_0/A, is 10^{-10} amp., cm.$^{-2}$ (*15*), far less than 10^{-7}. Thus, pE of oxygen is not measured directly with a platinum electrode in aerobic aqueous systems. Instead, it appears (*15*) that a Pt-electrode responds to processes such as $Pt(OH) + e^- = Pt + OH^-$, which has a potential (in acid solutions) of 0.84 volts. The situation that occurs with O_2 is shown schematically in Figure 6; over an extensive range of E the exchange current is so small that there is no observable electrode response. For such conditions, measured E_h values are unstable and erratic.

Another difficulty arises in E_h measurements. The balancing anodic and cathodic currents at the apparent "equilibrium" potential need not correspond to the same redox process and either may be a composite of two or more processes. An example of this is shown in Figure 7 for a Fe^{3+}–Fe^{2+} system in the presence of a trace of dissolved oxygen. The measured zero-current potential is that value where the rate of O_2 reduction at the electrode surface is equal to the rate of Fe^{2+} oxidation rather than the value of $E_{eq.}$ since at the latter point simultaneous O_2 reduction produces excess cathodic current. In addition, because the net reaction of E_m converts Fe^{2+} to Fe^{3+}, the measured potential exhibits a slow drift. Such "mixed" potentials are of little worth in determining equilibrium E_h values.

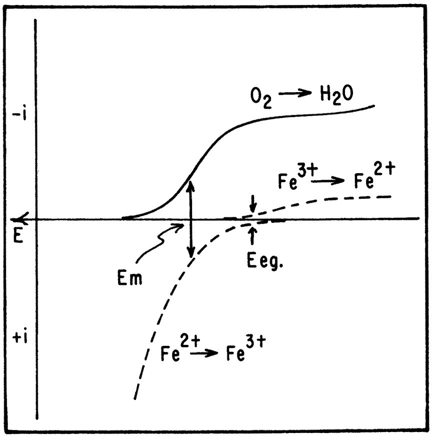

Figure 7. Electrode polarization curves for oxygen-containing solutions with a mixed potential resulting from oxygen reduction accompanied by Fe^{2+} oxidation. Curves are schematic but in accord with available data at significant points

Except for the Fe^{3+}–Fe^{2+} couple at concentrations greater than about $10^{-5}M$ and perhaps the $Mn^{(IV)}$–Mn^{2+} couple (*3*) the over-all redox systems important in natural waters are not electroactive. No reversible electrode potentials are established for the NO_3^-–NO_2^-–NH_4^+, SO_4^{2-}–H_2S, or CH_4–

org.–CO_2 systems. Moreover, few organic redox couples yield reversible potentials (*6*). An analysis of the data collected by Baas-Becking *et al.* (*2*), Mortimer (*11, 12*), and Kusnetzov (*9*) tends to corroborate the view that most measurements of E_h in natural waters represent mixed potentials not amenable to quantitative interpretation.

Indirect Evaluation of Redox Potential. In theory it is possible to evaluate the redox level in natural water systems by determining the relative concentrations of the members of one of the redox couples in the system and applying the electrochemical relations in reverse. In practice, however, there are severe limitations even on this basically sound procedure. First, the system must be in equilibrium or must be in a sufficiently constant metastable state to make the concept of a partial equilibrium meaningful. For example, although most aqueous media are not in equilibrium with regard to processes involving N_2, the inertness of these reactions may allow one to ignore them while treating the equilibrium achieved by other species. Second, results are not likely to be significant for oxygen-containing waters since, as previously shown, all the other couples exist at equilibrium essentially completely in their most highly oxidized states when O_2 is present. Only when reaction of O_2 is so slow that it can be considered inert like N_2 can determinations of concentrations of other species be meaningful reflections of redox potential level. Third, concordant values of E_h must be obtained for each of the redox couples in a multi-component system like the aquatic medium; otherwise the couples are not in equilibrium, and the concept of redox potential becomes meaningless.

Within these limitations analytical determination of the oxidized and reduced forms of a redox couple can provide quite precise values for E_h. Depending on the number of electrons transferred in the process, determinations accurate within a factor of 2 will give E_h values within 5 to 20 mv.

Conclusions

Equilibrium models are powerful tools for describing the conditions of stability of redox components in natural water systems. More extended quantitative inferences must be made with great caution because the systems are generally dynamic rather than equilibrated.

Electrochemical measurements of potential with inert metallic electrodes are not reliable indicators of E_h levels in most natural water systems, and even the concept of an E_h level is meaningless unless restrictive conditions are satisfied. Analytical determinations can in proper circumstances give more reliable information about E_h levels than potential measurements can.

Literature Cited

(1) Arnon, D. I., *Science* **149,** 1460 (1965).
(2) Baas-Becking, L. G. M., Kaplan, I. R., Moore, D., *J. Geol.* **68,** 243 (1960).
(3) Bricker, O. P., *Am. Mineralogist* **50,** 1296 (1965).
(4) Calvin, M., Bassham, J. A., "The Photosynthesis of Carbon Compounds," Benjamin, New York, 1962.
(5) Charlot, G., Badoz-Lambling, J., Trémillon, B., "Electrochemical Reactions," Chapter 7, Elsevier, Amsterdam, 1962.
(6) Clark, W. M., "Oxidation-Reduction Potentials of Organic Systems," Williams and Wilkins, Baltimore, 1960.
(7) Eck, R. V., Dayhoff, M. O., *Science* **152,** 363 (1966).
(8) Jörgensen, H., "Redox-malinger," Gjellerup, Copenhagen, 1945.
(9) Kusnetzov, S. I., *Arb. Limnol. Station Kossino* **20,** 55 (1935).
(10) Lehninger, A. L., "Bioenergetics," p. 35, Benjamin, New York, 1965.
(11) Mortimer, C. H., *J. Ecol.* **29,** 280 (1941).
(12) *Ibid.* **30,** 147 (1942).
(13) Sillén, L. G., Martell, A. E., *Chem. Soc. Spec. Publ.* **17** (1964).
(14) Sillén, L. G., "Chemical Equilibrium in Analytical Chemistry," Interscience, New York, 1962.
(15) Tanaka, N., Tamushi, R., *Eletrochim. Acta* **9,** 963 (1964).
(16) Vetter, K. J., "Elektrochemische Kinetik," Springer-Verlag, Berlin, 1961.
(17) Watanabe, W., Davanathan, M. A. V., *J. Electrochem. Soc.* **111,** 615 (1964).

RECEIVED July 11, 1966.

14

Some pH-Controlling Redox Reactions in Natural Waters

K. BOSTRÖM[1]

Scripps Institute of Oceanography, LaJolla, Calif.

Using stoichiometric model systems, it can be shown that some naturally occurring redox processes have a pronounced pH-controlling action, even in the presence of substances that act as buffers. High pH values can be reached particularly in systems where higher metal oxides act as oxidizers whereas an acid condition often develops when free oxygen is the oxidizer. However, in most natural systems carbonates and silicates have a more pronounced pH controlling effect than redox processes.

For more than a century it has been well-known that the course of many processes on the earth's surface, such as precipitation, dissolution, and redox reactions depend on the degree of acidity or alkalinity of the solutions involved. Conversely, it was also realized early that various geological processes may change the acidity of aqueous solutions. However, not until satisfactory methods to measure pH had been developed was it possible to understand fully how these processes depended on solution pH and vice versa. In the 1930's pH measurements became common in various geochemical studies; a general discussion of the importance of the concept of hydrogen ion activity in geochemistry was given by Atkins (*6*). More recently the influence of the medium's pH on the course of geological redox reactions has been discussed extensively by several workers, particularly Garrels. For a general summary and references the reader is referred to the work by Garrels and Christ (*18*). The acid-base definition used below will be the one proposed by Brönsted (*14*).

However, the processes by which pH is regulated in natural solutions is still not entirely clear despite extensive work. This circumstance

---

[1] Present address: University of Miami, Institute of Marine Sciences, Miami, Fla.

may be caused by several factors, such as incompletely known physicochemical constants for the pH-controlling species, particularly at high ionic strengths, and analytical difficulties, for instance in determining pH. Another possibility is that there are some pH-controlling reactions that have not been considered or have received only little attention.

It seems probable, for reasons given below, that some redox reactions constitute a group of such pH-controlling processes. The change in acidity of solutions owing to oxidation processes has long been known. Lindgren (*31*) and Smirnow (*48*) explained the acidity of solutions that percolate through the oxidation zone of sulfide ores as being caused by oxidation of sulfides. It is also well-known that the decomposition of organic matter releases CO_2, which tends to form acid conditions. Detailed discussions of such processes have been given by many authors, for example Richards (*42*).

In general, however, the change in pH owing to redox reactions has received little consideration. The main reasons are probably that (a) many studied systems have been assumed to be in intimate contact with the atmosphere—*i.e.*, it seems natural to assume that pH and CO_2-activity should remain constant in such systems—and (b) *e vs.* pH diagrams, which frequently are used to study redox reactions, show how these reactions are influenced by solution pH but do not show how the redox reactions themselves influence pH. [We shall define the redox potential *e* as the e.m.f. of the cell: $-$ Pt, H_2 (1 atm.) | H^+ (unit activity) || Redox system | Pt +.] However, the original amounts of reactants available will determine at which *e* and pH values the equilibrium is established although this statement may, *per se,* seem to be meaningless since stoichiometric and thermodynamic entities are not comparable. In closed systems and open systems that only slowly exchange material with their surroundings, it is known that redox processes may form strongly alkaline conditions (*8*). For example, the reduction of metal oxides such as Mn_2O_3, Mn_3O_4, and FeOOH (*8, 10*) in the presence of water produces large quantities of hydroxide ions as will be discussed more in detail below. In view of the fact that the oxidation states of certain elements vary considerably in the hydrosphere and in the earth's sediments, one can expect that several pH-controlling redox reactions occur in these environments, particularly during diagenesis and metamorphism.

This paper will discuss how redox processes may govern pH and phase composition of the system and to what extent they may control the chemistry of the aqueous solutions.

Much of the data required for a thorough discussion are still missing. Therefore, much of the following discussion will be devoted to studying the stoichiometry of possible pH-controlling reactions. This powerful approach is well-known in chemistry but has not been used as often to its full potential in geological and oceanographical studies as it deserves. However, studies by Richards (*42*) and Boström (*8*) show that the technique can be most practical.

Anoxic systems—*i.e.*, those in which no free oxygen exists—which commonly represent stagnant conditions, can in general because of their slow flushing be expected to be closer to equilibrium than oxygenated systems. Hence, we will emphasize mainly anoxic natural and model systems.

Anoxic conditions occur in deep sections of sediments, ground waters, and hot springs and in poorly flushed basins such as the Black Sea, Cariaco trench, Kaoe Bay, and in Norwegian and Canadian fjords. In these anoxic environments higher oxides of sulfur, iron, and manganese occur or are mechanically brought together with organic matter, but the reactions between the constituents are often complex and difficult to unveil, owing to the presence of buffering carbonates and silicates. However, in some hydrothermal vein environments, pH-controlling redox reactions between oxides and sulfides have developed with little interference from carbonates and silicates. Hence, one section will be devoted to reactions between manganese oxides and sulfides in such simpler hydrothermal vein systems. Later, the results from this section will be developed to cover more general redox situations; in subsequent sections these generalizations will be used to consider diagenetic and metamorphic processes in which organic matter interacts with manganese(III), iron(III), and sulfur (VI) compounds in pelagic sediments and sediments formed in stagnant basins. (The term pelagic sediment is rather loosely defined but generally refers to marine sediments in which the fraction derived from the continents indicates deposition from dilute mineral suspensions, distributed through the deep ocean water (*5*).) Finally, a general discussion is given of the significance of the redox processes in question. Table I gives the chemical compositions of the minerals discussed.

Since graphical displays of physicochemical relationships are convenient to use, much of the data in this paper are represented by *e vs.* pH diagrams. Redox potential and pH have been chosen as master variables only for convenience; this does not mean that *e* and pH always can be regarded as independent of each other.

Some physicochemical constants used here have been calculated (*9*) by various well-known thermodynamic techniques (*23, 30, 38*). The data for the calculations and for the construction of the diagrams are from various thermodynamic tables or other publications with thermodynamic data (*13, 15, 18, 23, 24, 25, 27, 29, 30, 38, 40, 45, 47, 50*).

Table I. Approximate Chemical Composition of Minerals Discussed

Allactite	$Mn_7(AsO_4)_2(OH)_8$
Armangite	$Mn_3(AsO_3)_2$
Barysilite	$Pb_3Si_2O_7$
Baryte	$BaSO_4$
Barytocalcite	$CaBa(CO_3)_2$
Bixbyite	Mn_2O_3
Brandtite	$CaMn_2(AsO_4)_2 \cdot 2\ H_2O$
Braunite	$(Mn,Si)_2O_3$
Brucite	$Mg(OH)_2$
Calcite	$CaCO_3$
Chamosite	$(Fe^{II},Fe^{III},Mg,Al)\ (Si,Al)O_{7.3\text{-}5}(OH)_{4\text{-}1}$
Dolomite	$CaMg(CO_3)_2$
Finnemannite	$Pb_5(AsO_3)_3Cl$
Fluorite	CaF_2
Galena	PbS
Goethite	$FeOOH$
Graphite	C
Gypsum	$CaSO_4 \cdot 2\ H_2O$
Hausmannite	Mn_3O_4
Hematite	Fe_2O_3
Hoernesite	$(Mg,Mn)_3(AsO_4)_2 \cdot 8\ H_2O$
Hydrocerussite	$Pb_3(CO_3)_2(OH)_2$
Hydrotroilite	$FeS \cdot nH_2O$
Limonite	$FeOOH \cdot nH_2O$
Magnetite	Fe_3O_4
Manganite	$MnOOH$
Margarosanite	$(Ca,Pb,Mn)SiO_3$
Native arsenic	As
Native bismuth	Bi
Native copper	Cu
Native iron	Fe
Native lead	Pb
Native sulfur	S
Nontronite	$Fe_2^{III}Na_{0.33}(Si,Al)_4O_{10}(OH)_2 \cdot 4\ H_2O$
Periclase	MgO
Pyrite	FeS_2
Pyroaurite	$Mg_{18}Fe_6(OH)_{48}(CO_3)_3 \cdot 12\ H_2O$
Pyrochroite	$Mn(OH)_2$
Pyrolusite	MnO_2
Quarts	SiO_2
Sarkinite	$Mn_2(AsO_4)OH$
Siderite	$FeCO_3$
Sjögrenite	$Mg_6Fe_2(OH)_{16}CO_3 \cdot 4\ H_2O$
Troilite	FeS

Redox Processes between Sulfides and Manganese Oxides

Vein deposits that originated from reactions between sulfides and manganese oxides have been observed in the Swedish iron-manganese ores at Långban, Harstigen, Pajsberg, Jakobsberg, and Sjögruvan (*33, 34, 49*). Probably, similar processes occurred in the zinc ores at Franklin and Sterling Hill, N. J. (*8*). The associations commonly referred to as the native lead-pyrochroite association are characterized by the occurrence of native lead, copper, and arsenic, baryte, calcite, pyrochroite, hydrocerussite, hematite, manganite, allactite, and brandtite (*3, 22, 39*). In addition, many other minerals occur in the veins (*3, 8*) (Table II and Figure 1). Because the Swedish associations are the best known to the author, they will be used as the example for discussion.

In the Swedish deposits, the native lead-pyrochroite veins are found exclusively within or close to hausmannite and braunite ores but not in iron ore except when a manganese ore is located in the vicinity (*34*). In

Table II. Minerals Present in the Vein Association and in the Vein-Wall in Långban

Vein-Association		*Vein-Wall*	
Galena	PbS		
Baryte	$BaSO_4$		
Anhydrous arsenates			
Allactite	$Mn_7(AsO_4)_2(OH)_8$		
Sarkinite	Mn_2AsO_4OH	Hausmannite	Mn_3O_4
Calcite	$CaCO_3$	Braunite	$(Mn,Si)_2O_3$
Native lead	Pb	Calcite	$CaCO_3$
Native copper	Cu	Barytocalcite	$CaBa(CO_3)_2$
Native arsenic	As		
Native bismuth	Bi		
Pyrochroite	$Mn(OH)_2$	Dolomite	
Arsenites		$CaMg(CO_3)_2$ (with impurities of Pb^{2+}, Ba^{2+}, Mn^{2+}, etc.)	
Armangite	$Mn_3(AsO_3)_2$		
Finnemannite	$Pb_5(AsO_3)_3Cl$	Skarn silicates	
Hydrocerussite	$Pb_3(CO_3)_2(OH)_2$		
Hydrous arsenates		Hematite	Fe_2O_3
Brandtite	$CaMn_2(AsO_4)_2 \cdot 2\ H_2O$	Magnetite	Fe_3O_4
Hoernesite	$(Mg,Mn)_3(AsO_4)_2 \cdot 8\ H_2O$		
Fluorite	CaF_2	Sulfides	PbS
Hematite	Fe_2O_3		FeS_2
Manganite	$MnOOH$		Cu_2S
Gypsum	$CaSO_4 \cdot 2\ H_2O$		
Lead silicates			
Barysilite	$Pb_3Si_2O_7$		
Margarosanite	$(Ca,Pb,Mn)SiO_3$		

addition to manganese minerals the manganese ores contain Ca-Mg-Mn-carbonates that are rich locally in Pb and Ba. After the ores were formed, they were subjected to intrusions of postmagmatic solutions from granites (*34*). The mineralogy of the veins indicates that the early postmagmatic solutions were rich in halogens and sulfides but that later carbon dioxide became the predominant volatile, aside from water. The presence of hematite and manganite indicates that the main phase of the mineral-forming processes took place in the temperature range 170°–270°C.; at temperatures above 270°C. bixbyte would have formed instead of manganite (*28*), and at temperatures below 170°C. goethite, not hematite, would have formed (*44*). In addition to manganite, the ubiquitous occurrence of hydrated minerals indicates that the reactions occurred in an aqueous system. Variations in pressure influence these temperature values only slightly. Pressure was probably not high, judging from the brittleness of the carbonate rocks during the tectonic events that occurred before and during the vein-forming processes.

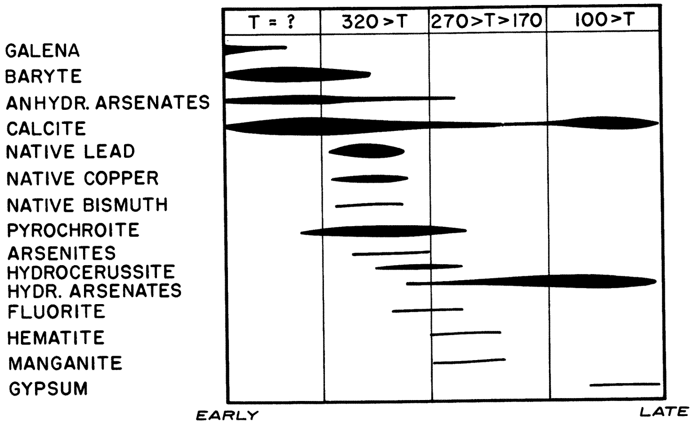

Figure 1. Order of formation of vein minerals in Långban. Variation in line thickness indicates approximately the quantities formed of the mineral in question. A thin line thus indicates that the mineral was formed in insignificant quantities.

Magnusson (*34*) pointed out that the occurrences of native metals in these veins probably were caused by oxidation of the sulfides by the manganese oxides. Furthermore, Mason (*35*) pointed out that the formation of native lead and pyrochroite took place in neutral, or more probably, in alkaline solutions. Similar conclusions were reached by Boström (*8*); as indicated by Figures 2 and 3, native lead, native arsenic, pyrochroite, and hydrocerussite probably form stable assemblages at fairly high pH values and reducing conditions. As far as can be deduced from available thermodynamic data, similar conditions hold for the temperature range 25°–300°C.

Several explanations can be suggested for the origin of this alkaline environment. One is that dolomites were metamorphosed by granites,

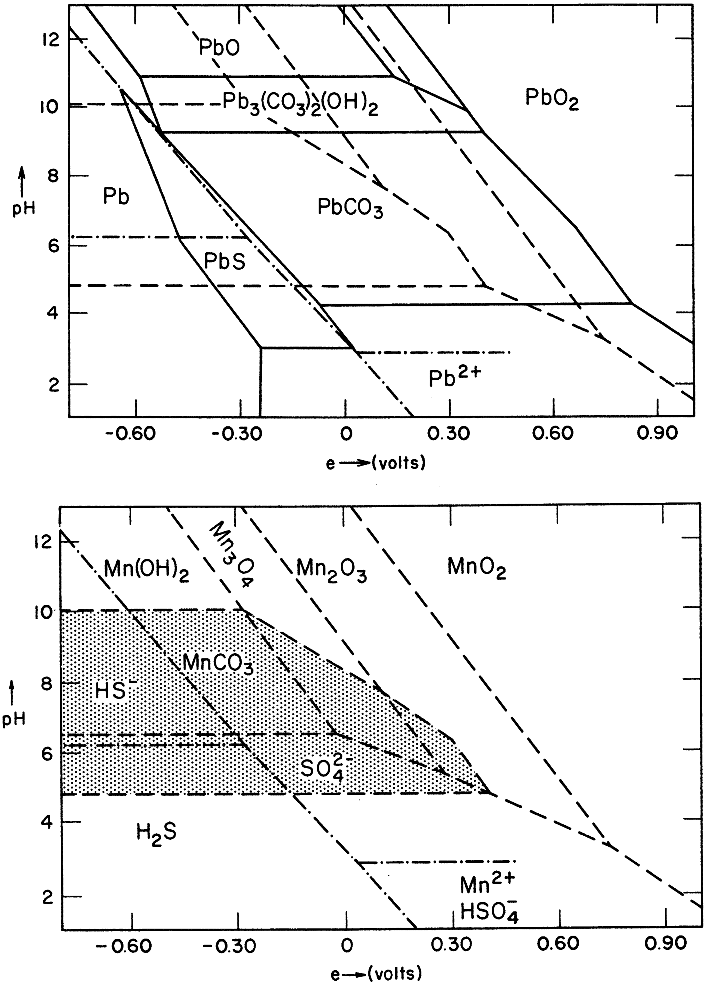

Figure 2. Plot of e vs. pH for two systems at 100°C. and 600 bars

(Top) Pb-S-Mn-CO_2-H_2O system
Total activities: Pb, Mn, $CO_2 = 10^{-2}$; $S = 10^{-8}$
———*Extent of stability and dominance regions for various Pb species*
– – – –*Corresponding regions for Mn species*
–•–•–*Limits of the dominance regions for H_2S, HS^-, SO_4^{2-}, HSO_4^-*
(Bottom) Mn-S-CO_2- H_2O system
Total activities: Mn, $CO_2 = 10^{-2}$; $S = 10^{-8}$
———*Mn species*
–•–•–S species

forming the periclase-spotted limestones that have been observed near the mines. Periclase later reacted with water, and the ensuing alkaline solution invaded the manganese ores together with the sulfidic granite emanations. The main objection to this explanation is that magnesium is not a characteristic element in the veins; frequently it seems to be completely absent. Where brucite does occur, it is found in separate veins, with minerals like magnetite but not with sulfides. The brucite veins are not confined to the vicinity of the manganese ores (*33, 34*). Possibly some of the other types of reduced veins with pyroaurite, sjögrenite, arsenites, and magnesium arsenates which have been observed were formed in connection with the slaking of periclase.

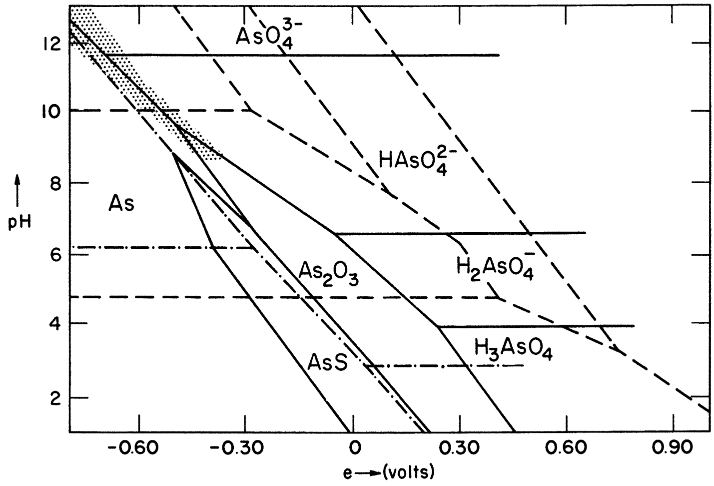

Figure 3. Plot of e vs. pH for the system As-S-Mn-CO_2-H_2O at 100°C. and 600 bars
Total activities: As = 10^{-1}, S = 10^{-8}, Mn and CO_2 = 10^{-2}
: : : : : Field represents possible dominance field for $H_2AsO_3^-$, $HAsO_3^{2-}$, and AsO_3^{3-}
——— As species
– – – – Mn species
–•–•– S species

Another explanation would be that dissolution of carbonates created an alkaline environment according to the reaction below.

$$CaCO_3 + H_2O \rightarrow Ca^{2+} + HCO_3^- + OH^-$$

At room temperature this process gives rise to a pH near 10, provided no CO_2 has been taken up from the atmosphere. As a consequence of this process the activity of HCO_3^- must also be high. However, at 25°C. and high total carbonate activity, pyrochroite is not stable at this pH value but requires a pH of 10.8 to form (*8*). This is also evident from the equation:

$$2H_2O + MnCO_3 \rightarrow Mn(OH)_2 + H_2CO_3 \qquad \log K_r = -8.63 \text{ at } 25°C.$$

A similar conclusion can be drawn for the formation of hydrocerussite. Thus, $PbCO_3$ from the carbonates in the vein wall could take part in the reaction

$$3PbCO_3 + 2OH^- \rightarrow Pb_3(CO_3)_2(OH)_2 + CO_3^{2-}$$

where the hydroxyl ions are formed when carbonates like calcite are dissolved in water. However, this process also builds up the activity of total carbonic acid so much that hydrocerussite becomes unstable. It can be shown (*8*) that this process is incapable of forming a sufficiently alkaline environment to form pyrochroite and hydrocerussite. These reactions also do not explain the extensive formation of calcite that has occurred in the veins. On the contrary, they assume that calcite is being dissolved in the veins. Furthermore, the implicit assumption that no CO_2 was originally dissolved in the water is most unlikely.

Still another explanation is that the thermal decomposition of $MnCO_3$ to MnO and the later slaking of MnO forms an alkaline environment. This process has occurred to some extent in the ore deposits; however, it does not explain the fact that many of the native lead-pyrochroite veins occur in hausmannite ores, where the manganese oxides are altered or completely leached away close to the vein.

The most probable suggestion seems to be that the reactions between sulfides like galena and manganese oxides like hausmannite or braunite created the alkaline environment necessary for pyrochroite and hydrocerussite to form (*8*):

$$PbS + 3\,Mn_3O_4 + 8\,H_2O \rightarrow Pb + SO_4^{2-} + 9\,Mn^{2+} + 16\,OH^-$$

$$PbS + 4\,Mn_3O_4 + 12\,H_2O \rightarrow Pb^{2+} + SO_4^{2-} + 12\,Mn^{2+} + 24\,OH^-$$

The equations show how hydroxyl ions are formed in quantities sufficient for forming pyrochroite, hydrocerussite, and allactite. These processes also explain how calcite and baryte can be among the early formed minerals in the veins. Any HCO_3^- in the original solutions could react with OH^- and Ca^{2+} as follows:

$$HCO_3^- + OH^- \rightarrow CO_3^{2-} + H_2O$$

$$Ca^{2+} + CO_3^{2-} \rightarrow CaCO_3(s)$$

Barium containing carbonates (*34*) probably were the source of barium in baryte:

$$BaCO_3 + SO_4^{2-} \rightarrow BaSO_4 + CO_3^{2-}$$

The chemistry of many of the veins is consistent with the reactions above and thus supports the sulfide-oxide reaction hypothesis. Thus, compounds of Mn, Ca, Ba, and Pb dominate the veins whereas, as pointed out above, Mg seems to be absent in many veins.

The stability conditions displayed in Figures 2 and 3 suggest that the processes discussed above are thermodynamically possible. To permit more exact calculations of the equilibrium constants for the processes, the reactions can be rewritten as follows:

$$PbS + 3\,Mn_3O_4 + 8\,H_2O + BaCO_3 \rightleftarrows Pb + 8\,Mn(OH)_2 + BaSO_4 + MnCO_3 \qquad (1)$$

$$PbS + 4\,Mn_3O_4 + 12\,H_2O + BaCO_3 \rightleftarrows PbCO_3 + 12\,Mn(OH)_2 + BaSO_4 \qquad (2)$$

log K_r for these reactions are (at 1000 bars):

$T°$,(K.)	400	500	600
Reaction 1	10.3	4.8	0.6
Reaction 2	14.4	6.7	0.9

The capacities to control pH of the redox reactions above have been studied (*8*) by a closed-system model for the vein-forming processes at 25°C. and 1 atm. By establishing a budget between consumed and formed species and using known solubility products, protolytic constants, proton and electroneutrality conditions, one can calculate which phases are stable and what the composition of the final solution will be. Such calculations show that reactions in this system indeed tend to produce OH^- and furthermore that the final solution is comparatively high in OH^- and low in HCO_3^-, as could be expected from the qualitative discussion above. It is of interest to note that these processes tend to form strongly alkaline conditions under non-stagnant conditions as well.

The absence of free silica in the veins is consistent with the model given above since, in addition to the increased solubility of silica at elevated temperatures, the process

$$SiO_2 + H_2O + OH^- \rightarrow H_3SiO_4^-$$

can explain the absence of quartz in the veins since any dissolved silica would tend to remain in solution and not precipitate. Silicates are scarce but not completely absent, however; silicates like margarosanite and barysilite are known in some native lead veins.

Redox Reactions in Anoxic Systems in General

In the previous section it was shown how alkaline conditions could arise from interactions between sulfides and manganese oxides. Indeed, many redox reactions have a pH-controlling tendency. A general survey of the oxidizers and reducers that are available for exogenic and metamorphic processes is therefore of interest.

Table III. Order of Atomic Abundance[a] of the Most Common Elements and Their Oxidation States in the Upper Lithosphere

Element	*Atom %*	*Valence States*
O	60.5	2−, 0
Si	19.8	4+
Al	5.98	3+
H	2.90	1+, 0
Na	2.41	1+
Ca	1.83	2+
Fe	1.81	(0), 2+, 3+
Mg	1.74	2+
K	1.32	1+
Ti	0.26	4+
C	0.16	4−, 2−, 0, 2+, 4+
P	0.08	5+
S	0.06	2−, 1−, 0, 6+
Mn	0.03	2+, 3+, 4+

[a] Values for the abundance of the elements vary somewhat from estimate to estimate (*7*), but these variations are small and insignificant for the present purpose.

Table III shows the abundance of various elements in the earth's crust and the oxidation states they frequently occupy. The table indicates that of the 14 most abundant elements, only six participate in redox reactions in the surface layers of the earth. [PH_3 seems to be extremely rare (*42*) and will not be discussed.] Because by definition free oxygen as O_2 is absent in the anoxic zone, it is evident that oxides of Fe(III) are the most important oxidizers in anoxic environment and that SO_4^{2-} and higher oxides of manganese are of importance only locally. Reducing compounds of importance are organic matter and sulfides, the latter frequently from volcanic emanations. Hydrogen is commonly combined with other elements, as in H_2O, CH_4, and NH_3 but may locally occur free as H_2. Since iron is the most widespread element that can serve as an oxidizer in the anoxic environment the distribution of the valence states of iron in various rocks is of interest (*see* Table IV). Sandstones frequently have a high Fe_2O_3/FeO ratio, but shales and clays may also be highly oxidized as shown in Tables IV and V. Since approximately 75% of the earth's surface is covered with sediments and since the sediments have a larger porosity than most igneous rocks, it is likely that processes in the sediments will have a pronounced influence on the chemistry of subterranean and deep ocean water. A detailed look at the composition of sediments is therefore of interest.

In sediments, oxidized iron is commonly present as the oxides magnetite, hematite, goethite, limonite, and as silicates such as ferric chamosite. In reduced form iron is present as siderite, several iron(II) silicates, sulfides, such as pyrite, FeS_2, and as undefined compounds of the general type $FeS \cdot nH_2O$, sometimes referred to as hydrotroilite. In rare cases iron occurs in native form in wood in bogs, in petrified wood mixed with limonite and organic matter, and in carbonaceous sediments.

Table IV. Oxidation State of Iron in Rocks (*21*)[a]

	$Fe_2O_3^*$		FeO		*Molar Ratio*
	%	*moles*	*%*	*moles*	Fe_2O_3/FeO
Igneous rocks	3.08	0.0171	3.80	0.0527	0.325
Shales	4.03	0.0224	2.46	0.0342	0.655
Terrigenous muds	5.07	0.0281	2.30	0.0320	0.878
Sandstones	1.08	0.0060	0.30	0.0042	1.43

[a] Abundances given in weight percent and in moles per 100 grams of rock.

Table V. Average Composition of Some Sediments and Sedimentary Rocks (*36*)

	Average shale, Middle West, U.S.	*Clay, mean of 712 analyses*
SiO_2	56.95	65.10
TiO_2	0.68	0.67
Al_2O_3	15.90	15.33
Fe_2O_3	4.36	3.53
FeO	1.56	0.55
MnO	—	—
MgO	2.15	1.18
CaO	4.58	2.85
Na_2O	0.56	1.03
K_2O	1.86	1.23
H_2O	2.64	3.05
P_2O_5	0.34	0.83
CO_2	3.96	3.10
SO_3	0.49	0.47
Organic	3.97	1.08

Manganese is mainly present as manganese(II) carbonates, but in some sediments and on weathering surfaces it is present as higher oxides such as manganite and pyrolusite. In some pelagic sediments the amount of highly oxidized manganese is appreciable, but only a few studies (*17*) have been made to determine the amount of manganese(II), (III), and (IV) compounds in such sediments. In view of these uncertainties, in the discussion below manganese will, as a cautious estimate, be assumed to be present in pelagic sediments mainly as manganese(III) compounds.

Sulfur is present in several oxidation states, usually as sulfide and sulfate. Locally native sulfur may occur in significant quantities. Sulfate is present in large concentrations in seawater and is probably the most important oxidizer in the water of anoxic basins such as the Black Sea, Kaoe Bay, and many fjords.

Carbon occurs frequently as carbon dioxide, either dissolved as carbonic acid or a protolytic product thereof, or bound as carbonate, or freely occurring as gas. Carbon dioxide is a weak oxidizer; the most important aspect of the redox geochemistry of carbon is the presence of carbon in the form of organic matter, which commonly is a strong reducing component in sediments and in the hydrosphere. Thus, although most sediments contain only a few percent organic matter, it is generally agreed that this component controls to a large extent the course of the redox processes which occur during diagenesis and metamorphism.

Hydrogen is almost exclusively present in combined form, as in water and organic compounds. Free hydrogen is brought into the anoxic environment by the decomposition of organic matter and in a few cases by volcanism.

The stability fields of the various iron, manganese, sulfur, carbon, oxygen, and hydrogen compounds discussed above are indicated in Figures 2–8. The stability conditions of these compounds do not vary much in the range 25°–200°C. For this reason most of the diagrams are for 100°C. only. The presence or absence of silica has a pronounced influence on the stability fields of many of the elements such as iron and manganese, but few thermodynamic data for silicates exist. In Figures 6–8 an attempt is made to illustrate the influence of SiO_2 on the stability relations for various iron compounds.

The constituents discussed above may participate in the following redox reactions. No attempt is made to cover every possible redox process in the sediments and in the hydrosphere but only to give an idea of how some different redox reactions may proceed, depending on the environments.

The pH-controlling tendency of a redox reaction depends primarily on the ratio, $R = \frac{\text{OH}^- \text{ produced}}{e^- \text{ consumed}}$, and not on the absolute number of OH^- ions produced. (The production of H^+ corresponds to a negative production of OH^-, the production of e^- to a negative consumption of e^-.) It is advantageous to treat the various half-cell reactions separately.

Reduction Processes. Metal oxides Me_nO_m, sulfates, and carbonates may be reduced as follows:

	R
$2\,e^- + 2\,H_2O + MeO_2 \rightarrow Me^{2+} + 4\,OH^-$	2.00
$2\,e^- + 3\,H_2O + Me_2O_3 \rightarrow 2\,Me^{2+} + 6\,OH^-$	3.00
$2\,e^- + 4\,H_2O + Me_3O_4 \rightarrow 3\,Me^{2+} + 8\,OH^-$	4.00
$2\,e^- + H_2O + 3\,Me_2O_3 \rightarrow 2\,Me_3O_4 + 2\,OH^-$	1.00
$8\,e^- + 4\,H_2O + Me_3O_4 \rightarrow 3\,Me^\circ + 8\,OH^-$	1.00
$e^- + Me^{4+} \rightarrow Me^{3+}$	0
$e^- + Me^{3+} \rightarrow Me^{2+}$	0
$2\,e + Me^{2+} \rightarrow Me^\circ$	0
$8\,e^- + 4\,H_2O + SO_4^{2-} \rightarrow S^{2-} + 8\,OH^-$	1.00
$6\,e^- + 4\,H_2O + SO_4^{2-} \rightarrow S^\circ + 8\,OH^-$	1.33
$4\,e^- + 3\,H_2O + CO_3^{2-} \rightarrow C + 6\,OH^-$	1.50

Since carbon monoxide is unstable and tends to form $C + CO_2$, it will not be discussed in the redox systems below.

Oxidation Processes. Sulfides may be oxidized according to the following equations.

	R
$8\,OH^- + MeS \rightarrow Me^{2+} + SO_4^{2-} + 4\,H_2O + 8\,e^-$	1.00
$8\,OH^- + MeS \rightarrow Me^\circ + SO_4^{2-} + 4\,H_2O + 6\,e^-$	1.33
$32\,OH^- + 3\,MeS \rightarrow Me_3O_4 + 3\,SO_4^{2-} + 16\,H_2O + 26\,e^-$	1.23
$22\,OH^- + 2\,MeS \rightarrow Me_2O_3 + 2\,SO_4^{2-} + 11\,H_2O + 18\,e^-$	1.22

Oxidation of Organic Matter. The thermodynamic data available for organic compounds are insufficient for a detailed study of redox processes involving organic compounds. Figure 4 shows the stability fields of some carbon compounds together with the conditions under which irreversible oxidation of some organic compounds occurs. The only thermodynamically stable carbon compounds are CH_4, C, and CO_2, depending on the oxygen pressure.

Many organic reactions are slow at low temperatures but are considerably accelerated by temperature increases (*1*). In addition, living organisms themselves, such as chemoautotrophic bacteria, may accelerate reactions involving dead organic matter.

The decomposition of organic matter leads to the formation of H_2, CH_4, CO_2, and H_2O and deposits more refractory organic matter, usually containing a higher fraction of graphitic material than was present in the original carbonaceous matter (*12*). Since the released H_2 and CH_4 are powerful reducing substances and are oxidized to H_2O and CO_2 by various oxidizers, the over-all oxidation of organic matter can be written as:

$$C_nH_mO_q + 2(2n + \frac{m}{2} - q)\ OH^- \rightarrow$$

$$nCO_2 + (2n + m - q)\ H_2O + 2(2n + \frac{m}{2} - q)\ e^-$$

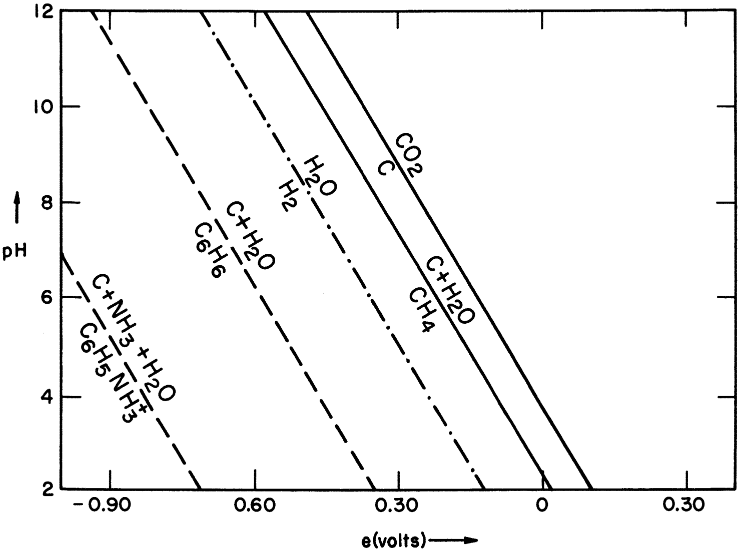

Figure 4. Plot of e vs. pH for the system C-H-O-N (incomplete) at 25°C. and 1 atm., showing stability and decomposition relations for various C-H-O-N compounds. H_2, H_2O, CH_4, C, and CO_2 represent thermodynamically stable phases

assuming H_2O and CO_2 to be the stable end products. If graphite is the stable end product, we can write the following equation for the oxidation of the reactive fraction.

$$C_nH_mO_q + 2(\frac{m}{2} - q)\ OH^- \rightarrow n\,C + (m - q)\ H_2O + 2(\frac{m}{2} - q)\ e^-$$

The oxidation and reduction processes mentioned above will now be studied in detail in some sediments.

Table VI. Composition of Pelagic Sediment plus Interstitial Water[a]

Compound	*Moles in 2500 grams of Sediment*	
	1	*2*
SiO_2	8.25	5.3–8.5
Al_2O_3	1.71	0.9–2.6
FeOOH	1.17	0.7–2.0
MnOOH	0.23	0.1–0.5
MgO	0.87	
CaO	0.73	0.2–3.5
Na_2O	0.87	
K_2O	0.32	
H_2O	82.00	
CO_2	0.73	0–~3.5
SO_3	0.057	
BaO	0.029	
Organic Matter	n.d.	0.2–0.6

[a] Average composition (Column 1) and the chemical variability (Column 2) in moles of 2500 grams typical pelagic sediment, recalculated after data from Goldberg and Arrhenius (*20*), Revelle (*41*), and other sources. For the calculations it is assumed that 1500 grams interstitial water is present. Content of CO_2 estimated assuming that all CaO is present as carbonate. The content of SO_3 estimated assuming that half of the BaO is present as sulfate; to this SO_3 value is added the quantity present in the 1500 grams interstitial water, assuming its composition to be identical to that of sea water. The number of moles of organic matter is based on an assumed average composition of $CH_{1.5}O_{0.5}$.

Redox Processes in Pelagic Sediments

Pelagic sediments cover a large area of the earth and constitute a considerable fraction of all sediments on the earth despite the fact that the average thickness probably is less than that for continental sediments. In pelagic sediments almost all iron is present as iron(III), and a large fraction of the manganese is in oxidation states higher than manganese(II) and frequently close to manganese(IV) (*17*). As an approximation, all iron and manganese will be assumed to be present as FeOOH and MnOOH. (A part of the iron is present in nontronite; the implication of this will be discussed later.) We will assume a sediment plus interstitial water of the composition given in Table VI, Column 1. Common variations in chemical composition of pelagic sediments are indicated in Table VI, Column 2. For the calculations below we also assume that the content of organic matter is 0.25 moles of carbon per 2500 grams of sediment (*see* Table VI). As a further approximation it is assumed that the system is closed. Unfortunately only some of the reactions during the diagenesis and metamorphism of pelagic sediments can be studied owing to our limited physicochemical data for silicates.

In treatises on geochemical processes involving carbonaceous matter, the simplified formula, CH_2O, is often used for organic matter. However, it is known that lignins and lipids are the primary species that survive microbiological decomposition in the sediment-water or sediment-air interface. It therefore seems more appropriate to use a formula between

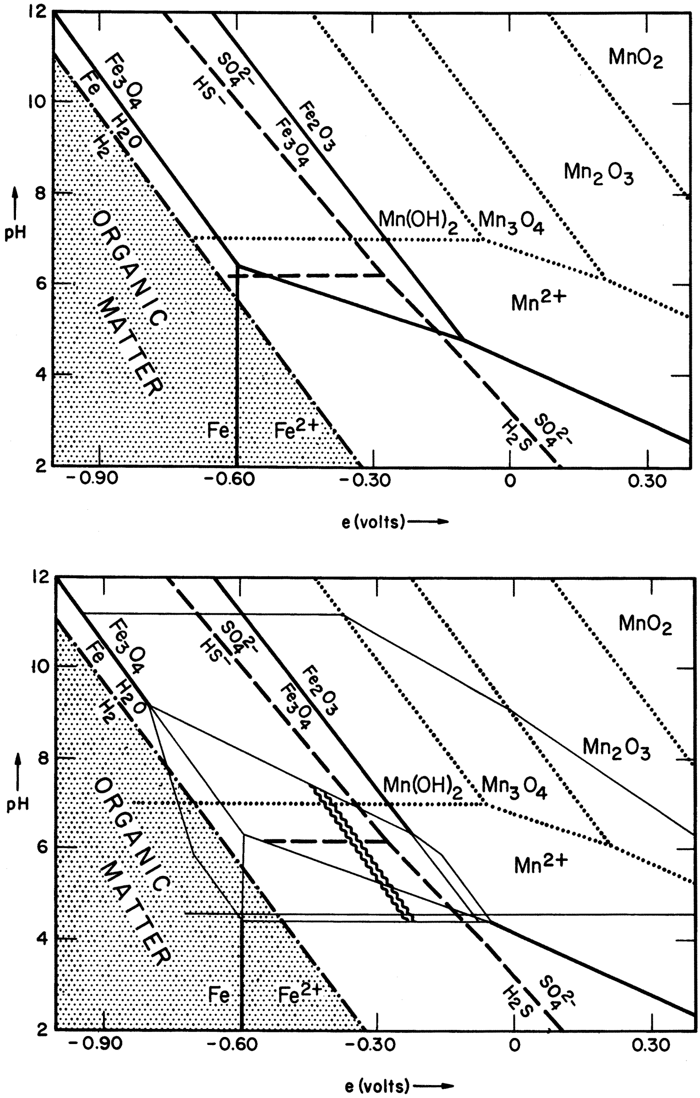

Figure 5. Plot of e vs. pH for the system Fe-Mn-S-H_2O (top) and Fe-Mn-SOCO_2-H_2O (bottom) at 100°C. and 600 bars
Total activities: Fe and Mn = 10^{-2}, S = 10^{-8}, CO_2 = 10^{-1}
: : : : : Negative redox potentials obtained by some organic compounds owing to their decomposition into hydrogen
~~~~ Approximate stability boundary between C and CO_2
Small carbonate field refers to $FeCO_3$, large field refers to $MnCO_3$

the one quoted above and those given for lignin, $CH_{0.9}O_{0.7}$ and $CH_{1.1}O_{0.4}$ (*2*, *43*). In the models below the simplified formula $CH_{1.5}O_{0.5}$ will be used to illustrate potential degradative reactions in the sediments.

We can now study the redox reactions that occur in two model pelagic sediments during the diagenesis and metamorphism. In Model I the average values in Table VI, Column 1 will be used. In Model II the maximum values in Table VI, Column 2 for FeOOH and MnOOH will be used. The content of organic matter will in both cases be assumed to be about 0.25 moles.

The following reactions are likely to occur (*see* Figure 5):

$$1.5\ H_2O + CH_{1.5}O_{0.5} + 4.5\ MnOOH \rightarrow 9\ OH^- + 4.5\ Mn^{2+} + CO_2 \quad (1)$$

Model						
I	0.077	0.051	0.23	0.46	0.23	0.051
II	0.17	0.11	0.50	1.00	0.50	0.11

$$CH_{1.5}O_{0.5} + 13.5\ FeOOH \rightarrow 4.5\ Fe_3O_4 + CO_2 + 7.5\ H_2O \quad (2)$$

Model I	0.087	1.17	0.39	0.087	0.65
Model II	0.14	1.90	0.63	0.14	1.05

For Model II all organic matter has been used up after Reaction 2 has taken place; at the same time almost all iron(III) has been consumed. For Model I, 0.112 mole organic matter still remains, which can react in the following ways with sulfate and magnetite (formed by Reaction 2):

$$1.78\ CH_{1.5}O_{0.5} + SO_4^{2-} \rightarrow S^{2-} + 1.78\ CO_2 + 1.35\ H_2O \quad (3)$$

Model I	0.101	0.057	0.057	0.101	0.077

$$4\ CH_{1.5}O_{0.5} + Fe_3O_4 \rightarrow 4\ C + 3\ Fe^{2+} + 6\ OH^- \quad (4)$$

Model I	0.011	0.003	0.011	0.009	0.017

After OH^- and CO_2 react, the following quantities (in moles) remain available for other processes:

	Model I	*Model II*
OH^-	—	0.50
CO_3^{2-}	0.239	0.25
Mn^{2+}	0.23	0.50
Fe^{2+}	0.009	—
S^{2-}	0.057	—
SO_4^{2-}	—	0.057

From these quantities one could expect that associations with $MnCO_3$ and FeS (Model I) and $MnCO_3$ and $Mn(OH)_2$ co-existing at pH = 9.52 at 25°C. (Model II) would develop. There is no evidence, however, that these assemblages are formed in real sediments; more probably other aqueous and solid chemical species in the sediment react with the generated OH^- and CO_3^{2-}. This is particularly the case for $CaCO_3$ and SiO_2:

$$x\,CaCO_3 + y\,Mn^{2+} \rightarrow Ca_{x-y}\,Mn_y\,(CO_3)_x + y\,Ca^{2+} \tag{5}$$

$$SiO_2 + H_2O + OH^- \rightarrow H_3SiO_4^- \tag{6}$$

Reactions 5 and 6 explain certain processes observed in pelagic sediments. For example, according to Lynn and Bonatti (*32*) manganese-containing carbonates form from interstitial solutions. Further, mobilization of silica and manganese that has been assumed to be caused by processes in the interstitial solutions in sediments, has been observed by Arrhenius (*4*).

The generated OH^- will probably attack silicates in an analogous way. Thus it is likely that silicate reactions tend to neutralize the formed hydroxyl ions by the following or some analogous process:

$$\begin{gathered} 3\,Al_2Si_2O_5\,(OH)_4 + 4\,SiO_2 + 2\,K^+ + 2\,Ca^{2+} + 7\,H_2O \leftrightarrows \\ 2\,KCaAl_3Si_5O_{16}\,(H_2O)_6 + 6H^+ \end{gathered} \tag{7}$$

Sillén (*46*) suggested that reactions of this type buffer the pH of sea water. From the discussion above they probably also tend to buffer the pH of the interstitial solutions in sediments. This conclusion is also implicit in the discussion by Sillén (*46*).

Reactions between organic matter and iron(III) silicates have not yet been considered in this discussion. In the models above, all iron was assumed to be present originally as FeOOH. However, in actual sediments some probably is present as nontronite, which possibly could react with organic matter, forming carbon dioxide and a hypothetical iron(II) sheet silicate:

$$\begin{gathered} CH_{1.5}O_{0.5} + 2.25\,Fe_2^{III}\,Na_{0.33}Al_{0.37}Si_{3.67}O_{10}(OH)_2 \cdot 4\,H_2O + 1.50\,H_2O \leftrightarrows \\ 2.25\,Fe_2^{II}\,Na_{0.33}Al_{0.37}Si_{3.67}O_{10}(H_2O)_2 \cdot 4\,H_2O + CO_2 \end{gathered} \tag{8}$$

Both Reactions 2 and 8 tend to form acid conditions; however, the ratio (Fe^{III} reduced / CO_2 produced) is different for the two reactions. Possibly the oxidation potential of nontronite is too small to form CO_2; in this case the following hypothetical reaction can be suggested:

$$\begin{gathered} Fe_2^{III}\,Na_{0.33}Al_{0.37}Si_{3.67}O_{10}(OH)_2 \cdot 4\,H_2O + 4\,CH_{1.5}O_{0.5} \leftrightarrows \\ Fe_2^{II}\,Na_{0.33}Al_{0.37}Si_{3.67}O_{10}(H_2O)_2 \cdot 4\,H_2O + 4\,C + 2\,H_2O \end{gathered}$$

The absence of thermodynamic data for many of the compounds discussed above and the uncertainty about which phases are formed under certain conditions makes it impossible to calculate the composition of the final aqueous and solid phases.

Redox Processes in Sediments Deposited under Anoxic or almost Anoxic Conditions

Anoxic or almost anoxic conditions are found in stagnant basins such as the Black Sea or in basins with sill depths in the oxygen minimum layer like the Santa Barbara or San Pedro basins off California (*16*). Under such conditions anoxic conditions may develop in the water under the sill depth or in the sediment just below the sediment-water interface.

The amount of organic matter deposited in sediments in the Los Angeles basins in California has been estimated by Emery (*16*). Of the total production of organic matter in the water over the sediment, only 6.4% was deposited in the sediment, and at a depth of 3 meters in the sediment only 4.2% of the originally produced organic matter remained. Furthermore, shales that presumably formed under similar conditions contain only 2.8% of the originally produced organic matter (*16*). Hence, it is probable that early diagenetic changes destroy 33% of all deposited organic matter and that another 23% is destroyed during late diagenetic changes, leading to the formation of shale. We will now discuss the redox processes which occur during the late diagenesis of carbonaceous sediments.

Since the reduction of sulfate to sulfide seems to be completed during the earliest part of the diagenesis (*26*), it is obvious that the decrease in organic matter during the later part of the diagenesis must be caused by other reduction processes. In view of the large amounts of iron buried in sediments, one could expect that iron(III) compounds could oxidize organic matter. Some evidence indicates that iron(II) compounds may also act as oxidizing agents under rare circumstances; this will be discussed later. Unfortunately Kaplan *et al.* (*26*) did not determine the oxidation state of iron in their sediment samples. Studies by Murty *et al.* (*37*) show that even in black shales with pyrite the content of iron(III) can be considerable. Similar observations have been made on carbonaceous chondrites, a type of meteorite containing up to 6% organic matter. Thus, studies of the Mössbauer effect (*19*), x-ray data, and microprobe analyses (*10*) show that Fe(III)-rich chamosite occurs together with troilite, FeS.

From the above it is likely that sulfate is reduced before ferric iron. This is contrary to what one would expect from the thermodynamic properties of Fe(III) compounds and sulfates. This may be caused by differences in reactivity between sulfates and iron(II) compounds. Analogous deviations owing to differences in reaction rates have been observed in the system PbS-Mn_3O_4-H_2O at elevated temperatures (*11*). It was found that the recrystallization of PbS proceeds much faster than the oxidation of S^{2-} to SO_4^{2-}, which is one of the final stable constituents in the system. Another possible explanation of course is that the stability boundaries for some ferric-ferrous silicates are displaced towards lower *e* values than the stability boundary for Fe_2O_3-Fe_3O_4.

The redox processes and processes linked to them in the basin sediments can be written in the following or some analogous way. At least some of these processes take place during the early diagenesis, as indicated by the presence of sulfides and iron(II) carbonate in many buried sediments:

$$1.78\ CH_{1.5}O_{0.5} + SO_4^{2-} \rightarrow S^{2-} + 1.78\ CO_2 + 1.33\ H_2O$$

$$CH_{1.5}O_{0.5} + 13.5\ FeOOH \rightarrow 4.5\ Fe_3O_4 + CO_2 + 7.5\ H_2O$$

$$3\ H_2O + 2\ CH_{1.5}O_{0.5} + 9\ FeOOH \rightarrow 9\ Fe^{2+} + 18\ OH^- + 2\ CO_2$$

$$Fe^{2+} + CO_3^{2-} \rightarrow FeCO_3$$

$$nH_2O + Fe^{2+} + S^{2-} \rightarrow FeS \cdot nH_2O$$

$$3.11\ CH_{1.5}O_{0.5} + 2\ SO_4^{2-} \rightarrow S_2^{2-} + 3.11\ CO_2 + 2\ OH^- + 1.33\ H_2O$$

$$Fe^{2+} + S_2^{2-} \rightarrow FeS_2$$

Some of the following reactions (or their analogs) can be expected to occur during the late diagenesis and in metamorphism:

$$8\ CH_{1.5}O_{0.5} + FeCO_3 \rightarrow Fe^{2+} + 9\ C + 2\ OH^- + 5\ H_2O$$

$$20\ CH_{1.5}O_{0.5} + 3\ FeCO_3 \rightarrow Fe_3O_4 + 23\ C + 15\ H_2O$$

$$2\ FeCO_3 + 4\ SiO_2 + 16\ CH_{1.5}O_{0.5} \rightarrow Fe_2Si_4O_{10} + 18\ C + 8\ H_2O$$

$$Fe_8^{III}\ Fe_{20}^{II}\ (Si_4O_{10})_{16} + 16\ CH_{1.5}O_{0.5} \rightarrow$$
$$14\ Fe_2\ Si_4O_{10} + 12\ H_2O + 16\ C + 8\ SiO_2$$

[$Fe_2Si_4O_{10}$ does not occur isolated but as component in clay minerals such as Fe(II) chamosite.]

It cannot be assumed *a priori* that conditions become acid when organic matter is oxidized; pH will be controlled by the extent to which hydroxide- and hydrogen ion-producing reactions balance each other. Possibly the final pH during late diagenesis and metamorphism is not controlled by carbonates which are unstable at low *e* values, owing to the reaction:

$$4\ e^- + CO_2 + 2\ H_2O \rightarrow C + 4\ OH^-$$

The stability limit between carbonates and graphite is indicated by a heavy zigzag line in Figures 5–7. The widespread occurrence of carbonates presumably even under severe reducing conditions may indicate, however, that the reduction of carbon dioxide to graphite has an appreciable overvoltage, as is the case for water (29). As Figures 5–7 show, this has some bearing on the problem of whether the final environment is neutral or slightly alkaline owing to the partial equilibria between carbonates and hypothetical iron silicates. If the final system is characterized by a large total activity of CO_2, the final pH may become fairly high. Under severe reducing conditions some bacteria may use the CO_2 in carbonates as an energy source (at least at low temperatures) and consequently increase the breakdown rate of carbonates.

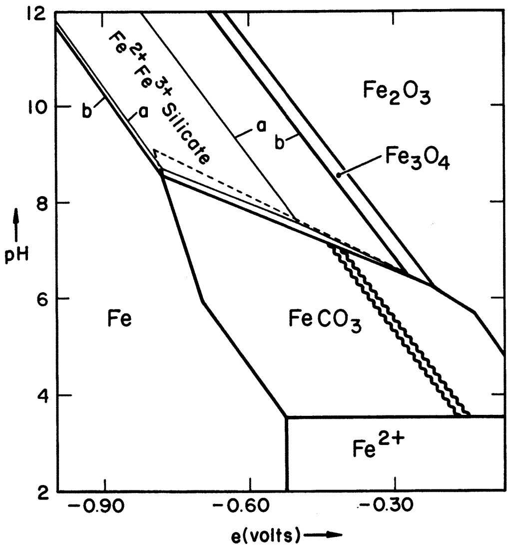

Figure 6. Hypothetical e vs. pH diagram showing how the presence of iron silicate may affect the stability relations in the Fe-Si-CO_2-H_2O system

— — —The part of the $FeCO_3$ field that is truncated owing to the presence of silicates

∿∿∿ *Approximate stability line between C and CO_2*

(a) Extent of the stability field for the silicate at low Si activities in the solution

(b) Extent of the stability field for the silicate at higher activities of Si in solution

Discussion

The preceding discussion shows that both protolytic and dissolution processes in carbonate and silicate systems and redox processes between oxidized and reduced constituents are pH controlling.

Important details that must be known before a more extensive discussion of such pH-controlling redox processes can be given are indicated below.

(1) The extent to which CO_2 may remain unaltered under severe reducing conditions despite its thermodynamic instability under these conditions

(2) The stability conditions of various iron-silicates

(3) The composition of the reactive fraction of the organic matter

(4) The quantities of Fe(II), Fe(III), S(II), S(VI) present and in which phases they occur

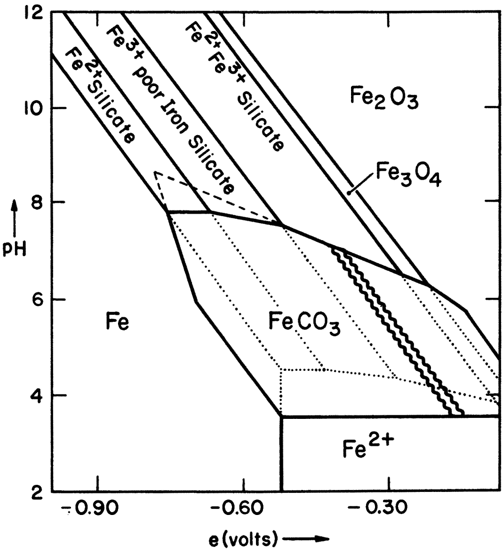

Figure 7. Similar to Figure 6 except that the hypothetical stability fields of additional silicates are shown

The instability of CO_2 in severe reducing systems was discussed to an extent above; it has already been pointed out that the final system may become fairly alkaline if the total activity of CO_2 is high (*see* Figures 6 and 7). Silicates will have a buffering action, however. If it is assumed that silicates of the compositions given in Figure 6–8 are stable with each other and with Fe and Fe_3O_4 at the *e*-pH conditions indicated in Figures 6–8, then the stability field of the silicates will cut off the upper sections

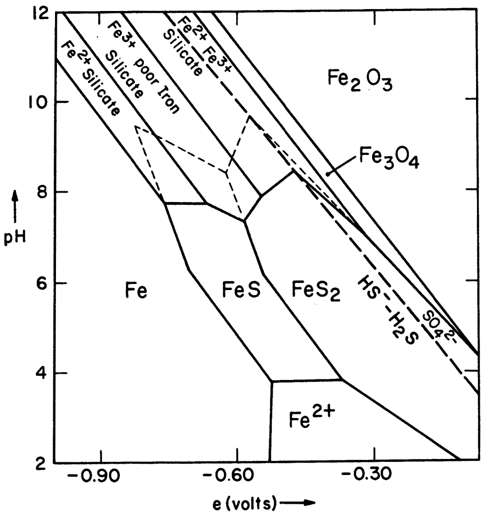

Figure 8. Hypothetical e vs. pH diagram showing how the presence of various iron silicates may affect the stability relations in the Fe-S-Si-H_2O system. The full lines refer to iron species, heavy dashed lines to the system H_2S-HS^--SO_4^{2-}. Thin dashed lines indicate how the presence of iron silicates may decrease the highest pH at which iron sulfides are stable

of the stability fields for $FeCO_3$, FeS, and FeS_2 (dashed lines in Figures 6–8). This means that the associations iron silicates-iron carbonates and iron silicates-iron sulfides are stable at lower pH values than the associations Fe_3O_4-$FeCO_3$ or Fe_3O_4-FeS-FeS_2, assuming identical total carbonate or total sulfur activities in the solutions. This is particularly well illustrated by the rare occurrences of terrestrial native iron. Native iron has been observed as incrustations in wood in bogs and is obviously authigenic, formed at quite low temperatures. Native iron has furthermore been found in petrified wood together with limonite; it also occurs in some shales. To be stable, iron evidently requires severe reducing conditions, but whether the final system is alkaline or neutral (*see* Figure 5) depends on whether or not CO_2 will remain unreduced. It can be objected that native iron is geochemically a rare mineral and consequently is of no general significance for understanding surface processes. In most surface deposits only little limonite and organic matter occur; redox reactions between these constituents will therefore have only slightly neutralizing effects on carbonated meteoric waters that flow through surface sediments and rocks. However, if large quantities of matter are present that can take part in redox reactions it is evident from the discussion above that redox reactions cannot *a priori* be neglected but must be considered when we wish to understand fully how pH is regulated in natural waters.

Acknowledgment

The author conveys his sincere thanks to G. Arrhenius, J. Hanor, L. G. Sillén, J. Sinkankas, and F. E. Wickman for stimulating discussions and critical reading of the manuscript.

This work was supported by a National Science Foundation grant, NSF–GP5112. The allocation of this support is gratefully acknowledged.

Literature Cited

(1) Abelson, P. H., "Researches in Geochemistry," P. H. Abelson, ed., Wiley, New York, 1959.
(2) Adler, E., *Z. Papier* **15,** 604 (1961).
(3) Aminoff, G., *Geol. Fören. Stockh. Förh.* **40,** 535 (1918).
(4) Arrhenius, G., "Reports of the Swedish Deep-Sea Expedition, 1947-1948," Vol. V, H. Pettersson, ed., Göteborgs Kungl. Vetenskaps-och Vitterhetssamhälle, Göteborg, 1952.
(5) Arrhenius, G., "The Sea," M. N. Hill, ed., Vol. 3, p. 655, Interscience, New York, 1963.
(6) Atkins, W. R. G., *Sci. Proc. Roy. Dublin Soc.* **19,** 455 (1930).
(7) Barth, T. F. W., "Theoretical Petrology," Wiley, New York, 1962.
(8) Boström, K., *Ark. Mineral. Geol.* **3,** 545 (1965).
(9) Boström, K., unpublished results.
(10) Boström, K., Fredriksson, K., *Smithsonian Inst. Misc. Collections* **151** (1966).
(11) Boström, K., Reid, A., in preparation.
(12) Breger, I. A., "Organic Geochemistry," Pergamon, New York, 1963.
(13) Bricker, O. P., *Am. Mineralogist* **50,** 1296 (1965).
(14) Brönsted, J. N., *Rec. trav. chim.* **42,** 718 (1923).
(15) Deer, W. A., Howie, R. A., Zussman, J., "Rock-Forming Minerals," Vol. 5, Wiley, New York, 1963.
(16) Emery, K. O., "The Sea Off Southern California; A Modern Habitat of Petroleum," Wiley, New York, 1960.
(17) Fomina, L. S., *Tr. Inst. Okeanol. Akad. Nauk SSSR* **54,** 158 (1962).
(18) Garrels, R. M., Christ, C. L., "Solutions, Minerals, and Equilibria," Harper and Row, New York, 1965.
(19) Gerard, A., Delmelle, M., *Compt. Rend.* **259,** 1756 (1964).
(20) Goldberg, E. D., Arrhenius, G., *Geochim. Cosmochim. Acta* **13,** 153 (1958).
(21) Goldschmidt, V. M., *Fortschr. Mineral. Krist. Petrogr.* **17,** 112 (1933).
(22) Haff, J. C., *Am. Mineralogist* **19,** 480 (1934).
(23) Hamann, S. D., "High Pressure Physics and Chemistry," Vol. 2, R. S. Bradley, ed., Academic Press, New York, 1963.
(24) "Handbook of Chemistry and Physics," 46th ed., The Chemical Rubber Co., Cleveland, 1965.
(25) "JANAF Thermodynamic Tables," Dow Chemical Corp., 1965.
(26) Kaplan, I. R., Emery, K. O., Rittenberg, S. C., *Geochim. Cosmochim. Acta* **27,** 297 (1963).
(27) Kelley, K. K., *U.S. Bur. Mines Bull.* **584** (1960).

(28) Klingsberg, C., Roy, R., *Am. Mineralogist* **44**, 819 (1959).

(29) Latimer, W. M., "The Oxidation States of the Elements and Their Potentials in Aqueous Solutions, 2nd ed., Prentice-Hall, Englewood Cliffs, 1952.

(30) Lewis, G. N., Randall, M., "Thermodynamics," rev. ed., McGraw-Hill, New York, 1961.

(31) Lindgren, W., "Mineral Deposits," McGraw-Hill, New York, 1933.

(32) Lynn, D. C., Bonatti, E., *Marine Geol.* **3**, 457 (1965).

(33) Magnusson, N. H., "Persbergs malmtrakt," Kungl. Kommerskolleg. Beskrivn Mineral-fyndigheter, No. 2, Stockholm, 1925.

(34) Magnusson, N. H., "Långbans malmtrakt," SGU Ser. Ca No. 23, Stockholm, 1930.

(35) Mason, B., *J. Geol.* **57**, 62 (1949).

(36) McKelvey, V. E., *U.S. Geol. Surv. Profess. Paper* **400-A** (1960).

(37) Murty, P. S. N., Aswathanarayana, U., Mahadevan, C., *Econ. Geol.* **57**, 614 (1962).

(38) Owen, B. B., Brinkley, S. R., *Chem. Rev.* **29**, 461 (1941).

(39) Palache, Ch., *U.S. Geol. Surv. Profess. Paper* **180** (1935).

(40) Palache, Ch., Berman, H., Frondel, C., "Dana's System of Mineralogy," Vols. I and II, Wiley, New York, 1944, 1951.

(41) Revelle, R., *Carnegie Inst. Washington Publ.* **556** (1944).

(42) Richards, F. A., "Chemical Oceanography," Vol. 1, pp. 611-645, J. P. Riley, G. Skirrow, eds., Academic Press, New York, 1965.

(43) Russel, A., *J. Am. Chem. Soc.* **70**, 1060 (1948).

(44) Schmalz, R. F., *J. Geophys. Res.* **64**, 575 (1959).

(45) Sharp, W. E., "The Thermodynamic Functions for Water in the Range −10 to 1000°C. and 1 to 250,000 Bars," U.S. Department of Commerce, Washington, D.C., 1962.

(46) Sillén, L. G., *Am. Assoc. Advan. Sci. Publ.* **67** (1961).

(47) Sillén, L. G., Martell, A. E., *Chem. Soc., London, Spec. Publ.* **17** (1964).

(48) Smirnow, S. S., "Die oxydations zone sulfidischer Lagerstätten," (German transl. 1954 of Russian edition of 1951; 1st Russian edition, 1936), Akademie Verlag, Berlin, 1951.

(49) Sundius, N., "Grythyttefältets Geologi," SGU Ser. C No. 312, Stockholm, 1923.

(50) Weller, W. W., Kelley, K. K., *U.S. Bur. Mines, Rept. Invest.* **6511** (1964).

RECEIVED January 20, 1967.

15

Equilibria and Nonequilibria in Organic Geochemistry

MAX BLUMER

Woods Hole Oceanographic Institution, Woods Hole, Mass.

Carbon compounds may have existed at or near thermodynamic equilibrium on the early, prebiological earth. The activity of organisms has converted most carbon in the earth's crust into thermodynamically unstable but long-lived compounds. During diagenesis a gradual, irreversible approach towards equilibrium occurs, but complete equilibrium between all components is not reached within time spans approaching the age of the earth. This does not preclude the participation of many metastable fossil organic compounds in reversible equilibria. Further study of these may lead to a tool for investigating chemical environments in the past.

Inorganic geochemistry is dominated by equilibrium processes. Most reactions are rapid, and thermodynamic equilibria are established within geologically short time spans. Many reactions which appear slow in the laboratory still proceed sufficiently fast to influence the composition of geological systems. Noteworthy exceptions involve certain metastable ions like CO_3^{2-}, SO_4^{2-}, and PO_4^{3-}, which may persist even in unfavorable environments for millions if not billions of years.

The equilibrium nature of most natural inorganic systems allows one to predict the stable ionic or mineral components of an environment if its pH, redox potential, pressure, and temperature are defined. Conversely, the reconstruction of a fossil physicochemical environment is often possible by studying fossil mineral assemblages (*1, 7*).

The organic geochemist encounters a quite different situation. Most organic products of organisms are thermodynamically unstable. When incorporated into sediments, they persist for long time spans because of the high degree of metastability inherent in carbon compounds under terrestrial environment conditions. The lack of equilibrium in the sedimentary organic matter is manifest within molecules, between different organic molecules, and between them and their inorganic matrix. Compounds with different oxidation states of carbon in one molecule, like propionic acid, are unstable; their disproportionation is thermodynamically favored but prevented by slow kinetics. A similar degree of metastability exists for mixtures of compounds of different oxidation state, both in purely organic systems and in mixed organic-inorganic systems. Thus, a 1:1 mixture of 1-pentane and formic acid is thermodynamically unstable at room temperature; likewise, the polynuclear aromatic hydrocarbons in manganese nodules (*8*) are preserved in association with Mn(IV) only because of their great degree of metastability.

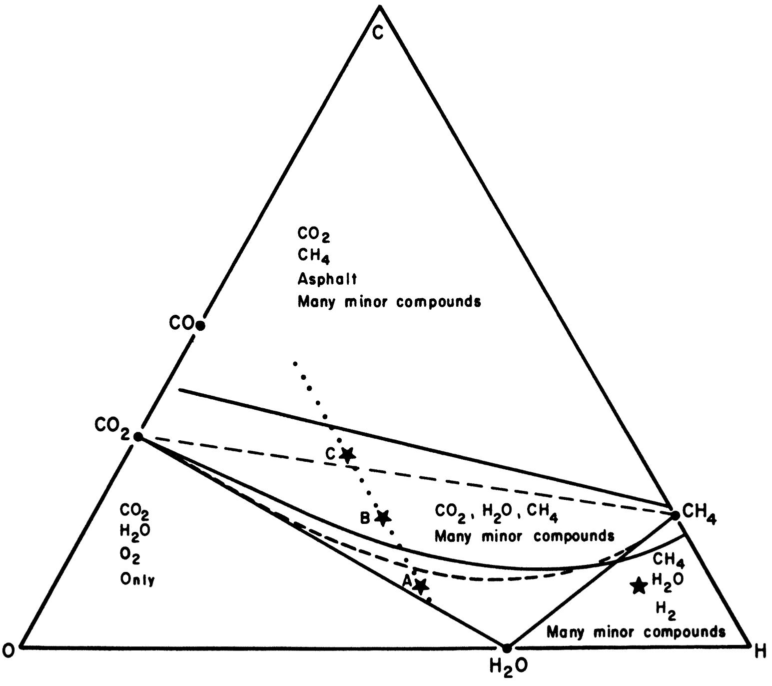

Science

Figure 1. Thermodynamic equilibrium in atmospheres of varying elemental proportions. The ternary diagram shows all compositions of systems containing carbon, hydrogen, and oxygen (each point represents 100% of the three components). Lower curves indicate the potential formation of solid carbon if equilibrium could be attained. Dashed curve holds at 500°K., the continuous one at 700°K. The upper lines indicate the "asphalt threshold," the dashed one at 500°K., and the continuous one at 700°K. Above this threshold, thermodynamic equilibrium favors the formation of large proportions of polycyclic aromatic compounds ("asphalt") and a lesser increase of most of the other families of compounds. The dots through points A to C indicate the points used in the computations for Figure 2 (6).

The thermodynamic equilibrium concentrations of numerous geochemically interesting compounds of C, H, O, and N have been computed by Dayhoff, Lippincott, and Eck for temperatures and pressures ranging from 300° to 1000°K. and 10^{-6} to 300 atm. (*6*). These authors conclude that starting from a hydrogen rich composition an increase in carbon content in this system (*see* Figure 1) leads to a threshold where the potential formation of elemental carbon becomes possible. The activation energy required to form solid carbon is quite high. A further increase in the carbon content of the system may therefore produce a metastable accumulation of tars and asphalt without the appearance of free carbon. Beyond this "asphalt boundary" large polycyclic aromatic systems become stable, and the concentration of many lower molecular weight organic compounds increases drastically (Figure 2). Relative to the aromatic hydrocarbons, aliphatics—especially the higher homologs of methane and ethane—are present in negligible concentrations. No combination of pressure, temperature, and elemental compositions was found which favors aliphatic over aromatic hydrocarbons.

This study lays the foundation for any consideration of the equilibrium composition of organic mixtures both on a prebiological earth and in biogenic sediments remote in time and space from the influence of living organisms. It is interesting to note the great similarity between the composition of the computed equilibrium mixture and the composition of organic compounds found in carbonaceous meteorites. This has been interpreted as suggesting the formation of these compounds by equilibrium reactions at an early stage of the formation of the solar system (*11, 12*).

Dayhoff's data quantitatively confirm earlier qualitative descriptions of petroleum (*13*) and of kerogen as nonequilibrium mixtures. Generally, sedimentary organic matter, especially at the time of deposition, is quite remote from equilibrium. During diagenesis the more reactive of the unstable compounds or substituents are gradually eliminated. The increasing aromaticity of coal and kerogen with increasing age and burial depth results in a gradual approach to equilibrium of the sedimentary organic matter. This process is extremely slow; thermodynamically unstable structures like higher normal alkanes, isoprenoids, steranes, and porphyrins have survived in sediments since the Precambrian (*5*).

The gross change in elemental composition and aromaticity of the sedimentary organic matter is much better understood than the detailed molecular changes leading to it. Much of our knowledge of sedimentary organic reactions comes from the study of the gradual conversion of sensitive biochemical products, especially pigments in the subsurface environment with increasing age and depth of burial (*2, 3, 4, 5, 9, 10*). Typical reactions (Figure 3) are eliminations of oxygen functions—often in sterically unfavorable positions—decarboxylations, hydrogenations, isomerizations, and some cleavage reactions. Many of these lead to a destruction of the ordered building pattern of biochemical structures.

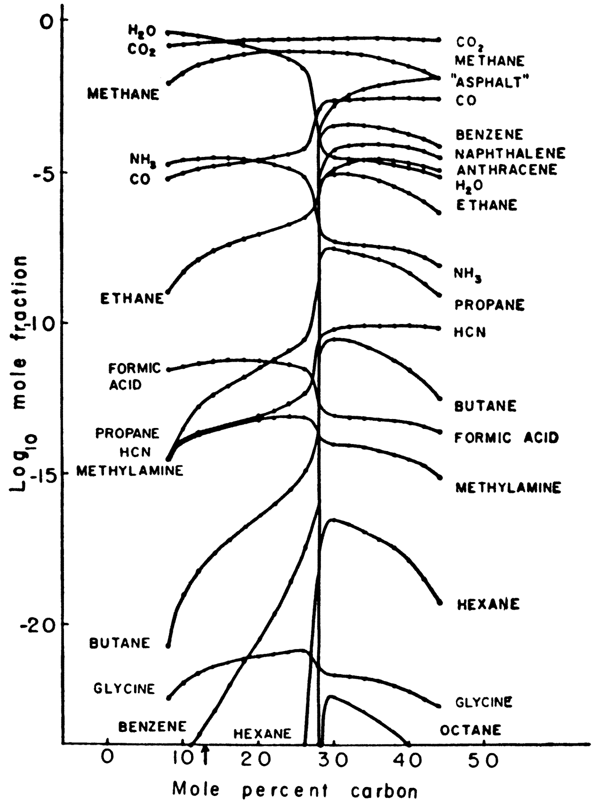

Science

Figure 2. Equilibrium concentrations in mole fractions of selected compounds at 500°K. and 1 atm. with composition of 40% oxygen, the indicated percentage of carbon, and the rest hydrogen. To this basic composition is added an amount of nitrogen equal to the amount of carbon. The nitrogen remains primarily as N_2 but produces significant quantities of some interesting compounds. The free energy of carbon in the system equals that of graphite at the composition indicated by the arrow. At this point solid carbon would be precipitated if it could be formed; there is no inflection of the curves at this point. The "asphalt threshold" is shown as a sharp inflection, sharpest of all for the aromatic and related heterocyclic compounds. If an atmosphere such as this were to condense, there would be about 1 molecule of glycine per droplet of condensate (6).

Inherently such reactions are irreversible: it is quite unlikely that under abiotic conditions a reverse reaction would possess the specificity to recreate the ordered building pattern initially created through biochemical pathways. In favorable environments geochemically irreversible reactions proceed to completion, and reaction intermediates are either unstable or metastable; their occasional preservation arises from kinetic, not thermodynamic factors.

Reaction	Type	Reversibility
R–COOH → R–H	Decarboxylation	Irreversible
R–COOH → R–H + shorter-chain acids and hydrocarbons	Cooper-Bray (6) degradation	
$R\text{-}\overset{\overset{C}{\vert}}{C}\text{-}R \rightarrow R\text{-}C\text{-}R$	Cleavage	Irreversible
R–C–C–R → R–C	Cleavage	Irreversible
$R_2C = CR_2 \rightarrow R_2HC\text{–}CHR_2$	Reduction	Irreversible
R–COH → RCH_3	Reduction	Irreversible
R–COOH → RCH_3	Reduction	Irreversible
$R_2\text{–}C{=}O \rightarrow R_2\text{–}CH_2$	Reduction	Irreversible
R-OH → R–H	Reduction	Irreversible
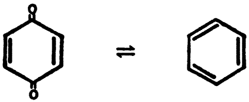	Reduction	Reversible
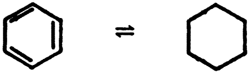	Reduction	Reversible
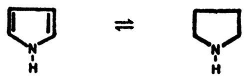	Reduction	Reversible
R–H ⇌ R–Me	Complexation	Reversible?
R–COOR ⇌ R–COOH	Hydrolysis	Reversible

Figure 3. Geochemically reversible and irreversible reactions. Only the reactions are listed for which we have evidence from the fringelites, the fossil porphyrins, and the phytol–derived hydrocarbons (5).

The mixture of sedimentary organic compounds, as a whole, is not in thermodynamic equilibrium. This does not preclude the participation of many metastable but long-lived compounds in reversible equilibria. A typical case is acetic acid; as a thermodynamically unstable compound it should disproportionate:

$$CH_3COOH \rightarrow CH_4 + CO_2$$

However, the disproportionation is so slow that it does not preclude the participation of the acid in the rapid equilibrium:

$$CH_3COOH \rightleftharpoons CH_3COO^- + H$$

In the same sense, many acid-base reactions in the sediments—possibly including esterifications and hydrolyses—are reversible. This also is true of some complexation reactions involving organic ligands, though stable complexes like those of porphyrins appear not to be in equilibrium with their components. Many purely organic redox systems may react sufficiently fast for equilibration with the environment to take place within geological time spans. At low redox potentials aromatic hydrocarbons and heteroaromatic compounds like porphyrins appear to equilibrate with partially hydrogenated derivatives (*2*, *5*, *10*).

In geochemically reversible reactions, environmental conditions determine the final ratio of starting material to end product; if conditions in the environment change, this ratio adjusts to the change. In cases of slow equilibration a molecular ratio of starting material to end product may be preserved, which is indicative of past environmental conditions. More data are needed to test this idea, but it is conceivable that analyses of aromatic and hydroaromatic hydrocarbons and pigments might be interpreted in terms of a fossil environment.

These considerations then lead us to the following conclusions: organic geochemistry, in contrast to inorganic geochemistry, is dominated by nonequilibrium processes. Equilibrium processes are believed to account for the composition of meteoritic organic matter. They also may have played a role on the prebiological earth. Abiotic equilibrium-type mixtures of organic compounds have not yet been found on earth. Their existence in igneous or metamorphic rocks appears possible and worthy of a systematic search. Most carbon in the earth's crust has been cycled through organisms; as a result, it has been incorporated into unstable but long-lived biochemical structures. During diagenesis the less stable compounds are eliminated by reactions which generally lead to a scrambling of the ordered structures created by organisms. Diagenesis results in gradual equilibration of the sedimentary organic matter, but at moderate temperatures equilibrium is not reached within time spans comparable to the age of the earth. Certain metastable but long-lived organic compounds may participate in acid-base, complexation and redox equilibria. The rates with which these equilibria adjust to changing environmental conditions varies widely in nature. Certain slow equilibrations may be of diagnostic value in determining fossil environmental conditions.

Acknowledgments

This work is supported by a research contract with the U.S. Office of Naval Research (Contract Nonr-2196(00)) and a grant from the National Science Foundation (GP-3250). We thank M. O. Dayhoff for permission to reproduce Figures 1 and 2, the former in a corrected version of that originally published (*6*).

Literature Cited

(1) Blumer, M., *Helv. Chim. Acta* **33**, 98 (1950).
(2) Blumer, M., Omenn, G. S., *Geochim. Cosmochim. Acta* **25**, 81 (1961).
(3) Blumer, M., *Geochim. Cosmochim. Acta* **26**, 225 (1962).
(4) *Ibid.*, p. 228.
(5) Blumer, M., *Science* **149**, 722 (1965).
(6) Dayhoff, M. O., Lippincott, E. R., Eck, R. V., *Science* **146**, 1461 (1964).
(7) Garrels, R. M., Christ, Ch., "Solutions, Minerals and Equilibria," Harper & Row, New York, 1965.
(8) Thomas, D. W., Blumer, M., *Science* **143**, 39 (1964).
(9) Thomas, D. W., Blumer, M., *Geochim. Cosmochim. Acta* **28**, 1147 (1964).
(10) *Ibid.*, p. 1467.
(11) Studier, M. H., Hayatsu, R., Anders, E., *Science* **149**, 1455 (1965).
(12) Studier, M. H., Hayatsu, R., Anders, E., *Science*, in press.
(13) Van Nes, K., Van Westen, H. A., "Aspects of the Constitution of Mineral Oils," Elsevier, Amsterdam, 1951.

RECEIVED April 4, 1966. Contribution No. 1785 of the Woods Hole Oceanographic Institution.

16

Biological Activity in Relation to the Chemical Equilibrium Composition of Natural Waters

G. FRED LEE and ALFRED W. HOADLEY

Water Chemistry Laboratory, University of Wisconsin, Madison, Wis.

For many elements, the concentration of a species in a given body of water can be predicted by abiotic chemical reactions such as protolysis, precipitation, complexation, redox, and sorption. Aquatic organisms can influence the concentration of compounds directly by metabolic uptake, transformation, storage, and release. Aquatic organisms may also cause chemical reactions by changing the concentrations of solutes which are important in abiotic equilibria. The two most important reactions of this type are changes in the pH of the water as a result of respiration and photosynthesis and the uptake and release of organic compounds. Both of these reactions can influence acid-base, precipitation, complexation, redox, and sorption reactions in natural waters.

The concentration of a particular species of an element in the aquatic environment is determined by the thermodynamics and kinetics of its chemical reactions. The concentrations of some elements present in a body of water can be predicted from abiotic chemical reactions such as protolysis, precipitation, complexation, redox, and sorption. However, the concentrations of other elements are influenced significantly by biochemical reactions. This concept has been emphasized by several authors. For example, Ruttner (*56*) has stated that "it is quite impossible to understand the chemistry of an aquatic biotope without taking into consideration the causal relationships in the metabolism of its community of organisms." This idea has been reiterated by Cushing (*12*), who lists the "quality and quantity of biota, particularly producers," among the factors influencing ionic changes in the aquatic environment, and it is the basis for Hynes' (*30*) view of a lake as a trap for fertility.

Biological populations are responsible to a great extent for cycling elements in natural waters. Although temperature and hydrologic cycles profoundly influence chemical equilibria in the aquatic environment, without the constant turnover provided by the aquatic fauna and flora, reactions would proceed largely in one direction. Aquatic organisms as well may influence the chemistry of an element in natural waters by altering concentrations of ions or compounds, such as H^+ ion, which in turn may alter the position of chemical equilibria in water.

We do not wish to argue the importance of the chemical *vs.* the biological role in specific equilibrium reactions but rather to bring to attention certain studies of biological material which suggest a role in determining the chemical composition of the aquatic environment, with special reference to the fresh water environment.

For the most part, ecologists have been concerned with studying the relationship of an organism to its physical, chemical, and biological environments. Hence, much effort has been devoted to examining the effects of various chemical compounds on aquatic organisms. We are concerned here, however, with the effects of aquatic biota on the concentrations of particular ions or compounds in natural waters. Few studies of fresh waters have been conducted from the latter point of view, however, although Redfield, Ketchum, and Richards (*53*) have reviewed the literature on the influence of organisms on the composition of sea water.

Since every organism may affect water chemistry, each should be considered. However, although occasionally higher plants and animals become significant when their numbers are large, bacteria and microscopic plants and animals ordinarily play dominant roles. Of particular importance is the high surface area to volume ratio of microorganisms and their biochemical versatility. Biochemical versatility is characteristic especially of bacteria of the genus *Pseudomonas,* one of the dominant genera in surface waters not significantly affected by sewage pollution. Pseudomonads are noted for their resistance to antibiotic substances and their production of antagonistic agents. Individual species may cause disease in fish, spoilage of food and dairy products, degradation of petroleum products, and the mineralization of algae.

Populations of bacteria in lakes determined by plate counts generally lie in the range of 10–100 organisms per ml. (*2, 60*). However, counts of 10,000–100,000 may be observed by this technique, particularly in shallow bay areas. The relation between plate and direct counts may vary greatly, however, and Collins (*11*) has reported ratios varying from 20 to 13,400. Thus, actual bacterial populations may be much higher than observed by direct plating techniques, often exceeding 10^6 cells per ml.

In open water, bacteria may exist freely as single cells or associated with particulate matter. The number living in a truly planktonic fashion is quite low, however, as can be seen in Table I. The surfaces of particulate matter, where organic substances are adsorbed and excreted products of other community members are available, afford the associated bacteria an opportunity to function in an enriched situation relative to the surrounding open water. Bacteria form the base of the ecological pyramid in attached communities. Colonization of surfaces may afford an opportunity to create special localized conditions, permitting solution of mineral constituents or the metabolism of certain organic materials by altering the pH, redox potential, or by preventing dispersal of extracellular enzymes.

Table I. Bacteria Populations in Water

Source	*Percent of Bacteria (free-living)*	*Reference*
Nile River	0.02–0.04	(*31*)
Experimental Stream		
Groundwater	0.005	(*70*)
Groundwater + 2% sewage	0.9	(*70*)
Lakes (Stuttgart Region)	10–30	(*3*)

The association of large numbers of bacteria with large populations of algae is evident from the data in Figure 1 (*50*). From work with *Chlorella pyrenoidosa* and *Thalassiosira nana,* Steemann-Nielsen (*61*) has suggested that during algal blooms occurring in the spring and summer, the bacterial populations actually are not associated with the surfaces of algae or with other surfaces because of the antibacterial activity of substances produced by the algae, but rather they exist in a truly planktonic state, metabolizing the excreted products of the photosynthetic organisms. Bacteria may be observed associated with the surfaces of dying algae, however. Golterman (*23*) showed that the mineralization of *Scenedesmus obliquus* depended on the presence of bacteria and that bacterial growth was promoted by substances released during autolysis of the algae. This author demonstrated the release of nitrogen comparable with that observed in the presence of natural bacterial populations caused by a pseudomonad which he isolated from decaying algae. Anaerobic and facultative bacteria active in the bottom sediments enriched with the remains of dead planktonic organisms influence the chemistry of natural waters, particularly those of the hypolimnion. Special conditions are created here as a result of oxygen depletion and the release of CO_2, H_2S, and many organic compounds.

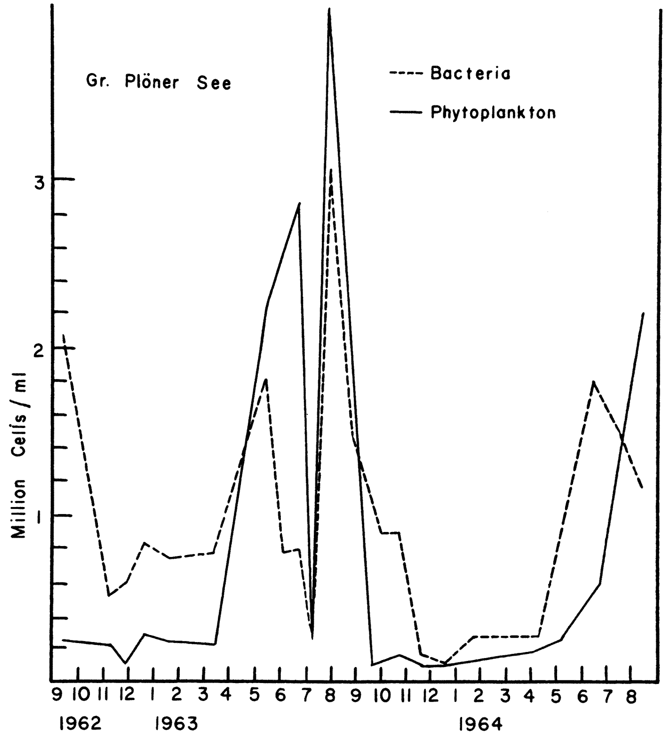

Figure 1. Total bacteria and phytoplankton at 1 meter below the surface in the Grossen Plöner Sea in 1962–1964 (50)

The algal populations differ from most bacteria present by being largely autotrophic. These organisms concentrate nitrogen, phosphorus, sulfur, and many mineral substances in water bodies, obtaining carbon from dissolved CO_2 and energy from sunlight. The algae exist as phytoplankton and as epiphytic, epipelic, and epilithic populations. Population levels may be influenced or controlled by temperature, enrichment, predation, and concentrating factors such as winds and currents. The distribution of phytoplankton is subject to many influences related to the morphometry of the water body, stratification, wind, current, and local availability of nutrient substances. The actively photosynthesizing population is restricted to the euphotic zone or must be carried into the euphotic zone for a period sufficient to permit a net gain of energy through photosynthesis during the day. Below the euphotic zone, in the profundal, the photosynthetic plankton enrich and support the metabolic activity of heterotrophic bacteria. The attached populations of the epiphytic, epipelic, and epilithic communities are restricted to the littoral zone where light penetrates to the bottom.

Rivers, ponds, small and large lakes represent quite different environments for algal populations, and these must be considered in interpreting the effects of algae on the chemistry of natural waters.

Direct Effects of Biota on Water Chemistry

In a grossly oversimplified model, an aquatic microorganism may be treated as a reaction site at which compounds are sorbed and are influenced by the organism. The sorbed compounds are transformed enzymatically into different compounds and are stored and/or released to the surrounding water. Biochemical literature shows that few, if any, elements are not influenced to some degree in natural waters by the aquatic biota. Therefore, in those waters where the rate of supply of an element controls its concentration—*i.e.*, where no precipitation and little or no abiotic sorption occurs—aquatic organisms may control the concentration of the element in solution. The most obvious examples of direct control occur for those elements that are major constituents of cellular materials —*e.g.*, carbon, nitrogen, and phosphorus. Also directly influenced by the aquatic biota are those elements which form principal components of the hard parts of many organisms, such as calcium in molluscs, silicon in diatoms, and certain testaceans (such as *Euglypha*). Studies by Lund *et al.* (*41, 42*) have demonstrated an inverse relationship between *Asterionella, Fragilaria,* and *Tabellaria* populations and the concentration of silicon in solution in Lake Windermere (Figure 2). These authors have observed decreases in the silicon concentration associated with large diatom populations. It appears, therefore, that diatoms may exert a significant influence on the silicon concentration in lakes. In Lake Windermere, the rate of uptake of silicon by diatoms exceeds the rate of supply of the element through geochemical processes and the rate of regeneration of the element upon death of the algae. Certain bacteria have been reported to enhance solution of aluminosilicates, coincidentally freeing other associated elements. Tesic and Todorovic (*63*) have suggested that such species are of the *Bacillus circulans* group, but they emphasize the need for study to determine whether these represent specific silicate bacteria and whether silicon and aluminum represent essential elements in the life of these bacteria. In this regard, Parés (*51*) has suggested bacterial involvement in the solution of many metals, either in the pure form or as ores.

The effect of biological activity on the chemistry of an element or compound in natural waters is interdependent upon (1) population of a particular group of organisms, (2) the lifetime of the organisms, (3) the rate of regeneration of the element upon death of the organisms, (4) concentration of the compound in the water, and (5) the biochemistry of the organisms. Each of these factors is considered below. Particular species of elements may be influenced by the organisms present, and these are not necessarily the species determined by the usual analytical procedures.

Numbers and Types of Organisms. The numbers of a particular group of organisms in a natural water represent a response to the environment and may be limited by factors such as concentrations of essential nutrients and toxic or inhibitory substances, reproduction rates, competition for available nutrients, predation, disease rate, and physical factors (light, temperature, pressure). The concentrations of certain elements may be reduced as a result of biological activity to such an extent that populations are limited (*42*), whereas the concentrations of other elements may be decreased significantly and yet never limit biological activity. It is extremely difficult, however, if not impossible at the present time, to determine the factors that limit the population of particular organisms in natural waters, as has been demonstrated during current research on the role of nitrogen and phosphorus in the eutrophication of natural waters.

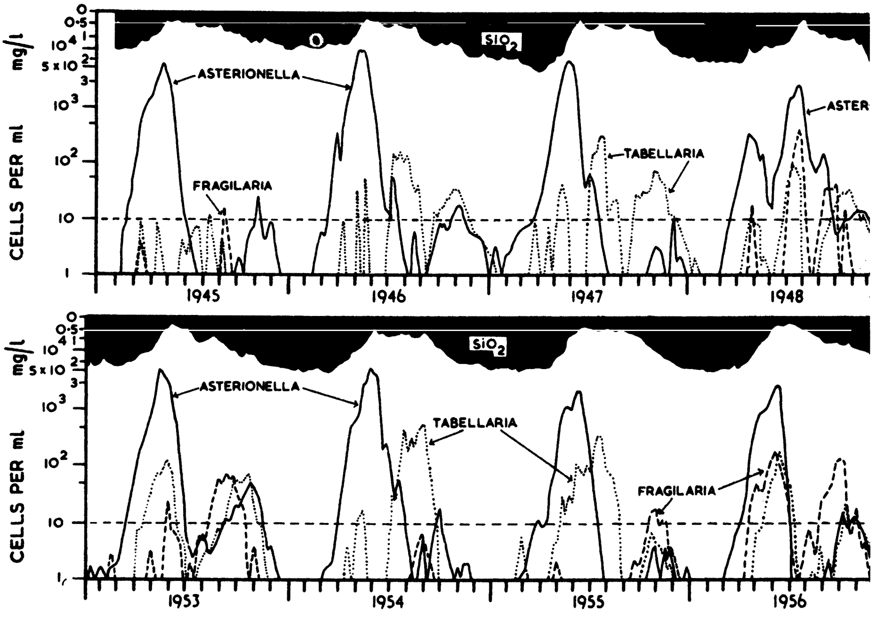

Figure 2. Periodicity of Asterionella formosa *Hass.,* Fragilaria Crotonensis *and fluctuations in the concentration of dissolved silica, in 0–5-meter water*

The role of photosynthesis in the carbon cycle is familiar, and the indirect effects on the chemistry of natural waters caused by removing or adding CO_2 during photosynthesis and respiration (particularly of photosynthetic microorganisms) are discussed below. A direct effect of these microorganisms, however, is selective removal of the light carbon and oxygen isotopes from the water, resulting in an enrichment of the heavy isotopes in the water body and of the light isotopes in the sediments (although enrichment of the sediments depends also upon the amount of marl deposited). Deevey and his associates (*13, 14*) have demonstrated the fractionation of carbon and oxygen in Linsley Pond, Conn., and Green Lake, N. Y.

Return of Elements to the Biological Cycle. The amount of an element bound in biological material and possible limits imposed on developing populations as a result of depletion in the water mass depend on the residence time of the element in the biomass and organism remains after death. Numerous studies have shown that the turnover rates of many elements are quite rapid so that the average residence time in the biomass is short. Phosphorus, for example, is released rapidly in water following death of the organisms (*55*). On the other hand, the return of the silicon composing diatom tests may be slow. As viewed by the water

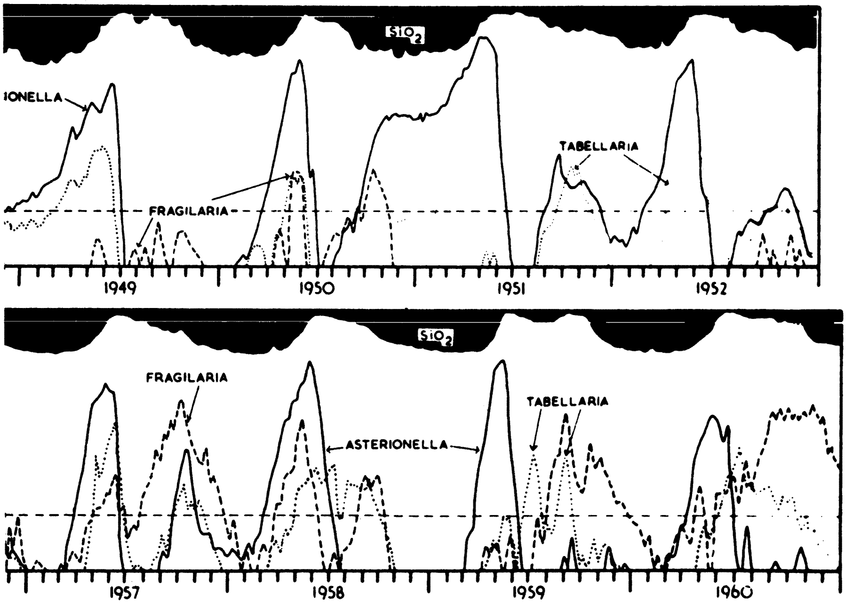

Kitton, Tabellaria flocculosa *(EHR) Grun. Var.* Asterionelloides *(Grun.) Knuds. column of the northern basin of Windermere from 1945–1960, inclusive* (*41*) chemist, the turnover time of an element is important since it determines the availability of the element for strictly chemical reactions as well as the availability for biological use. Those elements with long turnover times will remain as part of the particulate matter in the water and therefore will tend to accumulate in the sediments.

Concentration of Element. The role that the biota may play in the chemistry of natural waters requires considering the concentration of the element in the water relative to the amount of the element accumulated per unit weight of cell material. A population of organisms that has a high requirement for certain elements that occur in low concentrations in the water will tie up relatively large amounts of the element in the cell material and thereby significantly reduce the concentration in solution (—*e.g.*, the depletion of dissolved silicon by diatom populations in Lake Windermere). Ideally, some insight into this relationship could be gained by determining the numbers of organisms present in a body of water. The average composition of the organisms could be used to estimate the amount of the element present in the biomass. This relationship is complicated by the heterogeneous distribution and composition of organisms and the fact that they frequently will store up to 10 or more times their metabolic needs. The luxury consumption of phosphate by algae is well documented (*35*). Additional complications arise from apparent interactions between solutes which affect the uptake of nutrients by microorganisms. The so-called "phosphate sparing factor" (*29*) is an example of a solute interaction by which algae seem able to grow in laboratory cultures at lower phosphate concentrations, provided a little organic matter from natural water is added to the culture. The mechanism of this relationship is not understood.

Biochemistry of the Element. The biochemical function of an element in biological organisms may be significant in determining the concentration and forms of the element in the water. For example, organic compounds that are utilized during heterotrophic growth and metabolism are removed from water, transformed in part into cellular material, and partly excreted as CO_2. The net result is that an element in one form—*e.g.*, organic compound—is removed from the water, some of it is stored for a period of time, while the remainder is rapidly released to the environment in another oxidation state or chemical form. The reverse process occurs during photosynthesis and chemolithotrophic growth. During daylight, photosynthetic organisms remove CO_2 from the water and reduce it to carbohydrate *via* the Calvin-Benson cycle. Some investigators have reported that approximately 50% of the CO_2 fixed by algae appears as dissolved organic compounds in a short time (*19*).

Chemolithotrophic organisms can oxidize inorganic substances such as H_2S, elemental sulfur, or reduced nitrogen compounds, obtaining energy for growth. The iron bacteria provide a controversial example of cellular biochemical effects. It has been suggested that some members of this group can derive energy from the oxidation of ferrous to ferric iron (*69*). Other members appear to metabolize organic compounds that "hold" iron in suspension. The iron is released and deposited in the bacterial sheath as $Fe(OH)_3$. Oborn (*47, 48*) has recently reviewed the literature on the influence of organisms on the chemistry of iron and manganese.

Nitrogen's chemistry is controlled largely by biochemical reactions in natural waters. Although it has been suggested that the Van Slyke reaction (by which nitrite reacts with ammonia or amino acids to produce nitrogen gas) may take place in natural waters, Brezonik and Lee (*5, 6*) have shown that in natural waters this reaction proceeds at a significant rate only at pH of 3 or less. The oxidation and reduction of nitrogen compounds (nitrogen cycle) are all the result of enzymatic processes. Some of the transformations of nitrogen compounds in natural waters are brought about by specific organisms: *Nitrosomonas* oxidizes ammonia to nitrite, and *Nitrobacter* oxidizes nitrite to nitrate. Rheinheimer (*54*) attributed relatively high nitrite concentrations in the River Elbe during the summertime to a difference in the rates of nitrite and nitrate formation. More recently Bock (*4*) has studied the effects of light on *Nitrosomonas europaea* and *Nitrobacter winogradskyi* and found that *N. winogradskyi* was more light sensitive than *Nitrosomonas,* indicating a possible explanation.

The biochemical reduction of sulfate to sulfide by bacteria of the genus *Desulfovibrio* in anoxic waters is a significant process in terms of the chemistry of natural waters since sulfide participates in precipitation and redox reactions with other elements. Examples of these reactions are discussed later in this paper. It is appropriate now, however, to mention the enrichment of heavy isotopes of sulfur in lakes. Deevey and Nakai (*13*) observed a dramatic demonstration of the isotope effect in Green Lake, a meromictic lake near Syracuse, N. Y. Because the sulfur cycle in such a lake cannot be completed, depletion of $^{32}SO_4$, with respect to $^{34}SO_4$, continues without interruption, and ^{32}S sulfide is never returned to the sulfate reservoir in the monimolimnion. Deevey and Nakai compared the lake to a reflux system. H_2S-enriched ^{32}S diffuses to the surface waters and is washed out of the lake, leaving a sulfur reservoir depleted in ^{32}S. The result is an ^{34}S value of $+57.5\%$ in the monimolimnion.

The sulfide produced by sulfate reducers may be oxidized by several sulfur bacteria. Common among these are members of *Beggiotoales* and *Thiobacteriaceae,* as well as photosynthetic bacteria of *Thiorhodaceae* and *Chlorobacteriaceae,* which are common in eutrophic lakes in which the hypolimnion is depleted in oxygen. An example is the development of photosynthetic sulfur bacteria, particularly *Chromatium* spp., between the anaerobic and aerobic zones of Lake Windermere (*11*). Butlin and Postgate (*7*) examined four lakes in the Libyan Desert which were saturated with $CaSO_4$ but were low in organic matter. From three of these lakes, 200 tons of raw sulfur (50% sulfur) were removed yearly. The three productive lakes produced massive crops of the purple sulfur bacterium, *Chromatium* and the green sulfur bacterium, *Chlorobium,* whereas the fourth, which produced no elemental sulfur, did not. In laboratory experiments, Butlin and Postgate were able to establish symbiotic growth of sulfate reducers and *Chromatium.* The photosynthetic bacteria, in addition to oxidizing sulfide to elemental sulfur, provided organic matter for growing sulfate reducers.

The biochemical activity of an organism may be regulated by environmental factors. Fitzgerald and Nelson (*18*) have shown recently that planktonic algae grown in water containing a surplus of phosphorus do not possess alkaline phosphatase activity. However, if the same organisms are deprived of orthophosphate, they do develop it. The measure of alkaline phosphatase activity shows promise as a tool for determining whether or not algae have grown in the presence of limiting or surplus phosphorus concentrations in natural waters.

Another way in which organisms affect the chemistry of natural waters is by accelerating the rate of a reaction that normally proceeds by nonenzymic processes. Hydrolysis of pyrophosphate and tripolyphosphate to orthophosphate has been shown to proceed at a slow rate in the absence of microorganisms in natural waters. However, in the presence of microorganisms, the rate is greatly accelerated (*9, 10, 57*).

A reaction of considerable importance in water pollution is the production of high acidity waters in coal mines. The acidity of these waters seems to be the result of oxidation of pyritic compounds. Although the oxidation mechanism is not understood, several investigators feel that microorganisms accelerate this reaction rate (*25*).

In summary, there are few, if any, elements whose aqueous environmental chemistry is not directly influenced and/or controlled by biochemical reactions. In addition to the direct influence, microorganisms may also be significant in the chemistry of elements in natural waters by altering the composition of the water with respect to other elements or compounds. For the purpose of this discussion, this type of reaction will be termed indirect. Examples of these reactions are discussed below.

Indirect Effects of the Aquatic Biota in Water Chemistry

In general, the indirect influence of aquatic organisms on the chemistry of elements in natural waters is the result of assimilation or excretion of compounds that react chemically with the element in the water. The changes in the amount of CO_2 in the water that accompany respiration and photosynthesis deserve special consideration since many reactions are influenced by pH.

Indirect Effects as a Result of CO_2 Changes. ACID-BASE. Since respiration and photosynthesis cause changes in the carbon dioxide content of the water and since the carbonic system determines the pH of most natural waters, large populations of organisms may influence the pH markedly. The diurnal variation of pH in the euphotic zone is commonly ±0.5 pH units and in eutrophic lakes the epilimnion may have a pH that is several units higher than the hypolimnion (*39*). The surface variations are caused largely by the activity of photosynthetic organisms, and the pH gradient in eutrophic lakes by anaerobic metabolism of bacteria in the profundal. The magnitude of the pH effects attributable to the biota is determined by the numbers, types, and activity of the organisms present, as well as sunlight, turbidity, buffer capacity, pH, and turbulence. It is probable also that the magnitude of pH changes is greater at cell surfaces and that resulting reactions are more intense at these surfaces.

In addition to changing the pH of the water, the uptake and release of CO_2 alter the buffer capacity of the water. The effect upon buffer capacity is the result of two factors: (1) the dependence of buffer capacity on the hydrogen ion concentration, and (2) the dependence of buffer capacity on the total concentration of weak acid and conjugate base in solution (*67, 68*). The precipitation of $CaCO_3$ in natural waters reduces the buffer capacity to a value lower than that predicted on the basis of pH change and respiratory or photosynthetic changes in CO_2 content of the water.

DEGREE OF PROTOLYSIS. The most obvious effect of a pH change is the degree of protolysis of the acids present in solution. The distribution of carbonic species (CO_2, HCO_3^-, and CO_3^{2-}), phosphates, sulfide, hydrous oxides of iron and aluminum, and organic acids is determined by pH. Since many chemical reactions (precipitation and complexation) take place between the conjugate base and some other element, a change in the degree of protolysis many result in a change in the extent of these reactions.

PRECIPITATION REACTIONS. A change in the pH of a natural water may result in the precipitation from solution of those species that are at or near saturation if one of the precipitating species enters into acid-base reactions. The classical example is the photosynthetic precipitation of calcium carbonate. During photosynthesis, aquatic plants may remove sufficient CO_2 to raise the pH to the value at which the concentration of carbonate times that of calcium exceeds the solubility product for calcium carbonate. If nucleation occurs, calcium carbonate will be precipitated.

Bacteria have been reported to enhance the precipitation of $CaCO_3$ in sea water. Recently, Oppenheimer (*49*) has demonstrated an increase in the formation of aragonite in aged-filtered sea water enriched with 0.1% $NaNO_3$ and 0.67% $NaHCO_3$ when inoculated with washings from oolytic deposits. Greenfield (*24*) studied the influence of a marine pseudomonad on the precipitation of $CaCO_3$ from artificial sea water enriched with 1% peptone. Bacterial cells became enriched in calcium and magnesium with respect to the surrounding medium. Crystals of aragonite were formed in the presence of the bacteria but not in uninoculated controls. Single bacterial cells formed the nuclei of individual crystals, and Greenfield proposed that the bacterial surfaces—particularly the surfaces of dead cells—provided a concentrated calcium source. Raising the pH to values above that observed in the medium did not cause precipitation in the controls.

In addition to the removal of calcium and carbonate from solution, it is highly probable that other elements, such as Sr^{2+}, Pb^{2+}, and Zn^{2+}, are coprecipitated with $CaCO_3$. Normally, it would be expected that $CaCO_3$ precipitated during periods of high photosynthetic activity would be redissolved at night when pH is lower. However, Chave (*8*) has reported that $CaCO_3$ particles from the sea become coated with organic compounds that prevent solution of these particles in unsaturated water.

COMPLEXATION. A change in the pH of a natural water may change the degree of complexation of a species in solution since many complexing agents are also conjugate bases of weak acids and the stability of many complexes depends on pH. A change in pH may cause a change in degree of protolysis of the acid and therefore a change in the amount of complexing agent in solution. Since little is known about the nature of the complexing compounds in natural waters, it is impossible to estimate the significance of this effect.

REDOX REACTIONS. Changes in pH may significantly affect the rate of redox reactions. Stumm and Lee (*62*) have found that the rate expression for the reaction of dissolved oxygen and ferrous iron is:

$$-\frac{d\,(\mathrm{Fe(II)})}{dt} = k\,(\mathrm{Fe(II)})\,(\mathrm{O_2})\,(\mathrm{OH^-})^2$$

From this equation, it is evident that an increase of 1 pH unit will cause the rate of reaction to be increased 100 times. The rate of oxygenation of manganese(II) has been shown (*46*) to be pH dependent, the rate likewise increasing by a factor of 100 for each increase of 1 pH unit. The rate constant for the latter reaction is such that at the concentrations of manganese(II) and oxygen normally found in natural waters and in the pH range of 7–8, the reaction is quite slow. It is possible that the oxidation of manganese in natural waters occurs at the surface of algae during photosynthesis and at the surface of $CaCO_3$ crystals.

In addition to influencing the rate of a reaction, pH may also control the products where alternate or sequential pH-dependent reactions take place. An example of this type of reaction is the chlorination of phenol. Lee and Morris (*37*) have shown that the chlorination of phenol proceeds by the stepwise substitution at the 2, 4, and 6 positions of the aromatic ring. The rate of each of these reactions depends on the product of phenate or chlorophenate anion and the hypochlorous acid concentrations. Since each phenolic compound has a slightly different acid dissociation constant, the species of chlorophenols that are formed depend on the pH of the solution.

SORPTION. The sorption of a solute by particulate matter in natural waters may be highly pH dependent. Hydrogen ions may influence sorption by (1) competing for sorption sites, (2) modifying sorption sites, and (3) changing the degree of protolysis of the sorbing species. Since charged chemical species normally are more strongly sorbed at ionic sites (whereas uncharged species and large molecules are sorbed at van der Waals sites) and since both the nature of the sorption site and the sorbate may be altered by pH changes, the amount of sorption of a weak acid may be a function of water pH. The sorption of manganese(II) on freshly precipitated MnO_2 has been shown (*46*) to be influenced markedly by pH. They found that a fraction of a pH unit change around pH 7–8 could significantly change the amount of sorbed Mn(II). They proposed that this effect was caused by a change in the nature of sorption sites with pH. Studies should be conducted to determine whether or not sorption of Mn(II) on MnO_2 would behave similarly in the natural aquatic environment. If the laboratory results of Morgan and Stumm (*46*) are applicable to natural waters, several of the transition metals may show diurnal changes in the amount in solution as a result of diurnal pH changes.

The amount of sorption that occurs in natural waters may be influenced by pH by changing the amount of particulate matter present and the form of the precipitate. For example, if there is a diurnal precipitation and solution of $CaCO_3$, then the amount of compounds sorbed by this precipitate would exhibit a diurnal cycle.

FLOCCULATION. The precipitation of hydrous metal oxides—*e.g.*, iron and aluminum, may greatly influence the concentration of solutes in natural waters (*64*). Various studies have shown that the degree of incorporation of many solutes depends on the pH at which flocculation takes place (*44*).

Indirect Effects Other Than CO_2 Changes. In addition to altering the pH of natural waters, biological organisms may excrete and sorb compounds, particularly organic compounds, which enter into chemical reactions with other compounds in solution. There is little doubt but that a substantial part of the organic matter present in natural waters is produced by organisms in the water and to some extent in the watershed.

The nature of the organic compounds in natural waters has been the subject of considerable study (*15, 40, 52, 65, 66*). Only a few general comments are pertinent here. The fact that the greater part of the organic matter present in natural waters is nonliving is often overlooked by workers in water chemistry. Parsons (*52*) reported that in the euphotic zone of the sea, the relative proportions of organic matter are:

soluble organics	100
detritus	10
phytoplankton	2
zooplankton	0.2
fish	0.002

where the soluble organic matter is arbitrarily set at 100. According to Parsons (*52*), Duursma has reported an average dissolved organic carbon approximately 1 mg./liter near the surface of the North Atlantic Ocean. In many fresh waters, approximately 10 times this amount is normally found. Unpublished studies by Lee have shown that the concentration of dissolved organic carbon in Lake Mendota, Madison, Wis. is about 10 mg./liter and that of filterable solids about 2 mg./liter. The filterable solids in the surface waters are composed of approximately 10^6 phytoplankton cells/liter and 10^7 detritus (nonliving) particles/liter. The origin of this organic matter is believed to be the excretory and degradation products of plants and animals. In addition to aquatic organisms, terrestrial sources must be considered. Mackereth's (*43*) studies on the composition of lake sediments have shown that the sedimentary carbon probably reflects changes in the lake watershed rather than lake productivity. Also the organic matter in water may be significantly increased by domestic and industrial pollution.

Numerous studies have been conducted on the nature of the dissolved and particulate organic matter in natural waters. In general, these studies have shown that the composition of the bulk of the organic matter is undefined. Many of the laboratory studies on the nature of the dissolved organic matter in natural waters are of limited value owing to possible alteration of the compounds by the concentration and analytical methods used. The selectivity of the methods used to concentrate the solute to analytically detectable levels presents another problem in many analytical procedures used to study trace compounds in natural waters. Concentration procedures such as freezing, flocculation, sorption columns, and solvent extraction, have been shown to be selective for certain types of compounds (*32, 34, 38*). Extreme care must be exercised to insure that compounds found in concentrates of natural waters existed in the original sample.

Since the nature of the organic matter present in natural waters is not known, it is impossible to state with certainty the reactions that these compounds may influence or cause in natural waters.

ACID-BASE. The pH of natural waters is determined primarily by the carbonate equilibria. However, organisms may produce amounts of organic matter or ammonia sufficient to influence the pH and buffer capacity of the waters. It would be of interest to determine titration curves of high organic, high color, low alkalinity waters leached from some marshes. It is possible that these waters contain sufficient amounts of organic acids to be significant.

SOLUBILITY. Little is known about precipitation and dissolution of solutes in natural waters as a result of biological activity other than pH change. Possibly organic compounds excreted by organisms may form complexes with precipitates which would increase the concentration in solution. Evans (*16*) discussed the possible role that ATP, nucleic acids, and nucleotides may perform in solubilizing various minerals. Further study is needed before the significance of these reactions can be evaluated. Metallic ions also may be precipitated if the complexing organic substances holding them in solution are utilized as metabolic substrates by bacteria. Excessive blooms of algae in lakes are sometimes controlled by adding copper sulfate. In high alkalinity waters, copper is rapidly precipitated as a basic carbonate. To prevent its precipitation, copper may be added as a copper citrate complex. However, it has been found that the citrate is rapidly metabolized, and the copper is precipitated (*17*). Possibly this type of reaction may be significant in natural waters where dissolved organic matter could act as chelating agents forming complexes with metal ions, particularly iron.

Certain bacterial activities, such as denitrification and sulfate reduction, may be accompanied by $CaCO_3$ precipitation, apparently as a result of increases in the pH of the solution. However, it appears that some bacteria will precipitate $CaCO_3$ in amounts in excess of those which would be predicted by the pH change (*24*). The mechanism of this precipitation is not understood. As mentioned previously, the organic matter in natural waters appears to coat $CaCO_3$ particles and prevent their solution in undersaturated water (*8*). Kitano and Hood (*33*) have reported that the polymorphic form of calcium carbonate precipitated is influenced by certain organic compounds. Goldberg (*22*) has noted that the concentration profile of barium in the sea is similar to that of many nutrient elements. He suggested that the sulfate formed during the biochemical oxidation of organic sulfur compounds could lead to a subsequent formation of insoluble $BaSO_4$ within the decomposing biomass. As this mass sinks and decomposes, entraped $BaSO_4$ is released to the unsaturated water.

COMPLEXATION. Organic compounds excreted by aquatic organisms may result in the formation of complexes with transition metals in natural waters. Hood and Slowey (*28*) presented evidence indicating that appreciable amounts of copper in waters from the Gulf of Mexico exist in soluble complexes with organic matter. Since fresh waters, in general, contain larger amounts of dissolved organic matter, it is possible that copper and other transition metals exist as organic complexes. However, the demonstration of such complexes in natural waters must await further study.

One of the major difficulties encountered in studying complexes in natural waters is the inability to distinguish between compounds in true solution and those associated with particulate matter. This differentiation requires that some operational definition of "soluble" be adopted. A criterion based on the passage of the compound through a 0.45-μ pore size filter may lead to gross errors. Shapiro's (*58*) studies on the "holding capacity" of organic matter extracted from natural waters for iron and other metals have shown that iron and organic matter interact to form particles that will pass through a 0.45-μ pore, but are retained by 0.1-μ pores. It should be pointed out that complexation need not result in the formation of a soluble compound. Possibly ligand atoms which could form complexes with solutes are present on the "surfaces" of particulate matter present in natural waters. Such a reaction normally would be considered sorption.

Another example of an organometallic complex that has been found in natural waters is vitamin B_{12}. The stability constant of the cobalt in B_{12} must be large since both cobalt and B_{12} exist in natural waters at less than 1 μgram/liter.

SORPTION. One of the most important reactions involving organic matter present in natural waters is sorption. Biological organisms contribute organic matter that enters into these reactions and the detritus particles on which sorption of solutes may take place. There can be little doubt that the detritus particles influence the distribution of organic and inorganic compounds in natural waters. In addition, microorganisms may cause adhesion of particles forming aggregates as in soil [*see* review of Harris *et al.* (*26*)].

In addition to particulate organic matter, many natural waters contain large amounts of inorganic particulate matter which provide sorption sites for organic matter in water. Many rivers carry large amounts of suspended solids, especially during periods of high discharge. In lakes and oceans, turbidity currents may represent the transport of large amounts of suspended matter which is usually predominantly inorganic.

Bader (*2*) found that various clay minerals have large sorption capacities for dissolved organic compounds.

The sorbed organic substances can influence the distribution of other compounds in solution by changing the nature of the sorption sites. Fruh and Lee (*20*) have shown that the rate and extent of sorption of cesium by a stratified mica is influenced by inorganic and organic species in solution. In general, various organic compounds will compete for sorption sites, and the more strongly bound compounds will displace those with less affinity for the sites. In addition to competing for sites, the sorbed organics may activate or form new sites. Studies in the senior author's laboratory have shown that parathion is weakly sorbed by clay minerals. However, if these clay minerals are exposed to organic matter from natural waters, the amount of parathion sorbed will be increased. Similar reactions may occur with other organic and inorganic compounds. Shapiro's (*58*) studies on "holding power" of organics have shown that organics may control the particle size of precipitates.

A special case of sorption is the accumulation of surface-active compounds at the air-water interface. Surface-active compounds could affect the rates of gas transfer in natural waters. Mancy and Okun (*45*) have reported that surface-active compounds can markedly retard rates of gas transfer from air to water at low turbulence; however, these same compounds may increase the rate of gas solution at high turbulence.

REDOX REACTIONS. Aquatic organisms may alter the particular oxidation state of some elements in natural waters during activity. One of the most significant reactions of this type is sulfate reduction to sulfide in anoxic waters. The sulfide formed from this reaction can initiate several chemical reactions that can radically change the types and amounts of elements in solution. The classical example of this reaction is the reduction of ferric iron by sulfide. The resultant ferrous iron and other transition metals may precipitate with additional sulfide formed from further biochemically reduced sulfate. Iron reduction is often accompanied by a release of precipitated or sorbed phosphate. Gardner and Lee (*21*) and Lee (*36*) have shown that Lake Mendota surface sediments contain up to 20,000 p.p.m. of ferrous iron and a few thousand p.p.m. of sulfide. The biochemical formation of sulfide is undoubtedly important in determining the oxidation state and amounts of several elements in natural waters.

Organic matter in natural waters may enter into redox reactions with certain compounds in solution. Hem (*27*) has shown that tannic acid will reduce ferric iron to ferrous iron. Shapiro (*59*) has found ferric iron is reduced to ferrous iron in natural water samples boiled in acid. These reactions may proceed at slow rates in natural waters.

Organic materials in natural waters also may play an important part in redox reactions by complexing metal ions. Complex formation alters the free energy change of redox reactions. In general, a complexed metal ion will be a stronger oxidizing agent than the free species. Complexation of metals by organic compounds in natural waters could alter the redox potentials sufficiently to change the oxidation state of transition metals in natural waters relative to that which would be predicted based on the free species.

Summary

While the aqueous environmental chemistry of an element is determined by the thermodynamics and kinetics of its chemical reactions, and the amounts and forms of a particular element in pure water systems can possibly be predicted by chemical equilibria, in natural waters, aquatic organisms (particularly microorganisms) may significantly affect the concentrations of many elements. As in soil, the cycling of elements is largely the result of biological activity, and the many factors affecting the numbers or activity of organisms alter reaction rates and equilibrium concentrations. Effects of the aquatic biota upon the equilibrium composition of natural waters may be a direct result of biological activity, or they may result indirectly from changes in the pH, redox potential, or chemical composition of the water.

Although few investigations have led to reliable estimates of the actual influence of the biota upon the chemistry of natural waters and although much additional investigation is needed before the extent of biological influence upon chemical equilibria and involvement in geochemical cycles can be appreciated fully, it is clear that biota have dominant roles in water chemistry.

Acknowledgments

This paper was supported in part by a training grant, No. 5T1-WP-22-04, Federal Water Pollution Control Administration.

Literature Cited

(1) Babenzien, H., *Limnol.* **2,** 9 (1964).
(2) Bader, R. G., *Narragansett Marine Lab., Univ. R. I. Occas. Publ.* **1,** 42 (1962).
(3) Bardtke, D., *Naturwiss.* **52,** 401 (1965).
(4) Bock, E., *Arch. Mikrobiol.* **51,** 18 (1965).
(5) Brezonik, P. L., Lee, G. F., *J. Air Water Pollution* **10,** 145 (1966).
(6) *Ibid.*, p. 549.
(7) Butlin, K. R., Postgate, J. R., "Biology of Deserts," J. L. Cloudsley-Thompson, ed. Institute of Biology, London, 1954.

(8) Chave, K. E., *Science* **148**, 1723 (1965).

(9) Clesceri, N. L., Lee, G. F., *J. Air Water Pollution* **9**, 723 (1965).

(10) *Ibid.*, p. 743.

(11) Collins, V. G., *Proc. Soc. Water Treat. Exam.* **12**, 40 (1963).

(12) Cushing, C. E., Jr., *Ecology* **45**, 306 (1964).

(13) Deevey, E. S., Nakai, N., "Biogeochemistry of Sulfur Isotopes," M. L. Jensen, ed. Yale Univ., New Haven, pp. 169-178, 1962.

(14) Deevey, E. S., Jr., Nakai, N., Stuiver, M., *Science* **139**, 407 (1963).

(15) Duursma, E. K., "Chemical Oceanography," Vol. I, J. P. Riley and G. Skirrow, eds., pp. 433-475, Academic Press, New York, 1965.

(16) Evans, W. D., "Advances in Organic Geochemistry," U. Colombo and G. D. Hobson, eds., pp. 262-270, Pergamon Press, New York, 1964.

(17) Fitzgerald, G. P., Faust, S. L., *Water Sewage Works* **112**, 271 (1965).

(18) Fitzgerald, G. P., Nelson, T. C., *J. Phycology* **2**, 32 (1966).

(19) Fogg, G. E., "Physiology and Biochemistry of Algae," R. A. Lewin, ed., pp. 475-489, Academic Press, New York, 1962.

(20) Fruh, E. G., Lee, G. F., "Sorption of Cesium on Stratified Mica," in press.

(21) Gardner, W., Lee G. F., *J. Air Water Pollution* **9**, 553 (1965).

(22) Goldberg, E. D., "The Sea," Vol. II, M. N. Hill, ed., pp. 3-25, Interscience, New York, 1963.

(23) Golterman, H. L., *Verh. Internat. Verein. Limnol.* **15**, 544 (1964).

(24) Greenfield, L. J., *Ann. N.Y. Acad. Sci.* **109**, 23 (1963).

(25) Hanna, G. P., Brant, R. A., Lucas, J. R., Randles, C. I., Smith, E. E., *Ohio State Univ. Water Resources Center Rept.* **175** (1961).

(26) Harris, R. F., Chesters, G., Allen, O. N., "Dynamics of Soil Aggregation," in press.

(27) Hem, J. D., *U.S. Geol. Surv. Water Supply Paper* **1459-D** (1960).

(28) Hood, D. W., Slowey, J. F., *Texas A & M Progress Report, Proj.* **276**, AEC Contract No. AT-(40-1)-2799 (1964).

(29) Hutchinson, G. E., "A Treatise on Limnology—Geography, Physics, and Chemistry," Vol. I., Wiley, New York, 1957.

(30) Hynes, H. B. N., "The Biology of Polluted Water," Liverpool University Press, Liverpool, 1960.

(31) Jannasch, H., *Ber. Limnol. Flusstation Freudenthal* **7**, 21 (1956).

(32) Jeffrey, L. M., Hood, D. W., *J. Marine Res.* **17**, 247 (1958).

(33) Kitano, Y., Hood, D. W., *Geochim. Cosmochim. Acta* **29**, 29 (1965).

(34) Kobayashi, S., Lee, G. F., *Anal. Chem.* **36**, 2197 (1964).

(35) Kuhl, A., "Physiology and Biochemistry of Algae," R. A. Lewin, ed., pp. 211-229, Academic Press, New York, 1962.

(36) Lee, G. F., *Trans. Wisc. Acad. Sci. Arts Letters* **51**, 141 (1962).

(37) Lee, G. F., Morris, J. C., *J. Air Water Pollution* **6**, 419 (1962).

(38) Lee, G. F., Kumke, G. W., Becker, S. L., *J. Air Water Pollution* **9**, 69 (1965).

(39) Lee, G. F., Harlin, C. C., *Ind. Water Eng.* **2**, 36 (1965).

(40) Lee, G. F., ed., *Univ. Wis. Water Chem. Seminar*, Madison, Wis. Mimeo (1966).

(41) Lund, J. W. G., *Verh. Internat. Verein. Limnol.* **15**, 37 (1964).

(42) Lund, J. W. G., Mackereth, F. J. H., Mortimer, C. H., *Phil. Trans. Royal Soc.* **B246**, 255 (1963).

(43) Mackereth, F. J. H., *Proc. Royal Soc.* **B161**, 295 (1965).

(44) Malhotra, S. K., Lee, G. F., Rohlich, G. A., *J. Air Water Pollution* **8**, 487 (1964).

(45) Mancy, K. H., Okun, D. A., *J. Water Pollution Control Federation* **37**, 212 (1965).

(46) Morgan, J. J., Stumm, W., *Proc. Intern. Water Pollution Res. Conf. 2nd, Tokyo 1964* (1965).

(47) Oborn, E. T., *U.S. Geol. Surv. Water Supply Paper* **1459-F** (1960).
(48) *Ibid.*, **1667-C** (1964).
(49) Oppenheimer, C. H., *Geochim. Cosmochim. Acta* **23**, 295 (1961).
(50) Overbeck, J., *Naturwiss.* **52**, 145 (1965).
(51) Parés, Y., *Ann. Inst. Pasteur.* **107**, 136 (1964).
(52) Parsons, T. R., "Progress in Oceanography," Vol. I., pp. 205-239, M. Sears, ed. Pergamon Press, New York, 1963.
(53) Redfield, A. C., Ketchum, B. H., Richards, F. A., "The Sea," Vol. II, pp. 26-77, M. N. Hill, ed., Interscience, New York, 1963.
(54) Rheinheimer, G., *Arch. Mikrobiol.* **34,** 358 (1959).
(55) Rigler, F. H., *Limnol. Oceanog.* **9**, 511 (1964).
(56) Ruttner, F., "Fundamentals of Limnology," Univ. of Toronto Press, Toronto, 1953.
(57) Shannon, J. E., Lee, G. F., *J. Air Water Pollution* **10,** 735 (1966).
(58) Shapiro, J., *J. Am. Water Works Assoc.* **56,** 1062 (1964).
(59) Shapiro, J., *Limnol. Oceanog.* **11,** 293 (1966).
(60) Stark, W. H., McCoy, E., *Zentr. Bakteriol., Parasitenk., Infektiònsk. Abt. II.* **98,** 201 (1938).
(61) Steemann-Nielsen, E., *Deep-Sea Res., Suppl.* **3,** 281 (1955).
(62) Stumm, W., Lee, G. F., *Ind. Eng. Chem.* **53,** 143 (1961).
(63) Tesic, Z., Todorovic, M., *Rias. Comun. 6th Intern. Congr. Microbiol.* **3,** 149 (1953).
(64) Theobald, P. K., Jr., Lakin, H. W., Hawkins, D. B., *Geochim. Cosmochim. Acta* **27,** 121 (1963).
(65) Vallentyne, J. R., *J. Fish Res. Bd. Canada* **14,** 33 (1957).
(66) Wangersky, P. L., *Am. Scientist* **53,** 358 (1965).
(67) Weber, W. J., Stumm, W., *J. Chem. Eng. Data* **8,** 464 (1963).
(68) Weber, W. J., Stumm, W., *J. Am. Water Works Assoc.* **55,** 1553 (1963).
(69) Wolfe, R. S., "Principles and Applications in Aquatic Microbiology," H. Heukelekian and N. C. Dondero, eds., pp. 82-97, Wiley, New York, 1964.
(70) Wuhrman, K., *Ibid.*, pp. 167-192.

RECEIVED April 18, 1966.

INDEX

A

- Activation
  - energy 75
  - volume 77
- Activity
  - coefficient 96
  - definition 50
  - scales 45
    - infinite dilution 48
    - ionic medium 48
- Adsorption
  - and crystal structure 123
  - isotherms 139
    - linear 136
  - prediction 122
  - rates 176
  - sites on silica surfaces 171
  - specific 123
- Affinity 5
- Albite 250
- Alcoholic fermentation 279
- Algae 320
- Alkali metal chlorides, molal volumes of the 95
- Alkaline
  - environment 293
  - water 241
- Alkalinity 51
  - total 260
- Al_2O_3 133
- Aluminosilicates 143
- Aluminosilicate-solution equilibria 64
- Aluminum 192
  - species 21
- Ammonia 278
- Amorphous surface layer 168
- Anaerobic bacteria 321
- Anaerobic systems 279
- Analysis of water for trace metals 30
- Andalusite 148
- Andesine 223
- Anhydrite 235
- Anhydrous oxides 130
- Anoxic systems 288
- Apatite 153
  - equilibrium 253
- Aquatic
  - conditions, redox processes for 274
  - environment, potentials in the 270
  - organisms 320
- Aqueous surface chemistry of oxides and complex oxide minerals 121
- Aragonite 235, 247, 265
- Artinite 235
- *Asterionella* 323
- Atomic absorption spectroscopy 32
- Average composition of sediments 297

B

- *Bacillus circulans* 323
- Bacteria populations in water 321
- Barium in sea water 42
- *Beggiotoales* 327
- Biochemistry of elements 326
- Biological
  - activity *vs.* equilibrium composition of natural waters 319
  - cycle 325
  - enzymes 276
  - mediation of redox processes 271
- Biota on water chemistry, effects of 323
- Biotite 223
- Bismuth ion hydrolysis 189
- Brucite 236
- Buffer capacity 16, 184

C

- Calcite 235, 247, 265
- Calcium
  - carbonate equilibria 247
  - minerals 153
  - salts 155
  - in sea water 260
  - sulfate 277
- Carbonate
  - concentration 51
  - geochemistry 265
- Carbonates 299
  - heterogeneous equilibria involving 196
  - in sea water, solubility equilibria of 212
- Carbon dioxide, reduction to 307
- Carbonic acid, dehydration of 77
- Carbon system 278
- Cations
  - gallium-containing 184
  - isopoly- 184
- Charge
  - development 132

Charge *(Continued)*
  origin 123
  on oxides and hydroxides 124
  prediction 122
  reversal 132
Charging hydroxylated surfaces 125
Chelating agents 257
Chemical composition
  of minerals 289
  of springs and lakes 222
Chemical thermodynamics in natural water systems 1
Chemolithotropic organisms 326
Chlorella pyrenoidosa 321
Chloride coordination 259
Chlorite 62
Chlorobacteriaceae 327
Chlorobium 328
Chromatography, partition 185
Chromatium 328
Chrysotile 150
Clathrate-like cages 84, 88
Clay
  diagenesis 65
  minerals 134
Closed isothermal systems 3
Closed systems 2
Cluster models 84, 88
Coagulation 122
  effects 187
Coal 314
CO_2 changes 329
Coesite 164
Colorimetry 32
Common elements 296
Complexation 330
Complex oxide minerals, aqueous surface chemistry of 121
Composition
  of the Great Lakes 243
  of sea water 257
Concentration
  -dependent transitions 97
  of elements 326
  quotient 48
Coordination
  chemistry of the oceans 255
  entity 256
  fluoride 259
  number 128
Coprecipitates
  silica-alumina 150
  SiO_2-Fe_2O_3 151
Cristobalite 164
Critical concentration 95
Cryoscopy, fused salt 186
Crystal field stabilization energy 129
Crystallinity 132
Crystal structure, adsorption and 123
$Cu(OH)_2$, solubility constant of 209
CuO, solubility constant of 209
Cybotactic swarms 87

D

Debye-Hückle theory 92
Definition of pH 197
Dehydration of carbonic acid 77
Dense species 89
Detritus 62
Diagenetic processes 288
Dimers 86
Dissolution
  of carbonates 293
  patterns 172
Distribution coefficient 77
Dodecantimonates 190
Dodecatungstate 192
Dolomite 235, 251, 265
  equilibrium 249
Dynamic models 12

E

E_h 55
Elements
  biochemistry of 326
  common 296
  concentration of 326
Electrical double layer 125, 134
Electroanalytical methods 35
Electrode 271
  potential 279, 283
Electron activity 52, 272
Emission spectroscopy 31-32
Equilibria in organic geochemistry 312
Equilibrium
  composition of natural waters, biological activity *vs.* 319
  constant 6, 48
  model 8, 58, 68, 216
    of the Great Lakes 243
Errors in trace analysis 40
Eucken's polymer model 86
Eutrophic lakes 327
Evaporative concentration 232
e vs. pH diagrams 288
Exchange current 280

F

Facultative bacteria 321
Fe_2O_3 132
Fe_3O_4 132
Fe in sea water 54
Feldspars 223
Felsic rocks 232
Fermentation 275
Ferredoxin 274
Ferric oxide 279
Flame photometry 32
Flickering clusters 87
Flocculation 331
Florida red tide 262
Flotation
  ion 194
  precipitate 194
Fluidized vacancies 86
Fluoride coordination 259
Fluorite 153

Fragilaria 323
Frequency shifts 100
Fresh water scale 48
Fused salt cryoscopy 186

G

Galena 294
Gallium 193
  -containing cations 184
Geochemical balance 57
Geochemistry
  carbonate 265
  equilibria in organic 312
Gibbs energy 3
  of the solid-liquid interface 207
Gibbsite 223, 250
Gibbs phase rule 57, 244
Glauconite 63
Gran functions 51
Granitic rocks 223
Graphical presentation of solubility equilibria 203
Graphite 307
Great Lakes
  composition of the 243
  equilibrium models of the 243
Ground water 231
Gymnondinium breve 262
Gypsum 235

H

Hafnium 191
Heat of transport 78, 91
Heptamolybdate anions 186
Heterogeneous equilibria involving oxides, hydroxides, carbonates, and hydroxide carbonates 196
Hornblende 223
Humic acids 257
Huntite 235
Hydration
  of ions 92
  negative 93
  numbers 92
Hydrocarbons 313
Hydrogen bonds 106
  stabilization 103
Hydrogen ion concentration 198
Hydrolysis
  bismuth ion 189
  lead ion 188
  phenomena 183
Hydromagnesite 237
Hydrous oxides 130
Hydroxide carbonates
  heterogeneous equilibria involving 196
  in sea water, solubility equilibria of 212
Hydroxides
  charge on 124
  heterogeneous equilibria involving 196
Hydroxides *(Continued)*
  in sea water, solubility equilibria of 212
Hydroxo complexes 126, 259
Hydroxyapatite 253
Hydroxylated surfaces, charging 125
Hydroxyl number 189

I

Ice-lattice models 84
Ice structures 84
IEP(s) 123
Illite 62
Index of refraction of water 73
Infinite dilution activity scale 48
Infrared spectra of water 107
Inorganic solute species 183
Intrinsic viscosity 186
Inverse polarography 35
Ion
  exchange capacity 137
  flotation 194
Ionic
  diameter, mean 92
  medium activity scale 48
  medium method 47, 49
Iron
  (III) compounds 305
  native 309
  in rocks, oxidation state of 297
Isoelectric point 121, 126
Isolated systems 2
Isopolyanions 184
Isopolycations 184
Isopolymolybdates 193
Isopolytungstates 186
Isothermal compressibility of water 74

K

Kaolinite 60, 150, 223, 250
Kerogen 314
K-feldspar 223, 250
Kinetics of reactions 11
K^+-mica 250
Kyanite 148

L

Labile complex 258
Lakes
  chemical compositions of 222
  composition of the Great 243
  equilibrium models of the Great 243
  water chemistry 247
Langmuir isotherm 175
Lansfordite 235
Lead 294
  ion hydrolysis 188
Ligands 257
Light-scattering 186
Linear adsorption isotherms 136
Living organisms 274
Lizardite 150

Logarithmic diagram 45
Log K 52

M

Magnesite 235
Magnesium 261
Magnetic susceptibility of water .. 107
Manganese
  oxidation of 24
  oxides 279, 294
Marine sediments 57
Master variables 45
Mean ionic diameter 92
Membrane potentials 79
Meromictic lake 327
Metallic species, oceanic 261
Metal oxides 299
Metamorphic processes 288
Metastable solids 210
Metastability 313
Meteoritic organic matter 317
Methane fermentation 278
Mica 60, 223
Minerals
  aqueous surface chemistry of
    complex oxide 121
  chemical composition of 289
  in vein association in Långban .. 290
Mixed potentials 283
MnO, slaking of 294
MnO_2 ....122, 132, 135
Model sea water 49
MOH acidity 125
MOH groups 124
Molal volumes of the alkali metal
    chlorides 95
Molar surfaces 208
Molybdate-active silicic acid 161
Monolayers of palmitic acid 79
Monomeric water molecule 89
Monomers in water 104
Montmorillonite ..62, 64, 223, 228, 250
Moplis 57

N

Native
  iron 309
  lead 289
  metals 291
Natural water systems, chemical
    thermodynamics in 1
Negative hydration 93
Nernst potentials 279
Nesquehonite 235
Neutron
  activation 36
  inelastic scattering 110
  spectra 101
Nitrobacter winogradskyi 327
Nitrogen system 278
Nitrosomonas europaea 327
Nonelectrolyte solutions 111
Nonequilibrium processes 317
Nonstoichiometry 132
Nuclear magnetic resonance ...107, 187

O

Oceanic metallic species 261
Ocean models 60, 67
Oceans, coordination chemistry
    and the 255
Ocean sediments 62
Oligeneric silicic acid 161
Olivine 149
Open systems 12
Operational definition 50
Optical methods 31
Organic geochemistry, equilibria in 312
Organic matter, oxidation of 299
Organisms 314
Oxidation
  of manganese 24
  of organic matter 299
  processes 299
  -reduction systems 270
  state of iron in rocks 297
Oxide minerals, aqueous surface
    chemistry of complex 121
Oxides
  aqueous surface chemistry of ... 121
  charge on 124
  heterogeneous equilibria
    involving 196
  in sea water, solubility equilibria
    of 212
  and sulfides 288
  ZPC of complex 137
Oxidizing intensity 272

P

Palmitic acid, monolayers of 79
Particle size 208
  effect 206
Partition chromatography 185
PDI 126, 153
pE 52, 272
  scale 55
Pelagic sediments 288
  redox processes in 301
Periclase 293
Petroleum 314
pH 50
  -controlling redox reactions 286
  definition of 197
  in sea water 50
Phase rule, Gibbs 57
Phillipsite 62
Phosphate 45
  equilibria 249
  minerals 153-4
Photosynthesis 273
Pigments 317
Plagioclase feldspars 223

Plasma spectroscopy 32
Platinum 280
Polarization curve 280
Polarography 35
Polymorphous modifications,
  solubility of 206
Potential-determining
  ions 123, 126, 153
  rate 149
Potentials in the aquatic
  environment 270
Potentiometric titration 185
Precipitate flotation 194
Precipitation reactions 329
Protolysis 329
Pseudomonas 320

Q

Quartz 62, 164, 223

R

Raman spectra 107, 186
Redox
  couples 271
  equilibria 270
  potentials 52, 272
    for aquatic conditions 274
  processes in pelagic sediments 301
  processes, biological mediation of 271
  reactions 52, 330
Red tide 262
Reduction of
  carbon dioxide 307
  sulfate 305
Respiration 275
Robust complex 258

S

Saline waters 241
Salting out 111
Scale, fresh water 48
Scenedesmus obliquus 321
Scheelite 153
Sea water 46, 113
  barium in 42
  calcium in 260
  composition of 257
  model 49
  strontium in 42
Sedimentation 122
Sediments
  average composition of some 297
  marine 57
  ocean 62
Self-diffusion 186
Sepiolite 235
Serpentine 235
  minerals 150
Sierra Nevada spring waters 223
Sierra waters 232
Significant structure theory 86
Silica 124, 142, 235, 250
  -alumina co-gels 134
    coprecipitates 150
  modifications 164
Silicate
  equilibria 249
  reactions 304
  stability 250
Silicates 146, 223, 254
Silicic acid 161
  oligeneric 161
  molybdate-active 161
Silicon concentration 323
Sillimanite 148
SiO_2-Fe_2O_3 coprecipitates 151
Slaking of MnO 294
Soil waters 228
Solid-liquid interface, Gibbs
  energy of 207
Solid solution 211
Solubility
  constants 197
    of CuO 209
    of $Cu(OH)_2$ 209
    of $ZnCO_3$ 200
  equilibria
    graphical presentation of 203
    of oxides, hydroxides, carbonates, and hydroxide carbonates in sea water 212
  of polymorphous modifications 206
  product of ZnO 208
Solute-solvent interactions 70
Solute species, inorganic 183
Solution medium 190
Sorption 331
Space charge 132, 134
Specific adsorption 123, 133
Spectrophotometry 186
Springs, chemical compositions of 222
Stabilization
  hydrogen bond 103
  structural 103
  of water structure 112
Standard hydrogen electrode 52
Steady-state system 216
Stishovite 164
Stoichiometric constants 197
Strontium 261
  in sea water 42
Structural charge 134
Structural stabilization 103
Structure of water 70, 84
Sulfate, reduction of 305
Sulfates 299
Sulfides 294
  and manganese oxides 290
Sulfur system 276
Surface charge 126
Surface hydroxide groups 124
Surfaces, charging hydroxylated 125

T

Tabellaria 323
Talc 235
Tannins 257
Temperature and time 190
Ternary systems Me^{2+}-H_2O-CO_2 .. 196
Thalassiosira nana 321
Thermal conductivity of water ... 74
Thermodynamic constants 197
Thermodynamics in natural water
    systems, chemical 1
Thiobacteriaceae 327
Thorium solutions 187
Time and temperature 190
TiO_2 132
Total alkalinity 260
Trace
  analysis 31
    errors in 40
  metals, analysis of water for 30
Transport, heats of 91
Tridymite 164
Two-state theory of liquid water .. 85

U

Ultracentrifuge 186
Ultrasonic absorption 86

V

Variables, master 45
Vitreous silica 164

W

Water
  composition 229
  infrared spectra of 107
  index of refraction of 73
  isothermal compressibility of .. 74
  magnetic susceptibility of 107
  monomers in 104
  -solute interactions 70
  structure of 70
  structure, stabilization of 112
  thermal conductivity of 74
  two-state theory of liquid 85
  -water interactions 99
Weathering of rocks 223

X

X-ray analysis 32
X-ray crystal structure 185

Z

Zeolite 63
Zero point of charge 121, 134
Zinc carbonate 199
$ZnCO_3$, solubility constants of 200
ZnO, solubility product of 208
ZPC 123, 134
  of complex oxides 137
  non-oxides 153
Zircon 149
Zirconium 191